UNIVERSITÉ AIX-MARSEILLE II

Centre National de la Recherche Scientifique

Laboratoire d'Ingénierie des Systèmes Macromoléculaires

THÈSE

de Microbiologie Moléculaire et Biotechnologie

pour obtenir le grade de

Docteur de l'Université Aix-Marseille II

Présentée et soutenue par

Astrid WAHL

le 20 octobre 2010

L'Organisation moléculaire et la Réponse au Stress de la Voie de Biosynthèse des Phospholipides chez *Escherichia coli*

Membres du Jury :

Dr. Didier Zerbib	**Rapporteur**
Pr. Carlos Blanco	**Rapporteur**
Dr. Mireille Ansaldi	**Présidente du Jury**
Pr. James N. Sturgis	**Co-directeur de thèse**
Dr. Emmanuelle Bouveret	**Co-directrice de thèse**

Résumé
Les phospholipides sont à la base de l'architecture de la membrane plasmique bactérienne. La composition de celle-ci est en permanence contrôlée par les conditions extérieures afin d'adapter sa fluidité et maintenir l'homéostasie. Les différentes étapes de la voie de biosynthèse des phospholipides dans la membrane interne de *E. coli* sont bien connues. En revanche, on connaît peu l'organisation supramoléculaire et la régulation génétique des enzymes, ce qui correspond aux deux grands axes de recherche développés dans cette thèse.
Des études par double hybride bactérien ont mis en évidence un réseau d'interactions protéine-protéine, suggérant l'existence d'un complexe formé par les enzymes de la synthèse des phospholipides dans la membrane. Pour tester cette hypothèse, j'ai voulu étudier ces interactions en conditions natives, en utilisant des techniques comme le FRET, le BRET ou la purification TAP. Pour cela, j'ai développé de nouvelles cassettes permettant la construction systématique de souches de *E. coli* produisant des protéines étiquetées avec des rapporteurs fluorescents ou des tags d'affinité, en condition d'expression physiologique. Ceci m'a permis d'étudier la localisation et la stœchiométrie des enzymes de synthèse des phospholipides dans la membrane.
J'ai également étudié la régulation en réponse au stress du gène *plsB*, qui code pour la première enzyme de la voie de biosynthèse des phospholipides, et de *dgkA*, qui code pour une diacylglycerol kinase permettant le recyclage des phospholipides. Ces deux gènes, divergents sur le chromosome, sont régulés de façon antagoniste en réponse à trois types de stress : le facteur de réponse au stress extracytoplasmique σE active *plsB* et inhibe *dgkA*; le système à deux composants BasRS active *dgkA* et inhibe *plsB* ; la réponse stringente active *dgkA* et inhibe *plsB*. Ces résultats montrent que le locus *plsB-dgkA* est finement régulé par toute une série de régulateurs qui intègrent des signaux de stress multiples afin de contrôler l'activité de la voie de biosynthèse des phospholipides.

Summary
Phospholipids are the building blocks of the bacterial plasmic membrane. The composition of the membrane is continuously controlled by environment conditions, in order to adapt its fluidity and maintain the homeostasis. The enzymatic steps of the phospholipid synthesis pathway in the inner membrane of *E. coli* are well known. However, little is known about the supramolecular organization and the genetic regulation of the enzymes catalyzing these reactions, these questions constituting the two main axes developed in this thesis.
Two-hybrid studies have evidenced a network of protein-protein interactions, suggesting the existence of a membrane protein complex formed by phospholipid synthesis enzymes. To test this hypothesis, I wanted to assay these interactions in native conditions, by using techniques such as FRET, BRET or Tandem Affinity Purification. Toward this goal, I have developed novel cassettes permitting to systematically construct *E. coli* strains that produce proteins tagged with fluorescent or affinity tags, under physiological expression. This allowed me to study the localization and stœchiometry of phospholipid synthesis enzymes in the membrane.
Furthermore, I have studied the regulation in response to stress of the *plsB* gene that codes for the first enzyme of the phospholipid synthesis pathway, and of *dgkA* that codes for a diacylglycerol kinase that recycles phospholipids. These two neighboring and divergent genes are inversely regulated in response to three stress responses: the extracellular stress σE factor activates *plsB* and inhibits *dgkA*; the two-component system BasRS activates *dgkA* and inhibits *plsB*; stringent response activates *dgkA* and inhibits *plsB*. These results show that the *plsB-dgkA* locus is regulated by a series of regulators that integrate multiple stress signals, in order to control the activity of the phospholipids synthesis pathway.

Mots clés : phospholipides, interactions protéine-protéine, métabolisme des lipides, réponse au stress, RpoE, BasRS, *Escherichia coli*.

Discipline : Microbiologie Moléculaire

Laboratoire d'Ingénierie des Systèmes Macromoléculaires
CNRS UPR9027, 31 Chemin Joseph Aigiuer, 13402 Marseille Cedex 20

SOMMAIRE

LISTE DES ABREVIATIONS

ACP : acyl carrier protein
ADN : acide déoxyribonucléotide
ADP : adénosine diphosphate
ARN : acide ribonucléotide
ATP : adénosine triphosphate
BACTH : bacterial two hybrid
BG : β-galactosidase
B. subtilis : *Bacillus subtilis*
β-ME : β-mercaptoéthanol
CBP : calmodulin binding peptide
CDP : cytosine diphosphate
CTP : cytosine triphosphate
CL : cardiolipine
CoA : coenzyme A
DHAPAT : acyl-CoA:dihydroxyacetonephosphate-acyltransfrase
DOx nm : densité optique à x nanomètres
DTT : dithiothreitol
E. coli : *Escherichia coli*
ECFP : enhanced cyano fluorescent protein
EDTA : acide éthylènediaminotétraacétique
EGFP : enhanced green fluorescent protein
EGTA : éthylèneglycol-bis(ß-aminoéthyl ether)
EYFP : enhanced yellow fluorescent protein
FASI : fatty acid synthesis type I
FASII: fatty acid synthesis type II
G3P : glycérol-3-phosphate
GDP : guanosine diphosphate
GlcNac : Nacétyl-glucosamine
GMSA: gel mobility shift assay
GPAT : glycérol-3-phosphate acyltransférase
GTP : guanosine triphosphate
IgG : immunoglobulin G
IPTG : isopropyl-beta-D-thiogalactopyranoside
KAS : kétoacyl-ACP synthase
kDa : kilodaltons
KDO : 2-keto-3-déoxyoctonate
L-Ara4N : 4-amino-4-deoxy-L-arabinose
LPAAT : lysophosphatidate acyltransférase
LPEAT : 2-acylglycérophosphoéthanolamine acyltransférase
LPS : lipopolysaccharide
mRFP : monomeric red fuorescent protin
M. tuberculosis : *Mycobacterium tuberculosis*
N. meningitidis : Neisseria meningitidis
OMP : protéine de la membrane externe
OPG : glycanes périplasmiques osmoregulés
PA : phosphatase alkaline
PAP : complexe péroxydase anti-péroxydase
PBS : phosphate-buffered saline
PCR : réaction de polymérisation en chaîne

PE : phosphatidyléthanolamine
PG : phosphatidylglycérol
4'PP : 4'-phosphopantéthéine
ppGpp : guanosine 3'5'-bispyrophosphate
PLD : phospholipase D
ProtA : protein A of *Staphylococcus aureus*
RedGal : 6-Chloro-3-indolyl-β-D-galactoside
RMN : Nuclear Magnetic Resonance
S. cerevisae : *Saccharomyces cerevisae*
SDS : sodium dedocyl sulfate
SDS-PAGE : gel dénaturant au SDS
SPA : sequential peptide affinity
TAP : tandem affinity purification
TCS : système à deux-composants
TEV : tabacco etch virus
TMS : segment transmembranaire
ts : thermosensible
UDP-GlcNac : UDP-N-acétylglucosamine
X-Gal : 5-bromo-4-chloro-3-indolyl-beta-D-galactoside
Xphos : 2-Dicyclohexylphosphino-2′,4′,6′-triisopropylbiphenyl

AVANT-PROPOS

J'ai effectué ma thèse au Laboratoire d'Ingénierie des Systèmes Macromoléculaires sous la co-direction du Dr. Emmanuelle Bouveret et du Prof. James Sturgis. Mes travaux de thèse devaient s'intégrer au projet de recherche INMEMBRANE financé par l'ANR, en collaboration entre les deux groupes, consistant à développer des méthodes pour caractériser de nouveaux complexes protéiques membranaires. Le groupe d'Emmanuelle Bouveret travaille sur les liens existant entre la réponse au stress et le métabolisme des lipides chez *Escherichia coli*, et apportait au projet le modèle d'étude des enzymes de synthèse des phospholipides dans la membrane. En parallèle, le groupe de James Sturgis était intéressé par les développements technologiques nécessaires au projet, en particulier l'étude des protéines membranaires, et les techniques de transfert de fluorescence à appliquer à *Escherichia coli*.

Je me suis donc intéressée à la biosynthèse des phospholipides dans la membrane interne de *E. coli*. Les réactions enzymatiques successives de cette voie de biosynthèse sont bien décrites, mais l'organisation moléculaire dans la membrane des enzymes responsables et leur régulation génétique sont peu connues. Pendant sa thèse (2002-2005), Djamel Gully avait mis en évidence pour la première fois en utilisant le double hybride bactérien (BACTH) l'organisation en complexe protéique des enzymes impliquées dans la voie de biosynthèse et le recyclage des phospholipides. C'est à la suite de ces études que se situe mon sujet. Le but premier de ma thèse était de caractériser les enzymes de la synthèse des phospholipides au niveau de leur organisation supramoléculaire (localisation, topologie, interactions) dans la membrane interne. Toutefois, dans un deuxième temps, j'ai également étudié la régulation génétique en réponse au stress de deux gènes importants de cette voie de synthèse, et mis en évidence des connexions entre la synthèse des phospholipides et celle du LPS.

Dans l'introduction bibliographique, j'ai donc choisi de présenter l'ensemble du métabolisme des lipides, mais également celui du LPS, et leurs régulations génétiques. Le cycle de biosynthèse *de novo* des acides gras dans le cytoplasme et le cycle de dégradation des acides gras sont tout d'abord exposés (§ I). La voie de biosynthèse des phospholipides chez *E. coli* est ensuite décrite (§ II), suivie du peu d'information disponible sur l'organisation moléculaire des enzymes de la biosynthèse des phospholipides dans la membrane (§ III). Puis, je présente la synthèse du LPS et sa régulation (§ IV). Comme nous nous intéressons au laboratoire aux liens existant entre la réponse au stress et le métabolisme des lipides, je décris dans la dernière partie de l'introduction la régulation des gènes du métabolisme des (phospho)lipides (§ V).

La partie 'résultats' est organisée en deux grands chapitres qui correspondent aux deux axes de mon travail de thèse, suivis d'un chapitre 'matériel et méthodes'. Cette partie est écrite en anglais pour des raisons de commodité.

Pour étudier l'organisation moléculaire des enzymes de synthèse des phospholipides dans la membrane, j'ai construit une série de nouvelles cassettes permettant de fusionner les gènes de *E. coli* sur le chromosome avec les séquences de protéines fluorescentes et luminescentes. Ce travail a fait l'objet d'un article dans PROTEOMICS (article 1). Cet article est suivi de résultats complémentaires puis d'une discussion fournie qui expose les problèmes rencontrés. Dans ce chapitre sur l'organisation moléculaire des enzymes de synthèse des phospholipides, je présente ensuite les résultats de microscopie de fluorescence et de quantification que j'ai obtenus sur les enzymes de synthèse des phospholipides. Dans un deuxième temps, j'explique la stratégie v-TAP que nous voulons développer pour la purification de complexes membranaires natifs, et les résultats préliminaires que j'ai obtenus (résultats § II).

Dans le deuxième chapitre des résultats, je présente notre étude de la régulation des gènes *plsB* et *dgkA* en réponse à divers stress. Ce travail, présenté sous forme de manuscrit (article 2), a ouvert de nombreuses questions et de nombreuses pistes de travail. Nos résultats montrent qu'il reste énormément à comprendre et à découvrir sur le métabolisme des lipides, que ce soit sur sa régulation ou sur la participation de protéines de fonction inconnue. Ceci est discuté dans une conclusion et discussion générale du travail de thèse.

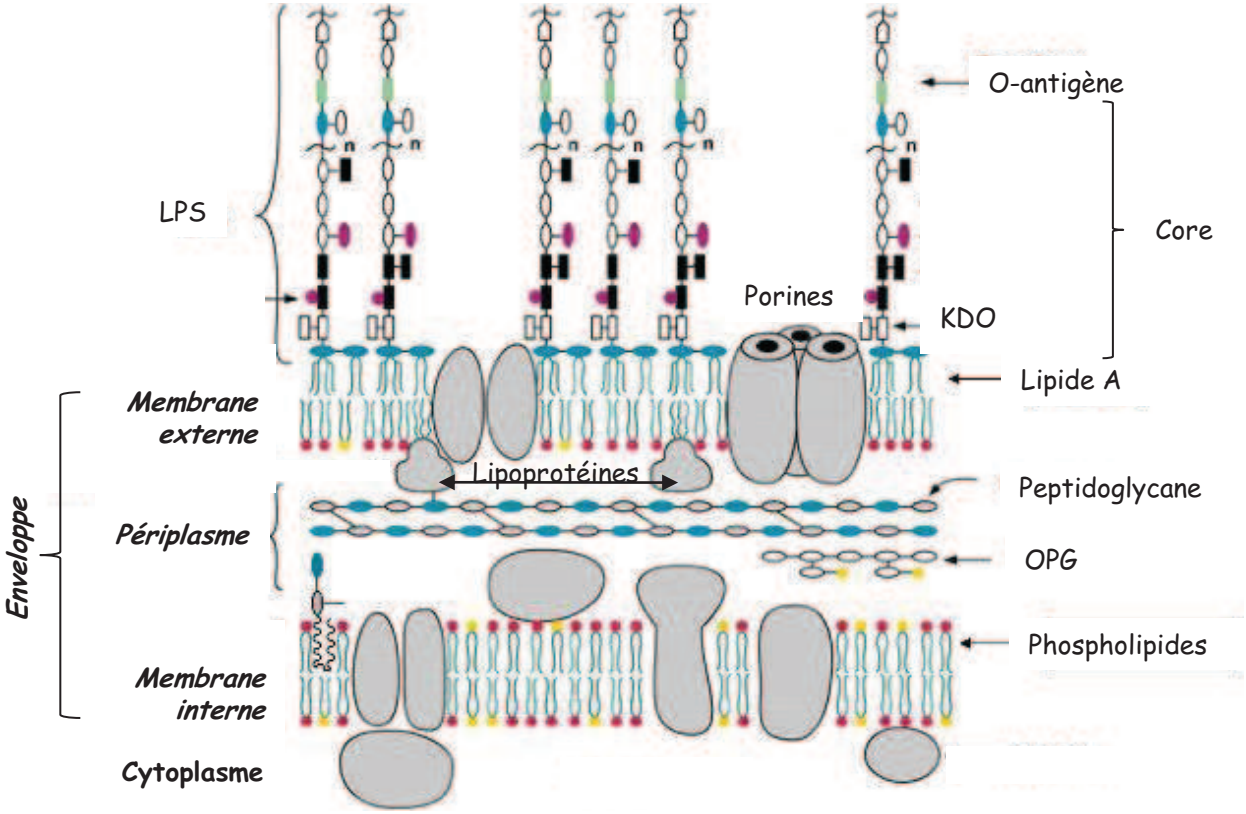

Figure 1: L'enveloppe cellulaire de *E. coli*, une bactérie à GRAM négatif (Raetz & Whitfield, 2002).
OPG: osmoregulated periplasmic glucan; LPS: lipopolysaccharide; KDO: 2-keto-3-déoxyoctonate.

INTRODUCTION BIBLIOGRAPHIQUE

L'enveloppe bactérienne peut être définie comme une frontière perméable protégeant la bactérie des agressions extérieures tout en permettant de nombreux échanges avec l'environnement. L'enveloppe cellulaire de *E. coli*, comme celle des différentes bactéries à GRAM négatif, est constituée de deux membranes, délimitant un espace périplasmique (figure 1). La membrane externe est formée par un feuillet asymétrique composé de phospholipides sur la face interne et en majorité de LPS sur la face externe. Le peptidoglycane, élément déterminant la morphologie bactérienne, est ancré à la face interne de la membrane externe. La membrane interne est formée par un feuillet symétrique de phospholipides. Chez *E. coli*, les espèces lipidiques se répartissent dans trois grandes classes: les phospholipides ($2x10^7$ molécules par cellule), le lipide A, composant du LPS ($2x10^6$ molécules par cellule), et les lipoprotéines. Ces espèces lipidiques chez *E. coli* sont principalement localisées au niveau de l'enveloppe cellulaire.

Dans un premier temps, je décrirai le métabolisme des acides gras (§ I) en détaillant le cycle de biosynthèse *de novo* (§ IB), la voie d'importation des acides gras exogènes (§ IC) et la voie de dégradation des acides gras (§ ID). Puis, je présenterai la biosynthèse des phospholipides (§ II), en incluant leur utilisation pour des biosynthèses secondaires dans l'enveloppe comme la modification du LPS, la biosynthèse des lipoprotéines, ou la biosynthèse des OPGs (osmoregulated periplasmic glucans). Le peu de données sur l'organisation moléculaire des enzymes de synthèse des phospholipides est exposé (§ III). Dans le quatrième chapitre, la voie de biosynthèse du LPS, les modifications du lipide A, et la régulation par des signaux de stress seront présentés (§ IV).

Finalement, je m'attacherai à montrer les mécanismes connus de la régulation des voies de synthèses des acides gras et des phospholipides, en insistant sur les mécanismes de réponse au stress (§ V).

Name (length)	Structure	[a] Fraction of total (%)
Major species		
Palmitic (16:0)	$CH_3(CH_2)_{14}COOH$	25–40
Palmitoleic (16:1)	$CH_3(CH_2)_5C(H)=C(H)(CH_2)_7COOH$	25–40
cis-Vaccenic (18:1)	$CH_3(CH_2)_5C(H)=C(H)(CH_2)_9COOH$	25–35
Minor species		
Lauric (12:0)	$CH_3(CH_2)_{10}COOH$	0–1
Myristic (14:0)	$CH_3(CH_2)_{12}COOH$	1–5
cis-9,10-Methylene-hexadecanoic (17:0)	$CH_3(CH_2)_5C(CH_2)C(H)(H)(CH_2)_7COOH$	1–20 [b]
Stearic (18:0)	$CH_3(CH_2)_{16}COOH$	0–1
Lactobacillic (19:0)	$CH_3(CH_2)_5C(CH_2)C(H)(H)(CH_2)_9COOH$	1–20 [b]
Unique to lipopolysaccharide		
3-D-Hydroxymyristic (14:0)	$CH_3(CH_2)_{10}CH(OH)—CH_2—COOH$	[c] -

Figure 2: Les acides gras dans la membrane de *E. coli* (Raetz & Newman, 1978). [a] Composition typique en acides gras chez *E. coli* K-12 en conditions de croissance de 30 à 37°C. [b] Des acides gras cycloprapanés s'accumulent pendant la phase stationnaire au détriment des acides palmitoléique et cis-vaccénique. [c] Pas detecté dans la fraction des phospholipides.

I. LE METABOLISME DES ACIDES GRAS CHEZ *E. COLI*

Les acides gras sont des acides carboxyliques de formule R-COOH où le radical R est une chaîne aliphatique de type hydrocarbure de longueur variable (C2 x n) qui donne à la molécule son caractère hydrophobe (DiRusso *et al.*, 1999). Les espèces des acides gras présents en majorité chez *E. coli* sont des acides gras avec 16 ou 18 atomes de carbone : palmitique (16:0; 25-40 %), palmitoléique (16:1; 25-40 %) et *cis*-vaccénique (18:1; 25-35 %) (figure 2) (Raetz & Newman, 1978). Mais les acides gras ne sont pas présents sous forme libre : soit ils sont liés à des cofacteurs comme l'acyl carrier protein (ACP) dans le cas de la synthèse des acides gras ou au Coenzyme A (CoA) pour leur dégradation dans le cytoplasme, soit ils sont intégrés dans les phospholipides. En effet, les acides gras sont les éléments de base nécessaires à la synthèse de phospholipides membranaires. En outre, les acides gras peuvent être utilisés pour des métabolismes secondaires, comme pour la synthèse de l'acide lipoïque ou des homoserinelactones.

La synthèse des acides gras est une combinaison de réactions enzymatiques nécessitant l'activité de nombreuses protéines. L'organisation des enzymes catalysant cette synthèse permet de différencier deux types distincts de synthèse suivant les organismes. D'un coté, les eucaryotes et certaines mycobactéries réalisent une synthèse grâce à des protéines multifonctionnelles (synthèse de type I ou FASI). D'un autre côté, dans les bactéries, les apicoplastes, les chloroplastes et les mitochondries d'eucaryotes, un système de synthèse des acides gras de type II (FASII) est présent dans lequel toutes les réactions enzymatiques sont réalisées par des protéines différentes.

La machinerie de synthèse des acides gras de type II a été étudiée depuis les années 60 en utilisant *E. coli* comme organisme modèle.

A. L'acyl carrier protein, co-facteur central pour la biogenèse des acides gras

ACP est la protéine centrale de la biosynthèse des acides gras pour les deux types de synthèse, FASI (fatty acid synthesis type I) et FASII (fatty acid synthesis type II). Dans les deux cas, ACP a pour fonction de présenter la chaîne acyle en formation à toutes les enzymes durant le processus de synthèse des acides gras. Durant cette synthèse, les chaînes d'acides gras sont liées par un groupement thioester à ACP. ACP est essentielle chez *E. coli* (De Lay & Cronan, 2006). C'est une petite protéine de 8 kDa (kilodaltons) très acide (point isoélectrique de 4,1) (figure 3). ACP est très abondante puisque avec environ 60000 copies par cellule elle représente 0,25% des protéines solubles de *E. coli* (Rock & Jackowski, 1982). ACP existe

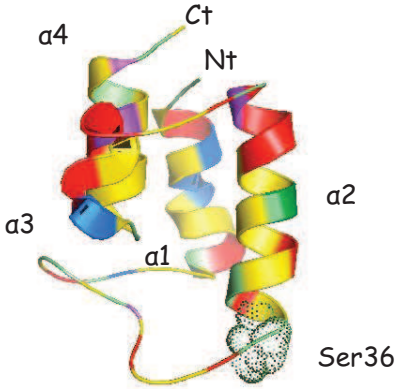

Figure 3: Structure de ACP d'après Kim & Prestegard (1990). La structure de ACP, représentée ici sous forme de structures secondaires, a été obtenue par RMN. ACP est constituée de quatre hélices α. Le résidu Serine 36 est représenté en nuage de points. C'est sur ce résidu que se fixe le groupement 4'-phosphopantéteine.

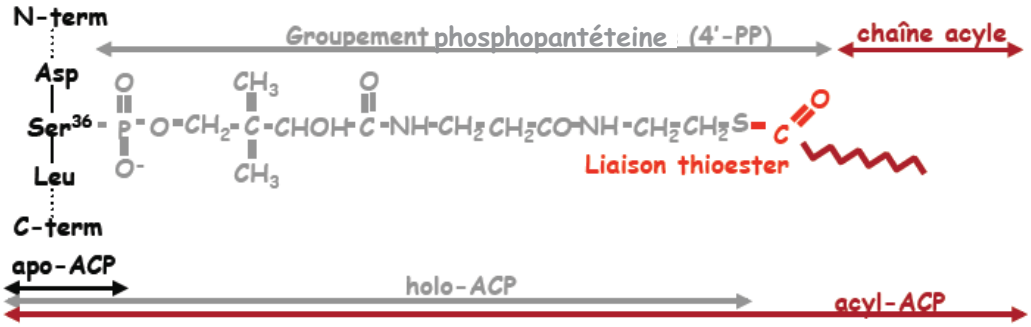

Figure 4: Modifications post-traductionnelles de ACP. ACP est modifiée au niveau du résidu Sérine 36 par addition d'un groupement 4'-phosphopantéteine (4'PP) composé d'une partie β-alanine et d'une partie β-mercaptoéthylamine se terminant par un groupement thiol libre, sur lequel une chaîne acylée peut être greffée par une liaison thioester.

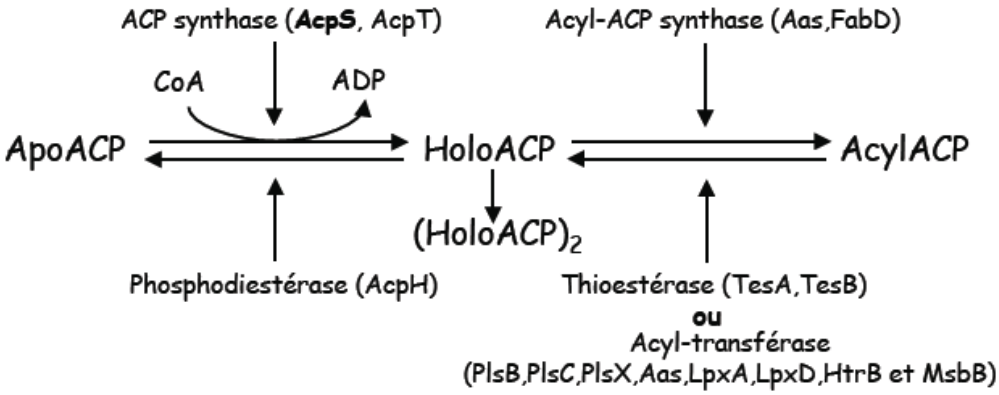

Figure 5: Enzymes catalysant les changement de forme d'ACP. ACP est synthétisée sous forme apo. Elle est modifiée post traductionnellemet en forme holo-ACP par l'ACP-synthase AcpS. Une autre ACP-synthase AcpT est capable de modifier ACP (Delay et Cronan, 2006), mais cette enzyme ne peut pas remplacer AcpS et son activité enzymatique est faible. La forme holo-ACP peut de nouveau être convertie en forme apo-ACP par la phosphodiesterase AcpH mais peut également être convertie en acyl-ACP par les acyl-ACP synthases Aas et FabD. La voie prioritaire pour la première étape de la synthèse des acides gras est FabD. L'acyl-ACP sert ensuite de substrat dans différents métabolismes comme celui des phospholipides (PlsB, PlsX, PlsC), des lipopolysaccharides (LpxA, LpxD, HtrB et MsbB), ou les thioestérases TesA et TesB.

sous trois formes: apo-ACP, holo-ACP et acyl-ACP qui coexistent dans la cellule (figure 4). ACP est tout d'abord synthétisée sous forme apo. Cette forme subit ensuite une modification post-traductionnelle par l'addition d'un groupement 4'-phosphopantéteine de 339 Da (4'PP) sur le résidu serine 36, conférant à ACP un groupement thiol réactif (figure 4). Cette modification est catalysée par AcpS (holo-ACP synthase) à partir de Coenzyme A (CoA) (figure 5) (Keating *et al.*, 1996). Le gène *acpS* codant pour cette enzyme est essentiel (Takiff *et al.*, 1992) démontrant que la modification d'ACP est indispensable à la survie.

ACP est une protéine structurellement flexible (Kim & Prestegard, 1989), ce qui semble nécessaire aux différentes interactions mettant en jeu cette protéine, tant avec des enzymes du métabolisme des lipides qu'avec des protéines non reliées à ce métabolisme. En effet, toutes les enzymes de la synthèse des acides gras utilisent des intermédiaires liés à ACP par une liaison thioester (DiRusso *et al.*, 1999 ; White *et al.*, 2005 ; Keatinge-Clay *et al.*, 2003 ; Heath & Rock, 1996 ; Zhang *et al.*, 2003). Dans le super complexe du FASI, la flexibilité du domaine ACP lui permet de faire la navette entre les différents sites réactionnels (Joshi *et al.*, 2005). De la même manière, la flexibilité de ACP pourrait lui permettre de jouer un rôle de navette entre les différentes enzymes du FASII organisées en complexe (Kim & Prestegard, 1989 ; Kim & Prestegard, 1990).

En plus de son rôle essentiel dans la synthèse des acides gras, ACP serait impliquée dans d'autres fonctions, comme le suggèrent les nombreuses interactions protéine-protéine trouvées par Tandem Affinity Purification sur ACP (Gully *et al.*, 2003 ; Butland *et al.*, 2005 ; Byers & Gong, 2007) (figure 6). En effet, ACP interagit avec la cystéine désulfurase IscS impliquée dans l'assemblage des centres Fe-S (Flint *et al.*, 1996; Gully *et al.*, 2003), mais le lien fonctionnel entre ces deux protéines n'est actuellement pas compris. De plus, ACP interagit avec la protéine MukB, impliquée dans la partition des chromosomes entre deux cellules filles (Niki *et al.*, 1992 ; Gully *et al.*, 2003) et serait également impliquée dans l'initiation de la transposition (Maekawa *et al.*, 1996 ; Sharpe & Craig, 1998). Ces deux derniers résultats indiquent que ACP pourrait jouer un rôle dans le métabolisme de l'ADN (acide déoxyribonucléotide), ce qui rappelle les liens connus entre l'initiation de la réplication et les phospholipides anioniques (Crooke, 2001). ACP est également substrat des enzymes LpxA, LpxD, LpxL, et LpxM auxquelles elle transfère des longues chaînes d'acides gras lors de quatre étapes de la biosynthèse du lipide A, composant du LPS (Raetz *et al.*, 2007) (cf. § IV). De plus, il a été montré au laboratoire que ACP interagit avec YbgC, une thioestérase du système Tol/PAL. YbgC est la seule protéine cytosolique de cet ensemble de protéines de l'enveloppe, et serait impliquée dans le métabolisme des phospholipides (Gully & Bouveret,

Protéines	Longeur de la chaîne acyle (acyl-ACP)[a]	Activité ou Fonction	Référence
AcpS	–	Holo-ACP synthase	Lambolat *et al.*, 1996
AcpH	–	Holo-ACP phosphodiesterase	Thomas *et al.*, 2007
FabA/B/D/E/F/G/H /I/K/L/Z	2-18	Enzymes de la synthèse des acides gras	White *et al.*, 2005
PlsB, PlsC, PlsX	16-18	Acylation des phospholipides	Rock & Jackoswki, 1982; Lu *et al.*, 2006
HlyC	14-18	Acylation de l'hémolysine	Issartel *et al.*, 1991
LipB	8	Biosynthèse des acides lipoiques	Jordan & Cronan, 1997
LpxA/D/L/M	10-14	Biosynthèse du lipide A	Raetz *et al.*, 2007
LuxI, AinS (*Vibrio fischeri*)	4-16	Quorum sensing: synthèse de AHL	Fuqua & Green berg, 2002
LuxD	14	Bioluminescence: acyl-ACP ésterase	Byers & Meighen, 1985
Aas	12-16	Réacylation des phospholipides avec acyl-ACP	Hsu *et al.*, 1991
Aas (*Vibrio harveyi*)	6-14	Ligation d'acyl-ACP	Fice *et al.*, 1993; Jiang *et al.*, 2006
MdoH	–	Synthèse des glucans périplasmiques osmorégulés (OPGs)	Therisod & Kennedy, 1987
SpoT	inconnu	Synthèse et hydrolyse du (p)ppGpp	Battesti & Bouveret, 2006
IscS	inconnu	Cystéine désulfurase	Flint et al., 1996; Gully *et al.*, 2003
MukB	inconnu	Ségrégation du chromosome	Gully *et al.*, 2003
PssA,YbgC	inconnu	Complexe de la synthèse des phospholipides	Gully & Bouveret, 2006

Figure 6: Les partenaires de ACP chez les bactéries à GRAM négatif (d'après Byers & Gong, 2007). Des interactions additionnelles non-montrées ont été identifiées par des approches protéomiques (Butland *et al.*, 2005). La source est *E. coli* sauf indiqué dans la première colonne. ACP: acyl carrier protein; AHL: acyl homosérine lactone; (p)ppGpp: guanosine 5'-(tri)diphosphate, 3'-diphosphate.
[a] spécificité des enzymes pour la longueur des chaînes acyles du substrat acyl-ACP. – pas applicable.

2006). Une autre fonction de ACP est qu'elle est essentielle lors de la synthèse des OPGs à l'étape de transglycosylation à partir d'UDP-glucose. Lors de cette synthèse, la forme active d'ACP serait une forme apo, car un mutant de la sérine 36 est toujours capable de promouvoir la réaction (Therisod & Kennedy, 1987).

B. Le cycle de biosynthèse des acides gras

B1. La synthèse des acides gras saturés

E. coli et la plupart des bactéries possèdent un système de synthèse des acides gras de type II (FASII) constitué par une série d'enzymes cytoplasmiques indépendantes (figure 7) (Rock & Cronan, 1996). Durant leur élongation, les chaînes d'acides gras sont portées par le co-facteur central ACP qui les transporte d'une enzyme à l'autre. La synthèse des acides gras se déroule en plusieurs cycles de réactions avec l'addition à la chaîne carbonée de deux nouveaux carbones à chaque cycle.

Chaque cycle d'élongation débute par la carboxylation d'une molécule d'acétyl-Coenzyme A (CoA) en malonyl-CoA par l'acetyl-CoA carboxylase (AccABCD). Cette enzyme hétérotétramérique réalise en fait deux demi-réactions catalysées par deux sous-complexes. La carboxy-biotine synthétisée par les enzymes AccB et AccC sert de donneur de groupement carboxyl aux enzymes AccA et AccD pour la formation de malonyl-CoA à partir d'acétyl-CoA. Le groupement malonyl est ensuite transféré du CoA à ACP par la malonyl-CoA:ACP transacylase FabD. Le malonyl-ACP ainsi formé est la brique de base à 2 carbones pour la synthèse des acides gras. Lors de l'étape d'initiation, la ß-kétoacyl-ACP synthase III FabH catalyse la condensation du malonyl-ACP avec un acétyl-CoA formant ainsi un ß-acétoacétyl-ACP, précurseur du cycle de synthèse des acides gras.

Chaque cycle d'élongation comprend quatre réactions successives de condensation, de réduction, de déhydratation et de réduction : la condensation d'un malonyl-ACP avec l'acyl-ACP en cours d'élongation est catalysée par la ß-kétoacyl-ACP synthase II (FabF). Le ß-kétoacyl-ACP formé est réduit en ß-hydroxyacyl-ACP par la ß-kétoacyl-ACP réductase FabG. Le ß-hydroxyacyl-ACP est ensuite converti en un trans-2-énoyl-ACP au cours d'une réaction de déshydratation catalysée par la ß-hydroxyl-ACP déshydratase FabZ. L'énoyl-ACP est ensuite réduit en un acyl-ACP par l'énoyl-ACP reductase FabI. La chaîne acyle s'est alors allongée de 2 carbones.

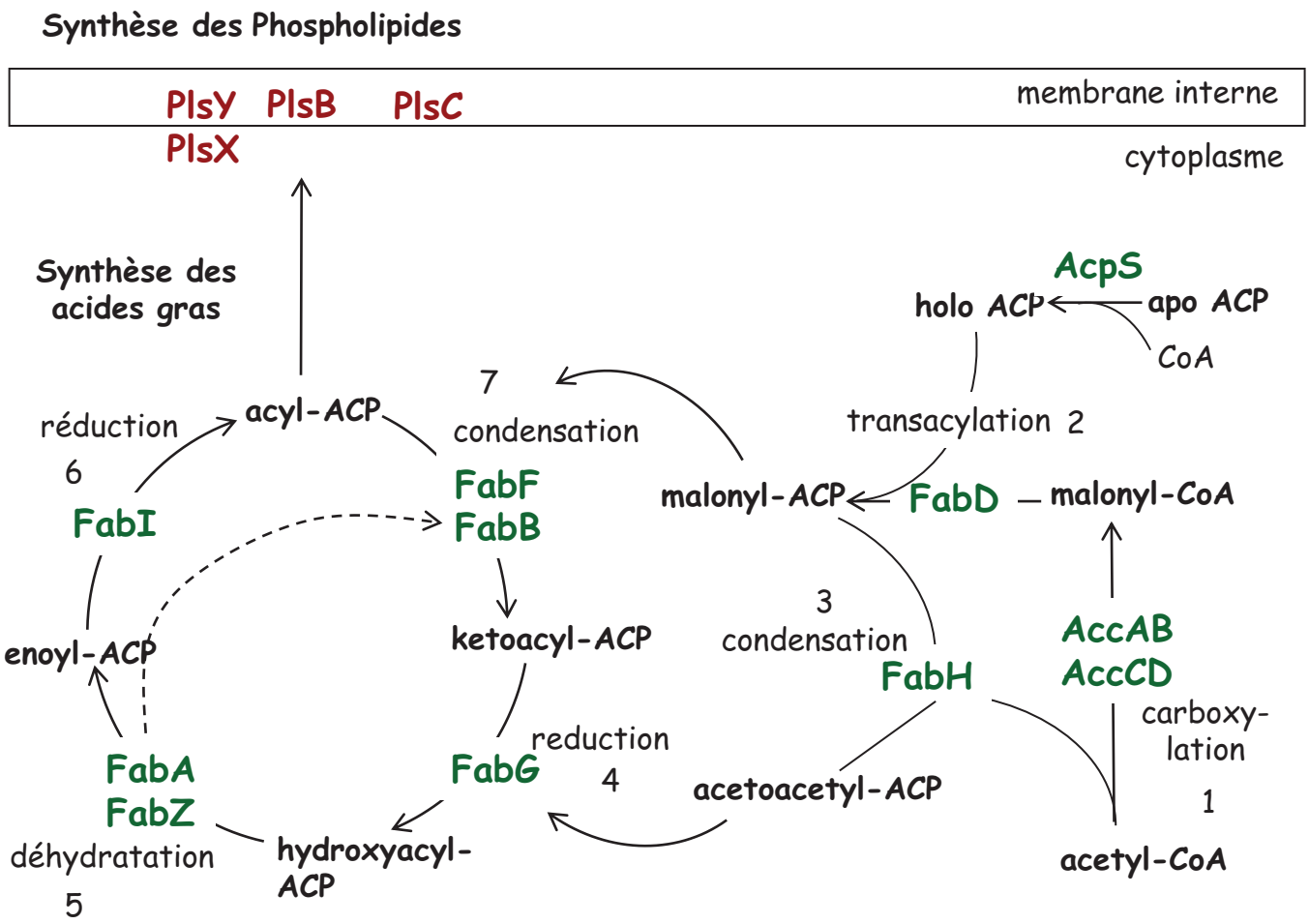

Figure 7: Cycle de synthèse des acides gras dans le cytoplasme. Le cycle de synthèse des acides gras de type II se décompose en deux étapes d'initiation et d'élongation. La première étape (1 à 3) conduit à la formation d'acétoacétyl-ACP ou de ketoacyl-ACP. La deuxième étape, regroupant les réactions 4 (ou 7 dans le cas du malonyl-ACP) à 6, conduit à la formation d'un acyl-ACP. Pour que le cycle de biosynthèse des acides gras débute, il faut une molécule d'ACP sous forme holo avec le groupement 4'-PP lié à la serine 36. À chaque cycle, 2 atomes de carbone sont ajoutés à la chaîne acyle.

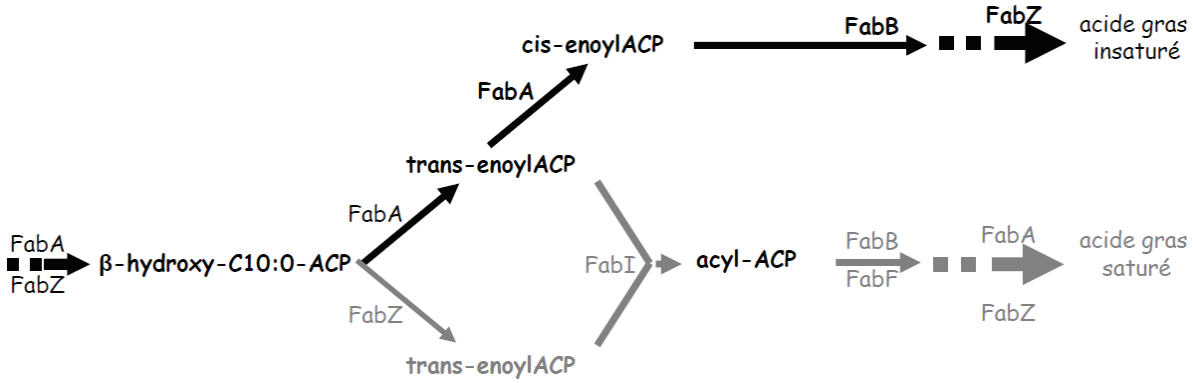

Figure 8: Synthèse des acides gras insaturés. La voie de biosynthèse des acides gras insaturés diffère de celle des acides gras saturés par l'isomérisation de la double liaison trans→cis par FabA ce qui stabilise la double liaison. Le cycle d'élongation continue directement par la condensation (réaction 7 dans la figure 7) d'un malonyl-ACP par FabB sans étape de réduction par FabI (réaction 6 dans la figure 7).

B2. La synthèse des acides gras insaturés

La synthèse des acides gras insaturés se déroule selon le même cycle de réactions que la synthèse des acides gras saturés, à la différence prêt qu'à l'étape de 8 (pour C16:1Δ^9) ou 10 (pour C18:1Δ^{11}) carbones, le ß-hydroxyacyl-ACP est déshydraté par la ß-hydroxyl-ACP déshydratase FabA au lieu de FabZ (figure 8) (Heath & Rock, 1996). Les ß-hydroxyl-ACP déshydratases FabA et FabZ sont deux enzymes homologues qui présentent une activité déhydratase commune, mais FabA catalyse en plus une réaction d'isomérisation de la double liaison de l'énoyl-ACP afin qu'elle ne soit pas réduite. Cet énoyl-ACP est directement et spécifiquement condensé avec un malonyl-ACP par la ß-kétoacyl-ACP synthase I FabB, sans subir de réduction. FabB est homologue à FabF, mais elle reconnaît spécifiquement un substrat comportant une insaturation. Chez *E. coli*, les enzymes FabA et FabB sont donc responsables de la synthèse des acides gras insaturés.

Après la biosynthèse des acides gras, qui a lieu dans le cytoplasme, ces acides gras sont transportés vers la membrane interne où ils sont incorporés dans les phospholipides synthétisés *de novo*. Lorsque la chaîne en cours d'élongation a atteint le nombre de carbones requis (C16 ou C18), elle est prise en charge par les acyltransférases PlsB, PlsX ou PlsC (cf. § IIB) pour la synthèse des phospholipides ou par une des acyltransférases impliquées dans la synthèse du lipide A (cf. § IV) (DiRusso *et al.*, 1999). Le cycle de synthèse des acides gras de *E. coli* dépend donc de l'activité d'un grand nombre d'enzymes distinctes, qui sont certainement organisées en complexe dans la cellule.

B3. Organisation supramoléculaire des enzymes de la synthèse des acides gras

Une voie de synthèse de type FASII, de type bactérienne, est également présente dans les apicoplastes, les mitochondries et les chloroplastes des organismes eucaryotes. En revanche, un système différent, le FASI, est présent dans le cytoplasme des eucaryotes non photosynthétiques et des mycobactéries. La synthèse des acides gras du type FASI est réalisée par une protéine multifonctionnelle, tandis que toutes les réactions enzymatiques de la synthèse du type FASII sont réalisées par des protéines distinctes. La structure du système FASI de mammifère a été résolue. C'est une grosse protéine (2.5×10^6 Da au total) multienzymatique, composée de domaines catalytiques nécessaires à la synthèse des acides gras connectés par des linkers (figure 9) (Maier *et al.*, 2008). En comparant les deux systèmes de synthèse des acides gras, on constate que les mêmes activités enzymatiques sont conservées malgré une organisation différente. Les enzymes distinctes du système bactérien de type FASII pourraient être organisées en un complexe macromoléculaire ressemblant à

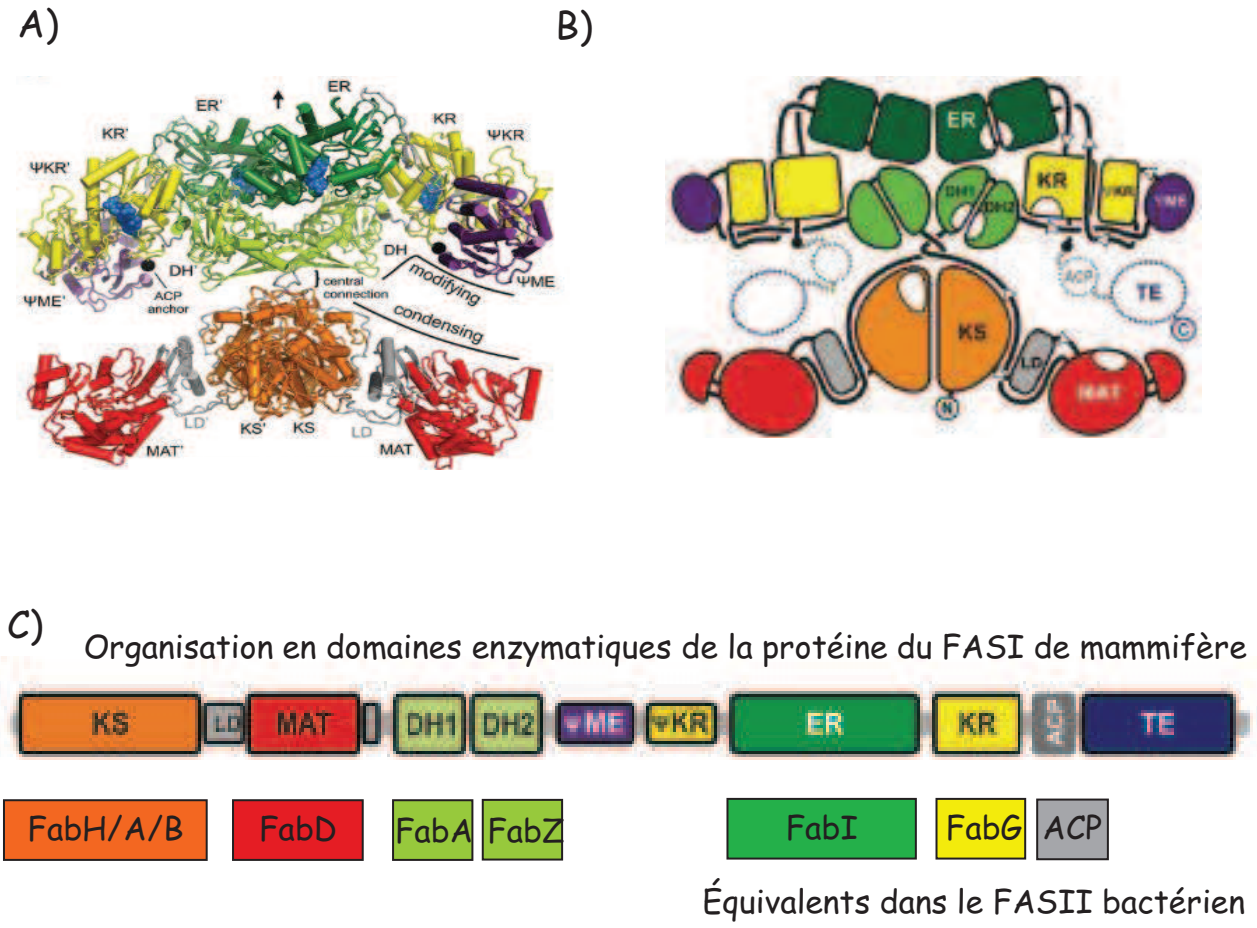

Figure 9: Représentation structurale des domaines du FASI de mammifère (Maier *et al.*, 2008). KS: kétoacylsynthase; MAT: malonyl-acetyl transférase; DH: déshydratase; ME: méthyltranférase; KR: kétoacylréductase; ER: enoylréductase; TE: thioestérase. **A)** Les domaines linkers (LD) sont représentés en gris. Les cofacteurs NADP+ et les sites de fixations pour les domaines C-terminaux ACP/TE sont indiqués sous forme de sphères bleues et noires respectivement. **B)** Diagramme schématique correspondant à A). **C)** Organisation linéaire de la séquence des domaines du FASI mammifère comparée avec les enzymes équivalentes du FASII bactérien.

l'architecture du super complexe FASI eucaryote. En ce sens, plusieurs interactions protéine-protéine ont déjà été observées entre les enzymes du système de type FASII de *Mycobacterium tuberculosis*, compatible avec une organisation en complexe (Veyron-Churlet *et al.*, 2004 ; Veyron-Churlet *et al.*, 2005). Au laboratoire, de nombreuses interactions ont été trouvées entre ces enzymes du FASII chez *E. coli* en utilisant le BACTH (Gully *et al.*, non-publié). De plus, la structure d'un complexe formé par des enzymes du FASII seraient superposable avec la structure de l'enzyme du FASI (Cantaloube *et al.*, non-publié).

Le FASI et le FASII posséderaient donc une architecture identique, mis à part l'organisation des domaines ACP. En effet, dans le FASI de mammifère, le domaine ACP est accroché par deux linkers à la protéine multi-enzymatique, tandis que chez les bactéries, ACP est une protéine isolée qui est présente à 60 000 molécules par cellule (Rock & Jackowski, 1982 ; Joshi *et al.*, 2005). ACP dans le FASII est donc en excès par rapport aux enzymes de la biosynthèse des acides gras, tandis que ACP est en quantité stœchiométrique dans le FASI. Cependant, dans le cas du FASI les substrats intermédiaires sont attachés d'une façon covalente via ACP et restent dans la machinerie catalytique. Ce processus pourrait augmenter l'efficacité catalytique en maintenant les substrats attachés à ACP à des concentrations locales importantes tout en maintenant de faibles distances entre les centres réactionnels (Leibundgut *et al.*, 2008).

C. La dégradation des acides gras

E. coli peut croître dans un milieu qui contient des acides gras comme seule source de carbone en les important à travers l'enveloppe puis en les dégradant par β-oxydation (DiRusso *et al.*, 1999).

C1. L'importation des acides gras exogènes à longue chaîne

Les acides gras exogènes à longue chaîne sont transportés par un mécanisme actif à travers l'enveloppe et sont ensuite activés pour être dégradés. Le transport requiert l'action des deux partenaires FadL et FadD (Dirusso & Black, 2004).

FadL joue le rôle de récepteur à la surface des bactéries des acides gras à longue chaîne et permet leur transport à travers la membrane externe. FadL est une protéine de membrane externe de 33 kDa (Black *et al.*, 1987) qui est structurée en tonneau avec 14 feuillets β et un domaine 'hatch' (clapet) qui bouche le tonneau (van den Berg *et al.*, 2004). Le transport des acides gras à longue chaîne s'effectuerait par un mécanisme de diffusion latérale (figure 10) (Hearn *et al.*, 2009) : le substrat se fixe avec une affinité faible et diffuse

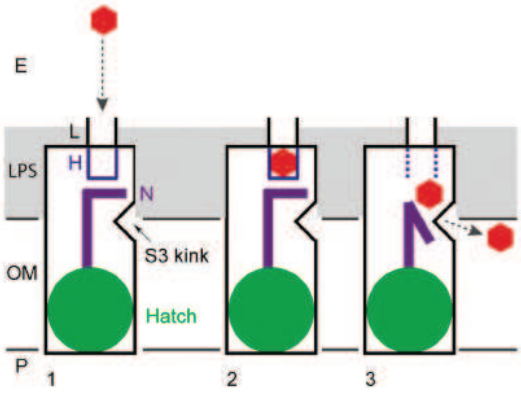

Figure 10: Modèle de diffusion latéral proposé pour l'import des acides gras à longue chaîne par FadL (Hearn *et al.*, 2009).
La partie polaire du LPS, barrière principale de ce processus de transport pour le substrat hydrophobe, est indiquée en gris. E: milieu extérieur; OM: membrane externe; P: périplasme.
(1) Le substrat (acides gras à longue chaîne; hexagone rouge) se fixe avec une affinité faible. **(2)** Le substrat diffuse ensuite vers un site de fixation d'affinité forte (H, bleu). **(3)** Un changement conformationnel dans le N-terminus de FadL (violet) provoque la libération du substrat et crée une ouverture à travers la paroi du tonneau formée par le pli dans le feuillet S3. Le substrat diffuse latéralement à travers l'ouverture vers la membrane externe.

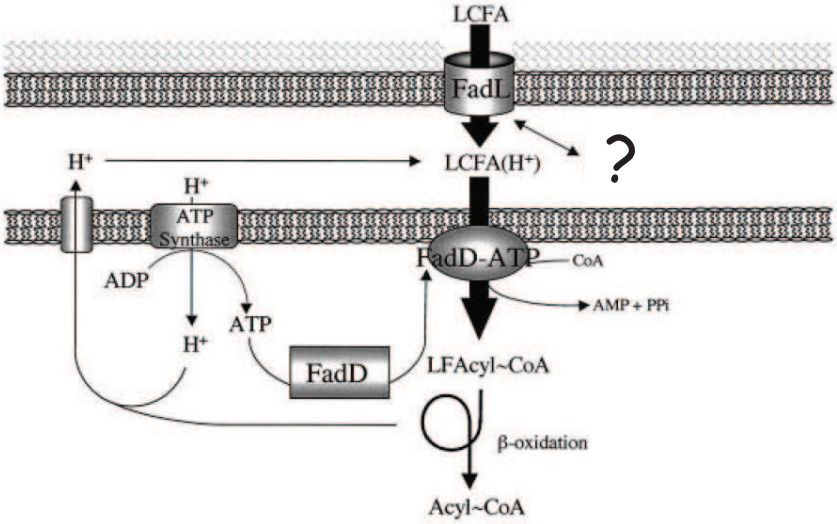

Figure 11: Transport vectoriel des acides gras à longue chaîne à travers l'enveloppe de *E. coli* (Black & DiRusso, 2003). Après avoir traversés la membrane externe grâce à FadL, les acides gras à longue chaîne entrent dans le périplasme où ils sont protonés ce qui leur permet de rentrer dans la membrane interne. La forme activée de FadD (FadD-ATP) pourrait détecter les acides gras libres (protonés) dans la membrane interne. La forme de FadD fixée à la membrane catalyse la formation de l'acyl-CoA à longue chaîne ce qui rend le processus unidirectionnel. Lorsque la cellule croît sur des acides gras à longue chaîne, l'énergie pour la génération du gradient électrochimique provient de la β-oxydation et de l'ATP synthase.

ensuite vers un site de fixation d'affinité forte. Un changement conformationnel dans le N-terminus de FadL provoque la libération du substrat et crée un passage continu à travers le tonneau vers la membrane externe. FadL a une affinité faible pour les acides gras de chaîne moyenne (C6-8), mais fixe spécifiquement des acides gras à longue chaîne (C10-16) (Kameda & Nunn, 1981). En utilisant FadL, ces substrats hydrophobiques contournent la couche hydrophilique du LPS sans être obligés de passer par un canal aqueux. Il est intéressant de noter que des acides gras à moyenne ou petite chaîne ne nécessitent pas FadL pour être importés chez *E. coli* parce qu'ils seraient relativement solubles dans l'eau et pourraient passer par d'autres canaux de la membrane externe (porines) (Black, 1990).

Le rôle de FadD dans la cellule est double (figure 11) : FadD est nécessaire à l'import des acides gras exogènes et possède également une activité acyl-CoA synthétase qui active les acides gras importés pour leur permettre de rentrer dans le métabolisme des lipides (Schmelter *et al.*, 2004). FadD a un large spectre d'activité pour la longueur de la chaîne acyle et son degrée d'insaturation, et elle requière du CoA et de l'ATP (adénosine triphosphate) pour son activité (Azizan *et al.*, 1999 ; Weimar *et al.*, 2002). FadD existe sous une forme dimérique dont le monomère est de 62 kDa (Kameda & Nunn, 1981). FadD est une protéine cytoplasmique liée à la face cytoplasmique de la membrane interne (Black & DiRusso, 2003). FadD serait activée par la fixation de l'ATP et la forme FadD-ATP serait capable de détecter le pool d'acides gras libres au niveau de la membrane interne. En catalysant la formation d'acyl-CoA, l'activité de FadD rend le transport des acides gras unidirectionnel (DiRusso *et al.*, 1999). Cette acylation vectorielle de FadD retire et active donc ces acides gras de façon concomitante avec le transport à travers la membrane interne (Black & DiRusso, 2003). Les acides gras formés sous forme d'acyl-CoA sont alors les substrats de la β-oxydation, mais ils peuvent également être incorporés dans les phospholipides membranaires (cf. § IIB).

C2. La β-oxydation des acides gras

La voie de β-oxydation aérobie, qui fait intervenir les enzymes codées par le régulon *fad* (fatty acid degradation), est la plus étudiée (DiRusso *et al.*, 1999 ; Overath *et al.*, 1969). Une deuxième voie de β-oxydation en condition d'anaérobie a été mise en évidence plus récemment et permet une croissance sur acides gras en condition anaérobie (Campbell *et al.*, 2003). La dégradation des acides gras chez *E. coli* est donc divisée en deux voies de β-oxydation cataboliques, l'une aérobie et l'autre anaérobie, qui ne font pas intervenir les mêmes enzymes.

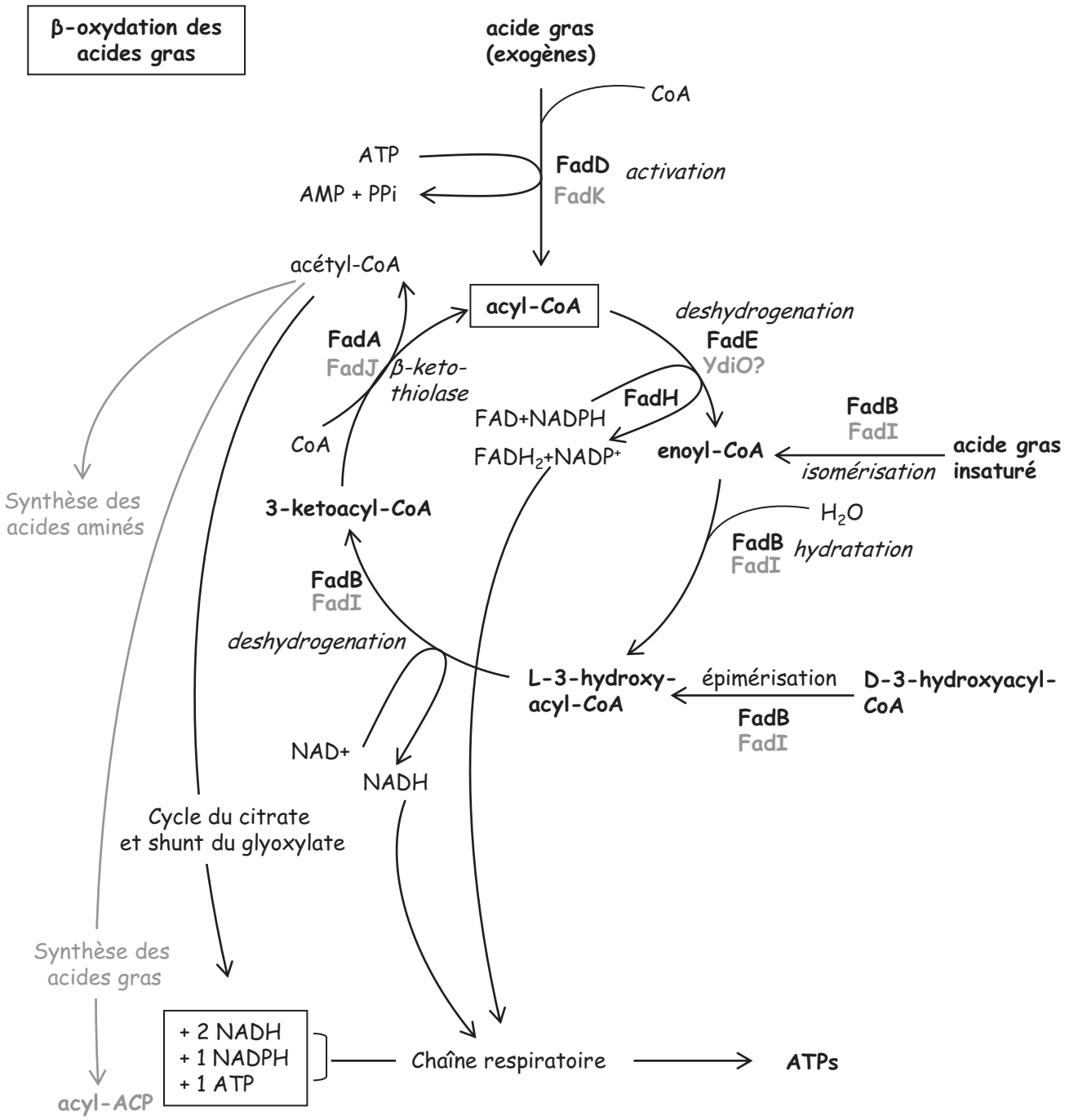

Figure 12: β-oxydation aérobie et anaérobie et devenir des métabolites secondaires. Les enzymes de la β-oxydation aérobie sont montrées en noir et celles de la β-oxydation anaérobie en gris clair. Un acide gras libre (exogène) est thioesterifié sur un CoA par FadD (FadK). Cet acyl-CoA devient le substrat de FadE (YdiO?) qui catalyse la formation d'enoyl-CoA et $FADH_2$. L'enoyl-CoA est transformé en kétoacyl-CoA par l'enzyme multifonctionnelle FadB (FadI) catalysant une hydratation puis une déshydrogenation en formant un NADH. Le kétoacyl-CoA est enfin clivé par FadA (FadJ) qui libère un acetyl-CoA et un acyl-CoA dont la chaîne carbonée a été réduite de deux carbones. Cet acyl-CoA réintègre un cycle de dégradation. L'acétyl-CoA peut être dégradé (cycle du citrate et shunt du glyoxylate) ou réutilisé lors de la biosynthèse d'acides gras. La voie de β-oxydation produit des cofacteurs réduits qui sont alors convertis en énergie (ATP) par la chaîne respiratoire.

1. La β-oxydation aérobie

La voie de β-oxydation suit un processus qui fonctionne comme l'envers en miroir de la synthèse des acides gras (figure 12). En revanche, les substrats sont fixés sur ACP ou CoA pour la synthèse ou la dégradation, ce qui permet la séparation des deux voies métaboliques. La β-oxydation des acides gras est divisée en deux étapes : l'activation des acides gras par FadD et le cycle de β-oxydation proprement dit au cours duquel 2 carbones sont enlevés à la chaîne acyle à chaque cycle (figure 12). Les activités enzymatiques successives d'un cycle sont catalysées par les 3 protéines suivantes : FadE (acyl-CoA déshydrogénase), FadB (enoyl-CoA hydratase et hydroxyacyl-CoA déshydrogénase) et FadA (kétoacyl-CoA thiolase).

Le cycle de β-oxydation commence par une déshydrogénation de l'acyl-CoA par FadE pour donner un trans-Δ2-enoyl-CoA (DiRusso *et al.*, 1999). FadB possède 4 activités enzymatiques différentes (Yang *et al.*, 1991). De plus, un cis-Δ3-enoyl-CoA peut intégrer la voie de β-oxydation grâce à l'activité cis-Δ3-trans-Δ2-enoyl-CoA isomérase de FadB. L'enoyl-CoA subit une hydratation catalysée par l'enoyl-CoA hydratase (crotonase), FadB, pour donner un (L)-3-hydroxyacyl-CoA. A ce stade, un (D)-3-hydroxyacyl-CoA peut intégrer la voie grâce à l'activité 3-hydroxyacyl-CoA épimérase de FadB. Le (L)-3-hydroxyacyl-CoA subit une déshydrogénation catalysée par une 3-hydroxyacyl-CoA déshydrogénase, FadB. FadA catalyse la dernière réaction (acyltransfert) conduisant à la formation d'un acétyl-CoA et d'un acyl-CoA raccourci de deux carbones. Il a été déterminé par purification des sous-unités α (FadB) et β (FadA) que FadB-FadA forment un complexe multienzymatique $\alpha_2\beta_2$ (Pawar & Schulz, 1981). Il est intéressant de noter que ce complexe n'est pas lié à la membrane, mais lors de sa purification, des phospholipides caractéristiques de la membrane interne sont co-purifiés (Kunau *et al.*, 1995). Dans le cas d'acides gras insaturés, les doubles liaisons doivent être réduites par une réductase possédant un cofacteur FAD (Kunau *et al.*, 1995). Une voie alternative a été mise en evidence dans laquelle une 2,4-dienoyl-CoA réductase (FadH) permet de réduire une double liaison en utilisant un NADPH comme donneur de proton (He *et al.*, 1997).

Chaque cycle produit donc un acétyl-CoA, un NADH et un $FADH_2$. Les cofacteurs réduits NADH et $FADH_2$ sont pris en charge par la voie de phosphorylation oxydative. L'acétyl-CoA peut suivre trois voies : soit rentrer dans la biosynthèse d'acides aminés comme l'arginine, la cystéine et la leucine, soit être de nouveau incorporé dans le cycle de synthèse des acides gras, soit subir le cycle du citrate et/ou le shunt du glyoxylate pour fournir de l'énergie sous forme de NADH et FADH2 (5 molécules d'ATP) (Sánchez *et al.*, 2005). Une

molécule d'acétyl-CoA produit 12 molécules d'ATP. Donc, à chaque fois qu'un cycle de β-oxydation est enclenché, 17 molécules d'ATP sont produites.

2. La β-oxydation anaérobie

Une deuxième voie de dégradation des acides gras, mise en place en condition anaérobie, a été mise en évidence en 2003 (Campbell *et al.*, 2003). Les composantes de ce système ne sont pas toutes identifiées mais l'acyl-CoA synthétase ainsi que le complexe multienzymatique de β-oxydation ont été mis en évidence. Les acides gras importés sont thioestérifiés au niveau d'un CoA par l'acyl-CoA synthétase FadK, l'homologue de FadD. FadK est spécifique des acides gras à petite chaîne (octanoate) (Morgan-Kiss & Cronan, 2004) (figure 12, enzymes en gris clair). Cette spécificité entraîne une perte de rendement lors de la valorisation des métabolites secondaires issus de la β-oxydation anaérobie ($FADH_2$, NADH et acétyl-CoA). Il est intéressant de constater qu'en condition anaérobie, les deux acyl-CoA synthases FadD et FadK sont fonctionnelles (Morgan-Kiss & Cronan, 2004). L'enzyme responsable de la deshydrogénation de l'acyl-CoA n'a pas été identifiée avec certitude dans le système anaérobie, mais YdiO, possédant 22% d'identité avec FadE, pourrait jouer ce rôle (Morgan-Kiss & Cronan, 2004). L'homologue pour la β-oxydation anaérobie du complexe multienzymatique de β-oxydation FadA-FadB est constitué des protéines YfcY et YfcX, respectivement renommées FadI et FadJ (Snell *et al.*, 2002) ; Campbell *et al.*, 2003]. De manière comparable au devenir des acétyl-CoA lors de la β-oxydation aérobie, les acétyl-CoA sont certainement dirigés en anaérobie vers le cycle du citrate. En effet, un mutant *aceA* (gène codant pour une enzyme permettant de catalyser la formation de glyoxylate à partir d'isocitrate pour donner du malate) ne croît plus en présence d'acides gras comme source unique de carbone (Campbell *et al.*, 2003).

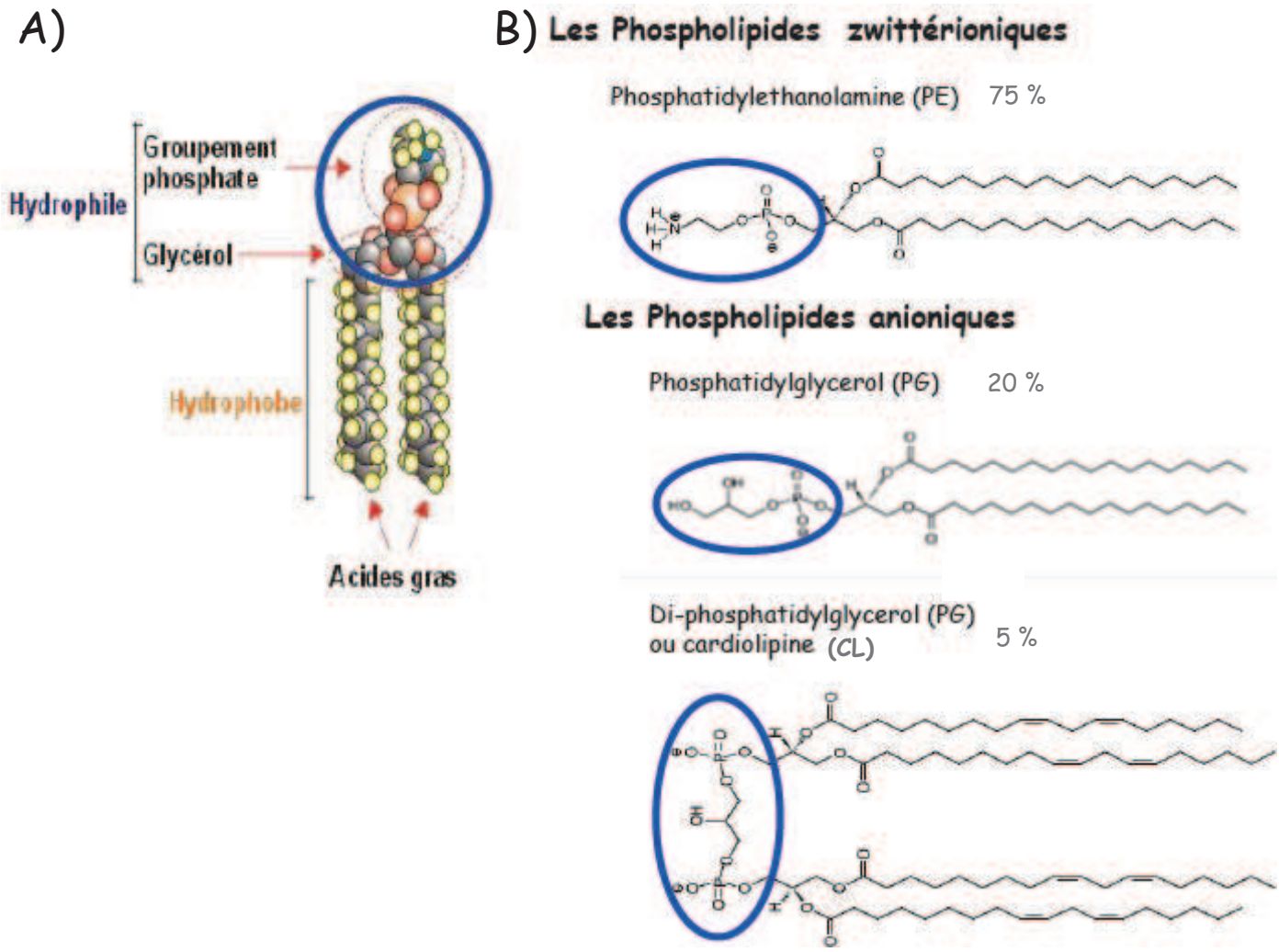

Figure 13: Les phospholipides majeurs de *E. coli*. A) Structure globale d'un phospholipide avec la tête polaire et les acides gras qui font la partie hydrophobe de cette molécule amphiphile. **B)** Les deux classes de phospholipides de *E. coli* : les phospholipides zwittérioniques (PE) et anioniques (PG, CL). La distribution naturelle des acides gras sur les positions 1 et 2 des phospholipides est très contrôlée. *In vivo*, les acides gras en position 1 du glycérol-3-phosphate sont en majorité saturés (acide palmitique C16) et insaturés en position 2 (acides palmitoléique C16:1Δ9 et cisvaccénique C18:1Δ11). L'acide cis-vaccénique C18:1Δ11 est également retrouvé en position 1 (Greenway & Silbert, 1983).

II. LA VOIE DE BIOSYNTHESE DES PHOSPHOLIPIDES CHEZ *E. COLI*

A. La structure des phospholipides majeurs de *E. coli*

Les phospholipides sont des molécules amphipatiques possédant une partie hydrophobe et une partie hydrophile (figure 13A) qui leur permettent de former une bicouche lipidique, base d'une membrane cellulaire. Les phospholipides de *E. coli* ont tous le même squelette de base, le glycérol. Ce glycérol est acylé au niveau des carbones C1 et C2. Le carbone C3 est modifié par un groupement glycérol, sérine ou éthanolamine formant la tête polaire spécifique des phospholipides. La nature de ces têtes polaires permet de classer les phospholipides en phospholipides anioniques, ou en phospholipides zwittérioniques. Les phospholipides anioniques représentent 15 à 20% des phospholipides de *E. coli*. Ils regroupent le phosphatidylglycérol (PG), le monoacylglycérol (en traces chez *E. coli*) et le diphosphatidylglycérol, également nommé Cardiolipine (CL) (figure 13B). Les phospholipides zwittérioniques représentent 80 à 85% des phospholipides de *E. coli*. Ils regroupent la phosphatidyléthanolamine (PE), qui est le phospholipide le plus abondant, et la phosphatidylsérine (en traces chez *E. coli*) (figure 13B). La distribution naturelle des acides gras sur les positions 1 et 2 des phospholipides est très contrôlée. *In vivo*, les acides gras en position 1 sont en majorité saturés (acide palmitique C16) et insaturés en position 2 (acides palmitoléique $C16{:}1^{\Delta 9}$ et cis-vaccénique $C18{:}1^{\Delta 11}$). L'acide cis-vaccénique $C18{:}1^{\Delta 11}$ est également retrouvé en position 1 (Greenway & Silbert, 1983). Les acides gras trouvés dans la membrane de *E. coli* ont été présentés dans la figure 2. La composition des chaînes acyles des phospholipides peut changer au cours de la croissance : lors de l'entrée en phase stationnaire les acides gras insaturés sont cyclopropanés (cf. § II *B3*).

B. La voie de biosynthèse *de novo* des phospholipides

La synthèse des trois phospholipides majeurs de *E. coli*, qui se déroule dans la membrane interne, est divisée en deux étapes (figure 14) (Cronan, 2003). Dans une première étape commune à tous les phospholipides, deux acides gras sont greffés sur les carbones C1 et C2 d'un glycérol-3-phosphate (G3P), puis le carbone C3 est activé par l'addition d'un groupement cytosine triphosphate (CTP). Dans une deuxième étape, la tête polaire du phospholipide est greffée en position C3 pour donner les deux grandes classes des phospholipides, anioniques (PG et CL) et zwittérioniques (PE et phosphatidylsérine).

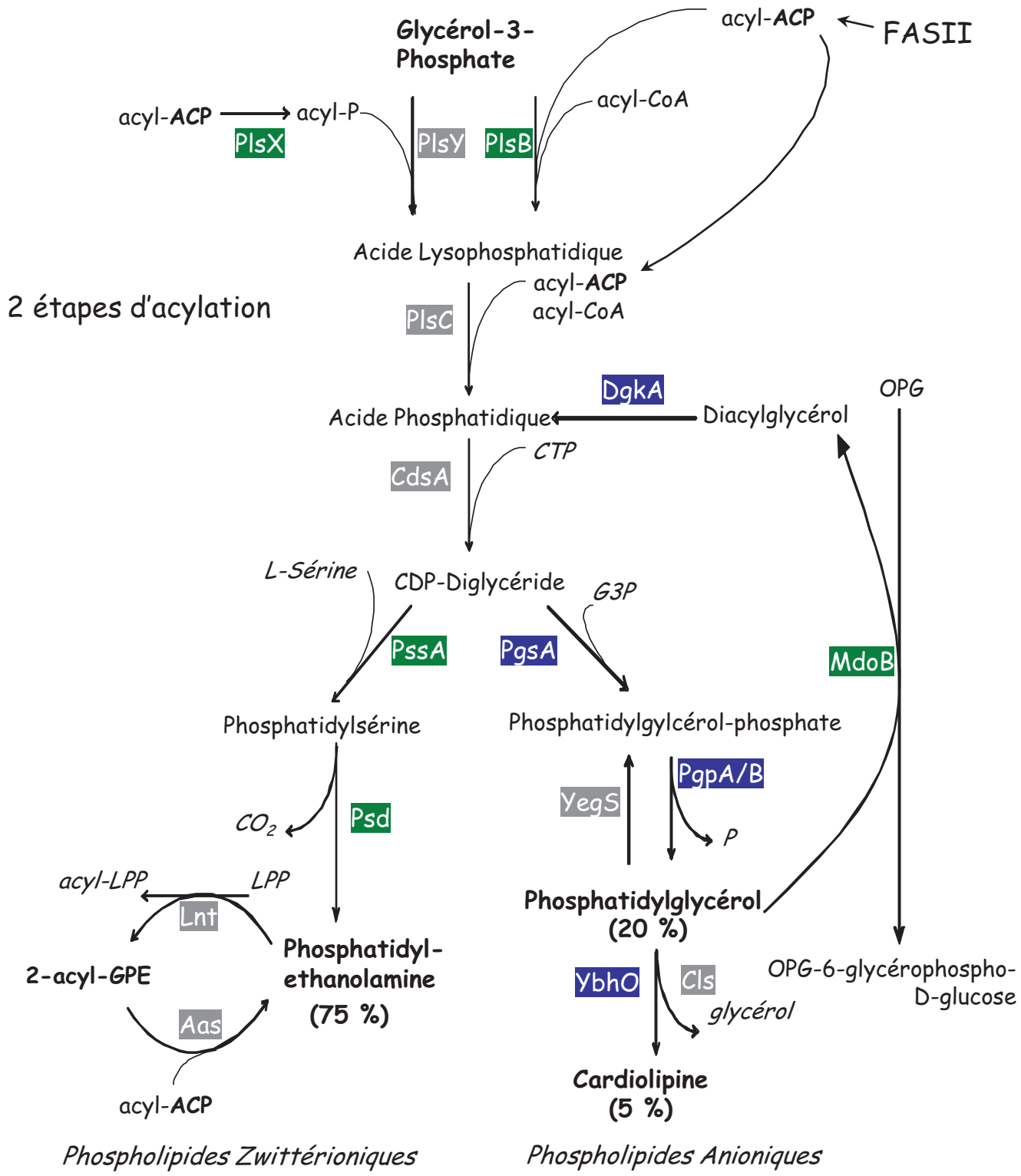

Figure 14: Les voies de biosynthèse et de recyclage des phospholipides dans la membrane interne chez *E. coli*. G3P: glycérol-3-phosphate; CoA: Coenzyme A; ACP: acyl carrier protein; OPG : glucan périplasmique osmorégulé. Colorées en bleu et en vert: enzymes dont les gènes sont activés ou réprimés, respectivement, par l'élévation de ppGpp durant la réponse stringente (d'après Traxler *et al.*, 2008).

B1. Les deux étapes d'acylation du glycérol-3-phosphate

1. Acylation du G3P par les voies PlsB ou PlsX/PlsY

La biosynthèse des phospholipides débute par l'acylation du G3P en position 1 pour former un acide lysophosphatidique (figure 14) (Cronan, 2003). La chaîne acyle utilisée lors de cette réaction est portée soit par ACP, s'il s'agit d'un acide gras synthétisé *de novo*, soit par le CoA, s'il s'agit d'un acide gras exogène importé d'une façon FadD-dépendante (cf. § I *C1*). Cette réaction essentielle chez *E. coli* est catalysée par la sn-G3P-acyltransférase (GPAT) PlsB qui est une enzyme membranaire de 91 kDa présente à 1400 copies par cellules (Green *et al.*, 1981). PlsB est organisée en 3 domaines (figure 15A). Une extension N-terminale cytoplasmique de 280 acides aminés est spécifique des GPATs et pourrait donc être impliquée dans la régulation de l'activité acyltransférase de PlsB (Wilkison & Bell, 1997). De plus, les résidus 150 à 251 présentent des similitudes avec des motifs de fixation de nucléotides qui pourraient réguler PlsB, comme des acyl-CoA ou le ppGpp (Heath *et al.*, 1994). Le site catalytique (Heath & Rock, 1998) avec le motif caractéristique $HisX_4Asp$ des acyltransférases (Lewin *et al.*, 1999) est situés dans un domaine central (Pfam 01553 ; résidus 280-424) conservé parmi toutes les acyltransférases (figure 16).

Récemment, une autre voie de synthèse de l'acide lysophosphatidique a été mise en évidence chez *Bacillus subtilis* (Lu *et al.*, 2006 ; Paoletti *et al.*, 2007). Cette deuxième voie necessite deux réactions enzymatiques et utilise un nouvel intermédiaire, l'acyl-phosphate, pour initier la formation des phospholipides (figure 17A et B). PlsX est une acyl-phosphate synthase cytoplasmique de 38 kDa ayant comme substrat l'acyl-ACP qui est produit par la synthèse *de novo* des acides gras. L'acyltransférase membranaire PlsY (22,2 kDa) acyle ensuite le G3P en position C1 à partir de l'acyl-phosphate.

Cette deuxième voie, qui fait intervenir les enzymes PlsX et PlsY, très conservée chez la plupart des bactéries, est également présente chez *E. coli* (figure 17C). Chez *E. coli,* PlsB est une enzyme essentielle ce qui n'est pas le cas des protéines PlsX et PlsY seules, tandis que chez *B. subtilis*, qui ne possède pas PlsB, PlsX et PlsY sont essentielles (Yoshimura *et al.*, 2007). La voie PlsB est trouvée surtout chez les γ-proteobacteries parmi lesquelles seules les *Xanthomonadales* ne possèdent pas PlsX/PlsY (figure 17C). La raison pour laquelle les deux voies de synthèse de l'acide lysophosphatidique coexistent chez la plupart des γ-proteobacteria comme *E. coli* n'est actuellement pas connue. Mais un avantage pourrait être que PlsB est capable d'utiliser l'acyl-CoA qui permet l'incorporation des acides gras exogènes (Lu *et al.*, 2006). Cependant, PlsX n'accepte que l'acyl-ACP provenant de la synthèse des acides gras *de novo*. L'avantage pour les γ-proteobacteria de posséder *plsB* et

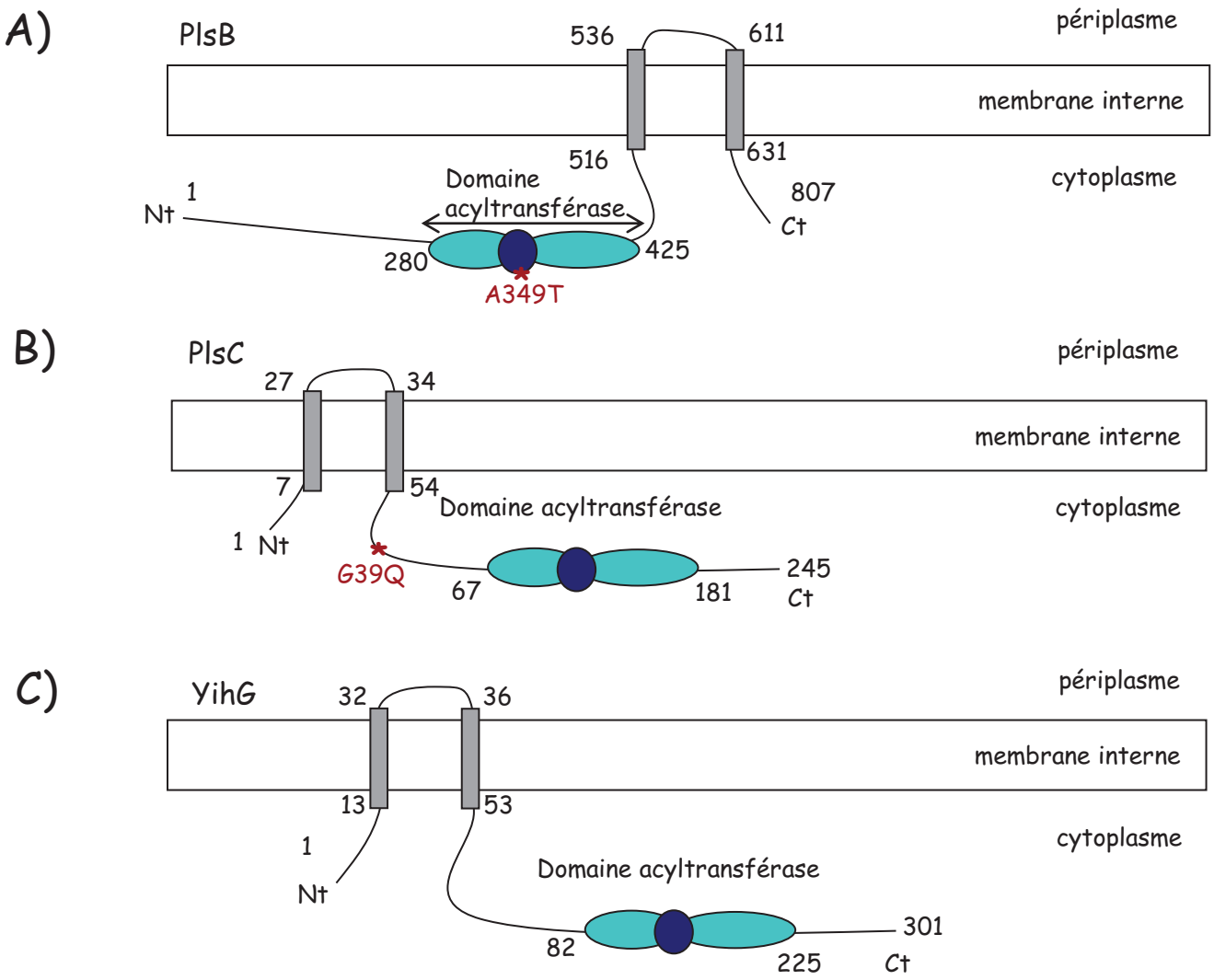

Figure 15: Topologies prédites des acyltransférases (A) PlsB, (B) PlsC et (C) YihG. Ct: C-terminus; Nt: N-terminus. Les numéros indiquent les limites des différents segments transmembranaires ou des domaine acyltransférases. Le domaine acyltransférase (Pfam01553) est indiqué en bleu et le site actif par une sphère bleue. Les mutations ponctuelles sont indiquées par une étoile rouge. La mutation A349T dans le site catalytique réduit l'activité enzymatique de PlsB (Heath & Rock, 1999). La mutation G39Q dans PlsC réduit l'activité enzymatique à la température non-permissive (42 °C) (Bouveret *et al.*, non-publié).

plsXY serait que des acides gras exogènes pourraient être utilisés au lieu des acides gras synthétisés *de novo* couteux en énergie (Cronan, 2003).

2. La deuxième acylation de l'acide lysophosphatidique par PlsC

Dans la deuxième étape d'acylation, une chaîne acylée est fixée sur l'acide lysophosphatidique en position C2 pour former un acide phosphatidique (Cronan, 2003). Cette deuxième réaction est catalysée par la 1-acyl-G3P acyltransférase (LPAT) PlsC qui est essentielle et conservée chez toutes les bactéries. PlsC est une protéine intégrale de membrane de 27 kDa présente en proportion équivalente à PlsB soit environ 1400 copies par cellules (Green *et al.*, 1981; Rock *et al.*, 1981). PlsC ne présente pas d'extension N-terminale comme PlsB (figure 15B), mais elle contient le même domaine acyltransférase (Pfam 01553) avec le site catalytique et son motif conservé $HisX_4Asp$ (figure 16) (Heath & Rock, 1998 ; Lewin *et al.*, 1999).

PlsC n'aurait pas de spécificité stricte de substrat, et PlsC pourrait incorporer les acides gras saturés et insaturés sur la position C2 en fonction de leur abondance (Zhang & Rock, 2008). Les acyltransférases PlsC des bactéries à GRAM positif, comme *B. subtilis* (Paoletti *et al.*, 2007), n'utilisent que l'acyl-ACP comme donneur des chaînes acyles. Chez *E. coli* en revanche, des expériences *in vitro* ont montré que PlsC, comme PlsB, pouvait utiliser comme substrat soit l'acyl-CoA soit l'acyl-ACP (Green *et al.*, 1981 ; Rock *et al.*, 1981). En conclusion, des bactéries à GRAM négatif, comme les γ-proteobacteria, sont capables d'utiliser acyl-ACP, acyl-phosphate, et acyl-CoA pour générer les phospholipides membranaires, tandis que des bactéries à GRAM positif n'utilisent que des acyl-phosphates, pour C1, et des acyl-ACPs, pour C2.

L'acide phosphatidique est ensuite activé par la cytosine-diphosphate(CDP)-diglycéride synthétase CdsA qui lie un groupement CTP (cytosine triphosphate) pour former un liponucléotide, le CDP-diacylglycérol (Cronan, 2003) (figure 14). CdsA est une protéine membranaire de 31,5 kDa présente à environ 1000 copies par cellule (Dowhan, 1997). Aucune donnée sur son site actif n'est disponible. Il existe une protéine homologue à CdsA chez *E. coli*, YnbB, mais dont l'activité n'a pas été étudiée jusqu'à maintenant (Cronan, 2003).

		Block I [a]	Block II	Block III	Block IV	Accession[b]
	GPAT	303[c]	348	382	417	
PlsB	*E. coli*	VPCHRSHMDYLLL	GAFFIRR	YFVEGGRSRTGR	ITLIPIYI	130326
	H. influenzae	VPCHRSHIDYLLL	GAFFIRR	YFIEGGRSRTGR	ISIVPVYV	1172533
	M. tuberculosis	AFSHRSYLDGMLL	GAIFIRR	WSIEGGRTRTGK	VYLVPTSI	2791522
	C. elegans	ICLHRSHLDILSM	NTIFIRR	FFLEGTRSRFGK	ISIIPVVF	1458332
	M. musculus	LPVHRSHIDYLLL	GGFFIRR	IFLEGTRSRSGK	ILVIPVGI	2498786
	R. norvegicus	LPVHRSHIDYLLL	GGFFIRR	IFLEGTRSRSGK	ILVIPVGI	2444459
PlsC	**LPAAT**					
	E. coli	IANHQNNYDMVTA	GNLLLDR	MFPEGTRSR.GR	VPIIPVCV	1789395
	S. typhimurium	IANHQNNYDMVTA	GNLLIDR	MFPEGTRSR.GR	VPIIPVCV	154236
	H. influenzae	IGNHQNNYDMVTI	GNIFLDR	MFPEGTRNR.GR	VPIIPVVC	1573737
	M. genitalium	VANHKSNLDPLVL	DCVFIDR	VFAEGTRIL.SN	VPILPVSI	1045898
	S. cerevisiae	IANHQSTLDIFML	GTYFLDR	VFPEGTRSTSEL	IPIVPVVV	464422
	C. elegans	ICNHQSSLDILSM	NTIFIDR	VFPEGTRNREGG	IPIIPVVF	1403001
	M. musculus	VSNHQSSLDLLGM	GIIFIDR	VFPEGTRNHNGS	VPIIPIVF	2467310
	H. sapiens alpha	VSNHQSSLDLLGM	GVIFIDR	VFPEGTRNHNGS	IPIIPVVF	2155238
	H. sapiens beta	VSNHQSILDMMGL	GVFFINR	IYPEGTRNDNGD	VPIVPVVY	2155240
	DHAPAT (*H. sapiens*)	LPSHRSYIDFLML	GAFFMRR	FFLEGTRSRSAK	TYLVPISI	3258645
	LPEAT (*E. coli*)	TPNHVSFIDGILL		IFPEGTRITTTG	ATVIPVRI	290403
	GPAT consensus	φ--HRS-φDφφ--	G-φFIRR	φFφEGTRSR-GK	φφφφPφφφ	
	LPAAT consensus	φ-NHQS-φDφφ--	G-φFIDR	φFPEGTR---G-	φPφφPφφφ	
	YihG	NHRSWA DIVVL		NFVEGSRFTQEK		

Figure 16: Blocs d'homologie[a] des acyltransférases (d'après Lewin *et al.*, 1999). GPAT : sn-glycérol-3-phosphate acyltransferase; LPAAT : lysophosphatidique acid acyltransferase; DHAPAT : acyl-CoA-dihydroxy-acetonephosphate-acyltransfrase; LPEAT : 2-acylglycerophosphatidylethanolamine acyltransferase; [a] Les blocs d'homologie ont été identifiés sur la base d'alignement des acides aminés en utilisant l'algorithm CLUSTAWL. [b] Les numéros d'accession sont pour le National Center for Biotechnology Information Protein Data Base. [c]Les numéros indiquent la position du résidu au début de chaque bloc de *E. coli* GPAT. Les blocs d'homologie de YihG ont été rajoutés en bas du tableau.

B2. Les modifications des têtes polaires

1. La voie de biosynthèse des phospholipides zwittérioniques

La voie de synthèse des phospholipides zwittérioniques débute par l'échange du CDP par une L-sérine par PssA (phosphatidylsérine synthase) donnant ainsi une phosphatidylsérine. Cette phosphatidylsérine est ensuite décarboxylée par Psd (phosphatidylsérine décarboxylase) formant ainsi la PE.

PssA est avec PlsX la seule protéine soluble de la voie de biosynthèse des phospholipides, associée de manière transitoire à la membrane (figure 18). PssA contient deux domaines phosphodiestérases homologues à ceux de la phospholipase D (PLD) (résidus 133-159 et 352-379) (Koonin, 1996). Le motif caractéristique dénommé HKD (figure 19) est essentiel pour l'activité enzymatique. Ces motifs HKD sont retrouvés chez les phosphatidylsérine synthases et cardiolipine synthases de bactéries et plantes. Mais leur rôle dans la réaction catalysée par PssA n'est pas connu, mis à part le fait que dans un mutant *cls*-1, PssA pourrait catalyser la synthèse de cardiolipine (Larson & Dowhan, 1976 ; Nishijima *et al.*, 1988).

L'étude bioinformatique de la séquence de PssA montre deux domaines hydrophobes (résidus 120-155 et 240-285) et des régions basiques à la suite de ces domaines hydrophobes (DeChavigny *et al.*, 1991). Les propriétés physicochimiques de ces régions pourraient être responsables de l'affinité de PssA pour les membranes contenant des phospholipides chargés négativement (PG et CL) (Louie *et al.*, 1986). Une localisation différentielle de PssA est responsable de la régulation de la synthèse de la PE : des associations plus nombreuses de PssA avec la membrane à cause d'un niveau trop élevé de PG et CL pourraient augmenter la synthèse de PE pour finalement compenser ce niveau trop élevé en phospholipides anioniques (Louie *et al.*, 1986).

Psd est synthétisée sous la forme d'une protéine précurseur de 322 acides aminés. Ce précurseur s'autoclive pour former deux sous-unités α et β (figure 18). La sous-unité β de 28,6 kDa (résidus 1-253) n'est pas modifiée. En revanche, la sérine 254, premier résidu de la chaîne α de 7 kDa est modifiée pour former un groupement pyruvoyl (Li & Dowhan, 1988 ; Li & Dowhan, 1990 ; Schmitzberger *et al.*, 2003). Quand la sérine 254 est mutée par une alanine, la protéine précurseur ne s'autoclive plus, et en conséquence l'activité décarboxylase de ce mutant est nulle (Li & Dowhan, 1990). L'activité décarboxylase de Psd *in vitro* nécessite la présence de phosphatidylsérine dans des micelles de détergent anionique, un phospholipide entièrement acylé et l'isomère L-sérine (Dowhan & Li, 1992). La décarboxylation de la phosphatidylsérine catalysée par Psd pourrait suivre le modèle proposé

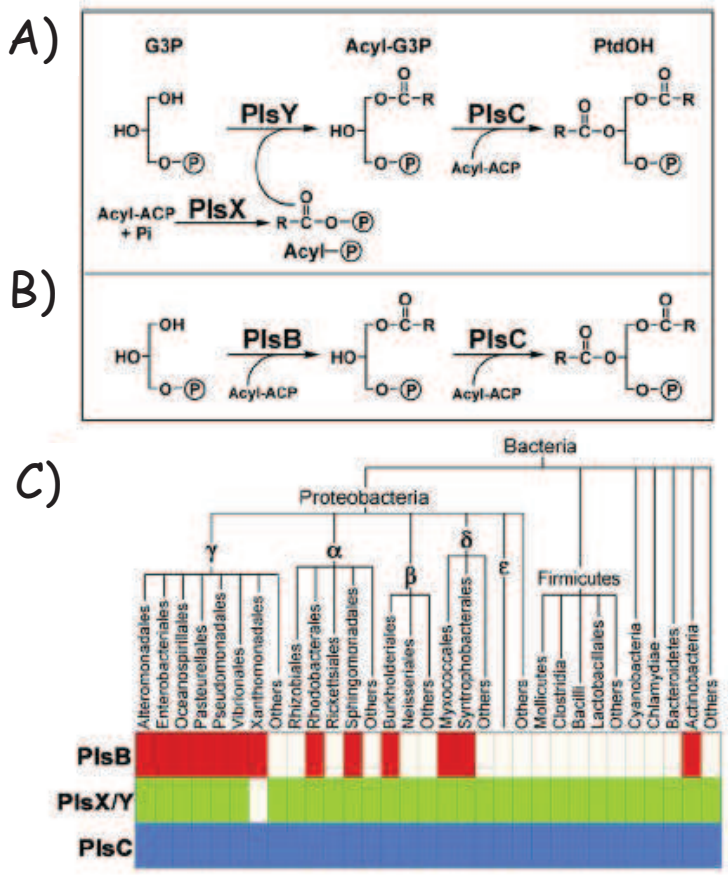

Figure 17: Les deux voies d'acylation du G3P, PlsB PlsX/PlsY (Lu *et al.*, 2006). G3P: glycérol-3-phosphate; PtdOH: acide phosphatidique. **(A)** La voie PlsXY commence pour la formation d'un acyl-phosphate (acyl-P), à partir d'un acyl-ACP, par PlsX. PlsY catalyse le transfert de l'acide gras de l'acyl-P sur le G3P. L'acyl-G3P est ensuite converti en PtdOH par PlsC en utilisant un acyl-ACP comme donneur. **(B)** La voie alternative PlsB commence avec le transfert d'un acide gras sur G3P par PlsB en utilisant un acyl-ACP suivie de l'acylation par PlsC. **(C)** Distribution des gènes codants pour les acyltransférases PlsB (rouge), PlsX/Y (vert), et PlsC (bleu) chez les bactéries.

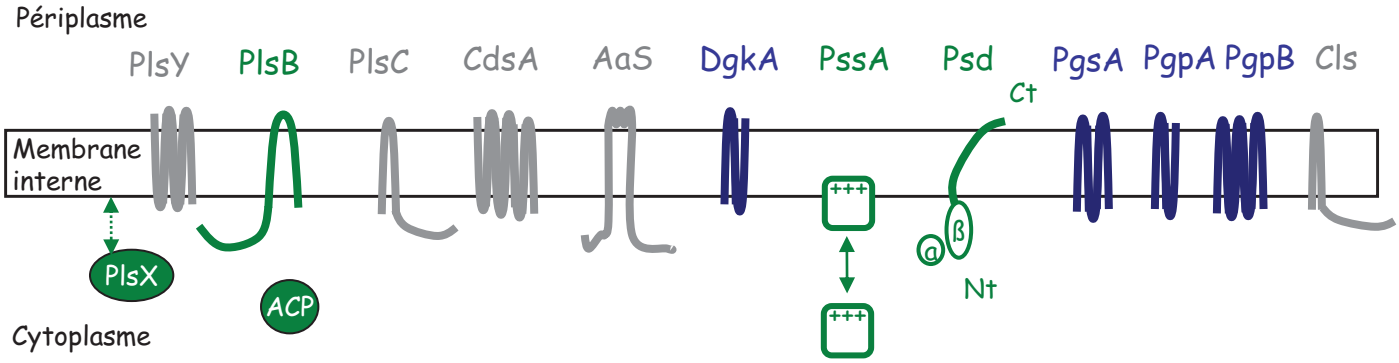

Figure 18: Topologies connues et prédites des enzymes de la biosynthèse des phospholipides dans la membrane interne de *E. coli*. La localisation du C-terminus de PlsY, PgsA, PgpA et PgpB a été déterminée (Daley *et al.*, 2005). PssA se fixe aux phospholipides anioniques; son accrochage est transitoire en fonction de la composition en phospholipides de la membrane. Psd est montrée avec ses deux sous-unités α et β. Les topologies ont été déterminées expérimentalement pour PlsY, DgkA et PgpB (Smith *et al.*, 1994; Lu *et al.*, 2007; Touzé *et al.*, 2008).

par Voelker (Voelker, 1997) : le groupement pyruvoyl forme une base de Schiff avec le groupement sérine de la phosphatidylsérine. La décarboxylation de la phosphatidylsérine est alors favorisée, avec un passage par un intermédiaire azométhine protoné, pour donner la PE.

2. La voie de biosynthèse des phospholipides anioniques

Dans la voie de synthèse des phospholipides anioniques, le groupement CDP de l'acide phosphatidique est remplacé par un G3P formant alors un phosphatidylglycérol phosphate. PgsA (phosphatidylglycérophosphate synthase), une protéine intégrale de membrane de 20 kDa, catalyse cette réaction (figure 14). De plus, PgsA qui est présente à environ 1400 copies par cellule (Larson & Dowhan, 1976) peut catalyser la réaction inverse, mais seulement en présence de CMP (Dowhan & Hirabayashi, 1981). L'étude enzymatique de PgsA purifiée a montré qu'elle pouvait catalyser le transfert de déoxy- ou de ribocytosine diphosphate (Hirabayashi *et al.*, 1976).

PgsA est essentielle, car un mutant de délétion n'est pas viable (Heacock & Dowhan, 1987). En revanche, il est possible de transduire une mutation *pgsA* dans un mutant *lpp*-2 (Kikuchi *et al.*, 2000 ; Matsumoto, 2001). La lipoprotéines majeur de la membrane externe (lipoprotéine de Braun) consomme le PG en transférant son groupement diacylglycéryl à la prolipoprotéine, le produit du gène *lpp* (Asai *et al.*, 1989 ; Sankaran & Wu, 1994). Cette souche *pgsA*3 *lpp*-2 serait viable en dessus de 40 °C et ne contient pas de PG ou de CL détectables (les deux 0,01% des phospholipides totaux) (Kikuchi *et al.*, 2000). L'essentialité de *pgsA* vient donc des fonctions essentielles du phospholipide anionique PG dans la cellule : le PG est consommé dans des réactions spécifiques à sa tête polaire, et le PG possède une charge négative qui peut recruter des protéines à la membrane interne (Matsumoto, 2001).

Les deux phosphatidylglycérophosphatases PgpA et PgpB réalisent la même réaction *in vitro* : déphosphoryler le phosphatidylglycérophosphate pour obtenir du PG. PgpA et PgpB sont des protéines intégrales de membrane interne, respectivement de 19,4 et 29 kDa (figure 18) (Daley *et al.*, 2005 ; Icho, 1988). La fonction physiologique de PgpA pourrait être autre que celle de phosphatidylglycérophosphatase, car *pgpA* est en operon avec des gènes impliqués dans la synthèse de la riboflavine (Torrents *et al.*, 2007). De plus, les deux enzymes PgpA et PgpB ne sont pas essentielles car le double mutant présente toujours une activité phosphatidylglycéro-phosphatase et la proportion en phospholipides (PE/PG/CL) ne varie guère (Funk *et al.*, 1992). L'enzyme responsable de cette activité résiduelle, localisée au niveau de la membrane interne, est nommée PgpC mais le gène codant cette activité n'a pas été identifié (Funk *et al.*, 1992).

```
            * *    *        *          * *    *
PssA  138:  HFKGFIIDDSVLYSGA     358:  HLKGMWVDDKWMLITG
YmdC  120:  HNKSFTVDGVVTLVGG     369:  HAKTFSIDGKTVFIGS
Cls   224:  HRKMIMIDNYIAYTGS     404:  HTKSVLVDGELSLVGT
YbhO  113:  HRKIVVIDARIAFIGG     290:  HGKVALMDDHWATVGS
```

Figure 19: Le domaine HKD (d'après Matsumotu *et al.*, 1999). Alignement de séquences du motif HKD (Pfam00614) de PssA, YmdC, un paralogue de PssA et Cls de fonction inconnue, Cls et YbhO chez *E. coli*. Ce domaine HKD est constitué de la séquence $H_{x2}K_{x4\text{-}6}D$ qui est retrouvé dans la superfamille des phospholipases D. Les numéros indiquent les résidus et les astérisques identifient les résidus très conservés.

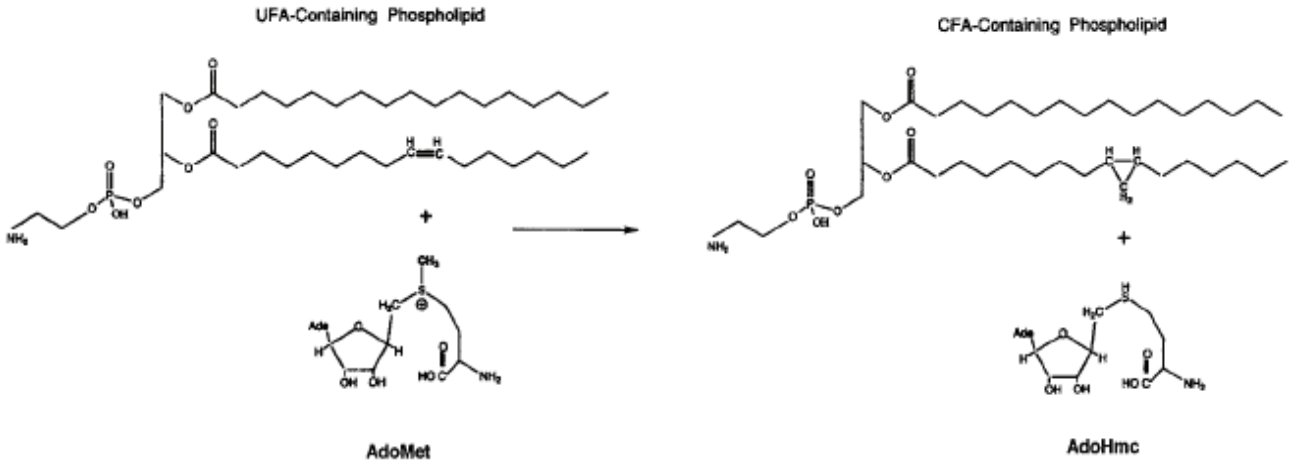

Figure 20: Réaction de cyclopropanation (Grogan &Cronan, 1997). Le phospholipide figuré (PE) présente un acide gras insaturé qui devient le substrat de la Cfa synthase nécessitant la présence de S-adénosyl-L-méthionine (AdoMet) pour donner un phospholipide avec un acide gras cyclopropané et un S-adenosyl-L-homocystéine (AdoHmc).

PgpB est multifonctionnelle car elle catalyse la déphosphorylation des acides lysophosphatidique et phosphatidique (Icho, 1988 ; Icho & Raetz, 1983) et présente une activité diacylglycérol pyrophosphate phosphatase (Dillon *et al.*, 1996). Mais son rôle physiologique est probablement de déphosphoryler l'undécaprenyl pyrophosphate (C55PP) en concert avec les autres enzymes BacA, LpxT et YbjG (Touzé *et al.*, 2008). PgpB, LpxT, et YbjG appartiennent à la famille des phosphatases PAP2 (Pfam01569). Il n'est pas compris pourquoi il existe quatre enzymes avec l'activité C55PP phosphatase, car l'expression de seulement *pgpB*, *bacA* ou *ybjG* suffit pour la synthèse d'undécaprenyl phosphate et la survie (El Ghachi *et al.*, 2005). L'expression de *lpxT* seule par contre ne suffit pas car LpxT possède une faible activité enzymatique (El Ghachi *et al.*, 2005). Des essais *in vitro* ont montré que son rôle physiologique pourrait être le transfert d'un phosphate de C55PP sur le Kdo2 (2-keto-3-déoxyoctonate) lipide A (Touzé *et al.*, 2008).

La synthèse de la CL est catalysée par la cardiolipine synthase Cls qui condense deux molécules de phosphatidylglycérol (figure 14) (Cronan, 2003). Tout comme PssA, Cls contient deux domaines phosphodiestérases homologues à ceux de la phospholipase D (résidus 219 à 246 et 399 à 426, Pfam PF00614) (Tropp, 1997). Les deux histidines des deux motifs HKD (figure 19) sont essentielles pour l'activité de ces enzymes et dans le cas de Cls, la mutation de ces histidines en glutamines entraîne une perte de l'activité (Guo & Tropp, 2000). L'activité enzymatique de Cls est inhibée par les produits de sa réaction: la CL et le glycérol (Ragolia & Tropp, 1994).

Un mutant de deletion Δ*cls* a pu être obtenu, ce qui suggére que le gène *cls* n'est pas essentiel. Dans ce mutant la CL est encore détectable, suggérant que PssA pourrait catalyser la synthèse de CL (Nishijima *et al.*, 1988). De plus, une deuxième activité CL synthase a été mise en évidence suggérant qu'une autre enzyme existerait avec cette activité (Guo & Tropp, 2000). Dans un mutant *cls*-1, codant pour une Cls défective, la présence de CL est encore observée (5 % des phospholipides totaux dans la phase stationnaire avancée), tandis que quand *cls*-1 est introduit dans un mutant thermosensible *pssA*-1(ts), la CL n'est plus détectable (Shibuya *et al.*, 1985). Cependant, il est impossible d'obtenir le double mutant Δ*cls pssA*-1(ts), où le gène *cls* est supprimé, du fait de l'essentialité de la CL chez *E. coli* (Nishijima *et al.*, 1988).

B3. Modification des chaînes acyles dans la membrane : cyclopropanation

En entrée en phase stationnaire, les chaînes acyles des phospholipides peuvent être modifiées après leur synthèse (Wang & Cronan, 1994). Parmi les trois grands types de modifications

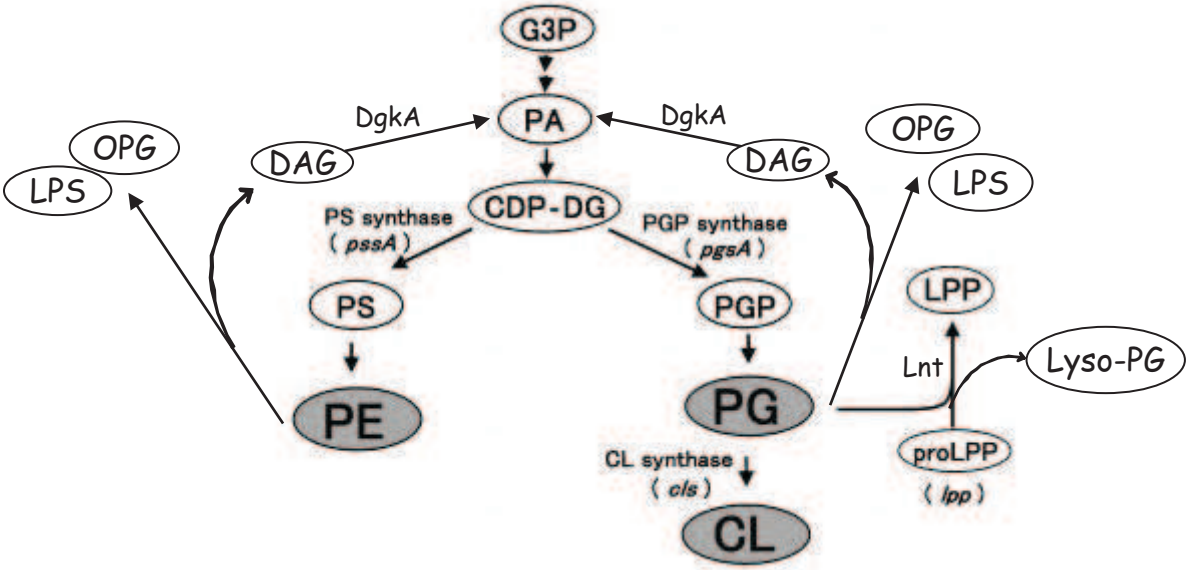

Figure 21: Utilisation des phospholipides pour des synthèses de l'enveloppe (d'après Matsumoto, 2001). G3P: glycérol-3-phosphate; PA, phosphatidic acid; CDP-DG: CDP-diacylglycérol; PS: phosphatidylserine; PE: phosphatidylethanolamine; PGP: phosphatidylglycerophosphate; PG, phosphatidylglycerol; CL, cardiolipin; proLPP, prolipoprotein; LPP: lipoprotéine de la membrane externe; OPG: osmoregulated periplasmic glucan; LPS: lipopolysaccharide.

décrites chez les bactéries (l'isomérisation cis → trans, la cyclopropanation et la désaturation des chaînes acyles), seule la cyclopropanation existe chez *E. coli*. La Cfa (cyclopropane fatty acid) synthase, une protéine de 44 kDa (Wang *et al.*, 1992), est responsable de la formation des cyclopropanes au niveau de la chaîne carbonée des phospholipides uniquement. Cette synthase est dépendante d'un donneur de méthylène, la S-adénosyl-L-méthionine (AdoMet) (figure 20) (Cronan *et al.*, 1979). A partir de la double liaison d'un acide gras insaturé (à partir de C9-11), la Cfa synthase 'ouvre' la double liaison grâce à son donneur de méthylène et forme un cyclopropane (Grogan & Cronan, 1997).

La Cfa synthase est présente dans la fraction cytoplasmique d'un lysat cellulaire, mais l'enzyme s'associe d'une façon réversible aux fragments membranaires et est stabilisée par des vésicules de phospholipides en s'y liant (Taylor & Cronan, 1979 ; Grogan & Cronan, 1997). L'enzyme a une affinité différente en fonction de la saturation des phospholipides. Elle interagit seulement avec des acides gras insaturés ou modifiés par cyclopropanation. Cfa est active sur tous les phospholipides majeurs de *E. coli*, et elle possède également une activité résiduelle *in vitro* sur des vésicules de phosphatidylcholine (Taylor & Cronan, 1979).

C. Dégradation et turnover des phospholipides

Les phospholipides anioniques sont sujets à la dégradation lors de la phase exponentielle alors que les phospholipides zwittérioniques sont relativement stables (Raetz & Newman, 1978). En effet, le marquage radioactif des phospholipides au P32 montre qu'à chaque temps de génération, 5 à 10% de PE et environ 30% de PG sont métabolisés (Raetz, 1986). Le renouvellement des PE pourrait refléter la dégradation par les phospholipases et le transfert du groupement phosphoéthanolamine au niveau des OPGs ou du lipide A (figure 21) (cf. § IVC). Le renouvellement de PG est dû à la formation de CL (spécialement lors de l'entrée dans la phase stationnaire), à la biosynthèse des lipoprotéines (LPP) et au transfert de glycérol-1-phosphate au niveau des OPGs (figure 21). Les phospholipides ainsi endommagés peuvent être soit recyclés directement en phospholipides soit dégradés par des phospholipases qui libèrent les chaînes acyles et la tête polaire du squelette glycérol.

C1. Utilisation des têtes polaires des phospholipides

Les OPGs sont des constituants de l'enveloppe des bactéries à GRAM négatif qui sont localisés dans l'espace périplasmique. Ce sont des molécules très anioniques importants pour la régulation osmotique de la bactérie (Kennedy, 1982). Les OPGs sont formés de 8 à 10

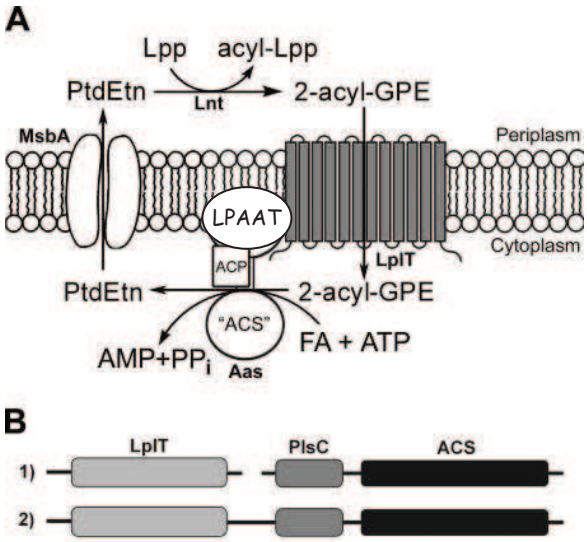

Figure 22: Réacylation d'une lysophosphatidyléthanolamine (2-acyl-GPE) par Aas (Harvat *et al.*, 2005). A) Un 2-acyl-GPE dans le périplasme est généré par transacylation, catalysée par Lnt, de la chaîne acyle sur la position 1 (de la PE ou PtdEtn) du N-terminus de la Lpp. Le 2-acyl-GPE est transporté par LplT (lysophospholipid transporteur) à travers la membrane interne où il est acylé par Aas utilisant un acyl-ACP comme acyl donneur. **B**) L'architecture associée avec la famille LplT chez les bactéries à GRAM négatif. 1) Chez *E. coli*, il y a 3 domaines fonctionnels présents dans 2 polypeptides. Le premier gène dans l'operon, *lplT* code pour LplT, qui appartient à la grande famille des faciliteurs et qui est exprimé comme une protéine distincte. Le deuxième gène dans l'operon, *aas*, code pour la lysophospholipid-acyltransférase/acyl-ACP synthétase, qui est bifonctionnelle. AaS possède deux domaines distincts: un domaine PlsC appartenant à la famille des lysophospholipid acyltransférase (LPAAT) et un domaine ACS appartenant à la famille des acyl-CoA synthétases impliquées dans le transfert sur le thiol via un intermédiaire acyl-AMP. 2) Un deuxième groupe de bactéries, les *Pseudomonaceaes* par exemple, possède les domaines LplT-PlsC-ACS fusionnés dans un seul polypeptide.

sous-unités glucosidiques liées entre elles par des liaisons β1->2 et β1->6 et contiennent des groupements succinate, glycérol-1-phosphate et phosphoéthanolamine (Kennedy *et al.*, 1976).

La synthèse de OPGs est responsable de 75 % de l'altération des phospholipides membranaires (Rotering & Raetz, 1983). La tête polaire (glycérol-1-phosphate) du PG est transférée sur un OPG par la phosphoglycérol transférase, MdoB. Cette réaction libère un diacylglycérol (DAG) (Fiedler & Rotering, 1985). La PE quant à elle est le donneur du groupement éthanolamine (tête polaire de la PE) mais l'enzyme catalysant ce transfert n'a pas été identifié (Miller & Kennedy, 1987). Par ailleurs, lors de la synthèse du LPS, le lipide A est décoré avec des groupements phosphoethanolamine dont le donneur est également la PE pour les enzymes de la famille EptA (cf. § IVC) (Reynolds *et al.*, 2005). Les DAGs relargués pendant la synthèse des OPGs et du lipide A peuvent être régénérés dans un cycle qui commence avec la phosphorylation des DAGs par la diacylglycérolkinase DgkA (figure 21). Le diacylglycérol-3-phosphate formé peut de nouveau être le substrat de CdsA et ainsi réintégrer la voie de biosynthèse des phospholipides.

Il a été montré qu'un mutant Δ*dgkA* entraînait une accumulation des DAGs (8 % des lipides totaux dont 75 % provenant de la synthèse des OPG et 25 % de celles du lipide A (Raetz & Newman, 1978). De plus, sur un milieu de faible osmolarité (LB sans NaCl par exemple) ce mutant ne croît plus. La diacylglycérolkinase DgkA est donc essentielle dans des conditions de faible osmolarité dû à son implication dans la synthèse des OPGs et la régénération des DAGs (Raetz & Newman, 1978). Par ailleurs, cette diacylglycérolkinase membranaire est un cas atypique conservé uniquement chez les prokaryotes, car elle ne possède pas d'homologie avec la grande famille des NAD kinases solubles conservées chez les eucaryotes (Van Horn *et al.*, 2009).

C2. Utilisation des chaînes acylées des phospholipides

Les phospholipides (PG) sont consommés comme donneurs de chaîne acyle, lors de la synthèse des lipoprotéines comme la Lpp (Sankaran & Wu, 1994). Lnt est une protéine membranaire catalysant le transfert du sn-1,2-diacylglycérol (à partir de PG) sur le groupement sulfhydryl de la cystéine N-terminale de la prolipoprotéine (Pro-Lpp) (Sankaran & Wu, 1994). Dans ce cas, les produits relargués sont le glycérol-1-phosphate et le lysophosphatidylglycérol. De plus, Lnt catalyse également la transacylation de la chaîne acyle (de la PE) sur la position 1 du N-terminus de la Lpp dans le périplasme. Dans ce cas, une 2-acyl-GPE est générée (figure 22A).

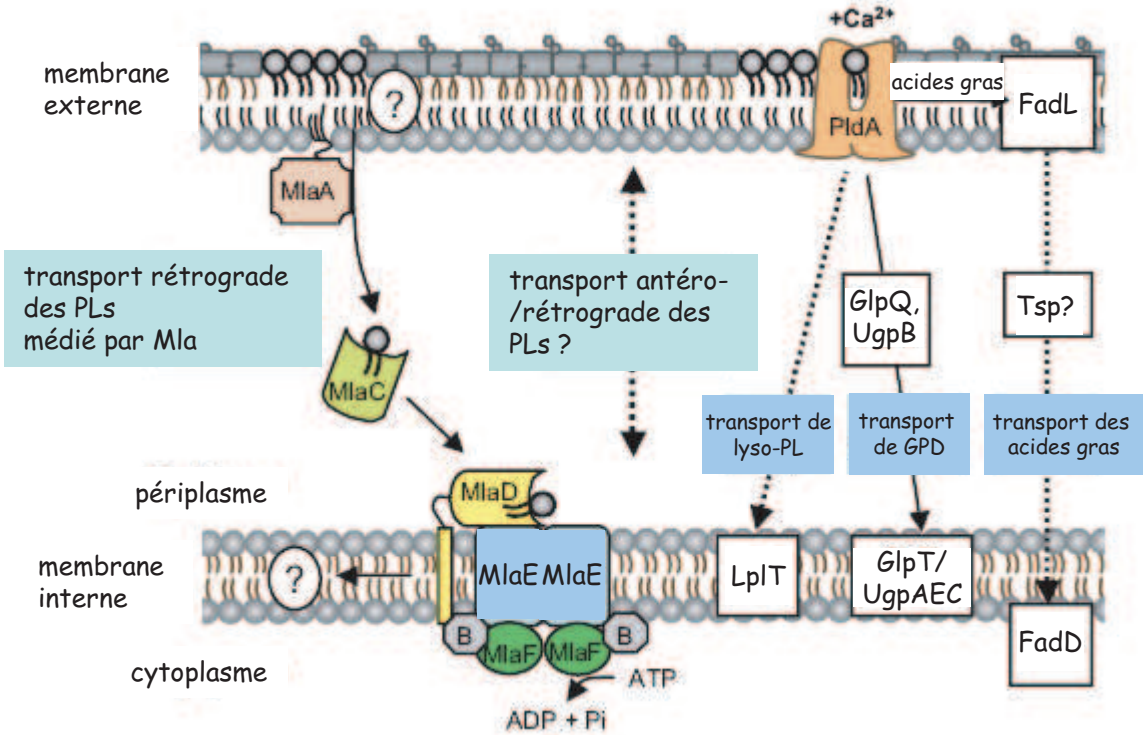

Figure 23: Modèle des voies Mla et PldA impliquées dans le turnover des phospholipides chez *E. coli* (Malinverni & Silhavy, 2009). La voie Mla extrait les phospholipides (PL) de la membrane externe (soit du feuillet interne avant la migration à la surface, soit directement de la membrane externe) et les transporte jusqu'au complexe MlaFEDB dans la membrane interne (IM) via la protéine périplasmique MlaC. Le devenir des PLs est inconnu, mais ils pourraient être réintroduits dans la IM. Probablement, d'autres systèmes de transport rétrogrades existent. Un niveau élevé de la phospholipase A (PldA) supprime des mutants de Mla en détruisant des PLs de la surface externe ce qui produit des acides gras libres, des lyso-PLs et des glycérophosphodiesters (GPDs). Chacune de ces molécules est transportée à la IM par des voies différentes, mais il n'est pas certain que les mêmes voies soient utilisées pour éliminer des produits de dégradation de PldA du feuillet externe. Les lignes pointillées représentent des modes de transport inconnus à travers le périplasme. L'implication des protéines dans les boites blanches est hypothétique.

Des chaînes acyles provenant des phospholipides sont également nécessaires pour des modifications du LPS dans la membrane externe. PagP est une enzyme utilisant des phospholipides comme donneurs de palmitate (à partir de la position *sn*-1) pour le transférer au lipide A (Bishop *et al.*, 2000). Dans ce cas, des esters de glycérol sont générés.

Les phospholipides sont également hydrolysés par la phospholipase A PldA de la membrane externe dont l'activité enzymatique est elle-même activée par la présence de (lyso - phospholipides (Dekker, 2000). Les acides gras libres, lyso-phospholipides et glycérophosphodiesters formés sont ensuite transportés à la membrane interne par plusieurs mécanismes possibles (figure 23 à droite). La fonction proposée pour PldA serait de maintenir l'asymétrie en phospholipides de la membrane externe en conditions de stress (Dekker, 2000).

Les seules données disponibles sur le recyclage d'un phospholipide endommagé lors de la synthèse des lipoprotéines est la réacylation de la lysophosphatidyléthanolamine (2-acyl-GPE) (à partir de la PE) par AaS (figure 22) (Jackowski & Rock, 1986). Aas est une enzyme bifonctionnelle membranaire qui possède deux domaines distincts responsables des deux activités nécessaires : une activité acyl-ACP synthétase (ACS) et une activité 2-acyl-GPE acyltransférase (LPAAT) (Cooper *et al.*, 1989). La 2-acyl-GPE traverse la membrane interne par transport facilité grâce à la protéine LplT (lysophospholipid transporter). Puis, elle est acylée par Aas qui utilise un acyl-ACP comme donneur de chaîne acyle. Aas utilise soit l'acyl-ACP provenant de la synthèse des acides gras, soit elle active un acide gras libre (ATP- et Mg^{2+}-dépendant) lequel est transféré sur un holo-ACP. En revanche, seule une petite partie du pool d'acides gras exogènes importés est disponible pour Aas (Rock & Jackowski, 1985). Le reste du pool subit la thioestérification sur un CoA par l'action de FadD (figure 11).

Il est intéressant de noter que *lplT* est en opéron avec *aas* chez la plupart des bactéries (figure 22B) (Harvat *et al.*, 2005). De plus, chez certaines bactéries, ces deux gènes sont même fusionnés et s'expriment sous frome d'un seul polypeptide avec les trois domaines fonctionnels LplT-PlsC-ACS fusionnés (figure 22).

D. Export des phospholipides vers la membrane externe

Le mécanisme d'exportation des phospholipides vers la membrane externe est peu connu. Deux questions se posent: comment passent les phospholipides du feuillet interne au feuillet externe de la membrane interne, et comment traversent-ils ensuite l'espace périplasmique vers la membrane externe? Malheureusement, ces questions restent sans réponses précises pour l'instant. Mais il semble que le transport des phospholipides est lié à celui du LPS (cf. § IVB). En effet, un mutant thermosensible du gène *msbA*(ts), qui code pour un transporteur du LPS,

Gène	Localisation Topologie	Caractéristiques	Références
yihG	Membrane interne 2 TMSs (prédit)	Domaine acyltransférase homologue à ceUX de PlsC et PlsB (Pfam01553); complémentation d'un mutant *plsC*(ts)	Neuwald, 1997
yegS	Cytoplasme	Homologue à NAD kinases eucaryotes (Pfam00781); Activité diacylglycérol kinase *in vitro*	Bakali *et al.*, 2006, 2007
ybhO	Association à la membrane	Domaine cardiolipine synthase (Pfam00614) et activité *in vitro*; Paralogue à Cls	Guo & Tropp, 2000 Quigley & Tropp, 2009
ynbA	Membrane interne 5 TMSs (prédit)	Domaine CDP-alcohol phosphatidyltransferase (Pfam01066); Paralogue à PgsA	Reed *et al.*, 2003
ynbB	Membrane interne 7-8 TMSs (prédit)	Domaine CDP-diglyceride synthase (Pfam01148); Paralogue à CdsA	Aiba *et al.*, 1996
ybjG (***bcrC***)	Membrane interne 6 TMSs (prédit)	Domaine undecaprenyl pyrophosphate phosphatase (Pfam01569); Paralogue à LpxT, PgpB et BacA	ElGhachi *et al.*, 2005
ymdC	?	Domaine phospholipase Dc (Pfam00614); Paralogue à PssA et Cls	Ponting & Kerr, 1996 Koonin, 1996

Figure 24: Gènes de fonction inconnue contenant des domaines prédits pour des activités enzymatiques dans le métabolisme des lipides chez *E. coli*. TMS: transmembrane segment; ts: thermosensible;

affecte non seulement le transport du LPS, mais également celui des phospholipides vers la membrane externe (Doerrler *et al.*, 2004). MsbA est une translocase pour de nombreuses molécules lipidiques ; elle est ATP-dépendante et activée par des lipides. Récemment, il a été montré qu'un flip-flop des phospholipides avait lieu dans des liposomes contenant seulement MsbA (Eckford & Sharom, 2010). Chez *Neisseria meningitidis* où le LPS et *msbA* ne sont pas essentiels, les phospholipides sont toujours transportés et une membrane externe est assemblée qui ne contient presque que des phospholipides (Sperandeo *et al.*, 2009). Le fait que *E. coli* a une croissance élevée par rapport à *N. meningitidis* pourrait expliquer pourquoi MsbA est importante pour un flip-flop rapide des phospholipides chez *E. coli* (Raetz *et al.*, 2007).

L'asymétrie en phospholipides des deux feuillets de la membrane externe doit être maintenue (Dekker, 2000). Dans ce contexte, l'identification d'un système impliqué dans le transport rétrograde des phospholipides de la membrane externe vers la membrane interne semble important (Malinverni & Silhavy, 2009) : le système Mla (maintance of OM lipid asymetry), un système de transport du type ABC aurait pour fonction de prévenir l'accumulation des phospholipides à la surface de la membrane externe (Malinverni & Silhavy, 2009). Les phospholipides retirés de la membrane externe par la voie Mla sont ensuite transportés à travers le périplasme liés à la protéine périplasmique MlaC qui les apporte au complexe MlaFEDB de la membrane interne (figure 23 à gauche). On peut penser que des systèmes analogues, mais dans l'autre sens – de la membrane interne vers la membrane externe – pourraient exister pour exporter les phospholipides.

E. Protéines de fonction inconnue impliquées dans le métabolisme des lipides

La plupart des enzymes de biosynthèse des phospholipides décrites plus haut sont essentielles. En revanche, il existe de nombreux homologues des enzymes impliquées dans le métabolisme des lipides, qui ne sont pas essentiels. Leurs fonctions sont pour la plupart inconnues. Ces gènes de fonction inconnus chez *E. coli* sont listés dans la figure 24. Seules les activités enzymatiques de YihG qui possède une activité acyltransférase, de YbhO, la cardiolipine synthase 2, et de la kinase YegS ont été caractérisées, toutefois sans apporter d'information sur leurs rôles physiologiques dans la cellule.

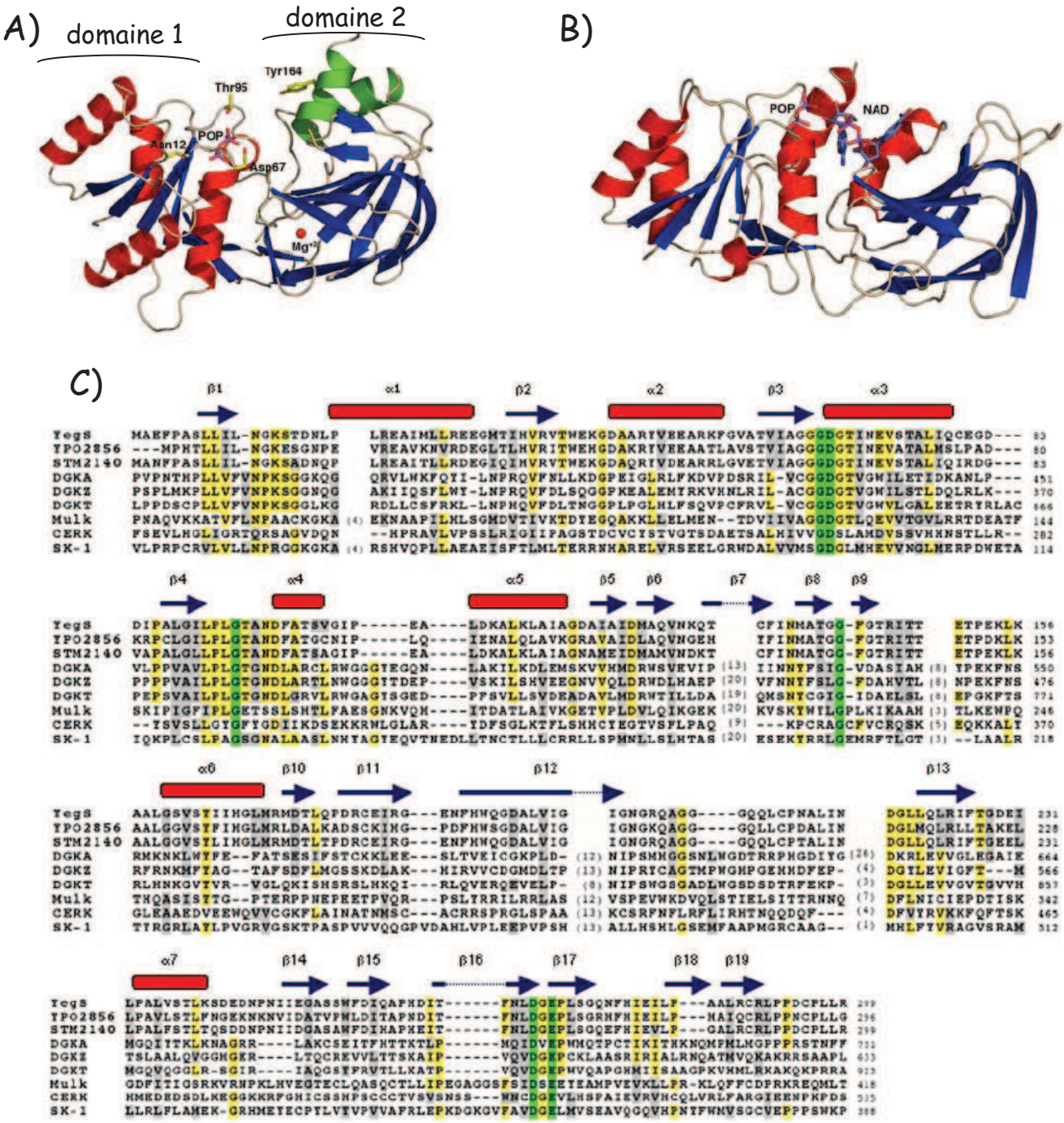

Figure 25: Structure de YegS et alignement comparatif avec les NAD kinases (Bakali *et al.*, 2007). (A) Structure de YegS de *E. coli*. **(B)** Structure de la NAD kinase eucaryote. **(C)** Alignement de séquences de YegS avec ses homologues proches, présenté avec les éléments de structure secondaires (feuillet ß en bleu, hélice α en rouge). YPO2856 est indiquée comme diacylglycérol kinase potentielle de *Yersinia pestis* (d'autres séquences procaryotes homologues ne sont pas inclues). Human DGK est une séquence réprésentative de la famille des diacylglycérol kinase; MulK est une multilipide kinase charactérisée recemment; CERK est la ceramide kinase humaine; SK-1 est une isoforme de la sphingosine kinase 1 humaine.

E1. L'acyltransférase YihG

YihG (36 kDa, 310 résidus) est prédite pour être une protéine de membrane interne avec deux segments transmembranaires (TMS) et avec son C-terminus localisé dans le cytoplasme (Daley *et al.*, 2005). De ces informations, on peut déduire une topologie préliminaire de YihG dans la membrane interne (figure 15 C). De plus, au laboratoire, il a été montré qu'une protéine fusion YihG-TAP se localise dans la membrane interne (résultats non-publiés).

YihG possède un domaine acyltransférase homologue à ceux de PlsC et PlsB (Pfam 01553). Des tests d'activité par complémentation de mutants *plsB* et *plsC* ont été réalisés en utilisant des mutants conditionnels : la souche BB2636 contenant un allele muté *plsBA349* est auxotrophe pour le glycérol (Bell, 1974) et la souche SM2-1contenant un allele *plsC*(ts) est thermosensible (Coleman, 1990). La surexpression de *yihG* complémente le phenotype thermosensible de la souche SM2-1, mais pas celui de la souche BB2636 (Bouveret *et al.*, non-publié). Ceci indique que YihG serait une acyltransférase du type PlsC, c'est à dire une lysophosphatidique acide acyltransférase (LPAAT ; figure 16). Par ailleurs, YihG serait activée par le facteur sigma alternatif SigmaS (RpoS) ce qui suggère un rôle de YihG en réponse au stress (Mohanty & Kushner, 1999).

E2. La cardiolipine synthase 2 YbhO

Les séquences en acides aminés de YbhO et YmdC possèdent les deux motifs HKD caractéristiques de la superfamille des phospholipases D (Pfam PF00614; figure 19) (Guo & Tropp, 2000). YbhO catalyse la formation de CL *in vitro*, mais pas *in vivo*, tout comme une forme tronquée de Cls sans N-terminus (premiers 60 résidus) (Guo & Tropp, 2000 ; Quigley & Tropp, 2009). Le N-terminus n'est donc pas essentiel pour l'activité enzymatique, mais jouerait un rôle dans l'insertion correcte de Cls dans la membrane interne. YbhO qui ne possède pas la séquence N-terminale serait donc une protéine cytoplasmique ou associée à la membrane (Guo & Tropp, 2000 ; Quigley & Tropp, 2009).

Cls, YbhO et la forme tronquée Cls' sans N-terminus (résidus 61 à 426) présentent les mêmes profils d'activité suivant le pH. Cls, YbhO et Cls' présentent toutes trois une stimulation par le phosphate et une inhibition par la cardiolipine et l'acide phosphatidique (Guo & Tropp, 2000 ; Ragolia & Tropp, 1994).

E3. La kinase cytosolique YegS

YegS est une protéine de fonction inconnue qui est homologue à des kinases retrouvées chez les eucaryotes. YegS possède *in vitro* une activité phosphatidylglycérol kinase et elle est

cytoplasmique (Bakali *et al.*, 2007). Bien qu'elle soit soluble, YegS devrait interagir avec la membrane car son substrat est lipidique. Effectivement, la structure de YegS (32 kDa) contient une région hydrophobe à la surface du domaine 1 qui pourrait représenter un site pour l'activation allostérique par des lipides (figure 25A) (Raben & Wattenberg, 2009). La séquence du domaine catalytique de YegS est similaire à celle d'une grande famille de NAD kinases eucaryotes (Pfam00781; figure 25B) (Bakali *et al.*, 2006 ; Bakali *et al.*, 2007). Il semble donc que YegS est un homologue proche de l'archétype structural de toutes les kinases solubles qui sont conservées parmi les eucaryotes et procaryotes (figure 25C) (Bakali *et al.*, 2007 ; Nichols *et al.*, 2007). En revanche, la diacylglycérolkinase DgkA ne montre aucune homologie avec ces kinases solubles (vanHorn *et al.*, 2009) et représente un cas particulier des bactéries à GRAM négatif, comme *E. coli*.

Il est intéressant de noter que l'expression de *yegS* est corégulée avec certains gènes impliqués dans la réponse à un stress acide (Masuda & Church, 2003). YegS pourrait ajouter des groupements phosphate chargés négativement au PG, ce qui pourrait compenser la perte de charge sur les têtes polaires pendant la formation de la CL par exemple (Bakali *et al.*, 2007).

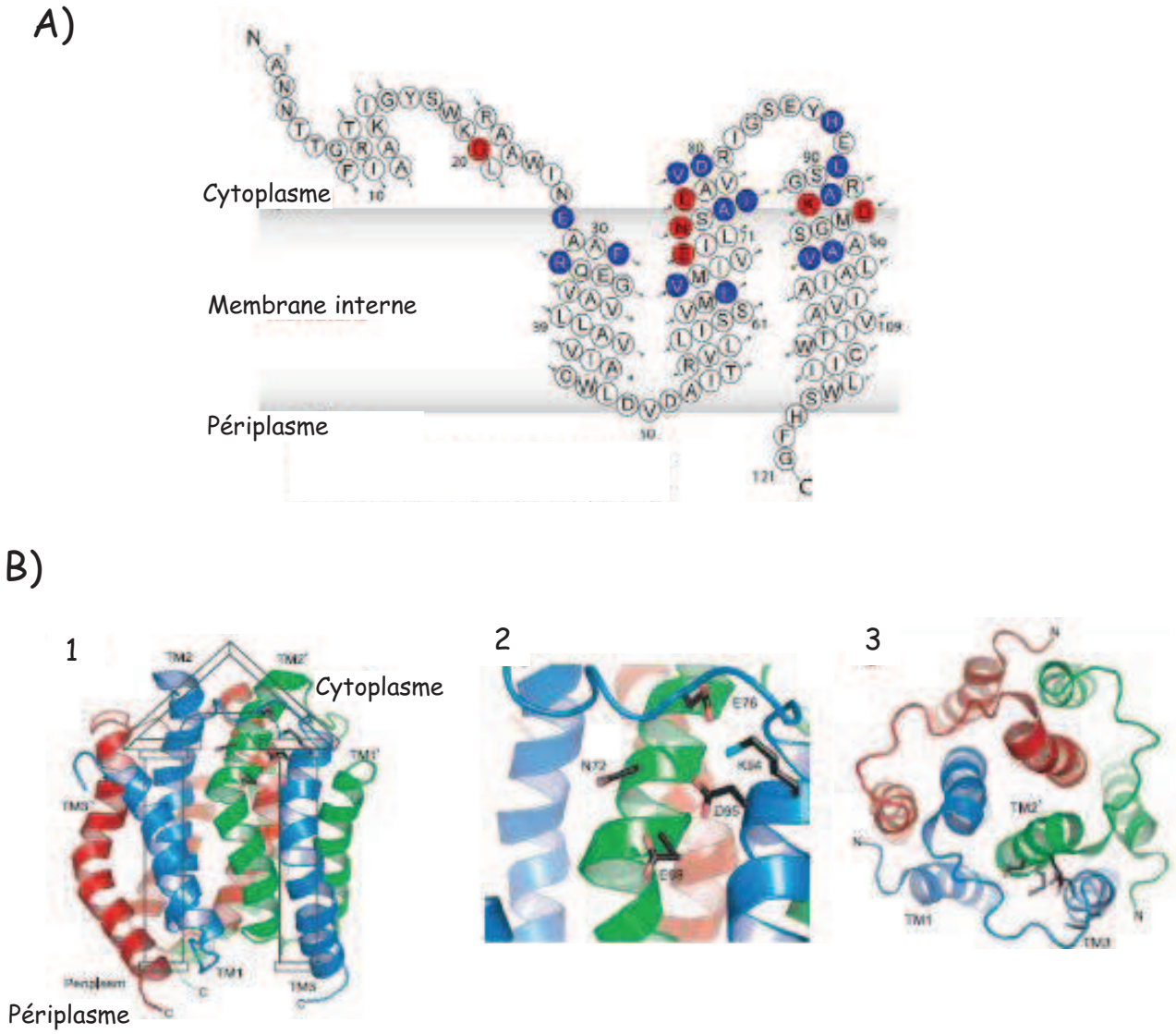

Figure 26: Structure de DgkA dans la membrane interne chez *E. coli* (Smith *et al.*, 1994; Van Horn *et al.*, 2009). (A) DgkA possède 3 segments transmembranaires avec le N-terminus (N) et une boucle dans le cytoplasme et le C-terminus dans le périplasme. Les résidus en bleu indiquent une identité de séquence de plus de 65 % parmi les orthologues; les résidus en rouge indiquent une identité de séquence de plus de 95 % parmi les orthologues. **(B1)** La structure de DgkA en trimère a été déterminée par RMN (Nuclear Magnetic Resonance) en solution. Les 3 domaines transmembranaires (TM) d'un monomère de DgkA sont représentés avec la même couleur. **(B2)** Site actif contenant les résidus le plus conservés. **(B3)** Diagramme en ruban, vu du cytoplasme, qui montre les chaînes de côtés des 5 résidus le plus conservés de DgkA (pour une colonnade).

III. ORGANISATION SUPRAMOLÉCULAIRE DES PROTÉINES DE LA BIOSYNTHESE DES PHOSPHOLIPIDES DANS LA MEMBRANE INTERNE

A. Topologie des protéines de la biosynthèse et du recyclage des phospholipides

Des études biochimiques ont montré que l'activité de biosynthèse de phospholipides est localisée dans la membrane interne chez *E. coli* (Cronan, 2003). Cela suggère que les enzymes sont des protéines membranaires ou associées à la membrane, comme c'est le cas pour PlsX et PssA (Paoletti *et al.*, 2007 ; Louie *et al.*, 1986). De plus, puisque les sites actifs des enzymes membranaires doivent être accessibles aux précurseurs solubles (e.g., G3P, CTP, acyl-ACP), la synthèse des phospholipides aurait lieu plus précisément au niveau du feuillet cytoplasmique de la membrane interne (Cronan, 2003). Il n'existe guère d'études spécifiques sur ces protéines, car il est souvent laborieux de travailler sur des protéines membranaires. Une approche globale du protéome de la membrane interne de *E. coli* a été faite pour faciliter ensuite la prédiction bioinformatique des topologies des protéines (Daley *et al.*, 2005). La localisation des C-termini de 601 protéines intégrales de la membrane interne a été déterminée en utilisant des protéines fusionnées à leur extrémité C-terminale soit à la GFP (green fluorescent protein) soit à la phosphatase alkaline (PA) (Daley *et al.*, 2005). La PA n'est active que dans le périplasme, tandis que la GFP n'est fluorescente que dans le cytoplasme. Dans cette étude, les C-termini des quatre enzymes PlsY, PgsA, PgpA et PgpB de la biosynthèse des phospholipides ont été trouvés côté cytoplasmique de la membrane interne (figure 18). La localisation du C-terminus de Cls n'a pas pu être déterminée. A présent, on ne connaît donc pas les topologies exactes de toutes les protéines de la biosynthèse des phospholipides. Seules les topologies de PlsY, PgpB, et DgkA sont connues en détail grâce à des approches classiques. De plus, la structure 3D de DgkA a été récemment déterminée.

DgkA est une protéine polytopique avec 3 TMS dans la membrane interne (figure 26A) (Smith *et al.*, 1994). Son extremité N-terminale est située dans le cytoplasme, son extremité C-terminale dans le périplasme, avec 2 hélices cytoplasmiques amphipathiques. De plus, la structure 3D de l'homotrimère de 40 kDa, qui est la forme active de DgkA, a été déterminée par RMN (Nuclear Magnetic Resonance) en solution (Van Horn *et al.*, 2009). Le troisième TMS de chaque sous-unité est échangé avec les premier et deuxième TMS de la sous-unité adjacente (figure 26B). Chacun des trois sites actifs de DgkA ressemble à une colonnade contenant des résidus critiques appartenant à deux sous-unités différentes (figure 26B) (Lau *et al.*, 1999). La corniche de la colonnade est déterminante de la spécificité de

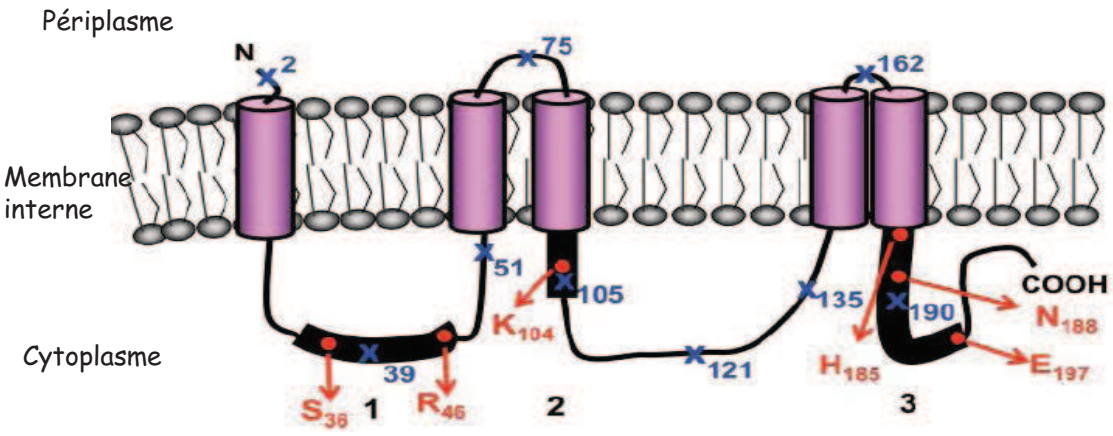

Figure 27: Topologie de PlsY dans la membrane interne chez *Streptococcus pneumoniae* (Lu *et al.*, 2007). La topologie a été déterminée par la méthode de l'accessibilité de cystéine substituée. PlsY possède 5 segments transmembranaires (cylindres) avec le N-terminus (N) et 2 courtes boucles dans le périplasme. Les 3 domaines plus larges dans le cytoplasme contiennent des motifs de séquence très conservés (barres noires) impliqués dans la catalyse; les X bleus indiquent les positions de substitution par des cystéines; les résidus catalytiques sont marqués par des points rouges.

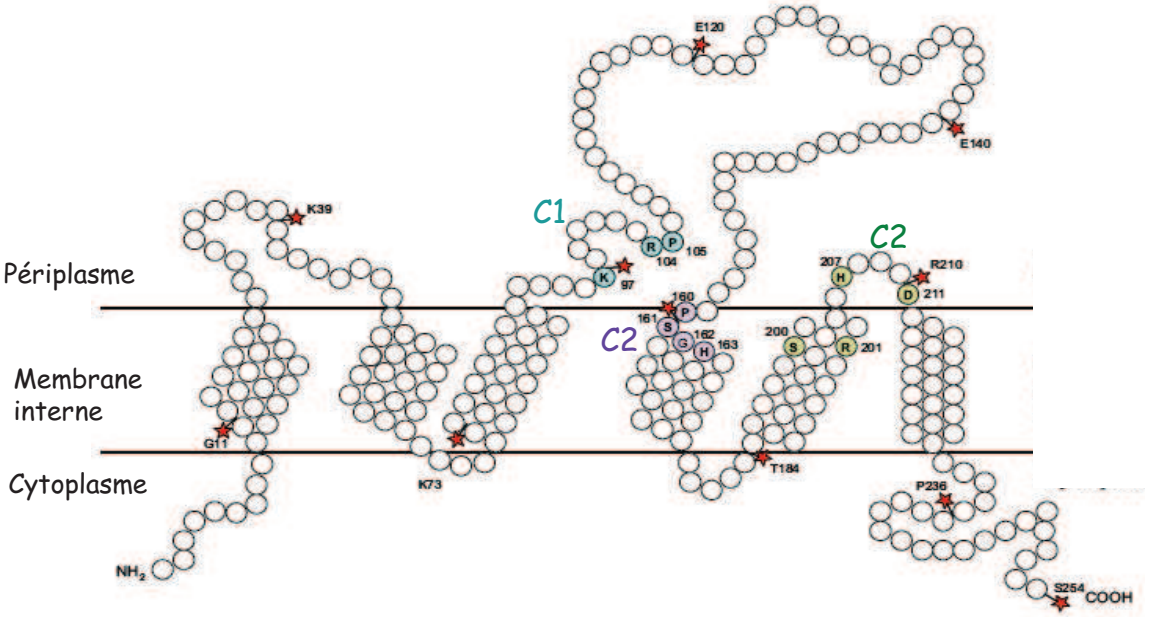

Figure 28: Topologie de PgpB dans la membrane interne chez *E. coli* (Touzé *et al.*, 2008). La topologie de PgpB a été déterminée par une approche de protéine de fusion avec la β-lactamase (limites des différentes protéines de fusion indiqué avec des étoiles rouges). PgpB possède 6 segments transmembranaires et une grande boucle périplasmique. Une signature de résidus périplasmiques a été identifiée (motif C1 en bleu, C2 en violet et C3 en vert). Elle est typique de la famille des PAP2 (phosphatidique acide phosphatase de type 2, Pfam01569), elle est également conservée dans YbjG et LpxT chez *E. coli*.

DgkA pour son substrat lipidique et chevauche le site de transfert du phosphoryle proche de l'interface eau-membrane. Des mutations dans ou proche du site actif causent des défauts de repliements, ce qui suggère que les différents sites des sous-unités qui se chevauchent sont impliqués dans le repliement correct et l'activité de DgkA (Van Horn *et al.*, 2009). Cette observation que la plupart des résidus importants pour le repliement de DgkA sont localisés prêt du site actif, explique pourquoi cette structure 3D spécifique de DgkA est très peu conservée. Bien que DgkA soit une enzyme efficace dans sa niche physiologique microbienne, elle serait donc un orphelin de l'évolution à cause de la relation proche entre son activité enzymatique et son repliement (Van Horn *et al.*, 2009).

La topologie de **PlsY** de *Streptococcus pneumoniae* a été déterminée par la méthode de l'accessibilité de cystéines substituées (Lu *et al.*, 2007). PlsY possède 5 TMS avec le N-terminus et 2 courtes boucles dans le périplasme (figure 27). De plus, chacun des 3 domaines plus larges dans le cytoplasme contient un motif de séquence très conservé qui serait critique pour l'activité de PlsY : le motif 1 possèderait une sérine et une arginine essentiels et le motif 2 correspondrait au site de fixation du G3P. Finalement, le motif 3 contient une histidine et une asparagine conservées qui sont importantes pour l'activité enzymatique et un glutamate qui est crucial pour l'intégrité structurale de PlsY (Lu *et al.*, 2007).

Finalement, la topologie de **PgpB** a été déterminée par une approche de protéines fusion avec la β-lactamase (Touzé *et al.*, 2008). PgpB possède 6 TMS, une grande boucle périplasmique, et une signature de résidus périplasmiques (figure 28, motif C1, C2 et C3) qui est typique pour la famille des PAP2 (phosphatidique acide phosphatase type 2, Pfam01569).

B. Localisation des phospholipides et des protéines de la biosynthèse des phospholipides

Les réactions de biosynthèse des phospholipides ont lieu au niveau de la membrane interne (Cronan, 2003). Toutefois, chez *E. coli*, peu d'études ont été menées pour étudier la localisation précise des enzymes dans la membrane. La question se pose si ces protéines présentent une localisation spécialisée et si elles sont organisées en complexes protéiques dans la membrane.

B1. Localisation des protéines de la biosynthèse des phospholipides

Dans une étude de localisation par microscopie fluorescente chez *B. subtilis*, il a été montré que les protéines Psd, PssA, PgsA, CdsA et Cls fusionnées à la GFP seraient localisées au niveau du septum des cellules en train de se diviser (figure 29) (Nishibori *et al.*, 2005). De

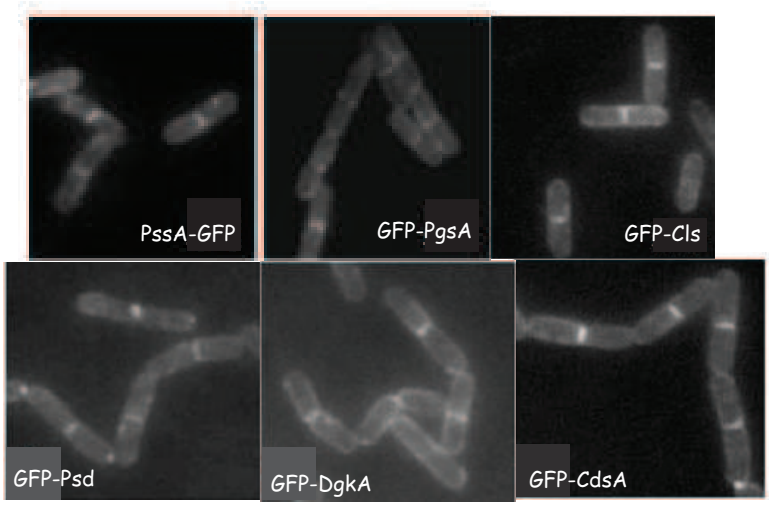

Figure 29: Localisation des protéines de la synthèse des phospholipides chez *B. subtilis* (Nishibori *et al.*, 2005). La localisation a été déterminée par des fusions avec la GFP exprimées à partir de plasmides. Les protéines PgsA, Cls, Psd et DgkA sont étiquetées au N-terminus. PssA est étiquetée au C-terminus.

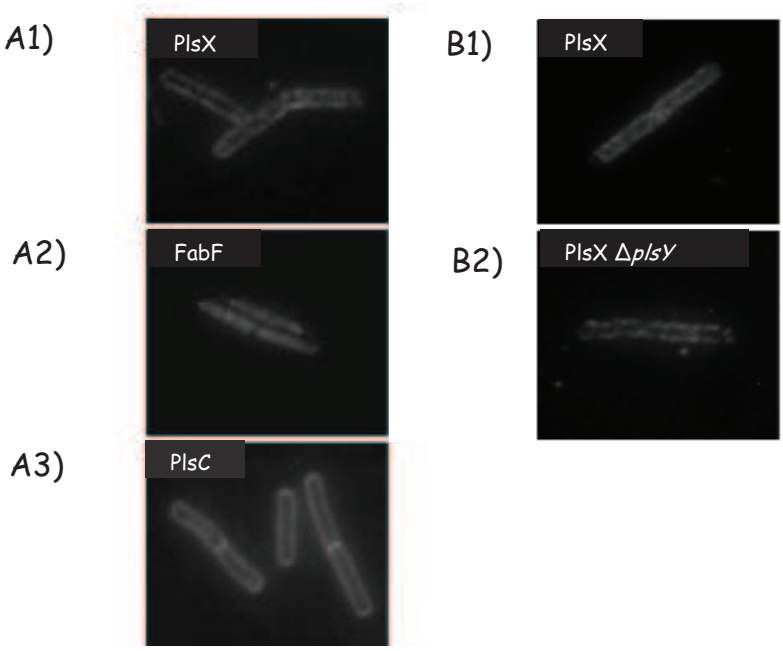

Figure 30: Localisation des protéines de la synthèse des phospholipides chez *B. subtilis* (Paoletti *et al.*, 2007). La localisation a été déterminée par immunodétection en utilisant des anticorps dirigés contre les protéines PlsX, FabF et PlsC.

plus, DgkA-GFP ne serait pas seulement localisée dans le septum, mais également sur les membranes latérales. La protéine de fusion GpsA-GFP utilisée comme contrôle a été retrouvée comme attendu dans le cytoplasme (non montré). Toutefois, il est difficile de généraliser ces résultats d'une bactérie à GRAM positif à une bactérie à GRAM négatif comme *E. coli*. De plus, dans cette étude, les protéines fusionnées à la GFP sont produites à partir de promoteurs artificiels inductibles ce qui pourrait provoquer une localisation non physiologique.

Une autre étude chez *B. subtilis* a utilisé la microscopie par immunofluorescence (Paoletti *et al.*, 2007). Contrairement à la première étude, l'avantage de cette approche est que des anticorps dirigés contre PlsX, PlsC et FabF sont utilisés et que les protéines sont donc détectées à leur niveau de production physiologique. L'enzyme du FASII FabF présente un signal diffus et spécifique qui est distribuée dans le cytoplasme (figure 30). PlsX, bien qu'elle soit une protéine soluble, est associée à la membrane d'une façon ponctuelle (figure 30) (Paoletti *et al.*, 2007). Il a été testé si l'association membranaire de PlsX résulterait d'une association avec PlsY dans la membrane. Mais la déplétion de PlsY ne modifie pas la distribution de PlsX (figure 30 B1 et B2). L'association de PlsX à la membrane ne dépend donc pas d'une interaction spécifique entre PlsX et PlsY, mais peut-être d'une interaction de PlsX avec une autre protéine membranaire ou directement avec les lipides. PlsC présente une localisation homogène dans la membrane (figure 30 A3).

Ces résultats bien que fragmentaires suggèrent que les enzymes de la synthèse des phospholipides pourraient avoir des localisations spécifiques dans la membrane en fonction de leur rôle. Une localisation au septum pourrait s'expliquer par la nécessité d'une synthèse *de novo* des phospholipides pendant la division cellulaire. De plus, il existe sans doute des interactions spécifiques entre les enzymes ou entre les enzymes et les phospholipides, comme c'est le cas pour PssA par exemple.

B2. Rôle des phospholipides dans la fonction et la localisation des protéines membranaires

Les protéines membranaires insérées dans le double feuillet de phospholipides sont soumises à leur influence, soit au niveau de leur fonction, soit de leur localisation.

Il a été montré par des marquages au NAO (10-N-nonyl-acridine orange) que la CL présente une localisastion irrégulière dans la membrane de *E. coli* (Mileykovskaya & Dowhan, 2000). De plus, elle serait préferentiellement localisée aux pôles et septum des bactéries en forme de bâtonnet, comme *E. coli* et *B. subtilis* (figure 31) (Nishibori *et al.*,

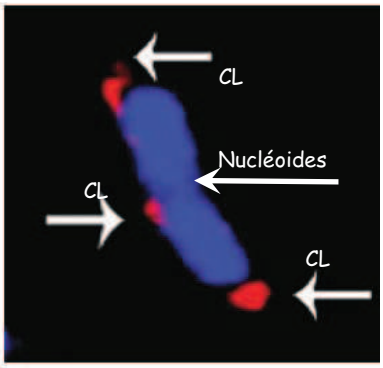

Figure 31: Localisation de la cardiolipine chez *E. coli* (Mileykovskaya & Dowhan, 2009). Microscopie de fluorescence d'une cellule marquée au NAO (10-N-nonyl-acridine orange) pour visualiser la cardiolipine (CL colorée en rouge) localisée aux pôles et septum. Un marquage au DAPI fait apparaître les nucléoides (bleu).

2005 ; Mileykovskaya *et al.*, 2005 ; Mileykovskaya *et al.*, 2009). Cette localisation spécifique serait dûe à des mécanismes physiques liés à la courbure de la membrane aux pôles et également à la courbure intrinsèque importante de la CL (Huang *et al.*, 2006). Des domaines de CL aux pôles sont favorisés de cette manière parce qu'ils réduisent l'énergie et la tension agissant aux membranes. Il pourrait exister d'autres types de domaines ou microdomaines avec des fonctions spécifiques.

La localisation des phospholipides pourrait influencer sur la localisation des protéines membranaire. ProP et MscC, des transporteurs membranaires, sont localisés d'une manière CL-dépendante aux pôles et septum de la cellule (Romantsov *et al.*, 2008 ; Romantsov *et al.*, 2010). Cette localisation CL-dépendante est spécifique de certaines protéines membranaires, car d'autres transporteurs membranaires, comme MscL et LacY, bien qu'ils présentent également une localisation aux pôles, ne dépendent pas de la CL pour cette localisation (Romantsov *et al.*, 2010).

Mis à part la machinerie de translocation, la composition des phospholipides jouent également un rôle dans l'insertion des protéines et leur topologie dans la membrane (van Klompenburg *et al.*, 1997). Ceci est dû à l'interaction des acides aminés chargés positivement de la protéine avec les phospholipides chargés négativement (anioniques). En effet, des régions avec de nombreux résidus d'acides aminés chargés positivement sont localisées en préférence côté cytoplasmique de la membrane interne (« positive-inside rule ») (von Heijne, 1989). L'interaction protéine-phospholipides peut modifier la topologie finale après translocation d'un TMS, comme il a été montré pour la protéine polytopique LacY (Bogdanov *et al.*, 2008).

Si la localisation des phospholipides et leur influence sur la localisation des protéines membranaires sont encore mal comprises, il est certain que les phospholipides influent sur l'activité de protéines membranaires. Par exemple, dans une souche Δ*pssA* de *E. coli* qui ne produit pas de PE, le repliement et l'insertion correcte de la lactose perméase LacY sont affectés (Bogdanov *et al.*, 1996 ; Bogdanov *et al.*, 2002 ; Cronan, 2003). Ce processus est spécifique de LacY et réversible quand on ajoute de la PE dans une vésicule. Il semble que la PE joue un rôle structural plutôt que chimique et serait donc un lipide chaperon spécifique pour certaines protéines membranaires.

Le PG est requit pour l'export correct de la lipoprotéine Lpp de la membrane interne à la membrane externe (Cronan, 2003). Dans une souche Δ*pssA* qui ne produit pas de PG, la cellule lyse dûe à une mauvaise localisation de la forme pro-lipoprotéine de Lpp qui cause un crosslink entre la membrane interne et la membrane externe (Suzuki *et al.*, 2002). De plus,

A)

	N°	354	375	836	622	718	724	637	854	861	958	815	952	988	1006	1007
N°	Construction	T25	T25 ACP	NT25 ACP	T25 PlsB	T25 PlsC	NT25 PlsC	T25 PssA	T25 PgsA	T25 PlsX	NT25 PlsY	T25 AaS	T25 DgkA	T25 YihG	T25 MalF	T25 MalG
355	T18										56					
379	T18ACP	49	45	86	2186	54	53	385	51	174	56	82	45	51	50	46
395	NT18ACP	60	778	61	182	56	58	58	57	61	53	54	58	38	45	56
621	T18PlsB	61	1676	210	3235	3440	70	62	3212	3581	92	2848	3134	3062	208	435
717	T18PlsC	61	63	54	2612	124	63	59	339	938	56	1464	64	111	151	65
636	T18PssA	48	1060	45	86	40	46	46	96	48	50	49	46	52	54	50
853	T18PgsA	47	47	45	665	138	40	46	291	54	50	108	64	50	51	52
856	T18PlsX	47	45	44	1563	53	45	43	408	1547	53	225	78	48	115	54
956	N18PlsY	49	43	52	3505	1957	49	49	1602	2678	52	3887	351	57	890	286
954	T18DgkA	41	43	40	1747	43	114	44	167	1042	54	1318	86	44	97	43
1104	TYihG	49	53	53	671	61	55	49	120	76	56	103	53	54	58	51
1004	T18MalF	42	44	45	88	80	45	44	73	54	54	76	79	63	204	1356
1005	T18MalG	51	50	49	118	60	50	49	73	290	58	85	84	67	3534	84

Activité	< 70	Entre 70 et 150	Entre 150 et 500	Entre 500 et 1500	> 1500

β-gal
[uMiller]

B)

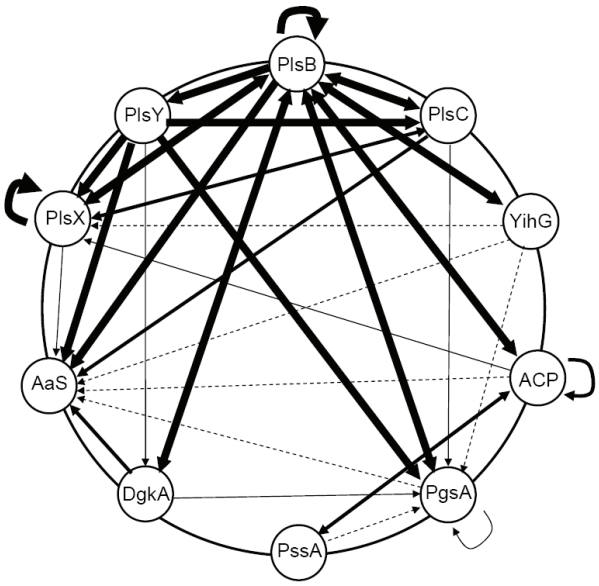

Figure 32: Interactions identifiées par BACTH entre les enzymes de la synthèse des phospholipides (Gully *et al.*, non-publié). A) Tableau systématique des interactions testées deux à deux. Les valeurs indiquées correspondent à l'activité β-galactosidase mesurée. La couleur des cases est fonction de l'intensité de l'activité selon la légende indiquée. Les protéines MalF et MalG sont des protéines membranaires du système de transport ABC du maltose chez *E. coli* et sont utilisées ici comme contrôle de spécificité. L'interaction entre MalF et MalG avait déjà été décrite (Karimova et al., 2005). **B)** Tentative de représentation du réseau d'interactions. Les flèches représentent les interactions détectées par double hybride bactérien. Les pointillés correspondent à une intensité d'interaction comprise entre 70 et 150, les traits fins à une intensité comprise entre 150 et 500, les traits noirs à une intensité comprise entre 500 et 1500 et les gros traits noirs à une intensité supérieure à 1500. Les flèches à double sens correspondent à des interactions mises en évidence quelque soit l'orientation des vecteurs utilisés. Une flèche simple correspond à une interaction détectée uniquement dans le sens T18→T25. Les flèches en dehors du cercle correspondent aux protéines capables d'oligomériser.

les phospholipides anioniques (PG, CL, acide phosphatidique) jouent un rôle dans la fonction de la protéine DnaA, impliquée dans l'initiation de la réplication du chromosome. L'interaction du complexe DnaA-ADP (adénosine diphosphate) avec les phospholipides anioniques active DnaA grâce à un échange de l'ADP par l'ATP (Crooke, 2001). La CL serait 10 fois plus efficace que le PG dans l'échange de l'ADP par l'ATP avec DnaA.

Le positionnement correcte des protéines FtsZ et MinD lors de la division cellulaire seraient également dépendante des phospholipides anioniques (Mileykovskaya *et al.*, 2005). La polymerisation à la membrane de FtsZ est une des premières étapes de l'assemblage de la machinérie de division. FtsZ possède une préférence pour la CL, mais FtsA serait également impliquée dans le processus. La machinérie de division MinCDE evite que le Z-ring est mal-situé aux pôles et ces trois protéines oscillent entre les pôles. Mais dans une souche Δ*pgsA* (et deficiente de Lpp) qui ne contient pas de PG et CL, MinD présente la même oscillation characteristique entre les pôles comme dans une souche sauvage (Mileykovskaya *et al.*, 2009). Ceci s'explique par le fait que d'autres phospholipides anioniques, comme l'acide phosphatique, peuvent substituer pour la CL et le PG.

Ces exemples sont intéressants car ils montrent l'implication majeure des phospholipides dans des mécanismes cellulaires essentiels ayant lieu dans les membranes. Les phospholipides ne jouent donc pas seulement un rôle dans la composition de la membrane, mais ils participent activement aux processus membranaires. Ces résultats montrent également que les phospholipides sont organisés de façon structurée en fonction de leur propriété physiquo-chimique dans la membrane et que les protéines associées avec la membrane pourraient se (co-)localiser spécifiquement en fonction des phospholipides.

C. Interactions entre les protéines de la biosynthèse des phospholipides

Dans une étude précédente faite au laboratoire (Gully & Bouveret, 2006), une interaction avait été détectée entre les protéines PlsB et PssA, deux enzymes de la biosynthèse des phospholipides qui pourtant n'agissent pas successivement dans la voie. De plus, une interaction a été également détectée entre PssA et ACP qui pourtant n'est pas un substrat de PssA (Gully & Bouveret, 2006). Ces résultats suggéraient l'existence d'un complexe protéique.

Les interactions protéiques existant entre ces enzymes ont été testées au laboratoire d'une manière systématique deux à deux par la technique du BACTH (Karimova *et al.*, 1998). Cette technique est basée sur la reconstitution de l'adénylate cyclase de *Bordetella pertussis*

qui permet de suivre une interaction *in vivo* entre protéines solubles ou même membranaires dans *E. coli* (Karimova *et al.*, 2005). Des vecteurs sont disponibles pour la production des protéines récombinantes fusionnées à leur extrémité N- ou C-terminale en fonction de leur topologie dans la membrane interne. Toutes les interactions possibles entre ces protéines ont été testées systématiquement et les résultats sont présentés dans la figure 32 (Gully *et al.*, non-publié). Toutes les interactions ne sont pas détectées dans les deux orientations de vecteurs possibles. Ceci pourrait s'expliquer par le fait que la technique de BACTH employée est sensible à l'organisation 3D et à la topologie des protéines fusion.

L'interaction entre PlsB et DgkA est intéressante car ce sont les seules enzymes de la synthèse des phospholipides dont les gènes sont voisins sur le chromosome, ce qui suggère une régulation coordonnée.

PlsB et PlsX interagissent, et ce dans les deux sens possibles d'utilisation des vecteurs de BACTH. Un lien génétique entre les deux gènes était déjà connu : un double mutant *plsB26plsX50* est auxotrophe pour le G3P, alors que les deux mutants simples ne le sont pas (Bell, 1974 ; Larson *et al.*, 1984). De plus, nos travaux et une autre étude (Hara *et al.*, 2008) chez *B. subtilis* ont montré une interaction entre PlsX et PlsY qui agisse successivement pour acyler le G3P. L'interaction est aussi intéressante parce que PlsX est soluble, mais associée à la membrane interne, tandis que PlsY est une protéine intégrale de membrane (Lu *et al.*, 2007). Ces résultats suggèrent que des événements de régulation entre les deux voies parallèles PlsB et PlsX/PlsY pourraient se passer au niveau enzymatique (Yoshimura *et al.*, 2007). Dans ce sens, PlsX interagit également avec les deux autres acyltransférases PlsC et Aas mais beaucoup plus faiblement.

ACP interagit fortement avec PlsB ce qui est cohérent avec le fait qu'un acyl-ACP est substrat de PlsB, tandis que ACP interagit plus faiblement avec PlsX et PssA. Par contre, ACP n'interagit pas avec PlsC, ce qui suggèrerait qu'un acyl-ACP n'est pas le substrat *in vivo* de cette acyltransférase, contrairement ce qu'il a été observé auparavant dans une étude *in vitro* (Rock *et al.*, 1981).

En conclusion, il existe donc un réseau d'interactions protéine-protéine entre les enzymes de synthèse des phospholipides dans la membrane interne. Ceci suggère l'existence d'un complexe protéique de membrane interne impliqué dans la synthèse des phospholipides, qui serait le pendant du réseau d'interactions entre les enzymes du FASII procaryote (cf. § IB) (Gully *et al.*, non-publié ; Veyron-Churlet *et al.*, 2005 ; Veyron-Churlet, non-publié).

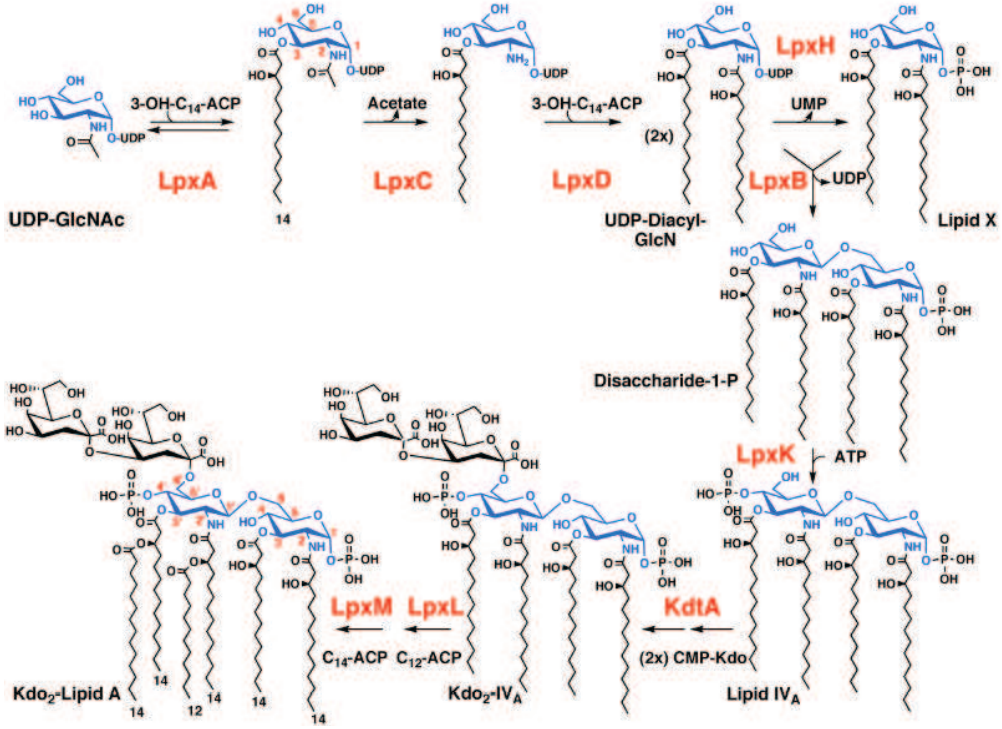

Figure 33: Voie de biosynthèse du Kdo_2-lipid A (Raetz *et al.*, 2007). Le glucosamine disaccharide du lipide A est représenté en bleu et le disaccharide KDO en noir. Le numéros rouges indiquent les positions de l'anneau du glucosamine du lipide A et ses précurseurs. Les numéros noirs indiquent la longueur prédominante des chaînes d'acide gras retrouvés dans le lipide A chez *E. coli*. L'espèce moléculaire montrée en bas à gauche représente environ 90% du lipide A total, le reste contenant majoritairement une chaîne acyle secondaire en position 3'.

IV. LA VOIE DE BIOSYNTHESE DU LIPOPOLYSACCHARIDE

Le LPS est un lipide de membrane externe qui est essentiel à la survie et à la virulence des bactéries à GRAM négatif. Le LPS est composé d'une ancre hydrophobique insérée dans la membrane, le lipide A (endotoxin) un saccharolipide à la base de glucosamine, et d'une extension polysaccharidique (= core qui comprend le disaccharide KDO (2-keto-3-déoxyoctonate) et d'autres saccharides), ainsi que la répétition de l'antigène O (figure 1). Sans l'antigène O, le LPS est nommé 'brut'.

La voie de biosynthèse du lipide A peut être considérée comme ayant une composante conservée et une composante variable : les enzymes de la synthèse du KDO_2-lipide A qui sont conservées et les enzymes de modification du lipide A qui varient d'un organisme à l'autre (Raetz *et al.*, 2007). Dans ce chapitre, nous traiterons brièvement la synthèse du lipide A pour illustrer l'implication des phospholipides dans cette synthèse, ainsi que les différentes modifications du lipide A chez les bactéries à GRAM négatif et leur régulation en fonction des conditions physiologiques.

A. La voie de biosynthèse du KDO_2-lipide A

La synthèse du LPS commence par celle du lipide A à partir d'acides gras ainsi que du précurseur UDP-[N-acétylglucosamine] (GlcNAc). Les neuf enzymes de la voie de biosynthèse constitutive du lipide A (figure 33) sont conservées chez les bactéries à GRAM négatif comme *E. coli* (Raetz & Whitfield, 2002 ; Riley *et al.*, 2006). Les trois premières (LpxA, LpxC and LpxD) sont solubles, tandis que LpxB et LpxH sont des protéines localisées du côté cytoplasmique de la membrane interne. Les quatre dernières enzymes (LpxK, KdtA, LpxL et LpxM) sont des protéines intégrales de la membrane interne. Leurs sites actifs sont situés à la surface cytoplasmique de la membrane interne, puisque leurs co-substrats solubles sont des molécules cytoplasmiques (Raetz *et al.*, 2007).

La première étape d'acylation de l'UDP-GlnNAc est catalysée par l'UDP-GlnNAc acétyltransferase (LpxA). LpxA nécessite un thioester 3-hydroxytétradécanoyl-ACP comme substrat (figure 33) et son site actif incorpore spécifiquement des chaînes d'hydroxyacyl C14. LpxC, l'UDP-3-hydroxymyristoyl N-acétylglucosamine désacétylase, désacétyle ensuite le 3-acyl-UDP-GlnNAc pour former un 3-myritoyl-UDP-glucosamine (3-myristoyl-UDP-GlcN). Après cette déacétylation, une deuxième chaîne de 3-hydroxymyristoyl, utilisant ACP comme donneur, est greffée au 3-myristoyl-UPD-GlcN par LpxD, l'UDP-3-hydroxylmyristoyl glucosamine N-acétyltransférase. Le produit de cette réaction, le dimyristoyl-UDP-GlcN, est hydrolysé par LpxH, l'UDP-2,3-diacylglucos-amine hydrolase, pour former un 2,3-bis(3-

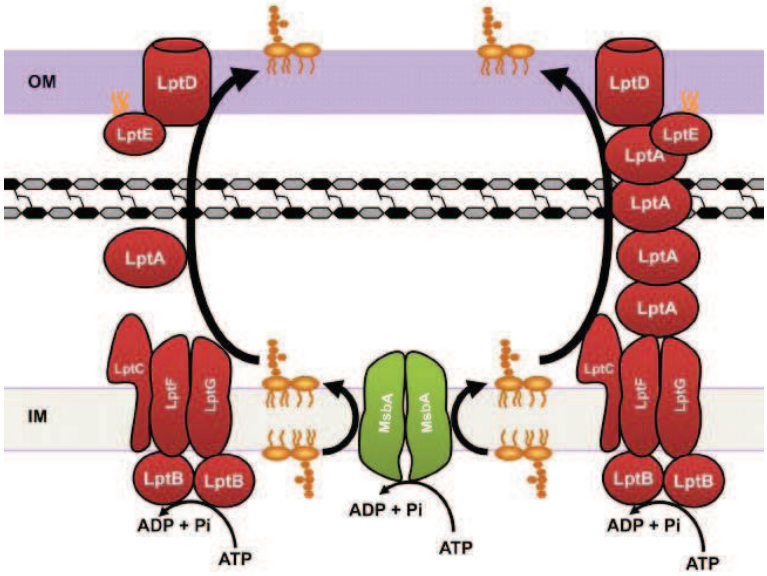

Figure 34: Modèle pour le transport du LPS à travers l'enveloppe (Ruiz *et al.*, 2009). Le LPS brut synthétisé *de novo* est transféré du feuillet interne au feuillet périplasmique par le transporteur ABC MsbA. Si l'antigène O est ajouté, il est ligué à la molécule par WaaL à cette étape (non montré). Ensuite, le LPS brut est extrait de la membrane interne par la protéine LptC et le transporteur ABC LptFGB. Dans le modèle de l'intermédiaire soluble (à gauche), LptA sert de un chaperon périplasmique transportant le LPS vers le site d'assemblage LptDE. Dans le modèle complexe trans-enveloppe (à droite), les facteurs Lpt constituent un complexe multi-protéique qui traverse l'enveloppe. Comme LptA crystalyse en fibre en présence de LPS, il est possible que LptA serve comme un pont entre les deux membranes. Mais il faut noter que seule l'interaction LptD / LptE a été démontrée.

hydromyristoyl)-glucosamine-1-phosphate (diacyl-GlcN-1-P ou lipide X, figure 33). Le diacyl-GlcN-1-P et un dimyristoyl-UDP-GlcN sont ensuite condensés par LpxB, la lipide A disaccharide synthase. Le produit de cette condensation est phosphorylé par LpxK, la tetraacyldisaccharide 4'-kinase pour former un précurseur important, le lipide IV_A. L'enzyme bifonctionnelle KdtA (WaaA) catalyse l'incorporation de deux molécules KDO sur le lipide IV_A. Ce KDO_2-lipide IV_A est de nouveau acylé à deux reprises par LpxL et LpxM, deux acyltransférases qui utilisent ACP comme donneur respectif de dodécanoyle et de myristoyle (figure 33). Il est intéressant de noter que lors de cette synthèse, ACP joue le rôle de donneur de chaîne acyle à six reprises.

B. L'export du LPS synthétisé *de novo*

Tout comme les phospholipides, le LPS synthetisé côté interne de la membrane cytoplasmique doit être transféré à travers l'enveloppe jusqu'à la face externe de la membrane. Il existe un peu plus de donnés sur le transport du LPS que sur celui des phospholipides, mais il n'est pas entièrement compris.

B1. Le transporteur ABC – MsbA

MsbA est une flipase essentielle qui transporte le LPS brut synthétisé *de novo* à travers la membrane interne d'une façon ATP-dépendante (ABC = ATP binding cassette) (figure 34) (Ruiz *et al.*, 2009). Il existe quatre structures cristallographiques de MsbA dans lesquelles elle est capturée dans des conformations différentes supportant son activité flipase (Ward *et al.*, 2007). Dans un mutant thermosensible *msbA*, le LPS brut s'accumule à la membrane interne à température non-permissive et n'est plus accessible à ArnT et EptA qui catalysent des modifications du LPS à la surface périplasmique de la membrane interne (Doerrler *et al.*, 2004). Par ailleurs, des études ont montré que MsbA fixe également des molécules amphipatiques, étant donc en même temps une flipase et un transporteur « multidrug » (Siarheyeva *et al.*, 2010). Bien que le LPS soit essentiel dans les bactéries à GRAM négatif, chez *Neisseria meningitidis* une croissance ralentie est possible sans LPS dans un mutant *msbA* (Tefsen *et al.*, 2005). Ce mutant maintient cependant la capacité d'assembler une membrane externe.

L'antigène O est transporté, lié à undécaprenol phosphate, d'une façon indépendante au LPS brut par la flipase Wzx (Ruiz *et al.*, 2009). Ensuite, à la surface périplasmique de la membrane interne, la ligase WaaL ajoute l'antigène O sur le LPS brut. Dans l'étape suivante,

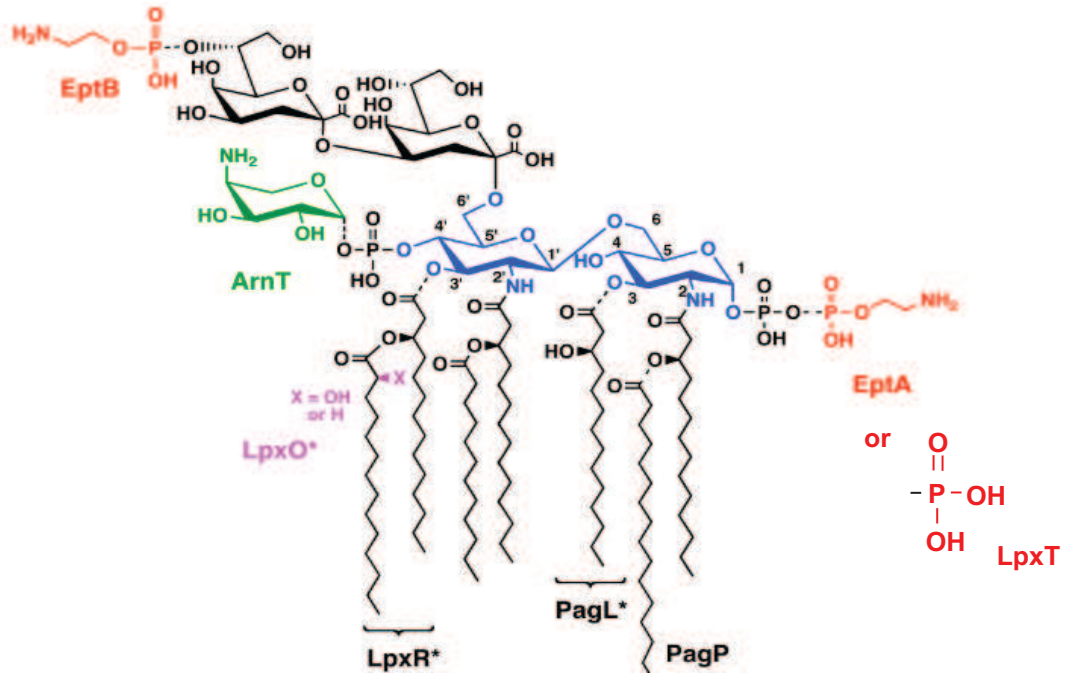

Figure 35: Modifications covalentes du Kdo$_2$-lipide A chez *E. coli* K-12 et *Salmonella* (d'après Raetz *et al.*, 2007; Herrera *et al.*, 2010). Les enzymes de modification du Kdo$_2$-lipide A avec un groupement phosphoethanolamine, 4-amino-4-deoxy-L-arabinose (L-Ara4N) et/ou palmitate sont indiquées respectivement en rouge, vert et noir.
Les enzymes PagL, LpxR et LpxO qui sont marquées avec une étoile (*) ne sont pas présentes chez *E. coli*.

le LPS (ou LPS brut dans le cas des souches *E. coli* K-12) interagit avec la voie Lpt pour être transporté à la membrane externe.

B2. La voie Lpt

Tous les facteurs de la voie Lpt impliqués dans le transport du LPS ont été identifiés et localisés (figure 34) (Ruiz *et al.*, 2009). De ces localisations, un ordre temporel de l'export de LPS a été prédit : MsbA, LptBCFG, LptA, et finalement LptDE. Le LPS est extrait de la membrane interne par LptC et LptFGB, un transporteur ABC. Jusqu'à présent, le mécanisme de la translocation du LPS par LptA à travers le périplasme reste incertain. Il existe deux modèles : un premier modèle décrit LptA comme étant une protéine chaperon soluble du périplasme qui transporte le LPS vers la membrane externe (figure 34 à gauche). Dans un deuxième modèle, qui est soutenu par le fait que LptA cristallise comme filament en présence de LPS, le LPS est transporté le long de quatre monomères LptA qui formeraient un pont entre les membranes interne et externe (figure 34 à droite) (Suits *et al.*, 2008). Finalement, le LPS est assemblé à la membrane externe par le complexe protéique LptDE (Ruiz *et al.*, 2009).

C. Les modifications du lipide A

Les modifications du lipide A existent chez toutes les bactéries à GRAM négatif et sont le mieux étudiées chez *E. coli* K12 et *Salmonella typhimurium*. Ces deux bactéries contiennent des enzymes qui peuvent modifier le lipide A avec des groupements phosphoethanolamine, 4-amino-4-deoxy-L-arabinose (L-Ara4N) ou palmitate (figure 35) (Raetz *et al.*, 2007). Deux déacylases sélectives et une dioxygénase sont en plus présentes chez *S. typhimurium*.

C1. Addition de groupements polaires sur le lipide A

Les gènes codants pour les enzymes qui catalysent l'addition du L-Ara4N sur le lipide A sont organisés dans l'opéron *arn* (*pmr*) (figure 36). Les noms entre parenthèses indiquent les gènes et protéines chez *S. typhimurium*.

La première étape de la biosynthèse du L-Ara4N est catalysée par l'UDP-glucose 6-déhydrogénase Ugd (PmrE) (figure 37) (Raetz *et al.*, 2007). Ensuite, l'UDP acide glucuronique est décarboxylé d'une manière oxydative par le domaine C-terminal de ArnA (PmrI). Le produit de cette réaction UDP-4-ketopentose est transaminé par l'UDP-L-Ara4O-C-4" transaminase, ArnB (PmrH), pour générer l'UDP-L-Ara4N. Ce dernier est ensuite formylé par le domaine N-terminal de ArnA. Seul ce dérivé N-formylé d'UDP-L-Ara4N peut être transféré à l'undécaprenyle phosphate par l'undécaprenyle phosphate-L-Ara4N transférase, ArnC (PmrF). Finalement, la déformylation par ArnD (PmrJ), qui génère 1-undé-

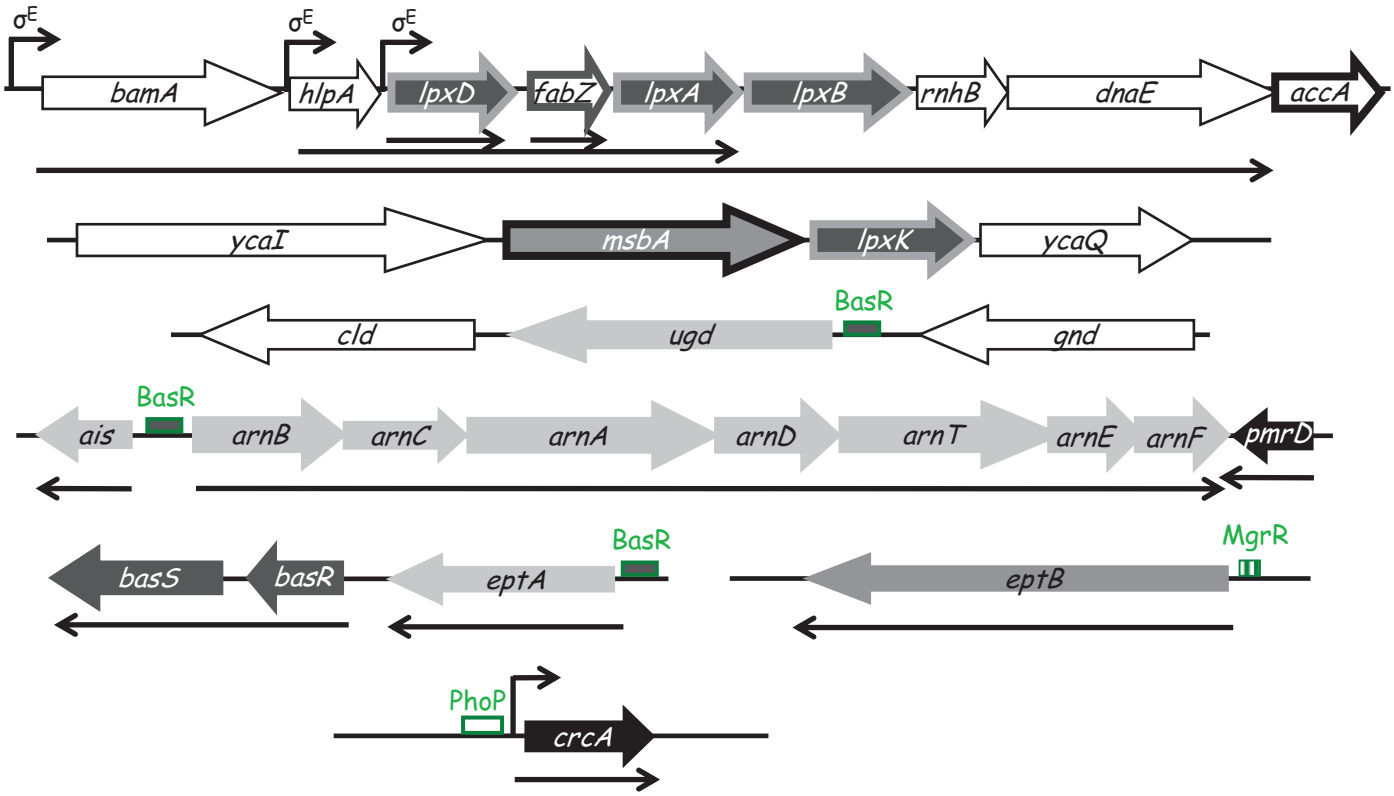

Figure 36: Gènes codants pour les enzymes des modifications covalentes du Kdo_2-lipide A chez *E. coli* K-12. L'organisation des gènes en opérons avec les sites de fixation des activateurs en vert. BasR et PhoP sont les régulateurs des TCS BasRS et PhoPQ (activateurs en vert) (Marchal *et al.*, 2004; Egushi *et al.*, 2004); MgrR est un petit ARN régulateur (Moon & Gottesmann, 2009). Les promoteurs identifiés expérimentalement sont représentés par une flèche. Les unités de transcription sont schématisées au dessous des gènes par des flèches.

caprenyle phosphate L-Ara4N, rend la voie irréversible. Les enzymes ArnE (YfbW) et ArnF (YfbJ) ont été identifiées chez *E. coli* comme étant des sous-unités d'une flipase qui transporterait l'undécaprenyl-phosphate-α-L-Ara4N à travers la membrane interne (Yan *et al.*, 2007). Après le transport de l'undécaprenyle phosphate-L-Ara4N du côté périplasmique de la membrane interne, ArnT (PmrK) transfère le L-Ara4N résidu au groupement 4'-phosphate du lipide A.

Chez *E. coli* et *S. typhimurium*, deux enzymes homologues peuvent greffer un groupement phosphoethanolamine sur le lipide A. Les phosphoethanolamine transférases EptA et EptB sont deux enzymes qui utilisent la PE comme donneur de phosphoethanolamine et le transfert s'effectue à la surface externe de la membrane interne (Lee *et al.*, 2004). Un diacylglycérol est généré comme produit secondaire (Reynolds *et al.*, 2005). EptA transfère le phosphoethanolamine en majorité au niveau du groupement 1-phosphate du lipide A, tandis que EptB le transfère au résidu externe de KDO (figure 35). Dans certaines conditions (concentration basse de Mg^{2+} et/ou pH acide) ou en absence de L-Ara4N, EptA peut modifier la position 4' du lipide A avec un deuxième groupement phosphoethanolamine. D'autres enzymes homologues à Ept sont probablement nécessaires pour transférer le phosphoethanolamine sur d'autres composants de l'enveloppe, comme les OPGs (Miller & Kennedy, 1987). De plus, il a été montré chez *Campylobacter jejuni* qu'une phospho-ethanolamine transférase modifie non seulement le lipide A, mais transfert également un groupement phosphoethanolamine au flagelle pour promouvoir son assemblage et sa motilité (Cullen & Trent, 2010).

Une partie des molécules du lipide A (20-30 %) chez *E. coli* et S. *typhimurium* contiennent un groupement diphosphate en position 1 (non montré) dans certaines conditions de croissance (10 mM Mg^{2+} et pH neutre) (Zhou *et al.*, 2001). Le groupement diphosphate est généré à la surface périplasmique de la membrane interne par LpxT (YeiU), une undécaprenyl pyrophosphatase (Touzé *et al.*, 2008).

La fonction des groupements polaires, comme L-Ara4N chargé positivement à pH 7, est de neutraliser la charge négative du groupement 4'-phosphate du lipide A. De cette manière, la susceptibilité de la bactérie aux peptides antimicrobiens cationiques, comme la polymyxine B, est réduite. Contrairement au groupement L-Ara4N, le rôle de la modification par le groupement phosphoethanolamine reste incertain. La modification avec le groupement diphosphate augmente la charge totale négative de la surface bactérienne (Herrera *et al.*, 2010). Ceci est en contraste avec la fonction de L-Ara4N qui neutralise la charge négative. Le rôle du groupement diphosphate pourrait être de stabiliser et/ou équilibrer les charges

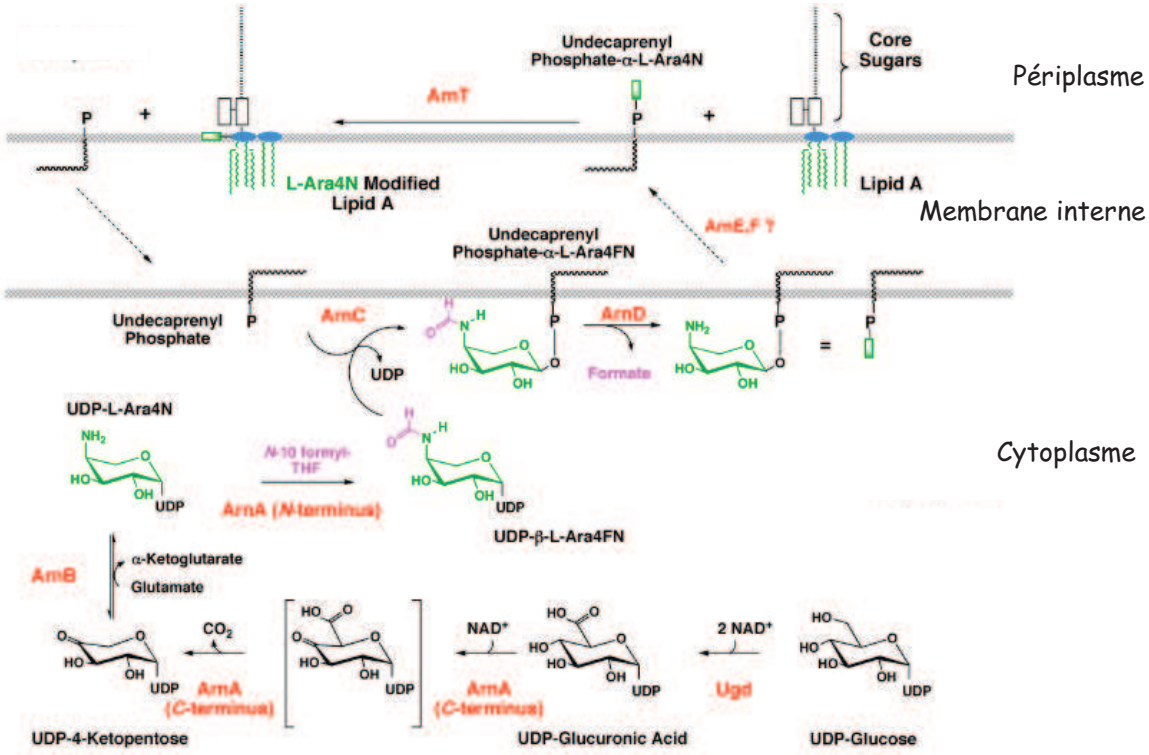

Figure 37: Voie de biosynthèse du L-Ara4N et attachement sur le lipide A (Raetz *et al.*, 2007).
UDP-L-Ara4N en vert; groupement formyle en magenta; groupement L-Ara4N en rectangle vert.

électrostatiques à la surface de la membrane externe en fonction des conditions environnementales.

C2. Modifications du lipide A par des chaînes acyles

PagP transfère un palmitate au lipide A à la surface externe de la membrane externe où elle utilise des phospholipides comme donneurs de palmitoyle (Bishop *et al.*, 2000). L'activité de PagP serait régulée par l'accès des phospholipides. En effet, le site actif de PagP est situé à l'extérieur de la membrane externe, or les phospholipides ne sont pas normalement présents à la surface externe de la membrane externe (Hwang *et al.*, 2002). PagP est structurée en 8 feuillets β formant un tonneau β qui traverse la membrane externe. PagP est capable de distinguer la longueur de la chaîne acyle à un atome de carbone prêt grâce à une « règle d'hydrocarbone » précise qui lui permet de sélectionner de préférence le palmitate pour le transfert au lipide A (Ahn *et al.*, 2004).

S. typhimurium contient des enzymes de modification du lipide A additionnels qui ne sont pas présentes chez *E. coli* (figure 35) : PagL et LpxR sont des lipases de la membrane externe, et LpxO est une hydroxylase de la membrane interne (Gibbons *et al.*, 2000 ; Trent *et al.*, 2001 ; Reynolds *et al.*, 2006). De façon intéressante, lors d'une production de LpxO, LpxR ou PagL chez *E. coli* K-12, des modifications du lipide A identiques à celles *S. typhimurium* sont observées.

D. Régulation de la voie de biosynthèse du LPS

D1. Régulation globale des gènes de la voie de biosynthèse du LPS

La voie de biosynthèse du KDO_2-lipide A est conservée chez les bactéries à GRAM négatif. L'expression des gènes codants pour les enzymes de cette biosynthèse est constitutive, car le LPS est essentiel chez les bactéries à GRAM négatif (Raetz *et al.*, 2007).

A la suite d'un stress extracytoplasmique (σ^E-dépendant), l'expression des gènes responsable de la synthèse *de novo* et l'assemblage des composants de la membrane externe, comme les OMPs, est activée. Ceci a pour but de réparer les mauvais repliements de protéines dans l'enveloppe. De plus, le LPS serait nécessaire pour l'assemblage des OMPs (Missiakas *et al.*, 1996). En effet, la voie de biosynthèse du KDO_2-lipide A est également sujette à une régulation lors d'un stress extracytoplasmique. Trois des neufs gènes organisés en opéron et codants pour les enzymes de cette voie (*lpxA*, *lpxB* et *lpxD*; figure 36) sont sous le contrôle d'un promoteur σ^E (Dartigalongue *et al.*, 2001 ; Rhodius *et al.*, 2006). Plus précisément, trois promoteurs σ^E sont présents dans ce locus : un en amont du gène *bamA*, codant pour une

protéine de la membrane externe, un en amont du gène *hlpA*, codant pour une protéine chaperon, et un en amont du gène *lpxD*. Par ailleurs, cet opéron contient également *fabZ*, un gène impliqué dans la biosynthèse des acides gras.

Il est intéressant de noter que *lpxK* est dans un opéron avec le gène *msbA* codant pour le transporteur ABC impliqué dans le transport du KDO-lipide A à travers la membrane interne (cf. § IV B). Les autres gènes de la voie de biosynthèse du LPS ne sont pas regroupés en opéron ou se situent dans des contextes génétiques non-liés au métabolisme des lipides.

D2. Régulation des gènes de modification du lipide A

Contrairement à la voie de biosynthèse constitutive du LPS brut, les modifications du lipide A sont très variables en fonction des souches (*E. coli* (non-) pathogènes, *S. typhimurium*) et en fonction des conditions de croissance.

1. Rôle des TCSs PhoPQ et BasRS dans la régulation des modifications du LPS

Les TCSs (two-component system) bactériens sont des facteurs clefs de régulation pour l'adaptation de la cellule dans des conditions environnementales variées. Typiquement, ces systèmes sont composés d'une histidine kinase membranaire et d'un régulateur de réponse cytoplasmique (Mascher *et al.*, 2006). La kinase possède souvent une grande boucle externe (localisé dans le périplasme chez les bactéries à GRAM négatif) qui est capable de sentir des signaux environnementaux d'une manière directe ou indirecte. En présence d'un signal, la structure du domaine de phosphorylation cytoplasmique est altérée par un changement conformationnel. Cela provoque l'autophosphorylation de l'histidine conservée de la kinase et ce phosphate est ensuite transféré à un aspartate conservé situé dans le N-terminus du régulateur cytoplasmique. La phosphorylation du régulateur augmente l'affinité pour son site de fixation à l'ADN. Finalement, le régulateur peut également être déphosphorylé par une activité phosphatase du senseur.

Régulons PhoPQ et BasRS (PmrAB)

Les TCSs PhoPQ et PmrAB ont été beaucoup étudiés chez *S. typhimurium* dans le cadre de leur implication dans la resistance à des peptides antimicrobiens. Le TCS PmrAB est nommé BasRS chez *E. coli*. Ces deux TCSs contrôlent l'expression de nombreux gènes de modification du LPS :

Le régulon du TCS BasRS comprend les gènes *anr* (synthèse du L-Ara4N), ainsi qu'*ugd* et *eptA* (Wösten & Groisman, 1999). Les gènes de la synthèse du L-Ara4N sont organisés dans l'opéron *arn* avec *ais* (*pmrG*) en amont et *pmrD* en aval (figure 36). Seul le

A)

ugd	(*S. typhimurium*)	CTTAAT ATTAA CTTAAT
pmrC	(*S. typhimurium*)	CTTAAG GTTCA CTTAAT
pmrC	(*E. coli*)	CTTAAG GTTGG CTTAAT
pmrH	(*S. typhimurium*)	CTTAAT GTTAA TTTAAT
pmrH	(*E. coli*)	CTTAAG GTTAA GTTAAT
pmrH	(*Y. pestis*)	CCTAAG GTTCA TTTAAG
pmrD	(*S. typhimurium*)	ATTAAT GTTAG GTTAAT
mig-13	(*S. typhimurium*)	CTTTAA GGTTA ATTTAA
mig-13	(*E. coli*)	CTTTAA GTTTT ATTTAA
STM1269	(*S. typhimurium*)	CTTAAT GTTAT CTTAAT
yibD	(*S. typhimurium*)	CTTAAT AGTTT CTTAAT
sseJ	(*S. typhimurium*)	CTTAAG AAATA TTTAAT

B)

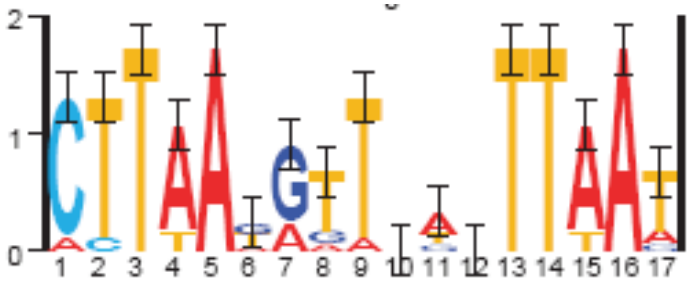

Figure 38: Régulon et motif consensus de PmrA (BasR) déterminé chez *Salmonella (*Marchal *et al.*, 2004). (A) Alignement des séquences du site de fixation de PmrA vérifiés expérimentalement chez *S. typhimurium*. Les séquences des orthologues de *E. coli* et *Yersinia pestis* sont représentées également. **(B)** Motif du site de fixation de PmrA adapté sur la base des 12 séquences représentées en (A).

gène *ugd* (*pmrE*) n'est pas localisé dans ce même locus. *eptA* (*pmrC*) est le premier gène dans un opéron avec les gènes *basRbasS* codant pour le TCS BasRS. Dans une approche *in silico* suivie d'une validation expérimentale dans *S. typhimurium* et d'autres souches apparentées, un motif consensus de fixation du régulateur PmrA/BasR a été décrit (figure 38) (Marchal *et al.*, 2004).

Le TCS PhoPQ régule le gène *crcA* (*pagP*) (figure 36) qui code pour l'enzyme CrcA (PagP) responsable du transfert d'un palmitate sur le lipide A. *crcA* (*pagP*) n'est donc ni sous le contrôle de PmrAB ni de RpoE, contrairement à la majorité des gènes de modifications du lipide A. PhoPQ contrôle de plus chez *S. typhimurium* les gènes *pagL* et *lpxR* impliqués comme *pagP* dans les modifications palmitate du lipide A (figure 35) et le gène *pmrD* qui active le TCS PmrAB (Gunn, 2008).

Mécanismes d'activation

PhoQ forme un dimer et est un senseur typique qui possède une grande boucle périplasmique (145 acides aminés; figure 39B) (Cheung *et al.*, 2008). La surface du domaine senseur de cette boucle périplasmique est chargée négativement, tout comme la membrane et donc, le cation Mg^{2+} peut s'intercaler entre ce domaine de PhoQ et la membrane interne et stabiliser ainsi le senseur (figure 40A) (Hancock & McPhee, 2005). En absence de Mg^{2+} ou en présence de Mg^{2+} et des peptides cationiques (figure 40B et C), PhoQ est déstabilisé et s'autophosphoryle (Bader *et al.*, 2005). Ensuite, PhoP est phosphorylé par PhoQ ce qui active le régulon PhoPQ.

PmrB est un senseur atypique qui possède une boucle périplasmique plus petite que PhoQ (30 acides aminés; figure 39A) (Perez & Groisman, 2007). La boucle périplasmique de PmrB possède 9 résidus conservés. Parmi ces 9 résidus, 4 glutamates forment deux motifs ExxE de fixation de Fe^{2+} (figure 39C) (Wösten *et al.*, 2000) qui pourraient également fixer d'autres cations, comme Al^{3+} ou Zn^{2+}. De plus, une histidine et ces quatre glutamates sont importants pour sentir le pH extracytoplasmique (Perez & Groisman, 2007). En effet, la substitution de l'histidine et de chacun des 4 glutamates abolit la réponse au pH acide et à Fe^{2+} de PmrB (Perez & Groisman, 2007). Le mécanisme d'activation n'est pas compris entièrement, mais ces résultats suggèrent que la protonation de l'histidine et/ou des glutamates périplasmiques activerait PmrB. Les résidus cruciaux pour sentir le pH et les métaux cationiques sont conservés chez *E. coli* et *S. typhimurium* (figure 39C), on peut donc considérer le même mécanisme pour *E. coli* où la réponse au pH est indépendante d'une réponse PhoPQ-dépendante.

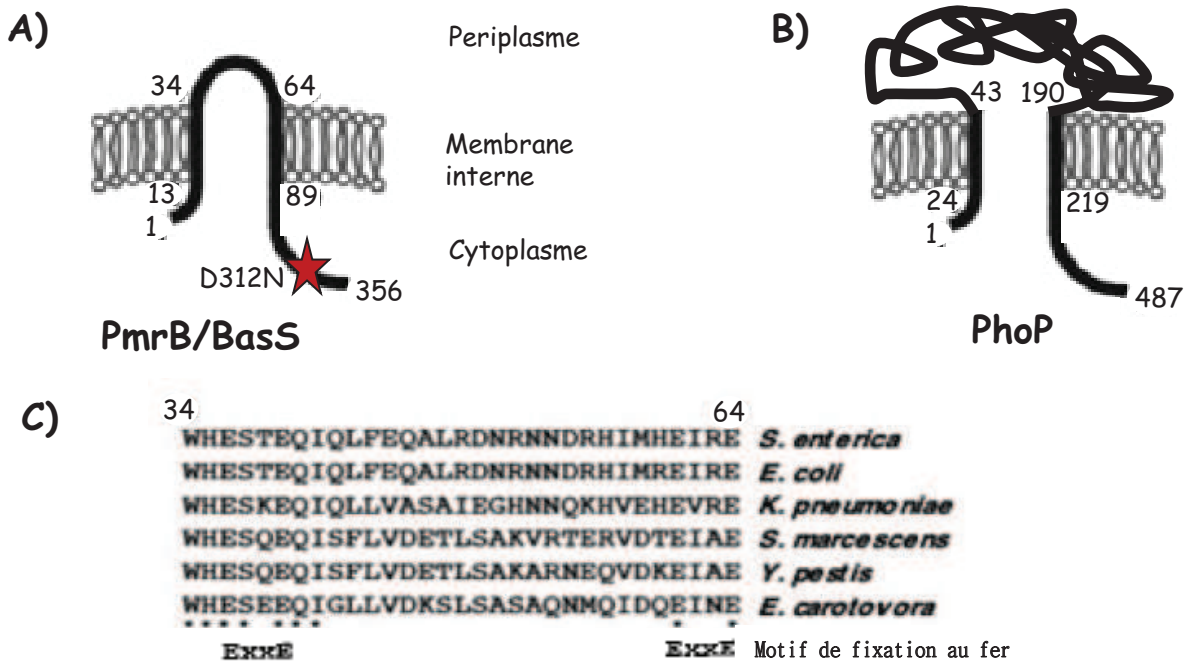

Figure 39: Les TCSs PmrAB/BasRS et PhoPQ (Perez & Groisman, 2006; Cheung *et al.*, 2008). A) Topologie prédite de PmrB. Le senseur atypique PmrB possède une petite boucle périplasmique (30 acides aminés). L'étoile rouge indique la mutation ponctuelle d'une asparagine en une aspartat au résidu 312 du mutant '*dgkR*' (Raetz *et al.*, 1981) **B)** Le senseur typique PhoQ possède une grande boucle (145 acides aminés) périplasmique. La surface du domaine senseur de cette boucle périplasmique est chargée négativement. **C)** La boucle périplasmique de PmrB possède 9 résidus conservés. Parmi ces 9 résidus, 4 glutamates forment deux motifs ExxE de fixation de Fe^{2+} qui pourraient également être responsables de la fixation d'autres cations, comme Al^{3+} ou Zn^{2+}. De plus, une histidine et quatre glutamates sont importants pour sentir le pH extracytoplasmique.

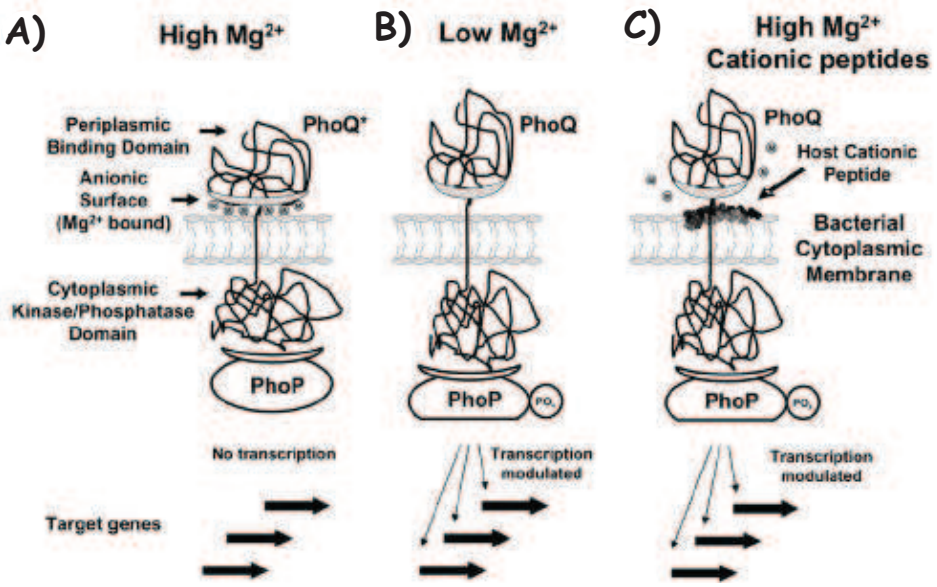

Figure 40: Activation du TCS PhoPQ chez *Salmonella* (Hancock & McPhee, 2005). A) En présence de Mg^{2+} à forte concentration, le cation divalent forme un pont entre les phospholipides chargés négativement du feuillet externe de la membrane interne et la surface anionique du domaine de fixation de PhoQ. PhoP reste déphosphorylé et donc inactif. **B)** À basse concentration en cations divalents, la conformation de PhoQ se modifie, ce qui active le domaine kinase cytoplasmique. Ensuite, PhoP phosphorylé se fixe sur l'ADN et modifie la transcription des gènes de son régulon. **C)** Des peptides antimicrobiens cationiques de l'hôte traversent la membrane externe de la bactérie et se fixent au domaine anionique de PhoQ (remplaçant Mg^{2+}, si sa concentration est importante) ce qui résulte en une activation de l'activité kinase.

Chez *S. typhimurium*, PhoP active également le TCS PmrAB de façon indirecte. En effet, PhoPQ active le gène *pmrD* et la protéine PmrD active le TCS PmrAB d'une manière post-transcriptionnelle (Kato & Groisman, 2004). PmrD se lie à la forme phosphorylée de PmrA et empêcherait ainsi sa déphosphorylation par PmrB (Kato & Groisman, 2004). Ceci déclenche alors la transcription des gènes PmrA-dépendant chez *S. typhimurium*. C'est le premier exemple d'une protéine qui permet à un TCS de répondre au signal gouvernant un autre TCS en protégeant l'état phosphorylé du régulateur. Mais la phosphorylation initiale de PmrA par PmrB est toujours nécessaire pour son activation (Perez & Groisman, 2007).

Chez *E. coli*, la protéine PmrD est présente, mais elle n'interagit pas avec BasR (Winfield & Groisman, 2004). Les protéines PmrD présentes chez *E. coli* et *S. typhimurium*, possèdent seulement 55 % d'identité de séquence, ce qui est rare pour des homologues de ces espèces très proches. Ceci suggére que ces deux protéines ont évolué différemment dû aux niches écologiques distinctes des deux bactéries (Winfield & Groisman, 2004). Il est intéressant de noter que *Citrobacter rodentrium*, une autre entérobactérie, ne possède pas le gène *pmrD* (Bader *et al.*, 2005). De façon intéressante, chez ces entérobactéries assez proches phylogénétiquement, une grande diversité de régulation des modifications du LPS est donc présente.

Réponses PhoPQ- et BasRS-dépendantes aux différents signaux physiologiques

Chez *S. typhimurium*, PhoPQ répond aux peptides antimicrobiens (Bader *et al.*, 2005). Ces peptides cationiques font partie d'une immunité innée et sont conservés chez les eucaryotes, comme les plantes et mammifères (Hancock & Diamond, 2000 ; Ganz, 2003). Ils sont très différents en séquence, mais possèdent des caractéristiques structurales en commun : ces molécules amphipatiques ont une charge nette positive qui leur permet d'interagir avec des membranes des bactéries chargées négativement pour les perméabiliser et causer la lyse cellulaire (Dathe & Wieprecht, 1999). Par ailleurs, plusieurs signaux physiologiques ont été identifiés dont le point commun est de posséder des charges positives et de pouvoir interagir avec des phospholipides anioniques (charges négatives) de la membrane. Le but de la bactérie est donc d'empêcher une interaction de la membrane avec des peptides antimicrobiens en neutralisant la charge nette de la membrane. Le nom des gènes de l'opéron *pmr* chez *S. typhimurium* provient de leur implication dans la résistance à la polymyxine, un de ces peptides antimicrobiens. La présence des peptides antimicrobiens provoque donc l'activation du TCS PhoPQ, ainsi que celle du TCS PmrAB dans le cas de *S. typhimurium* (Kato & Groisman, 2004), ce qui conduit à une décoration du lipide A par des modifications neutralisant la charge totale de la membrane.

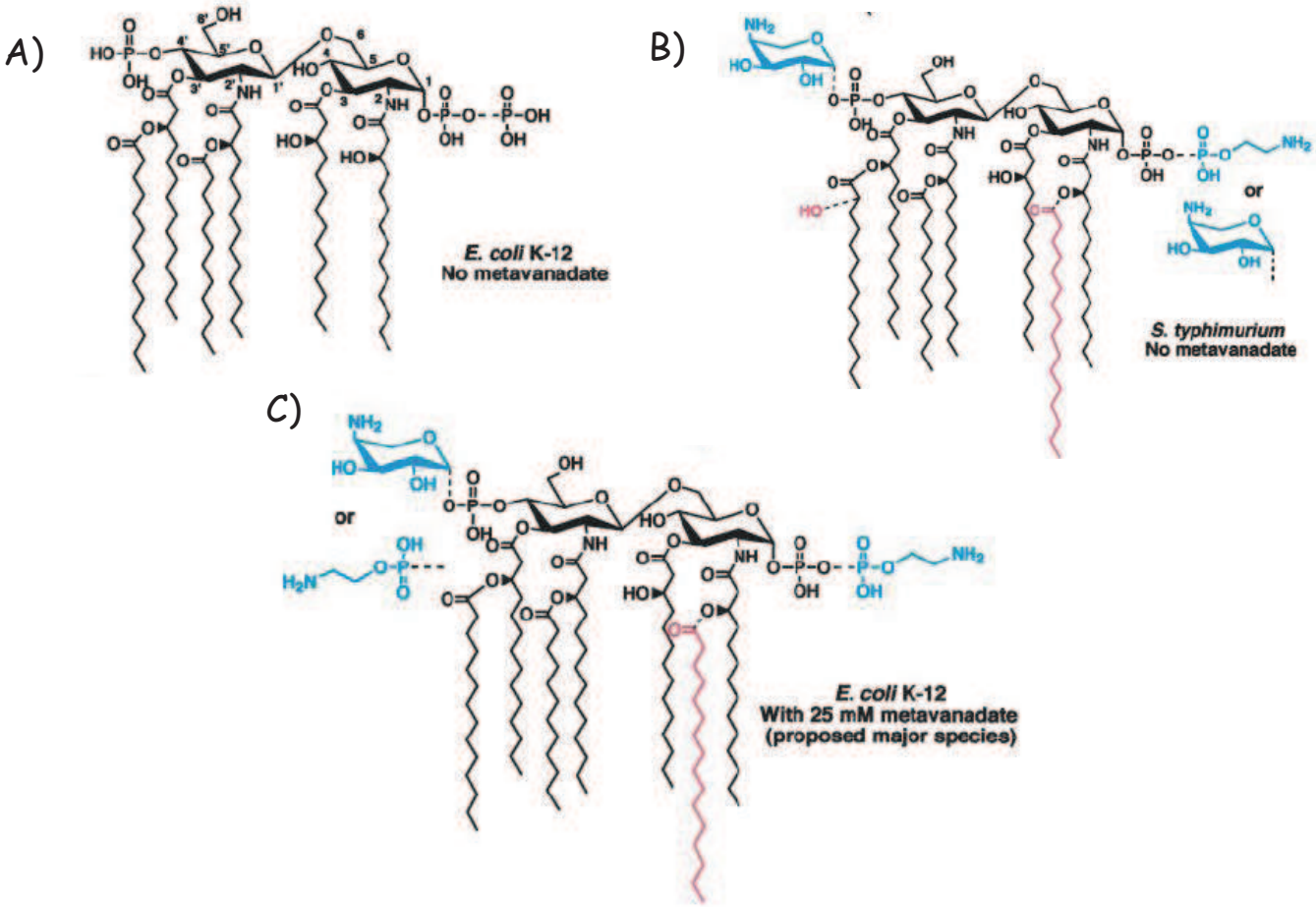

Figure 41: Structures du lipide A retrouvées chez *E. coli* K-12 et *S. typhimurium* (Zhou *et al.*,1999). A) Environ 2/3 du lipide A chez *E. coli* en conditions normales de croissance dans du LB est le 1,4'-bis-phosphate hexa-acylé. Le reste est une espèce contenant du 1-pyrophosphate (pointillé). **B)** Quand *S. typhimurium* croît en LB, le lipide A est beaucoup décoré seul ou en combinaison avec les quatre composants indiqués en pointillé. Les groupements palmitoyl et S-2-OH sont représentés en rouge; les groupements L-Ara4N et phosphoethanolamine sont représentés en bleu. **C)** En présence de NH_4VO_3 (25 mM) les modifications retrouvées chez *E. coli* K12 sont globalement les mêmes que celles produites par *S. typhimurium*, sauf que le S-2-OH n'est pas détecté.

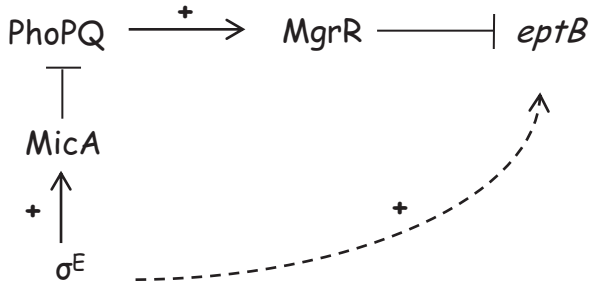

Figure 42: Activation de *eptB* par σ^E via le TCS PhoPQ. Le TCS PhoPQ inhibe l'expression du gène *eptB* via l'activation du petit ARN non-codant MgrR (Moon & Gottesmann, 2009). Le facteur sigma alternatif σ^E inhibe le TCS PhoPQ via l'activation du petit ARN MicA (Coornaert *et al.*, 2010). σ^E active donc de façon indirecte l'expression de *eptB* (flèche en pointillé).

Chez *S. typhimurium*, PhoPQ est induit également par des faibles concentrations de Mg^{2+} (10 µM), ce qui reflète les conditions dans les macrophages de l'hôte (Soncini & Groisman, 1996). Chez *S. typhimurium*, la biosynthèse de L-Ara4N est induite dans un milieu carencé en Mg^{2+} indépendamment du pH, tandis que chez *E. coli* BasRS répond à des concentrations basses de Mg^{2+} comme stimulus pour la décoration par L-Ara4N (operon *arn*), mais seulement dans un milieu acide (Gibbons *et al.*, 2005). Il semble donc que BasRS réponde plutôt au pH acide et pas à la concentration de Mg^{2+}, ce qui est soutenu par le fait que BasS possède un motif senseur pour le pH.

Une étude transcriptomique chez *E. coli* à montré que la présence de $FeSO_4$ (200-400 µM) induit l'operon *arn* (Hagiwara *et al.*, 2004), ce qui a été confirmé par des fusions transcriptionnelles (Froelich *et al.*, 2006). De la même façon, il a été montré que la présence de $ZnSO_4$ (200 µM) active l'induction BasR-dépendante de l'opéron *arn* et de *eptA* (Lee *et al.*, 2005) et en conséquence induit la biosynthèse de L-Ara4N chez *E. coli*.

Des concentrations élevées d'ammonium metavanadate (NH_4VO_3; 25 mM) qui n'affecte pas la croissance induisent les modifications du lipide A chez *E. coli*, qui ressemblent à celles présentes naturellement sur le lipide A de *S. typhimurium* (figure 41) (Zhou *et al.*, 1999). Le mécanisme d'activation n'est pas compris, mais il est connu que le NH_4VO_3 est un inhibiteur aspécifique des phosphatases (Zhou *et al.*, 1999). Le NH_4VO_3 pourrait donc inhiber l'activité phosphatase de BasS, ce qui maintiendrait BasR active en empêchant sa déphosphorylation.

2. Régulation de eptB par RpoE et MgrR

L'expression du gène *eptB* codant pour la phosphoethanolamine transférase est activée par le facteur sigma alternatif RpoE (Figueroa-Bossi *et al.*, 2006). Cependant, la séquence promotrice du gène *eptB* ne contient pas le consensus pour un promoteur σ^E (figure 36) (Rhodius *et al.*, 2006), ce qui suggère une régulation indirecte.

Le petit ARN (acide ribonucléotide) non-codant MgrG est activé par PhoPQ chez *E. coli* et inhibe l'expression de *eptB* dont la séquence promotrice contient une séquence d'appariement de MgrR (figure 36) (Moon & Gottesman, 2009). En conséquence, *eptB* est inhibé de façon indirecte par PhoPQ via MgrR. De plus, il a été démontré que σ^E activerait le petit ARN non-codant MicA qui inhibe le TCS PhoPQ (Coornaert *et al.*, 2010). Donc, le facteur sigma alternatif σ^E active *eptB* de façon indirecte via le TCS PhoPQ et les petits ARN non-codants MicA et MgrR (figure 42).

Dans ce contexte, il est intéressant de noter que le TCS BasRS active le géne *eptA*, codant pour l'homologue de EptB. EptB transfère un groupement phosphoethanolamine au résidu externe de KDO, tandis que EptA au groupement 1-phosphate du lipide A (figure 35) (Raetz *et al.*, 2007). Ces modifications aux différentes positions pourraient influer sur les propriétés du lipide A et ceci pourraient expliquer leur régulation génétique dans différentes réponses au stress.

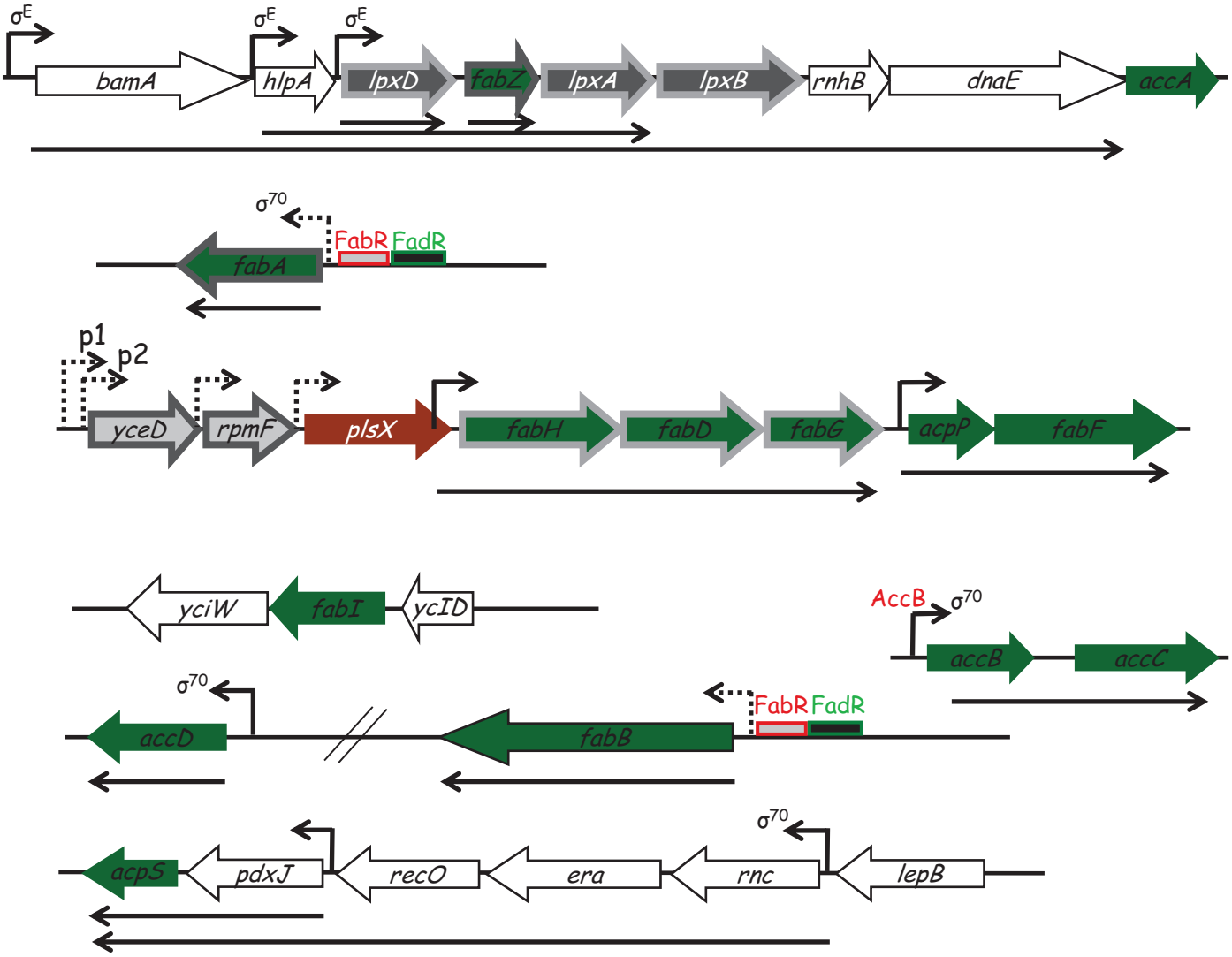

Figure 43: Organisation chromosomique des gènes de la biogenèse des acides gras (Tanaka *et al.*, 1989; Podkovyrov *et al.*, 1996; Zhang & Cronan. 1996). Les sites de fixation des régulateurs FabR et FadR sont indiqués en rouge et vert. Les promoteurs identifiés expérimentalement sont représentés par une flèche et les promoteurs potentiels sont représentés par une flèche pointillée. Les unités de transcription sont schématisées au dessous des gènes par des flèches.

V. REGULATION DU METABOLISME DES LIPIDES CHEZ *E. COLI*

La composition en acides gras des lipides membranaires est sujette à une régulation fine en réponse à des variations environnementales, comme la température, dans le but de maintenir une fluidité de la membrane. En revanche, la composition en phospholipides reste relativement stable (DiRusso & Nyström, 1998). La régulation du métabolisme des lipides implique donc une régulation coordonnée des voies de biosynthèses des acides gras et des phospholipides en fonction du taux de la croissance et en réponse à des changements dans le milieu extérieur.

A. Organisation des gènes codants pour les enzymes du métabolisme des lipides

Le cluster *fab* est formé des sept gènes *rpmF*, *plsX*, *fabH*, *fabD*, *fabG*, *acpP* et *fabF* (figure 43). *rpmF*, premier gène de l'opéron code pour la protéine ribosomale RpmF et *plsX* code pour la protéine PlsX qui catalyse avec PlsY la première acylation du G3P de la voie de synthèse des phospholipides. Ce lien génétique entre des gènes de la biogenèse des lipides et un gène codant pour une protéine ribosomale suggére une régulation coordonnée (Podkovyrov & Larson, 1995). L'expression des gènes de l'opéron *fab* est complexe. Aucun transcrit correspondant à la totalité des gènes de l'opéron n'a pu être mis en évidence jusqu'à présent. Des expériences de mutagenèse, de protection à la RNAse et des Northern blot ont permis de localiser cinq promoteurs potentiels contrôlant l'expression des gènes de cet opéron (Podkovyrov & Larson, 1996 ; Zhang & Cronan, 1998) (figure 43). Les gènes de l'opéron *fab* sont exprimés à partir d'une série de transcrits chevauchants où chaque gène est transcrit avec au moins un autre gène de l'opéron (Zhang & Cronan, 1996). De plus, le gène *yceD*, en amont de l'opéron *fab*, codant pour une protéine conservée de fonction inconnue, possède deux promoteurs (p1 et p2) et est co-transcrit avec *rpmF* (Tanaka *et al.*, 1989). Le promoteur qui contrôle la transcription d'*acpP* et *fabF* est suffisant pour la transcription forte nécessaire à la synthèse du pool de ACP dans la cellule (Zhang & Cronan, 1996). La quantité de promoteurs présents ainsi que la variété des transcrits possibles laisse imaginer l'importance et la complexité de la régulation de cet opéron.

En ce qui conserne les gènes codant pour la dégradation des acides gras par β-oxydation aérobie et anaérobie, les gènes *fadBA* et leurs homologues de la β-oxydation anaérobie *fadIJ* sont transcrits en opéron (Yang *et al.*, 1991; Bradley *et al.*, 2007). En revanche, les gènes *fadE* et *fadD*, *fadK*, *ydiO*, *fadM* et *fadH* sont isolés sur chromosome de *E. coli*.

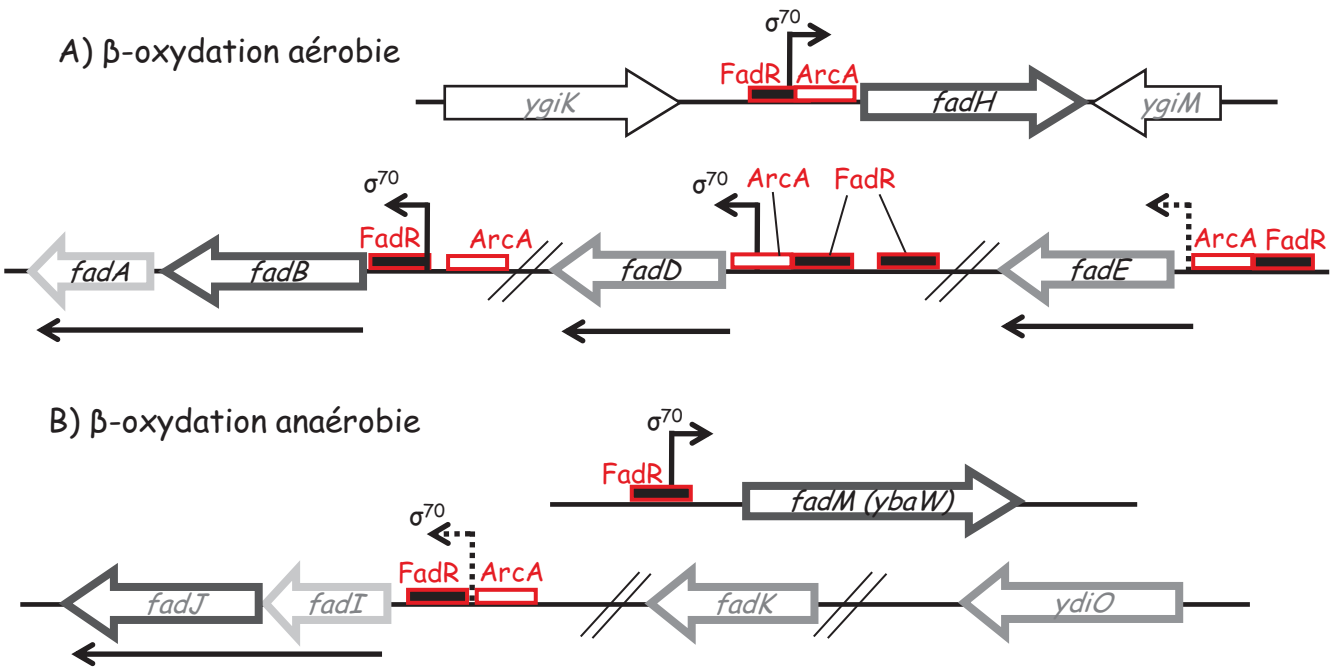

Figure 44: Organisation des gènes de la β-oxydation aérobie (A) et anaérobie (B) (Yang *et al.*, 1991; DiRusso *et al.*, 1999; Campbell *et al.*, 2003). En rouge: inhibiteur; en vert: activateur. FadR: Régulateur de la dégradation des acides gras (Black *et al.*, 1992); ArcA: Régulateur du système à deux composants ArcAB (Cho *et al.*, 2006). Les promoteurs identifiés expérimentalement sont représentés par une flèche et les promoteurs potentiels sont représentés par une flèche pointillée. Les unités de transcription sont schématisées au dessous des gènes par des flèches.

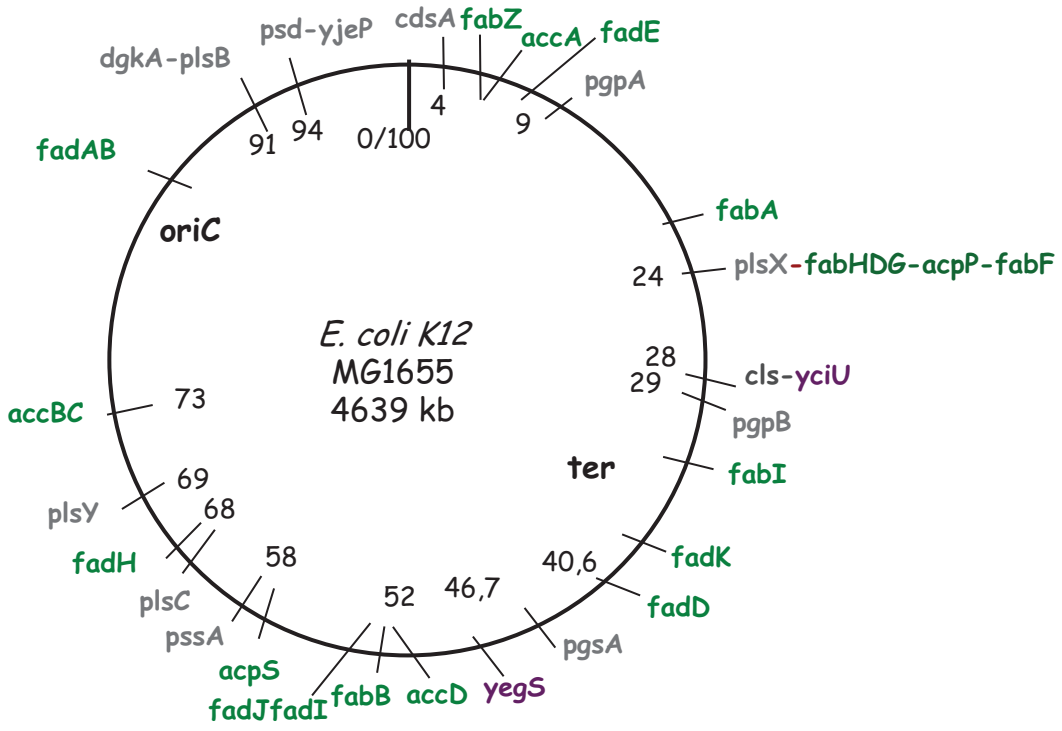

Figure 45: Organisation génétique des gènes codants pour les enzymes du métabolisme des acides gras et des phospholipides chez *E. coli* K-12. Les chiffres indiquent la position des gènes en minutes sur le chromosome de *E. coli*.

Les gènes codants pour la biosynthèse des phospholipides sont dispersés sur le chromosome de *E. coli* (figure 45), mis à part : *plsX*, *plsB* et *dgkA*. *plsX* fait partie de l'opéron *fab* et *plsB* est organisé d'une manière divergente avec *dgkA* sur le chromosome.

Comme les gènes de la synthèse des phospholipides sont dispersés sur le chromosome bactérien, la question se pose de savoir comment tous ces gènes sont régulés de façon coordonnée, cruciale pour l'homéostasie lipidique de l'enveloppe. De plus, s'agit-il d'une régulation génétique et/ou également enzymatique? On connait bien les mécanismes de régulation génétique de dégradation des acides gras, mais étonnamment très peu sur les voies de biosynthèse *de novo* des acides gras et des phospholipides.

B. Régulation transcriptionnelle des gènes du métabolisme des lipides

B1. Les régulateurs du métabolisme des acides gras: FadR et FabR

Le gène *fadR* (Fatty Acid Degradation Repressor) a d'abord été décrit comme un répresseur de la dégradation des acides gras et de l'import des acides gras exogènes (Overath *et al.*, 1969). De plus, FadR est en même temps un activateur de la biosynthèse des acides gras insaturés (Nunn *et al.*, 1983). Des domaines de fixation du régulateur de réponse FadR sont en effet présents en amont des gènes *fadD*, *fadE*, *fadBA*, *fadH*, *fadM*, *fadIJ* et *fadL* permettant la β-oxydation aérobie ainsi qu'en amont des gènes *fabA* et *fabB* permettant la biosynthèse *de novo* des acides gras insaturés (figures 43 et 44). En absence d'acides gras à longue chaîne (≥ C12) dans le milieu, FadR se lie sur ces domaines ce qui réprime l'expression de la transcription des gènes *fad* et active l'expression des gènes *fabA* et *fabB* (figure 46A) (van Aalten *et al.*, 2000). En revanche, en présence d'acides gras à longue chaîne, les acides gras sont convertis en thioester d'acyl-CoA qui se fixent sur FadR. Le complexe FadR-acyl-CoA se dissocie des promoteurs et la transcription des gènes *fad* est activée, tandis que la transcription de *fabA* et *fabB* est réprimée. C'est la position du site de fixation de FadR dans le promoteur du gène cible qui détermine si FadR est activateur ou répresseur. En effet, le domaine de fixation de FadR est localisé dans la région -40 du promoteur de *fabA* pour lequel FadR est activateur (figure 47B) (Cronan *et al.*, 1988 ; Henry & Cronan, 1992). En revanche, le site de fixation de FadR se situe respectivement en +9 et -17 des gènes *fadBA* et *fadL*, sur lesquels FadR agit comme répresseur (figure 47B).

De la même façon, FadR inhibe la transcription des gènes *fadIJ* dans des conditions aérobie. En revanche, la transcription du gène *fadK* ne semble pas être dépendante de FadR (Campbell *et al.*, 2003 ; Morgan-Kiss & Cronan, 2004).

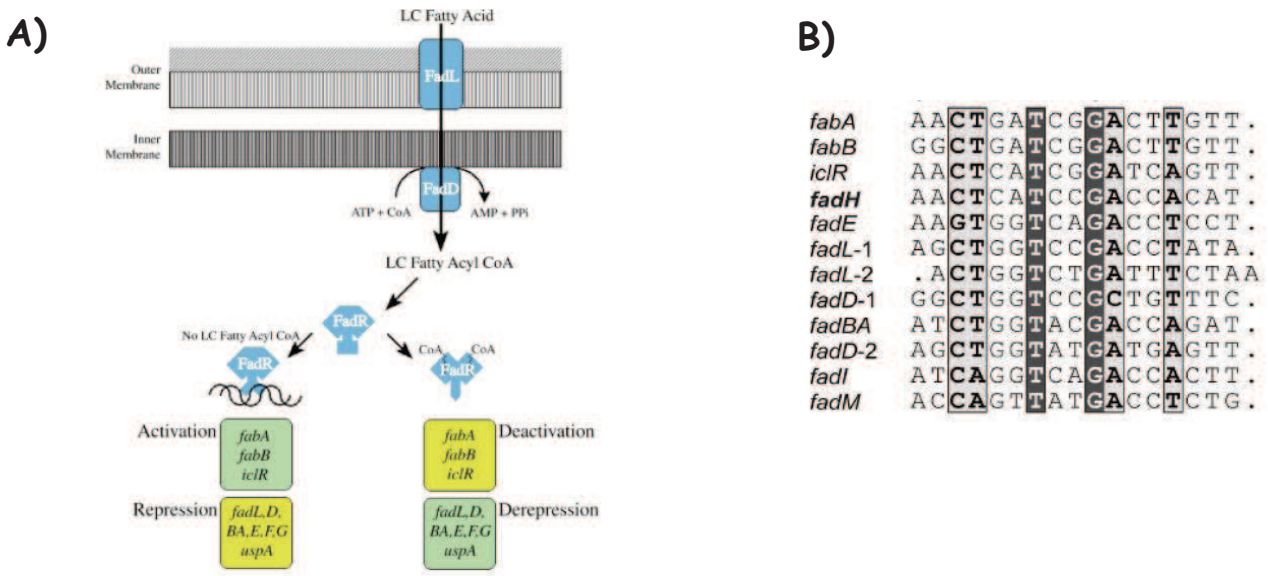

Figure 46: Régulation de la dégradation des acides gras par FadR (vanAalten *et al.*, 2000). A) Les protéines impliquées dans l'import et l'activation des acides gras sont colorées en bleu. Des gènes activés sont représentés en vert et des gènes inhibés sont représentés en jaune. LC fatty acid: acide gras à longue chaîne. **B**) Alignement des séquences du site de fixation de FadR déterminé chez *E. coli* (Feng & Cronan, 2010). Les lettres blanches avec un fond noir dans la séquence du consensus motif indiquent les nucléotides qui sont conservés à 100 %, tandis que les lettres noires avec un fond gris indiquent les nucléotides qui sont conservés.

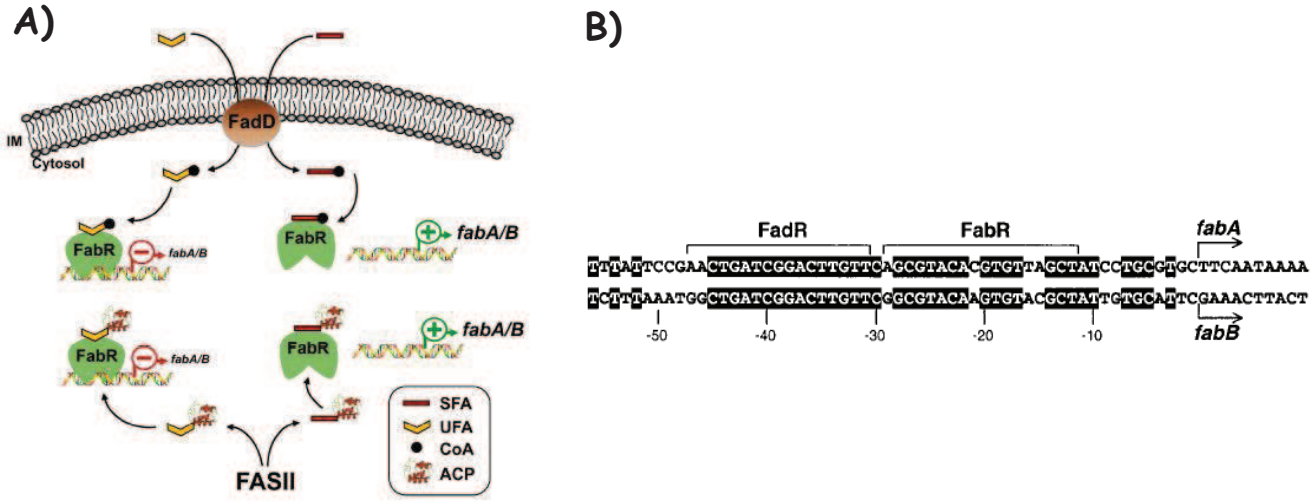

Figure 47: Régulation de la synthèse des acides gras insaturés par FabR et FadR (Zhang et *al.*, 2002; Zhu *et al.*, 2009). A) *fabB* et *fabA* sont responsables de la synthèse des acides gras insaturés (UFA: unsaturated fatty acid).Le répresseur FabR possède deux conformations: l'une se fixe avec une affinité faible à l'ADN, tandis que l'autre conformation a une forte affinité pour son palindrome de fixation sur l'ADN localisé dans les promoteurs de *fabB* et *fabA*. FabR se lie au pool entier des acyl-ACPs à longue chaîne étant produits par le FASII et /ou aux acyl-CoAs venant des acides gras exogènes. Des thioesters d'acides gras saturés (SFA: saturated fatty acid) maintiennent FabR dans la forme de faible affinité pour l'ADN ce qui permet une transcription élevée de *fabA* et *fabB*. Des thioesters d'UFAs au contraire stabilisent la conformation de FabR de forte affinité pour l'ADN ce qui résulte en la répression de *fabA* et *fabB*. FabR permet donc de détecter les pools des thioesters d'acyl-ACP et d'acyl-CoA qui sont disponibles pour la glycérophospholipide acyltransférase (PlsB) et module en conséquence l'expression des gènes *fabB* et *fabA* pour équilibrer le ratio UFA:SFA des chaînes acyles produites par le FASII. **B)** Les séquences des régions promotrices des *fabA* et *fabB* sont très similaires. Le +1 de transcription est indiqué par une flèche. Les sites de fixation de FadR et FabR sont indiqués par les parenthèses.

FabR (Fatty Acid Biosynthesis Repressor) est un deuxième régulateur transcriptionnel de la biosynthèse des acides gras. En présence d'acides gras insaturés, FabR réprime *fabA* et *fabB* qui sont essentiels à la formation des acides gras insaturés (figure 47A) (Zhu *et al.*, 2009). Le site de fixation de FabR est en aval du site de fixation de FadR sur les deux promoteurs de *fabA* et *fabB* (figure 47B).

Pour conclure, les régulateurs FadR et FabR assurent une régulation orchestrée de la dégradation des acides gras et de la biosynthèse des acides gras insaturés en fonction de la présence d'acides gras à longue chaîne (in-)saturés dans le milieu extérieur. Grâce à la régulation coordonnée de *fabAB*, une composition équilibrée des acides gras est présente pour l'incorporation au niveau des phospholipides *via* les acyltransferases PlsB et PlsC (cf. § IIB) et pour finalement maintenir l'homéostasie membranaire. En revanche, jusqu'à présent FadR et FabR n'ont pas d'action décrite sur la biosynthèse des acides gras saturés ou des phospholipides.

B2. Le TCS ArcAB

Le TCS ArcAB joue un rôle essentiel dans la régulation de nombreux gènes impliqués dans le métabolisme anaérobie (Liu & De Wulf, 2004). En effet, ArcA est également un répresseur global du cycle du citrate, du shunt du glyoxylate et de la phosphorylation oxydative dans des conditions anaérobies afin de mettre en place le métabolisme anaérobie. En présence d'oxygène, ArcAB est inactivé par un potentiel redox élevé, tandis qu'en absence d'oxygène, le senseur ArcB active le régulateur ArcA (Liu & De Wulf, 2004).

Le régulon *fad* est réprimé par ArcA (Cho *et al.*, 2006 ; Feng & Cronan, 2010). En présence d'oxygène (ArcA inactif), le régulon *fad* est uniquement sous le contrôle de FadR. En absence d'oxygène, les gènes de la β-oxydation aérobie des acides gras sont donc inhibés par ArcA et la β-oxydation anaérobie des acides gras se met en place. Mais en même temps, FadR reste actif en absence des acides gras à longue chaîne dans les conditions anaérobies (Cronan, 1997). Récemment, il a été trouvé que *fadH* est réprimé par FadR et ArcA de façon additive et il a été proposé que cela est dû au fait fait que les sites de fixation de FadR et ArcA se chevauchent (Feng & Cronan, 2010). Pour l'expression des gènes *fadBA* en revanche, la répression de FadR et ArcA semble synergétique et cela serait dû au fait que leurs sites de fixation sont séparés par 42 pb (Feng & Cronan, 2010). Le TCS ArcAB et FadR contrôlent donc de façon coordonnée la mise en place des systèmes de β-oxydation, mais d'autres régulateurs globales comme l'AMP cyclique interviennent également.

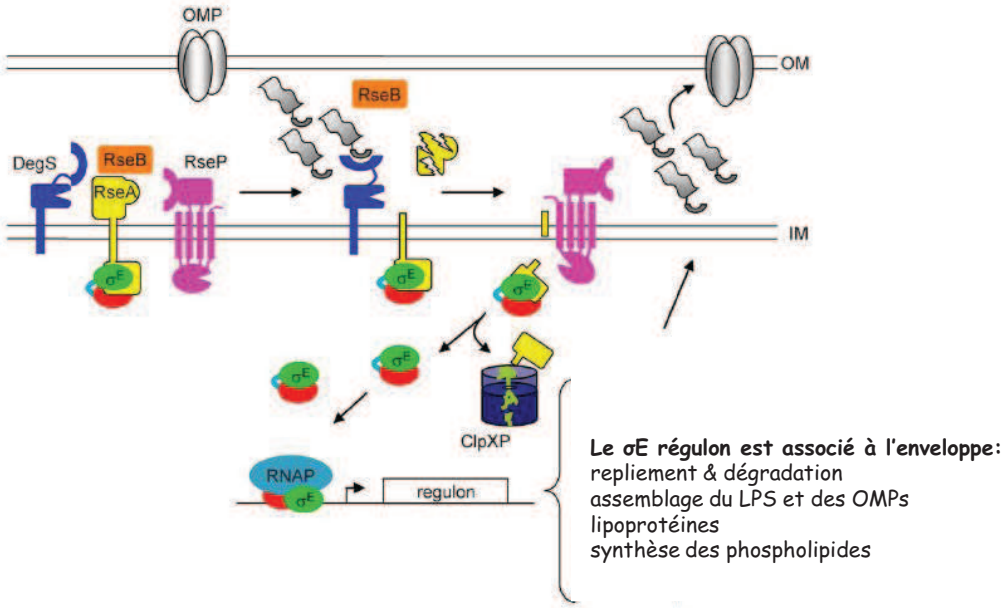

Figure 48: Réponse au stress extracytoplasmique σ^E-dépendant (Hayden & Ades, 2008). σ^E est séquestré à la membrane par RseA. RseB se fixe sur le domaine périplasmique de RseA et protège RseA de la protéolyse. Des OMPs mal-repliés activent la protéase DegS qui clive le domaine périplasmique de RseA. RseP clive ensuite la RseA dégradée déjà en partie et libère le domaine cytoplasmique de RseA lié à σ^E. Ce domaine de RseA est enfin dégradé par ClpXP en libérant σ^E qui va ensuite interagir avec l'ARN polymérase (RNAP) et réguler la transcription de son régulon. Le ppGpp et la protéine DksA peuvent activer la transcription σ^E-dépendante, une fois que σ^E est libéré de RseA (pas montré).

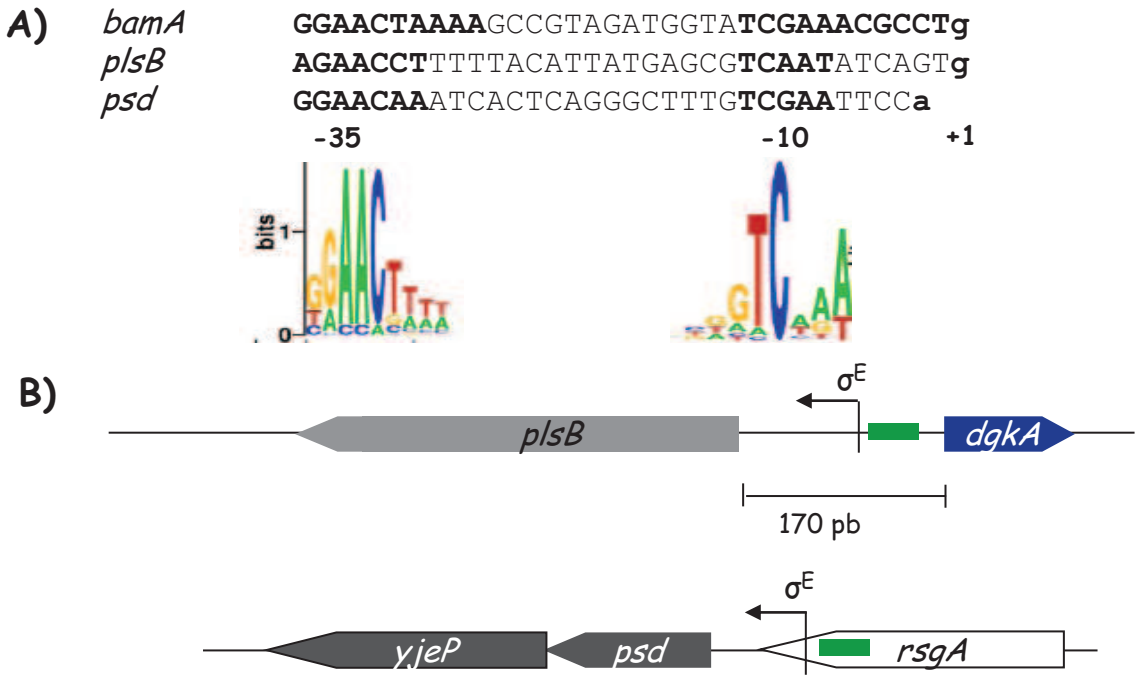

Figure 49: Promoteur consensus de RpoE et organisation génétique de *plsB* et *psd* (d'après Rhodius *et al.*, 2006). (A) Les régions -10 et -35 pour les promoteurs σ^E, ainsi que le + 1 sont représentés. Le motif consensus est indiqué en dessous. **(B)** Les gènes *plsB* et *dgkA* sont organisés d'une manière divergente sur le chromosome avec une séquence intergénique de 170 pb. *psd* et *yjeP* forment une unité de transcription. Le promoteur σ^E est coloré en vert pour son rôle d'activateur.

B3. Régulation RpoE-dépendante du métabolisme des lipides

Le facteur sigma alternatif RpoE aussi nommé σ^E (SigmaE) ou σ^{24} est une protéine de 21,6 kDa. Chez *E. coli*, un stress sur l'enveloppe (= stress extracytoplasmique) qui endommage les OMPs active une réponse RpoE-dépendante (Hayden & Ades, 2008). Le régulateur CpxR du TCS CpxRA peut également entraîner cette réponse, mais ce mécanisme n'est pas entièrement compris. RpoE est activé par une cascade protéolytique résultant dans la dégradation du facteur antisigma membranaire RseA (figure 48) et ensuite, RpoE est libéré dans le cytoplasme où il contrôle la transcription des gènes de son régulon (Hayden & Ades, 2008).

Le régulon RpoE contient des gènes codant pour des protéases et protéines chaperons de l'enveloppe et pour la synthèse des composants membranaires avec le but ultime de réparer et réinsérer les composants endommagés dans la membrane, comme les OMPs, lors du stress extracytoplasmique. Des études transcriptomiques ont identifié des gènes de la synthèse des acides gras, des phospholipides et du lipide A comme membre du régulon RpoE (Rhodius *et al.*, 2006) : le gène *plsB*, l'unité de transcription *psd-yjeP*, et l'opéron *hlpA-lpxD-fabZ-lpxA* sont activés par RpoE. Le motif consensus du promoteur RpoE-dépendant est en effet retrouvé en amont de *plsB* et *psd* (figure 49). L'opéron *hlpA-lpxD-fabZ-lpxA* contient un gène de la synthèse des acides gras et deux gènes impliqués dans la synthèse du lipide A (figure 43). De plus, il existe trois promoteurs σ^E dans cet opéron, un en amont de *bamA*, un en amont d'*hlpA* et un en amont de *lpxD* (figure 43) (Dartigalongue *et al.*, 2001). HlpA est un chaperon périplasmique qui se fixe sur des protéines de la membrane externe mal-repliés et améliore le transport et/ou l'insertion des protéines à travers et/ou dans la membrane (Kleinschmidt, 2003 ; Bulieris *et al.*, 2003).

Si on regarde plus précisément, c'est surtout la voie de biosynthèse de la PE qui est activée, par l'induction de *plsB* et *psd* lors d'un stress extracytoplasmique. Les OMPs nécessitent en même temps des phospholipides et du LPS synthétisés *de novo* pour l'insertion dans la membrane externe (Ried *et al.*, 1990 ; Kloser *et al.*, 1998). De plus, il a été proposé que les phospholipides et le LPS pourraient agir comme des lipo-chaperons assurant le repliement correct des OMPs dans la membrane externe (Mogensen & Otzen, 2005). Pour conclure, le rôle de RpoE serait d'assurer le transport et le repliement correct des protéines de la membrane externe synthétisées *de novo* en activant la synthèse des composants lipidiques de membrane (phospholipides et LPS) en parallèle de l'action des chaperons.

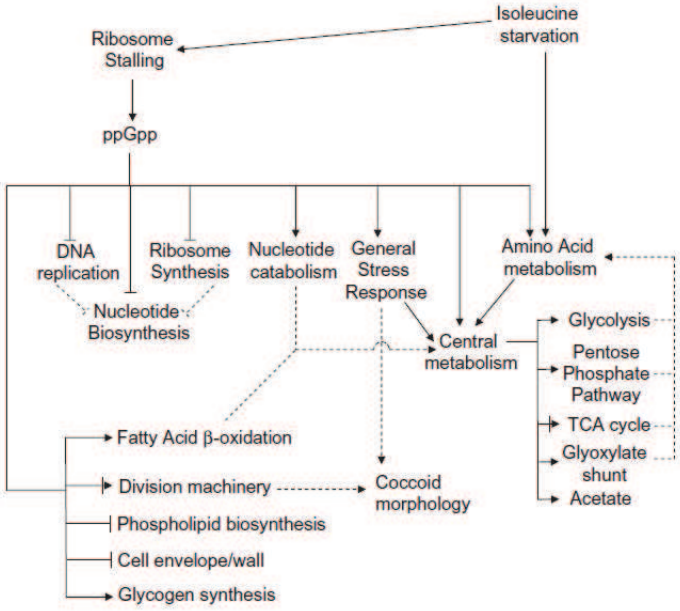

Figure 50: Modèle des modifications physiologiques lors de la réponse ppGpp-dépendante à une carence en isoleucine (Traxler *et al.*, 2008). Les flèches pleines représentent des activations, les lignes pleines des inhibitions et les lignes en pointillées représentent des effets fonctionnels. Ces régulations ne sont pas toutes directes.

C. Régulation du métabolisme des lipides par la réponse stringente et le ppGpp

Lors d'une carence nutritionnelle, la croissance bactérienne est arrêtée et l'énergie cellulaire et les ressources du milieu sont dédiées à la survie des bactéries en attendant le retour à des conditions plus favorables à la croissance. Ce processus conservé chez toutes les bactéries est nommé la réponse stringente et est essentiel à l'adaptation des bactéries à un milieu carencé. Les effecteurs principaux de cette réponse sont deux nucléotides à guanine, le guanosine 5'-triphosphate, 3'-diphosphate (pppGpp) et le guanosine 3'5'-bispyrophosphate (ppGpp), dérivés du GTP (guanosine triphosphate) et du GDP (guanosine diphosphate) respectivement, et communément appelés ppGpp. Le ppGpp est un régulateur global de la transcription qui contrôle des processus cellulaires centraux tels que la biogenèse des ribosomes ou des lipides, la réplication et la division cellulaire (figure 50).

L'élévation du taux de ppGpp dans la cellule lors d'une carence en acides aminés provoque non seulement un arrêt de la synthèse des ARN stables, mais également un arrêt immédiat de la biosynthèse des phospholipides *de novo* (figure 50). Lors de cette inhibition, toutes les espèces de phospholipides sont affectées (Pizer & Merlie, 1973). Après cet arrêt de synthèse, un système de remodelage est mis en route : lors de l'entrée en phase stationnaire, la composition en phospholipides varie, avec une augmentation des phospholipides anioniques et de la cyclopropanation.

C1. La régulation transcriptionnelle par le ppGpp

Il a été montré que le promoteur situé dans le gène *plsX* dont dépend l'expression des gènes *fabH*, *fabD* et *fabG* est inhibé par le ppGpp (figure 43) (Podkovyrov & Larson, 1996). Ce promoteur contient par ailleurs une séquence discriminatrice riche en GC, caractéristique des promoteurs régulés par le ppGpp (Travers, 1980).

Plus récemment, une étude transcriptomique a comparé l'expression globale des gènes d'une souche sauvage avec une souche qui ne produit pas de ppGpp (= Δ*relA*Δ*spoT*; ppGpp°) lors d'une carence en acide aminés (figure 51B) (Traxler *et al.*, 2008). L'expression des gènes de l'opéron *fab* est réprimée dans la souche sauvage produisant du ppGpp, tandis que l'expression est induite dans la souche ppGpp°. *fadE*, qui est impliqué dans la β-oxydation des acides gras, est induit dans la souche sauvage, mais pas dans la souche ppGpp°, tandis que l'expression de *fadD* est plus importante dans la souche ppGpp° que dans la souche sauvage (Traxler *et al.*, 2008). Ces résultats sont en accord avec le passage de la synthèse des phospholipides vers la dégradation des acides gras durant la réponse stringente (DiRusso &

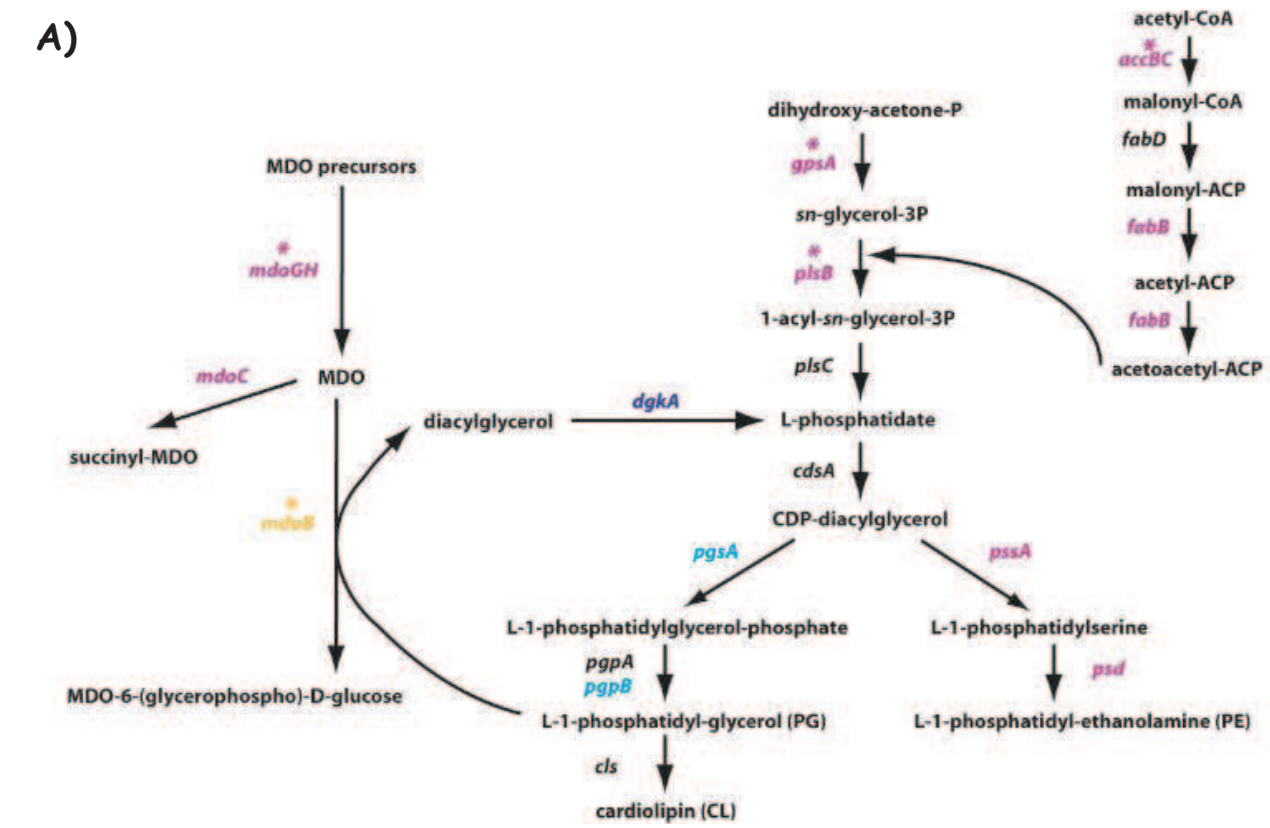

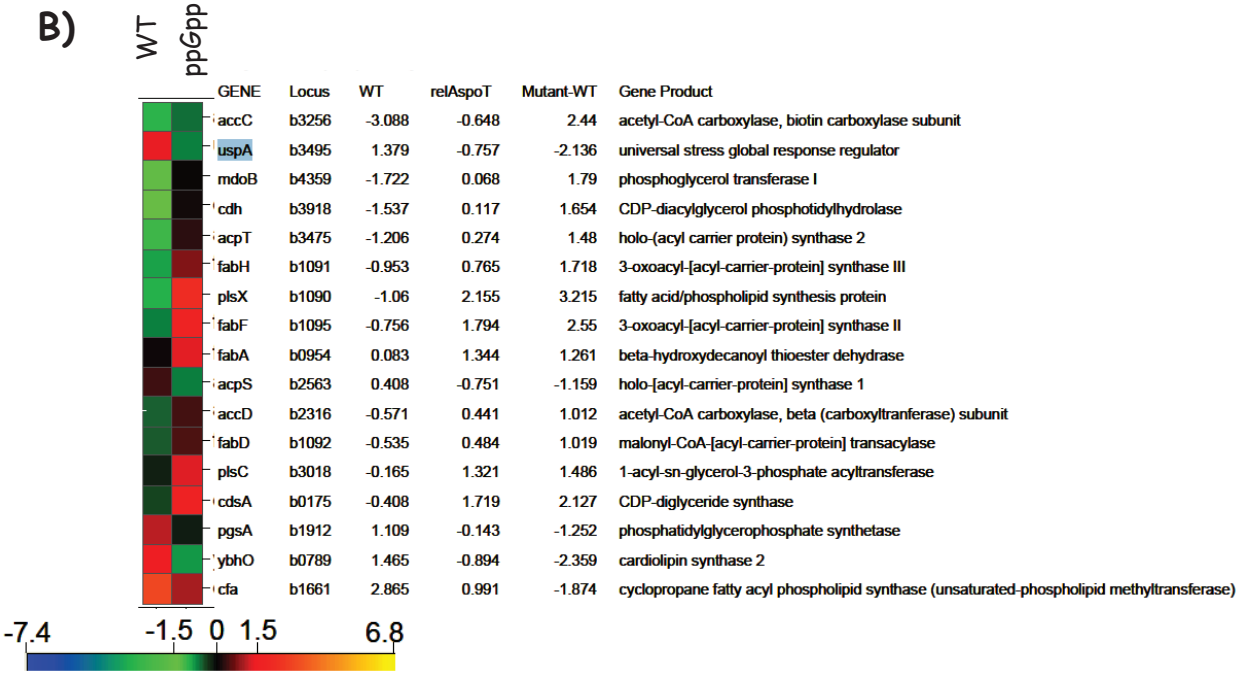

GENE	Locus	WT	relAspoT	Mutant-WT	Gene Product
accC	b3256	-3.088	-0.648	2.44	acetyl-CoA carboxylase, biotin carboxylase subunit
uspA	b3495	1.379	-0.757	-2.136	universal stress global response regulator
mdoB	b4359	-1.722	0.068	1.79	phosphoglycerol transferase I
cdh	b3918	-1.537	0.117	1.654	CDP-diacylglycerol phosphotidylhydrolase
acpT	b3475	-1.206	0.274	1.48	holo-(acyl carrier protein) synthase 2
fabH	b1091	-0.953	0.765	1.718	3-oxoacyl-[acyl-carrier-protein] synthase III
plsX	b1090	-1.06	2.155	3.215	fatty acid/phospholipid synthesis protein
fabF	b1095	-0.756	1.794	2.55	3-oxoacyl-[acyl-carrier-protein] synthase II
fabA	b0954	0.083	1.344	1.261	beta-hydroxydecanoyl thioester dehydrase
acpS	b2563	0.408	-0.751	-1.159	holo-[acyl-carrier-protein] synthase 1
accD	b2316	-0.571	0.441	1.012	acetyl-CoA carboxylase, beta (carboxyltranferase) subunit
fabD	b1092	-0.535	0.484	1.019	malonyl-CoA-[acyl-carrier-protein] transacylase
plsC	b3018	-0.165	1.321	1.486	1-acyl-sn-glycerol-3-phosphate acyltransferase
cdsA	b0175	-0.408	1.719	2.127	CDP-diglyceride synthase
pgsA	b1912	1.109	-0.143	-1.252	phosphatidylglycerophosphate synthetase
ybhO	b0789	1.465	-0.894	-2.359	cardiolipin synthase 2
cfa	b1661	2.865	0.991	-1.874	cyclopropane fatty acyl phospholipid synthase (unsaturated-phospholipid methyltransferase)

Figure 51: Voies métaboliques impliquées dans la synthèse des acides gras, des phospholipides et du MDO régulées par le ppGpp (Durfee *et al.*, 2008; Traxler *et al.*, 2008). A) Analyse transcriptomique de la réponse à la carence en acides aminés induite par l'ajout de sérine hydroxamate. Les gènes en bleu foncé sont activés au temps 10 minutes après ajout de sérine hydroxamate. Les gènes en bleu clair sont activés à 30 min, les gènes en jaune sont inhibés à 10 min, les gènes en rose sont inhibés à 10 min, les gènes en noir ne sont pas affectés. Les astérisques signalent que les gènes sont régulés dans une souche Δ*relA* comme dans une souche sauvage. B) Ratio de l'expression des gènes impliqués dans la biosynthèse des acides gras et des phospholipides dans une souche sauvage (WT) comparée à une souche ppGpp°. Couleur rouge : induction de l'expression ; couleur verte : inhibition de l'expression.

Nyström, 1998), qui accompagne la formation de cellules plus petites et rondes à l'entrée en phase stationnaire. De plus, l'expression de 17 gènes impliqués dans la synthèse des phospholipides est altérée dans la souche ppGpp° (Traxler *et al.*, 2008). Une autre étude du transcriptome de *E. coli* en condition de carence en acides aminés suggère également que plusieurs gènes de la voie de synthèse des phospholipides seraient régulés par la réponse stringente (figure 51A) (Durfee *et al.*, 2008). En condition de carence, la voie de synthèse des phospholipides serait globalement inhibée au niveau des premières étapes : le gène *gpsA* codant pour la G3P synthase et *plsB*. De plus, l'expression des gènes de la voie de synthèse de PE serait réprimée, tandis que les gènes de la voie de synthèse des phospholipides anioniques seraient activés. Cette activation de la synthèse des gènes de synthèse des phospholipides anioniques est renforcée par l'activation de l'expression du gène *dgkA* qui code pour une enzyme impliquée dans le recyclage du diacylglycérol issu de la dégradation du PG.

Les gènes de synthèse des phospholipides et des acides gras sont donc régulés lors de la réponse stringente, mais le mécanisme de régulation de tous ces gènes est inconnu et on ne sait pas si cette régulation en réponse stringente est directe ou indirecte (via RpoS par exemple). L'inhibition conjointe des gènes des composants de la membrane externe et des phospholipides suggère que l'assemblage de la membrane interne et externe est largement interrompu pendant la réponse stringente.

uspA est un autre gène régulé directement par le ppGpp qui est impliqué dans le métabolisme des lipides (Kvint *et al.*, 2003). Il code pour la protéine UspA (Universal Shock Protein), une protéine cytoplasmique nommée ainsi car son expression est induite dans de nombreuses conditions de stress (Nyström & Neidhardt, 1994 ; Nyström & Neidhardt, 1992). Cette protéine est par ailleurs la protéine de *E. coli* majoritairement exprimée en phase stationnaire. Le gène *uspA* fait également partie du régulon FadR et pourrait donc jouer un rôle dans le métabolisme des acides gras (Farewell *et al.*, 1996). La régulation de *uspA* en condition de carence dépend en fait d'une compétition entre FadR et le ppGpp. En condition normale de croissance, FadR inhibe l'expression d'*uspA*. Lors d'une carence, l'augmentation de ppGpp dans la cellule active l'expression de *uspA* malgré la présence de FadR dans la cellule (Kvint *et al.*, 2000). Le ppGpp passe donc au dessus de la régulation FadR dépendante pour imposer sa propre régulation.

Le ppGpp peut également contrôler d'une façon indirecte la transcription via le facteur sigma alternatif RpoS (figure 52). Ce facteur est présent en quantité basale dans la cellule durant la phase exponentielle de croissance mais sa quantité augmente lors de l'entrée en phase stationnaire ou pendant la réponse stringente (Lange & Hengge-Aronis, 1994). Plus de

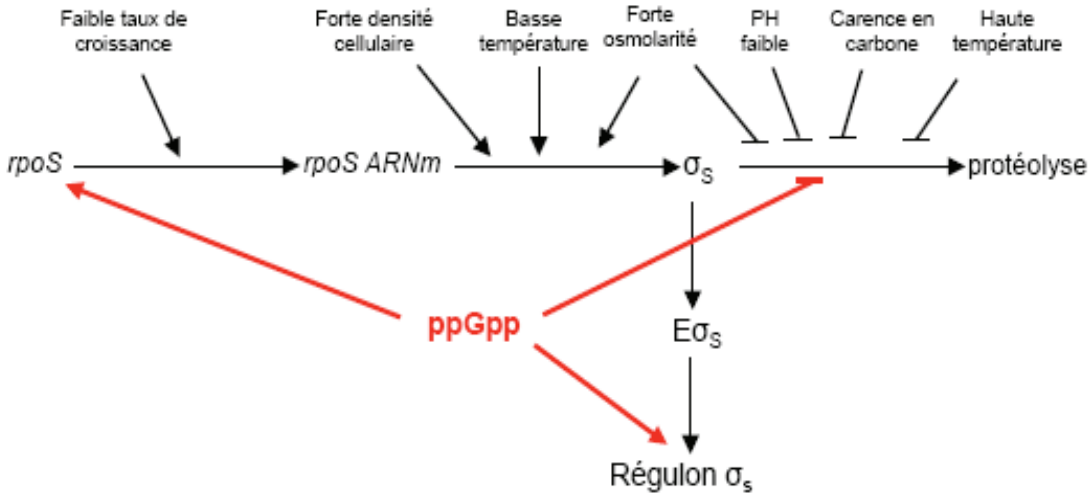

Figure 52: Régulation du facteur σ^s (d'après Hengge-Aronis, 2002). Le facteur σ^s est un facteur régulé à plusieurs niveaux en fonction des conditions environnementales. Le ppGpp active son expression, inhibe sa dégradation et participe à l'activation des gènes σ^s-dépendants.

10% des gènes de *E. coli* sont régulés directement ou indirectement par le facteur RpoS (Weber *et al.*, 2005). Plus qu'un facteur sigma alternatif, RpoS est donc un deuxième facteur primaire. Une séquence consensus claire présente dans les promoteurs des gènes régulés par RpoS n'a pas pu être établie. En effet, ce facteur est similaire au facteur végétatif σ^{70} (Lonetto *et al.*, 1992) et les séquences des promoteurs reconnus par ces deux facteurs σ ne sont pas distinguables.

En entrée en phase stationnaire, on observe une accumulation de la Cardiolipine au dépend du PG, dû à une activation de Cls (Hiraoka *et al.*, 1993). Une souche Δ*cls* perd sa viabilité (10^{-4} comparé à la souche sauvage) après incubation pendant 5 jours, suggérant un rôle pour la survie de la cellule. Une fusion transcriptionnelle de *cls* est également activée lors de l'entrée en phase stationnaire (Heber & Tropp, 1991), soutenant une régulation stringente. Cette activation de *cls* n'est pas retrouvée en carence en acides aminés (Traxler *et al.*, 2008). En revenche, de manière intéressante, le gène codant pour la cardiolipine synthase 2, *ybhO*, est activé par le ppGpp (Traxler *et al.*, 2008).

Durant l'entrée en phase stationnaire ou en condition de réponse stringente, la composition en acides gras des phospholipides est également modifiée. La proportion d'acides gras saturés (C16:0) augmente et les acides gras insaturés sont convertis en dérivés du cyclopropane (CFA) par l'action de la CFA synthase qui agit directement sur les phospholipides de la membrane (Wang & Cronan, 1994). L'activité CFA synthase serait activée lors d'une carence (Taguchi *et al.*, 1980), suggérant une régulation stringente. Bien que l'enzyme soit produite pendant toutes les phases de croissance, son activité enzymatique est instable *in vivo* et une protéine fusion possède une demi-vie de moins de 5 minutes. La région promotrice de *cfa* contient deux promoteurs : un promoteur est σ^{70}-dépendant, tandis que le deuxième promoteur serait régulé par le σ^{S} dont l'expression est activée par le ppGpp durant la transition entre les phases de croissance exponentielle et stationnaire (Rosenthal *et al.*, 2008). En phase stationnaire plus avancée, l'activité enzymatique de Cfa redescend à un niveau basal (Wang & Cronan, 1994).

Par ailleurs, l'expression de *yihG* est activée dans la phase stationnaire (Mohanty & Kushner, 1999).

L'ensemble de ces résultats montre que le ppGpp peut exercer un contrôle direct ou indirect (via RpoS) sur la régulation génétique de différents processus impliqués dans des modifications membranaires au cours d'un stress nutritionnel, mais il peut également réguler de façon directe le métabolisme des lipides en agissant au niveau enzymatique.

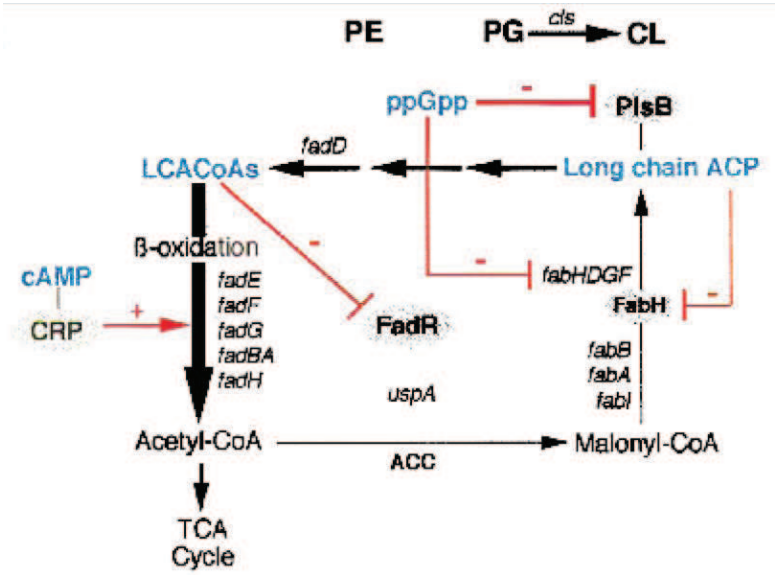

Figure 53: Représentation schématique et hypothétique de l'interconnexion entre les régulations des acides gras et des phospholipides durant la réponse stringente (DiRusso & Nyström, 1998). Le sens des voies métaboliques est indiqué par les larges flèches noires, tandis que les lignes et les flèches rouges indiquent des régulations positives ou négatives de l'expression de gènes ou des activités enzymatiques. Les composés en bleu sont importants pour la régulation. LCA: acides gras à longue chaine. CoA: coenzyme A. PE: phosphatidyléthanolamine. PG: phosphatidylglycérol. CL: cardiolipine.

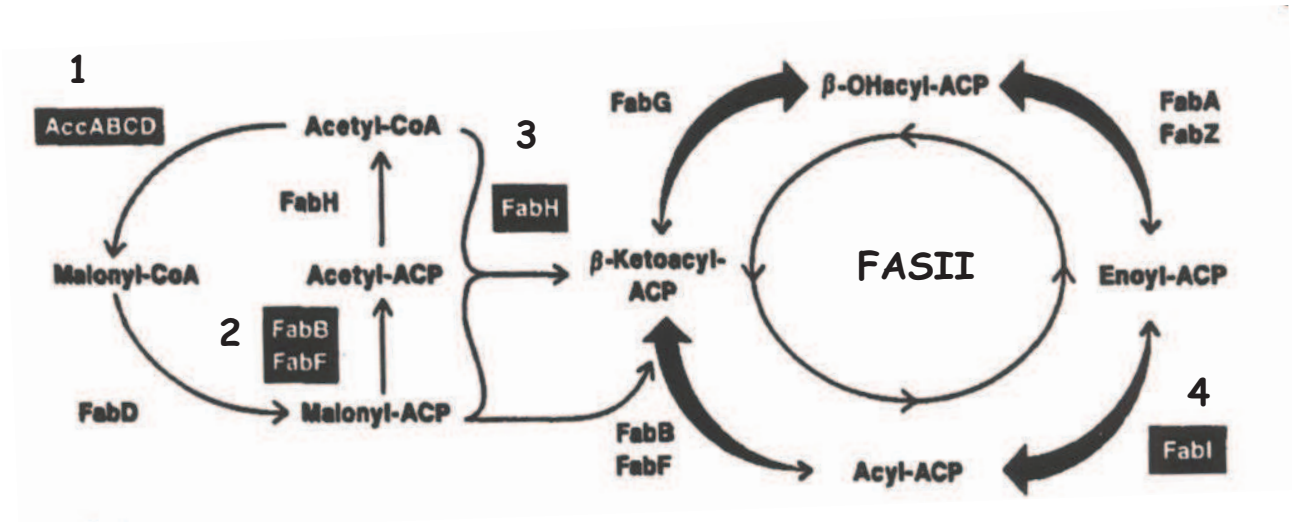

Figure 54: Représentation schématique des sites potentiels de régulation de la biosynthèse des acides gras par l'acyl-ACP (Rock & Cronan, 1996). Il y a quatre enzymes candidates pour la régulation par l'acyl-ACP: **1.** L'inhibition de AccABCD par l'acyl-ACP inhiberait la synthèse des acides gras en limitant le pool de malonyl-CoA. **2.** La stimulation de FabB et FabF par l'acyl-ACP limiterait la synthèse en détruisant le malonyl-ACP. **3.** L'inhibition de FabH par acyl-ACP bloquerait l'initiation de la synthèse des acides gras. **4.** FabI joue un rôle déterminant en complétant les cycles d'élongation des acides gras, car l'équilibre de la réaction deshydratation est en faveur des intermédiaires β-hydroxyacyl-ACP. L'inhibition de FabI par acyl-ACP pourrait empêcher la finalisation des cycles d'élongation.

C2. La régulation au niveau enzymatique par le ppGpp

Des études enzymatiques menées *in vitro* ont montré que le ppGpp pouvait inhiber directement l'activité d'enzymes impliquées dans le métabolisme des lipides comme l'acétyl-CoA carboxylase (Polakis *et al.*, 1973) ou PlsB et PgsA (Merlie & Pizer, 1973). L'inhibition de la synthèse des phospholipides durant la réponse stringente pourrait être la conséquence de l'action inhibitrice du ppGpp à différents niveaux de la synthèse des lipides (figure 53) (Nunn & Cronan, 1974). L'inhibition de PlsB qui fait le lien entre la synthèse des acides gras (synthétisés *de novo* ou importés) et la synthèse des phospholipides entraine une cascade de régulation qui modifie entièrement le métabolisme des lipides dans la cellule. Etant la première étape, PlsB est le point crucial pour la régulation de toute la voie de biosynthèse *de novo* des phospholipides chez *E. coli*. L'inhibition de l'activité de PlsB par le ppGpp provoque l'accumulation des acides gras à longue chaîne liés à ACP provenant de la synthèse *de novo* des acides gras (figure 53) (DiRusso & Nyström, 1998). Par une boucle de feedback négative sur l'étape de ACC et FabH, cette accumulation provoque l'inhibition de la synthèse des acides gras (figure 54) (Heath *et al.*, 1994). Deux autres points de régulations pourraient être FabB/FabF, qui consomment le malonyl-ACP et FabI, qui complète les cycles d'élongation des acides gras. L'acyl-ACP stimule FabB/FabF ce qui détruit le malonyl-ACP et inhibe FabI ce qui empêche la finalisation des cycles d'élongation. La synthèse des acides gras est donc inhibée en second lieu, en conséquence de l'arrêt de la synthèse des phospholipides. L'accumulation des acyl-ACPs à longue chaîne pourrait provoquer une accumulation conjointe de molécules d'acyl-CoA par transfert de la chaîne acyle (figure 53) (DiRusso & Nyström, 1998). Cette augmentation d'acyl-CoA conduirait alors à la dérepression des gènes *fad*, conduisant à activer la dégradation des phospholipides membranaires et fournissant ainsi une source de carbone et d'énergie pour assurer les activités de maintenance de la cellule. PlsB fonctionne donc comme un senseur du statut de la cellule pour coordonner la synthèse des phospholipides avec la synthèse des macromolécules et la croissance (Zhang & Rock, 2008).

A défaut d'une protéine PlsB chez la plupart des eubactéries (cf. §II *B1*), PlsX devrait être le point de contrôle du niveau d'acyl-ACP dans la voie PlsX/PlsY. Des bactéries à GRAM positif produisent également le ppGpp lors d'une réponse stringente, mais il n'est pas connu pour le moment si le ppGpp a un rôle dans la régulation de l'activité de PlsX (Zhang & Rock, 2008). L'inactivation de PlsX conduit à l'inhibition coordonnée des synthèses des acides gras et également des phospholipides chez *B. subtilis* sans accumulation d'un intermédiaire lipidique (Paoletti *et al.*, 2007). Ce résultat suggère là aussi que, l'accumulation

d'acyl-ACP à longue chaîne pourrait inhiber la biosynthèse des acides gras, comme c'est le cas chez les bactéries qui possèdent PlsB.

Characterization of the supramolecular organization of phospholipid synthesis enzymes:

Localisation Amount/ Regulation | **Interaction**

***in vivo* Fluorescence**

MICROSCOPY:
- cellular localization
- protein-protein interactions (FRET by FLIM)

SPECTROFLUORIMETER (TECAN):
- fluorescence and bioluminescence
- relative quantification
- follow protein amount dynamically
- protein-protein interactions (FRET/BRET)

v-TAP

- physiological conditions
- high specifity
- new possible protein-protein interactions
- membrane proteins

Figure 55: Representation of the goals of my thesis and techniques set up to fulfill these goals.

CONTEXT AND OBJECTIVES OF THE THESIS

Despite the extensive knowledge existing on the biochemical pathway of phospholipid synthesis, there is still little data available on the molecular characteristics of the proteins involved. From early biochemical studies, it is known that *de novo* phospholipid synthesis takes place in the cytoplasmic membrane (Raetz, 1986; Raetz & Dowhan, 1990; Wickner, 1989). Consistently, the phospholipid synthesis enzymes are predicted to be inner membrane proteins with predicted transmembrane domains for some of them. However, the exact topologies are not determined, except for PlsY (Lu *et al.*, 2007), DgkA (Smith *et al.*, 1994) and PgpB (Touzé *et al.*, 2008). More generally, the supramolecular organization of the enzymes in the inner membrane is unknown: the information concerning localization, amount, and interactions of the phospholipid synthesis enzymes is very scarce. Although the biochemical reactions that take place are well understood, even the active sites of the enzymes are often not determined.

When I arrived in the laboratory of Dr. Emmanuelle Bouveret, Djamel Gully had already tested systematically all the possible molecular interactions between the enzymes of the phospholipid synthesis, and ACP, using the BACTH technique (Karimova *et al.*, 1998). He had found indeed numerous interactions between these enzymes (figure 33) (Gully *et al.*, unpublished). This was the first evidence for an interaction network of phospholipid synthesis enzymes in the inner membrane, and for a physical connection with fatty acid synthesis enzymes in the cytoplasm. Following this work, the initial objectives of my thesis under the co-direction of Prof. James N. Sturgis and Dr. Emmanuelle Bouveret were to demonstrate and characterize the associations between the phospholipid synthesis proteins *in vivo* in native conditions.

To fulfil this goal, two main strategies were considered. We rationalized a biochemical approach for isolating membrane complexes in native membrane by affinity purification (v-TAP). We also envisaged *in vivo* fluorescent approaches such as FRET or BRET (figure 55). All these approaches required tagging of proteins (affinity tags like TAP or SPA and fluorescent reporters like EGFP or luciferase). As I wanted to work under physiological conditions, the coding gene should still be expressed from its natural promoter. Therefore, I designed new cassettes permitting the insertion of the sequences coding for these tags at the 3' end of the gene on the chromosome of *E. coli* (article 1). Using this procedure, I succeeded in obtaining a series of strains where phospholipid synthesis proteins are tagged at their C-terminus with the 5 cassettes EGFP, EYFP, ECFP (respectively enhanced green, yellow,

cyano fluorescent protein), mRFP (monomeric red fluorescent protein), and Rluc (*Renilla* luciferase). These strains were used to obtain the first *in vivo* results of quantification and localization, and now we can dynamically follow the fluorescent and bioluminescent proteins. Concerning v-TAP, I constructed strains producing proteins that are fused with the TAP tag and that are correctly inserted in the inner membrane. I then started the set up of this new technique.

Compared to the initial goal, I did not obtain data that would have allowed me to confirm the existence of a complex for phospholipid synthesis in the inner membrane. However, during this study, I developed several valuable techniques and accumulate new data on the molecular aspect of phospholipid synthesis enzymes: localization, quantification, and topology.

During the course of the study, we became interested in the regulation of phospholipid synthesis genes. Indeed, as it is the case for the molecular characteristics of the enzymes, the genetic regulation of this pathway is generally unknown despite its fundamental importance in membrane homeostasis. Curiously, the phospholipid synthesis genes are not organized as a cluster like other pathways such as fatty acid synthesis, but are rather scattered around the chromosome. Yet, some genetic regulation must occur, as it has been shown that the genes of the phospholipid synthesis pathway are co-ordinately regulated during stringent response. Moreover, mutants have been described that affect gene expression, but that were never identified.

We took an interest in *plsB* and *dgkA* genes that are the only phospholipid synthesis genes that are co-localized on the chromosome of *E. coli*. The second goal of my thesis was to understand the genetic regulation of this locus, and particularly the response to stress signals mediated by the regulators σ^E, BasRS, and ppGpp (article 2).

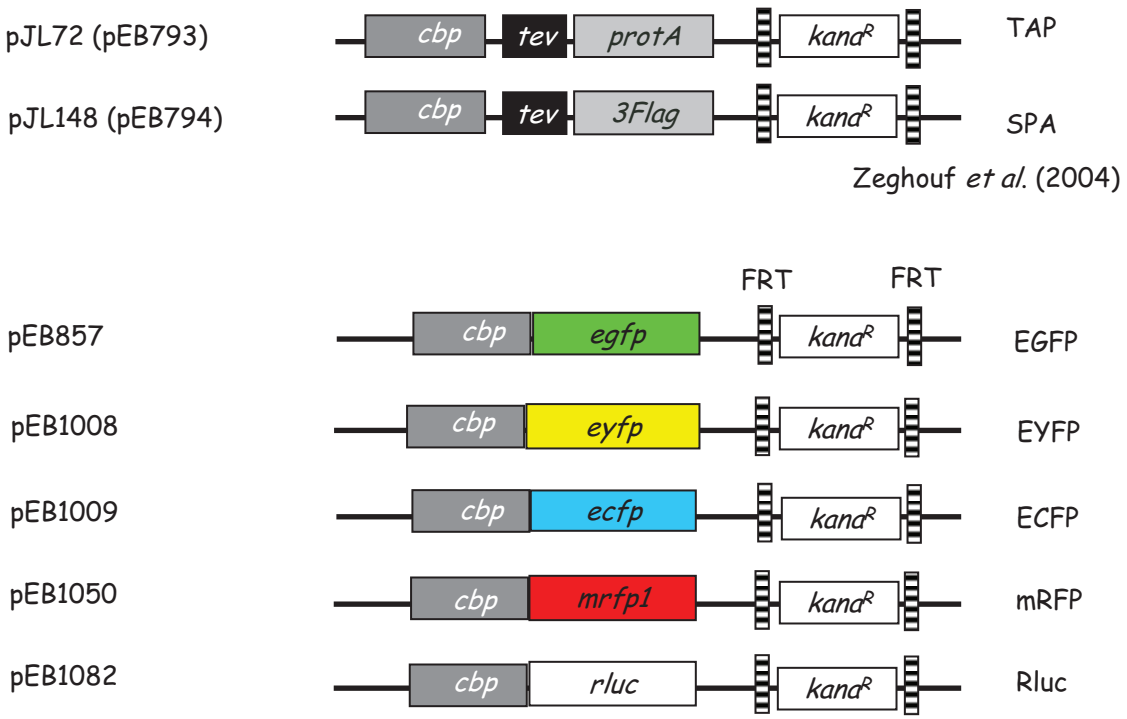

Figure 56: Cassettes for chromosomal tagging in *E. coli*. TAP: Tandem Affinity purification; SPA: Sequential Peptide Affinity; CBP: Calmodulin binding peptide; Tev: Tobacco etch virus cleavage sequence; ProtA: protein A; 3Flag: 3x octapeptide tag; kana^R: resistance to kanamycin; *egfp*: enhanced green fluorescent protein; *eyfp*: enhanced yellow fluorescent protein; *ecfp*: enhanced cyano fluorescent protein; *mrfp1*: monomeric red fluorescent protein; *rluc*: Renilla luciferase; FRT: Flipase recognition target.

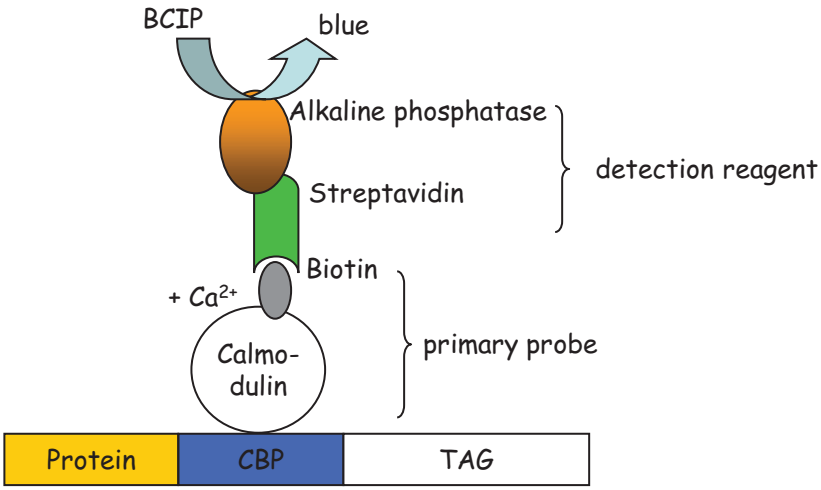

Figure 57: Principle of the CBP detection method (Stratagene®). The detection method is based on a far Western blot technique using biotinylated calmodulin (bio-CaM) as the primary probe and streptavidin conjugated to alkaline phosphatase (AP) as the detection reagent. There is a single biotinylated protein (22.5 kDa) in *E. coli* that is recognized by the streptavidin AP detection reagent.
CBP: Calmodulin binding peptide.

I. SUPRAMOLECULAR CHARACTERIZATION OF PHOSPHOLIPID SYNTHESIS ENZYMES

A. New cassettes allowing systematic fluorescent and luminescent detection, and purification from physiological expression levels

A1. Introduction and summary of article 1

Any new protein interaction found by a given approach (BACTH or TAP for example) has to be validated by different techniques and its physiological relevance must be verified. In our case, we wanted to explore the possibility of an interaction network constituted of phospholipid synthesis enzymes, which had been evidenced only by BACTH (Gully *et al.*, unpublished). We wanted to use affinity co-purifications and/or FRET/BRET techniques. For fluorescence experiments, plasmids expressing the genes *egfp*, *eyfp*, and *ecfp*, were purchased from clontech® and then all parental plasmids were modified as described below. The plasmid expressing the monomeric red fluorescent protein (*mRFP*1) was already available in the laboratory (Campbell *et al.*, 2002). For BRET techniques, we used a plasmid expressing the gene coding for Renilla luciferase (*rluc*) coupled with *eyfp*, which has been used successfully in bacteria (Xu *et al.*, 1999).

Additionally, we wanted to study the localization and the amounts of the phospholipid synthesis proteins, as well as their genetic regulation. Affinity purification or fluorescent and bioluminescent experiments both required the use of recombinant proteins fused with various types of tags, such as TAP and SPA or EGFP, EYFP, mRFP, and Rluc (figure 56). Furthermore, our goal was to work in conditions as physiological as possible, and therefore the tagged proteins were to be produced at their physiological level. In order to follow these requirements, we designed new cassettes derived from the TAP and SPA cassettes already described for use in *E. coli* (Zeghouf *et al.*, 2004). These cassettes described in article 1 allow the systematic fusion of fluorescent or luminescent proteins preceded by the calmodulin binding peptide (CBP) tag to the C-terminus of *E. coli* proteins (figure 56). These cassettes were inserted by recombination on the chromosome, at the 3' end of each tagged gene by the Datsenko & Wanner (2000) technique. Therefore, the fusion protein is expected to be produced at physiological level. This approach permits the study of protein localization by fluorescent microscopy and protein quantification, *in vivo* and dynamically in diverse conditions. Furthermore, the CBP tag (which is present in all the cassettes we constructed) makes it possible to perform various additional biochemical experiments on a given recombinant strain (Stofko-Hahn *et al.*, 1992): first, recombinant proteins can be detected

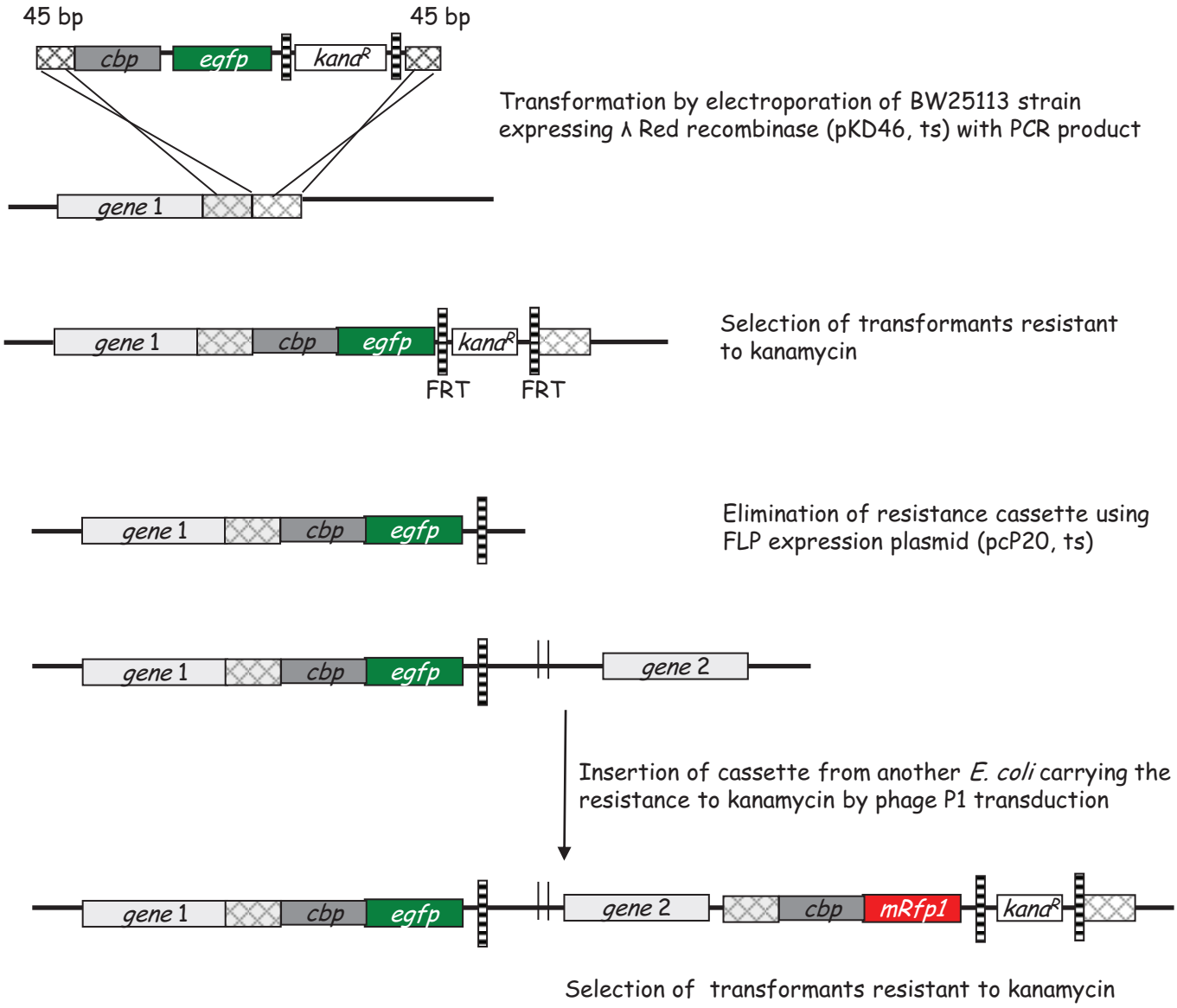

Figure 58: Combination of two genes with different fluorescent cassettes in a single cell by phage P1 transduction. Modified according to Datsenko & Wanner (2000). CBP: Calmodulin binding peptide; kana^R: resistance to kanamycin; *egfp*: enhanced green fluorescent protein; *mrfp1*: monomeric red fluorescent protein; The hatched boxes represent the 45-base pair sequences of homology between the oligonucleotides and the sequence targeted on the chromosome. FRT: Flipase recognition target .
After insertion by homologous recombination of the first cassette in the chromosome (here *cbp-egfp-kana^R*), the resistance cassette was removed by plasmid pCP20 (pEB266) expressing a flipase, which recognizes the FRT sites. This permitted the easy combination in one strain of multiple tagged proteins by successive introduction by phage P1 transduction of new-tagged constructs into the host.

using the CBP detection kit that can be purchased from Stratagene. The principle of this detection kit is that the CBP tag is recognized by biotinylated Calmodulin in presence of Calcium (figure 57). Alkaline phosphatase (AP) bound to streptavidin is used as the detection reagent. It has to be mentioned that an endogenous biotinylated protein (22.5 kDa) is present in *E. coli*, which is recognized by streptavidin. Second, affinity purification and co–purification experiments can be performed thanks to Calmodulin affinity resin (Stratagene). The described cassettes are very valuable for the versatility of experiments they make available for a given strain. Another advantage is that no artificial over-production of proteins is used, which keeps the physiological stoechiometry between enzymes.

The results obtained on the cytoplasmic protein ACP and on phospholipid synthesis enzymes in the inner membrane of *E. coli* illustrate the use of different fluorescent reporters to determine their localization. They further show how the cassettes can be used in order to follow dynamic processes, protein detection or purification using the CBP tag, and relative quantification by luciferase assay. ACP protein was successfully tagged with CBP-EGFP, CBP-EYFP, and CBP-mRFP1. A cytoplasmic and diffuse labelling was clearly seen (article 1, figure 2A); PgsA and PlsY enzymes have also been successfully tagged by CBP-mRFP1 and CBP-EGFP, respectively, and were detected in the membrane as expected from the literature (article 1, figure 2B). We have followed the amount of PlsB upon induction by the envelope stress factor RpoE, using a strain producing PlsB-CBP-EYFP. The observed increase of PlsB protein quantity in response to RpoE induction confirms published transcriptome results (Rhodius *et al.*, 2006) (article 1, figure 3). Furthermore, an example of the utility of the CBP moiety of the cassettes for detection and purification is shown in figure 4B of article 1. By Western blot on total cell extracts and using the Affinity® CBP protein fusion detection kit (Stratagene), various proteins (ACP, Psd, PlsB, and PlsC) tagged with different reporters (CBP-Rluc, CBP-EGFP, CBP-mRFP1, or CBP-EYFP) can be detected together by the same assay. Finally, *in vivo* relative quantification of all the proteins can be performed by bioluminescence measurement with the Rluc fusions.

In conclusion, we have designed cassettes allowing us to study *in vivo* the enzymes of the phospholipid synthesis pathway in the membrane of *E. coli*. The combination of CBP and fluorescent or luminescent tags is very valuable by the diversity of the experiments that can be performed on a given strain, from biochemistry to dynamic and *in vivo* studies.

TECHNICAL BRIEF

Tagging of *Escherichia coli* proteins with new cassettes allowing *in vivo* systematic fluorescent and luminescent detection, and purification from physiological expression levels

Astrid Wahl, Pierre Hubert, James N. Sturgis and Emmanuelle Bouveret

LISM, CNRS, Aix-Marseille University, Marseille, France

We designed cassettes allowing the systematic fusion of fluorescent or luminescent proteins preceded by the calmodulin binding peptide tag to the C–terminus of *Escherichia coli* proteins. The chromosomal insertion, and thus physiological expression level of these fusions, permits the study of protein localization by fluorescent microscopy and protein quantification, *in vivo* and dynamically in diverse conditions. Furthermore, the calmodulin binding peptide tag allows standard detection, affinity purification, and co–purification experiments. These cassettes are therefore very valuable for the versatility of experiments they make available for a given strain, from biochemistry to dynamic and *in vivo* studies.

Received: April 15, 2009
Revised: August 24, 2009
Accepted: September 1, 2009

Keywords:
Fluorescent proteins / Microbiology / Protein detection / Protein–protein interactions

In this technical brief, we present a set of new cassettes for tagging proteins of *Escherichia coli* with visible fluorescent proteins (VFPs, standing for EGFP, ECFP, EYFP, or mRFP1) or the luciferase luminescent protein from *Renilla reniformis*. In these cassettes, the sequence coding for the fluorescent or luminescent proteins is preceded by the sequence coding for the 5 kDa calmodulin binding peptide (CBP) [1]. The characteristics of our tagging approach are as follows: tag sequences are inserted on the chromosome, *in situ* at the 3′ extremity of the ORF, in order to produce a protein tagged at its C-terminus; cells thus produce only the tagged copy of the protein, presumably at a physiological expression level. It is then possible to follow *in vivo* the protein amounts thanks to their fluorescence or luminescence, and the localization of proteins by fluorescence microscopy. When the functionality of the tagged proteins is preserved, this approach therefore allows the obtaining of physiological information about protein localization and amounts, systematically and dynamically in different genetic or growth conditions. The novelty and usefulness of the cassettes described in this paper reside in the CBP tag that allows standard detection (Affinity CBP detection kit from Stratagene), and standard affinity purification or co-purification experiments (on Calmodulin columns), independent of the type of fusion with any VFP or luminescent protein. Furthermore, such a cassette for *R. reniformis* luciferase tagging using the λRed technique has not been described before to our knowledge. Finally, fluorescent and luminescent proteins have been chosen with *in vivo* protein–protein interaction applications in mind, such as FRET or BRET (fluorescent or bioluminescent resonance energy transfer) by combination of two VFPs in the same strain for FRET, or by combination of VFP and luciferase-tagged proteins in the same strain for BRET [2]. One technical advantage of our cassettes is that they all possess the same 5′ and 3′ extremities. Indeed, they all begin with the CBP tag and finish with the FRT recombination site after

Correspondence: Dr. Emmanuelle Bouveret, LISM, CNRS, Aix-Marseille University, 31 chemin Joseph Aiguier, 13402 Marseille Cedex 20, France
E-mail: bouveret@ifr88.cnrs-mrs.fr
Fax: +33-4-91-71-21-24

Abbreviations: ACP, acyl carrier protein; **BRET,** bioluminescence resonance energy transfer; **CBP,** calmodulin binding peptide; **FRET,** fluorescent resonance energy transfer; **Rluc,** *Rennilla reniformis* luciferase; **VFP,** visible fluorescent protein (color variants of green fluorescent protein)

the Kanamycin resistance gene (Fig. 1). Therefore, with a single pair of oligonucleotides, a given gene can be tagged with the five different reporters in one experiment.

The CBP-VFP(or Rluc)-FRT-Kana^R-FRT cassettes were obtained by modification of the pJL72 plasmid containing the tandem affinity purification cassette described previously [3] (Fig. 1). The sequences of EGFP, EYFP, ECFP (Clontech), mRFP1 [4], and Rluc (*Rennilla reniformis* luciferase) [2] were amplified with oligonucleotides adding NheI and EcoRV restriction sites and then inserted into pJL72 [3] between the NheI and EcoRV sites, thereby replacing the Protein A and TEV cleavage sequence portions of the tandem affinity purification tag.

For insertion into the genome, the cassettes are amplified with a forward oligonucleotide composed of the 45 last bases of the ORF before the stop codon followed by the TCCATGGAAAAGAGAAG sequence and a reverse oligonucleotide composed of the reverse-complement of the 45 bases following the stop codon followed by the CATATGAATATCCTCCTTAG sequence. Note that, if necessary, it is possible to design a forward oligonucleotide hybridizing at any position in the cassette, for example, avoiding the CBP coding sequence that we have found in some rare cases to affect the functionality of the tagged protein. The amplified cassette is then introduced into *E. coli* genome using the Datsenko and Wanner technique, applicable to any type of *E. coli K12* strain transformed with the pKD46 plasmid [5]. Correct recombination of the cassette at the desired site in the chromosome is then verified by two PCRs, one upstream and one downstream the site of insertion, using respectively the ebm25 and ebm282 oligonucleotides (Fig. 1). We also verify that no undesired insertion events have occurred and that the tag sequence cannot be expressed on its own (data not shown).

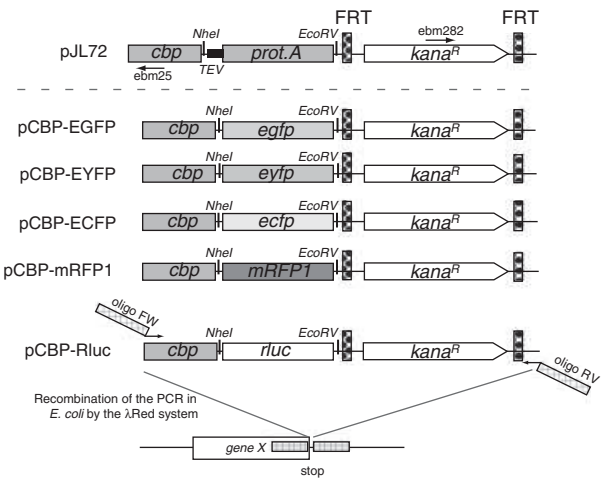

Figure 1. Description of the cassettes and oligonucleotide design for chromosomal tagging in *E. coli.* Oligo FW: forward oligonucleotide. Oligo RV: reverse oligonucleotide. Tev: TEV cleavage sequence. The hatched boxes represent the 45-base pair sequences of homology between the oligonucleotides and the sequence targeted on the chromosome. FRT: recombination site for the Flipase. The ebm25 (5′ GCGGTTGGCTGCTGAGACGGC 3′) and ebm282 (5′ ACGCTTGATCCGGCTACCTGCCC 3′) primers (whose binding positions are indicated on the pJL72 cassette) are used for controlling the correct recombination of the cassettes in the chromosome, in combination with primers binding respectively upstream or downstream the insertion point.

The resistance to kanamycin can then be removed by transforming the strain at 30°C with the pCP20 plasmid, which shows temperature-sensitive replication, confers ampicillin resistance, and permits FLP synthesis [5]. After growth at non-permissive temperature (42°C) on a non-selective medium, loss of ampicillin and kanamycin resistance indicates loss of both the pCP20 plasmid and the FRT-flanked kanamycin resistance gene. Removing the kanamycin resistance permits the easy combination in one strain of multiple tagged proteins by successive P1 transduction of new-tagged constructs into a kanamycin sensitive host. Thus, the various combinations needed for co-localization experiments or for FRET or BRET techniques can be rapidly constructed.

The enzymes of phospholipid synthesis located in the inner membrane of bacteria have been well characterized for their enzymatic properties, but the molecular information on these proteins is scarce. Localization studies of phospholipid synthesis enzymes have been performed in *Bacillus subtilis*, but using plasmid encoded fluorescent fusion proteins and artificial expression [6]. A recent work by immunolocalization of phospholipid synthesis enzymes still in *B. subtilis* has allowed the visualization at the membrane of PlsX and PlsC [7], but one difficulty with this technique is the limitation to proteins for which antibodies are available and the impossibility to follow the localization of proteins dynamically. Our goal was to develop a standardized and systematic approach for all enzymes of the phospholipid biosynthesis pathway allowing us to perform diverse *in vivo* studies. We present here the results obtained on acyl carrier protein (ACP) and on phospholipid synthesis enzymes in the inner membrane of *E. coli*, illustrating (i) different fluorescent reporters and different localizations, (ii) how they can be used in order to follow dynamic processes, (iii) protein detection or purification using the CBP tag, and (iv) relative quantification by luciferase assay.

(i) ACP protein was successfully tagged with CBP–EGFP, CBP–EYFP, and CBP–mRFP1 (Fig. 2A). However, it has to be noted that in each case, tagging of ACP resulted in a strong filamentation phenotype, indicative of a negative effect on the functionality of the protein, a negative behavior that can happen for some constructions. Yet, in the filamentous cells or in rod-shape cells, a strong cytoplasmic and diffuse labeling was clearly seen for ACP–EGFP, ACP–EYFP, and ACP–mRFP1 fusions, consistent with the high abundance of ACP (60 000 molecules *per* cell) [8]. PgsA and PlsY enzymes have also been successfully tagged by CBP-mRFP1 and CBP–EGFP, respectively, in this case without producing

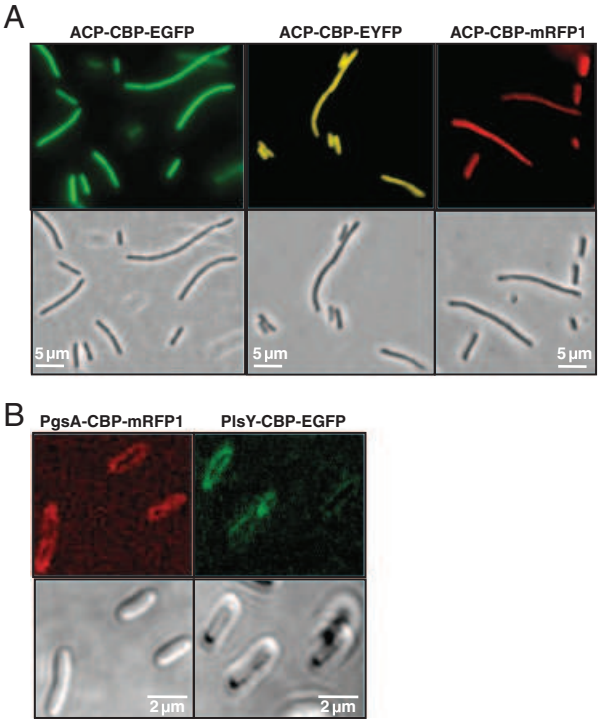

Figure 2. Localization by fluorescent microscopy of ACP, PgsA, and PlsY. W3110 *E. coli* K12 strains expressing different VFPs, ACP–CBP–EGFP, ACP–CBP–EYFP, ACP–CBP–mRFP1, PlsY–CBP–EGFP, and PgsA–CBP–mRFP1 were grown in LB rich medium at 37°C. Exponentially growing cells were immobilized with 0.25% agarose, and observed either with an Zeiss Axiovert microscope (A) or a confocal Olympus FV1000 microscope (B). In both cases, a 100 × oil immersion objective was used, with default filters and acquisition settings for each VFP. Tagged proteins produced by each strain are indicated on the figure. Upper row for each panel shows the fluorescent image, while the lower row is the differential interference contrast image.

any apparent physiological or morphological defaults, and detected in the membrane as expected from the literature (Fig. 2B) [9].

(ii) Apart from localization studies, the fluorescent fusion proteins, expressed at physiological levels, can be used to follow the effect of varying parameters such as growth conditions or genetic background on their abundance. As an example, we have followed the amount of PlsB upon induction by the envelope stress factor RpoE, using a strain producing PlsB–CBP–EYFP. This strain was transformed by the pBAD–*rpoE* plasmid that permits the overexpression of RpoE. Using a microplate reader that can read both absorbance and fluorescence and can shake and incubate the plates, the fluorescence due to PlsB–CBP–EYFP can be followed dynamically throughout growth and induction of *rpoE* (Fig. 3). The observed increase of PlsB protein quantity in response to RpoE induction confirms published transcriptome results [10].

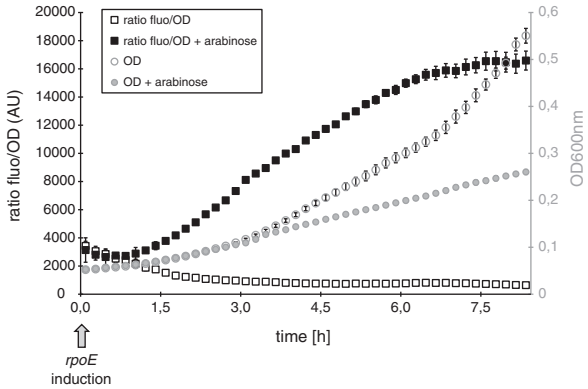

Figure 3. Increase of PlsB-CBP-EYFP amount upon *rpoE* induction. W3110 *E. coli* K12 strain producing PlsB–CBP–EYFP was transformed by pBAD24 [12] or pBAD-*rpoE* (this study) plasmids. Clones were grown overnight in LB at 32°C, then several 100 × dilutions were prepared in M9 minimal medium supplemented with amino acids and incubated at 32°C with continuous shaking in a TECAN M200 microplate reader. OD_{600nm} and fluorescence (excitation 510 nm, emission 550 nm) were continuously measured. After 1 h 20min of incubation, *rpoE* expression was induced in half of the replicates with 0.2% arabinose, and OD_{600nm} and fluorescence were measured during ongoing incubation and growth. AU: arbitrary units for specific fluorescence, corresponding to the ratio fluorescence (in arbitrary units)/OD_{600nm}. Specific fluorescence over time is shown with black and square labels, whereas OD_{600nm} is shown with grey and circle labels.

In parallel, an increased signal of fluorescence is observed by microscopy in the membrane of the PlsB–CBP–EYFP producing strain when RpoE is overexpressed (data not shown), and this increase can also be observed by Western blot (see below, Fig. 4A). We are now using this approach to systematically study regulation processes controlling the expression of phospholipid synthesis enzymes (Wahl *et al.*, to be published).

(iii) An example of the utility of the CBP moiety of the cassettes for detection and purification is shown in Fig. 4A and B. The CBP tag is recognized by biotinylated calmodulin. Therefore, by Western blot on total cell extracts using the Affinity® CBP protein fusion detection kit (Stratagene), various proteins (ACP, Psd, PlsB, and PlsC) tagged with different reporters (CBP–Rluc, CBP–EGFP, CBP–mRFP1, or CBP–EYFP) can be detected together by the same assay (Fig. 4A). The same bands corresponding to the tagged proteins are detected with anti-luciferase or anti-GFP antibodies (this could not be performed on the Psd–CBP–mRFP1 fusion). Two distinct strong bands are detected for the ACP–CBP–Rluc and ACP–CBP–EGFP proteins, corresponding to the natural high abundance of ACP, and different post-translational modifications by the phosphopantetheine prosthetic group and acyl chains [8]. A small amount of cleavage (less than 5%)

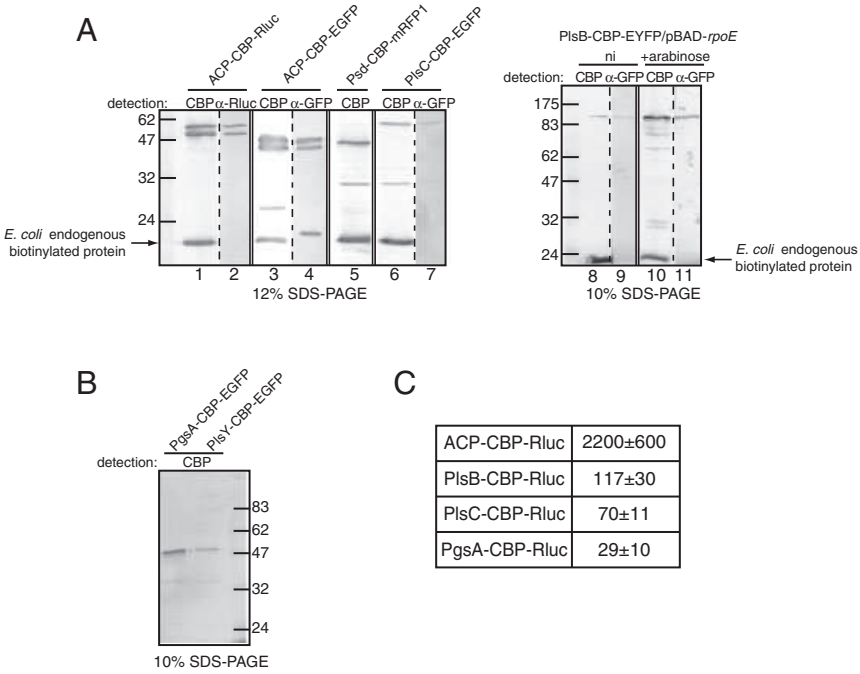

ACP-CBP-Rluc	2200±600
PlsB-CBP-Rluc	117±30
PlsC-CBP-Rluc	70±11
PgsA-CBP-Rluc	29±10

Figure 4. Relative quantification of phospholipid synthesis enzymes by Western blot and luciferase assay. (A) The W3110 *E. coli* strains containing the constructions ACP–CBP–Rluc (lanes 1 and 2), ACP–CBP–EGFP (3, 4), Psd–CBP–mRFP1 (5), or PlsC–CBP–EGFP (6, 7) were grown in LB rich medium at 37°C till $OD_{600nm} = 1$. Strain W3110 PlsB–CBP–EYFP transformed with pBAD-*rpoE* plasmid was grown in LB rich medium at 37°C till $OD_{600nm} = 1$ (ni (not induced): lanes 8 and 9) and *rpoE* expression was then induced with 0.05% arabinose for 1 h (lanes 10 and 11). Total cell extracts were analyzed in double by Western blot using the CBP detection kit from Stratagene (CBP) and anti-luciferase from Millipore(α–Rluc) or anti–GFP antibodies from Roche (α–GFP). Molecular weight markers are indicated on the side of the blots. The extracts of ACP–CBP–Rluc and ACP–CBP–EGFP strains were diluted four times compared to the other strains. The detected band sizes correspond to the expected molecular weight of the fusion proteins: 49 kDa for ACP–CBP–Rluc, 40 kDa for ACP–CBP–EGFP, 37 kDa for Psd–CBP–mRFP, 122 kDa for PlsB–CBP–EYFP, and 59 kDa for PlsC–CBP–EGFP. (B) For low abundance proteins, membrane protein extracts were prepared from 200 mL cultures of *E. coli* strains producing PgsA–CBP–EGFP and PlsY–CBP–EGFP proteins grown in LB rich medium at 37°C till $OD_{600nm} = 1.5$. The proteins were then purified on Calmodulin beads (Affinity® Purification System from Stratagene) and analyzed on a 10% SDS–PAGE followed by Western blot using the CBP detection kit (Stratagene). The band sizes correspond to the expected molecular weight of the fusion proteins: 50 kDa for both constructions. (C) The W3110 *E. coli* strains producing the constructions ACP–CBP–Rluc, PlsB–CBP–Rluc, PlsC–CBP–Rluc, and PgsA–CBP–Rluc were grown on LB-agar plates at 37°C overnight. Cells directly harvested from the LB-agar plates were resuspended in minimal medium at the same concentration (estimated by their OD_{600nm}) and analyzed *in vivo* in a microplate reader (M200 TECAN) for luciferase activity by addition of 5 μM coelenterazine (SIGMA) to the cultures. Numbers are the mean of the measured luminescence (arbitrary unit) in triplicate, with the SD indicated.

between the CBP and EGFP domains is observed for ACP–CBP–EGFP protein (Fig. 4A, lanes 3 and 4). For the other tagged proteins, a band is detected at the expected size (Fig. 4A, lanes 5–11). It has to be noted that the CBP detection kit systematically reveals an additional band corresponding to an endogenous biotinylated 20 kDa protein of *E. coli*. Increase in PlsB production upon induction of *rpoE* followed dynamically by fluorescence measurement (see above, Fig. 3) is also clearly detected by Western blot (Fig. 4A, lanes 8–11). In this last case, several degradation products are observed (lane 10).

For some low-abundance proteins (PlsY and PgsA), their quantities do not allow direct CBP detection without overloading the gel. However, from purified and solubilized membranes, we were able to purify these proteins on calmodulin beads and then detect them by Western blotting (Fig. 4B). It has to be noted that it should be possible to perform localization microscopy using the same CBP affinity binding principle.

(iv) Finally, *in vivo* relative quantification of all the proteins can be performed with the luciferase fusions (Fig. 4C). Indeed, for quantification purposes, luciferase assay is more recommended than fluorescence measurement because it is less dependent on the optical properties of the bacteria. While it has to be kept in mind that luciferase activity depends on the oxygen availability, *R. reniformis* luciferase presents the advantage of not requiring ATP, therefore of being less sensitive to the metabolic state of the cells than firefly or *Vibrio fisheri*

luciferases. The ratio that we obtained for ACP compared to the other enzymes (about 30 times more abundant, Fig. 4C and data not shown) is in accordance with published literature evaluating ACP amount to 60 000 molecules per cell [8] and phospholipid synthesis enzymes to 1400 molecules per cell based on enzymatic activities [11]. This assay of protein amount measurement is rapid and easily amenable to multiple growth conditions.

In conclusion, we have designed cassettes allowing us to study *in vivo* the enzymes of the phospholipid synthesis pathway in the membrane of *E. coli*. We think that the combination of CBP and fluorescent or luminescent tags is very valuable by the diversity of the experiments that can be performed on a given strain, from biochemistry to dynamic and *in vivo* studies. The plasmids containing the cassettes are described in our website (http://lism.cnrs-mrs.fr/Bouveret) and will be available *via* addgene (http://www.addgene.org/).

We are grateful to Dr. J. Greenblat for the gift of pJL72 plasmid. Dr. Damien Leduc has helped setting up the recombination method in our laboratory. We thank researchers from Bouveret's, Sturgis's, and Lloubes' groups for discussion and feedback on the use of the cassettes. This work was funded by CNRS and ANR. A. W. is funded by the Antibiotarget Marie-Curie European training network.

The authors have declared no conflict of interest.

References

[1] Stofko-Hahn, R. E., Carr, D. W., Scott, J. D., A single step purification for recombinant proteins. Characterization of a microtubule associated protein (MAP 2) fragment which associates with the type II cAMP-dependent protein kinase. *FEBS Lett.* 1992, *302*, 274–278.

[2] Xu, Y., Piston, D. W., Johnson, C. H., A bioluminescence resonance energy transfer (BRET) system: application to interacting circadian clock proteins. *Proc. Natl. Acad. Sci. USA* 1999, *96*, 151–156.

[3] Zeghouf, M., Li, J., Butland, G., Borkowska, A. *et al.*, Sequential Peptide Affinity (SPA) system for the identification of mammalian and bacterial protein complexes. *J. Proteome Res.* 2004, *3*, 463–468.

[4] Campbell, R. E., Tour, O., Palmer, A. E., Steinbach, P. A. *et al.*, A monomeric red fluorescent protein. *Proc. Natl. Acad. Sci. USA* 2002, *99*, 7877–7882.

[5] Datsenko, K. A., Wanner, B. L., One-step inactivation of chromosomal genes in *Escherichia coli* K-12 using PCR products. *Proc. Natl. Acad. Sci. USA* 2000, *97*, 6640–6645.

[6] Nishibori, A., Kusaka, J., Hara, H., Umeda, M., Matsumoto, K., Phosphatidylethanolamine domains and localization of phospholipid synthases in *Bacillus subtilis* membranes. *J. Bacteriol.* 2005, *187*, 2163–2174.

[7] Paoletti, L., Lu, Y. J., Schujman, G. E., de Mendoza, D., Rock, C. O., Coupling of fatty acid and phospholipid synthesis in *Bacillus subtilis*. *J. Bacteriol.* 2007, *189*, 5816–5824.

[8] Rock, C. O., Cronan, J. E., *Escherichia coli* as a model for the regulation of dissociable (type II) fatty acid biosynthesis. *Biochim. Biophys. Acta* 1996, *1302*, 1–16.

[9] Zhang, Y. M., Rock, C. O., Membrane lipid homeostasis in bacteria. *Nat. Rev. Microbiol.* 2008, *6*,222–233.

[10] Rhodius, V. A., Suh, W. C., Nonaka, G., West, J., Gross, C. A., Conserved and variable functions of the sigmaE stress response in related genomes. *PLoS Biol.* 2006, *4*,e2.

[11] Cronan, J. E., Bacterial membrane lipids: where do we stand? *Annu. Rev. Microbiol.* 2003, *57*,203–224.

[12] Guzman, L. M., Belin, D., Carson, M. J., Beckwith, J., Tight regulation, modulation, and high-level expression by vectors containing the arabinose PBAD promoter. *J. Bacteriol.* 1995, *177*, 4121–4130.

Fusion	BW25113 Kana^R	W3110 Kana^R	W3110 Δ°	Comment on detection and functionality of the fusion protein
CBP-EGFP	PlsB (493)	PlsB (495)	PlsB (497)	Detectable; growth phenotype; filamentation, even more when induced by RpoE; membrane
	PgsA (262)	PgsA (264)	PgsA (271)	Detectable; growth phenotype; no filamentation; membrane
	PlsY (391)	PlsY (399)	PlsY (414)	Detectable, low signal; no growth phenotype; no filamentation; membrane
	PlsX (402)	PlsX (419)		Detectable, low signal; no growth phenotype; no filamentation, no clear localization
		PlsC (417)		Detectable; slight growth phenotype; no filamentation; membrane?
	ACP (276)	ACP (342)		Detectable; strong growth phenotype; strong filamentation; cytoplasm
	YjeP (519)	YjeP (521)		Detectable only with induction by RpoE; filamentation
EGFP	Psd (515)	Psd (531)		Detectable; no growth phenotype; no filamentation, even upon induction by RpoE; membrane
ECFP		PlsC (416)		Detectable; no phenotype
CBP-EYFP	PlsB (293)	PlsB (300)	PlsB (382)	Detectable; growth phenotype; filamentation, even more when induced by RpoE; membrane
	PlsX (398)	PlsX (403)		Detectable, very low signal; no growth phenotype; no filamentation
		PlsC (418)		Detectable; slight growth phenotype on plate; no filamentation
	ACP (322)	ACP (344)	ACP (345)	Detectable; strong growth phenotype; strong filamentation; cytoplasm
CBP-mRFP	PgsA (361)	PgsA (362)		Detectable; no growth phenotype; no filamentation; membrane
	PlsB (389)	PlsB (393)	PlsB (409)	Detectable; slight growth phenotype; filamentation, even more when induced by RpoE; membrane
	Psd (498)	Psd (499)		Detectable; no growth phenotype; no filamentation, even when induced by RpoE; membrane
	PssA (518)	PssA (523)		Detectable, very low signal; no growth phenotype; no filamentation
	PlsY (394)	PlsY (496)		n.d.; no growth phenotype on plate;
		PlsC (423, 500)		Detectable; no growth phenotype on plate; no filamentation
	ACP (363)	ACP (364)	ACP (368)	Detectable; slight growth phenotype; less filamentation than EGFP and EYFP tags; cytoplasm
CBP-Rluc	PlsX (396)	PlsX		Detectable; strong growth phenotype on plate;
	PlsY (422)	PlsY (411)		Detectable; no growth phenotype on plate;
	PlsB (405)	PlsB (410)		Detectable; no growth phenotype on plate;
		PlsC (182)		Detectable; no growth phenotype on plate;
	PgsA (373)	PgsA (376)		Detectable; slight growth phenotype on plate;
	ACP (383)	ACP (392)	ACP (407)	Detectable; strong growth phenotype on plate;
Rluc	DgkA (377)	DgkA (387)		No signal;

Figure 59: *E. coli* strains obtained during this work that produce different fluorescent and bioluminescent fusion proteins at physiological expression level. kana^R: kanamycin resistance cassette; Δ°: the kanamycin resistance cassette has been removed from this strain using pCP20;
n.d.: not detectable. The numbers in brackets after the protein names indicate the lab code.

A2. Supplementary results to article 1

Since article 1 is a short technical paper, not all constructions and results obtained were described. I will present them in the following chapter and discuss at the same time problems that had to be faced.

1. Combination of two reporter cassettes in one cell

Fluorescent and luminescent proteins have been chosen for *in vivo* protein-protein interaction applications, such as FRET or BRET (fluorescent or bioluminescent resonance energy transfer). These techniques require the combination of two fluorescent reporters (ideally EYFP and ECFP for example) in the same strain for FRET, or the combination of EYFP and Rluc tagged proteins in the same strain for BRET (Xu *et al.*, 1999).

Thanks to the presented cassettes, it was possible to combine two different reporters in one cell (figure 58). In total, 4 proteins were fused with EGFP, 3 with EYFP, 1 with ECFP, 5 with mRFP and 7 with RLUC in the *E. coli* strain BW25113 (figure 59). Then, most of the recombinant alleles were transduced by phage P1 into the *E. coli* wild type strain W3110. Finally, the resistance cassette was removed by plasmid pCP20 expressing a flipase, which recognizes the FRT sites. This permitted the easy combination in one strain of multiple tagged proteins by successive introduction by phage P1 transduction of new-tagged constructs into the host (figure 58). This is only possible for genes that are <u>not</u> co-localized on the chromosome, which is the case for most phospholipid synthesis genes (figure 45). If the two genes are co-localized, the second cassette fused at the 3' end of the second gene cannot be introduced by phage P1 transduction. In this case, we used the Datsenko & Wanner method (2000) on the strain containing already the first fusion gene. Eventually, 11 strains were constructed in which two fluorescent colors are combined in one cell by tagging two different genes (figure 60).

For example, I transduced the cassette *acp*-CBP-mRFP::*kana*^{R} in strain W3110 producing PgsA-CBP-EGFP° (strain without the resistance cassette). Correct insertion and production of both fusion genes and proteins was checked (data not shown). Fluorescent imaging was performed on a confocal Olympus FV1000 microscope. First, the mRFP (ACP) signal was measured; second, the EGFP (PgsA) signal was measured. The measurements were done in this order to avoid bleaching of the mRFP signal by the laser used for excitation of EGFP. The cytosolic signal for ACP-CBP-mRFP and a membrane localization of PgsA-CBP-EGFP were detected, as expected (figure 61). When the two independent pictures are

Combinations in W3110	Lab code
PgsA-CBP-EGFP::kana^R / ACP-CBP-EYFP°	EB360
PgsA-CBP-EGFP::kana^R / ACP-CBP-mRFP°	EB371
ACP-CBP-mRFP::kana^R / PlsB-CBP-EYFP°	EB390
PgsA-CBP-Rluc::kana^R / PlsB-CBP-EYFP°	EB386
ACP-CBP-Rluc::kana^R / PlsB-CBP-EYFP°	EB400
ACP-CBP-EGFP::kana^R / PlsB-CBP-mRFP°	EB507
PlsY-CBP-EGFP::kana^R / PlsB-CBP-mRFP°	EB506
PlsC-CBP-ECFP::kana^R / PlsB-CBP-EYFP°	EB456
Psd-EGFP::kana^R / YjeP-CBP-mRFP°	EB551

Figure 60: *E. coli* strains producing two different fusion proteins at physiological expression level. kana^R: kanamycin resistance cassette; °: the kanamycin resistance cassette has been removed from this strain using pCP20 (pEB266).

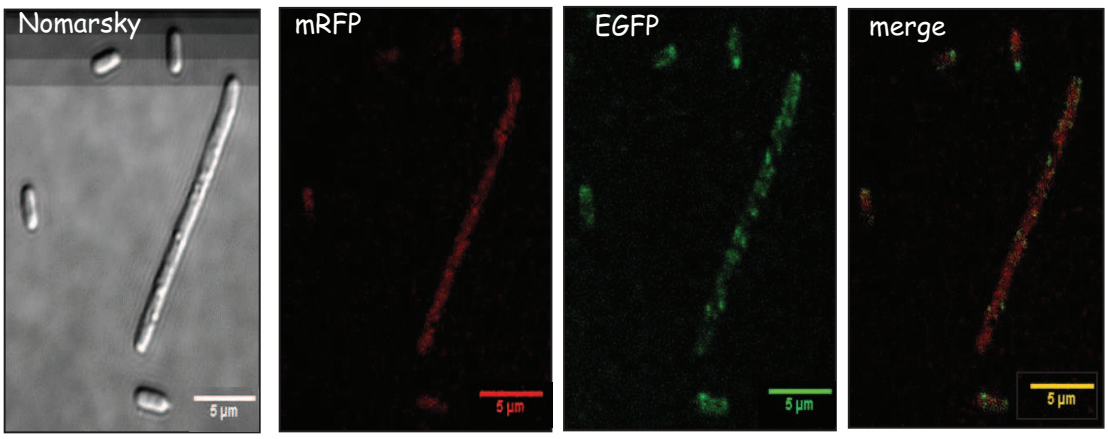

Figure 61: W3110 producing both ACP-CBP-mRFP and PgsA-CBP-EGFP in the same strain (EB371). Exponentially growing cultures (37 °C in LB supplemented with kanamycin (25 µg/mL) were harvested by centrifugation, washed once with M9 (1X, pH7,2) and resuspended in fresh M9. The cells were immobilized with 0,25% agarose on a microscope glass slide. A 100X oil immersion objective was used for a confocal Olympus FV1000 microscope with default filters and acquisition settings for mRFP (excitation = 605 nm; emission = 670 nm) and GFP (excitation = 498 nm; emission = 516 nm).

merged, the two fusion proteins do not co-localize. However, the cell presents a strong filamentation phenotype as do all the ACP tagged strains.

In conclusion, it is possible with this technique to combine two genes that are fused with the coding sequence for two different fluorescent reporters at their 3' end on the chromosome, in order to do localization studies on the produced fluorescent fusion proteins.

2. Shuffling technique

In the laboratory, a collection of *E. coli* strains producing proteins that are already tagged with affinity tags (SPA, TAP) is available (Butland *et al.*, 2005). This collection contains a total of 857 strains, including 198 corresponding to highly conserved, soluble, and essential proteins. Most of the proteins are tagged with the SPA affinity tag. In order to take advantage of these already constructed strains, we developed a new tagging strategy that we named the "shuffling technique", which permits to replace the SPA tag by any of our cassettes. First, we designed a universal primer pair (ebm415/416) that hybridizes at the 5' end of the *cbp* sequence and 6 bp after the 3' end of the second FRT site, respectively (figure 62). All the cassettes can be amplified with this primer pair. Second, the kanamycin resistance cassette has to be removed from a given strain of the Butland collection using plasmid pCP20. Then, the newly amplified cassette can be introduced by recombination in this strain, thanks to the regions of homologies that remain: there will be recombination at the *cbp* sequence and at the scar of the FRT site. This recombination results in an exchange of a sequence coding for ProtA (protein A of *Stapyhlococcus aureus*) or 3Flag for a sequence coding for a fluorescent or bioluminescent protein.

plsC was chosen as a candidate gene, as our first attempts at tagging *plsC* did not work using a primer pair specific for *plsC* (Datsenko & Wanner, 2000). An *E. coli* strain producing PlsC-CBP-TEV-3Flag (TEV= tabacco etch virus) already exists in the Butland collection (Butland *et al.*, 2005). Thanks to the shuffling technique, I could obtain *E. coli* strains W3110 producing PlsC-CBP-Rluc, PlsC-CBP-EGFP, PlsC-CBP-EYFP, and PlsC-CBP-ECFP, for which I verified the correct insertion in the *E. coli* chromosome by PCR (polymerase chain reaction) on colony. Then, I performed production tests of the different strains producing these fusion proteins. I could detect PlsC-CBP-EGFP with the CBP detection kit as well as with an antibody raised against GFP (article 1, figure 4A) and by fluorescence measurement with a fluorimeter that measures emitted fluorescence signal from live cells (data not shown). I could also detect a PlsC-CBP-Rluc bioluminescence signal in

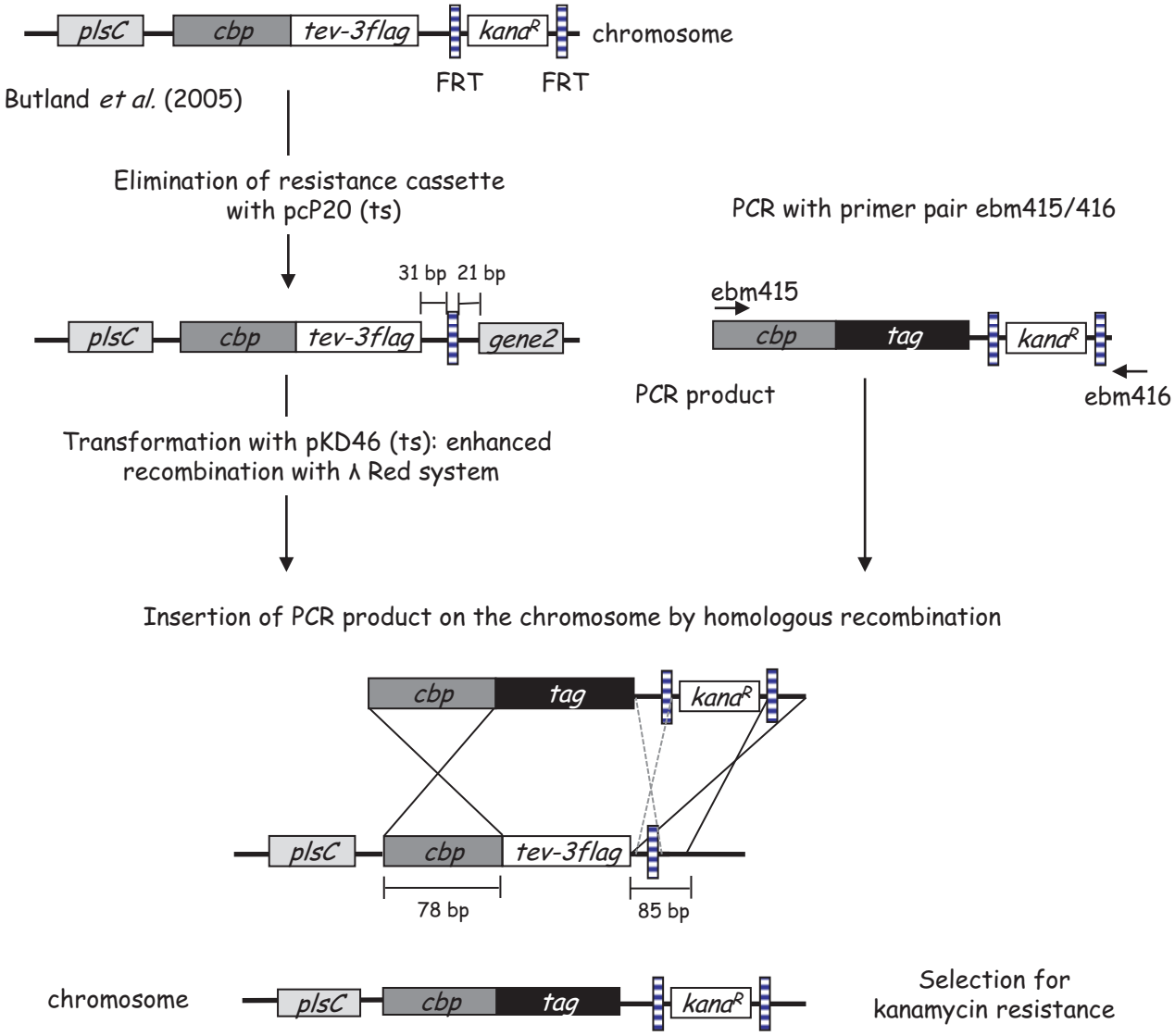

Figure 62: The shuffling technique for exchanging cassettes in *E. coli* strains existing already in the Butland collection tagged with SPA or TAP (Butland *et al.*, 2005). First, a universal primer pair (ebm415/416) was designed that hybridizes at the 5' end of the *cbp* sequence and 6 bp after the 3' end of the second FRT site, respectively. Any of our cassettes can be amplified with this primer pair. Second, the kanamycin resistance cassette has to be removed from the strain of the Butland collection using the plasmid pCP20 (pEB266). Then, the amplified cassette ("tag"), such as a fluorescent or bioluminescent one, can be introduced by recombination in this strain. There will be recombination at the *cbp* sequence and after the FRT site. This recombination results in an exchange of sequences coding for ProtA or 3Flag with a sequence coding for a fluorescent or bioluminescent protein.
Dashed lines indicate a possible (and unwanted) region of homologous recombination.

order to relatively quantify it compared to other enzymes of the phospholipids synthesis pathway (article 1, figure 4C).

In conclusion, the shuffling technique is a valuable variant of our standard tagging strategy that takes advantage of already available tagged strains, like the strains of the Butland collection, and avoid the synthesis of gene specific long oligonucleotides (Butland *et al.*, 2005).

3. Relative quantification by fluorescence or bioluminescence

Relative quantification of proteins tagged with Rluc can be performed using a luciferase assay *in vivo*. The relative quantification of 6 proteins (PlsC, PgsA, PlsX, PlsB, PlsY, and ACP) was performed on strains *plsC*-CBP-Rluc (EB180), *pgsA*-CBP-Rluc (EB376), *plsX*-CBP-Rluc (EB376), *plsB*-CBP-Rluc (EB410), *plsY*-CBP-Rluc (EB422), and *acp*-CBP-Rluc (EB392). The ratio that we obtained for ACP compared to the other enzymes (about 30-50 times more abundant, figure 63) is in accordance with published literature evaluating ACP amount to 60000 molecules per cell and phospholipid synthesis enzymes to 1400 molecules per cell based on enzymatic activities (Rock & Cronan, 1996; Cronan, 2003).

For quantification purposes, on one hand luciferase assay has an advantage over fluorescence measurement because it is less dependent on the optical properties of the bacterial cell. But on the other hand, luciferase activity depends on oxygen availability and needs its substrate, the coelenterazine. The necessity of a substrate is a problem as the timing and dosage are crucial when adding to the cells. Then, the substrate has to enter the cell and therefore a maximum of the enzymatic reaction is reached approx. 5 min after adding the substrate. So, the reaction is variable over time with characteristic fluctuations and does rapidly decrease when monitored in a kinetic measurement (data not shown). To evaluate the significance of the *in vivo* measurement, I tried to lyse the cells, which releases the protein fused with Rluc and permits direct and immediate contact with the substrate coelenterazine in the buffer. However, the lysis did not enhance the result or change the kinetic characteristics (data not shown).

In conclusion, the luciferase assay is a valuable tool for relative quantification of protein amount if the timing of addition of the substrate coelenterazine and of the kinetic properties of the enzymatic reactions is kept in mind during measurement and analysis.

Fusion protein	Rluc activity [AU]
PlsC-CBP-Rluc	64 ± 27
PgsA-CBP-Rluc	23 ± 3
PlsX-CBP-Rluc	123 ± 42
PlsB-CBP-Rluc	159 ± 43
PlsY-CBP-Rluc	72 ± 24
ACP-CBP-Rluc	26215 ± 12405

Figure 63: Relative quantification of phospholipid synthesis enzymes by luciferase assay. W3110 *E. coli* strains producing the fusion proteins PlsC–CBP–Rluc (EB180), PgsA–CBP–Rluc (EB376), PlsX–CBP–Rluc (EB376), PlsB–CBP–Rluc (EB410), PlsY–CBP–Rluc (EB422), and ACP–CBP–Rluc (EB392) were grown in LB at 37°C overnight. Cells were harvested by centrifugation and were resuspended in minimal medium at the same concentration (estimated by their OD_{600nm}) and analyzed *in vivo* in a microplate reader (M200 TECAN) for luciferase activity by addition of 5 mM coelenterazine (SIGMA) to the cultures.
Numbers are the mean of the measured luminescence (arbitrary unit) in triplicate, with the SD indicated.

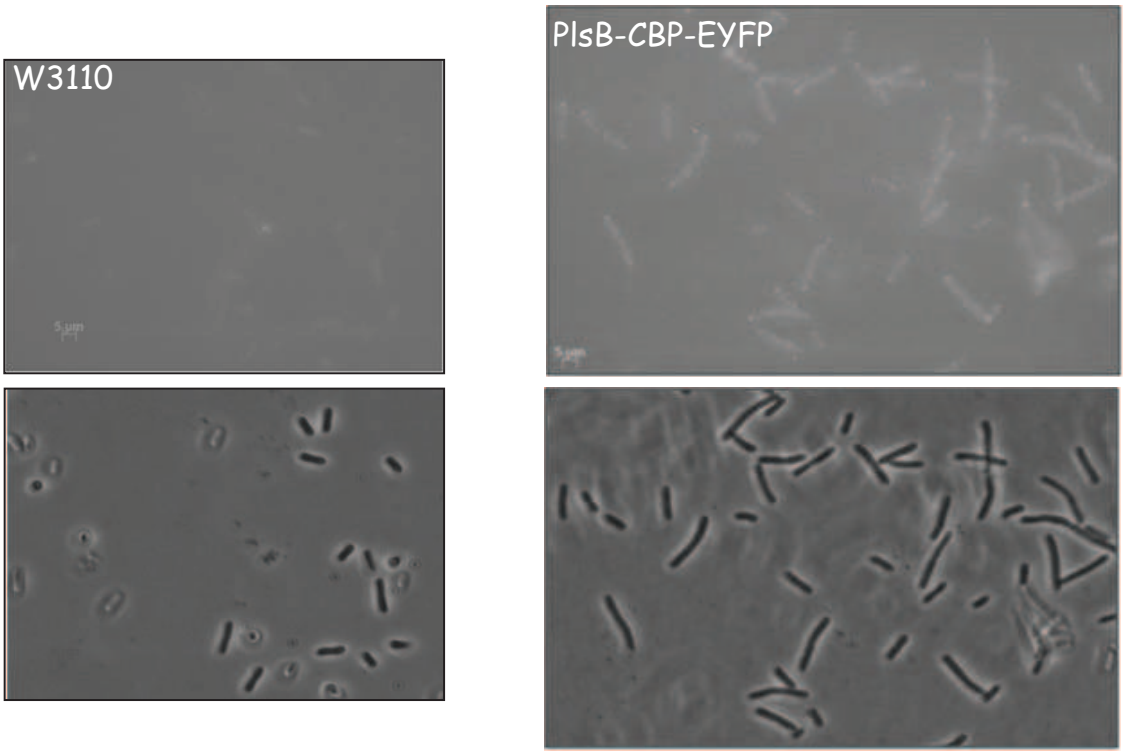

Figure 64: Cell morphology of W3110 compared to W3110 producing PlsB-CBP-EGFP (EB495). W3110 and W3110 producing PlsB-CBP-EGFP (EB495) were grown in LB supplemented with kanamycin (25 µg/mL) till late stationary phase at 37°C. Cells were harvested by centrifugation, washed once with M9 (1X, pH7,2) and resuspended in fresh M9. The cells were immobilized with 0,25 % agarose on a microscope glass slide. A 100X oil immersion objective was used for the Zeiss Axiovert 200M microscope, with default filters and acquisition settings for GFP: excitation = BP450-490 nm; emission = BP515-565 nm; exposure time = 500 ms.

A3. Discussion of article 1

1. Functionality of the fusion proteins

Some fusion proteins were not (fully) functional. Since most of the phospholipid synthesis enzymes are essential for growth, tagging of some of them resulted in smaller colony size on plates and/or a filamentation phenotype (especially in the case of PlsB and ACP). Tagging of ACP resulted in smaller colonies on plate (data not shown) and a strong filamentation phenotype (about 30 % for EGFP, length 2 to 10 µm) (article 1, figure 2 and data not shown). A strain with PlsB fused to EGFP or EYFP formed smaller colonies on plate than a strain with PlsB fused to mRFP and than the wild type strain (data not shown). It also presented a filamentation phenotype (about 20 % for EGFP, length 2 to 8 µm) (figure 64), which became even stronger at higher temperature (37°C compared to 30 °C) and upon induction by RpoE.

Interestingly, for many strains producing protein fusions, these phenotypes were weaker when fused to mRFP instead of EGFP or EYFP. Psd for example could not be obtained in fusion with CBP-EGFP or any other fluorescent or bioluminescent reporter, but only in fusion with CBP-mRFP. The resulting recombinant strain presented no growth phenotype on plate and no filamentation (data not shown). So, what makes the difference between these reporter proteins? The only differences between EGFP and EYFP are some point mutations in or near the chromophore, but they form the same β-barrel structure. Although, mRFP has a similar structure (β-barrel) as EGFP and EYFP, there is no similarity in the amino acid sequences. The structural properties of the EGFP and EYFP tags may still be different and affect the protein functionality more than the mRFP tag, or the difference in their sequence may influence protein folding during translation.

There are several possible reasons that may cause these phenotypes: first, when fusing an essential enzyme with a tag, this can attenuate or abolish its catalytic activity and lead to the strain phenotypes mentioned above. Alternatively, the insertion of a cassette in the chromosome might have an effect on the expression of gene(s) located downstream, and the phenotype results from a default independent of the tagged gene. Similarly, when the kanamycin resistance cassette is removed, we ignore the effects of the remaining cassette and the FRT scar on expression of downstream genes. However, in most cases it did not seem to change the behaviour of the strain without the kanamycin resistance cassette compared to the parental tagged strain. Finally, problems might occur both from a functionality default and a folding default in the membrane: indeed, unrelated membrane proteins may be impaired due to aggregates formed by the tagged protein at the membrane.

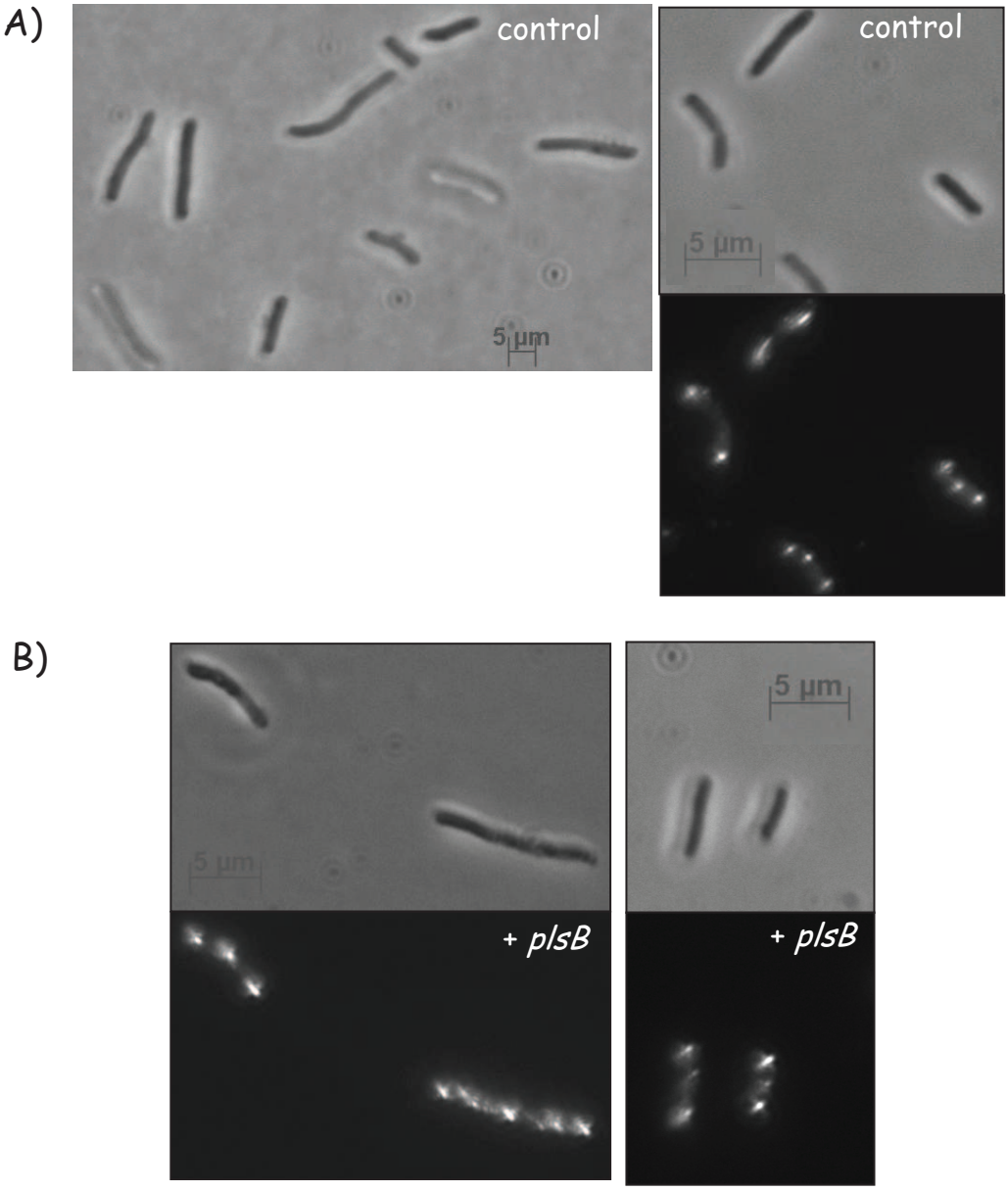

Figure 65: W3110 producing PlsB-CBP-EGFP° (EB497) and complementation test. W3110 producing PlsB-CBP-EGFP° (EB497) was transformed with pUT18linker ((**A**) control; pEB355) or pUT18linker-*plsB* ((**B**); pEB621). Exponential growing cultures in 2YT were incubated at 37°C and induced for 3 h with 0,1 mM IPTG for pUT18 derivatives. Cells were harvested by centrifugation, washed once with M9 (1X, pH7,2) and resuspended in fresh M9. The cells were immobilized with 0,25 % agarose on a microscope glass slide. A 100X oil immersion objective was used for the Zeiss Axiovert 200M microscope, with default filters and acquisition settings for GFP: excitation = BP450-490 nm; emission = BP515-565 nm; exposure time = 500 ms.

1.1 Complementation of PlsB and ACP tagged strains

In order to find out where the growth problem came from, we first tested if the phenotypes (small colony size, filamentation) could be complemented by *plsB* expression in trans. If the phenotype can be complemented, this would suggest that PlsB tagged proteins are not fully functional. But if there is no complementation, the phenotype is due to another problem than PlsB activity. In the laboratory, we possess BACTH plasmids pUT18linker-*plsB* or pKT25linker-*plsB*, which had been shown to be functional as they complement strain BB2636 (*plsB*26*plsX*50) that is glycerol auxotroph (Gully *et al.*, unpublished). Strain W3110 producing PlsB-CBP-EGFP° was transformed with the following plasmids: pUT18linker or pKT25linker and pUT18linker-*plsB* or pKT25linker-*plsB.* No complementation was observed on the colony size when grown on plate (data not shown). Additionally, with or without induction of plasmids pUT18linker-*plsB* or pKT25linker-*plsB* the filamentation phenotype was not complemented (figure 65 and data not shown). These results suggest that the smaller colony size and filamentation are not only due to an attenuated functionality of PlsB fusion protein as there was no complementation by the *plsB* allele in trans. Alternatively, the PlsB tagged protein might have a dominant negative effect, due to aggregation or competition for interactions.

Similarly, I tested whether the phenotypes of ACP tagged strains could be complemented by expressing *acpP* from a plasmid. In the laboratory, we provide a BACTH plasmid that had been shown to complement an *acpP*^{ts} mutant (data not shown) (Battesti & Bouveret, 2009). When the three strains in which ACP is tagged with CBP-EGFP, CBP-EYFP, or CBP-mRFP were transformed by pUT18linker-*acpP*, it complemented the growth phenotype on plate in the case of ACP tagged with CBP-mRFP and CBP-EGFP (figure 66A), but not of ACP tagged with CBP-EYFP. However, it did not change the filamentation phenotype observed by light microscopy (figure 66B). Indeed, cells producing ACP tagged strains with CBP-EGFP and transformed with an *acpP* gene in trans were longer than wild type cells and some filamentous cells were present. Cells producing ACP tagged with CBP-EGFP and transformed with the control plasmid cells were longer than wild type (2-3 times), some “star” cells were present, and some cells were filamentous (not shown in figure 66B). In conclusion, there was no difference between the phenotypes of the strains transformed or not with a functional *acpP* gene in trans. So, the phenotypes of smaller colony size on plate and of filamentous cells were not caused only by an impaired functionality of the tagged *acpP* gene.

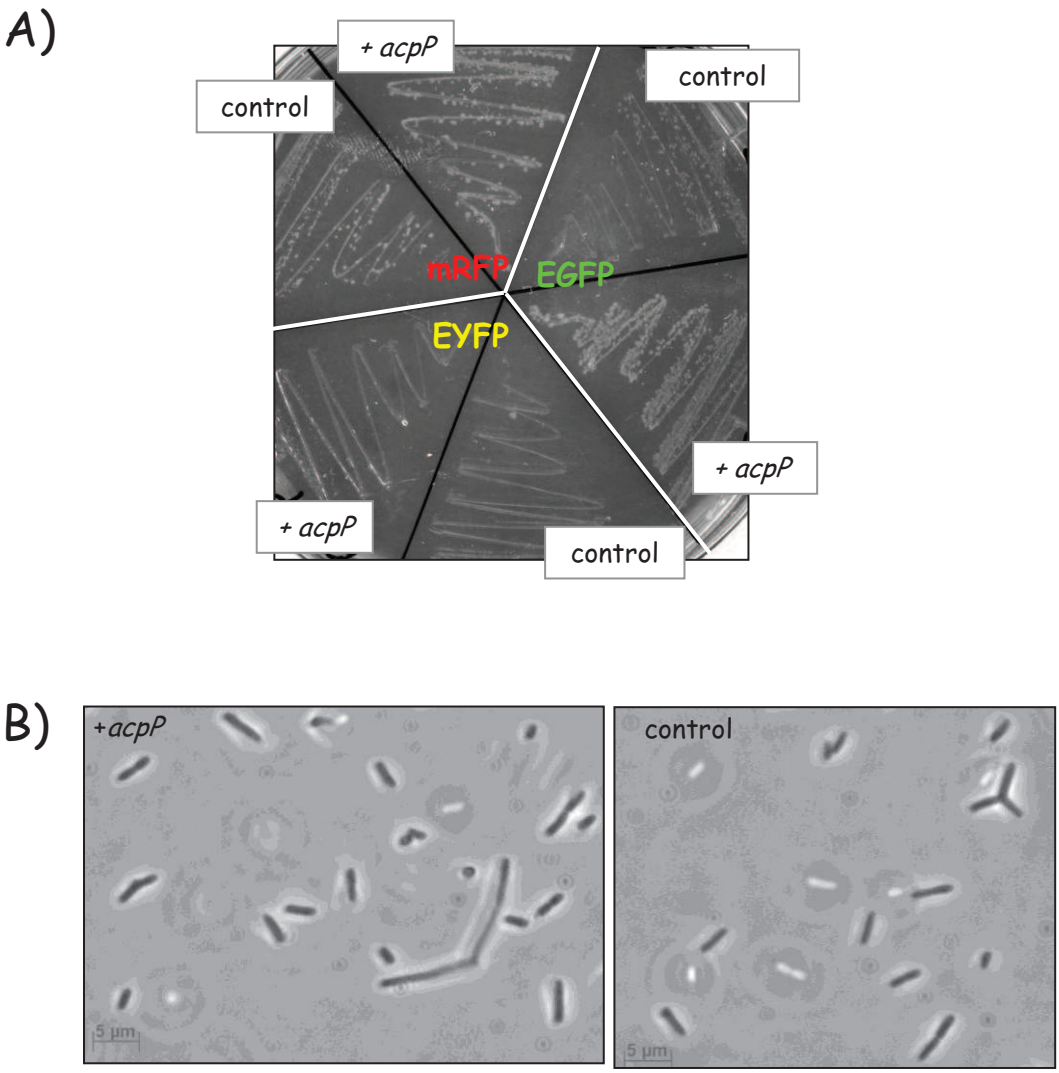

Figure 66: W3110 strains producing ACP tagged with CBP-EGFP (EB342), CBP-EYFP (EB344), and CBP-mRFP (EB364) and complementation test. A) Complementation of growth phenotype on plate: isolated colonies from transformation plates LB supplemented with ampicillin (100 µg/mL) and kanamycin (25 µg/mL) are plated on the same medium without induction of the pUT18linker (= control; pEB355) and pUT18linker-*acpP* (pEB379) plasmids and grown overnight at 37°C. **B)** Complementation of filamentation phenotype of W3110 producing ACP-CBP-EGFP: isolated colonies from transformation plates LB supplemented with ampicillin (100 µg/mL) and kanamycin (25 µg/mL) were grown overnight at 37°C in 3 mL LB without induction of the pUT18linker (= control; pEB355) and pUT18linker-*acp* (pEB379) plasmids. The next day cells are harvested by centrifugation, washed and resuspended in M9 (1X, pH7,2) and observed in a Zeiss Axiovert 200M microscope in phase contrast and an 100X oil immersion objective.

In the cases of ACP and PlsB fusion strains the phenotypes did not seem to be caused by tagging these enzymes. They must be at least partly functional, since they are essential enzymes for growth and the strains were viable. It rather seems that the whole lipid and membrane metabolism was disturbed. One has to keep in mind that ACP is very abundant (60000 molecules/cell) and so will be the reporter protein. Both ACP and PlsB are involved in a series of important cellular processes and form various protein-protein interactions. This could lead to disturbance by the tag of other proteins which interact with ACP or are located near PlsB in the inner membrane, which could then cause specific aggregations of these proteins.

1.2 Construction of a strain expressing *acpP*STOP-CBP-EYFP::kana^R

When we submitted article 1, a reviewer's comment regarding the filamentation phenotype of ACP tagged strains was to perform repeated recombinations with the same *acpP-cbp-eyfp* construct and note if the same abnormal phenotype is produced. Regarding this point, the experiment was not done as the reviewer suggested, however, three different fluorescent tags (EGFP, EYFP, and mRFP) were transformed and in all cases, the filamentation phenotype occurred. Furthermore, I tested for all constructions by PCR with primers hybridizing in the cassette and in the sequences up or down stream of the gene to verify the correct insertion on the chromosome. For *acpP* constructions, I also performed PCRs with a primer pair hybridizing at the 3' and 5' end of *acpP* sequence to verify that no gene duplication had been taken place somewhere else on the chromosome. Only fragments corresponding to the full length fusions were amplified, suggesting that no duplication had occurred.

Another comment of the reviewer was to insert the cassette downstream of *acpP*, but to keep the stop codon of *acpP*. This control would demonstrate both the absence of low level expression from the tags caused by any potential cryptic initiation codons in the tag sequences, and also the absence of random insertion into another gene followed by expression of the insert leading to an abnormal phenotype. Additionally, we ought to test if filamentation still occurred due to the chromosomal insertion and effects on genes in the same orf down stream of *acpP*. To answer to this second comment, we designed a new forward primer (ACPstop) that keeps the stop codon after *acpP* (figure 67A). First, the correct insertion of cassette *cbp-eyfp::kana^R* on the chromosome in strain BW25113 was checked by PCR on colony (data not shown). When we measured the specific fluorescence of BW25113 producing ACP tagged with CBP-EYFP compared to the corresponding strain with the stop codon, there was only a residual signal for BW25113 producing ACP tagged with CBP-EYFP

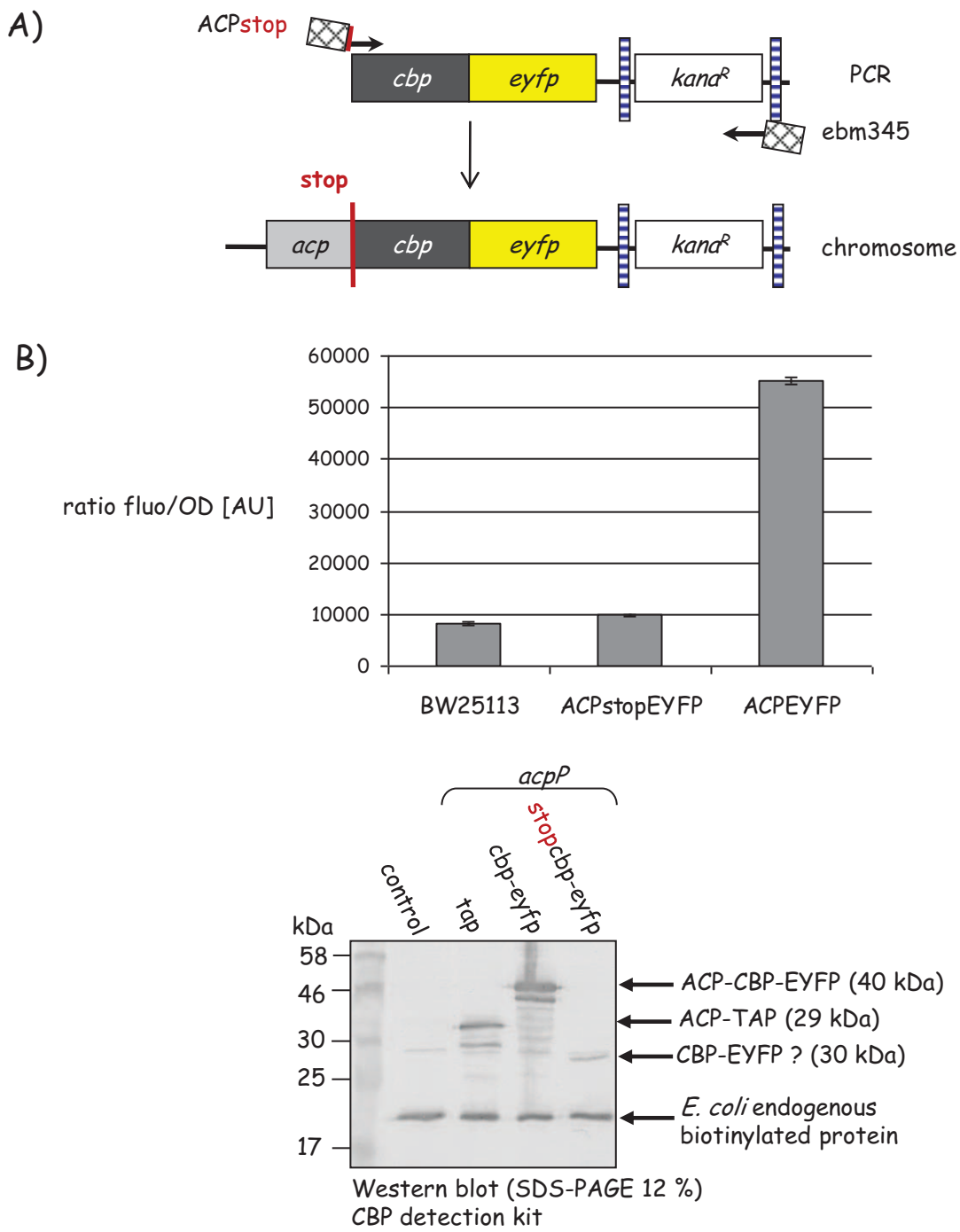

Figure 67: Strain BW25113 *acpP*STOP-CBP-EYFP*::kana*^{R} (EB580) and tag detection. A) Design of the forward primer to insert the cassette CBP-EYFP::kana after the stop codon of *acpP* on the chromosome of *E. coli* strain BW25113. **B)** On the top: overnight cultures grown at 32°C in 2YT supplemented with kanamycin (25 µg/mL), if necessary; OD_{600nm} and fluorescence (excitation= 510 nm, emission= 550 nm) were measured using a TECAN M200. AU: arbitrary units for specific fluorescence, corresponding to the ratio fluorescence (in arbitrary units)/OD_{600nm}. On the bottom: overnight cultures were grown at 32°C in 2YT supplemented with kanamycin (25 µg/mL) and total cell samples were prepared to do a Western blot using the CBP detection kit (Stratagene). The molecular weight in kilo Dalton (kDa) is indicated at the left hand side of the blot.

and with stop codon (figure 67B). Furthermore, in a production test by Western blot with the CBP detection kit, no full length fusion protein was detected; however, there was a faint band corresponding to the molecular weight of CBP-EYFP (30 kDa, lane 4) only. This band might be due to a weak translation initiation only of CBP-EYFP. In this context, it has to be mentioned that ACP migrates at a higher molecular weight in a SDS-PAGE (Hill *et al.*, 1995) and that the two detectable bands represent its two forms occurring in the cell: the apo and holo form of ACP (Rock *et al.*, 1981). This behavior remains when ACP is tagged.

The morphology of the new strain BW25113 in which *acpP* has still its stop codon was compared to the parental strain and the strain BW25113 producing ACP tagged with CBP-EYFP using a Zeiss light microscope (100 X objective). Already, the BW25113 parental strain showed about 5 % filamentous cells when grown overnight at 37 °C (data not shown). 30 % of the cells of BW25113 producing ACP tagged with CBP-EYFP presented a filamentation phenotype, while only 10 % of the cells of the strain with the stop codon presented a filamentation phenotype (data not shown).

These results suggest that the phenotype came mostly from tagging *acpP*. Together with the complementation experiments, this suggests that the problems came from perturbations provoked by the tag of other cell processes.

2. Improving functionality of produced fusion proteins

Because obviously problems occurred regarding the functionality of the fusion proteins, we tried to improve their functionality by changing the tag size (without CBP), or by tagging at the N-terminus rather than C-terminus of the protein.

2.1 New cassette without the CBP tag

E. coli W3110 strains producing PssA or Psd tagged with CBP-mRFP were obtained. However, strain producing PssA or Psd tagged with EGFP or EYFP could not be obtained. As we found that the structural properties of the tags CBP-EGFP and CBP-EYFP may affect the protein functionality, we wondered if reducing the tag size could improve it. So, we tried to reduce the cassette size by cutting off the 5kDa CBP tag. New forward primers were designed that hybridize in the linker sequence between the CBP and tag sequence and then our standard tagging method followed. PssA and Psd were chosen as candidates, as their tagging with CBP-EGFP or CBP-EYFP was not successful and DgkA was also chosen, as the fusion protein DgkA tagged with TAP (CBP-Tev-ProtA) or SPA (CBP-Tev-3Flag) were not functional. Only strain producing Psd-EGFP could be obtained. We have no specific test for the functionality of Psd, but already the fact that I could obtain a strain producing Psd-EGFP

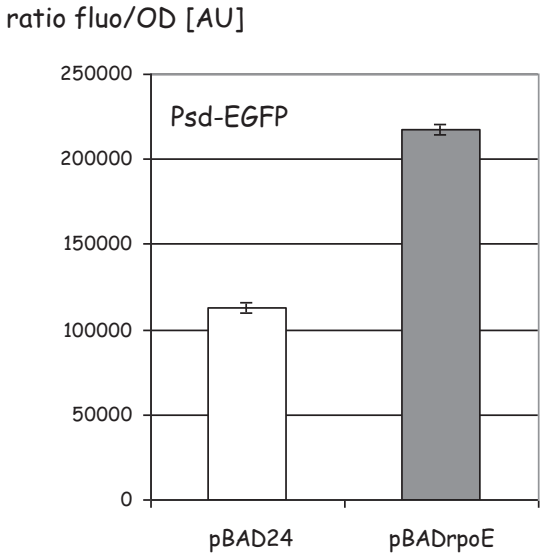

Figure 68: Psd-EGFP (EB531) production. *E. coli* strain W3110 producing Psd-EGFP transformed with pBAD24 (pEB227) or pBAD-*rpoE* (pEB1102) was grown in LB supplemented with kanamycin (25 µg/mL), ampicillin (100 µg/mL), and 0,01 % arabinose overnight at 32°C. Then, the overnight culture was transferred into a 96 well plate for measurement in a fluorimeter (TECAN M200 microplate reader). OD_{600nm} and fluorescence (excitation= 485 nm, emission= 530 nm) were measured. AU: arbitrary units for specific fluorescence, corresponding to the ratio fluorescence (in arbitrary units)/OD_{600nm}.

(detectable with an antibody raised against GFP; data not shown) indicated that Psd is still functional since it is an essential protein. Furthermore, the protein amount of Psd-EGFP increased upon induction by RpoE (figure 68) as expected from the literature (Rhodius *et al.*, 2006) and from experiments of Psd-CBP-mRFP (data not shown), which also confirmed the functionality of the fusion protein.

To conclude, for *psd*, a functional fusion with a fluorescent reporter could be obtained by removing the 5 kDa CBP tag. Additionally, the *dgkA* gene was fused with Rluc and ProtA or 3Flag without the CBP tag. The fusion protein was only obtained without the CBP tag in the case of Rluc and its functionality was improved in the case of ProtA or 3Flag compared to TAP and SPA, respectively (cf. § III B4).

2.2 New cassette permitting to tag at N-terminus

Another reason for loss of function of a fusion protein could be that the protein may not tolerate tagging its C-terminus, for example because its active site is in this domain or because the tag prevents interactions. This is true for soluble as well as for membrane proteins. The possibility of tagging a membrane protein depends also on its topology in the inner membrane and sometimes requires an N-terminal tag. Furthermore, there are techniques that require a certain orientation of the tags, such as FRET or BRET techniques where the tags ought to be at the same side of the inner membrane to determine a protein-protein interaction; for correct fluorescence activity of GFP, the tag needs to be located in the cytoplasm (Feilmeier *et al.*, 2000). Finally, the expression of the downstream orf of the tagged gene could be attenuated by introducing the tag between two genes and therefore change or stop transcription signals.

We therefore decided to construct a cassette that permits tagging at the N-terminus of any protein. However, the insertion of a fusion sequence at the beginning of an orf is in any way more complex than for a C-terminal tag, because the chromosomal N-terminal tag can attenuate or abolish upstream transcription signals and the physiological expression of the target gene. In yeast, the galactose inducible plasmid pBS1761 has been designed for N-terminal tagging with TAP (Puig *et al.*, 2001). The principle is the same as for the C-terminal tagging: a PCR product is amplified whose extremities possess homology to the insertion site in the chromosome where the recombination ought to take place. After chromosomal insertion, the selection marker and the artificial promoter can be removed thanks to LoxP sites (Puig *et al.*, 2001). We decided to develop a similar tagging strategy in *E. coli*, and to start with the fluorescent reporter EGFP (figure 69). In the cassette, an artificial promoter is to be provided and so, the *egfp* fused gene is under the arabinose inducible promoter. The PCR

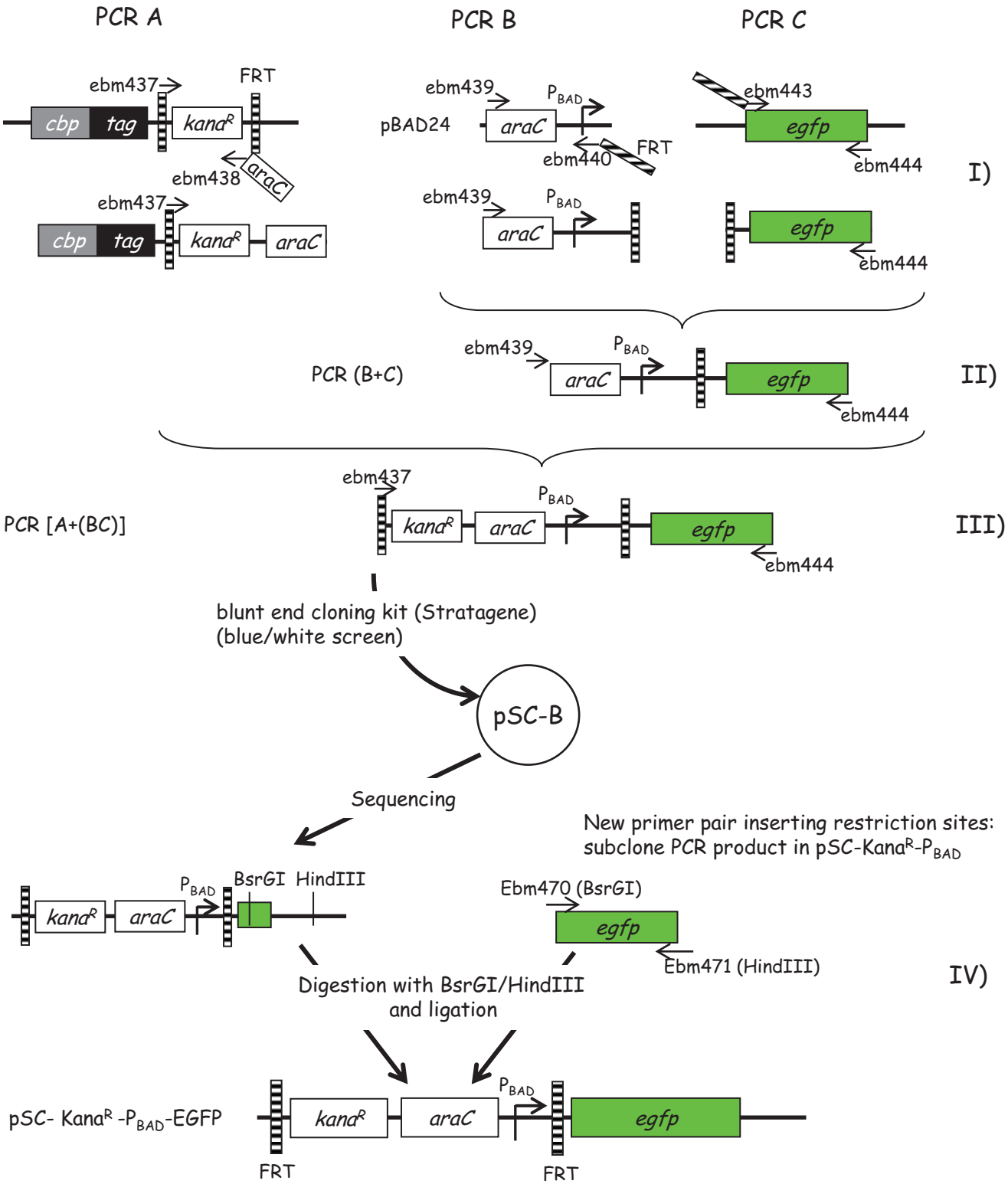

Figure 69: Construction of the cassette for tagging with EGFP at the N-terminus. First, single PCRs (I) were performed: PCR A amplifies the kana^R cassette with FRT flanking site (ebm437/438), PCR B amplifies the PBAD promoter (ebm439/440), and PCR C amplifies the *egfp* sequence (ebm443/444). Then, successive PCRs were used to combine single PCRs A, B, and C in one PCR product (II). The resulting PCR product was then cloned into pSC-B with a blunt end cloning kit (Stratagene®) and a blue/white screen (step III). A clone was obtained with a large part of the sequence of *egfp* missing (IV). However, we took advantage of two restriction sites for BsrGI and HindIII to insert the missing *egfp* sequence in plasmid pSC-Kana^{R}P$_{BAD}$ (pEB1124) using a new primer pair (ebm470/471) and to finally give plasmid pSC-Kana^{R}P$_{BAD}$-*egfp* (pEB1129).

amplified cassette can be inserted in the *E. coli* chromosome using the λRed system. The kanamycin resistance cassette together with the artificial promoter P_{BAD} can be taken out thanks to pCP20 expressing the flipase FLP. In the end, the tagged gene is expressed from its natural promoter preceded by the *egfp* sequence.

To construct the cassette as shown in figure 69, we performed overlapping PCRs. First, I performed single PCRs (step I) to amplify the *kana*^{R} cassette with FRT flanking site (ebm437/438), the P_{BAD} promoter (ebm439/440), and the *egfp* sequence (ebm443/444). Then, successive PCRS were used to combine single PCRs A, B, and C in one PCR product (step II). The resulting PCR product was then cloned into pSC-B with a blunt end cloning kit (Stratagene) and a blue/white screen (step III). Strangely, I obtained a clone with a large part of the *egfp* sequence missing (step IV). However, we took advantage of two restriction sites for BsrGI and HindIII to insert in this plasmid (pSC-*kana*^{R}P_{BAD}; pEB1124) the missing *egfp* sequence using a new primer pair (ebm470/471) and to finally give plasmid pSC-*kana*^{R}P_{BAD}-*egfp* (pEB1129).

We tried to use this cassette for DgkA tagging. Indeed, the N-terminus of DgkA is situated in the cytoplasm, while its C-terminus is situated in the periplasm (Smith *et al.*, 1994). Additionally, the DgkA fusion protein produced from the BACTH pKT25linker-*dgkA* plasmid and tagged at its N-terminus had been shown to be functional (Gully *et al.*, unpublished). As we wanted to perform fluorescent experiments, such as FRET techniques, cytoplasmic tagging was needed. With a primer pair (ebm490/494) designed to tag DgkA at its N-terminus and using the standard protocol according to Datsenko & Wanner (2000), *E. coli* strain EB536 was obtained in which *egfp-dgkA* is under the P_{BAD} promoter. It was first tested whether DgkA fused at its N-terminus with EGFP was functional on LB without NaCl with or without arabinose induction of P_{BAD}. Strain EB536 did not grow on LB without NaCl, like a Δ*dgkA* mutant (figure 70A) (Raetz & Newman, 1978). With induction of P_{BAD} by arabinose, this strain expressing *egfp-dgkA* under the P_{BAD} promoter grew in small colonies, indicating that the protein is not fully functional (figure 70A). We decided to take out the artificial P_{BAD} promoter and the kanamycin resistance cassette by transformation with pCP20. We tested again on LB without NaCl the phenotype of the resulting strain BW25113 °EGFP-DgkA, in which *egfp-dgkA* is under the natural promoter of *dgkA*. This strain formed small colonies on LB-NaCl (figure 70A). The growth of this strain was not significantly better than that of P_{BAD}-EGFP-DgkA upon induction with arabinose. A reason that the growth was not improved despite the presence of the natural *dgkA* promoter, might be that its expression is affected by the remaining FRT site and *egfp* sequence that attenuate transcription signals

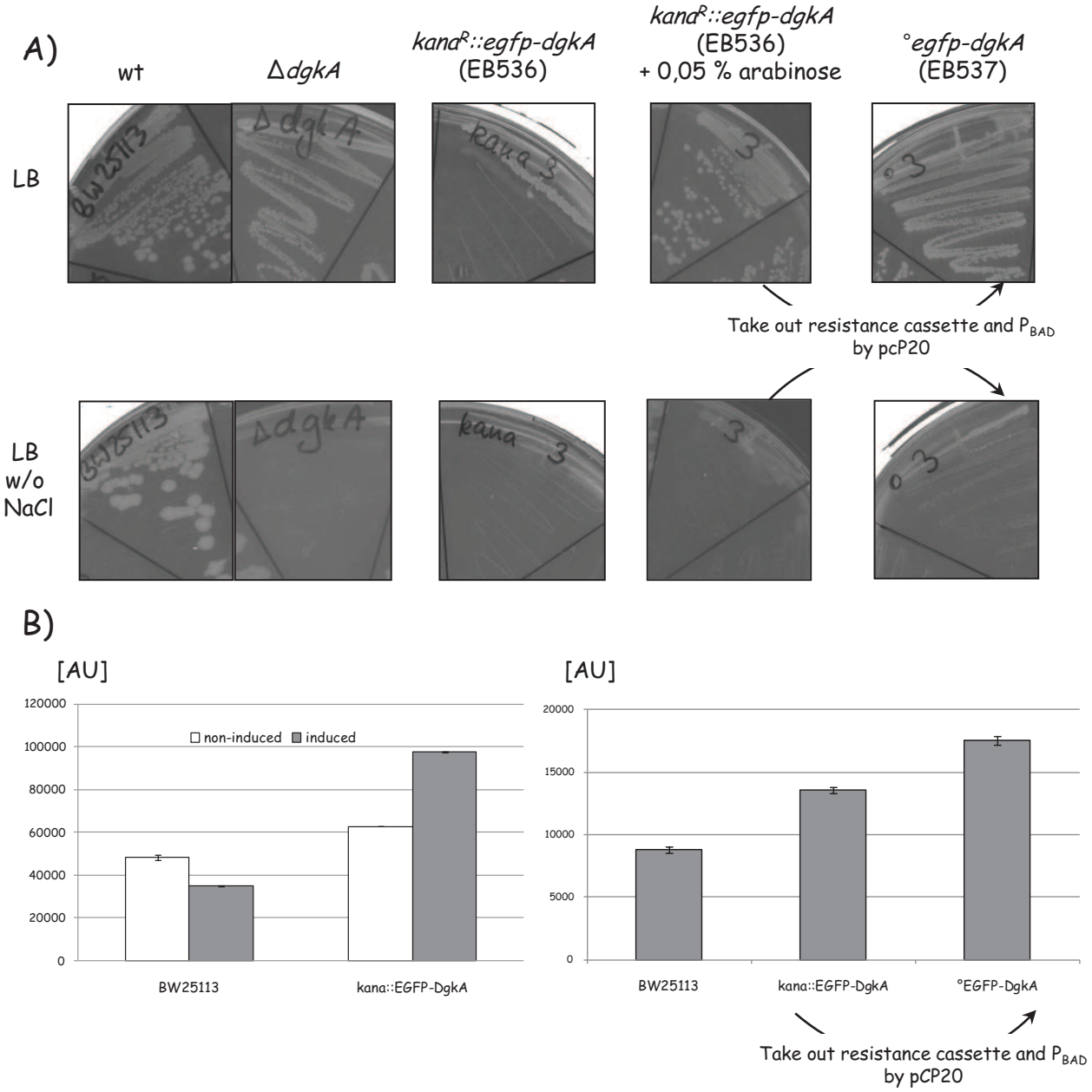

Figure 70: Tagging of DgkA with N-terminal EGFP tag. A) Different strains were shown on plates containing LB or LB without NaCl supplemented or not with 0,05 % arabinose and incubated overnight at 37°C. **B)** Production test of DgkA tagged at its N-terminus: On the left: overnight cultures grown at 37 °C supplemenetd with kanamycin (25 µg/mL) are diluted 1/100 in 3 mL of 2YT without antibiotics, grown at 37 °C till OD_{600nm}= 0,5 and induced with 0,01 % arabinose during 4 h. On the right: overnight cultures grown in 3 mL 2 YT at 37°C with or without kanamycin (25µg/mL). Then, in both cases the cultures are set to OD_{600nm} = 1 in PBS (1X) and using a TECAN M200 the OD_{600nm} and fluorescence (excitation= 485 nm, emission= 530 nm) were measured. AU: arbitrary units for specific fluorescence, corresponding to the ratio fluorescence (in arbitrary units)/OD_{600nm}.

upstream of *dgkA*. Additionally, I was not able to detect the fusion protein EGFP-DgkA in either strains (with P_{BAD} or natural promoter) with an antibody raised against GFP, suggesting that the protein was not produced correctly in fusion with EGFP (data not shown) or that the production level was too low. Finally, I tried to detect the specific fluorescence of the fusion protein using the TECAN plate reader and I could detect a stronger signal in the case of the P_{BAD} promoter upon induction with arabinose compared to the wild type and non-induced culture (figure 70B). After taking out the resistance cassette and the P_{BAD} promoter, I could detect a specific fluorescence signal for EGFP-DgkA under its natural promoter (figure 70B).

In conclusion, the fusion protein DgkA tagged with EGFP was not well produced neither under an artificial nor its natural promoter. Furthermore, these fusion proteins were also not fully functional on LB-NaCl. These results were not convincing at all. Maybe the design of the N-terminal cassette should be refined in order to improve transcriptional signals (avoid FRT scar, a smaller or different tag). Moreover, another protein than DgkA would have been more suitable for testing this N-terminal tagging. Indeed, DgkA is active as a trimer with shared TMSs between the monomers in the inner membrane (Van Horn *et al.*, 2009). Therefore, any tag that affects its correct folding and quaternary structure could affect the enzymatic activity of DgkA. We therefore plan to test tagging with this cassette on other proteins, soluble proteins like ACP or membrane proteins like PgsA.

B. Cellular localization of phospholipid synthesis enzymes

Localization studies were shown for the soluble protein ACP tagged with CBP-EGFP, CBP-EYFP, and CBP-mRFP, and for the inner membrane proteins PlsY and PgsA tagged with CBP-EGFP and CBP-mRFP, respectively (article 1, figure 2). We then wanted to localize systematically all phospholipid synthesis proteins fused to fluorescent reporters (EGFP, EYFP, mRFP) by fluorescence microscopy.

PgsA

W3110 strain producing PgsA-CBP-EGFP presented a weak and diffuse signal all over the cell, which was concentrated in some cells at the poles or membrane (figure 71). In contrast, PgsA tagged with CBP-mRFP was localized in the membrane homogenously (article 1, figure 2B). Again, tagging with mRFP appears to be better than with EGFP. Indeed, PgsA is expected to be localized in the membrane. Topology predictions have determinded 4 to 6 TMSs for PgsA indicating that it is an integral membrane protein. In biochemical studies, the enzymatic activity of PgsA has been found in the inner membrane fraction of purified membranes (Cronan, 2003).

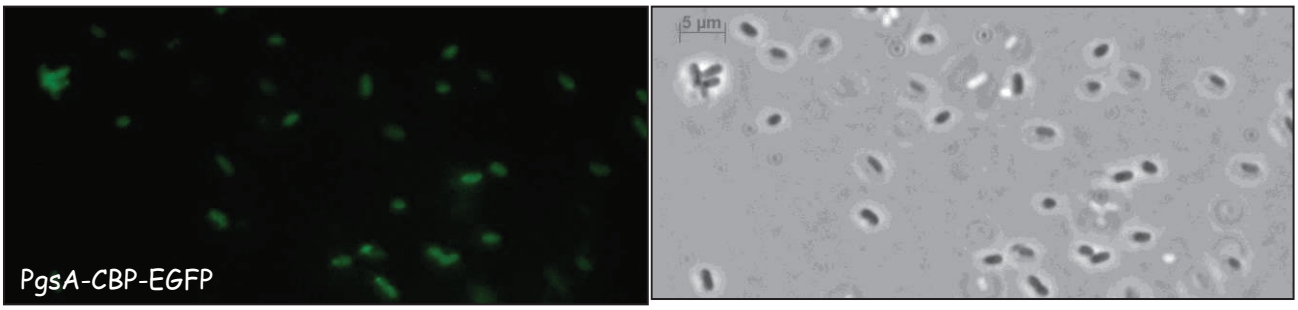

Figure 71: Localization of PgsA-CBP-EGFP (EB264). Late stationary culture was grown at 30 °C in LB supplemented with kanamycin (25 µg/mL) and then harvested by centrifugation, washed once with M9 (1X, pH7,2) and resuspended in fresh M9. The cells were immobilized with 0,25 % agarose on a microscope glass slide. A 100X oil immersion objective was used for the Zeiss Axiovert 200M microscope, with default filters and acquisition settings for GFP: excitation = BP450-490 nm; emission = BP515-565 nm; exposure time = 3600 ms.

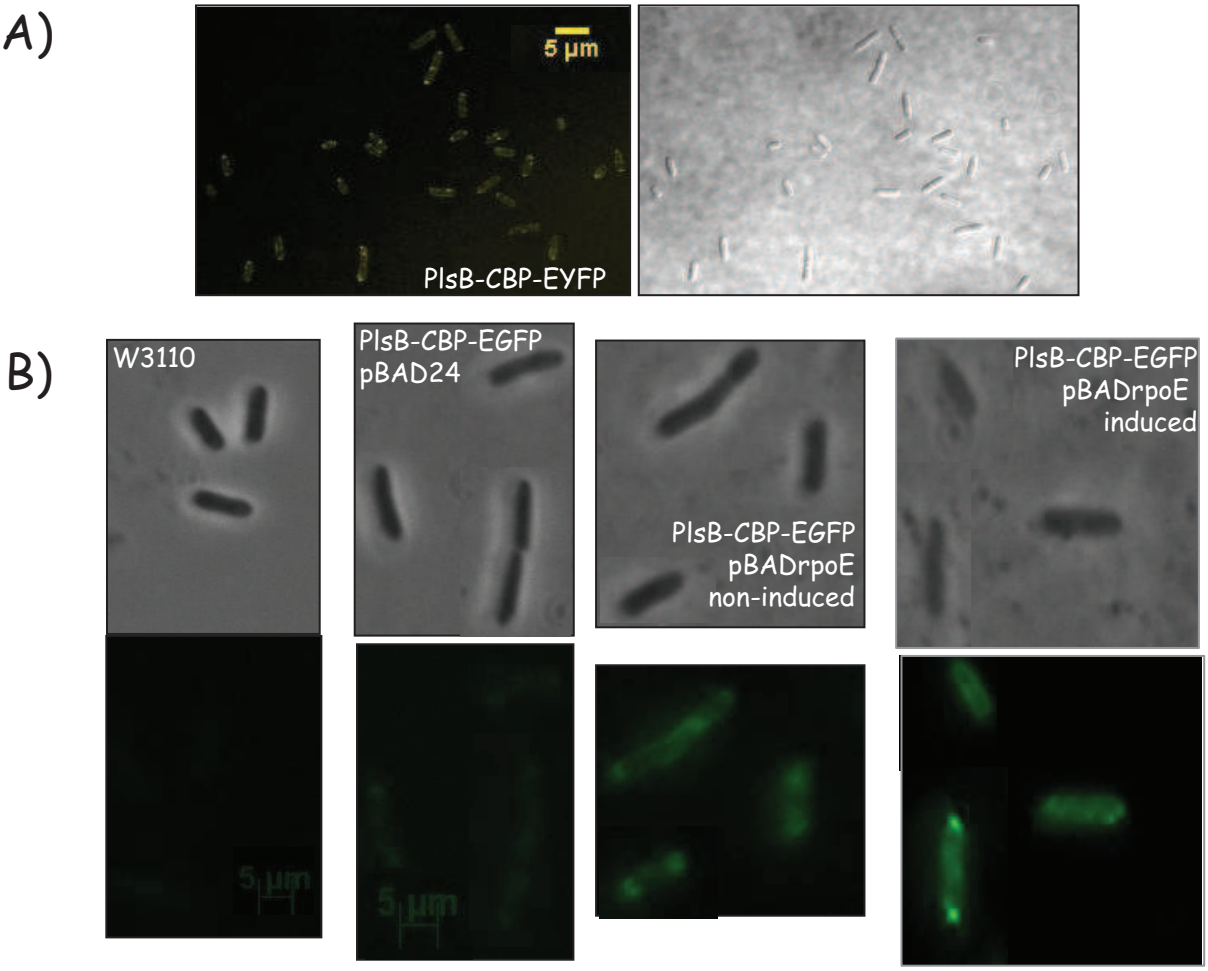

Figure 72: Localization of PlsB-CBP-EYFP (EB300) and PlsB-CBP-EGFP (EB495). A) Late stationary culture was grown at 30 °C in 2YT supplemented with kanamycin (25 µg/mL) and then harvested by centrifugation, washed once with PBS (1X) and resuspended in fresh PBS. The cells were immobilized with using a poly-lysinated microscope glass slide. A 100X oil immersion objective was used, with default filters and acquisition settings for YFP of the confocal Olympus FV1000 microscope: excitation = BP500 ± 20 nm; emission = BP535 ± 30 nm; **B)** Exponentially growing cultures (37 °C in LB supplemented with kanamycin (25 µg/mL), ampicillin (100 µg/mL), and arabinose (0,2 % = induced)) were harvested by centrifugation, washed once with M9 (1X, pH 7,2) and resuspended in fresh M9. The cells were immobilized with 0,25 % agarose on a microscope glass slide. A 100X oil immersion objective was used for the Zeiss Axiovert 200M microscope, with default filters and acquisition settings for GFP: excitation = BP450-490 nm; emission = BP515-565 nm; exposure time for all samples = 1500 ms.

PlsB

In the case of W3110 strain producing PlsB-CBP-EYFP, the fluorescent fusion protein was detected and localized at the membrane as expected (figure 72A). However, the cells presented a filamentation phenotype (figure 64) and they were about double sized compared to the parental strain W3110 for 30 % of the population (figure 72B). Furthermore, the same localization and distribution in spots around the cells was observed for all three PlsB strains tagged with EYFP (figure 72A), EGFP, or mRFP (data not shown). The localization pattern of the PlsB-CBP-EGFP fusion showed a concentration at the poles and its signal became stronger upon induction by RpoE (figure 72B; constant exposure time t = 1500 ms). Although the cells became more filamentous (50 %) with RpoE induction, especially at 37°C compared to 30°C (data not shown), the characteristic spotty patterns of PlsB fusion proteins did not change.

In order to test whether the spots detected by microscopy might correspond to aggregates of the fusion protein PlsB-CBP-EYFP, I tried to solubilize it. It has been shown that PlsB can be easily solubilized using Triton at low concentrations (Green *et al.*, 1981). Therefore, membranes from strain EB300 with or without induction by RpoE were purified and solubilized with 2 % Triton (figure 73). PlsB-CBP-EYFP could be solubilized from the membrane fraction for both conditions, induced or not induced. However, for the RpoE induced PlsB-CBP-EYFP, a band in the insoluble fraction was detected. This insoluble fraction corresponds to aggregates that could not be solubilized. Still, the ratio of aggregates to membrane fraction of PlsB-CBP-EYFP protein seems to be reasonable. Therefore, the spots seen by microscopy does not seem to correspond to aggregates in the membrane and might correspond to a specific localisation of PlsB in the membrane.

It has to be noted that the localization and the characteristic spotty pattern of PlsB tagged with fluorescent fusions was similar for all tested conditions: its aspect did not change with or without induction of RpoE (data not shown), nor did it with expression in trans of *plsB* with the pUT18linker-*plsB* or pKT25linker-*plsB* plasmids (data not shown).

Psd

Strain W3110 producing the fusion protein Psd-EGFP showed a weak specific and diffuse signal (figure 74A). The distribution in the cell suggested a cytosolic localization similar to ACP. However, when the production of Psd-EGFP was induced by RpoE, the fluorescence signal of the fusion protein was located around the cell and was concentrated at the poles and formed spotty patterns (figure 74A). The same behaviour was found for a strain producing Psd-CBP-mRFP (data not shown). Psd fusion proteins induced by RpoE showed a similar

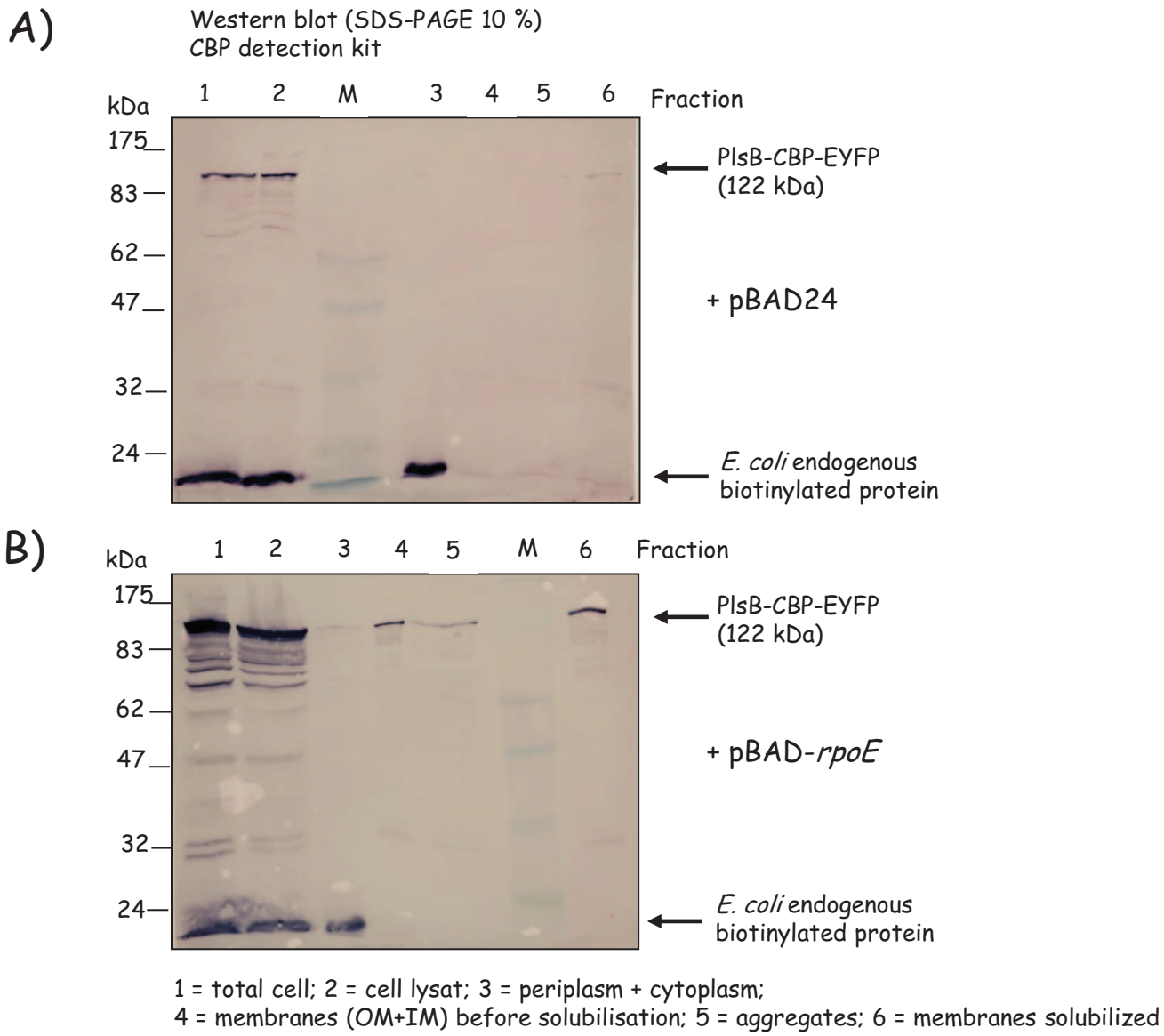

Figure 73: Fractionation and membrane solubilization of strain W3110 producing PlsB-CBP-EYFP (EB300). Strain W3110 producing PlsB-CBP-EYFP was transformed with either **(A)** pBAD24 (pEB227) or **(B)** pBAD-*rpoE* (pEB1102). A 200 mL LB culture supplemented with ampillicin was grown at 37°C, induced at OD_{600nm}= 0,5 for 2,5 h with 0,01 % arabinose. Cells were harvested, lysed by sonication, and membranes were collected by centrifugation (1h at 50 K at 4 °C). The membrane fraction was then incubated 2 h at 4 °C on a wheel with 2 % Triton to solubilize membrane proteins. Samples were prepared for Western blot analysis by heating 5 min at 96 °C in Laemmli buffer (1X) and the Stratagene CBP detection kit was used.
M: molecular weight marker.

localization to PlsB fusion proteins. So, it seems that the induction with RpoE changes the localization of Psd tagged with EGFP or mRFP, which then resembles to PlsB localization. Another possibility is that the induction leads to aggregation of the fusion protein.

We wanted to verify if Psd-CBP-mRFP formed aggregates in the membrane by making a solubilization test. The fusion protein Psd tagged with CBP-mRFP could be detected in a Western blot analysis using the Affinity® CBP protein fusion detection kit (Stratagene) (figure 75). We can assume that Psd tagged with CBP-mRFP is functional because the fusion protein autocleaves its polypeptide post-translationally at the Ser253, producing an α-subunit tagged with CBP-mRFP and an αβ-subunit (uncleaved). Psd tagged with CBP-mRFP was present in the membrane fraction and could be solubilized from membranes with detergent (Triton 2%) (figure 75). In the total cell extract both the cleaved α-CBP-mRFP and the uncleaved Psd-CBP-mRFP were detected. The α-subunit was detected in the solubilized membrane fraction, while the uncleaved Psd-CBP-mRFP was detected in the aggregate fraction. The majority of fusion protein was cleaved correctly and the ratio of aggregates (uncleaved Psd-CBP-mRFP) to membrane fraction of α-CBP-mRFP protein seems to be reasonable. In conclusion, the spots seen by microscopy might correspond to a specific localisation of Psd in the membrane.

psd is co-transcribed with *yjeP* (Rhodius *et al.*, 2006), a gene of unknown function homologous to mechanosensitive channels (Touzé *et al.*, 2001). The fusion protein could only be detected upon induction by RpoE (cf. § III D). Using a fluorimeter, its specific fluorescence could be measured; however, the signal was much weaker than for Psd tagged strains. Strain W3110 producing the fusion protein YjeP-CBP-EGFP was observed by fluorescence microscopy. However, an exact localization was hard to determine due to the low signal (figure 74B).

PlsC and PlsX

Strain W3110 producing the fusion protein PlsC-CBP-EGFP showed a quite low signal (figure 76). A work using immunolocalization of phospholipid synthesis enzymes in *B. subtilis* allowed the visualization at the membrane of PlsX and PlsC (Paoletti *et al.*, 2007). For fusion proteins PlsX-CBP-EGFP/-EYFP the signal was unfortunately also too low to detect (data not shown).

DgkA

Strain BW25113 producing DgkA tagged with EGFP at the N-terminus under the arabinose inducible P_{BAD} promoter presented a signal that was too low (with or without induction by arabinose) to exactly localize the fusion protein by fluorescence microscopy (data not shown).

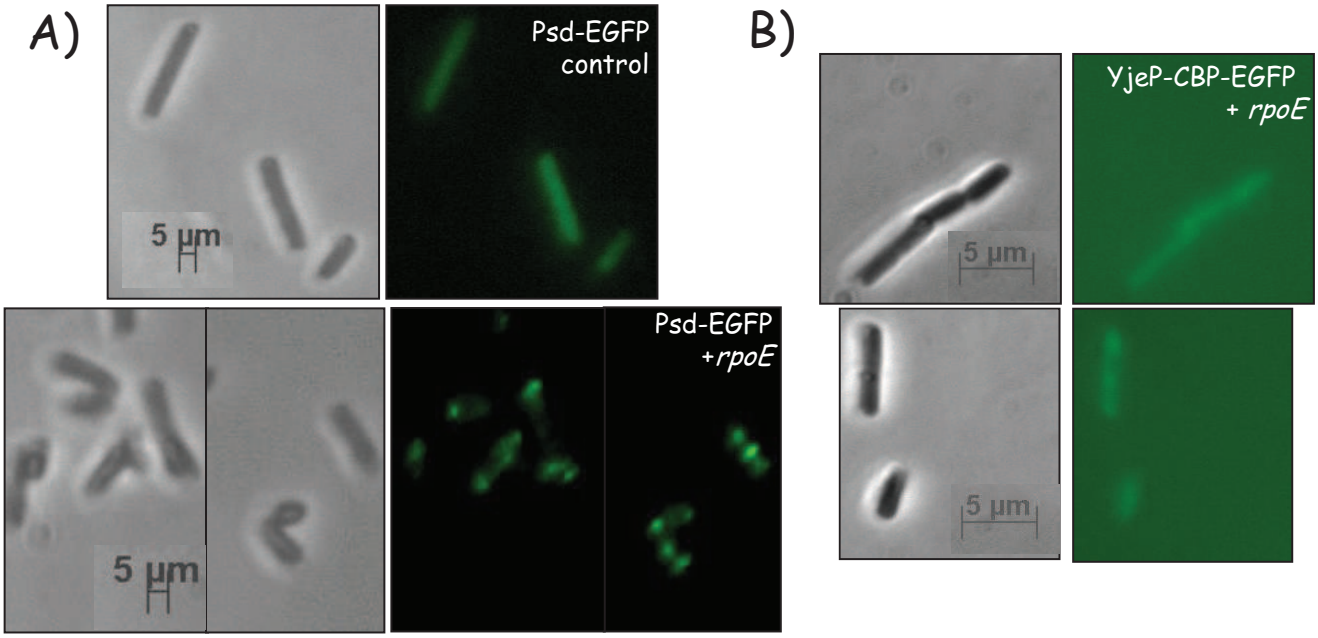

Figure 74: Localization of Psd-EGFP (EB531) and YjeP-CBP-EGFP (EB521). A) Late stationary growing cultures (30°C in LB supplemented with kanamycin (25 µg/mL) and ampicillin (100 µg/mL)) harboring plasmids pBAD24 (= control; pEB227) or pBAD-*rpoE* (pEB1102) were induced with 0,01 % arabinose. Cells were harvested by centrifugation, washed once with M9 (1X, pH 7,2) and resuspended in fresh M9. The cells were immobilized with 0,25 % agarose on a microscope glass slide. A 100X oil immersion objective was used for the Zeiss Axiovert 200M microscope, with default filters and acquisition settings for GFP: excitation = BP450-490 nm; emission = BP515-565 nm; exposure time for non-induced = 3000 ms; for induced = 700 ms. **B**) Late stationary growing cultures (30°C in LB supplemented with kanamycin (25 µg/mL) and ampicillin (100 µg/mL) harboring plasmid pBAD-*rpoE* were induced with 0,01 % arabinose. Cells were harvested by centrifugation, washed once with M9 (1X, pH 7,2) and resuspended in fresh M9. The cells were immobilized with 0,25 % agarose on a microscope glass slide. A 100X oil immersion objective was used for the Zeiss Axiovert 200M microscope, with default filters and acquisition settings for GFP: excitation = BP450-490 nm; emission = BP515-565 nm; exposure time = 2000 ms.

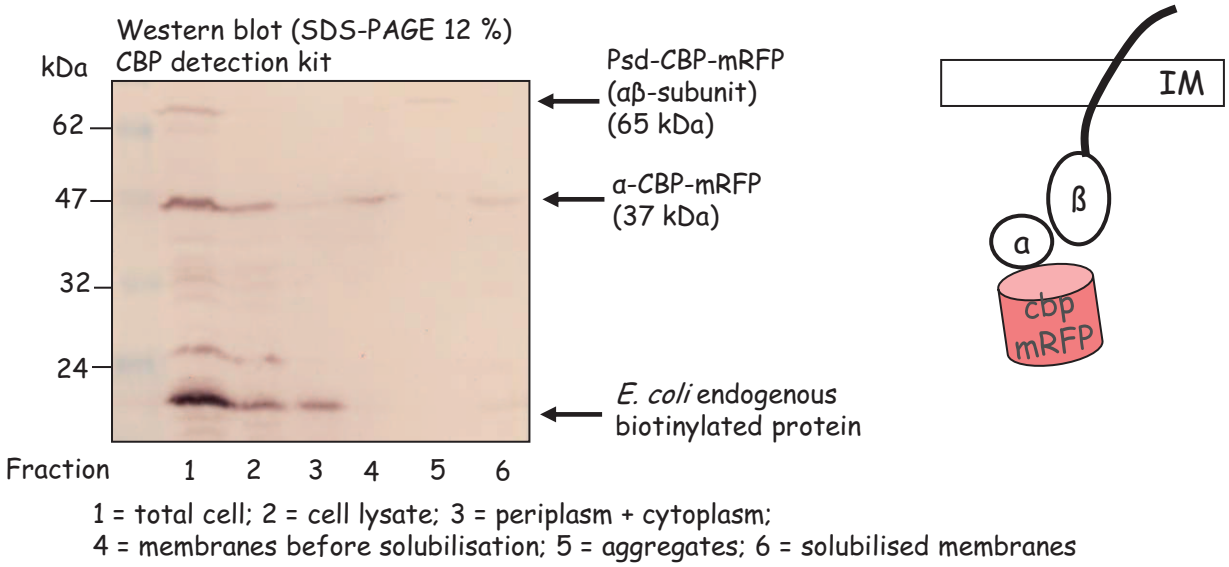

Figure 75: Psd-CBP-mRFP (EB499) production. A) *E. coli* strain W3110 producing Psd-CBP-mRFP transformed with pBAD-*rpoE* (pEB1102) was grown in 200 mL LB culture at 37°C till OD_{600nm}= 0,8 and expression of *rpoE* was induced for 2 h by adding 0,01 % arabinose. Cellular fractionation was performed by sphaeroplast preparation (according to Isnard *et al.*, 1994).

The same was the case for strain BW25113 producing °EGFP-DgkA, where *egfp-dgkA* is under the physiological *dgkA* promoter (figure 77).

To conclude, different phospholipid synthesis enzymes could be localized thanks to fluorescent fusion proteins that were detected using fluorescence microscopy: PgsA and PlsY presented membrane localization. PlsB and Psd (upon induction by RpoE) also showed membrane localization, with a concentration at the poles and/or a spotty pattern. For the other proteins of the phospholipid synthesis (PlsX, PlsC, and DgkA) the production level was too low to detect a specific signal. This was certainly due to the low physiological expression level from their natural promoter. However, PlsB formed partly aggregates and Psd only showed spotty pattern upon induction with RpoE. Furthermore, PlsB and Psd fusion proteins were induced by RpoE and presented this characteristic spotty pattern, which is not due to aggregation of PlsB and Psd fusion protein.

Paoletti *et al.* (2007) used immunolocalization to detect PlsC and PlsX with antibodies raised against these two proteins. We chose to use fluorescent reporters under physiological expression of the corresponding tagged gene, because thus there is no need for specific antibodies for each protein. This was a technical advantage for our global approach to localize all phospholipid synthesis enzymes, which was, however, inconvenient due to low signal and functionality problems of the physiological fusion proteins.

C. Topology of phospholipid synthesis enzymes

Except for PlsY (Lu *et al.*, 2007), DgkA (Smith *et al.*, 1994) and PgpB (Touzé *et al.*, 2008) (cf. Introduction § IIIA), the topologies of the phospholipid synthesis enzymes are only inferred from TMS predictions. In some cases (such as CdsA), combining TMS predictions and knowledge of the localization of the C-terminus (Daley *et al.*, 2005) give a good topology model. However, in other cases (PgsA, PlsC), the predictions vary very much from one webserver to another and are therefore not clear. It is important for us to know the exact topology, or at least the positions of the N- and C-terminus, in order to choose to which extremities the tag must be fused for v-TAP, FRET, or BACTH. In order to determine the topologies we needed to know, we chose to use a dual reporter consisting of both *E. coli* alkaline phosphatase (AP, residue 22-472) and the α-fragment of the β-galactosidase (BG, residue 4-60), fused at various positions in the sequence of the membrane protein (Alexeyev & Winkler, 1999; Karimova *et al.*, 2009). The sequence is cloned upstream the two sequences coding for AP and BG fragments in pKTop, a low copy plasmid carrying the resistance to kanamycin (figure 78A). The principle of the dual reporter lies in the fact that AP is only

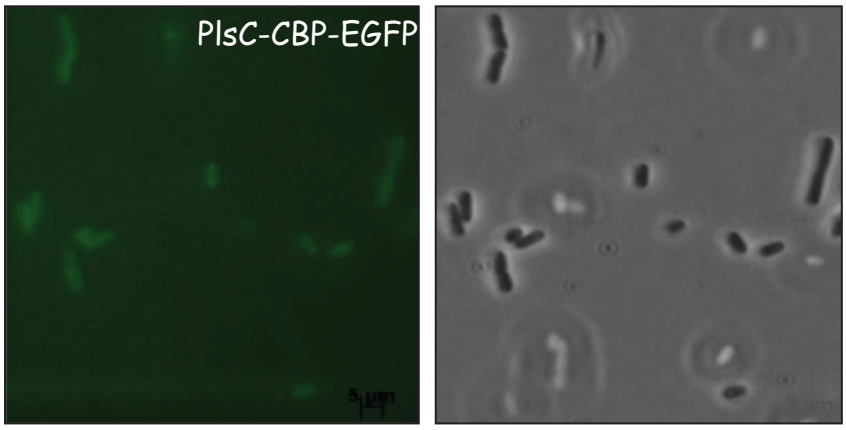

Figure 76: Localization of PlsC-CBP-EGFP (EB417). Strain W3110 PlsC-CBP-EGFP. Exponentially growing cultures (30°C in LB supplemented with kanamycin (25 µg/mL). Cells were harvested by centrifugation, washed once with M9 (1X, pH 7,2) and resuspended in fresh M9. The cells were immobilized with 0,25 % agarose on a microscope glass slide. A 100X oil immersion objective was used for the Zeiss Axiovert 200M microscope, with default filters and acquisition settings for GFP: excitation = BP450-490 nm; emission = BP515-565 nm; exposure time = 2900 ms.

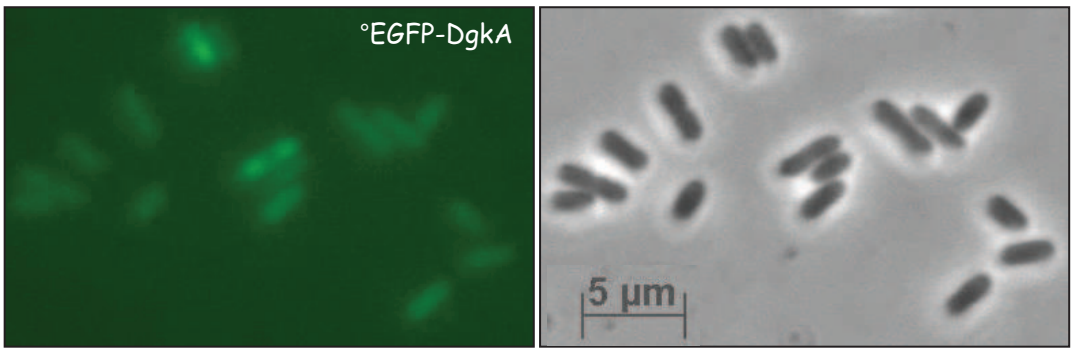

Figure 77: Localization of EGFP-DgkA produced in strain BW25113 (EB537). Strain BW25113 °EGFP-DgkA exponentially growing cultures (30°C in LB supplemented with kanamycin (25 µg/mL). Cells were harvested by centrifugation, washed once with M9 (1X, pH 7,2) and resuspended in fresh M9. The cells were immobilized with 0,25 % agarose on a microscope glass slide. A 100X oil immersion objective was used for the Zeiss Axiovert 200M microscope, with default filters and acquisition settings for GFP: excitation = BP450-490 nm; emission = BP515-565 nm; exposure time = 3000 ms.

active in the periplasm and BG only in the cytoplasm. On dual indicator plates supplemented with two different chromogenic substrates Xphos (2-Dicyclohexylphosphino-2′,4′,6′-triisopropylbiphenyl) and RedGal (6-Chloro-3-indolyl-β-D-galactoside), protein fusions with their C-terminus located in the cytoplasm appear red (RedGal, BG activity), while protein fusions with their C-terminus located in the periplasm appear blue (Xphos, AP activity) (figure 78B). For AP and BG activity assays of the protein fusions, *E. coli* strains capable of α-complementation (like TG1 or DH5α) are used as a host strain.

It was necessary to know the topology of **PgsA**, especially the position of the C-terminus, as it was a candidate for the v-TAP technique. In the v-TAP protocol, we use "inside-out" membrane vesicles, in which the cytosolic side of the inner membrane faces the exterior of the vesicle. The prediction of PgsA topology is clearly not well defined. Depending on topology prediction programmes, 3 (TopPred, Sosui) or 4 (TMHMM, DAS) TMSs are predicted at various positions with the C-terminus in the cytoplasm (Daley *et al.*, 2005). We decided to construct 9 truncated fusions of PgsA with AP-BG after residue 37, 51, 61, 85, 107, 127, 146, 166, or 183 (full length). Then, *E. coli* strain DH5α was transformed with the resulting plasmids and plated on dual indicator plates. Residues 37, 85, and 166 showed a blue coloration indicating AP activity and a periplasmic location (figure 79A). However, the fusion of residue 37 to AP-BG not always showed the blue colour as seen in figure 79A (on the right), suggesting an intermediate (= membrane) position. All the other residues showed a red coloration indicating BG activity and a cytoplasmic location.

We propose a topology model (figure 79B) in which PgsA has 6 TMSs with the N- and C-terminus facing the cytoplasm. The determined position of the C-terminus is in agreement with the study of Daley *et al.* (2005). However, these 6 TMSs are in contrast with the bioinformatic programmes that predicted 3 or 4 TMSs. This difference could be explained by the fact that we found 2 TMSs, whereas different programmes predicted 1 big TMS in different regions. Furthermore, a point mutation at residue 60 (*pgsA*3 = Thr60Pro) lowered the enzymatic activity of PgsA *in vitro* (Usui *et al.*, 1994), suggesting that this residue is part of the catalytic site. This result is in agreement with the cytoplasmic localization of residue 60 in our model and the knowledge that the active site ought to be localized at the inner membrane facing the cytoplasm (Cronan, 2003).

Topology prediction programmes predicted 3 TMSs for **PlsC** with its C-terminal acyltransferase domain in the cytoplasm. However, these TMS predictions were very uncertain. The topology of PlsC was of interest for us, as it could be a model, or compared to topologies of other acyltransferase homologues, such as the GPAT PlsB and the LPAAT

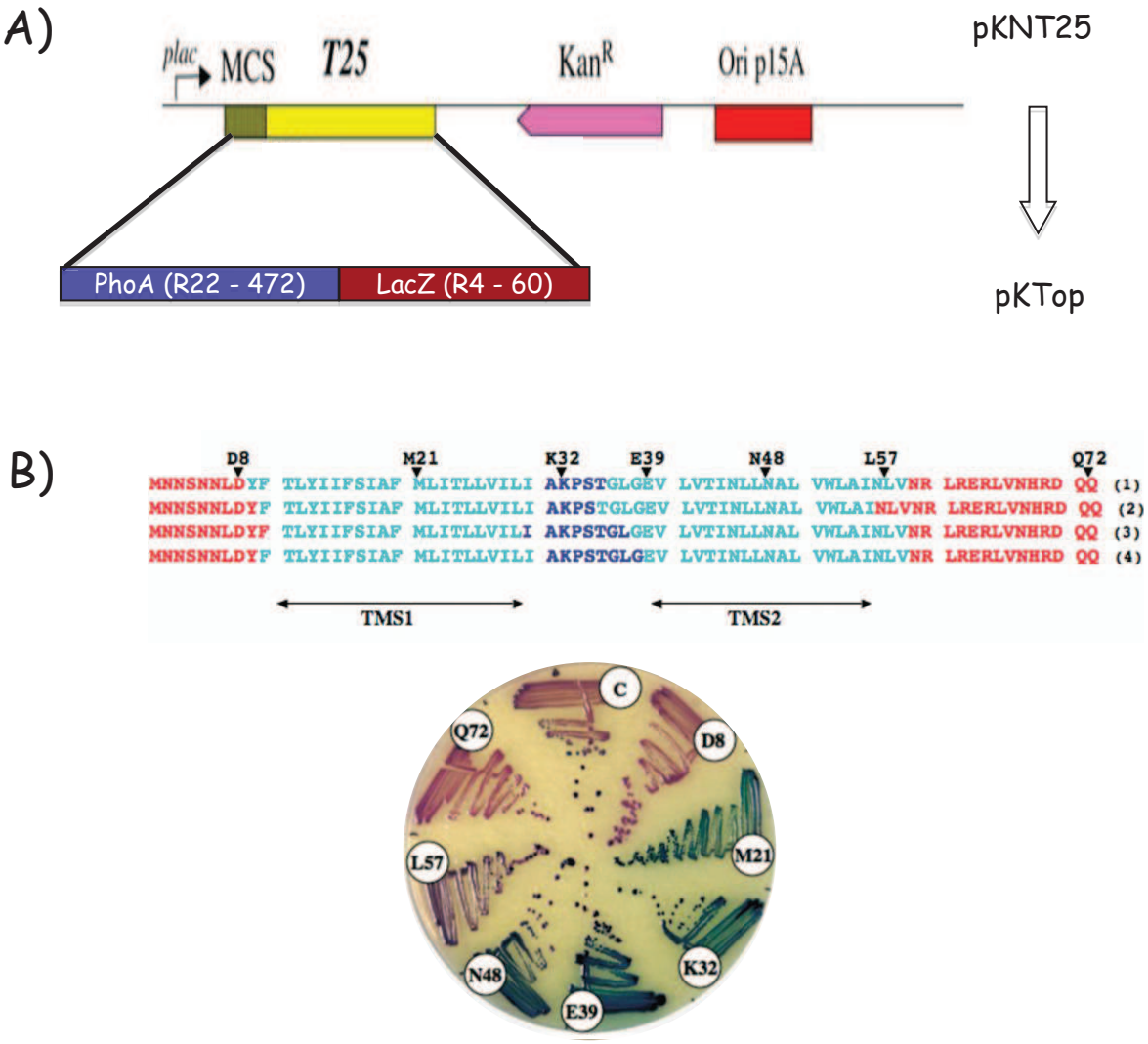

Figure 78: Dual reporter system for the determination of membrane protein topology (Karimova *et al.*, 2009). A) Cloning of *phoA* (residues 22-472) and *lacZ* (residues 4-60) sequences in pKNT25 to give pKTop (pEB1121), a low copy plasmid with a dual reporter carrying the resistance to kanamycin **B)** YmgF topology analysis as an example. On the top: *In silico* models that predict the membrane topology of YmgF. TMS: transmembrane segment. The small black arrowheads indicate the positions of different fusions with the AP-BG reporter. On the bottom: Experimental determination of YmgF membrane topology in *E. coli* DH5α cells. Blue coloration of the colonies (high AP activity) indicates a membrane or periplasmic location of the fusion point. Red coloration of the colonies (high BG activity) indicates cytosolic location of the fusion point. Control cells (*E. coli* DH5α/pKTop) are indicated by the C label.

YihG. Finally, the position of the C-terminus of PlsC has not been determined in the study by Daley *et al.* (2005) because there was no clear TMS prediction. Therefore, we wanted to determine its topology experimentally.

We constructed 8 truncated fusions of PlsC with AP-BG after residue 30, 70, 126, 208, 185, and 246. Transformation was performed in DH5α and ΔPhoA° to test if in ΔPhoA° the result would be clearer, as this strain is less affected in growth than DH5α. But there was no big difference between DH5α and ΔPhoA°, and it has to be noted that growth was strongly affected in both strains for most constructs, except for fusions at residues 30 and 70, and interfered therefore with the analysis of the results. Truncated PlsC at residues 30 and 70 showed blue and red colour, respectively, indicating periplasmic and cytoplasmic location (figure 80A). Thus, we propose a topology model of PlsC with 2 TMSs and its C-terminus as well as its catalytic domain (residues 73-78) in the cytoplasm (figure 80B).

Interestingly, the crystal structure of the soluble catalytic domain of glycerol-3-phosphate-acyltransferase (GPAT) from the squash *Cucurbita moschata* corresponding to Pfam01553 is available (Turnbull *et al.*, 2001), suggesting that domain Pfam01553 is situated integrally in the cytoplasm. Furthermore, a study on mitochondrial rat liver glycerol-3-phosphate-acyltransferase (GPAT) proposed a topology model that contains 2 TMSs with the active site in the N-terminal domain facing the cytosolic face of the outer mitochondrial membrane (Gonzalez-Baro *et al.*, 2001). This suggests in general that it is the N-terminal extremity with the catalytic site of GPAT acyltransferases that locates in the cytoplasm, while it is the C-terminal extremity with the catalytic site of LPAAT acyltransferases locates in the cytoplasm.

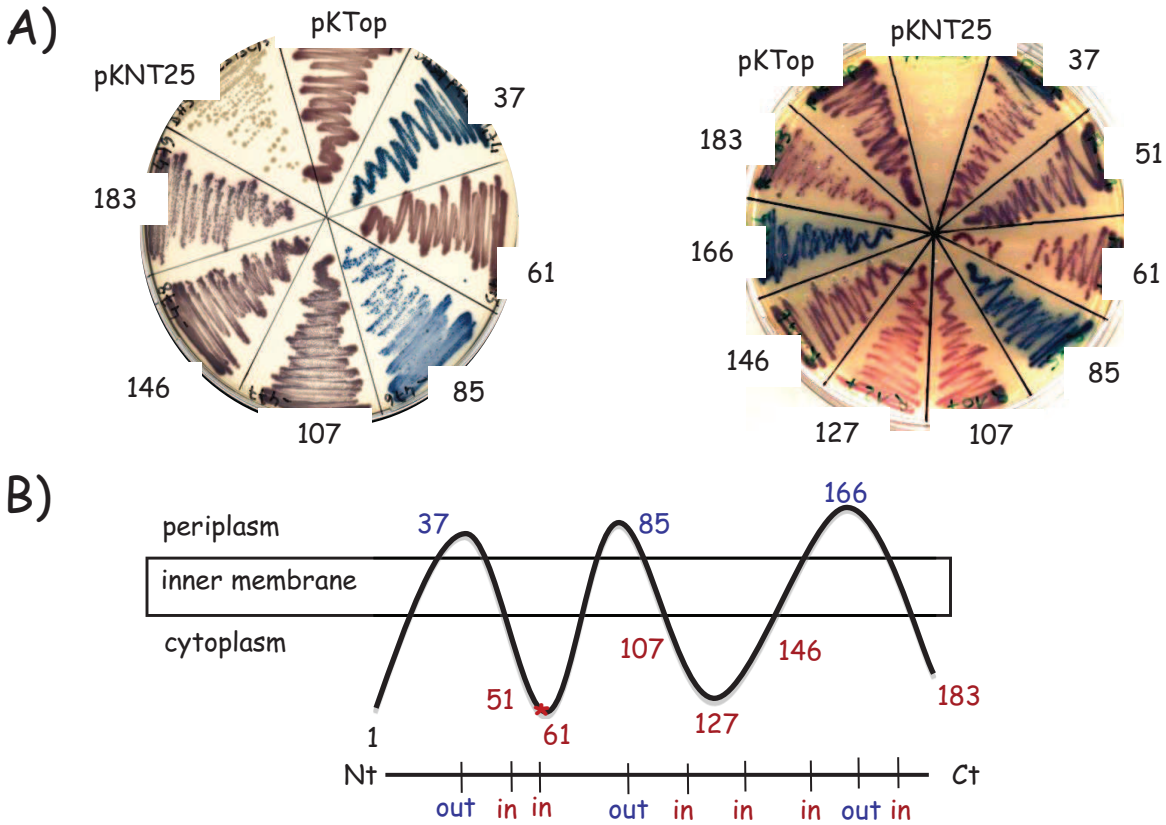

Figure 79: Topology of PgsA in the inner membrane. A) AP-BG fusion activity: DH5α cells were grown overnight at 37°C on dual indicator plates containing LB agar with 5-bromo-4-chloro-3-indolyl phosphate disodium salt (X-Phos (80 µg/ml), for AP activity) and 6-chloro-3-indolyl-β-D-galactoside (Red-Gal (100 µg/ml), for BG activity) as indicators and IPTG (1 mM), and 50 µg/ml kanamycin. Plasmid pKNT25 is a negative control that has no activity. Blue coloration of the colonies (PA activity) indicates a membrane or periplasmic location. Red coloration of the colonies (BG activity) indicates cytosolic location. **B)** Topology model of PgsA in the inner membrane. The red star indicates the point mutation Thr60Pro in mutants strain *pgsA*3 (Usui *et al.*, 1994), which leads to decreased PgsA activity. Numbers correspond to amino acid residue. Nt: N-terminus; Ct: C-terminus.

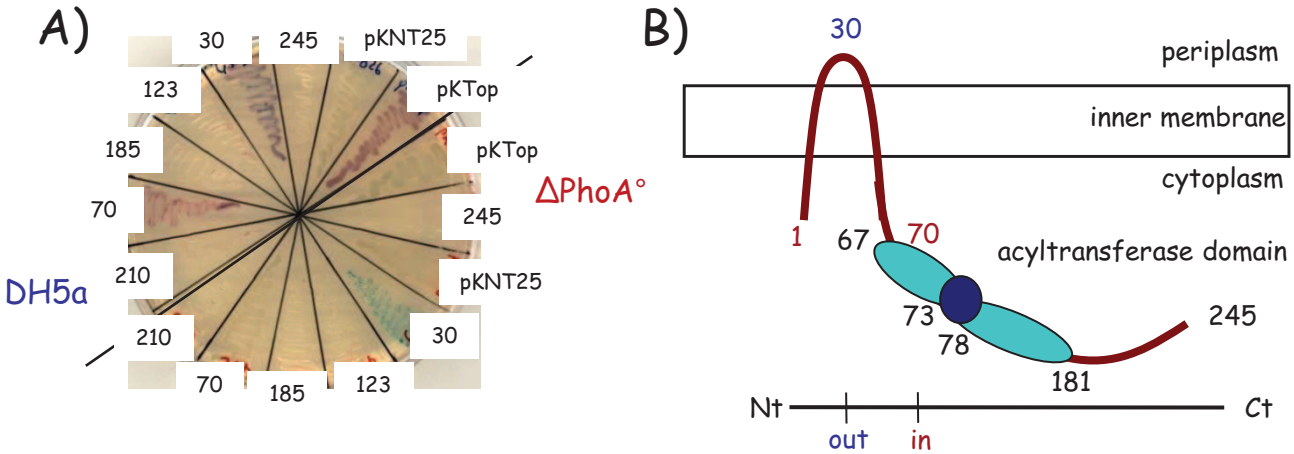

Figure 80: Topology model of PlsC in the inner membrane. A) AP-BG fusion activity: Cells were grown overnight at 37°C on dual indicator plates (see composition figure 79). Plasmid pKNT25 is a negative control that has no activity. **B)** Topology model of PlsC in the inner membrane with 2 TMSs. The blue circle indicates the catalytic site (residues 73-78) with the motif of the acyltransferase domain. Numbers correspond to amino acid residue. Nt: N-terminus; Ct: C-terminus.

II. PURIFICATION OF PHOSPHOLIPID BIOSYNTHESIS ENZYMES BY THE TAP METHOD

In our laboratory, interactions between the enzymes of the phospholipid synthesis pathway have been tested systematically using the BACTH method. The high number of identified interactions suggested the existence of an interaction network within the inner membrane (Gully & Bouveret, 2006). However, the BACTH method presents some limits: generation of wrong positives and wrong negatives as well as the limitation to test interactions of proteins only two by two and not protein complexes involving more than two interacting partners. The question was if these numerous interactions found by BACTH had a physiological relevance. One objective of my thesis was therefore to validate these protein interactions and a possible interaction network of the phospholipid synthesis enzymes by another technique, such as the TAP. The TAP purification (Tandem Affinity Purification) has the advantage that protein complexes can be isolated in physiological conditions (Rigaut *et al.*, 1999). This technique has been set up in the laboratory of Dr. Séraphin in the yeast *Saccharomyces cerevisae* (Rigaut *et al.*, 1999) and has since then permitted the description of the full interactome of yeast (Gavin *et al.*, 2002; Gavin *et al.*, 2006). In *E. coli*, an interaction network of conserved and essential proteins has been found by the TAP technique (Butland *et al.*, 2005; Babu *et al.*, 2009). This technique is a powerful tool to purify native and functional protein complexes in physiological conditions. Thanks to the native purification and elution conditions during the whole process, the members of a complex can be identified and they can be used further for *in vitro* studies. The identity of the different partners of the protein used as the bait is determined by mass spectrometry, which requires the knowledge of the genome of the organism studied.

When I arrived in the laboratory of Dr. Emmanuelle Bouveret, the Tandem Affinity Purification had been set up in *E. coli* on Acyl Carrier Protein. ACP is the central co-factor of lipid biogenesis and a very abundant soluble protein (Gully *et al.*, 2003). Among the numerous partners of ACP identified by this technique, were found PlsB and PssA that are involved in phospholipid synthesis (Gully *et al.*, 2003). Together with the BACTH results, this strengthened the evidence for a physical connection of the fatty acid and phospholipid synthesis enzymes.

However, the TAP technique can only be used on soluble protein complexes. In order to be able to study the phospholipid enzymes, we needed to set up a new technical approach, the vesicle Tandem Affinity Purification (v-TAP), a variant of the TAP method.

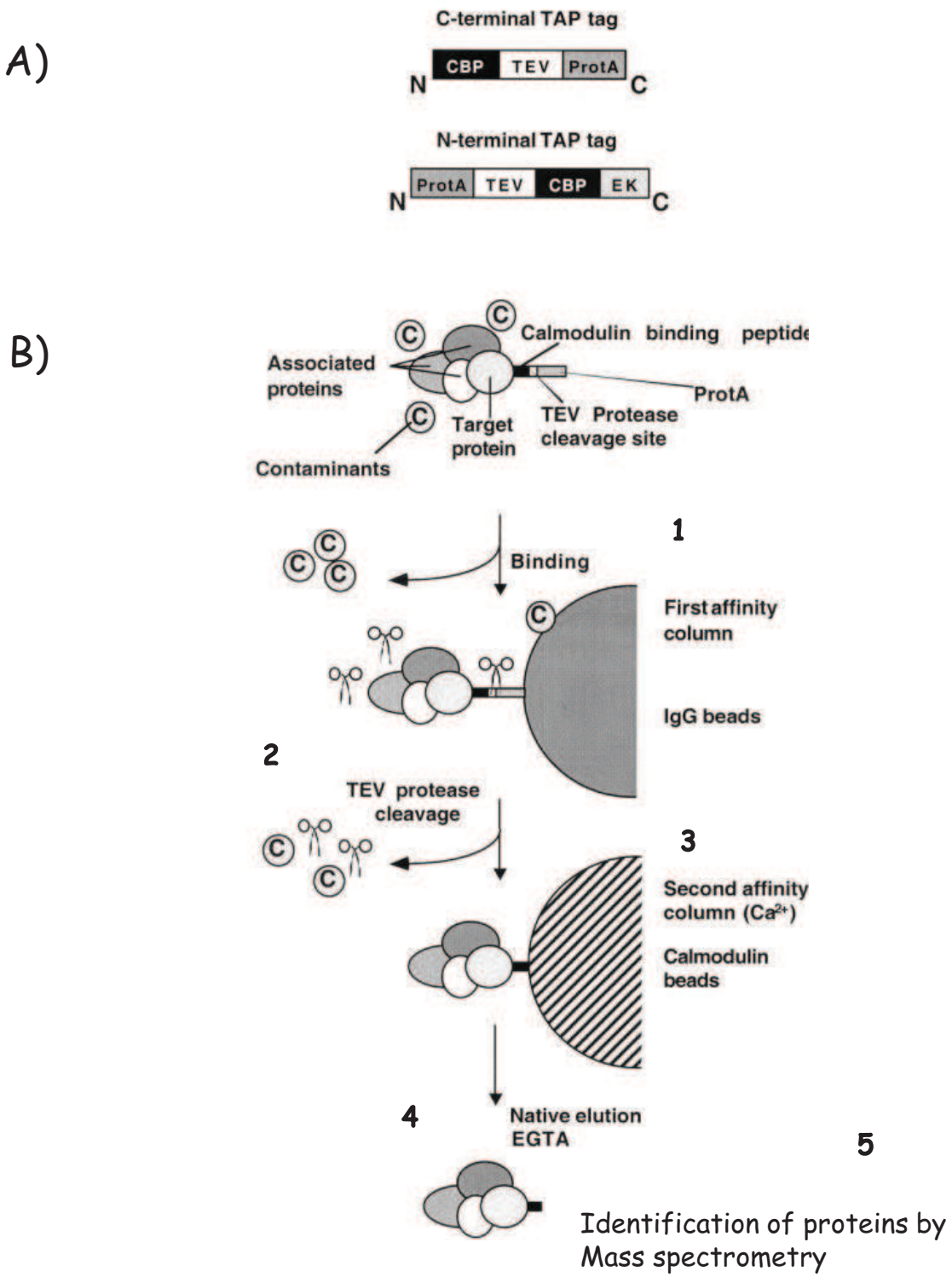

Figure 81: The TAP purification (Puig *et al.*, 2001). A) Schematic representation of the C- and N-terminal TAP tags. **B)** Overview of the TAP purification strategy for soluble complexes.

A. Rational for a native membrane complex purification by affinity: the v-TAP method

A1. The TAP method in E. coli

The TAP method was first developed in yeast for soluble complexes (Rigaut *et al.,*1999) and has later been set up in *E. coli* (Gully *et al.*, 2003). TAP is an affinity purification method based on the TAP tag (20 kDa), formed itself by two tags in tandem, two IgG binding domains of the protein A of *Staphylococcus aureus* (ProtA), permitting a purification on IgG beads, and the CBP tag permitting a purification on Calmodulin beads in the presence of calcium (Puig *et al.*, 2001). The two tags are separated by a TEV (tobacco etch virus) cleavage site (figure 81A). The ProtA tag, the TEV cleavage site, and the CBP tag are separated by flexible linker regions. The TAP tag can be fused either at the N-terminal (ProtA-TEV-CBP) or the C-terminal (CBP-TEV-ProtA) extremities of a protein. Ideally, the gene coding for the bait protein is fused to the TAP tag sequence on the *E. coli* chromosome, which assures a physiological expression of the fusion protein. For this purpose, plasmid pJL72 containing the TAP and a kanamycin resistance cassette embraced by FRT sites can be used in *E. coli* and related bacteria (Zeghouf *et al.*, 2004). In this method, *E. coli* strain DY330, which contains a chromosomal λRed recombination system, is used to place the tag at the C-terminal of a target protein on the chromosome (Zeghouf *et al.*, 2004). However, fusion proteins that are tagged at their N-terminus with the TAP tag and still under the control under of their endogenous promoter cannot be easily produced. In any case, the gene coding for the protein fusion with the TAP tag at its N- or C-terminus can also be (over-)expressed using a plasmid.

A protein extract is prepared from a 500 mL – 1 L culture of *E. coli* strains producing the fusion protein. The purification consists of two successive affinity steps separated by a TEV cleavage step (figure 81B). First, the ProtA affinity tag of the fusion protein X (X-CBP-TEV-ProtA) binds to the IgG beads (**1**). Then, the fusion protein X-CBP is eluted in a mild and native manner from the IgG beads by the TEV protease that cleaves the TAP tag between CBP and ProtA (**2**). Now, the elution is composed of the fusion protein X-CBP and its interacting partners, as well as contaminant proteins and the TEV protease. The CBP affinity tag of the fusion protein X (X-CBP) then binds to Calmodulin beads depending on Ca^{2+} (**3**), from which it is eluted in mild and native conditions using EGTA (ethyleneglycol-bis(ß-aminoethyl ether) (**4**). EGTA chelates Ca^{2+} ions and hence, releases the bond protein. Finally,

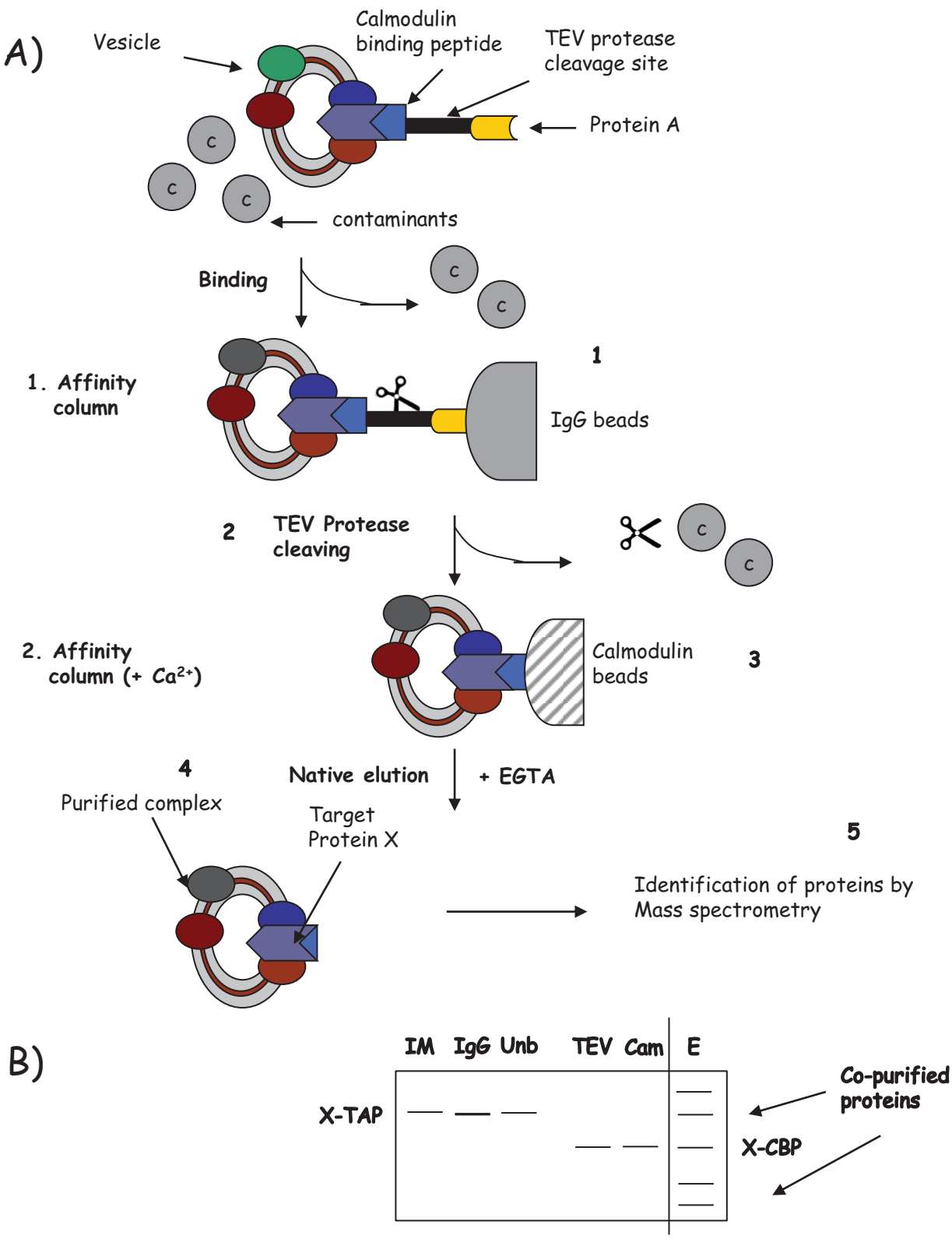

Figure 82: The TAP purification (Puig *et al.*, 2001). A) Overview of the TAP purification strategy for complexes in vesicles. (see text for details) **B)** Theoretical result of a TAP purification with (far) Western blot and Coomassie Blue staining: IM: inner membrane, IgG: bound to IgG beads, Unb: flowthrough of IgG coloumn, TEV: TEV cleavage, E: elution step (Coomassie Blue staining). The antibody used to detect the fusion protein tagged with TAP is PAP that recognizes ProtA. After the TEV cleavage step, the fusion protein with CBP can only be detected with the CBP detection kit (Stratagene).

the fusion purified proteins are analyzed by Western blot and/or protein staining and the identity of these proteins is determined by mass spectrometry (**5**).

The advantages of the TAP purification technique are that new protein interactions can be identified under native and physiological conditions. Furthermore, the TAP technique can be used in any organism. However, this protocol can be only used for soluble proteins. To cope with this limitation, solubilization protocols have been set up especially for membrane protein purification using the TAP tag (Gavin *et al.*, 2006). However, as we wanted to stay in conditions as physiological as possible, we chose to develop a novel technique without using detergent.

A2. TAP method for membrane vesicles (v-TAP)

In order to resolve the problem of membrane complex purification, we designed a new method called v-TAP, in which membrane protein complexes are enriched with the tagged membrane protein in their native environment. The purification steps for the v-TAP are in principle the same as for the soluble TAP, but the purification is performed on inner membrane vesicles containing the TAP-tagged protein X and its possible interacting partners (figure 82). The membrane vesicles are prepared by the following procedure (figure 83): After breaking the cells with a French Press (**1**), inner membranes are purified using differential ultra-centrifugations (**2**). These vesicles are "inside-out", that means that the cytoplasmic side of the inner membrane now faces the outside. Homogenous membrane vesicles are prepared by successive passages through an extruder (**3**) (cf. Materials & Methods). The extruder was designed for the pharmaceutical industry to prepare liposomes of defined size. In the laboratory, we have polycarbonate membranes with different pore sizes (1 µm – 100 nm). The resulting vesicles of defined size (**4**) with the targeted protein are then enriched by two purifications steps on first IgG beads and second Calmodulin beads separated by a TEV cleavage step (figure 82A). The whole purification is performed under native conditions meaning that no detergent is used to solubilize proteins from the membrane vesicles. In theory, in the final elution a membrane protein complex is enriched in its native environment - inner membrane domains. The theoretical result of a v-TAP purification is shown in figure 82B.

B. v-TAP purification of PlsB-, PgsA-, and PlsY-TAP

My goal was to validate the interactions found by BACTH between the phospholipid synthesis enzymes, using the v-TAP technique.

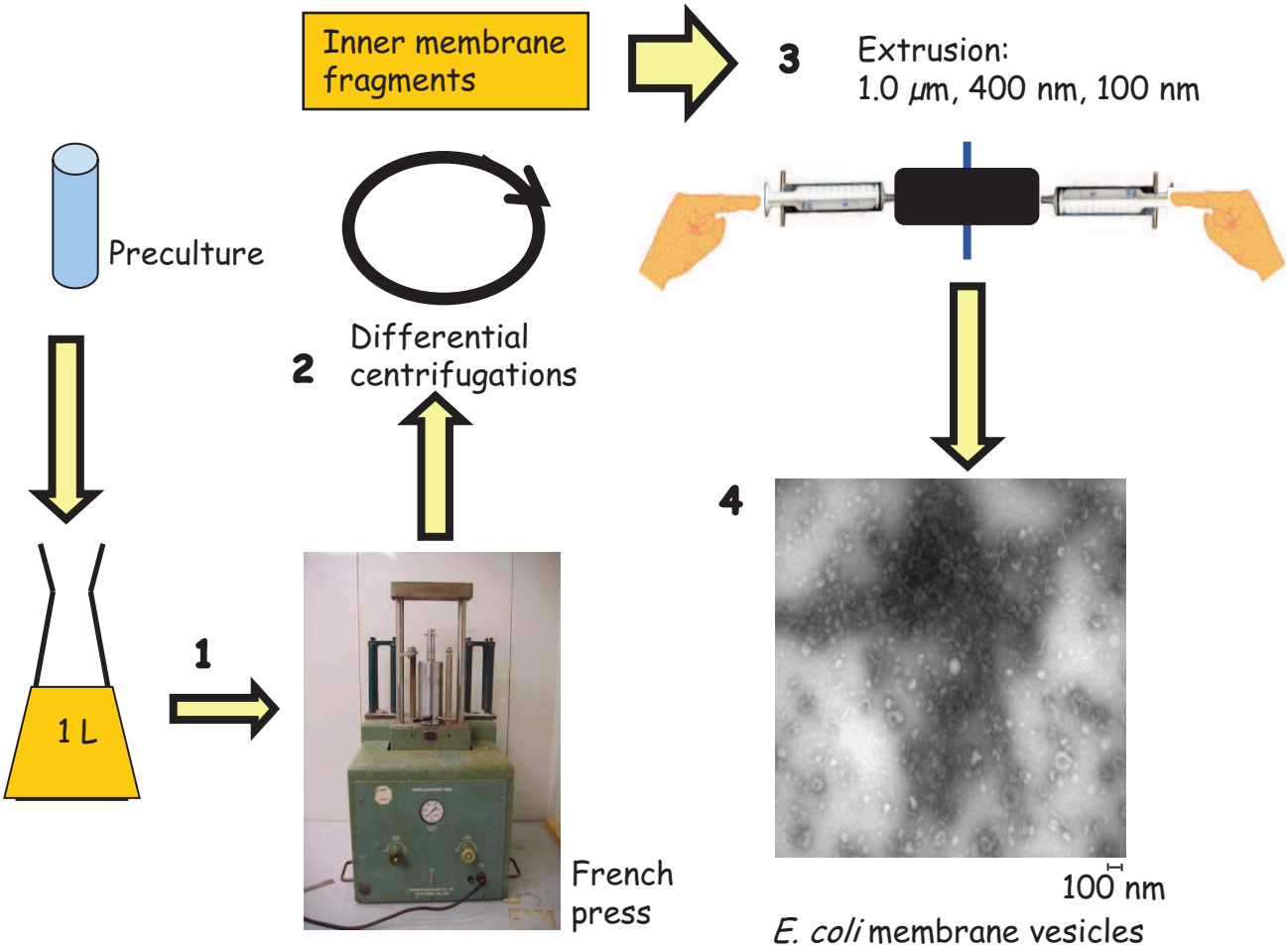

Figure 83: Preparation of membrane fragments. *E. coli* cells from a 1 L culture are broken using a French press (1). The outer and inner membrane fragments are then separated by differential centrifugation taking advantage of the fact that the outer membrane fragments are heavier than the inner membrane fragments (Duquesne & Sturgis, 2008). Then, the resulting inner membrane fragments are homogenized by successive extrusion (3) using polycarbonate membranes of decreasing pore size to give *E. coli* inner membrane vesicles of defined size (4).

PlsB was chosen as a candidate for v-TAP purification because it has been found in the ACP-TAP purification together with PssA (Gully *et al.*, 2003). In the BACTH screen, PlsB interacts with almost all of the other proteins from the phospholipid pathway (Gully et al., unpublished), which makes PlsB a good bait protein. Furthermore, PlsB is the first and commitment step of the phospholipid synthesis pathway and might be an important point of regulation for other enzymes of the pathway.

PlsY was chosen because it is one of the few phospholipid synthesis proteins whose exact topology in the inner membrane is known (Lu *et al.*, 2007). Additionally, PlsY makes part of the second pathway parallel to PlsB and might be therefore also a key point of regulation. It interacts in the BACTH screen also with numerous other enzymes of the pathway, such as PlsB, PgsA, PlsX, and PlsC.

PgsA was chosen as it catalyses the first step of the pathway of anionic phospholipids at the branching point between anionic and zwitterionic phospholipids. Thanks to this position within the phospholipid pathway, PgsA might be a point of interaction with other enzymes of the pathway, such as PlsB and PlsY, in order to regulate the enzymatic activity.

In the ideal case of the v-TAP technique, the purification is realized on a protein tagged with the TAP tag on the chromosome. However, the physiological expression levels of the phoshoholipid genes are quite low and we first needed to set up the v-TAP protocol. Hence, the first tests of the v-TAP purification were done on a recombinant protein encoded by a plasmid and by using expression from an inducible promoter.

B1. Setting up the v-TAP purification with a plasmid expressing tap-pgsA

The pBAD-NtTAP (pEB587) plasmid permits N-terminal tagging with the TAP tag and expression from an arabinose inducible P_{BAD} promoter. A pBAD-NtTAP-*pgsA* plasmid was constructed. The exact topology of PgsA is not known, however, its C-terminus is predicted to be situated in the cytoplasm (Daley *et al.*, 2005). Furthermore, since we have determined 6 TMSs, it can be assumed that the N-terminus is located in the cytoplasm. Therefore, the N-terminal TAP tag of the TAP-PgsA fusion protein should be located at the cytoplasmic side of the inner membrane and will hence be located at the outer surface of the future membrane vesicles ("inside-out") after the extrusion step. However, the functionality of the TAP-PgsA fusion protein was not tested. To do so the pBAD-NtTAP-*pgsA* could be transformed in a *pgsA* mutant to test if this plasmid complements and if the produced fusion protein TAP-PgsA is fully functional.

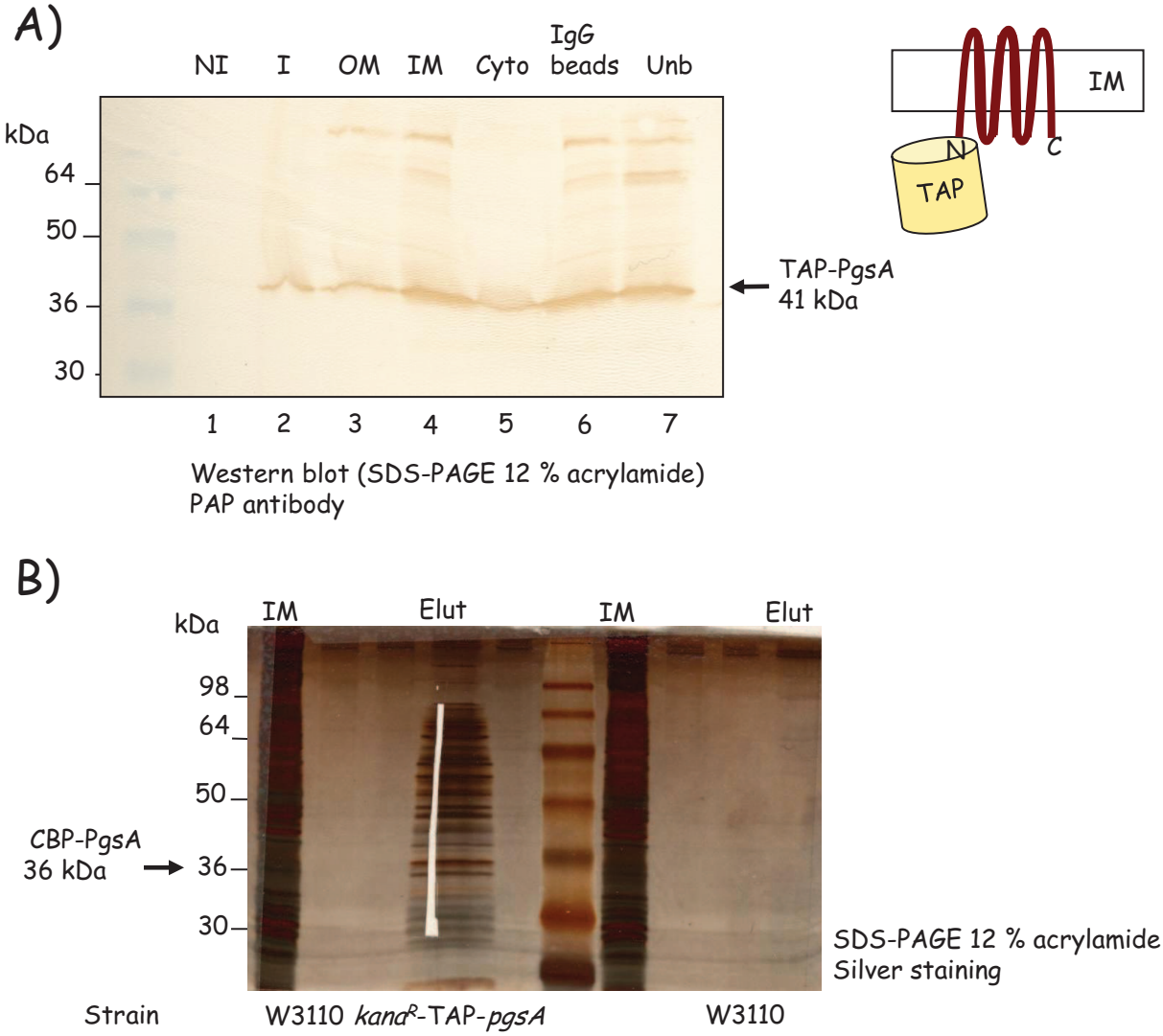

Figure 84: Cellular fractionation of TAP-PgsA producing W3110 *E. coli* cells and v-TAP purification. A) A 1L culture of W3110 *E. coli* cells expressing *tap-pgsA* from a plasmid were induced with 0,005 % arabinose for 1 h at 37°C. Fractionation and separation of OM et IM by differential ultra-centrifugations and resuspended in 1mL ammonium bicarbonate (10 mM) each. NI: Non-induced; I: Induced; OM: Outer membrane; IM: Inner membrane; Cyto: Cytoplasm; IgG beads: material still bound after elution to IgG beads thanks to ProtA tag; Unb: Unbound. **B**) v-TAP purification from strain W3110 (as negative control) or W3110 producing TAP-PgsA. Elutions (5x200 µL) are pooled and precipitated with TCA. The lane corresponding to the precipitated elution was cut vertically into 4 parts (96-64 kDa, 64-42 kDa, 42-33 kDa, and 33-16 kDa) indicated by white arrows.

W3110 *E. coli* cells were transformed with the pBAD plasmid expressing *tap-pgsA*. The production of the fusion protein TAP-PgsA in whole cell extract was analyzed. TAP-PgsA could be detected by Western blot at the expected molecular weight of 41 kDa (figure 84A, lane 2). Then, the localization of the fusion protein was determined by cellular fractionation using differential centrifugations (separation of inner and outer membranes). Although the fusion protein TAP-PgsA was found in every fraction, TAP-PgsA was clearly enriched in the inner membrane fraction (figure 84A, lane 4). The fact that the fusion protein TAP-PgsA was found in every fraction might be due to the over-expression and production of too much protein which could then not be separated properly. Nevertheless, the v-TAP purification was performed on the inner membrane fraction following the protocol, in parallel with a W3110 control strain (figure 84B): first, membrane vesicles (Ø 100 µm) were prepared using the extruder and an ammonium bicarbonate buffer (10 mM) containing no detergent. Then, this membrane vesicle preparation was enriched by two successive affinity purification steps on IgG and Calmodulin beads separated by a TEV cleavage step. In the final step, the bait protein CBP-PgsA with the membrane vesicle was eluted by EGTA (2mM). This final elution was then analyzed by Silver staining (figure 84B). The lane corresponding to the elution was cut vertically into 4 parts (96-64 kDa, 64-42 kDa, 42-33 kDa, and 33-16 kDa), which were sent to the Proteomics service IMM-IFR88 on the CNRS campus. These 4 parts of the total gel containing the enriched proteins was digested using 10 µl of Trypsin (c = 0.33µg/µL) (Gold Promega) in a buffer based on ammonium bicarbonate (25 mM) for 6 hours at 37°C. The digested peptides from the dried supernatant were then resuspended in 10 µl formic acid (5 %) and then analyzed on a ion trap MS-MS (mass spectrometry) (MS). The spectra of the peptides were compared to the data bank collection "Ecoli" of NCBI in order to identify the proteins.

Two enzymes of the phospholipid synthesis were identified (figure 85): PgsA itself and Psd pro-enzyme. Additionally, other inner membrane proteins were identified, such as ATP synthase subunits, Cytochrome bd, and NADH dehydrogenase. The fact that other inner, but no outer membrane proteins were co-purified, suggests that inner and outer membrane were correctly separated. However, these proteins are relatively abundant compared to phospholipid synthesis enzymes and so they may be unspecific contaminats. The purification could be realized in *pgsA* mutant transformed by pBAD-NtTAP-*pgsA* to see if this changes the resulting copurifed proteins. When we perform the purification in a wild type background, the wild type PgsA protein competes with the PgsA fusion protein and the latter may be affected in its capacity to interact with other proteins because of its tag.

A)

E. coli Protein	Score	MW [kDa]	Localization
ATP synthase, gamma chain	50	31,6	Cyto, IM
Galactitol permease IIC component	40	48,3	IM
Dihydroorotate dehydrogenase	20	36,7	IM
ATP synthase, alpha chain	20	55,2	Cyto, IM
Hypthetical protein YefG	20	37,8	p: IM
Phosphatidylserine decarboxylase proenzyme, **Psd**	20	35,9	Cyto? , IM
Probable glutamate/gamma-aminobutyrate decarboxylase	20	55,1	IM
Chain length determinant	10	36,5	IM
Translocase SecY subunit	10	48,5	IM
Low affinity tryptophan permease	10	45,2	p: IM
Transketolase 2	10	73,0	Cyto
ATP synthase, beta chain	10	50,2	IM
Probable 3-hydroxybutyryl-CoA dehydrogenase	10	51,7	p: Cyto

B)

E. coli Protein	Score	MW [kDa]	Localization
Membrane-bound ATP synthase, subunit beta	100	17,2	IM
Membrane-bound ATP synthase, subunit delta	50	19,3	Cyto, IM
Fumarate reductase, anaerobic, iron-sulfur subunit	40	27,1	p: IM
Succinate dehydrogenase, iron-sulfur protein	40	26,7	p: IM
Orf, hypthetical protein	40	15,2	-
yiaF gene product	30	30,8	p: IM
Phophatidylglycerophosphate synthetase, **PgsA**	30	20,7	IM
Putative transport protein	30	30,8	-
Orf, hypthetical protein	30	11,1	-
Hypthetical protein	20	23,1	-
Putative O-acetyl transferase	20	21,7	-
NADH dehydrogenase I chain I	20	20,5	p: IM

Figure 85: Proteins identified by mass spectrometry from the TAP-PgsA purification. The lane corresponding to the elution (figure x) was cut vertically into 4 parts (96-64 kDa, 64-42 kDa, 42-33 kDa, and 33-16 kDa), which were sent to mass spectrometry (MS) analysis (ion trap MS-MS). The total gel containing the enriched proteins is digested using 10 µl of Trypsin (c = 0.33µg/µL) (Gold Promega) in a buffer based on ammonium bicarbonate (25 mM) for 6 hours at 37°C. The digested peptides from the dried supernatant were then resuspended in 10 µl formic acid (5 %). The spectra of the peptides were compared to the data bank collection "Ecoli" of NCBI in order to identify the proteins. **A**) Identified proteins from part 3 (42-33 kDa). In this part, Psd pro-enzyme was identified with a molecular weight of 35,9 kDa **B**) Identified proteins from part 4 (33-16 kDa). In this part, PgsA (the bait protein) was identified with a molecular weight of 20,7 kDa.
MW: molecukar weight in kilo Dalton (kDa). Localization: Cyto = cytoplasm; IM = inner membrane; p: localization is predicted.

It was encouraging that PgsA (the bait) could be identified and was co-purified with another phospholipid synthesis enzyme, Psd. It is interesting that these two proteins were co-purified, because Psd catalyses the last reaction of the branch leading to PE, while PgsA makes part of the second branch leading to PG and CL. As this result was encouraging, we started to set up the v-TAP with proteins that are produced at their physiological level.

B2. Production and localization of the physiologically expressed chromosomal fusions

For purification experiments at physiological expression level, a series of strains were constructed in which the proteins are tagged at their C-terminus with the TAP, SPA, ProtA, or 3Flag tag (figure 86). 4 strains were constructed in which the proteins PlsB, PlsY, PgsA, and DgkA are tagged at their C-terminus with the TAP tag. The topologies of PlsY and DgkA are known and the C-terminus of PlsY is located in the cytoplasm, while the C-terminus of DgkA is located in the periplasm (Smith *et al.*, 1994; Lu *et al.*, 2007). We have determined the topology of PgsA and the topology of PlsB is only a prediction with two TMS and its N- and C-termini in the cytoplasm (figure 15). First, the correct insertion of the cassettes in the *E. coli* chromosome was verified by PCR on colony (data not shown). Furthermore, the production of the tagged protein could be validated for the four strains by Western blot analysis (total cell fractions in figures 87 and 88). The localization (expected in the inner membrane) of the fusion proteins PlsB, PlsY, and PgsA tagged with TAP was then verified by cell fractionation. In the laboratory a couple of techniques are used for cell fractionation: Sphaeroplast preparation or French Press lysis followed by differential ultra-centrifugation (cf. Materials & Methods). The principle of the sphaeroplast preparation is that cells are lysed by osmotic shock, while with French Press cells are broken physically by applying high pressure (1200 psi). Strain W3110 producing PgsA tagged with TAP was fractionated using the sphaeroplast technique (figure 87), while strains W3110 producing PlsB or PlsY tagged with TAP were fractionated using differential ultra-centrifugation in order to separate inner and outer membranes (figure 88A and B). In these localization experiments by cell fractionation, it could be shown that the three fusion proteins are localized in the (inner) membrane fraction as expected. However, for PlsB a band is found in the outer membrane fraction (OM) which might either be aggregates (see solubilization PlsB-CBP-EYFP figure 73) or due to a bad separation of inner and outer membranes.

Cterminal Tag	BW25113 Kana^R	W3110 Kana^R	W3110 Δ°	Comment on detection and functionality of the fusion protein
TAP	PlsB	PlsB	PlsB	Detectable; no obvious growth phenotype
	PgsA	PgsA	PgsA	Detectable; no obvious growth phenotype
	PlsY	PlsY		Detectable, no obvious growth phenotype
	DgkA	DgkA	DgkA	Detectable; not functional on LB-NaCl
	ACP	ACP		Detectable; no obvious growth phenotype
SPA	PssA	PssA		n.d.
	DgkA	DgkA	DgkA	Detectable; not functional on LB-NaCl
	PlsC			n.d.
	PlsB	PlsB		Detectable; no obvious growth phenotype
ProtA	DgkA	DgkA	DgkA	Detectable; functional on LB-NaCl
3Flag	DgkA	DgkA	DgkA	Detectable; functional on LB-NaCl

Figure 86: Proteins fused with different affinity tags. BW25113 Kana^R: *E. coli* strain BW25113 in which recombination took place to insert the cassette carrying the resistance against kanamycin; W3110 Kana^R: cassette carrying the resistance against kanamycin transduced by phage P1 in *E. coli* W3110 strain; W3110 Δ°: *E. coli* strain W3110 after taking out the kanamycin resistance cassette with plasmid pCP20 (pEB266); TAP: Tandem Affinity Purification tag; SPA: Sequential Peptide Affinity tag; ProtA: protein A; 3Flag: 3x octapeptide tag; kana^R: resistance to kanamycin; n.d.: not determined.

In conclusion, strains producing fusion proteins PlsB, PgsA, and PlsY tagged with TAP were obtained and all proteins were found at their expected molecular weight and in the (inner) membrane fraction.

B3. v-TAP purifications of PgsA-TAP and PlsB-TAP

We first tried the v-TAP on a strain producing PgsA-TAP because of the good results obtained with the plasmid pBAD-NtTAP-*pgsA*. However, in the final elution step, no material was left, and PgsA-TAP (or PgsA-CBP) was not detectable (data not shown).

Therefore, we dissected the purification, step by step, and found that already after the TEV cleavage step no protein at all could be detected. When incubating the vesicle fraction with IgG beads, the PgsA-TAP fusion protein could be detected bound to the IgG beads (data not shown). However, in the elution with TEV, hardly any fusion protein could be detected, indicating that the material was lost during the TEV cleavage (data not shown). After the second purification step, the Calmodulin beads, PgsA-CBP was not detectable anymore (data not shown).

When we tested whether the entire fusion protein PgsA-TAP was able to bind to the Calmodulin beads. The vesicle fraction (after extrusion) containing PgsA-TAP was directly incubated with Calmodulin beads. As seen in figure 89, PgsA-TAP did bind to the beads. However, PgsA-CBP alone did not bind to the beads as shown above. We cannot explain this strange behavior. An explanation may be that most of the material got lost between the TEV cleavage and the second purification step on Calmodulin beads. As PgsA is a protein of low abundance, the problem might be also that there was not enough bait protein in the beginning.

We continued our effort with a strain producing PlsB-TAP, as this protein seemed to be more abundant than PgsA from production tests by Western blot. Furthermore, PlsB is good as candidate bait, as many interaction partners of PlsB have been found using the BACTH (Gully *et al.*, unpublished). A v-TAP purification on *E. coli* cells W3110 expressing *plsB-tap* was performed according to the protocol on a 1 L culture (see Materials & Methods). The fusion protein PlsB-TAP was detected by Western Blot analysis in the inner membrane fraction as expected (data not shown). Then, extracts were analyzed before and after passage through the extruder in order to determine the loss of material in this step. As it can be seen in figure 90A, there was only minimal loss in the extrusion step. PlsB-TAP bound to IgG beads in the first purification step. Then, the cleaved PlsB-CBP could be detected in the TEV cleavage (figure 90B). However, PlsB-CBP could not be detected in the next step, neither on the Calmodulin beads nor in the unbound and in the last elution step. We verified whether

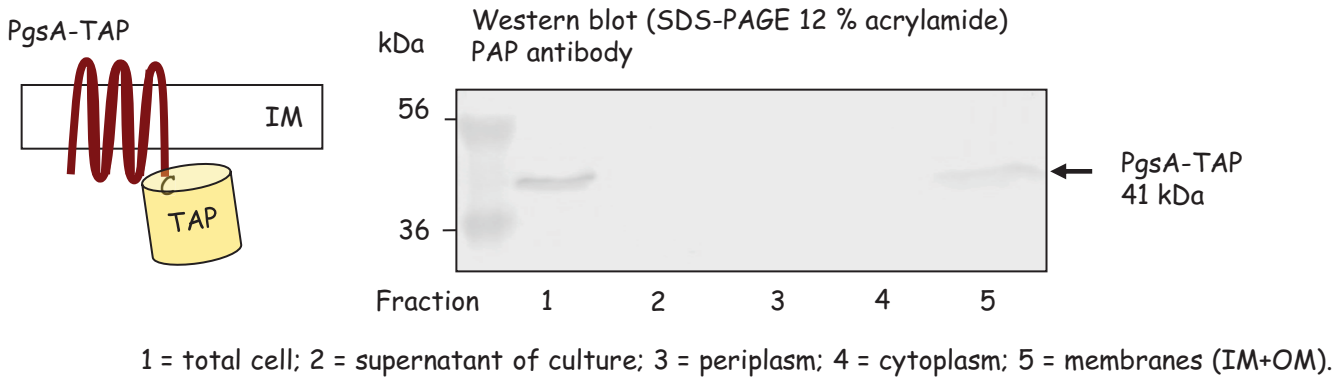

Figure 87: Cellular fractionation of PgsA-TAP producing W3110 *E. coli* cells by sphaeroplast preparation (according to Isnard *et al.*, 1994). The fractionation is realized with a culture grown in 2YT at 37 °C till an OD600nm = 1. The preparation was performed on1 mL of the culture. Exact preparation see materials & methods. The samples of the fractions 1, 2, 3, 4, and 5 are loaded onto a SDS-PAGE. Western blot was done with antibody PAP recognizing the ProtA in the TAP tag.

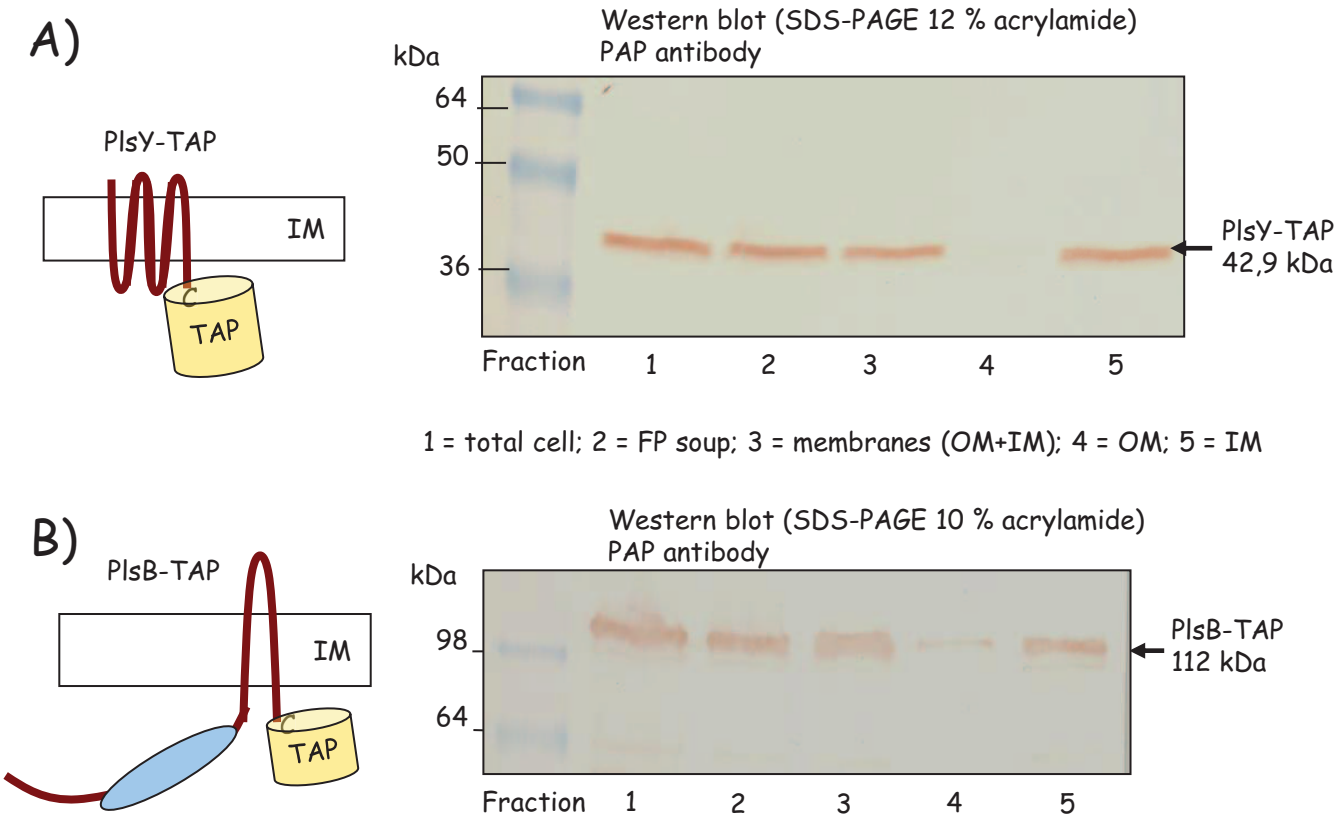

Figure 88: Fractionation of PlsY-TAP and PlsB-TAP producing W3110 *E. coli* cells by separation of OM and IM. FP soup = extract after breaking the cells in the French Press; OM = outer membrane IM = inner membrane. Preparation was done on a culture in 1 L LB grown at 37 °C till an OD_{600nm}=1. Exact preparation see materials & methods. The pellet corresponding to the outer membrane fraction (4) and is resuspended in 1 mL Ammonium bicarbonat (10 mM). The pellet corresponding to the inner membrane fraction (5) and is resuspended in 1 mL 50 mM TEA, 250 mM sucrose, 1 mM DTT (pH = 7,5). **A)** W3110 PlsY-TAP is detected in the inner membrane fraction (5). **B)** W3110 PlsB-TAP is detected in the inner membrane fraction (5).

PlsB-TAP could bind to Calmodulin beads by incubating the vesicle fraction directly with these beads. However, PlsB-TAP did not bind to Calmodulin beads (data not shown). This suggests that the CBP tag in PlsB-CBP fusion protein was not accessible for binding with the Calmodulin bead. However, PlsB-CBP-TEV-ProtA (=TAP) bound to the IgG beads. There might be some folding problems between the CBP tag and PlsB, although the tag possesses linker sequences to assure flexibility.

A point of improvement would be to add a flexible linker sequence between the CBP tag and the tagged protein to increase its accessibility. But on the other hand, this would increase the length of the tag and could also have negative effects. PlsB might not be the best candidate as bait to purify a membrane protein complex, as it is seems to be only loosely attached to the inner membrane and can therefore be easily solubilized (Green *et al.*, 1981): PlsB has been found together with PssA in the soluble protein complex in the ACP-TAP purification, which was performed with low amounts of detergent. Therefore, it could be difficult to purify a stable membrane complex using PlsB-TAP as bait.

C. Discussion and Prospect

During the first year of my PhD we developed the v-TAP method, a variant of the TAP purification technique that ought to enable us to purify membrane protein complexes under native conditions and at their physiological level.

First, PgsA tagged at the N-terminus with the TAP tag and produced from a plasmid was successfully purified using the v-TAP technique. Two enzymes of the phospholipid synthesis were identified: PgsA and Psd pro-enzyme together with other inner membrane proteins, such as ATP synthase subunits, Cytochrome bd, and NADH dehydrogenase. It is interesting that Psd was co-purified with PgsA. Psd catalyses the last reaction to form phosphatidylethanolamine (zwitterionic phoshpholipid). By interacting, Psd and PgsA could regulate the enzymatic activities in the branches of the two pathways leading to the anionic and zwitterinonic phospholipids. There are no BACTH data about Psd because in the laboratory the BACTH plasmids have not been constructed yet. This is also due to its particular post-translational modification at the Ser253 and the auto cleavage into an α- and β-subunit, which could be problematic for interaction studies. Despite these encouraging results, there were some major problems: first, the fusion protein TAP-PgsA was enriched as expected in the inner membrane fraction, but it was found in all cell fractions. We reasoned that the problem was the over-expression from a plasmid, as it produced a not physiological amount of the fusion protein and can therefore lead to mislocalization. The N-terminal tag

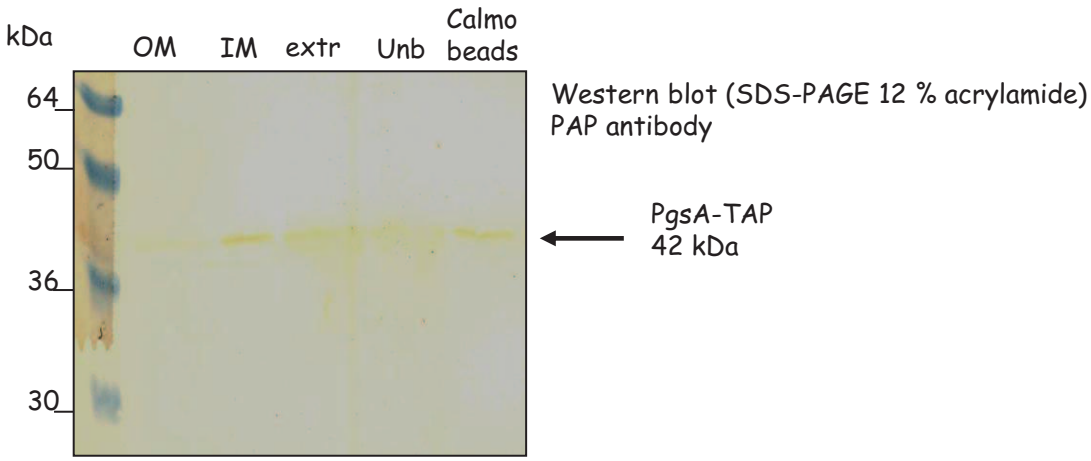

Figure 89: Binding of purified inner membrane fraction containing PgsA-TAP to Calmodulin beads. 30 µL of Calmodulin beads were incubated 2 h at 4 °C with 1,4 mL of a diluted extract of PgsA-TAP. Then, Laemmli buffer was added to the beads and samples were loaded on gel. OM: Outer membrane; IM: Inner membrane; extract= after extrusion; Unb: Unbound; Calmo beads: fusion protein that is bound to the Calmodulin beads.

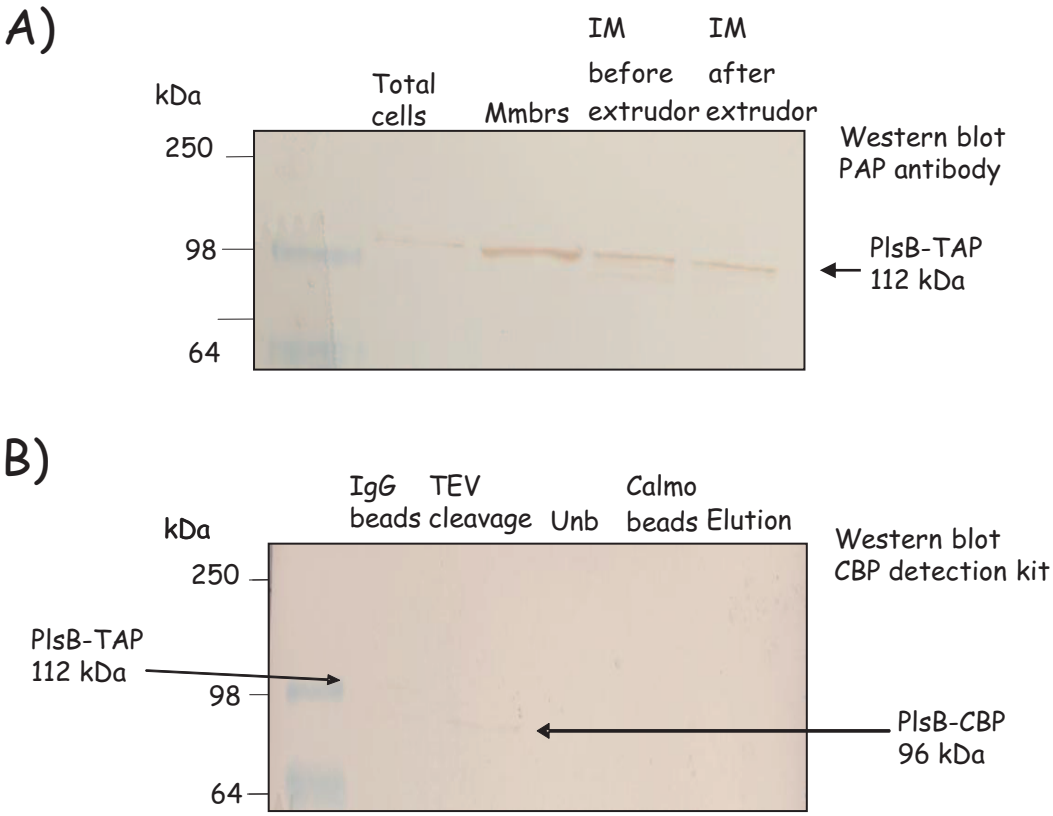

Figure 90: v-TAP purification on strain W3110 producing PlsB-TAP. FP soup = extract after breaking the cells in the French Press; OM = outer membrane IM = inner membrane. Preparation was done on a culture in 1 L LB grown at 37 °C till an OD_{600nm}=1. The pellet corresponding to the outer membrane fraction (4) and is resuspended in 1 mL Ammonium bicarbonat (10 mM). The pellet corresponding to the inner membrane fraction (5) and is resuspended in 1 mL 50 mM TEA, 250 mM sucrose, 1 mM DTT (pH = 7,5).
A) Analysis of extract before and after extrusion by Western blot with antibody PAP **B)** Detection after TEV cleavage of fusion protein PlsB-CBP using the CBP detection kit (Stratagene).

could also lead to problems in PgsA functionality if it affects for example its correct folding and insertion in the inner membrane. Therefore, tagging PgsA at its C-terminus with the TAP tag might improve the localization problem as well. Second, most of the co-purified proteins seem to be unrelated to PgsA or the (phospho)lipid synthesis. The problem was probably the over-production of the bait protein, which can lead to the identification of unspecific interactions in the vesicle complex. So, we decided to set up the v-TAP with a protein that is produced at its physiological level.

For v-TAP purification, 3 strains were constructed in which the proteins PlsB, PlsY, and PgsA are tagged at their C-terminus with the TAP tag. PlsB, PlsY, and PgsA tagged with TAP tag were localized as expected in the inner membrane fraction. When purifying PgsA tagged with TAP the fusion protein could only be detected till the TEV cleavage step, after this step no material was left. It seems that when over-expressing *pgsA-tap* by plasmid there was too much material, while at physiological expression level, there was too little material. For the v-TAP purification of PlsB-TAP, the problem was that the fusion protein could not bind to the second column, the Calmodulin beads. This problem might be solved by changing the tag, such as a Streptavidin and 6xHistidine tag separated by a protease cleavage site for example. It would be also interesting for PlsB to induce it in a more physiological way by over-expressing *rpoE*. In this way, there would be more material of the bait protein, but in a less artificial manner than by over-expression from a plasmid directly.

We think it is a promising technique, but as a technological project, the v-TAP development was not adapted to a thesis project, and another researcher in our laboratory took up the project and continues to work on it. The v-TAP protocol is currently adapted and improved, by refining for example the separation of inner and outer membranes and verification of preparation of inner membrane by a NADPH assay. *plsY* was successfully tagged with the TAP tag on the chromosome, the fusion protein PlsY-TAP could also be purified (data not shown), but no concluding results with co-purified proteins were achieved.

In prospect, the project of the v-TAP shall be continued with all enzymes of the phospholipid synthesis pathway in order to confirm the interaction network found by BACTH. Then, the v-TAP developed in the model organism *E. coli* can be applied to study other (membrane) protein systems. In the laboratory, a project for purifying the photosynthetic complex of *Roseobacter* has been started as well.

III. DIFFERENT STRESS RESPONSES REGULATE THE *PLSB – DGKA* GENES

A. Introduction and summary of Article 2

The mechanisms of genetic regulation of the phospholipid synthesis pathway are unknown despite its fundamental importance in membrane homeostasis. The composition of the bacterial membrane must be precisely regulated in order to adapt to different growth conditions, such as nutritional starvation (= stringent response) or diverse stress responses. For example, during stasis the relative CL content increases and unsaturated fatty acids are condensed to cyclopropane groups (Zhang & Rock, 2008), which as a result decreases membrane fluidity.

Furthermore, transcriptome studies in *E. coli* have shown that phospholipid synthesis genes are globally inhibited during stringent response, excepted the genes of the anionic phospholipid pathway that are activated, together with *dgkA* coding for an enzyme recycling diacylglycerol (Traxler *et al.*, 2008; Durfee *et al.*, 2008; Aberg *et al.*, 2009). These data suggest the existence of a complex regulatory mechanism of response to stress. Curiously, the phospholipid synthesis genes are not organized as a cluster, but are rather scattered all over the chromosome which renders their coordinated regulation all the more puzzling (figure 91). However, there is one exception: the *plsB* and *dgkA* genes are next to each other in divergent directions. The promoters of *plsB* and *dgkA* overlap in the intergenic region of 170 base pairs (figure 91).

In a transcriptomic study, *plsB* and *dgkA* were shown to be regulated by ppGpp in an opposite way (Traxler *et al.*, 2008). *dgkA* was activated, while *plsB* was inhibited by ppGpp. Moreover, another transcriptome study has shown that the alternative sigma factor SigmaE (RpoE) activates *plsB* (Rhodius *et al.*, 2006). RpoE responds to extracellular stress which damages outer membrane proteins (OMPs). The newly synthesized OMPs are thought to be translocated across the envelope together with PE. Hence, RpoE activates the branch catalysing the *de novo* synthesis of PE, in particular *plsB* and *psd*. An RpoE-dependent *plsB* promoter has been described and its transcription start site has been mapped (Rhodius *et al.*, 2006). Finally, other unknown regulators might exist that regulate phospholipid synthesis. A *dgkR-1* mutant was isolated in which the DgkA activity was activated, while the PlsB activity was inhibited, suggesting an antagonist regulation of the two genes (Raetz *et al*., 1981; Walsh *et al*., 1986). However, no corresponding gene has been assigned, and the mutated allele was only crudely mapped to 93-94 min position on the chromosome (Raetz *et al.*, 1981).

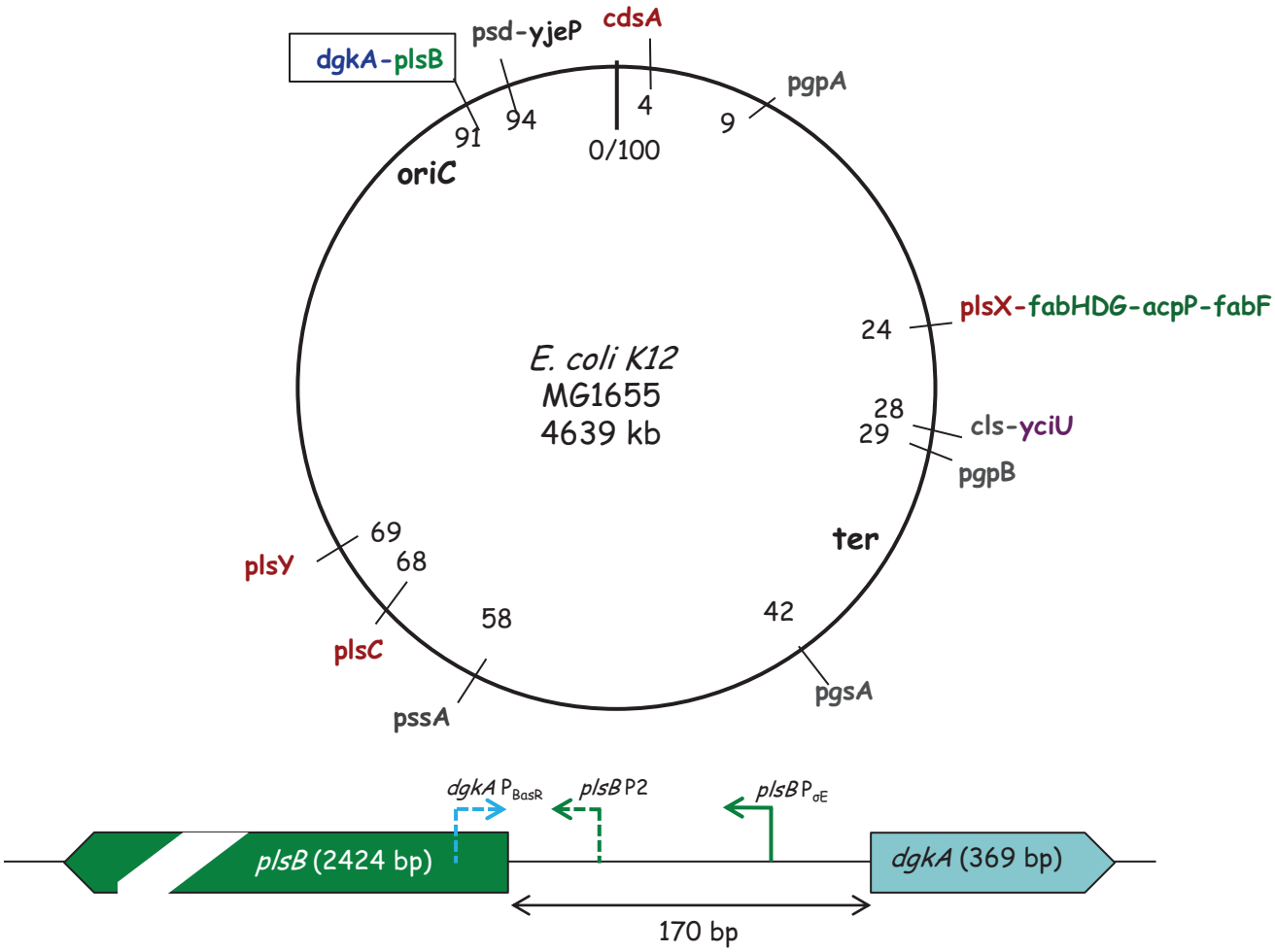

Figure 91: Genetic organization of phospholipid synthesis genes on the chromosome of *E. coli* K-12 MG1655. The intergenetic region of genes *plsB* and *dgkA* contains an RpoE-dependent promoter (filled line; Rhodius *et al*., 2006) and two new promoters (dashed lines) identified in article 2: a second promoter for *plsB* constitutive expression and a *dgkA* promoter that is activated by BasR.
Numbers indicate the gene position on the *E. coli* chromosome in minutes.

cttaagattcatttaat tg a	BasR consensus (Marchal *et al.*, 2004)
CTTAAGGTTGG**CTTAAT**	*eptA*
CTTAATA**TT**A**ACTTAAT**	*ugd*
CTTAAGGTTA**A**G**TTAAT**	*arnB*
CTTAATAG**TT**T**CTTAAT**	*yibD*
CTTAATGGTAAATTCAG	*dgkA*

Figure 92: Regulon of the BasRS TCS in *E. coli* and alignment of the BasR consensus sequences. Bold letters in the sequences of the *E. coli* genes indicate conserved nucleotides from the aligned sequences. The predicted –35 consensus of the *dgkA* promoter is indicated by a line.

Therefore, we wanted to decipher the regulation of the two genes *plsB* and *dgkA*. They seem to be key points of regulation for the whole phospholipid synthesis pathway because PlsB catalyzes the first and commitment step of the synthesis and DgkA is involved in recycling damaged phospholipids.

Using an *E. coli* library of transcriptional fusions with *gfp* (Zaslaver *et al.*, 2006) and our fusion proteins, we have found that *dgkA* and *plsB* are regulated by a diversity of stress responses. First, we could confirm that RpoE induction resulted in an increase of PlsB protein amount. On the contrary, the amount of DgkA decreased upon induction by RpoE, suggesting an antagonistic regulation of *dgkA* and *plsB* by RpoE thanks to the σ^E dependent promoter. Furthermore, we described here for the first time a second promoter for *plsB* expression that is responsible for the high basal *plsB* expression. When mutating its predicted – 10 consensus, the basal expression level was drastically lowered, but expression was still induced in response to RpoE. Furthermore, we have shown that expression of this second promoter is inhibited during stringent response and that it contains a GC rich sequence upstream of the predicted transcription start site characteristic of stringently regulated promoters (Travers, 1980).

Concerning the regulation of *dgkA*, we noticed the *basRS* and *dcuRS* genes coding for two TCSs in the *dgkR* region around 93,7 minutes on the *E. coli* chromosome. Using a set of programs for promoter prediction, a putative *dgkA* promoter was found, at the beginning of the reverse *plsB* coding sequence, that is preceded by a BasR binding box, corresponding to the consensus binding site described for PmrA of *S. typhimurium*, the homolog of *E. coli* BasR (Marchal *et al.*, 2004) (figure 92). Eventually, we have shown that *dgkA* is activated by the TCS BasRS and that the *dgkR*-1 mutation corresponds to a point mutation D312N in the sensor BasS leading to constitutive activation of the BasRS TCS. When mutating the BasR binding box in the putative promoter region of *dgkA*, the BasR response of *dgkA* was abolished. Therefore, we concluded that *dgkA* activation by BasR is specific.

The TCS BasRS activates expression of LPS modifications genes coding for enzymes that decorate the lipid A with L-4AraN (ArnBCADTEF) and phosphoethanolamine (EptA). BasR induces the gene coding for EptA. EptA uses PE as donor for phosphoethanolamine. The reaction releases a diacylglycerol, which can be reintroduced by DgkA into the phospholipid synthesis pathway. Therefore, BasR induces LPS modifications and in parallel *dgkA* to guarantee the recycling of the damaged PE.

We have shown in this article that the genetic regulation of *plsB* and *dgkA* depends on three different stress response regulators: σ^E, ppGpp, and BasR. Several promoters were

identified each responsible for the expression of *plsB* and *dgkA* in response to a different kind of stress regulator (figure 91). Our results showed that the *plsB* and *dgkA* expression is a key point of integration for different stress mecanisms. The complex regulation suggests that the integration of these different signals on *plsB* and *dgkA* expression results in an optimized balance between *de novo* phospholipid synthesis and phospholipid recycling.

Multiple stress signals are integrated at the *dgkA-plsB* locus for control of phospholipid synthesis in *Escherichia coli*

Astrid Wahl, Laetitia My, Romain Dumoulin[1], James N. Sturgis, Emmanuelle Bouveret*

LISM, CNRS, Aix-Marseille University, 31 chemin Joseph Aiguier, 13402 Marseille Cedex 20, France.

*Corresponding author

Email : bouveret@ifr88.cnrs-mrs.fr

Tel: +33 (0)4 91 16 45 04

Fax: +33 (0)4 91 71 21 24

1 Present address: UMR1319, INRA, 78352 Jouy-en-Josas, cedex France.

Keywords

Phospholipid biosynthesis – envelope biogenesis - bacterial stress response - σE - ppGpp - BasRS – *dgkR* - LPS modification

Abbreviations

G3P: glycerol-3-phosphate; ppGpp: guanosine 5'-diphosphate ; 3'-diphosphate – TAP: Tandem Affinity Purification; ProtA: Protein A; GFP: Green Fluorescent Protein; MDO: membrane derived oligosaccharide; σE: Sigma E

Abstract

The phospholipid composition of the bacterial membrane must be finely tuned depending on the environment. However, very little is known about the regulation of phospholipid synthesis genes. They appear to be constitutively expressed in different growth conditions, but they might be differentially regulated during stress response. Indeed, specific genes are activated by alternative Sigma factors, and transcriptome analyses have shown that phospholipid synthesis genes are coordinately regulated during the stringent response. In *E. coli*, the genes coding for glycerol-3-phosphate acyltransferase and diacylglycerol kinase (*plsB* and *dgkA*) are found next to each other in divergent orientations, suggesting a coordinated regulation. We investigated their regulation and found that these two genes are inversely regulated by a diversity of stress response pathways. *plsB* activation by σE is concomitant with a reduced DgkA amount. A second proximal promoter for *plsB* expression is responsible for the basal *plsB* expression and is inhibited during stringent response. Finally, *dgkA* is activated by a specific two-component regulator, BasR, linking *dgkA* function of phospholipid recycling to LPS modifications. In *E. coli*, PlsB and DgkA are key enzymes in the phospholipid synthesis pathway and our results show that their expression is a crucial point of integration for different stress signals.

INTRODUCTION

The biochemical pathway for phospholipid biosynthesis in the inner membrane has been extensively studied in *E. coli* for nearly 40 years, giving a clear picture of the enzymes and catalytic activities involved (Zhang and Rock, 2008a). Phospholipids constitute the building blocks of the plasma membrane of bacteria, and the composition of this membrane is robustly maintained in any growth condition. The constant ratio between anionic (Phosphatidylglycerol and Cardiolipin) and zwitterionic (Phosphatidylethanolamine) phospholipids is maintained by a direct activation of Phosphatidylserine synthase PssA by the anionic phospholipids in the inner membrane (Saha et al., 1996). The nature of the fatty acid chains incorporated in phospholipids is determined by the specificities of the glycerol-3-phosphate (G3P) acyltransferases, and their degree of unsaturation is controlled at the level of fatty acid biogenesis by the FabR transcriptional regulator in *E. coli* (Fujita et al., 2007; Zhu et al., 2009). Finally, the phospholipid synthesis pathway is under growth rate control, since the phospholipid content does not vary with growth rate. However, how this is achieved remains an almost complete black box (Cronan, 2003). The effector of the stringent response, ppGpp, has been shown to inhibit the activity of the G3P-acyltransferase PlsB, the first enzyme of the phospholipid synthesis pathway in *E. coli* (Heath et al., 1994). Because ppGpp concentration inversely correlates with growth rate (Baracchini and Bremer, 1988; Hernandez and Bremer, 1990), this may explain how the activity of the whole pathway is correlated with growth rate. However, if and how other phospholipid synthesis enzymes than *plsB* are coordinately regulated by growth rate is not known.

Very little is known about the regulation of phospholipid synthesis genes. In parallel to the constitutive expression of phospholipid synthesis enzymes described above, some data indicate that these genes might be differentially regulated in response to a variety of stresses.

The whole phospholipid synthesis pathway might be regulated by ppGpp during the stringent response to starvation events. While it was reported that ppGpp inhibits the enzymatic activity of PlsB (Heath et al., 1994), genetic regulation might also occurs. Indeed, transcriptome studies in *E. coli* have shown that there is a global genetic regulation of phospholipid biosynthesis genes upon stringent response and growth arrest due to amino acid starvation. Furthermore, the majority of this regulation was dependent on SpoT and RelA enzymes controlling ppGpp amounts (Durfee et al., 2008; Traxler et al., 2008; Aberg et al., 2009). Globally, the genes involved in phospholipid biosynthesis were inhibited, which is consistent with an arrest of macromolecular synthesis during growth arrest. However, the genes of the anionic phospholipid pathway seemed to be specifically activated, which is consistent with a relative increase in anionic phospholipids and especially cardiolipin during stationary phase (Zhang and Rock, 2008a). Other genes were activated during stringent response, such as *dgkA* coding for diacylglycerol kinase, an enzyme that permits the reinsertion of diacylglycerol into the phospholipid synthesis pathway, and *ybhO*, coding for an homolog of cardiolipin synthase (Durfee et al., 2008; Traxler et al., 2008). The phospholipid synthesis genes are not grouped in clusters or operons (in contrast with fatty acid biosynthesis genes). It is thus mysterious how they might be coordinately regulated despite their dispersion on the chromosome.

In addition, specific genes are activated by alternative Sigma factors. During stationary phase, σS activates the expression of cyclopropane fatty acid synthase (*cfa*), which is responsible for the conversion of acyl chain unsaturations into cyclopropane groups (Eichel et al., 1999). In response to envelope stress, σE activates *plsB* and *psd* genes, consequently activating *de novo* phosphatidylethanolamine synthesis (Rhodius et al., 2006). Finally, other unknown regulators

might participate in phospholipid synthesis regulation, as suggested by the existence of *dgkR* and *pssR* mutants still without assigned genes (Raetz et al., 1981; Sparrow and Raetz, 1983).

We were especially interested in the genetic organization and regulation of *plsB* and *dgkA* genes. Indeed, PlsB is the central control point for lipid biosynthesis arrest during stringent response (Heath et al., 1994). Furthermore, *plsB* is down-regulated during stringent response, whereas *dgkA* is up-regulated (Durfee et al., 2008), suggesting coordinated and opposite regulation, reinforced by the fact that *plsB* and *dgkA* are the only genes of phospholipid synthesis to be clustered on the chromosome in *E. coli*. PlsB enzyme transfers a fatty acid chain from an acyl-ACP to G3P in the first acylation step of the phospholipid synthesis pathway (Zhang and Rock, 2008b). DgkA is an atypical integral membrane diacylglycerol kinase, which recycles diacylglycerol produced by membrane derived oligosaccharide (MDO) synthesis into the phospholipid synthesis pathway (Badola and Sanders, 1997).

The *plsB* and *dgkA* genes are transcribed divergently, with an intergenic sequence of 170 base pairs (Figure 1A). *plsB* expression is activated by σE and the σE-dependent promoter has been precisely described and its transcription start mapped (Rhodius et al., 2006). On the contrary, no specific study has been performed on the transcription of *dgkA*. Yet, one study once reported the possibility of a specific regulation of *dgkA* (Raetz et al., 1981). A *dgkR-1* mutant was isolated in which the enzymatic activity of DgkA was enhanced, whereas the activity of PlsB was reduced, suggesting the possibility of an antagonist regulation of the two genes (Raetz et al., 1981; Walsh et al., 1986). However, this potential *dgkR* regulator was never identified, and the mutated allele was only crudely mapped to 93-94 min position on the chromosome (Raetz et al., 1981). When browsing the genetic map of the corresponding region of the chromosome, we could spot many potential regulators, but no obvious choice appeared for a regulator of

phospholipid synthesis. Recently, a paper reported that in *Pseudomonas fluorescens*, *dgkA* expression is induced by the ColRS two-component system specific of Pseudomonas species (Kivistik et al., 2009). This suggested to us that *dgkA* may be regulated by specific regulators, such as two-component systems. Looking back at the large potential *dgkR* region around 93,7 minutes (ECGSC reference) on the chromosome, we noticed *basRS* genes encoding the BasRS two-component system that activates genes involved in LPS modification, and that is induced in response to high iron concentrations in *E. coli* (Hagiwara et al., 2004; Froelich et al., 2006). We then realized that upstream the *dgkA* gene, at the beginning of the reverse *plsB* coding sequence, a sequence corresponded to the consensus binding site described for PmrA of *Salmonella typhimurium*, the homolog of *E. coli* BasR (Marchal et al., 2004) (Figure 1). Strangely, despite its conservation in the upstream sequence of *dgkA* from *Salmonella*, this site has never been listed in the systematic studies of PmrAB in *Salmonella* (Marchal et al., 2004) or of BasRS in *E. coli* (Hagiwara et al., 2004).

In this paper, we aimed at elucidating the genetic regulation of *plsB* and *dgkA* by three stress response regulators: σE, ppGpp, and BasR. We measured the effect of these regulators both on gene expression using transcriptional fusions with *gfp*, and on physiological protein amounts. We identified several promoters, each sensitive to different kind of stress regulators, which are responsible for the expression of *plsB* and *dgkA*. This complex regulation suggests that the *plsB-dgkA* locus is a crucial point for regulating phospholipid synthesis as it integrates various stress signals, resulting in an optimized balance between de novo phospholipid synthesis and phospholipid recycling.

RESULTS

Antagonistic regulation of *plsB* and *dgkA* by RpoE

In order to follow the regulation of *plsB* and *dgkA* by the alternative sigma factor σE, we used a pBAD-*rpoE* plasmid (pEB1102) permitting the artificial expression of *rpoE*, inducible with arabinose. We planned to assess the effects of σE over-production on gene expression, but also to be able to detect its effects on the amount of proteins produced. We therefore engineered *E. coli* strains in which PlsB or DgkA proteins were tagged at their C-terminus, in order to detect these proteins by Western blotting using antibodies specific for the tags. In such strains, the amounts of tagged proteins and their variation are expected to reflect physiological regulation events, because the sequence coding for the tag is inserted at the 3' end of the target gene on the chromosome, without altering the natural promoter sequence. We used cassettes that contain the sequences coding for the TAP (CBP-Tev-ProteinA) or SPA (CBP-Tev-3Flag) tags followed by the gene coding for kanamycin resistance (Zeghouf et al., 2004). These cassettes were introduced by recombination thanks to the λRed system in *E. coli* BW25113/pKD46 strain followed by transduction in W3110 strain (Datsenko and Wanner, 2000), in order to tag either DgkA or PlsB with the TAP or SPA tags (Table 2).

We observed that the DgkA-TAP and DgkA-SPA proteins were not functional, as the corresponding strains were unable to grow on LB devoid of NaCl, which is a characteristic phenotype of a *dgkA* mutant (Raetz and Newman, 1978) (data not shown). Therefore, we engineered two new strains producing either DgkA-ProteinA(ProtA) (EB395) or DgkA-3Flag (EB401) (Table 2). These last recombinant DgkA proteins could be detected in low amounts by Western blot (Figure 2B and Figure 4), and were functional as shown by the correct growth of the engineered strains on LB agar without NaCl (data not shown). The W3110/PlsB-TAP (EB367)

and W3110/PlsB-SPA (EB385) strains showed no obvious growth phenotypes and permitted a clear detection of the PlsB recombinant proteins (Figure 2A and data not shown).

Upon σE over-production, levels of PlsB-TAP and PlsB-SPA recombinant proteins strongly increased (Figure 2A, compare lanes 1 and 2, and data not shown), as was expected from the known induction of *plsB* gene by σE (Rhodius et al., 2006). Interestingly, the levels of DgkA-ProtA and DgkA-3Flag recombinant proteins, already low compared to PlsB, were reduced (Figure 2B and data not shown). This inhibitory effect of σE on DgkA production has never been described before. Due to the organization of the *plsB* and *dgkA* genes on the chromosome, the inhibitory effect of σE on DgkA may be explained by the occupancy of the σE-dependent promoter of *plsB* (Figure 1A).

We wanted to confirm the antagonist regulation of *dgkA* and *plsB* by σE by looking at the expression of the two genes. We used transcriptional fusions with the sequence coding for *gfp*, in the low copy vectors pUA66 and pUA139 (Zaslaver et al., 2006). Using this technique, promoter activity can be followed by measuring the fluorescence of GFP directly in living cells with a fluorimeter (Zaslaver et al., 2006) (see Material and Methods). We first tested the *plsB* and *dgkA* transcriptional fusion plasmids available in the *E. coli* promoter library constructed by Uri Alon's laboratory (Zaslaver et al., 2006). These two plasmids correspond to an identical *plsB-dgkA* intergenic sequence cloned in one orientation or the other upstream the *gfp* coding sequence (Figure 1A). Unfortunately, the *dgkA* transcriptional fusion did not give any measurable signal (data not shown). On the reverse, the signal obtained with the *plsB* transcriptional fusion was strong, and clearly induced by σE (Figure 3A). Furthermore, we mutated, in this transcriptional fusion, the -10 region of the previously described σE-dependent promoter of *plsB* (Rhodius et al., 2006), and verified that σE no longer induced the expression of *gfp* (Figure 3A, *plsB**). However,

despite the mutation of the -10 region of this σE-dependent promoter, the level of *gfp* expression measured without σE induction was identical to those of the wild type sequence (Figure 3A, compare *plsB* and *plsB** with pBAD). This suggested the existence of a second promoter for *plsB* expression, located in the *plsB-dgkA* intergenic sequence.

A second stringent promoter is responsible for basal *plsB* expression

We therefore constructed a new transcriptional fusion with *gfp* of a sequence comprising the 91 base pairs before the start codon of *plsB* (*plsBΔ*), which does not include the upstream σE-dependent promoter of *plsB* (Figure 1A). This shortened construction still gave a strong expression signal, equivalent to the basal signal of the previous transcriptional fusion (Figure 3A, compare *plsB*Δ and *plsB*, with pBAD), strengthening the hypothesis that a second promoter and transcription start site for *plsB* expression may exist downstream of the σE-dependent promoter, in the 91 base pairs before the start codon of *plsB*. We ran a search on the *dgkA-plsB* intergenic sequence for a putative promoter using a set of bioinformatic servers and got a low hit using BPROM (*http://www.softberry.com/berry.phtml*). A +1 transcription start site at a G is predicted, 36 base pairs before the start codon of *plsB*, with a predicted -10 consensus (TGCTATCCT), but no clear -35 consensus (Figure 1, *plsB*P2).

Despite the low prediction score, we decided to verify this promoter prediction by mutating the predicted -10 consensus sequence. We modified 3 nucleotides, both in the transcriptional fusion comprising the sequence of the σE-dependent promoter (*plsB**2), and in the shortened version (*plsBΔ**2) (Figure 1). The signal was drastically lowered with the mutation in the putative -10 for the full-length intergenic sequence (*plsB**2), and was totally abolished for the shortened version (*plsBΔ**2) (Figure 3A). However, the signal given by the full-length

transcriptional fusion mutated in this second putative promoter (*plsB**2) was still amplified by the over-production of σE (Figure 3A). These results demonstrate that there are two independent promoters for *plsB* expression. The newly described proximal one (*plsB*P2) may be a basal promoter responsible for strong expression of *plsB* during growth. The distal one (*plsB*PσE) is the previously described σE-dependent promoter, and our results show that it is only active upon σE induction.

In order to demonstrate that the two promoters characterized with transcriptional fusions corresponded to physiological promoters, we followed the amount of PlsB protein in a strain where PlsB is tagged at its C-terminus with the TAP tag, and its expression under the control of the physiological promoter region. We then introduced point mutations in the *plsB*P2 and *plsB*PσE promoter sequences, in the chromosomal DNA of these strains, with the following procedure: we cloned a 1650 bp genomic region encompassing the *plsB-dgkA* intergenic sequence in pKO3 plasmid (Link et al., 1997), and then introduced the mutations in pKO3-*plsBdgkA* (pEB1207) by site directed mutagenesis (see Tables 2 and S1). The plasmids were then used to introduce the mutations in the *plsB-dgkA* intergenic regions in the chromosome of *E. coli* PlsB- or DgkA-tagged strains, by two successive steps of homologous recombination (Link et al., 1997).

The mutation in the σE-dependent promoter could be obtained easily, and this did not affect the basal amount of PlsB-TAP protein (Figure 2, compare lanes 1 and 3). However, when the strains were transformed with pBAD-*rpoE* and induced, there was no longer any increase of PlsB-TAP amount in the strain with the mutation in the *plsB*PσE promoter (Figure 2, compare lanes 2 and 4). This demonstrated that the σE-dependent promoter is not responsible for the basal amount of PlsB produced during normal growth. We were not able to introduce directly the

mutation in the second promoter *plsB*P2. We hypothesized that because *plsB* is essential (Yoshimura et al., 2007), this second promoter responsible for basal production of PlsB, might be essential. Therefore, we transformed the W3110PlsB-TAP strain with the pBAD-*rpoE* plasmid and tried again to mutate the *plsB*P2 promoter in condition of *rpoE* induction, reasoning that the production of PlsB by the σE-dependent promoter should compensate for the loss of the *plsB*P2 promoter. In this case, we obtained the desired mutant. The amount of PlsB-TAP was drastically reduced in the mutant compared to the wild type (Figure 2, compare lanes 5 and 6). However, the production was still enhanced with *rpoE* induction (Figure 2, lanes 6 and 8). The low amount of PlsB-TAP present without *rpoE* induction could be due to a leaky production of σE from the pBAD-*rpoE* plasmid, or from the σE-dependent promoter even in the absence of extracytoplasmic stress. We did not observe any growth defect of the mutant strain, suggesting that the low amount of PlsB-TAP was still sufficient to sustain growth. In conclusion, the results obtained by comparing PlsB-TAP amounts in the strains containing mutation in the *plsB*P2 and *plsB*PσE promoters, mirrored exactly the results obtained with the transcriptional fusions (compare Figures 2A and 3A). This demonstrated the presence of 2 distinct promoters for *plsB* expression (Figure 1).

Both the transcriptional fusions and the tagged strains experiments show that a proximal promoter, distinct from the σE-dependent promoter, is responsible for basal *plsB* expression. Phospholipid content does not vary with growth rate, and *plsB* has been shown to be the point of control for all lipid biogenesis during growth arrest (Heath et al., 1994). However, it remained unclear whether the inhibition of PlsB activity during growth arrest was due to direct inhibition of PlsB enzymatic activity or due to the inhibition of *plsB* gene expression. Recent transcriptome

studies of the stringent response showed that *plsB* expression was indeed inhibited in case of amino acid starvation (Durfee et al., 2008; Traxler et al., 2008), and a systematic study of *E. coli* promoter activity showed that *plsB* expression follows growth rate (Zaslaver et al., 2009). These global studies suggested to us that *plsB* transcription might be regulated by ppGpp. Therefore, we tested if the two promoters controlling *plsB* expression were under stringent control. We studied the activity of the *plsB*PσE and *plsB*P2 promoters and the corresponding mutant ones in a Δ*relA*Δ*spoT* strain (EB425) devoid of ppGpp. In this strain, there was an increase in reporter expression for both the full length and shortened transcriptional fusions (Figure 3B, *plsB* and *plsBΔ*). The mutation in the proximal *plsB*P2 promoter abolished this increase, in both constructions (Figure 3B, *plsB**2* and *plsBΔ**2*). Conversely, the mutation in the σE-dependent promoter did not affect the Δ*relA*Δ*spoT* effect (Figure 3B, *plsB**). We obtained the same results when we performed the experiment in a Δ*dksA* strain instead of Δ*relA*Δ*spoT* (data not shown). In a Δ*dksA* strain, ppGpp is still present, but for most stringently controlled promoters, DksA acts as a cofactor of RNA polymerase (RNAP) that is required for the inhibitory action of ppGpp on RNAP, and its deletion can mimic an absence of ppGpp (Potrykus and Cashel, 2008; Srivatsan and Wang, 2008). These results suggest that the proximal *plsB*P2 promoter is under stringent control and might continuously link *plsB* expression to growth rate. Despite the very low score of the prediction, the sequence upstream the predicted transcription start site for *plsB*P2 is GC rich, which is characteristic of the discriminative sequence of stringently regulated promoters (Travers, 1980).

In conclusion, there are 2 independent promoters driving *plsB* expression : the proximal *plsB*P2 promoter is responsible for the basal production of PlsB and its activity might be linked to

growth rate, and the *plsB*PσE distal one is only activated during envelope stress triggering a σE stress response.

***dgkA* expression is activated by the two-component system BasRS**

We wanted to test if the potential BasR binding site that we noticed at the beginning of *plsB* coding sequence, homolog to the PmrA consensus described in *Salmonella*, might control *dgkA* expression. We therefore decided to test the effect of BasR over-production on the amount of the DgkA protein and on *dgkA* gene expression. We cloned the coding sequence of *basR* in the pBAD expression vector. We also cloned a mutated *basR53* allele coding for a BasR protein with a single amino acid substitution (residue 53 Glycine replaced by a Valine), which constitutively activates the *basRS* (*pmrAB)* regulon in *E. coli* (Froelich et al., 2006). Finally, we cloned *dcuR*, a response regulator homologous to *basR*, to use it as a control for specificity. All the proteins were correctly produced upon induction with 0,01% arabinose (Figure 4A).

We observed that BasR over-production increased DgkA-Flag production, whereas DcuR had no effect (Figure 4A). This stimulating effect of BasR on DgkA-Flag was further increased in the case of the BasR53 mutant protein (Figure 4A). The same result was obtained in the W3110DgkA-ProtA strain (data not shown).

In order to follow expression, we used transcriptional fusions with *gfp* (Zaslaver et al., 2006). However, the limits of the DNA region cloned in the *dgkA* transcriptional fusion available in the *E. coli* promoter library (Zaslaver et al., 2006) did not include the potential BasR binding site (Figure 1A). Therefore, we constructed new transcriptional fusions of different lengths, comprising the potential BasR binding site: *dgkA2* includes the BasR binding site and the full *plsB-dgkA* intergenic region, *dgkA3* excludes the *plsB*PσE promoter sequence, and *dgkA4*

excludes both the *plsB*PσE and *plsB*P2 promoter regions (Figure 1A). Contrary to the initial *dgkA* plasmid from the *E. coli* promoter library, a weak but detectable signal (above the pUA66 negative control) could be measured for the *dgkA4* construct (Figure 5A). Moreover, while the over-production of BasR53 had no effect on the expression of the *dgkA* initial construct, it enhanced the expression of the three new transcriptional fusions comprising the potential BasR binding site, *dgkA2*, *dgkA3*, and most strongly the shorter *dgkA4* (Figure 5A). For the same three constructions, the signal was enhanced with BasR or BasR53 over-production, but not with DcuR over-production, showing the specificity of this activation (Figure 5B and data not shown). These results locate the promoter of *dgkA* inside the fragment of 160 base pairs cloned in the *dgkA4* transcriptional fusion, comprising the consensus for BasR(PmrA) binding (Figure 1). We ran a search on this sequence for a putative promoter using a set of bioinformatic servers (Reese, 2001; Gordon et al., 2003) and got a strong hit. The predicted promoter has a +1 transcription start site 180 base pairs before the start codon of *dgkA*, good -10 and -35 consensus sequences, and the BasR(PmrA) binding site is located on top of the -35 region, as described for other promoters regulated by PmrA (Marchal et al., 2004) (Figure 1B).

In order to demonstrate that the induction by BasR was due to the identified BasR binding site, we introduced a mutation in the *dgkA3* transcriptional fusion, in the BasR consensus site (*dgkA3#*). As an additional negative control, we also mutated a T repeat located just upstream (*dgkA3*T), which might correspond to the consensus described for ColR binding, a regulator that has been shown to induce *dgkA* expression in *Pseudomonas fluorescens* (Kivistik et al., 2009). The mutation in the BasR binding consensus abolished the response of the transcriptional fusions to BasR53 overproduction, whereas the mutation in the T repeat did not modify the response (Figure 5C).

In the same way that we followed PlsB-TAP protein amounts in strains carrying mutations in *plsB* promoters, we verified that DgkA-ProtA was under the control of the identified BasR activated promoter *in vivo*. We introduced a mutation in the BasR consensus, in the pKO3-*plsBdgkA* plasmid (mut#, pEB1267) in order to insert this mutation in the chromosome of the W3110/DgkA-ProtA strain. DgkA-ProtA amounts in strains containing a wild type (EB401) or mutated (EB637) BasR binding site followed exactly the changes observed in the activities of the transcriptional fusions: there was a slight increase in the basal DgkA-ProtA amount in the strain carrying the mutation (Figure 4B, compare lanes 1 and 3), and there was no increase upon BasR53 production, contrary to the wild type promoter (Figure 4B).

To definitively demonstrate the direct regulation of *dgkA* by BasR, we performed gel mobility shift assays. BasR, BasR53, and DcuR proteins were purified as recombinant proteins with a 6His-Tev N-terminal tag (Materials and Methods). The binding of these proteins on DNA fragments obtained by PCR was then tested by gel mobility shift assay. 6His-Tev-BasR provoked a clear shift of a DNA fragment comprising the *arnB* promoter region, whereas there was no effect of the 6His-Tev-DcuR protein at the same concentration (Figure 6, left hand panel). This showed the direct binding of BasR on the *arnB* promoter of *E. coli*, which was already described for *S. typhimurium* (Wosten and Groisman, 1999) and expected in *E. coli* because *arnB* is activated by BasR (Hagiwara et al., 2004; Froelich et al., 2006). The assay was then performed with a DNA fragment corresponding to the region cloned in the *dgkA2* transcriptional fusions (Figure 1A). 6His-Tev-BasR53 provoked a shift of the DNA, whereas there was no effect with the 6His-Tev-DcuR protein at the same concentration (Figure 6). Finally, to demonstrate the specificity of this shift (which unfortunately did not show a clear shifted band), we tested the

binding of 6His-Tev-BasR53 on the same fragment, but containing the mut# mutation in the predicted BasR binding motif. A weak amount of retarded material was observed, but the band corresponding to the mutated *dgkA* promoter did not disappear (Figure 6, compare *dgkA2* and *dgkA2*mut# with BasR53). This set of gel shift assays demonstrated that BasR directly bind the BasR consensus sequence in the promoter of *dgkA* that we have evidenced.

***dgkR*, epilogue**

The results reported above demonstrated that the response regulator BasR activates *dgkA* expression. The *dgkR-1* mutant allele reported previously, which provokes an increased in DgkA enzymatic activity and a reduced PlsB activity (Walsh et al., 1986), was mapped crudely in the vicinity of *basRS* on the chromosome (Raetz et al., 1981). This suggested to us that *dgkR-1* might correspond to a point mutation in *basR* or *basS* genes, resulting in a constitutive activation of the 2-component system.

We first tested if *dgkA* expression was indeed induced in the GK1 (*dgkR-1*) strain compared to the parental strain R477. Using the *dgkA4* transcriptional fusion, we verified that *dgkA* was indeed induced in the *dgkR-1* mutant (figure 7A). We further checked the expression of *ais*, *ugd,* and *arnB*, three genes that are known to be activated by BasR (PmrA) in *E. coli* or *Salmonella* (Wosten and Groisman, 1999; Froelich et al., 2006). The induction of the whole BasR regulon (Figure 7A) strengthened the hypothesis that *dgkR-1* might be a constitutively active *basRS* mutant. Therefore, we sequenced the *basRS* locus in R477 (parental strain) and GK1 (*dgkR-1*) *E. coli* strains. We identified a point mutation in *basS* open reading frame, corresponding to a mutation of Aspartate 312 to Asparagine in BasS protein.

We then cloned wild type *basS* and *basS*(D312N) alleles in pBAD24 in order to verify that this point mutation alone was responsible for the activation of *dgkA* and the whole BasR regulon. Overexpression of wild type *basS* complemented the phenotype of up-regulation of *dgkA* and *ais* in GK-1 (figure 7B), demonstrating that the D312N mutation was involved in this up-regulation. Furthermore, over-production of the mutated BasS(D312N) protein in a MG1655Δ*basS* strain induced the expression of *dgkA* and *ais* (figure 7C), showing that the mutation alone was sufficient to constitutively induce the BasR regulon. Interestingly, over-production of BasS(D312N) protein in MG1655Δ*basS* decreased the expression of *plsB*, which is consistent with the reduced PlsB activity described in *dgkR-1* strain GK-1 (figure 7C).

In conclusion, we showed that *dgkR-1* mutant is a constitutively active *basS(D312N)* mutant, triggering the activation of the whole BasR regulon, including *dgkA*.

DISCUSSION

In the present paper, we have dissected the regulation of the *plsB* and *dgkA* genes in response to different stress regulators. We have demonstrated that *dgkA* is part of the BasRS regulon and identified the BasR binding sequence, at the beginning of the reverse *plsB* coding sequence. As already known, *plsB* is activated by σE, but we have further shown that this induction is accompanied by an inhibition of DgkA production. Finally, we have evidenced a second promoter for *plsB* transcription. This second promoter is responsible for the basal and strong activity during growth, whereas the σE dependent promoter is only activated during σE specific stresses.

dgkA is activated by BasR.

That *dgkA* is part of the BasRS regulon appeared as a surprise, because it was never identified before in transcriptomic or bioinformatic approaches aimed at defining this regulon, either in *S. typhimurium* or in *E. coli*. In depth studies have been performed mainly in *S. typhimurium*, and differences between the two bacteria may explain this absence. However, the PmrA(BasR) binding site consensus we identified upstream *dgkA* in *E. coli* is exactly conserved in *S. typhimurium* sequence, and match well enough the refined consensus sequence proposed for *S. typhimurium* (Figure 1B) (Marchal et al., 2004). The BasR binding site overlaps the -35 region of the predicted *dgkA* promoter. This is similar to the organization of all the promoters activated by PmrA(BasR) that have been described before (Marchal et al., 2004). Yet, the position of the *dgkA* promoter, so far away from the start codon (180 bp) and located at the beginning of *plsB* ORF (Figure 1A), might explain the fact that this potential site was not taken into account. It has still to be understood why the leader sequence of *dgkA* is so long. The *dgkA* gene was not

identified either in the transcriptome performed in *E. coli* (Hagiwara et al., 2004). Yet, this study consisted in comparing the Δ*basRS* mutant strain to a wild type strain, and the level of *dgkA* expression might have been too low already in the wild type strain to see any difference. This seems consistent with the fact that we were not able either to see any effect of the Δ*basR* or Δ*basS* deletion on the DgkA protein amounts (data not shown). Furthermore, using transcriptional fusion with *gfp*, the basal signal given by the *dgkA* fusions in standard growth conditions was always hardly detectable above the pUA66 background. Strong expression of *dgkA* was only observed in condition of BasRS activation: by overproducing BasR or BasR53 regulators, or in the *dgkR*-1 (*basS*(D312N)) genetic context. A new approach of transcriptomic definition of the BasRS regulon might be to compare Δ*basRS* strain with a strain overproducing BasR, as it has been done for defining σE regulon in *E. coli* (Rhodius et al., 2006). Finally, one has to remain cautious when comparing regulation mechanisms in *S. typhimurium* and *E. coli*, as it has been shown that all regulatory circuits may not be interchangeable and identical in the two bacteria (Perez and Groisman, 2009). Furthermore, there seems to be a great diversity in the 2 component systems that are used for controlling LPS modification genes or *dgkA*. For example, in *Pseudomonas aeruginosa*, the ParR-ParS system is used (Fernandez et al., 2010), in *Pseudomonas fluorescens*, the ColR-ColS has been suggested to control *dgkA* expression (Kivistik et al., 2009), and the PmrAB two-component system does not control at all LPS modification genes in *Legionella pneumophila* (Al-Khodor et al., 2009).

So, why *dgkA* would be activated by the BasRS two-component regulatory system? It has been shown in the last years that many of the genes of the regulon code for enzymes involved in LPS modifications (Raetz et al., 2007). Indeed, during their export to the outer face of the outer membrane of bacteria, LPS molecules can be modified with several decorations, such as

phosphoethanolamine, 4-amino-4-deoxy-L-arabinose, or palmitate (Raetz et al., 2007). One of the enzymes of the regulon, *pmrC* (*eptA* in *E. coli*), is involved in the transfer of phosphoethanolamine from phosphatidylethanolamine to the 1-phosphate group of the heptose residue in lipid A (Lee et al., 2004). This reaction releases a diacylglycerol, the substrate of the diacylglycerol kinase DgkA. DgkA recycles diacylglycerol into phosphatidic acid, which can then reenter the phospholipid biosynthesis pathway (Raetz and Newman, 1978). Until now, DgkA has been involved only in the recycling of diacylglycerol produced by MDO biosynthesis (Zhang and Rock, 2008a). But, it was observed that MDO biogenesis could be accounted for only ⅔ of the diacylglycerol that accumulates upon *dgkA* inactivation (Rotering and Raetz, 1983). It was then already proposed that the remaining ⅓ of diacylglycerol accumulation might result from LPS modification by phosphoethanolamine, catalysed by enzymes of the *eptA* family (Reynolds et al., 2005). Therefore, it is logical that *dgkA*, as the recycling enzyme, would be part of a group of enzymes producing diacylglycerol. Strikingly, in some proteobacteria such as Vibrios and Campylobacter, *dgkA* and *eptA* are neighboring genes, together with *basR* and *basS*. Consequently, the STRING server predicts a functional association between *dgkA* and *eptA* based on neighborhood and cooccurrence, with a score of 0.82 (Jensen et al., 2009). This strengthens our finding of a genetic and functional association of DgkA with the enzymes of LPS modifications.

Antagonist roles of BasR and RpoE stress responses on envelope remodeling?

Our results show that *dgkA* expression is activated by BasR, whereas it is inhibited by σE. Conversely, *plsB* expression is activated by σE, whereas it is at least partially inhibited by BasR as can be seen in GK1 strain (Figure 7C and Walsh et al., 1986). Other data from the literature

point to opposite effects triggered by the σE and BasRS (PmrAB) stress responses on the regulation of LPS modifications. EptA and EptB are homolog enzymes that catalyze the transfer of a phosphoethanolamine from phosphatidylethanolamine to the LPS, but they are responsible for the modification of two different positions of the lipid A molecule (outer Kdo residue of Kdo2-lipid A in the case of EptB and the 1-phosphate group in the case of EptA) that might have different consequences on LPS biochemical properties (Reynolds et al., 2005). In contrary to *eptA* that is activated by BasR (Wosten and Groisman, 1999; Froelich et al., 2006), *eptB* is not. But, it is activated indirectly by σE both in *E. coli* and in *S. typhimurium* (Rhodius et al., 2006; Figueroa-Bossi et al., 2006). This indirect activation might be explained by the fact that *eptB* is inhibited by the small RNA MgrR, which is part of the PhoPQ regulon (Moon and Gottesman, 2009), and that the small RNA MicA, induced by σE, inhibits PhoPQ (Coornaert et al., 2010). In *Salmonella*, PhoPQ activates indirectly *eptA* expression by activating PmrAB (Kox et al., 2000). Therefore, it seems that EptA and EptB driven LPS modifications may be antagonist, and more generally that BasRS or σE stress responses may trigger different modifications of LPS. Despite the fact that PhoPQ and BasRS are not similarly regulated in *S. typhimurium* and *E. coli* (Perez and Groisman, 2009), and that the above references are a mix of studies in *S. typhimurium* and *E. coli*, it appears that regulatory cascades involving PhoPQ, BasRS, σE, and small RNAs fine-tune LPS modifications in response to a variety of stress and growth conditions (Overgaard et al., 2009).

Yet, both EptA and EptB activities produce diacylglycerol, so DgkA that recycles diacylglycerol is expected to be required in both cases of *eptA* or *eptB* activation. In *E. coli*, whereas BasR logically activates *dgkA* (this paper) together with *eptA* (Froelich et al., 2006), σE inhibits *dgkA* (this paper) in conjunction with the activation of *eptB* (Rhodius et al., 2006).

Therefore, the fate of the diacylglycerol produced by *eptB* during RpoE stress response remains to be elucidated.

***plsB* expression is driven by two promoters.**

We have shown that in addition to its already described σE promoter (Rhodius et al., 2006), *plsB* expression is driven by a second proximal promoter. In fact, our results demonstrate that it is this second promoter that is responsible for the basal expression of *plsB* when there is no extracellular stress signal. *plsB* is an essential gene (Yoshimura et al., 2007), and we reasoned that this second promoter might be required for growth. However, when we mutated it in strain W3100P*2*plsB*-TAP, we did not detect obvious effect on growth (data not shown). Maybe this was because this mutation did not abolish completely the production of PlsB (Figure 2).

We propose that this second promoter P2 links *plsB* expression to growth rate, through a control by ppGpp. Indeed, we found that the activity of the promoter was increased in a ppGpp° strain (Figure 3B). This result is strengthened by a global study of promoter activities in *E. coli* grown under two growth rate conditions, showing higher activity of *plsB* promoter at higher growth rate (Zaslaver et al., 2009). As the first step in the pathway of de novo phospholipid synthesis, control of *plsB* expression by ppGpp may explain how phospholipid synthesis is maintained under growth rate control, ensuring that phospholipid content remains constant. It was already described that PlsB is the crucial point of inhibition of phospholipid synthesis during stringent response, but it was suggested that ppGpp inhibited the enzymatic activity of PlsB (Heath et al., 1994). While our results do not rule out this possibility, they clearly indicate that there is a control at the expression level. It will be interesting to test if other phospholipid synthesis genes than *plsB* are under growth rate or ppGpp control, as already suggested by the

transcriptome studies of the stringent response (Durfee et al., 2008; Traxler et al., 2008; Aberg et al., 2009).

plsB expression is activated by σE, whereas it is inhibited by ppGpp. Because full σE activity requires the presence of ppGpp (Costanzo and Ades, 2006; Costanzo et al., 2008), the opposite effect of the two stress response regulators on *plsB* expression may appear paradoxical. Yet, the presence of two distinct promoters resolves this apparent paradox. They can integrate different kind of stress responses, and for example permit *plsB* expression when required, despite a global stringent response.

Global conclusion

In conclusion, the *plsB-dgkA* locus integrates three distinct types of stress signals: global stringent response, BasRS two-component system, and extracytoplasmic stress, thanks to 3 different promoters. For these three types of stress responses, the two genes might be regulated in opposite manners: we have shown here that it is the case for σE (*dgkA* down and *plsB* up) and transcriptome results suggest that it is the case for the stringent response (*plsB* down and *dgkA* up) (Durfee et al., 2008). Finally, *plsB* expression is reduced when BasS(D312N) is overproduced, whereas *dgkA* is activated (this work), consistent with the corresponding enzymatic activities reported in the GK-1 mutant (Raetz et al., 1981). This specific organization of *plsB* and *dgkA* genes is restricted to enterobacteria, and might reflect a specific need for coordinated envelope and LPS biogenesis regulation in the lifestyle of these bacteria.

Our results show that phospholipid biogenesis is clearly subjected to genetic regulation in response to stress. Yet, we only investigated here the regulation of *plsB* and *dgkA*. It suggests that there are still a lot of stress response mechanisms to uncover in this metabolic pathway. For

example, a *pssR* regulator has been suggested but never identified (Sparrow and Raetz, 1983) and several genes homolog to phospholipid synthesis genes have yet no clear physiological function and might be required for stress adaptation as suggested by their up-regulation during stringent response (Traxler et al., 2008).

EXPERIMENTAL PROCEDURES

Media and antibiotics

Cells are grown at 37 °C in Lysogeny Broth (LB) medium unless otherwise stated. The plasmids are maintained with ampicillin (100 μg/ml), chloramphenicol (50 μg/ml), or kanamycin (50 μg/ml).

Plasmid construction

Transcriptional fusions with gfp. Gene expression was monitored using transcriptional fusions with *gfp* using the pUA66 and pUA139 plasmids (Zaslaver et al., 2006). The transcriptional fusions with promoters of *plsB*, *arnB*, *ais*, *ugd*, and *rpoE* were taken from the *E. coli* promoter library (Zaslaver et al., 2006). The other intergenic regions tested between *plsB* and *dgkA* were amplified by PCR with different primer pairs (see table S1) using purified genomic DNA of MG1655 strain for the matrix. PCR products were then digested by BamHI/XhoI restriction enzymes and cloned into pUA139 or pUA66 depending on the desired orientation (Zaslaver et al., 2006). Mutagenesis was performed using the QuikChange® Site-Directed Mutagenesis Kit (Stratagene), to introduce mutations in the *plsB*PσE (mut*) or *plsB*P2 (mut*2) promoters of *plsB*, in the PmrA consensus site (mut#) and in the upstream T repeat (mutT) using oligonucleotide pairs Ebm433/434, Ebm586/587, Ebm547/548, and Ebm545/546 respectively (see table S1).

Protein expression and purification. The expression vector pET-6His-Tev (pEB1188) was obtained by inserting hybridized oligonucleotides Ebm577 and Ebm578 in pET22 (Novagen) digested by NdeI/EcoRI. Sequences coding for *rpoE*, *basR*, *basS*, *basS*(D312N) or *dcuR* genes were amplified by PCR on genomic DNA (MG1655 or GK1 for *basS*(D312N)) using the

oligonucleotides indicated in table 1, digested by EcoRI/XhoI and cloned into pBAD24 (Guzman et al., 1995) digested by EcoRI/SalI or into pET6-His-Tev (pEB1188) digested by EcoRI/XhoI. pBAD-*basR53* and pET6HisTev-*basR53* plasmids were constructed by performing site directed mutagenesis on both pBAD-*basR* and pET-6His-Tev-*basR* plasmids with oligonucleotides Ebm542 and Ebm543 (see table S1).

Strain construction

Tagging on the chromosome. In order to introduce the sequences coding for TAP, SPA, ProtA, or Flag tags (Zeghouf et al., 2004) downstream of *plsB* or *dgkA* genes on the chromosome, we amplified the corresponding cassettes from plasmids pJL72 and pJL148. We used oligonucleotides Ebm332/333 for tagging *plsB* with TAP and SPA cassettes, and oligonucleotides Ebm398/409 for tagging *dgkA* with ProtA or 3Flag (Table S1). Then, the cassettes were introduced in BW25113/pKD46 cells following the protocol of Datsenko and Wanner (Datsenko and Wanner, 2000). The recombinant genes were transferred to the desired strain background by P1 transduction (Miller, 1992). When required (for transformation with the transcriptional fusion plasmids carrying resistance to kanamycin), the resistance to kanamycin gene was removed using the pCP20 plasmid (Cherepanov and Wackernagel, 1995), allowing the transduction of other alleles linked to kanamycin resistance. Likewise, the Δ*basR::kana*^{R} allele was combined with *dgkA-flag*° allele in W3110. MG1655Δ*relA*°*spoT*207 (EB425) was constructed by transducing *spoT207* allele (from CF1693) in MG1655Δ*relA*° (EB421).

Insertion of point mutation in the promoter sequences on the chromosome. A sequence of 1650 base pairs comprising the *plsB-dgkA* intergenic region was cloned between BamHI and SalI restriction sites of pKO3 (Link et al., 1997). Mutations in the σE-dependent promoter of *plsB* (*),

in the second promoter of *plsB* (*2), and in the PmrA consensus site (#) were introduced by directed mutagenesis in the pKO3-*plsBdgkA* plasmid (pEB1207), using oligonucleotides Ebm433/434, Ebm586/587, and Ebm547/548 respectively. The point mutations were then introduced in the chromosome of W3110/plsB-TAP° (EB367), W3110/*dgkA*-flag° (EB401), and W3110/*dgkA*-ProtA° (EB395) strains following the method described previously (Link et al., 1997).

Protein purification

BL21(DE3)Lys strain was transformed with plasmids pET-6His-Tev-*dcuR* (pEB1190), pET-6His-Tev-*basR* (pEB1189), or pET-6His-Tev-*basR53* (pEB1192) (Table 1). Strains were grown in 500 ml LB at 30°C. At OD_{600nm}=0.9, 1 mM IPTG was added and the cultures incubated during 6 hours at 23°C. After pelleting, the cells were broken by sonication in 10 ml of buffer 1 (20 mM Tris-HCl pH 8, 200 mM NaCl, 2 mM ß-mercaptoethanol, 10 mM imidazole, 0.2 % NP40) and the extract was then centrifuged during 30 min at 27000 g before incubation on 500 µl of Talon beads (Clontech) on a wheel during 2 hours at 4°C. The beads were washed with 15 ml buffer 1, 5 ml buffer 1 with 1 M NaCl, and 10 ml buffer 1. Proteins were eluted in 5 steps of 500 µl buffer 1 with 200 mM imidazole. The protein concentrations determined by a Bradford assay was about 0.5 mg/ml.

Gel mobility shift assay

Gel mobility shift assays were performed using DNA fragments obtained by PCR. 6His-Tev-BasR, -BasR53 or -DcuR purified proteins (see figure legend for quantities) were mixed with 100 ng of the DNA fragments to be tested and 200 ng of an unspecific PCR

preparation in 20 µl of 25 mM Tris-HCl (pH 7.2), 10 mM $MgCl_2$, 1 mM $CaCl_2$, 0.5 mM EDTA (pH 8.0), 50 mM KCl and 5 % glycerol. The reaction mixture was allowed to stand at room temperature (20°C) for 30 minutes and then loaded onto a 10% polyacrylamide gel (polyacrylamide/bisacrylamide, 29:1, w/w). The gel was pre run in TBE 0.5X for 30 minutes at 80 V, loaded and run for 2h30 at room temperature. The shift was revealed by coloration of the gel with Gel Red.

Measure of promoter activity with *gfp* transcriptional fusions

We used several clones from the *E. coli* transcriptional fusion library (Zaslaver et al., 2006), obtained through Open Biosystems, and we constructed the required additional transcriptional fusions (see above for plasmid construction and table 1). MG1655 wild type *E. coli* strain or isogenic mutant strains were transformed with plasmids carrying the *gfp* transcriptional fusions and maintained with kanamycin. For co-transformation, compatible plasmids (pBAD24 and derivatives) were used and ampicillin added. Selection plates were incubated at 37°C for 16 hours. 600 μL of LB medium supplemented with required antibiotics, and with arabinose (0,01 % or 0,05 %) when necessary for PBAD-driven expression, were inoculated (4 to 6 replicate each assay) and grown for 16 hours at 30°C in 96-well polypropylene plates of 2.2 ml wells under aeration and agitation. Fluorescent intensity measurement was performed in a TECAN© infinite M200. 150 μL of each well were transferred into a black Greiner 96 well plate for reading absorbance at 600nm and fluorescence (excitation: 485 nm; emission: 530 nm). The expression levels were calculated by dividing the intensity of fluorescence by the absorbance at 600nm. These results are given in arbitrary units because the intensity of fluorescence is acquired with a variable gain and hence varies from one experiment to the other.

SDS-PAGE and Western blot

SDS-PAGE, electrotransfer onto nitrocellulose membranes, and Western-blot analyses were performed as previously described (Gully et al., 2003). TAP and ProtA tags were detected with the PAP antibody from Sigma. Monoclonal anti-Flag M2 was purchased from Sigma. Anti-σE was purchased from Neoclone.

ACKNOWLEDGMENTS

We thank C.R. Raetz who sent us the R477 and GK-1 strains, so long after their original publication in 1981. We are very grateful to U. Alon for the distribution of the *E. coli* transcriptional fusions library, and to the researchers of the Keio university for the library of *E. coli* deletion mutants. We also thank JF Greenblat's lab for the SPA and TAP plasmids for tagging proteins in *E. coli* strains. We thank Jennifer Spagnolo who performed some plasmid constructions. We thank Eric Cascales for helpful technical advices and the Cascales', Lloubès', and Sturgis' lab members for discussion. A.W. was recipient of Marie Curie and FRM fellowships. Research was funding by the CNRS and the ANR.

REFERENCES

Aberg, A., Fernandez-Vazquez, J., Cabrer-Panes, J.D., Sanchez, A., and Balsalobre, C. (2009) Similar and divergent effects of ppGpp and DksA deficiencies on transcription in *Escherichia coli*. *J Bacteriol* **191**: 3226-3236.

Al-Khodor, S., Kalachikov, S., Morozova, I., Price, C.T., and Abu Kwaik, Y. (2009) The PmrA/PmrB two-component system of *Legionella pneumophila* is a global regulator required for intracellular replication within macrophages and protozoa. *Infect Immun* **77**: 374-386.

Baba, T., Ara, T., Hasegawa, M., Takai, Y., Okumura, Y., Baba, M., Datsenko, K.A., Tomita, M., Wanner, B.L., and Mori, H. (2006) Construction of *Escherichia coli* K-12 in-frame, single-gene knockout mutants: the Keio collection. *Mol Syst Biol* **2**: 2006.0008.

Badola, P., and Sanders, C.R.n. (1997) *Escherichia coli* diacylglycerol kinase is an evolutionarily optimized membrane enzyme and catalyzes direct phosphoryl transfer. *J Biol Chem* **272**: 24176-24182.

Baracchini, E., and Bremer, H. (1988) Stringent and growth control of rRNA synthesis in *Escherichia coli* are both mediated by ppGpp. *J Biol Chem* **263**: 2597-2602.

Cherepanov, P.P., and Wackernagel, W. (1995) Gene disruption in Escherichia coli: TcR and KmR cassettes with the option of Flp-catalyzed excision of the antibiotic-resistance determinant. *Gene* **158**: 9-14.

Coornaert, A., Lu, A., Mandin, P., Springer, M., Gottesman, S., and Guillier, M. (2010) MicA sRNA links the PhoP regulon to cell envelope stress. *Mol Microbiol* **76**: 467-479.

Costanzo, A., and Ades, S.E. (2006) Growth phase-dependent regulation of the extracytoplasmic stress factor, sigmaE, by guanosine 3',5'-bispyrophosphate (ppGpp). *J Bacteriol* **188**: 4627-4634.

Costanzo, A., Nicoloff, H., Barchinger, S.E., Banta, A.B., Gourse, R.L., and Ades, S.E. (2008) ppGpp and DksA likely regulate the activity of the extracytoplasmic stress factor sigma(E) in *Escherichia coli* by both direct and indirect mechanisms. *Mol Microbiol* **67**: 619-632.

Cronan, J.E. (2003) Bacterial membrane lipids: where do we stand? *Annu Rev Microbiol* **57**: 203-224.

Datsenko, K.A., and Wanner, B.L. (2000) One-step inactivation of chromosomal genes in *Escherichia coli* K-12 using PCR products. *Proc Natl Acad Sci U S A* **97**: 6640-6645.

Durfee, T., Hansen, A.M., Zhi, H., Blattner, F.R., and Jin, D.J. (2008) Transcription profiling of the stringent response in *Escherichia coli*. *J Bacteriol* **190**: 1084-1096.

Eichel, J., Chang, Y.Y., Riesenberg, D., and Cronan, J.E.J. (1999) Effect of ppGpp on *Escherichia coli* cyclopropane fatty acid synthesis is mediated through the RpoS sigma factor (sigmaS). *J Bacteriol* **181**: 572-576.

Fernandez, L., Gooderham, W.J., Bains, M., McPhee, J.B., Wiegand, I., and Hancock, R.E. (2010) Adaptive resistance to the "last hope" antibiotics polymyxin B and colistin in Pseudomonas aeruginosa is mediated by the novel two-component regulatory system ParR-ParS. *Antimicrob Agents Chemother* **54**: 3372-3382.

Figueroa-Bossi, N., Lemire, S., Maloriol, D., Balbontin, R., Casadesus, J., and Bossi, L. (2006) Loss of Hfq activates the sigmaE-dependent envelope stress response in *Salmonella enterica*. *Mol Microbiol* **62**: 838-852.

Froelich, J.M., Tran, K., and Wall, D. (2006) A pmrA constitutive mutant sensitizes *Escherichia coli* to deoxycholic acid. *J Bacteriol* **188**: 1180-1183.

Fujita, Y., Matsuoka, H., and Hirooka, K. (2007) Regulation of fatty acid metabolism in bacteria. *Mol Microbiol* **66**: 829-839.

Gordon, L., Chervonenkis, A.Y., Gammerman, A.J., Shahmuradov, I.A., and Solovyev, V.V. (2003) Sequence alignment kernel for recognition of promoter regions. *Bioinformatics* **19**: 1964-1971.

Gully, D., Moinier, D., Loiseau, L., and Bouveret, E. (2003) New partners of acyl carrier protein detected in *Escherichia coli* by tandem affinity purification. *FEBS Lett* **548**: 90-96.

Guzman, L.M., Belin, D., Carson, M.J., and Beckwith, J. (1995) Tight regulation, modulation, and high-level expression by vectors containing the arabinose PBAD promoter. *J Bacteriol* **177**: 4121-4130.

Hagiwara, D., Yamashino, T., and Mizuno, T. (2004) A Genome-wide view of the *Escherichia coli* BasS-BasR two-component system implicated in iron-responses. *Biosci Biotechnol Biochem* **68**: 1758-1767.

Heath, R.J., Jackowski, S., and Rock, C.O. (1994) Guanosine tetraphosphate inhibition of fatty acid and phospholipid synthesis in *Escherichia coli* is relieved by overexpression of glycerol-3-phosphate acyltransferase (*plsB*). *J Biol Chem* **269**: 26584-26590.

Hernandez, V.J., and Bremer, H. (1990) Guanosine tetraphosphate (ppGpp) dependence of the growth rate control of *rrnB* P1 promoter activity in *Escherichia coli*. *J Biol Chem* **265**: 11605-11614.

Jensen, L.J., Kuhn, M., Stark, M., Chaffron, S., Creevey, C., Muller, J., Doerks, T., Julien, P., Roth, A., Simonovic, M., Bork, P., and von Mering, C. (2009) STRING 8--a global view on proteins and their functional interactions in 630 organisms. *Nucleic Acids Res* **37**: D412-6.

Kivistik, P.A., Kivi, R., Kivisaar, M., and Horak, R. (2009) Identification of ColR binding consensus and prediction of regulon of ColRS two-component system. *BMC Mol Biol* **10**: 46.

Kox, F.F.L., Wösten, M.M.S.M., Groisman E.A., (2000) A small protein that mediates the activation of a two-component system by another two-component system. *EMBO Journal* **19**: 1861-1872.

Lee, H., Hsu, F.F., Turk, J., and Groisman, E.A. (2004) The PmrA-regulated *pmrC* gene mediates phosphoethanolamine modification of lipid A and polymyxin resistance in *Salmonella enterica*. *J Bacteriol* **186**: 4124-4133.

Link, A.J., Phillips, D., and Church, G.M. (1997) Methods for generating precise deletions and insertions in the genome of wild-type *Escherichia coli*: application to open reading frame characterization. *J Bacteriol* **179**: 6228-6237.

Marchal, K., De Keersmaecker, S., Monsieurs, P., van Boxel, N., Lemmens, K., Thijs, G., Vanderleyden, J., and De Moor, B. (2004) In silico identification and experimental validation of PmrAB targets in *Salmonella typhimurium* by regulatory motif detection. *Genome Biol* **5**: R9.

Miller, J.H. (1992) A short course in bacterial genetics : a laboratory manual and handbook for *Escherichia coli* and related bacteria. (ed). Plainview, N.Y: Cold Spring Harbor Laboratory Press, pp. 2 v.

Moon, K., and Gottesman, S. (2009) A PhoQ/P-regulated small RNA regulates sensitivity of *Escherichia coli* to antimicrobial peptides. *Mol Microbiol* **74**: 1314-1330.

Overgaard, M., Kallipolitis, B., and Valentin-Hansen, P. (2009) Modulating the bacterial surface with small RNAs: a new twist on PhoP/Q-mediated lipopolysaccharide modification. *Mol Microbiol* **74**: 1289-1294.

Perez, J.C., and Groisman, E.A. (2009) Evolution of transcriptional regulatory circuits in bacteria. *Cell* **138**: 233-244.

Potrykus, K., and Cashel, M. (2008) (p)ppGpp: still magical? *Annu Rev Microbiol* **62**: 35-51.

Raetz, C.R., Kantor, G.D., Nishijima, M., and Jones, M.L. (1981) Isolation of *Escherichia coli* mutants with elevated levels of membrane enzymes. A trans-acting mutation controlling diglyceride kinase. *J Biol Chem* **256**: 2109-2112.

Raetz, C.R., and Newman, K.F. (1978) Neutral lipid accumulation in the membranes of *Escherichia coli* mutants lacking diglyceride kinase. *J Biol Chem* **253**: 3882-3887.

Raetz, C.R., Reynolds, C.M., Trent, M.S., and Bishop, R.E. (2007) Lipid A modification systems in gram-negative bacteria. *Annu Rev Biochem* **76**: 295-329.

Reese, M.G. (2001) Application of a time-delay neural network to promoter annotation in the *Drosophila melanogaster* genome. *Comput Chem* **26**: 51-56.

Reynolds, C.M., Kalb, S.R., Cotter, R.J., and Raetz, C.R. (2005) A phosphoethanolamine transferase specific for the outer 3-deoxy-D-manno-octulosonic acid residue of *Escherichia coli* lipopolysaccharide. Identification of the *eptB* gene and Ca2+ hypersensitivity of an *eptB* deletion mutant. *J Biol Chem* **280**: 21202-21211.

Rhodius, V.A., Suh, W.C., Nonaka, G., West, J., and Gross, C.A. (2006) Conserved and variable functions of the sigmaE stress response in related genomes. *PLoS Biol* **4**: e2.

Rotering, H., and Raetz, C.R. (1983) Appearance of monoglyceride and triglyceride in the cell envelope of *Escherichia coli* mutants defective in diglyceride kinase. *J Biol Chem* **258**: 8068-8073.

Saha, S.K., Nishijima, S., Matsuzaki, H., Shibuya, I., and Matsumoto, K. (1996) A regulatory mechanism for the balanced synthesis of membrane phospholipid species in *Escherichia coli*. *Biosci Biotechnol Biochem* **60**: 111-116.

Sparrow, C.P., and Raetz, C.R. (1983) A trans-acting regulatory mutation that causes overproduction of phosphatidylserine synthase in *Escherichia coli*. *J Biol Chem* **258**: 9963-9967.

Srivatsan, A., and Wang, J.D. (2008) Control of bacterial transcription, translation and replication by (p)ppGpp. *Curr Opin Microbiol* **11**: 100-105.

Travers, A.A. (1980) Promoter sequence for stringent control of bacterial ribonucleic acid synthesis. *J Bacteriol* **141**: 973-976.

Traxler, M.F., Summers, S.M., Nguyen, H.T., Zacharia, V.M., Hightower, G.A., Smith, J.T., and Conway, T. (2008) The global, ppGpp-mediated stringent response to amino acid starvation in *Escherichia coli*. *Mol Microbiol* **68**: 1128-1148.

Walsh, J.P., Loomis, C.R., and Bell, R.M. (1986) Regulation of diacylglycerol kinase biosynthesis in Escherichia coli. A trans-acting *dgkR* mutation increases transcription of the structural gene. *J Biol Chem* **261**: 11021-11027.

Wosten, M.M., and Groisman, E.A. (1999) Molecular characterization of the PmrA regulon. *J Biol Chem* **274**: 27185-27190.

Xiao, H., Kalman, M., Ikehara, K., Zemel, S., Glaser, G., and Cashel, M. (1991) Residual guanosine 3',5'-bispyrophosphate synthetic activity of *relA* null mutants can be eliminated by *spoT* null mutations. *J Biol Chem* **266**: 5980-5990.

Yoshimura, M., Oshima, T., and Ogasawara, N. (2007) Involvement of the YneS/YgiH and PlsX proteins in phospholipid biosynthesis in both *Bacillus subtilis* and *Escherichia coli*. *BMC Microbiol* **7**: 69.

Zaslaver, A., Bren, A., Ronen, M., Itzkovitz, S., Kikoin, I., Shavit, S., Liebermeister, W., Surette, M.G., and Alon, U. (2006) A comprehensive library of fluorescent transcriptional reporters for *Escherichia coli*. *Nat Methods* **3**: 623-628.

Zaslaver, A., Kaplan, S., Bren, A., Jinich, A., Mayo, A., Dekel, E., Alon, U., and Itzkovitz, S. (2009) Invariant distribution of promoter activities in *Escherichia coli*. *PLoS Comput Biol* **5**: e1000545.

Zeghouf, M., Li, J., Butland, G., Borkowska, A., Canadien, V., Richards, D., Beattie, B., Emili, A., and Greenblatt, J.F. (2004) Sequential Peptide Affinity (SPA) system for the identification of mammalian and bacterial protein complexes. *J Proteome Res* **3**: 463-468.

Zhang, Y.M., and Rock, C.O. (2008a) Membrane lipid homeostasis in bacteria. *Nat Rev Microbiol* **6**: 222-233.

Zhang, Y.M., and Rock, C.O. (2008b) Acyltransferases in bacterial glycerophospholipid synthesis. *J Lipid Res* **49**: 1867-1874.

Zhu, K., Zhang, Y.M., and Rock, C.O. (2009) Transcriptional regulation of membrane lipid homeostasis in *Escherichia coli*. *J Biol Chem* **284**: 34880-34888.

Name	Lab code[a]	Relevant characteristics[a]	Reference
pCP20	pEB266	ts, Cm^R, Amp^R, FLP recombinase gene	(Cherepanov and Wackernagel, 1995)
pKD46	pEB267	ts, Amp^R, lambda Red genes	(Datsenko and Wanner, 2000)
pJL72	pEB793	Amp^R, Km^R, TAP tag cassette	(Zeghouf et al., 2004)
pJL148	pEB794	Amp^R, Km^R, SPA tag cassette	(Zeghouf et al., 2004)
pBAD24	pEB227	Amp^R, ColE1 replication origin, P_{BAD} promoter	(Guzman et al., 1995)
pBAD24-*rpoE*	pEB1102	PCR ebm399/400 (EcoRI/XhoI) in pBAD24 (EcoRI/SalI)	this work
pBAD24-*basR*	pEB1149	PCR ebm516/517 (EcoRI/XhoI) in pBAD24 (EcoRI/SalI)	this work
pBAD24-*basR53*	pEB1165	Point mutation G53V	this work
pBAD24-d*cuR*	pEB1150	PCR ebm519/520 (EcoRI/XhoI) in pBAD24 (EcoRI/SalI)	this work
pBAD24-*basS*	pEB1195	PCR ebm582/583 (EcoRI/XhoI) in pBAD24 (EcoRI/SalI)	this work
pBAD24-*basS(D312N)*	pEB1276	PCR ebm582/583 on GK-1 (EcoRI/XhoI) in pBAD24 (EcoRI/SalI)	this work
pUA66	pEB898	Km^R, Transcriptional fusion GFP, cloning sites BamHI->XhoI	(Zaslaver et al., 2006)
pUA139	pEB987	Km^R, Transcriptional fusion GFP, cloning sites XhoI->BamHI	(Zaslaver et al., 2006)
pUA66-*dgkA*	-		(Zaslaver et al., 2006)
pUA66-*dgkA2*	pEB1115	PCR ebm431/432 in pUA66 (BamHI/XhoI)	this work
pUA66-*dgkA3*	pEB1171	PCR ebm541/432 in pUA66 (BamHI/XhoI)	this work
pUA66-*dgkA3#*	pEB1175	mutation in the PmrA consensus	this work
pUA66-*dgkA3T*	pEB1177	mutation T upstream the PmrA consensus	this work
pUA66-*dgkA4*	pEB1241	PCR ebm647/432 in pUA66 (BamHI/XhoI)	this work
pUA139-*plsB*	-		(Zaslaver et al., 2006)
pUA139-*plsBmut**	pEB1116	mutation in the *plsB*PSigE promoter	this work
pUA139-*plsBmut*2*	pEB1201	mutation in the *plsB*P2 promoter	this work
pUA139-*plsB*Δ	pEB1172	deletion of the *plsB*PSigE promoter	this work
pUA139-*plsB*Δmut*2	pEB1172	mutation in the *plsB*PSigE promoter	this work
pUA66-*rpoE*	-		(Zaslaver et al., 2006)
pUA66-*arnB*	-		(Zaslaver et al., 2006)
pUA66-*ais*	-		(Zaslaver et al., 2006)
pUA66-*ugd*	-		(Zaslaver et al., 2006)
pET22	pEB70	Amp^R, T7 promoter	Novagen
pET-6His-Tev	pEB1188	Ebm577/578 in pET22 (NdeI/EcoRI)	This work
pET-6His-Tev-*basR*	pEB1189	PCR ebm516/517 on *basR* in pEB1188 (EcoRI/XhoI)	This work
pET-6His-Tev-*basR53*	pEB1192	PCR ebm516/517 on *basR53* in pEB1188 (EcoRI/XhoI)	This work
pET-6His-Tev-*dcuR*	pEB1190	PCR ebm519/520 in pEB1188 (EcoRI/XhoI)	This work
pKO3	pEB232	*repA*(ts) Cm^R M13ori *sacB*	(Link et al., 1997)
pKO3-*plsBdgkA*	pEB1207	Ebm592/593 in pKO3 (BamHI/SalI)	this work
pKO3-*plsBdgkAmut#*	pEB1267	mutation ebm547/548 in the PmrA consensus	this work

pKO3-*plsBdgkAmut**	pEB1265	mutation ebm433/434 in the *plsB*PSigE promoter	this work
pKO3-*plsBdgkAmut**2	pEB1266	mutation ebm586/587 in the *plsB*P2 promoter	this work

Table 1: **Plasmids**. ts : thermosensitive. Amp^R Cm^R Km^R : genes coding respectively for ampicillin, chloramphenicol and kanamycin. a: Lab codes correspond to our stock numbering. b: the characteristics are given only for the vectors or the reference plasmids. Vectors and reference plasmids are in grey shade. Transcriptional fusions from the *E. coli* promoter library (Zaslaver et al., 2006) do not have lab codes.

Name	Relevant characteristics	Reference
R477	*F- thr-1 leu-6 his-4 rpsL136*	(Raetz et al., 1981)
GK-1	Diglyceride kinase hyperactive mutant *dgkR-1*, R477 derivative	(Raetz et al., 1981)
BL21(DE3) pLysS	F– *omp*T *hsd*SB(rB–, mB–) *gal dcm* (DE3) pLysS (CamR)	Novagen
BW25113	*rrnB3 ΔlacZ4787 hsdR514* Δ(*araBAD*) Δ(*rhaBAD*)568 *rph*-1	(Datsenko and Wanner, 2000)
EB428	BW25113 Δ*basR::kana*^{R}	(Baba et al., 2006)
EB427	BW25113 Δ*basS::kana*^{R}	(Baba et al., 2006)
EB126	BW25113 Δ*relA::kana*^{R}	(Baba et al., 2006)
CF1693	MG1655Δ*relA251::kana*^{R} Δ*spoT207::cam*^{R}	(Xiao et al., 1991)
EB132	BW25113 Δ*dksA::kana*^{R}	(Baba et al., 2006)
W3110	F- LAM-IN(*rrnD-rrnE*)1 rph-1	Bachmann (1987)
EB385	W3110*plsB*-SPA°::*kana*^{R} - pKD46 mediated TAP-kana recombination	this work
EB367	W3110*plsB*-TAP° - pKD46 mediated TAP-kana recombination	this work
EB613	W3110*plsB*P2mut**plsB*-TAP°, mut* insertion, pEB1265 mediated	this work
EB624	W3110*plsB*P2mut*2*plsB*-TAP°, mut*2 insertion, pEB1266 mediated	this work
EB388	W3110*dgkA*-ProtA::*kana*^{R} , pKD46 mediated ProtA-kana recombination	this work
EB395	W3110DgkA-ProtA°, *kana*^{R} removed from EB388 with pCP20	this work
EB612	W3110*dgkA*Pmut#DgkA-ProtA°, mut# insertion in EB395, pEB1267 mediated	this work
EB381	W3110*dgkA*-Flag::*kana*^{R} Flag-kana recombination, pKD46 mediated	this work
EB401	W3110*dgkA*-Flag°, *kana*^{R} removed from EB381 with pCP20	this work
EB637	W3110*dgkA*Pmut#*dgkA*-Flag°, mut# insertion, pEB1267 mediated	this work
EB431	W3110Δ*basR::kana*^{R} , P1 transduction from EB428 to W3110	this work
EB566	W3110*dgkA*-Flag°Δ*basR::kana*^{R}, P1 transduction from EB428 to EB401	this work
MG1655	F- lambda- *ilvG- rfb-50 rph-1*	Bachmann (1996)
EB421	MG1655Δ*relA*°, P1 transduction from EB126 to MG1655 and *kana*^{R} removed with pCP20	this work
EB425	MG1655Δ*relA*°*spoT*207*::cam*^{R} – P1 transduction from CF1693 to EB421	this work
EB559	MG1655Δ*dksA*°, P1 transduction from EB132 to MG1655 and *kana*^{R} removed with pCP20	this work
EB634	MG1655Δ*basS*°, P1 transduction from EB427 to MG1655 and *kana*^{R} removed with pCP20	this work

Table 2: ***E. coli* K12 strains**. The ° character after a strain name means that the kanamycin cassette was removed using the pCP20 plasmid.

FIGURE LEGENDS

Figure 1: *plsB-dgkA* intergenic region.

A. The consensus regions for BasR binding, promoters, and transcription start sites are indicated by boxes and arrows, in blue for *dgkA* elements and in green for *plsB* elements. Predicted +1 transcription sites are shown in dashed lines, the known +1 transcription site for σE promoter of *plsB* in plain line. Limits of the regions cloned in transcriptional fusions with *gfp*, in pUA66 or pUA139 plasmids, are shown below the scheme, by blue and green horizontal arrows. Mutations introduced in the promoter regions of *dgkA* and *plsB*, either in the transcriptional fusions with *gfp*, or in the chromosome of W3110/PlsB-TAP or W3110/DgkA-ProtA strains, are indicated by red stars. All element sizes and distances are represented on scale, except for *dgkA* and *plsB* ORF external limits.

B. Sequences of the promoters of *dgkA* and *plsB*. For *dgkA* promoter, an alignment of the BasR binding region with the consensus sequence for PmrA binding of *Salmonella* (Marchal et al., 2004) is shown. The exact mutations introduced in the promoters are indicated below the sequences in red.

Figure 2: Effect of σE overproduction on PlsB and DgkA protein amounts

A. *E. coli* strains producing a TAP tagged PlsB protein with wild type promoters (EB367) or the indicated mutations in the *plsB*PσE and *plsB*P2 promoters (EB613 and EB624 respectively) were transformed by pBAD or pBAD-*rpoE* plasmids and grown at 37°C in LB complemented with ampicillin and 0,01% arabinose. Proteins were separated by SDS-PAGE 10% and detected by Western blot with PAP antibody. **B.** W3110DgkA-Flag° strain (EB401) transformed by pBAD24 or pBAD-*rpoE* plasmids was grown at 37°C in LB complemented with ampicillin and 0,01%

arabinose. Proteins were separated by SDS-PAGE 12% and detected by Western blot with anti-Flag antibody.

Figure 3: *plsB* transcription

MG1655 strain transformed by the indicated transcriptional fusions and pBAD-*rpoE* plasmid was grown overnight. The values show the ratio of fluorescence over optical density at 600nm, giving the relative amount of GFP produced, in arbitrary units (A.U.). The values are the mean of 3 to 6 replicas. **A**. MG1655 strain was transformed with pUA66, or *plsB*, *plsB**, *plsBΔ,* or *rpoE* transcriptional fusions together with pBAD24 or pBAD-*rpoE* plasmids. The cultures were grown overnight at 30°C in LB supplemented with Ampicillin, Kanamycin, and 0,01% arabinose. **B.** MG1655 and EB425 (Δ*relA*Δ*spoT*) strains were transformed by the same series of transcriptional fusions as in **A** and the *gfp* expression was assayed similarly after overnight growth at 30°C in LB.

Figure 4: Effect of BasR on DgkA protein amounts

A. The W3110/DgkA-Flag° recombinant strain (EB401) was transformed with pBAD24, -*rpoE*, -*basR*, -*basR53*, or -*dcuR* plasmids. The strains were grown at 37°C in LB complemented with ampicillin and 0,05% arabinose. Proteins were separated by 12% SDS-PAGE and detected by Western blot with anti-Flag antibody. **B**. W3110/DgkA-ProtA strains with or without the mut# mutation introduced in the BasR consensus binding site (EB395 and EB612) were transformed with pBAD and pBAD-*basR53* plasmids. The strains were grown at 37°C in LB complemented with ampicillin and 0,05% arabinose. Proteins were separated by SDS-PAGE 12% and detected by Western blot with PAP antibody.

Figure 5: *dgkA* transcription

The values show the amount of GFP produced after overnight growth of MG1655 strain transformed by the indicated transcriptional fusions and pBAD plasmids. The values are the mean of 3 to 6 replicas. The cultures were grown overnight at 30°C in LB supplemented with Ampicillin, Kanamycin, and 0,05% arabinose. **A.** MG1655 strain was transformed with pUA66, or *dkgA*, *dgkA2*, *dgkA3,* or *dgkA4* transcriptional fusions together with pBAD24 or pBAD-*basR53* plasmids. **B.** MG1655 strain was transformed with pUA66 and *dgkA4* transcriptional fusion together with pBAD24, pBAD-*dcuR*, pBAD-*basR*, or pBAD-*basR53* plasmids. **C.** MG1655 strain was transformed with pUA66 or *dgkA3, dgkA3mut#, dgkA3mutT,* or *arnB* transcriptional fusions together with pBAD24 or pBAD-*basR53* plasmids.

Figure 6: BasR binding on *plsB-dgkA* intergenic region

The DNA fragments were obtained by PCR with oligonucleotides Ebm600/601 (see Table S1) for *arnB* and oligonucleotides Ebm431/432 for *dgkA2* and *dgkA2mut#*. For the experiment on *arnB*, 2μg of 6His-Tev-BasR or 6His-Tev-DcuR proteins were used. For the experiment on *dgkA2*, 3μg of 6His-Tev-BasR53 or 6His-Tev-DcuR proteins were used. A DNA Ladder (Smart Ladder Eurogentec) has been loaded on the gels (left lane). The images of the two panels are edited for the figure, but in a given panel, all the lanes originate from the same gel shift assay.

Figure 7: up-regulation of the BasR regulon in *dgkR-1* mutant

The values in arbitrary units are the ratio of the fluorescent signal produced by GFP divided by the OD600. The values are the mean of 4 or 6 replicas. **A.** R477 and GK1 strains transformed

with pUA66, *dkgA4*, *ais*, *ugd, arnB,* or *plsB* transcriptional fusions were grown overnight at 30°C in LB supplemented with kanamycin. **B.** R477 and GK1 strains transformed with pUA66, *dkgA4*, or *ais* transcriptional fusions together with pBAD24 or pBAD-*basS* were grown overnight at 30°C in LB supplemented with kanamycin, ampicillin, and 0,05% arabinose. **C.** MG1655Δ*basS*° strain (EB634) transformed with pUA66, *dkgA4*, *ais*, or *plsB* transcriptional fusions together with pBAD24, pBAD-*basS*, or pBAD-*basS*(D312N) was grown overnight in LB supplemented with kanamycin, ampicillin, and 0,05% arabinose.

Figure 1

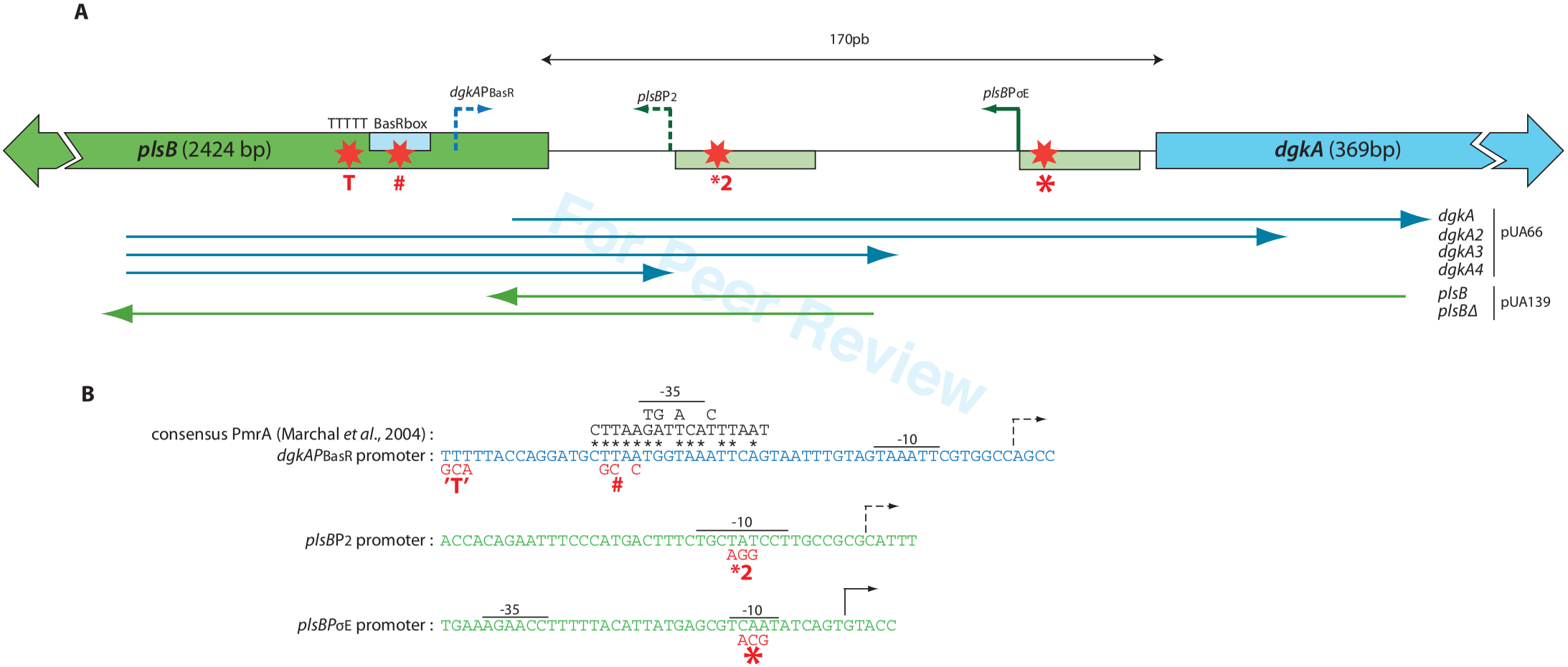

Figure 2

A

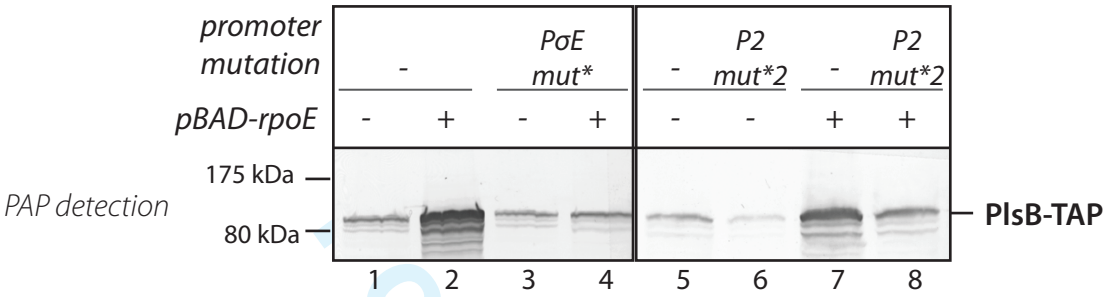

B

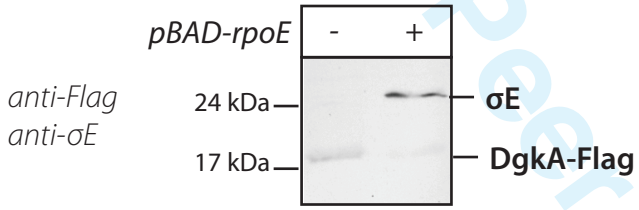

Figure 3

A

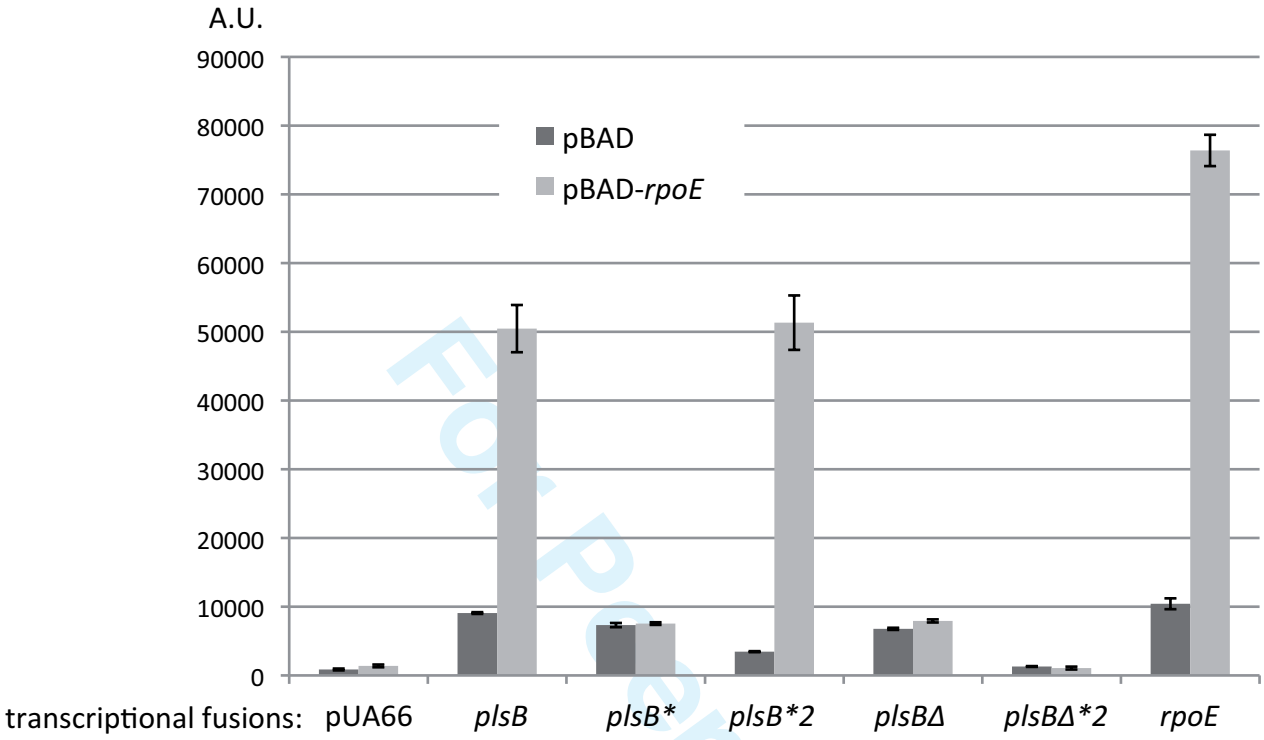

B

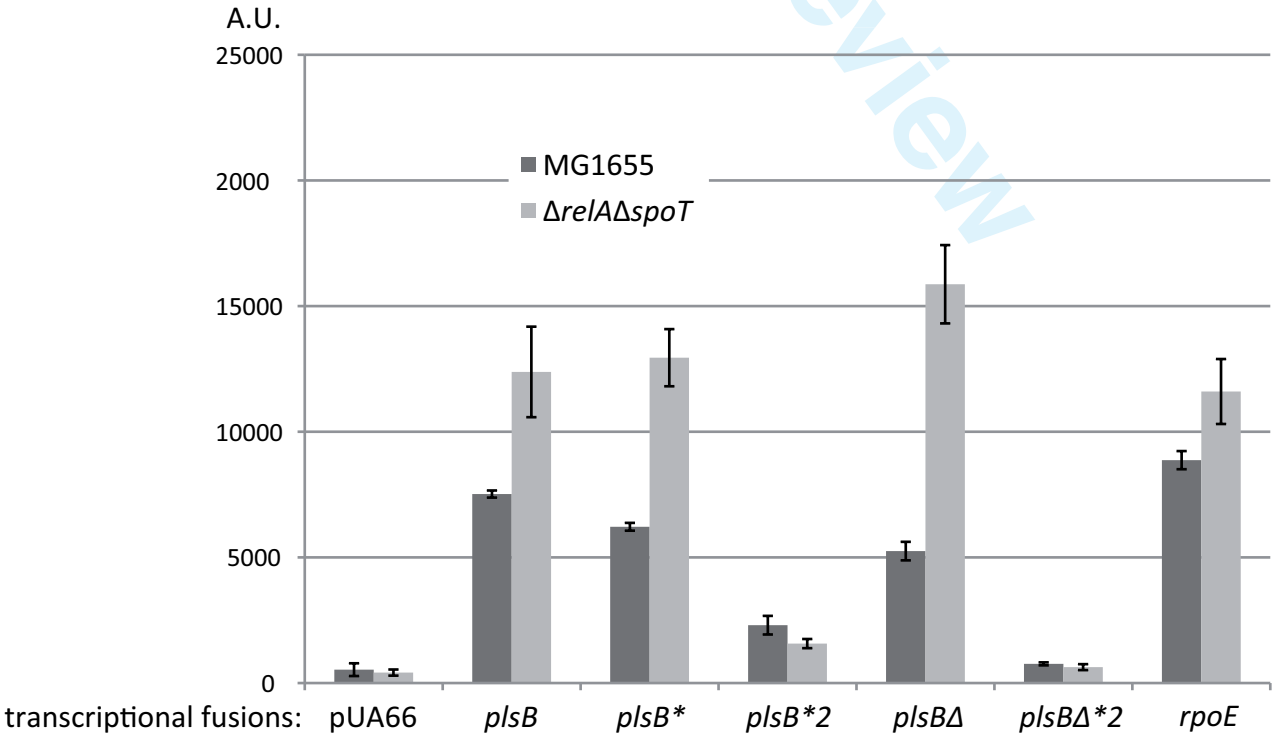

Figure 4

A

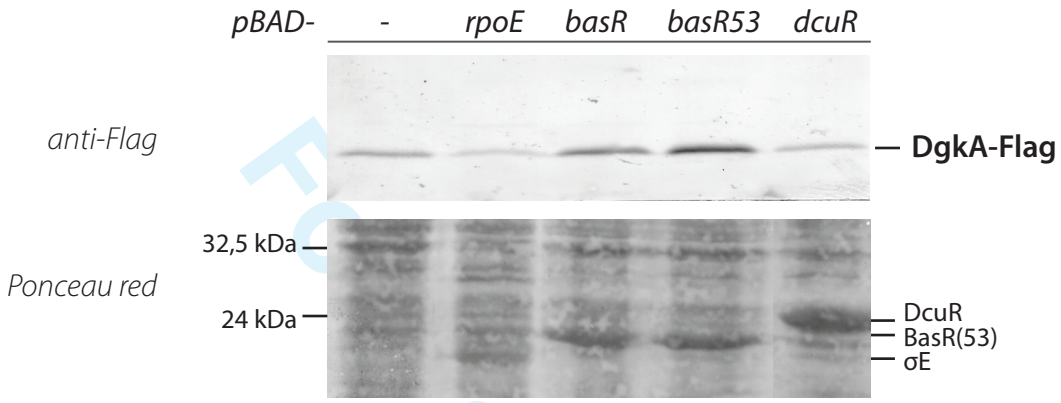

B

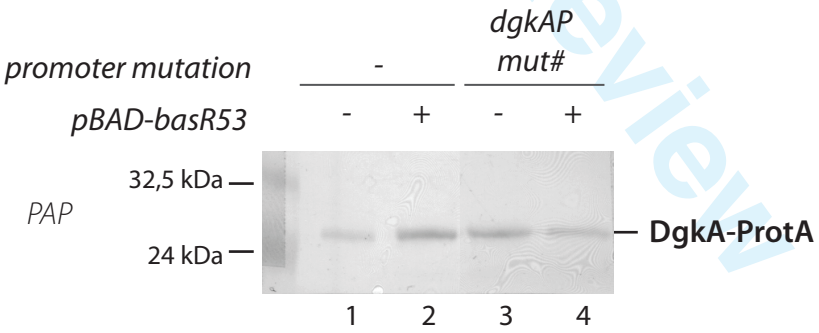

Figure 5

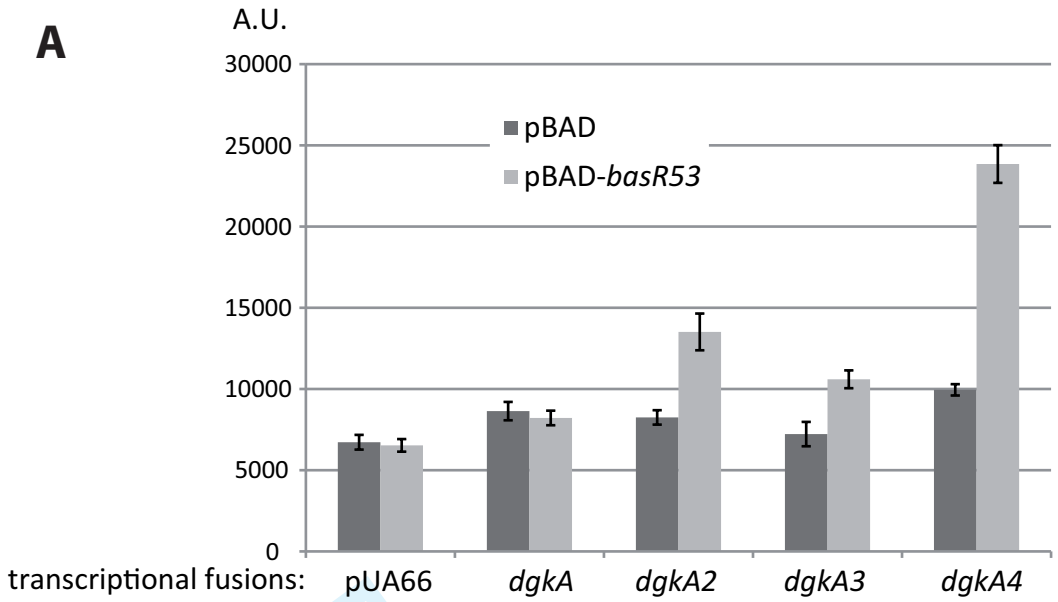

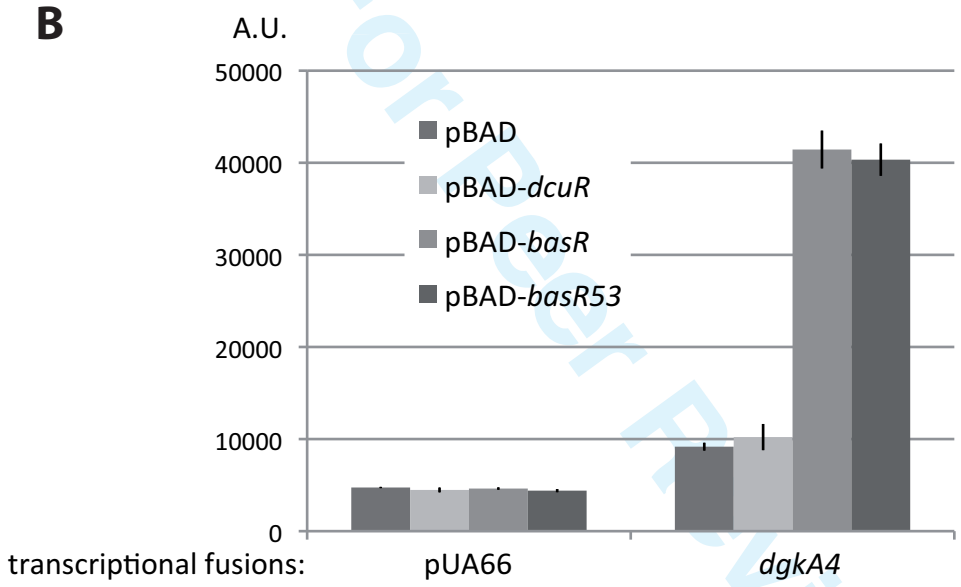

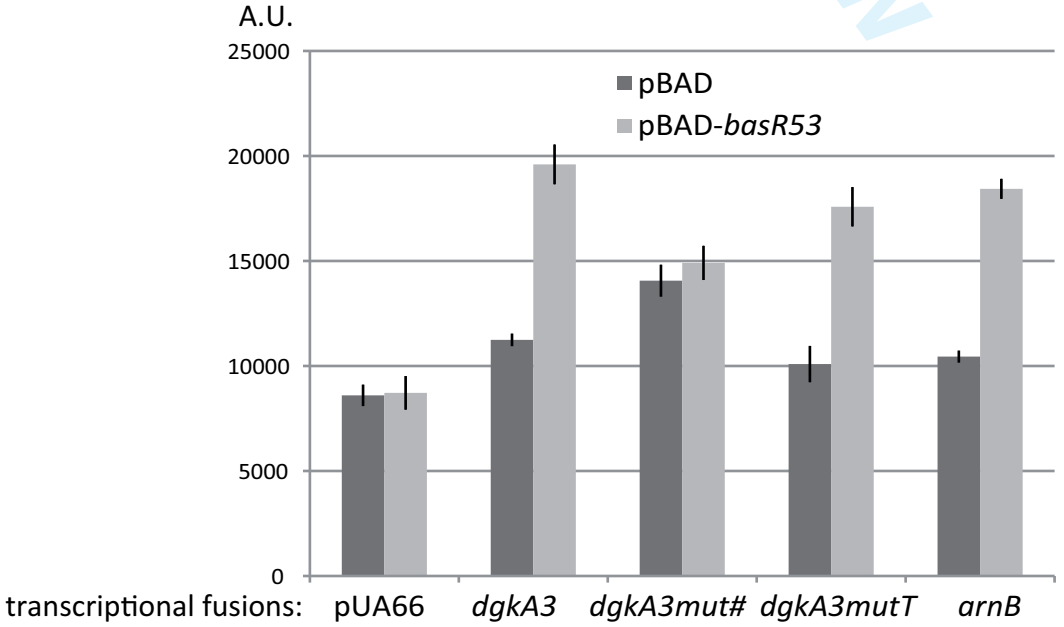

Figure 6

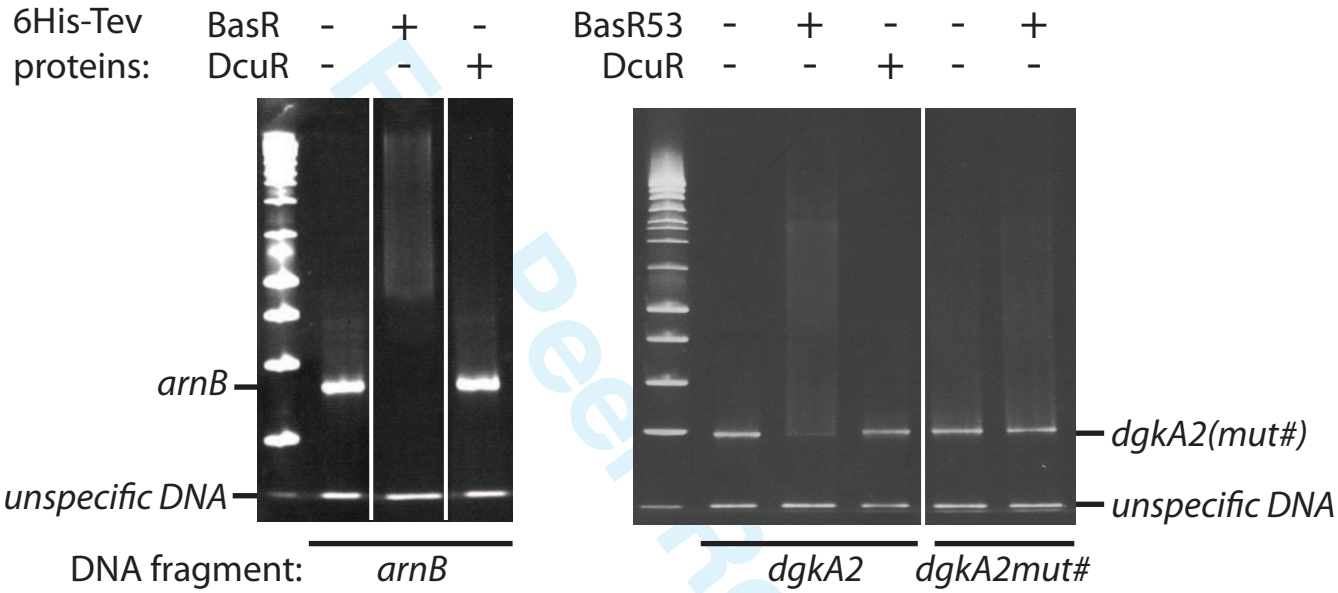

Figure 7

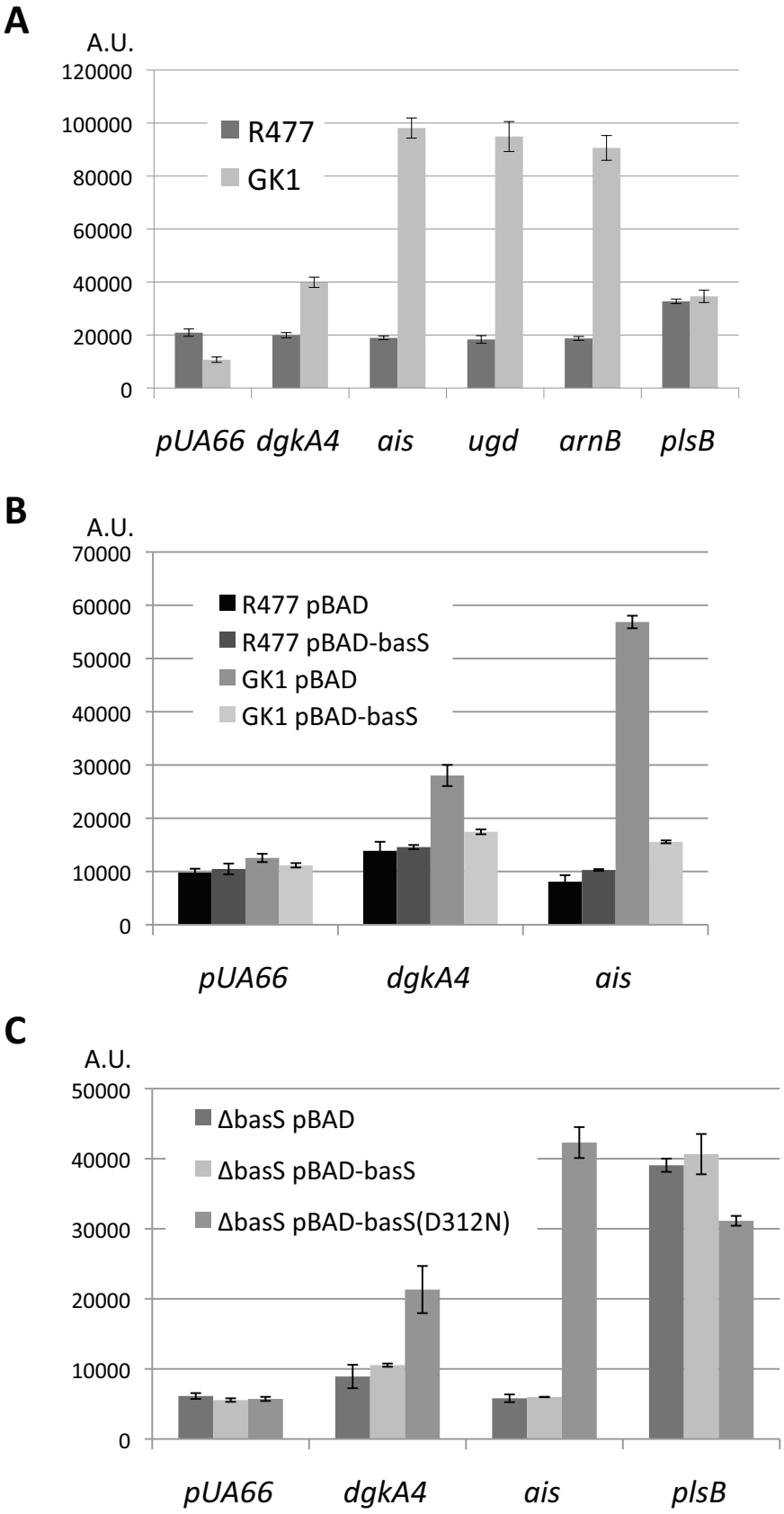
A
A.U.
120000
100000
80000
60000
40000
20000
0
R477
GK1
pUA66
dgkA4
ais
ugd
arnB
plsB
B
A.U.
70000
60000
50000
40000
30000
20000
10000
0
R477 pBAD
R477 pBAD-basS
GK1 pBAD
GK1 pBAD-basS
pUA66
dgkA4
ais
C
A.U.
50000
40000
30000
20000
10000
0
ΔbasS pBAD
ΔbasS pBAD-basS
ΔbasS pBAD-basS(D312N)
pUA66
dgkA4
ais
plsB

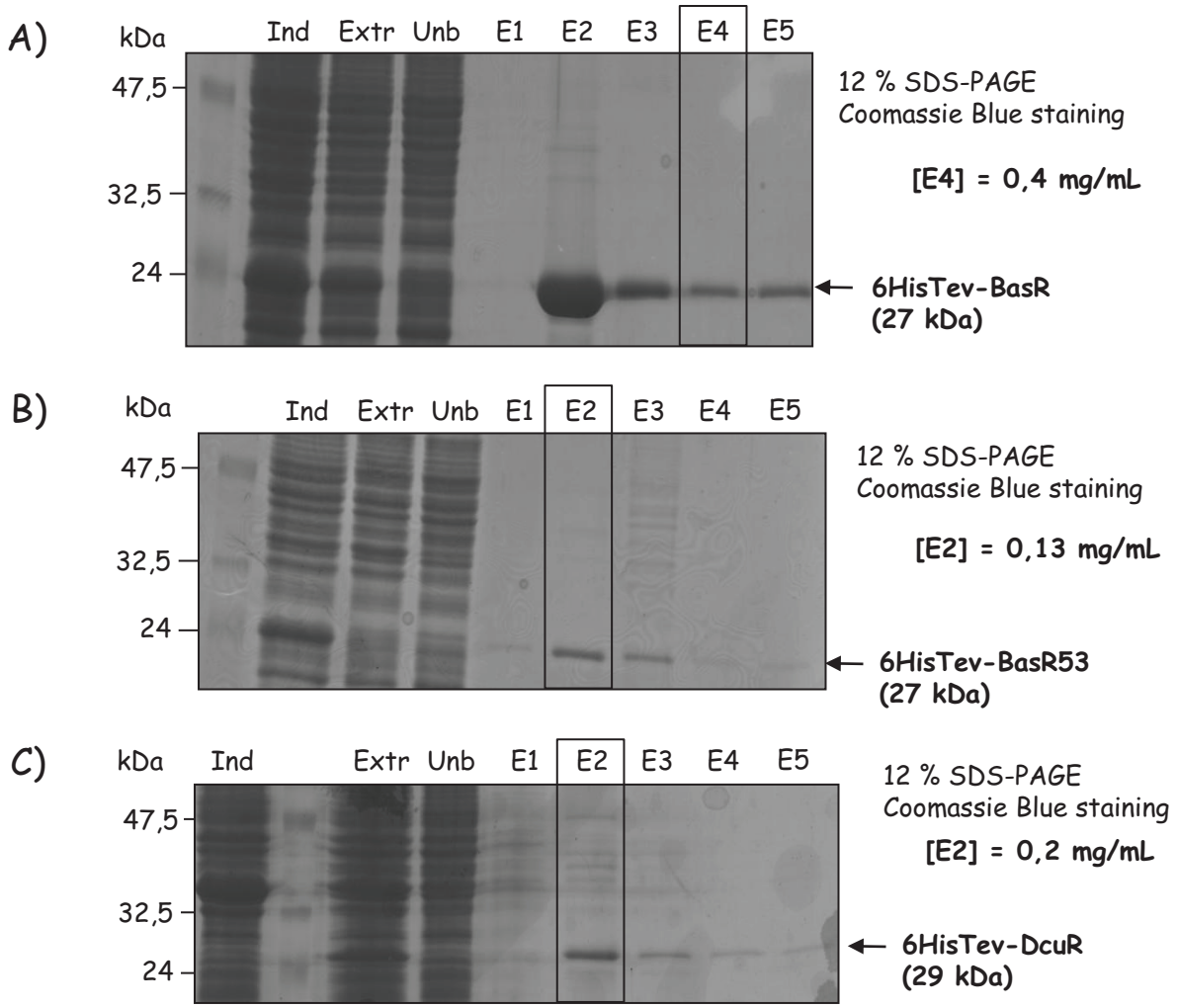

Figure 93: Purification of 6HisTev-BasR, -BasR53, -DcuR. Strain BL21(DE3)Lys was transformed with plasmids pET6his-tev-*basR, basR53,* and *dcuR* (pEB1189, pEB1192, and pEB1190, respectively) . For protein purification from a 500 mL culture using Talon beads see Materials & Methods. **A - C)** Approx. 0,3 OD units of induced, extract, and unbound samples and 2 µL of E1-E5 (500 µL each) were resuspended in 1X Laemmli buffer, heated 5 min at 96 °C, and loaded on an SDS-PAGE. Then, fractions (A) E4 and (B-C) E2 were chosen by estimation of their similar amount from the Coomassie Blue staining and quantified excactly using the Bradford assay. or further experiments E4 was chosen (c= 0,4 mg/mL). **B)** For further experiments E2 was chosen (c= 0,13 mg/mL). **C)** For further experiments E2 was chosen (c= 0,2 mg/mL).
Ind: Induced total cell extract; Extr: sonication extract; Unb: unbound; E1-E5: elution 1 till 5.

B. Supplementary results of article 2

B1. Gel mobility shift assay

As we have shown that BasR activates *dgkA* using *in vivo* methods such as transcriptional fusions and fusion proteins, we wanted to show that this activation was direct, using an *in vitro* approach. It has been shown in *Salmonella* that the sequence of the PmrA binding box includes an imperfect 9 bp inverted repeat, similar to the DNA-binding sites of many prokaryotic regulators that consist of 5–10 bp inverted repeat sequences (Wösten & Groisman, 1999). In *S. typhimurium*, direct binding of PmrA to the promoter regions of *pmrG*, *pmrH*, and *pmrC* has been demonstrated (Wösten *et al.,* 1999). *In silico* analysis comparing close relatives of *S. typhimurium* has shown that in *E. coli*, the binding box is conserved upstream of the genes *eptA* (*pmrC*), ugd (*pmrE*), *arnB* (*pmrH*), and *yibD* (figure 92) (Marchal *et al.*, 2004; Froelich *et al.*, 2006). However, in *E. coli* they have not all been confirmed experimentally.

We decided to test if the response regulator BasR (*E. coli*), as well as the constitutively active mutant BasR53, binds to the promoter regions of *arnB* (positive control) and *dgkA* by gel mobility shift assay (GMSA). The response regulator DcuR should serve as a negative control. First, BasR, BasR53, and DcuR (a homolog of BasR (26 %)) were purified as 6His tagged recombinant proteins. Plasmids pET22-*6his-tev–basR,-basR53,-dcuR* were constructed. *E. coli* strain BL21(DE3)lys permitting overproduction with the pET system was then transformed with these plasmids. Each recombinant protein was produced with a 6His-TEV tag at its N-terminus. The standard protocol of 6His purification on Cobalt beads is described in Materials & Methods. The proteins were purified to near homogeneity, at a sufficient concentration for GMSA, about 0,2-0,4 mg/mL (figure 93).

Then, binding of the purified proteins was tested on DNA fragments obtained by PCR, corresponding to the regions cloned in the transcriptional fusions with *gfp*. Constant amount of these DNA fragments at constant molarity were mixed *in vitro* with increasing protein molarity, to give an increasing ratio of protein to DNA (approx. 1:1 to 1:250). This DNA-protein mixture was incubated at 20 °C to allow binding of the protein to the DNA sequence. Then, electrophoresis was performed in a native acrylamide gel with following revelation of the DNA fragments by Gel Red (cf. Materials & Methods).

As expected, we detected a shift for the PCR corresponding to the *arnB* promoter when incubated with BasR, but not with the same amount of DcuR (figure 94A). Yet, a faint shift was visible for DcuR at high concentration. This could be explained by an unspecific binding of DcuR at high protein concentration. Then, we tested the binding of BasR or

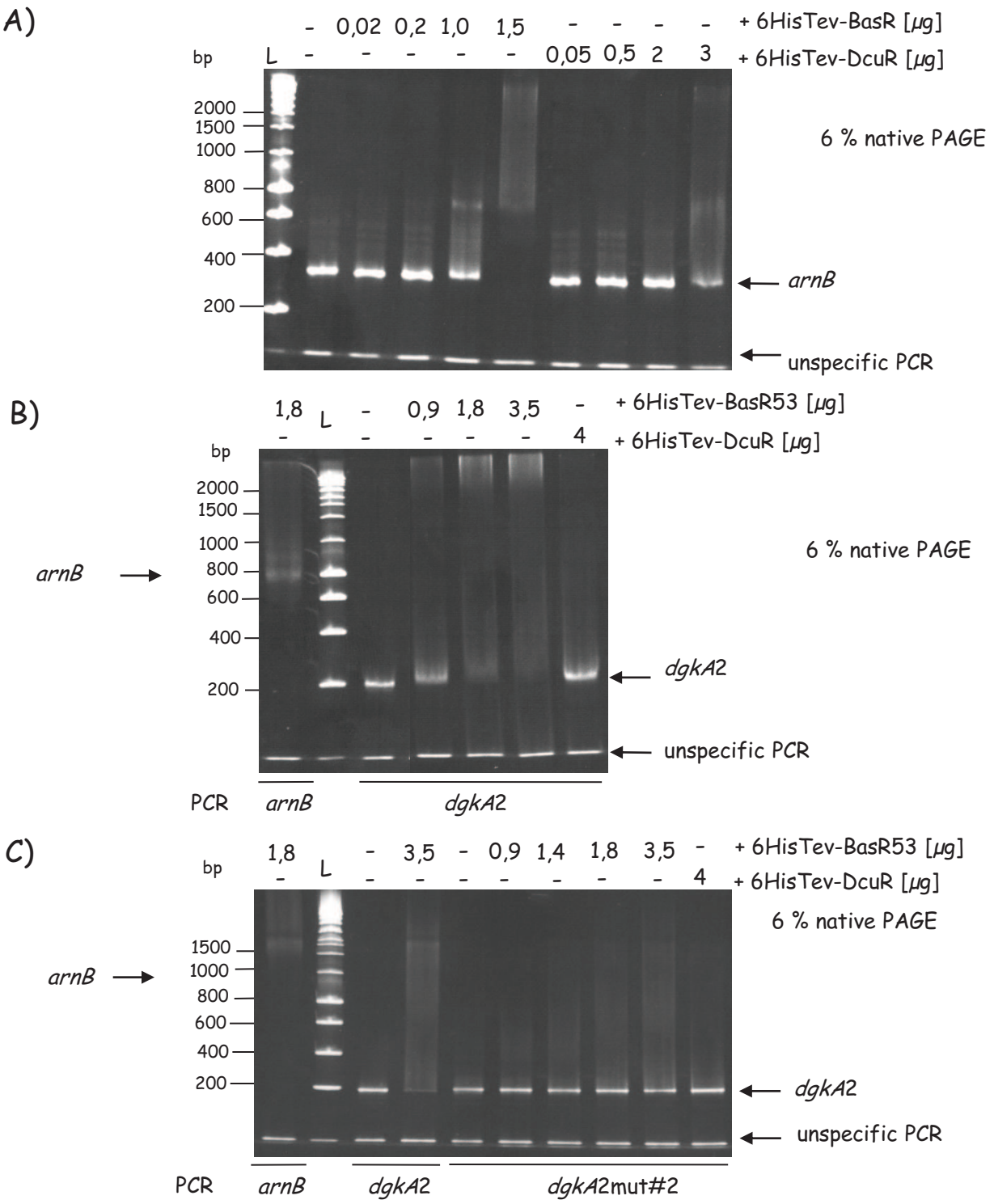

Figure 94: BasR binds to *arnB* and *dgkA* promoter regions. A) A constant amount (170 nM) of PCR product (ebm600/601) corresponding to the promoter region of *arnB* and an unspecific PCR product (ebm423/424) (190 nM) were mixed with an increasing amount of 6HisTev-BasR or -DcuR recombinant protein. **B)** A constant amount (150 nM) of PCR product *dgkA*2 (ebm431/432) corresponding to the promoter region of *dgkA* and an unspecific PCR product (ebm423/424) (190 nM) were incubated with an increasing amount of 6HisTev-BasR53 or –DcuR recombinant protein. **C)** Constant amounts (150 nM) of PCR products *dgkA*2 and *dgkA*2mut#2 (ebm431/432), which was amplified using pUA66-*dgkA*2mut#2 (pEB1174), and an unspecific PCR product (ebm423/424) (190 nM) were incubated with an increasing amount of 6HisTev-BasR53 or –DcuR recombinant protein. L: DNA ladder.

BasR53 on the *dgkA* promoter region. Both BasR and BasR53 bound to the promoter region of *dgkA* (figure 94B and data not shown) as suggested by the disparition of the band. However, in contrast with *arnB* where the band clearly shifted to form another band, there is no clear shift of the DNA fragment corresponding to the *dgkA* promoter region, but it disappeared. This fact questions the significance of this result. A reason for this behaviour could be that different types of binding are present for *arnB* and *dgkA*. Indeed, the consensus sequence of the BasR binding box for *dgkA* differs for 5 nucleotides compared to *arnB*, which could change the binding properties.

In order to show that this shift corresponded to a specific BasR binding, we used a DNA fragment containing a mutation in the BasR binding box (*dgkA2*mut#2). At identical BasR53 concentrations, there was no shift with the mutated DNA fragment (*dgkA2*mut#2*;* figure 94C), whereas a shift was detected for *dgkA*2. This suggests that the BasR binding to the promoter region of *dgkA* is specific to the BasR binding box. DcuR did not bind to neither of the promoter sequences (figure 94B and C). We cannot explain why the shifts of the bands corresponding to the *dgkA* DNA fragments were always diffuse and not as clear as for *pmrH*. Furthermore, the gel shift experiments were not always reproducible. Among other factors (ratio DNA:protein, concentration in bis/acrylamide), it depended on how many times the purified proteins were (de-)frozen, which can affect their binding activity. To overcome this problem, small aliquots could be kept at -80 °C and defrozen only once or freshly purified proteins could be used for each GMSA series.

These experiments confirmed that BasR activation of *arnB* and *dgkA* is direct and specific. These results are consistent with the literature (Wösten *et al.,* 1999) and with our *in vivo* results using transcriptional fusions (article 2, figure 5). It strengthens the fact that *dgkA* belongs to the BasRS regulon.

B2. 6His-Tev-BasR and 6His-Tev-BasR53 proteins formed dimers

The dyad symmetry in the PmrA-binding sequence suggests that the PmrA protein binds to its binding box as a dimer, and consistent with this notion it has been found that the PmrA protein dimerizes under non-reducing conditions (Wösten & Groisman, 1999). In the same idea, we wanted to test if the purified 6His-Tev tagged BasR and BasR53 proteins from *E. coli* could form dimers stabilized by disulfide bridges as described for *S. typhimurium* PmrA. 6His-Tev-BasR and 6His-Tev-BasR53 were resuspended in SDS (sodium dedocyl sulfate) sample buffer without 2-mercaptoethanol (β-ME), with or without heating, and analyzed on a SDS-PAGE stained with Coomassie Blue. Both BasR and BasR53 proteins formed dimers in

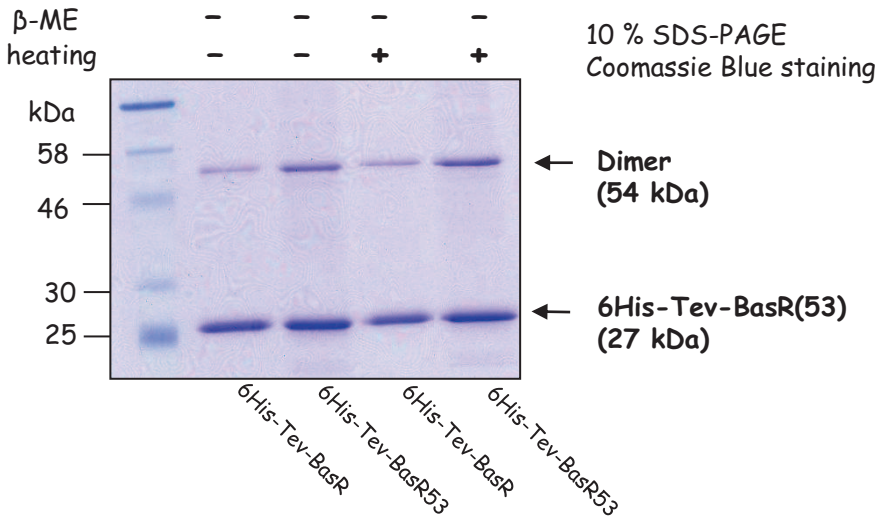

Figure 95: Dimerization of BasR and BasR53 protein (according to Wösten & Groismann, 1999). 6His-Tev tagged BasR or BasR53 protein (1 µg) was resuspended in SDS sample buffer without 2-mercaptoethanol (β-ME), with or without heating, and loaded on a 10% SDS-PAGE then stained with Coomassie Blue.

non-reducing conditions (figure 95). In contrast, in reducing conditions (with β-ME) only the monomers were present (figure 93). This result is consistent with the study by Wösten & Groismann (1999) and confirmed that the purified recombinant proteins 6HisTev-BasR and -BasR53 were behaving like PmrA of *S. typhimurium* and suggest a similar mechanism.

B3. Additional mutation in the putative BasR binding box in dgkA promoter region

We showed that *dgkA* expression is activated by BasR. We further showed that this activation resulted from the BasR binding box by introducing a mutation in the – 35 region (mut#2, figure 96). No more activation was visible (figure 6, article 2). In addition to what is described in the paper, we performed another mutation in the BasR binding box (mut#1) and in a T repeat upstream of the predicted –35 consensus that might correspond to the consensus described for ColRS in *Pseudomonas* (Kivistik *et al.*, 2009). 3 nucleotides have been changed in each case (figure 96). The mut#2 mutation, the mut#1 mutation, but not the mutT mutation, abolished the response to BasR (figure 97A). However, this mut#1 mutation increased the basal level of *dgkA* 6-fold compared to *dgkA*2. The mut#2 mutation as well as mutT had only a very little effect of increasing the basal level. The mut#1 and mut#2 mutations were introduced on the chromosome of strain W3110 producing DgkA-Flag. In the resulting strains, the (basal) protein amount analyzed by Western blot followed exactly the expression profile of the transcriptional fusion plasmids (figure 97B): W3110 *dgkA*-Flag° with mutation mut#1 produced more DgkA-Flag protein at physiological level than W3110 *dgkA*-Flag° and *dgkA*-Flag° with mutation mut#2. Upon induction by BasR53 DgkA-Flag° was induced, while both strains with mutations #1 and #2 on the chromosome did not respond anymore.

The putative – 35 consensus of the *dgkA* promoter comprises the BasR binding box. It is possible that mutation mut#1 changes the basal *dgkA* expression level because it modifies the sequence of the – 35 consensus is changed, which might make stronger. The binding position of BasR to the *dgkA* promoter is comparable with other genes of the BasR regulon (Marchal *et al.*, 2004)

B4. Functionality test of DgkA fusion proteins

Strain BW25113 in which DgkA is tagged at its C-terminus with TAP or SPA, was constructed according to the technique of Datsenko & Wanner (2000) (cf. Materials & Methods) (figure 98). A phenoytpic test is available to test the functionality of DgkA protein: a Δ*dgkA* mutant does not grow in medium depleted in NaCl, because DgkA activity is needed for production of OPGs which are essential for growth in low osmolarity medium (Raetz & Newman, 1978). To test the functionality of DgkA tagged with TAP or SPA, we plated the

CTTTTTACCAGGATGCTTAATGGTAAATTCAG *dgkA*

CTTTTTACCAGGATGC**caAt**TGGTAAATTCAG *dgkA*mut#1
CTTTTTACCAGGATGC**gcAc**TGGTAAATTCAG *dgkA*mut#2
C**gca**TTACCAGGATGCTTAATGGTAAATTCAG *dgkA*mutT

Figure 96: Position and sequence of mutations mut#1, mut#2, and mutT in the dgkA promoter. The predicted –35 consensus of the *dgkA* promoter is indicated by a line. Bold letters indicate exchanges of nucleotides for mutations mut#1, mut#2, and mutT, which were introduced in the *dgkA* promoter region.

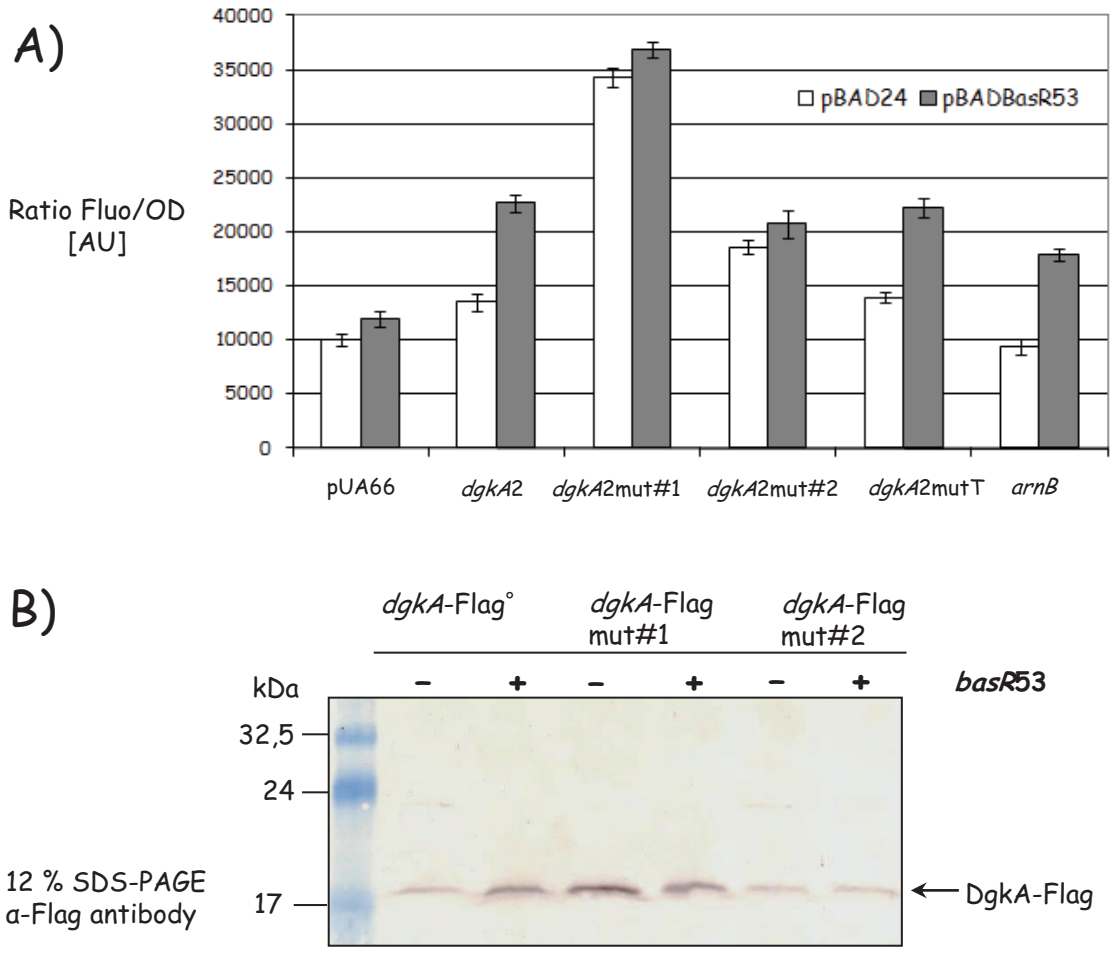

Figure 97: Mutations mut#1 and mut#2 abolish activation of *dgkA* by BasR. A) Strain MG1655 was co-transformed by plasmids as indicated. Overnight cultures were grown in LB at 30°C supplemented with kanamycin (25µg/mL) and ampicillin (100 µg/mL) and 0,01 % arabinose. Then, using a TECAN M200 the OD_{600nm} and fluorescence (excitation= 485 nm, emission= 530 nm) were measured. AU: arbitrary units for specific fluorescence, corresponding to the ratio fluorescence (in arbitrary units)/OD_{600nm}. **B)** Strains W3110 *dgkA*-Flag°, *dgkA*-Flag#1, and *dgkA*-Flag#2 were transformed by pBAD24 or pBAD-*basR*53. Late stationary cultures were grown at 37°C in LB supplemented with kanamycin (25µg/mL; if necessary) and arabinose (0,05%). Total cell extracts were analyzed by Western blot with appropriate antibodies.

strains on LB or LB without NaCl agar plates. Both strains producing these fusion proteins did not grow on LB without NaCl and hence, DgkA-TAP and -SPA fusion proteins were not functional (figure 99). This could be due to the size and or structural properties of the tags provoking misfolding or problems of protein insertion in the inner membrane. In our experience with membrane proteins, removing the 5 kDa CBP sequence from the TAP or SPA tag (TAP=CBP-TEV-ProtA; SPA=CBP-TEV-3Flag) could enhance in some cases the enzyme functionality. Therefore, we constructed new strains in which DgkA is tagged with ProtA or 3Flag at its C-terminus (figure 98A). The fusion proteins were produced at their expected molecular weight (figure 98B). As shown in figure 99, both strains grew on LB without NaCl and hence, DgkA-ProtA and -Flag fusion proteins were functional. To conclude, fusion proteins DgkA-ProtA and DgkA-3Flag were functional and were used as reporters to follow DgkA protein amount *in vivo* (article 2, figure 2).

B5. Dependence of dgkA expression to the TCS BasRS

dgkA is induced by the response regulator BasR of the TCS BasRS. I wanted to test whether overproduction of the sensor BasS alone would also activate *dgkA*. *E. coli* strain MG1655 was transformed by pBAD24, pBAD-*basR*53, or pBAD-*basS* with pUA66 or *dgkA*2 and the effect of overproduction of BasS and BasR53 on *dgkA*2 was monitored. Only BasR53 overproduction, but not BasS, induced expression of *dgkA*2 (figure 100A).

Then, we wanted to test the effect of the deletion of either *basR* or *basS* on production of DgkA. The allele Δ*basR::kana*^{R} or Δ*basS::kana*^{R} was transduced in strain W3110 *dgkA*-Flag° and Western blot analysis was performed. There was a slight increase of DgkA-Flag protein amount in W3110 *ΔbasS::kana*, but not in W3110 *ΔbasR::kana* (figure 100B). The increase of DgkA in *ΔbasS* strain, could be due to the absence of a phosphatase activity on BasR. When we transformed Δ*basR::kana*^{R}, Δ*basS::kana*^{R} or an isogenic wild type strain with *dgkA* transcriptional fusions, no difference in expression was measured (data not shown). Since DgkA and PlsB are regulated by RpoE in an antagonistic way, we reasoned that might be the case also for BasR. Therefore, we tested the effect of the deletion of either *basR* or *basS* on production of PlsB. There was also no change for production of PlsB-TAP in strain W3110 *plsB*-TAP° combined with deletions of *ΔbasS* and *ΔbasR*.

B6. Validation of the BasR regulon in E. coli and its response to metavanadate

In *S. typhimurium*, the PmrAB regulon contains genes responsible for lipid A modifications (Wösten & Groisman, 1999). The BasRS regulon contains the same genes responsible for lipid A modifications in *E. coli* (Froelich *et al.*, 2006; Hagiwara *et al.*, 2004): *arnB*, *ais*

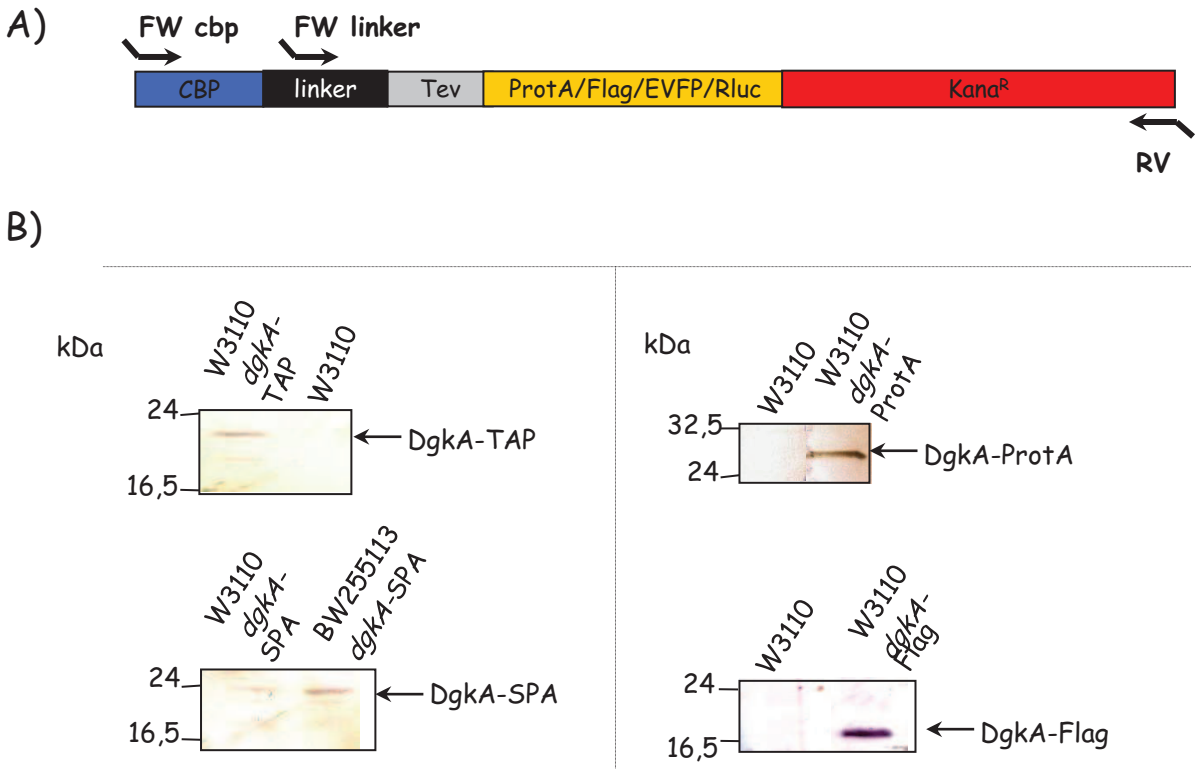

Figure 98: Construction of strains producing DgkA with different tags with or without the CBP sequence. A) Primer pairs used for amplification of the different tags of DgkA: CBP: Calmodulin Binding Protein; Tev: cleavage sequence by Tev protease; TAP, SPA, ProtA, Flag et Rluc: different tags used (see figure). **B)** Production test of tagged proteins: strains producing the tagged protein were grown in 2YT supplemented with kanamycin (12,5 mg/mL) at 37°C. Then, total cell extracts are analyzed by Western blot with appropriate antibodies.

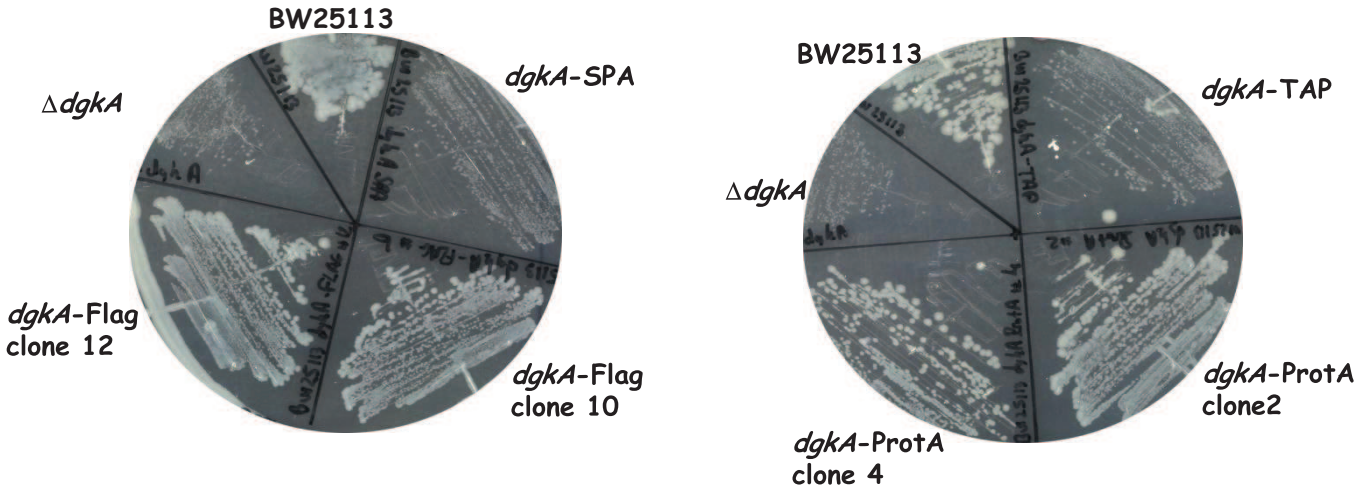

Figure 99: Growth of strains in which *dgkA* is tagged with different cassettes on LB plates without NaCl. *E. coli* strains BW25113 wild type, BW25113 Δ*dgkA*, BW25113 *dgkA*-TAP, BW25113 *dgkA*-SPA, BW25113 *dgkA*-ProtA and BW25113 *dgkA*-Flag were restriked on LB agar plates depleted of NaCl and were grown overnight at 37°C. Then, the different growth phenotypes of the strains can be compared.

(transcribed divergently with *arnB*), *ugd*, and *eptA*, and a gene of unknown function, *yibD*. The Zaslaver's library of *E. coli gfp* transcriptional fusions contains most of the promoters of the genes of the BasRS regulon (Zaslaver *et al.*, 2006). We verified that the cloned sequences in the library all contain the predicted BasR consensus box (Marchal *et al.*, 2004). We have shown that *arnB* is induced with overproduction of BasR53 (article 2, figure 5C), which is consistent with the knowledge that it is a member of the BasRS regulon and *arnB* can therefore serve as a positive control for the BasRS response. Additionally, we wanted to screen the expression of all these genes upon BasR overproduction. In the first place, *E. coli* MG1655 strain was co-transformed with pBAD24 or pBAD-*basR*53 and pUA66, *ais*, *ugd*, or *arnB*. *ais*, *ugd*, and *arnB* transcriptional fusions were induced upon BasR53 overproduction (figure 101A). However, there was no response of *eptA* transcriptional fusion upon BasR53 overproduction although it contains the BasR binding box (data not shown).

It has been reported that lipid A modifications in *E. coli* can be induced by addition of the chemical metavanadate (NH_4VO_3) (Zhou *et al.*, 1999). It could be that metavanadate prevents dephosphorylation of BasR by BasS thanks to its phosphatase activity. It was suggested that metavanadate provoked LPS modifications independently from the TCS BasRS, except for one modification, which has been shown to be BasRS dependent (Tam & Missiakas, 2005). We wanted to test if the whole BasRS regulon (including *dgkA*) would be induced by metavanadate and if it was dependent of BasRS. *E. coli* BW25113 wild type, Δ*basS*°, or Δ*basR*° strains were transformed with pUA66, *ais*, *ugd*, *eptA*, *arnB* (Zaslaver *et al.*, 2006), *dgkA*2, or *dgkA*3 (this work). The genes of the BasRS regulon were all induced by metavanadate in a wild type strain context, except of *eptA* and *dgkA*. In both Δ*basS*° and Δ*basR*° strains, transcriptional fusions *ais*, *ugd*, and *arnB* were not induced, suggesting that their activation by metavanadate is dependent on TCS BasRS (figure 101B).

Because we did not detect a metavanadate effect on *dgkA* expression, I wanted to test whether an increase in DgkA protein amount could be detected in response to metavanadate. Strains W3110 expressing *dgkA*-Flag°, *dgkA*-Flag°/Δ*basR::kana*^{R}, and *dgkA*-Flag°/ Δ*basS::kana*^{R} were grown in LB supplemented or not with 25 mM metavanadate. In all strains there was an increase in DgkA-Flag protein with addition of metavanadate (figure 102A), but which was not dependent on BasRS.

But the situation might be even more complicated by the fact that LPS modifications themselves, induced by BasRS, have been proposed to activate the RpoE response (Tam & Missiakas, 2005). Therefore, we wanted to test if metavanadate that induces LPS modifications has an effect on *rpoE*. *E. coli* MG1655 was transformed with transcriptional

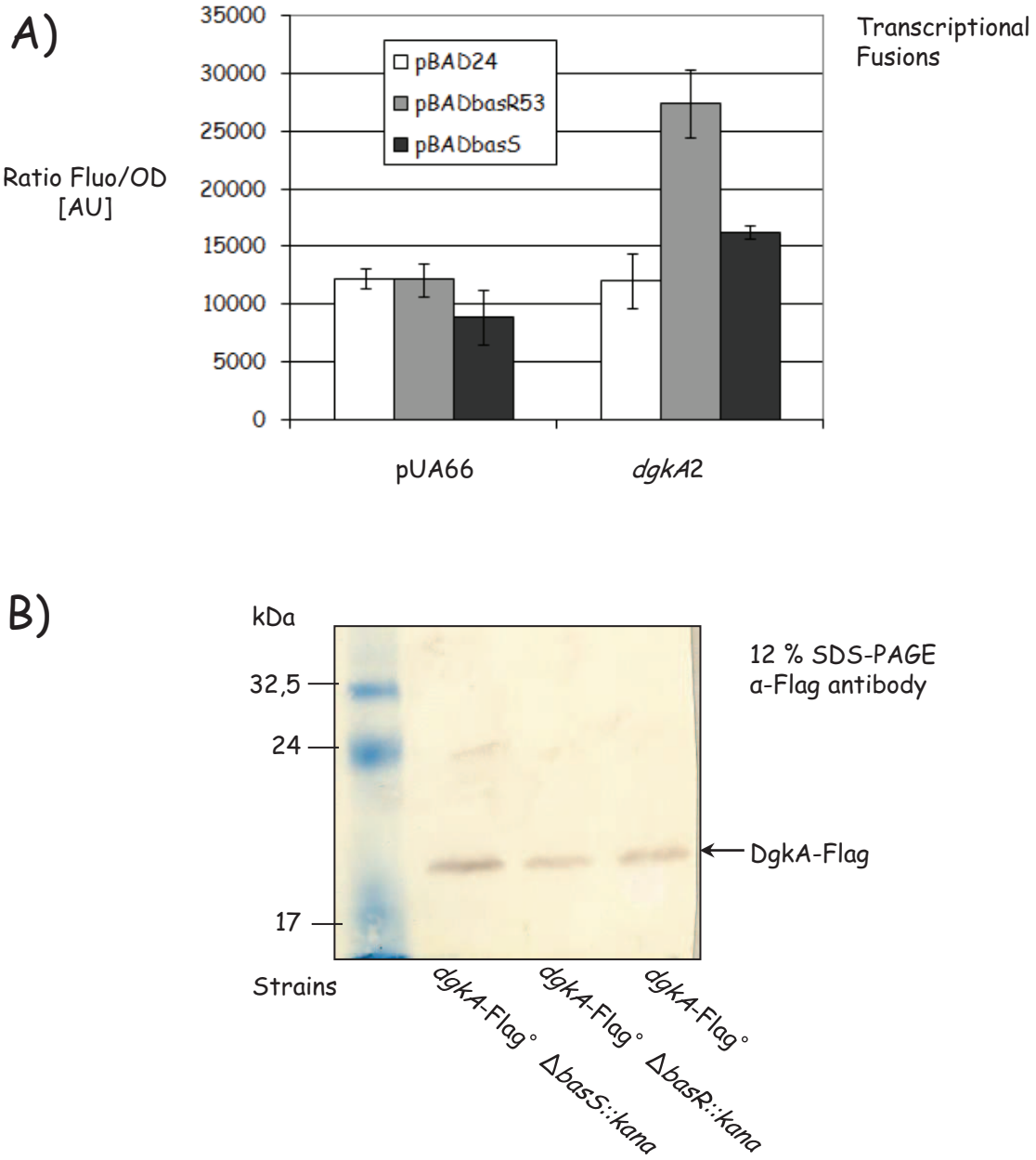

Figure 100: Effect of over-expression or deletion of *basR* and *basS* on *dgkA* expression. A) *E. coli* strain MG1655 was co-transformed with pBAD24 (pEB227), pBAD-*basR53* (pEB1165), or pBAD-*basS* (pEB1195) and with pUA66 (pEB898) or pUA66-*dgkA*2 (pEB1115). Overnight cultures were grown in LB at 30°C supplemented with kanamycin (25µg/mL) and ampicillin (100 µg/mL) and 0,01 % arabinose. Then, using a TECAN M200 the OD_{600nm} and fluorescence (excitation= 485 nm, emission= 530 nm) were measured. AU: arbitrary units for specific fluorescence, corresponding to the ratio fluorescence (in arbitrary units)/OD_{600nm}. **B)** Late stationary cultures were grown at 37 °C in LB supplemented with kanamycin (25µg/mL) if necessary. Total cell extracts were analyzed by western blot with antibodies anti-Flag and anti-mouse.

fusions *rpoE*, *plsB* (Zaslaver *et al.*, 2006), and *plsB*mutP_{rpoE} (this work) and the effect of metavanadate (25 mM) was tested on their expression. The expression of *rpoE* increased with metavanadate. However, *plsB* transcriptional fusions did not change significantly with addition of metavanadate (figure 102B), suggesting that these conditions reflect not a RpoE response. This result does not agree with the study of Tam & Missiakas (2005).

In conclusion, our results showed that LPS modification induced by metavanadate do not activate an RpoE response. We found that the BasRS regulon is induced by metavanadate in a BasRS-dependent manner. However, the mechanism of this BasRS activation by metavanadate remains unclear.

Strangely, we did detect no activation neither of *eptA* or *dgkA* by metavanadate nor of *eptA* by BasR. This could be due to a sensitivity problem of the *gfp* transcriptional fusion detection. When a *dgkR*1 strain with a constitutive sensor BasS(D312N), was transformed with the *eptA* transcriptional fusion plasmid, *eptA* expression was slightly induced (data not shown), suggesting that it is the case.

B7. Regulation of plsB and dgkA in response to ppGpp

plsB expression is regulated by a second stringent promoter that follows the growth rate and is inhibited by ppGpp (article 2, figure 3). Furthermore, there are indications in transcriptome studies that *dgkA* is activated by ppGpp while *plsB* is inhibited during stringent response (Durfee *et al.*, 2008). Here, I will detail the results obtained with *E. coli* strains that are impaired in controlling the level of the alarmone ppGpp: a ppGpp° (EB425) strain does not synthesize ppGpp, since it lacks RelA and SpoT ppGpp-synthase activity (Δ*relA*°*spoT*207). In strain Δ*dksA*° (EB559), ppGpp is still present, but for most stringently controlled promoters, DksA is a RNA polymerase cofactor required for the inhibitory action of ppGpp on the RNA polymerase (Potrykus & Cashel, 2008; Srivatsan & Wang, 2008). Finally, a strain $ppGpp^{++}$ (EB544) produces more ppGpp compared to an *E. coli* MG1655 wild type strain, because the mutation *spoT*203 abolishes the ppGpp degradation activity of SpoT.

All four strains MG1655, EB425, EB559, and EB544 were transformed with *plsB* and *dgkA*2 transcriptional fusion plasmids (Zaslaver's library or this work). Unfortunately, the basal signal of the transcriptional fusion *dgkA*2 was already almost at the background pUA66 level and therefore no decrease could actually be measured. But we did not detect an increase of *dgkA*2 in strain EB544 either, which is in contrast with the result from the transcriptome study (Durfee *et al.*, 2008). The same result was obtained for *dgkA*3 or *dgkA*4 transcriptional fusion (data not shown).

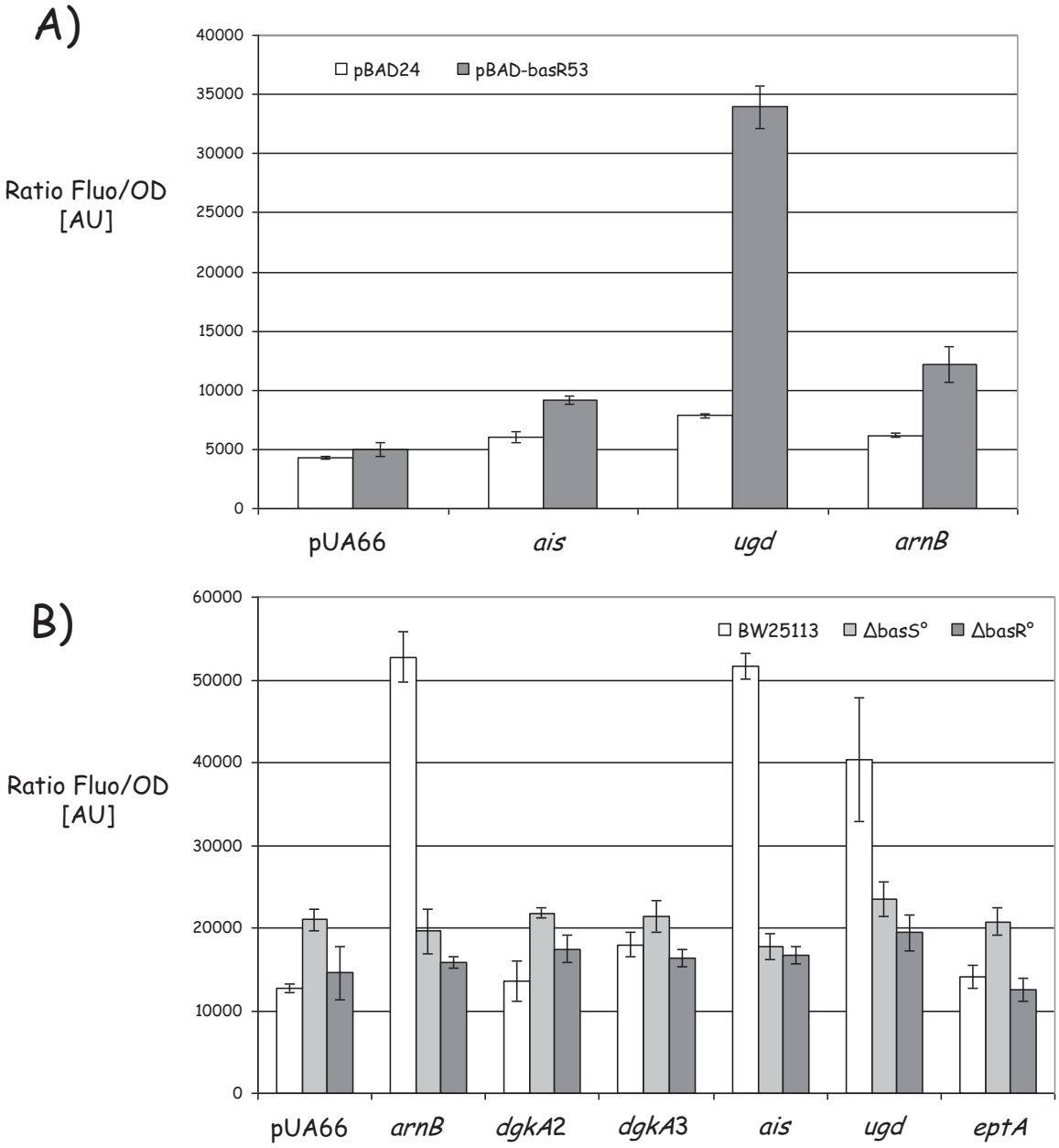

Figure 101: The BasRS regulon and its response to metavanadate is *basR*- and *basS*-dependent. A) *E. coli* strain MG1655 was co-transformed with pBAD24 or pBAD-*basR53* and transcriptional fusion plasmids pUA66, *ais*, *ugd*, and *arnB* (Zaslaver *et al.*, 2006). Single colonies were inoculated in LB medium supplemented with kanamycin (50 µg/mL), ampicillin (100 µg/mL), and arabinose (0,001 %) and were grown overnight at 30°C. Then, using a TECAN M200 the OD_{600nm} and fluorescence (excitation= 485 nm, emission= 530 nm) were measured. AU: arbitrary units for specific fluorescence, corresponding to the ratio fluorescence (in arbitrary units)/OD_{600nm}. **B)** *E. coli* wt BW25113, Δ*basS*°, and Δ*basR*° were transformed by pUA66, *ais*, *ugd*, *eptA*, *arnB* (Zaslaver *et al*., 2006), *dgkA*2, and *dgkA*3 (this work). Single colonies were inoculated in LB medium supplemented with kanamycin (50 µg/mL) and metavanadate (25 mM) and were grown overnight at 30°C. Then, using a TECAN M200 the OD_{600nm} and fluorescence (excitation= 485 nm, emission= 530 nm) were measured. AU: arbitrary units for specific fluorescence, corresponding to the ratio fluorescence (in arbitrary units)/OD_{600nm}.

The expression level of all *plsB* transcriptional fusions followed the level of ppGpp in the different strains (figure 103): *plsB* expression was up regulated in the absence of ppGpp action (ppGpp° (EB425) and Δ*dksA*° (EB599) had similar effects), while it was slightly down regulated in the ppGpp^{++} (EB544) strain. These effects of ppGpp were acting on the second promoter of *plsB*, because they still occurred in transcriptional fusions *plsB*Δ and *plsB*mutP$_{rpoE}$ that, respectively, does not contain the σ^E-dependent promoter or in which it is mutated.

In conclusion, we did not find the same results as the transcriptome studies for *dgkA*, since there is no effect of ppGpp on *dgkA* expression. Durfee *et al.* (2008) compared a wild type strain with a Δ*relA* mutant upon adding serine hydroxymate (SHX) and found that *dgkA* was up-regulated after 10 minutes. The authors reasoned that a response after 10 minutes suggests a direct transcriptional regulation by ppGpp. This could lead to differences in the response profile compared to our study, which has been performed overnight and in a ppGpp° strain. On the other hand, we found that *plsB* expression is inhibited by ppGpp which is consistent with other transcriptome studies and the known inhibition of *de novo* phospholipid synthesis during stasis.

B8. Effect of overproduction of RseAB on dgkA and plsB expression

At the beginning of my thesis, only the σ^E-dependent promoter was known for *plsB*. As we had shown the activation of PlsB by RpoE overproduction experiments, we also wanted to test the effects of a deletion mutant *rpoE* strain. But since RpoE is essential in *E. coli* (De Las Peñas *et al.*, 1997), a deletion mutant cannot be obtained. However, it has been shown that the overproduction of the anti sigma factors RseA and RseB (short RseAB because *rseA* and *rseB* form an operon) sequester RpoE at the membrane and therefore mimic a Δ*rpoE* phenotype (De Las Peñas *et al.*, 1997).

I constructed the pBAD-*rseAB* plasmid to overproduce RseAB. In the study of De Las Peñas *et al.* (1997) it has been described that overproduction of RseAB leads to growth retardation because of the essential nature of RpoE. *E. coli* MG1655 strain was transformed with pBAD24 or pBAD-*rseAB* and its growth was followed with or without *rseAB* induction. Growth was retarded with induction of RseAB (black squares in figure 104A) as expected 2-4h after induction with arabinose, but it finally reached the same final OD_{600nm} as controls. When I analyzed the protein profile of this experiment by SDS-PAGE and Coomassie Blue staining, I could not detect a band corresponding to RseAB overproduced protein(s) (data not shown). This might be due to the fact that RseA is a membrane spanning protein whose over-

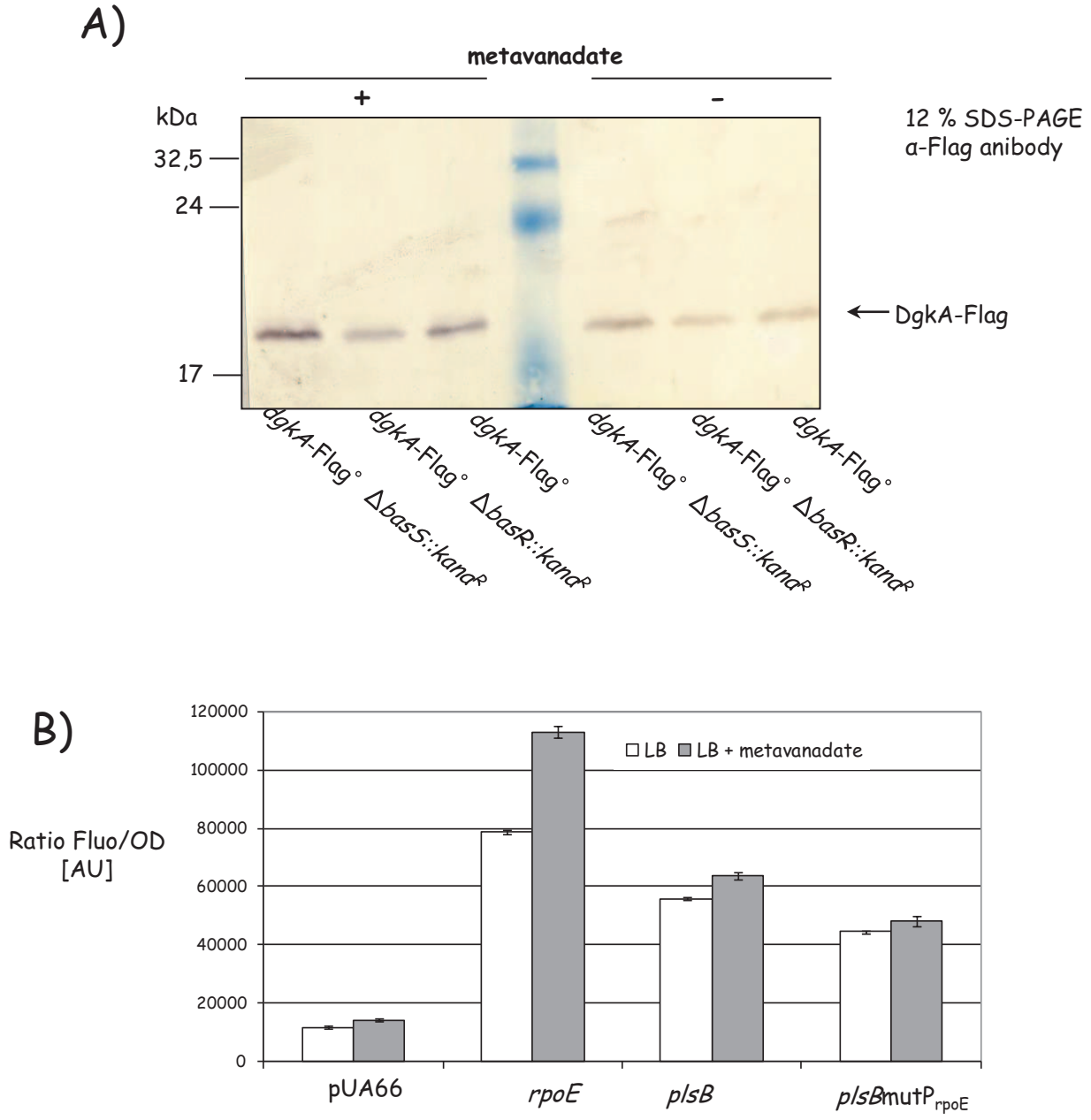

Figure 102: Effect of metavanadate on expression of *dgkA*, *plsB* and *rpoE*. A) Late stationary cultures were grown at 37 °C in LB supplemented with kanamycin (25µg/mL) if necessary and 25 mM metavanadate as indicated. Total cell extracts were analyzed by western blot with appropriate antibodies. **B)** Strain MG1655 was transformed by transcriptional fusion plasmids pUA66, *rpoE*, *plsB*, *plsB*mutP_{rpoE} (Zaslaver *et al.*, 2006; this work). Single colonies were inoculated in LB or LB + 25 mM metavanadate supplemented with kanamycin (50 µg/mL) and were grown overnight at 30°C. Then, using a TECAN M200 the OD_{600nm} and fluorescence (excitation= 485 nm, emission= 530 nm) were measured. AU: arbitrary units for specific fluorescence, corresponding to the ratio fluorescence (in arbitrary units)/OD_{600nm}.

production is difficult. The low expression of *rseAB* might explain the relatively low effect on growth.

In order to see if overproduction of RseAB has an effect on RpoE reporters and phospholipid synthesis gene expression, *E. coli* MG1655 strain was co-transformed by pBAD24 or pBAD-*rseAB* and transcriptional fusion plasmids pUA66 (control), *rpoE*, *rpoH*, *plsB* (Zaslaver *et al.*, 2006), *psd*2 or *dgkA*2 (this work). The clone *psd* from the Zaslaver's library did not contain the RpoE promoter, we therefore constructed a new clone, *psd*2, that does. The expression of *rpoE* and *rpoH* was decreased with overproduction of RseAB as expected (figure 104B), but there was no effect on *plsB*, *psd*2 and *dgkA*2 expression. But we now know that the second constitutive *plsB* promoter drives *plsB* expression under normal growth conditions, while this experiment was done in non-RpoE inducing conditions. In fact, we now do not expect a change for *plsB*. It would be necessary to do the same experiment in a condition in which RpoE stress response is activated.

B9. PlsB and DgkA interact by BACTH

The genes *plsB* and *dgkA* are one of the rare cases where phospholipid synthesis genes are co-localized on the *E. coli* chromosome. Furthermore, they are transcribed divergently, consistent with the antagonistic regulation we have evidenced. We wanted to test if PlsB and DgkA proteins interact. During his PhD, Djamel Gully has tested systematically the interactions of all phospholipid synthesis enzymes, but DgkA was not included in the study.

In the laboratory, different techniques are available to study protein-protein interactions. Among these techniques, the BACTH technique is used frequently (Karimova *et al.*, 1998). This technique consists in the reconstitution of the adenylate cyclase activity in a *cya*$^-$ *E. coli* strain (figure 104). Proteins whose interaction is tested are fused with the subunits T18 and T25 of the catalytic domain of the adenylate cyclase of *Bordetella pertussis.* When interacting, the fusion proteins permit the contact of the two subunits T18 and T25 and so adenylate cyclase activity is reconstituted. The produced cAMP associates to the CAP protein and regulates numerous genes in the cell, among which are the lactose and maltose operons. The activity of these two operons is detected thanks to a blue coloration on LB medium containing X-Gal or a violet coloration on McConkey medium containing maltose (figure 105).

To test an interaction between PlsB and DgkA protein, *E. coli* strain BTH101 *cya*$^-$ was co-transformed with different pairs of plasmids: pUT18linker-*dgkA* with pKT25linker-*dgkA*, pKT25linker-*plsB*, pKT25linker-Ntr*plsB*, or pKT25linker-Ctr*plsB* and pKT25linker-*dgkA*

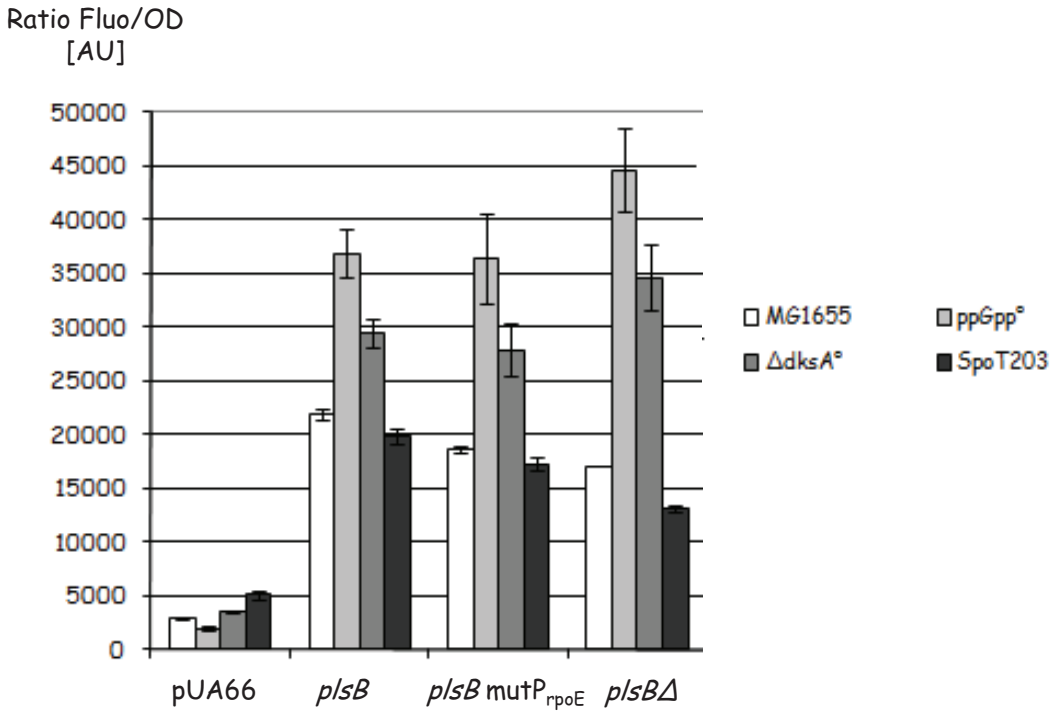

Figure 103: Effect of ppGpp on expression of *dgkA* and *plsB*. Strains MG1655, ppGpp° (EB425), Δ*dksA*° (EB559) or SpoT203 (EB544) were transformed by transcriptional fusion plasmids as indicated. Overnight cultures were grown in LB at 30°C supplemented with kanamycin (25µg/mL). Then, using a TECAN M200 the OD_{600nm} and fluorescence (excitation= 485 nm, emission= 530 nm) were measured.
AU: arbitrary units for specific fluorescence, corresponding to the ratio fluorescence (in arbitrary units)/OD_{600nm}.

with pUT18linker-*plsB*, pUT18linker-Ntr*plsB*, or pUT18linker-Ctr*plsB*. The N-terminal region of PlsB corresponds to residues 1 to 279 and is located in the cytoplasm (figure 16). The C-terminal region of PlsB corresponds to residues 280 to 807 and contains its acyltransferase domain and its two predicted TMDs. PlsB fusion proteins produced from pUT18linker-*plsB* or pKT25linker-*plsB* had been shown to be functional because the two plasmids complement strain BB2636 (*plsB*26*plsX*50) that is glycerol auxotroph (Gully *et al.*, unpublished). Furthermore, DgkA fusion proteins produced from pUT18linker-*dgkA* with pKT25linker-*dgkA* had also been shown to be functional as the Δ*dgkA* strain transformed with the two plasmids could grow on LB without NaCl (data not shown).

On the McConkey plate, the violet coloration specific of the protein interaction appears only for the clone co-transformed with pUT18linker-*dgkA* and pKT25linker-*plsB* as well as for the clone co-transformed with pKT25linker-*dgkA* and pUT18linker-*plsB*, which showed that the full length fusions of PlsB and DgkA interact (figure 106). These results were confirmed also on a LB plate containing X-Gal indicating by its specific blue coloration an interaction between the proteins. It is interesting to note that neither the C-terminus nor the N-terminus of PlsB alone interacted with DgkA. This could be due to a limited production of the domains of PlsB alone or the need for a particular folding of some regions of PlsB for the interaction with DgkA.

These results suggest that regulation takes place both at transcriptional and protein level between *plsB* and *dgkA*. We were not able to detect an oligomerization of DgkA by BACTH, although it forms a trimer (Van Horn *et al.*, 2009). So, these results should be taken with caution. Another reason might be that DgkA is susceptible to tagging which could lead to conformational changes and misfolding of its quaternary structure. But as shown here with the BACTH plasmids, DgkA did tolerate tagging at its N-terminus and DgkA fusion proteins were functional. This is in contrast with the EGFP-DgkA chromosal N-terminal fusion protein that was not functional.

C. Discussion to article 2

The regulation of the *plsB* and *dgkA* genes in response to different stress regulators was dissected. We have demonstrated for the first time that *dgkA* is part of the TCS BasRS regulon and identified a conserved BasR binding site upstream the *dgkA* orf. However, *dgkA* was never found in transcriptomic approaches or bioinformatic searches, neither in *S. typhimurium* - in which most of the studies were performed - nor in *E. coli* (Hagiwara *et al.*, 2004). A reason for this absence might be that there are differences in the activation mechanisms of the

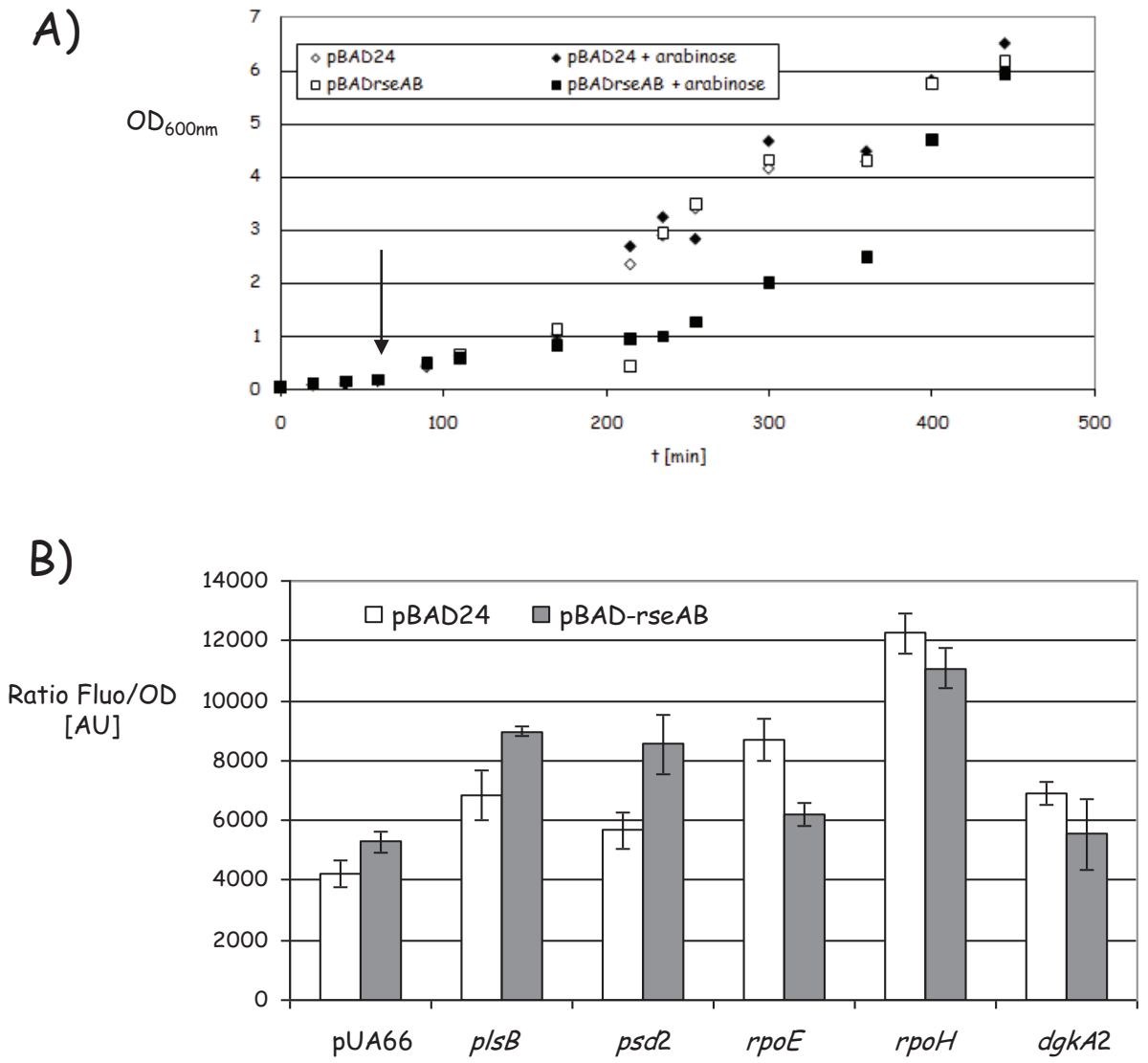

Figure 104: Effect of RseAB overproduction on RpoE-dependent genes. A) Growth curve: *E. coli* strain MG1655 was transformed with pBAD24 or pBAD-*rseAB*. Overnight cultures were grown in LB supplemented with ampicillin (100 µg/mL) at 37°C, diluted to an OD_{600nm}= 0,05 in 50 mL LB and were grown 1 h at 37°C. Then, each of the two cultures was divided into two cultures and half of them were induced with 0,1 arabinose. Growth was monitored every 20 min by measuring $OD_{600\ nm}$. **B)** *E. coli* strain MG1655 was co-transformed with pBAD24 or pBAD-*rseAB* and transcriptional fusion plasmids pUA66, *rpoE*, *rpoH*, *plsB* (Zaslaver *et al.*, 2006), *psd*2, and *dgkA*2 (this work). Single colonies were inoculated in 4 replica and grown without induction overnight at 30°C. Cultures were diluted 100X in fresh LB medium, grown till exponential phase (OD_{600nm}= 0,1) and induced during 2 h with 0,01 % arabinose at 30°C. Then, using a TECAN M200 the OD_{600nm} and fluorescence (excitation= 485 nm, emission= 530 nm) were measured. AU: arbitrary units for specific fluorescence, corresponding to the ratio fluorescence (in arbitrary units)/OD_{600nm}.

2 TCSs BasRS and PmrAB in the two bacteria and because of its strainge localization at the beginning of the *plsB* coding sequence. The only transcriptome study in *E. coli* (Hagiwara *et al.*, 2004) consisted in comparing the double Δ*basRS* mutant strain to a wild type strain. In this case, the basal level of *dgkA* expression might have been too low already in the wild type strain to measure any decrease. This is consistent with our finding that the basal signal of *dgkA* transcriptional fusion was always low compared to other promoters and that DgkA protein amount was not changed in a Δ*basR* mutant compared to a wild type strain (figure 100B). In our work, we observed the activation of *dgkA* by overproducing the BasR regulator which could be a new approach for a transcriptomic study.

We identified the promoter of *dgkA* using prediction programs and we found that the predicted – 35 consensus comprises the BasR binding box (figure 91). Furthermore, using GMSA we could show that BasR binds specifically to this BasR binding box in the promoter region of *dgkA*. The position of the BasR binding box on the *dgkA* promoter at the predicted – 35 consensus is consistent with the positions determined for PmrA in *S. typhimurium*: the transcription start sites of *pmrC*, *pbgPE*, and *pmrG* genes have been determined, and the PmrA binding boxes are located around – 40, – 38, or – 80 nucleotides before the respective start sites (Marchal *et al.*, 2004). We plan to definitely determine the transcription start site of *dgkA* experimentally.

What is the physiological meaning of the activation of *dgkA* by BasRS? Many genes that are regulated by BasRS code for enzymes involved in modifying LPS with different decorations, such as phosphoethanolamine, L-Ara4N, or palmitate (Raetz *et al.*, 2007). Among them, EptA (PmrC in *S. typhimurium*) transfers a phosphoethanolamine from phosphatidylethanolamine to the 1-phosphate group of the heptose residue in lipid A. DgkA recycles diacylglycerol to phosphatic acid, which can then reenter the phospholipid biosynthesis pathway (Raetz & Newman, 1978). It has been found that 75 % of the diacylglycerol recycled by DgkA is produced during OPG biosynthesis (Rotering & Raetz, 1983; Zhang & Rock, 2008). It has then been proposed that the remaining 25 % diacylglycerol accumulated from phosphoethanolamine modifications of the lipid A are catalyzed by enzymes of the *eptA* family (Reynolds *et al.*, 2005). When LPS is modified with phosphoethanolamine, diacylglycerol is produced as a by-product. So, *dgkA* is activated together with the BasRS regulon. These results suggest genetic and functional associations of DgkA with the enzymes of the LPS modifications.

We have shown that *dgkA* is activated by BasR, while it is inhibited by RpoE. In a similar way, there are different effects of the RpoE and BasRS responses on the regulation of

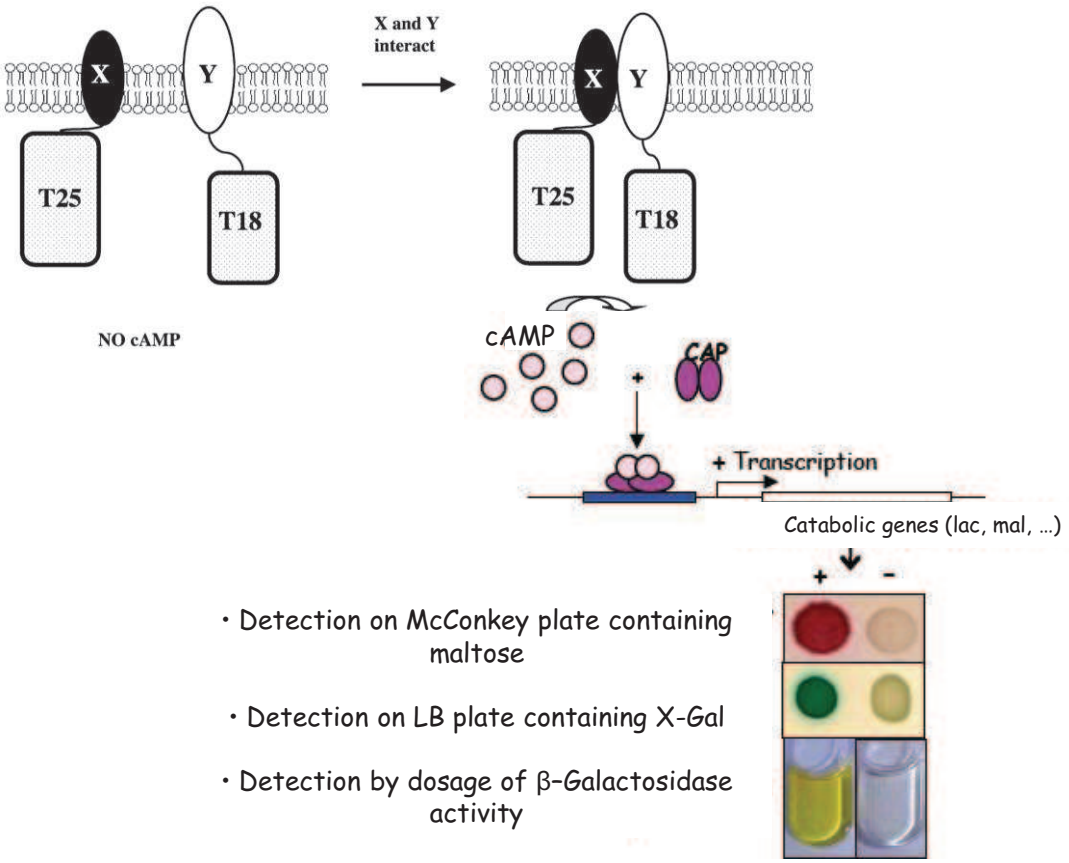

Figure 105: The BACTH (Karimova *et al.*, 1998). Proteins whose interaction is tested are fused with the subunits T18 and T25 of the catalytic domain of the adenylate cyclase of *Bordetella pertussis*. When interacting, the fusion proteins permit the contact of the two subunits T18 and T25 and so adenylate cyclase activity is reconstituted. The produced cAMP associates to the CAP protein and regulates numerous genes in the cell, among which are the lactose and maltose operons. The activity of these two operons is detected thanks to a blue coloration on LB medium containing X-Gal or a violet coloration on McConkey medium containing maltose, and a yellow coloration in a liquid assay dosage in the presence of ONPG.

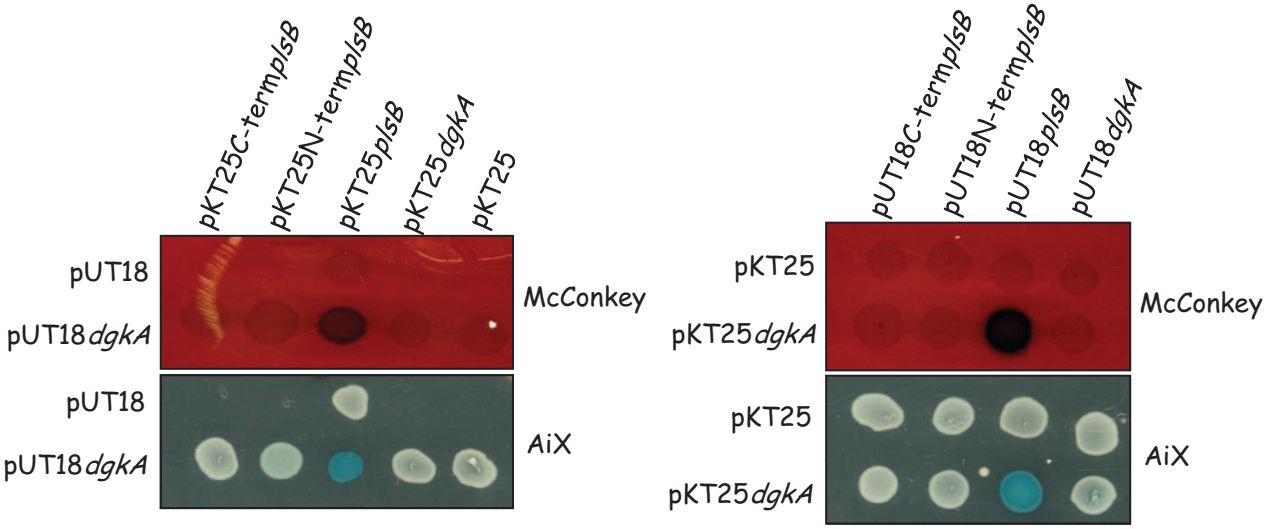

Figure 106: PlsB and DgkA interact. *E. coli* strain BTH101 was co-transformed with the pairs of plasmids indicated. One clone of every co-transformation is grown in LB supplemented with 0,5 mM IPTG, and then 2 µL of these cultures were dropped on McConkey supplemented with 1 % maltose or on AiX. After 24 h of incubation at 30°C, the resulting interactions appear in violet if there is an interaction on McConkey supplemented with maltose or in blue on AiX.
AiX: LB agar supplemented with ampicillin, IPTG [0,5 mM] and X-Gal [40 µg/mL].

LPS modifications. Indeed, *eptB*, a homologue of *eptA* that is not part of the BasRS regulon, is activated by RpoE both in *E. coli* and *S. typhimurium* (Rhodius *et al.*, 2006; Figueroa-Bossi *et al.*, 2006). Both EptA and EptB catalyze the transfer of phosphoethanolamine from PE to the LPS, but they modify two different positions of the lipid A molecule: outer Kdo residue of Kdo2-lipid A for EptB and the 1-phosphate group for EptA (Reynolds *et al.*, 2005). These two modifications might not have the same effects on the LPS properties. The regulation of LPS modifications is even more complicated by the fact that small RNAs (MgrR inhibits *eptB* and is part of the PhoPQ regulon and MicA, which is induced by RpoE, inhibits PhoPQ) make part of these regulatory loops (Moon & Gottesman, 2009; Coornaert *et al.*, 2010). Keeping in mind that the regulation mechanisms of PhoPQ and BasRS TCSs in *E. coli* and *S. typhimurium* are not strictly identical (Perez & Groisman, 2007), and that the references above are from both studies in *E. coli* and *S. typhimurium*, it appears that regulatory cascades involving PhoPQ, BasRS, RpoE, and small RNAs fine-tune LPS modifications in response to a variety of stress and growth conditions (Overgaard *et al.*, 2009). However, one questions remains: what is the fate of the diacylglycerol produced by *eptB* that is activated during RpoE stress response? DgkA is expected to be required in both cases of *eptA* or *eptB* activation to recycle diacylglycerol. Strangely, while *dgkA* is logically activated during the response to BasRS together with *eptA*, it is inhibited in response to RpoE.

In addition to the already described RpoE promoter (Rhodius *et al.*, 2006), we have shown that *plsB* expression is driven by a second proximal promoter. Our results demonstrate that this second promoter is responsible for the basal expression of *plsB* when there is no extracellular stress signal. As *plsB* is an essential gene, we reasoned that this second promoter might be required for growth. However, when we inactivated it by introducing a mutation on the chromosome, there was no obvious effect on growth (data not shown). This suggests that this second promoter is not essential for growth. Another reason might be that residual activity of RpoE was sufficient to maintain growth. We propose that this second promoter P2 links *plsB* expression to growth rate, through a control by ppGpp. Indeed, we found that the activity of this promoter was increased in a ppGpp° strain, which is strengthened by a global study of promoter activities in *E. coli*, showing higher activity of *plsB* promoter at higher growth rate (Zaslaver *et al.*, 2009). As the first step in the pathway, it was already described that PlsB is the crucial point of inhibition of phospholipid synthesis during stringent response, but it was suggested that ppGpp inhibited the enzymatic activity of PlsB (Heath *et al.*, 1994). While our results do not rule out this possibility, they clearly indicate that there is a control at the expression level as well. *plsB* expression is inhibited by ppGpp, whereas it is activated by

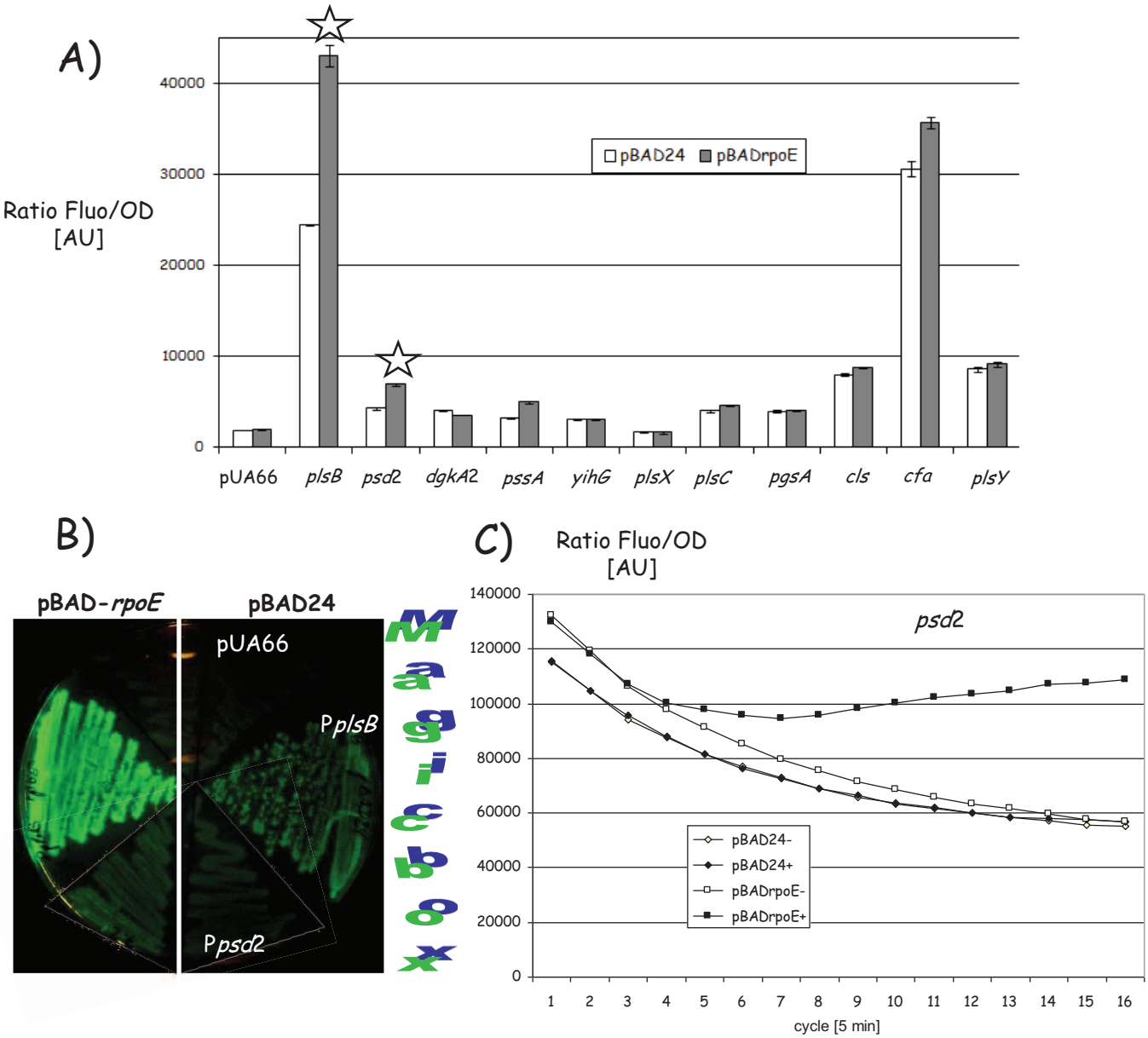

Figure 107: Effect of RpoE overproduction on expression of phospholipid synthesis genes. A) Strain MG1655 was co-transformed by transcriptional fusion plasmids and pBAD24 or pBAD-*rpoE* as indicated. Overnight cultures were grown at 30°C in LB supplemented with kanamycin (25µg/mL) and ampicillin (100 µg/mL). Then, using a TECAN M200 the OD_{600nm} and fluorescence (excitation= 485 nm, emission= 530 nm) were measured. The star indicates significant and reproducible measurements. **B)** Strain MG1655 was co-transformed by transcriptional fusion plasmids as indicated. Single colonies from transformation plates were restriked on LB plates supplemented with kanamycin (25µg/mL) and ampicillin (100 µg/mL) and grown overnight at 37 °C. Then, using a black box (= "Magic box") with filters permitting to detect GFP fluorescence (excitation= 488 nm, emission= 515 nm) a picture was taken of the cells emitting fluorescence (EGFP) with a numeric camera. **C)** Strain MG1655 was co-transformed by transcriptional fusion plasmid *psd*2 (this work) and pBAD24 or pBAD-*rpoE*. Overnight cultures were grown at 30°C in LB supplemented with kanamycin (25µg/mL), ampicillin (100 µg/mL). The next morning, cultures were diluted 1/100 in fresh LB with or without induction by arabinose as indicated by – or + (0,1 %) and grown at 30 °C. Then, using a TECAN M200 the OD_{600nm} and fluorescence (excitation= 485 nm, emission= 530 nm) were measured in kinetic cycles of 5 minutes during growth.
AU: arbitrary units for specific fluorescence, corresponding to the ratio fluorescence (in arbitrary units)/OD_{600nm}.

RpoE. The opposite effect of the two stress response regulators on *plsB* expression might appear paradoxical because full RpoE activity requires the presence of ppGpp (Costanzo & Ades, 2006; Costanzo *et al.*, 2008). Yet, the presence of two distinct promoters resolves this apparent paradox. They can integrate different kind of stress responses, and for example permit *plsB* expression when required (RpoE stress response), despite global stringent response.

The *plsB-dgkA* locus integrates three distinct types of stress signals: the global stringent response, the specific TCS BasRS, and the RpoE-dependent extracytoplasmic stress, thanks to three different promoters. For these three types of stress responses, the two genes might be regulated in opposite manners: this is the case in the *dgkR*1 strain which contains a mutation in the *basS* gene (Raetz *et al.*, 1981), we have shown that it is the case for RpoE (*dgkA* down and *plsB* up), and transcriptome results suggest that it is the case for the stringent response (*dgkA* up and *plsB* down) (Durfee *et al.*, 2008). By regulation of these two points of control, the whole phospholipid synthesis pathway can be tuned according to environmental conditions in order to keep a balanced membrane homeostasis.

D. Regulation of the phospholipid synthesis pathway by RpoE

psd codes for phosphatidylserine decarboxylase which is the branching point leading to PE. It has been reported that *psd* and *plsB* are activated by RpoE (Rezuchova *et al.*, 2003; Rhodius *et al.*, 2006). Our question was if the activation of these two genes is sufficient to activate the PE synthesis during RpoE stress response. We therefore wanted to screen systematically all phospholipid synthesis genes upon induction by RpoE. Most of these genes are available as transcriptional fusions in the Zaslaver's library. Additionally, I constructed the plasmids pUA66-*pssA*, because it was not in the Zaslaver's library, and pUA66-*psd*2, because the initial *psd* clone of the Zaslaver's library did not include the RpoE promoter sequence. *E. coli* strain MG1655 was co-transformed by plasmids pBAD24 or pBAD-*rpoE* and all the transcriptional fusion plasmids of phospholipid synthesis genes. We showed that only *plsB* and *psd*2 were activated by RpoE at transcriptional level (figure 107). The measurements for the other transcriptional fusions were not significantly changed and not reproducible. Despite the fact that we found DgkA decreased upon RpoE induction, we could not show that *dgkA* is down regulated at transcriptional level. But here again the reason might be the low basal expression level of *dgkA* and therefore no decrease could be monitored.

By taking advantage of the transcriptional fusions, we could follow the activation of *plsB* and *psd*2 expression by RpoE dynamically *in vivo*. *E. coli* strain MG1655 was co-

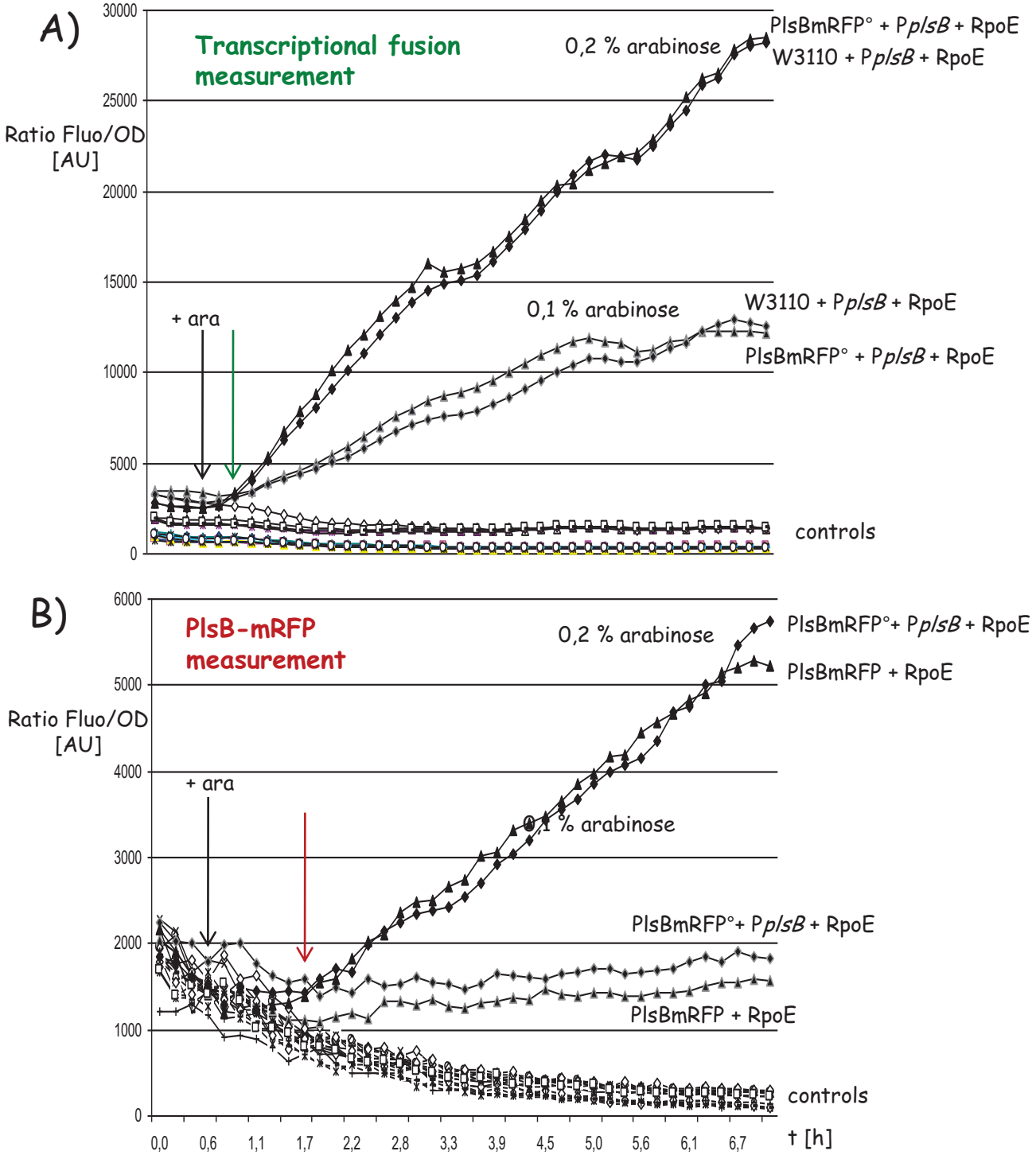

Figure 108: Activation of *plsB* transcription and accumulation of PlsB-CBP-mRFP upon RpoE overproduction followed dynamically *in vivo*. Strains W3110 and W3110 *plsB*-CBP-mRFP° (EB409) were co-transformed by transcriptional fusion plasmid P*plsB* and pBAD24 or pBAD-*rpoE* as indicated. Strain W3110 *plsB*-CBP-mRFP::kana^R (EB393) was transformed by pBAD24 or pBAD-*rpoE*. Cultures were grown at 30 °C in LB supplemented with kanamycin (12,5 (strains) or 25µg/mL) and ampicillin (100 µg/mL), without or with different concentrations of arabinose. Then, using a TECAN M200 the OD_{600nm} and fluorescence (**A)** GFP: excitation= 485 nm, emission= 530 nm; **B)** mRFP: excitation= 560 nm, emission= 610 nm were measured. AU: arbitrary units for specific fluorescence, corresponding to the ratio fluorescence (in arbitrary units)/OD_{600nm}. The arrows in green (EGFP) and red (mRFP) indicate when an activation of the signal is detected.

transformed by plasmids pBAD24 or pBAD-*rpoE* and transcriptional fusions *plsB* and *psd*2 (this work). Transcription of *psd*2 is activated about 20 min after induction (figure 107C) and a similar result was found for *plsB* (data not shown).

We could follow the effect of RpoE overproduction on the PlsB and Psd protein amount using our chromosomal fusions with fluorescent reporters. An increase of the protein amount of PlsB-CBP-EYFP upon *rpoE* overexpression was detected for the first time (article 1, figure 3). Moreover, by transforming an mRFP tagged PlsB strain by the *plsB* transcriptional fusion with GFP, we could monitor at the same time the expression and protein amount in the same experiment using two settings for fluorescent measurement. *plsB* expression is activated about 24 min after induction of RpoE with arabinose, and then the increase of protein amount of PlsB-CBP-mRFP can be detected about 1,1 h after induction (figure 108).

In the same way, it was possible to monitor the increase upon RpoE induction *in vivo* of Psd tagged with EGFP or mRFP by measuring the specific fluorescence with the TECAN dynamically (data not shown). The gene *psd* forms a transcription unit with *yjeP* (Rhodius *et al.*, 2006), which codes for a predicted membrane protein of unknown function. We therefore tested whether the protein amount of YjeP would also increase upon induction of RpoE. Strain W3110 *yjeP*-CBP-EGFP::$kana^R$ was constructed and transformed with pBAD-*rpoE*. The fusion protein YjeP-CBP-EGFP cannot be detected at its physiological production level, but by Western blot analysis, YjeP-CBP-EGFP was detected upon induction with RpoE (data not shown). Furthermore, the specific fluorescence signal of YjeP-CBP-EGFP was induced by RpoE (data not shown). These results strengthen the fact that *psd* and *yjeP* form an operon that is activated by the same σ^E-dependent promoter. They also suggest that YjeP has a role during RpoE induced stress response. However, the function of YjeP remains unknown as well as its link with Psd activity.

To conclude, we could show using *in vivo* dynamic fluorescent techniques that *plsB* and *psd* (together with *yjeP*) are up regulated upon induction by RpoE both at transcriptional and protein level. DgkA in contrast is down regulated by RpoE. These results suggest that regulation both at transcriptional and protein level is finely tuned at this crucial locus *plsB-dgkA* in order to equilibrate between *de novo* synthesis in particular of PE (PlsB and Psd) and recycling (DgkA) pathways of phospholipids during RpoE stress response.

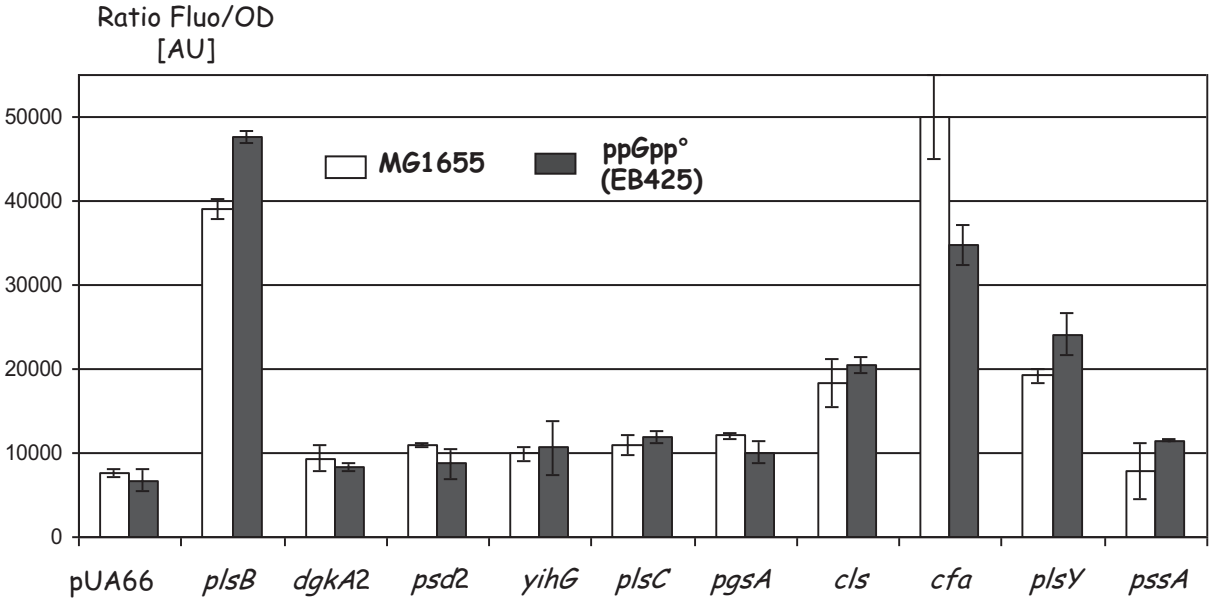

Figure 109: Effect of ppGpp on expression of phospholipid synthesis genes. Strains MG1655 or MG1655 ppGpp° (EB425) were transformed by transcriptional fusion plasmids as indicated. Overnight cultures were grown in LB at 30°C supplemented with kanamycin (25µg/mL). Then, using a TECAN M200, the OD_{600nm} and fluorescence (excitation= 485 nm, emission= 530 nm) were measured.
AU: arbitrary units for specific fluorescence, corresponding to the ratio fluorescence (in arbitrary units)/OD_{600nm}.

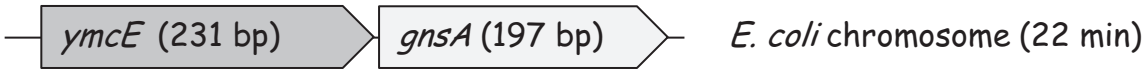

Figure 110: Genetic organization of *gnsA* and *ymcE*. bp: base pairs.

E. Regulation of phospholipid synthesis genes in response to ppGpp

We have shown that *plsB* expression is regulated by a second stringent promoter that follows the growth rate and the ppGpp level of the bacterial cell. There are indications in transcriptome studies that other phospholipid synthesis genes are regulated as well during stringent response (Traxler *et al.*, 2008; Durfee *et al.*, 2008; Aberg *et al.*, 2009). Therefore, I tested the response of all transcriptional fusions of phospholipid synthesis genes in *E. coli* strains that are impaired in controlling the level of ppGpp. *E. coli* MG1655 or ppGpp° (EB425) strains were transformed by transcriptional fusion plasmids with *gfp* (Zaslaver *et al.*, 2006, or this work). Expression of *cfa* was decreased in ppGpp° (figure 109). This is consistent with the known activation of *cfa* by the alternative sigma factor SigmaS that is itself induced by ppGpp during stasis (Zhang & Rock, 2008). Except *plsB*, the expression of other phospholipid synthesis genes, however, did not change significantly (figure 109). This is not consistent with results of transcriptome studies (Traxler *et al.*, 2008; Durfee *et al.*, 2008; Aberg *et al.*, 2009). Expression tests of all reporters were not performed in strains Δ*dksA*° or SpoT203, but may give clearer results that are in agreement with these studies. A reason might be that the limits of the used transcriptional fusions did not contain the correct promoter sequences. Another explanation could be that the detection of the fluorescent signal of the *gfp* transcriptional fusions is not sensitive enough to detect small changes. The reasons for these different results could also be differences in how the experiments were performed (different strains, time point).

F. Regulation of phospholipid synthesis genes by GnsA and YmcE

During my thesis, we were looking for clues about potential regulators of phospholipid synthesis. That was how we became interested in *dgkA* regulation. We found a paper about the *dgkR1* mutant strain in which DgkA enzymatic activity was induced 7-fold and PlsB activity repressed (Raetz *et al.*, 1981). The identified "DgkR" regulator appeared to be the TCS BasRS. But during the course of my thesis, we came around other candidates in the literature.

We found information about two possible regulators of phospholipid synthesis: *ymcE* and *gnsA*. GnsA (*secG* null mutant suppressor) was isolated as a multicopy suppressor of a cold-sensitive *secG* mutant (Sugai *et al.*, 2001). The suppressor was originally thought to localize to the *ymcE* gene, which is located immediately upstream of *gnsA* (Rock *et al.*, 1996) (figure 110). It has been found that after a temperature downshift from 37 °C to 20 °C and by

detecting radio-labelled phospholipid moieties, overexpression of *gnsA* inhibited PE synthesis and thus caused a proportional increase of anionic phospholipids (Sugai *et al.*, 2004).

In order to test the possibility of a regulation of phospholipid synthesis genes by GnsA or YmcE, I constructed plasmids pBAD-*ymcE* (pEB1111) and pBAD-*gnsA* (pEB1112) permitting over-production of YmcE and GnsA. In the first place, *E. coli* MG1655 strain was co-transformed by pBAD24 or pBAD-*gnsA* and pUA66, *plsB*, *dgkA*, *psd*, *cls*, *plsX*, *pgsA*, *yihG*, *plsC* or *plsY*. However, there were no effects upon over-production of GnsA on gene expression (data not shown). A similar result was obtained with pBAD-*ymcE* (data not shown).

Then, we wanted to see if there was an effect of GnsA overproduction on PgsA protein amount. W3110 strain producing PgsA-CBP-EGFP (EB264) was transformed by pBAD24 or pBAD-*gnsA* and grown with or without induction at 20 or 37 °C. However, there was no effect on PgsA upon over production of GnsA in any condition (data not shown).

A null mutation of *gnsA* had no effect on phospholipid composition (Sugai *et al.*, 2004). But we wanted to test the effect of either Δ*gnsA* or Δ*ymcE* strains on the expression of the phospholipid synthesis genes. *E. coli* BW25113 Δ*gnsA*° or Δ*ymcE*° strains were by transformed with all the *gfp* transcriptional fusion plasmids of phospholipid synthesis genes. However, there was no effect of the two strains (data not shown).

To conclude, our results are not consistent with the literature that overproduction of GnsA (or YmcE) has an effect on *pgsA*. However, we did not measure the phospholipid composition of the membranes upon overproduction of GnsA and thus the results cannot be compared directly.

CONCLUSION GENERALE

Les travaux de thèse de Djamel Gully avaient suggéré que les enzymes de synthèse des phospholipides pouvaient être organisées en complexe protéique dans la membrane interne (Gully *et al*., 2006, thèse 2005). Pendant ma thèse, je me suis donc attachée à comprendre l'organisation moléculaire de ces protéines membranaires, c'est à dire à étudier leur topologie et leur localisation, et à essayer de confirmer l'existence de complexes protéiques dans la membrane interne. Pour cela, j'ai développé des cassettes permettant d'étiqueter facilement les protéines d'intérêt avec des rapporteurs fluorescents ou luminescents, par recombinaison sur le chromosome (article 1).

De plus, j'ai étudié la régulation génétique des enzymes de synthèse des phospholipides en conditions de stress, car peu d'études ont été menées à ce sujet jusqu'à présent. En utilisant des rapporteurs transcriptionnels et protéiques, j'ai montré que parmi tous les gènes de biosynthèse des phospholipides, seuls les gènes *plsB* et *psd* sont induits par le facteur sigma alternatif RpoE. Cet effet se retrouve au niveau de la quantité des protéines PlsB et Psd qui est augmentée, ce que j'ai pu visualiser avec les rapporteurs fluorescents. En revanche, la quantité de protéine DgkA est réduite lors de la surproduction de RpoE. A l'inverse, j'ai montré que *dgkA* est activé par le régulateur de réponse BasR. Ces résultats mettent en évidence un lien entre la synthèse des phospholipides et l'incorporation de modifications dans le LPS, impliquées dans la résistance aux peptides microbiens (article 2).

Lors de ma thèse, plusieurs problèmes et questions se sont posés. Tout d'abord, les approches envisagées pour la caractérisation de complexes protéiques dans la membrane interne et pour la localisation des enzymes de synthèse des phospholipides n'ont pas été totalement fructueuses. Ensuite, les résultats décrits dans l'article 2 ont ouvert un nouveau sujet de recherche, et ils soulèvent de nombreuses perspectives concernant la régulation génétique de la voie de biosynthèse des phospholipides en réponse au stress. Finalement, bien que toutes les enzymes nécessaires à la voie principale de synthèse des phospholipides soient a priori identifiées, il existe de nombreux homologues des différentes enzymes qui pourraient également participer à ce métabolisme, pour la synthèse d'espèces minoritaires, ou en réponse au stress. Ces trois grands points sont ici discutés.

Étude et importance des protéines membranaires

Il existe de nombreux exemples de complexes protéiques membranaires. Ils correspondent à des machineries complexes, effectuant des fonctions bien précises. On peut citer par exemple

les complexes constituant les chaînes de transfert d'électrons, comme les complexes LH2 (light harvest) des bactéries photosynthétiques ou le complexe de l'ATP-synthase bactérienne. Les machineries de sécrétion sont également de bons exemples. A l'inverse de ces machineries bien caractérisées, plusieurs voies de biosynthèse qui se déroulent dans la membrane, comme les voies de biosynthèse des phospholipides, du lipide A, de l'undecaprenyl-phosphate etc…, sont assurées par des séries d'enzymes membranaires dont on ne connaît pas l'organisation moléculaire. Ces enzymes effectuent des séries de réactions qui doivent être coordonnées, et on peut donc soupçonner l'existence de complexes protéiques ou à tout le moins d'interactions protéine-protéine. C'est la question que nous avons voulu étudier dans le cas de la synthèse des phospholipides.

Malheureusement, bien qu'environ 25-30 % des protéines bactériennes soient prédites pour être membranaires, et malgré leur importance dans les fonctions cellulaires, la protéomique de la membrane est notoirement sous-étudiée (Poetsch & Wolters, 2008). Cela est dû à plusieurs facteurs, dont la difficulté dans la solubilisation des composants de la membrane (phospholipides, LPS, peptidoglycane) et l'hydrophobicité des protéines membranaires contenant des segments transmembranaires, ce qui rend difficile leur séparation et leur identification (Cordwell, 2006).

Plusieurs techniques ont été développées pour essayer d'étudier les interactions protéine-protéine entre protéines membranaires. La purification par affinité ou par immunoprécipitation peut être tentée, en utilisant une protéine étiquetée ou un anticorps spécifique, et en la purifiant dans des conditions de solubilisation douce pour maintenir les interactions avec ses partenaires. Des purifications simples ou plus élaborées comme la Tandem Affinity Purification sont envisageables. La technique des gels au bleu natifs constitue une autre approche. Dans tous les cas, l'utilisation de détergents « doux » (Triton-X100, digitonin) est nécessaire afin de solubiliser les protéines membranaires.

L'approche de Tandem Affinity Purification est basée sur deux purifications d'affinité successives grâce à une étiquette en tandem (tag TAP). Par cette approche, un réseau d'interactions protéique a été décrit chez *E. coli* (Butland *et al.*, 2005; Hu *et al.*, 2009). L'étiquette en tandem rend cette purification spécifique, avec peu de contaminants. De plus, des complexes protéiques stables peuvent être isolés dans des conditions de purification et d'élution natives. Le désavantage de cette méthode est qu'elle n'est applicable que si les partenaires protéiques sont solubles. On peut imaginer appliquer cette méthode à des extraits de protéines membranaires solubilisées, comme cela a été décrit dans le cas de l'interactome

de levure (Gavin *et al.*, 2006). Toutefois, l'étape de solubilisation risque toujours de provoquer la perte d'interactions spécifiques qui ont lieu dans la membrane. Il est également envisageable d'effectuer un pontage chimique sur les membranes, avant l'étape de solubilisation pour ensuite effectuer la purification TAP sur des échantillons solubilisés voir dénaturés puisque le pontage maintient les interactions (Stingl *et al.*, 2008).

Une technique alternative pour l'identification de complexes membranaires est la technique des gels au bleu natifs (Helbig *et al.*, 2010). Le colorant bleu est utilisé pour charger les complexes protéiques négativement afin d'améliorer leur mobilité dans le gel. Les complexes sont séparés par électrophorèse en deux dimensions : la première dimension est un gel d'acrylamide natif avec un détergent doux afin de séparer les complexes en fonction de leur taille. Les complexes sont alors séparés dans la deuxième dimension par SDS-PAGE classique. Chez *E. coli*, cette technique a été utilisée pour déterminer des complexes formés par des protéines de l'enveloppe (Stenberg *et al.*, 2005). De plus, des nouveaux colorants ou des marquages avec des isotopes radioactifs permettent une quantification des protéines dans ces complexes.

Finalement, la technique du BACTH bactérien a été utilisée pour de nombreuses études d'interactions entre protéines membranaires. Cette technique est basée sur la reconstitution enzymatique des sous-unité T18 et T25 de l'adenylate cyclase de *Bordetella pertussis* dans une souche *E. coli cya*$^-$ (Karimova *et al.*, 1998). Le BACTH est applicable aux protéines membranaires dont la topologie est connue et peut être utilisé comme système hétérologue chez d'autres bactéries. Mais, cette technique pourrait générer de nombreux faux négatifs dans le cas des protéines de membrane, en particulier dus à la surproduction des protéines hybrides. De plus, des interactions qui nécessiteraient plus de deux partenaires ne pourraient pas être détectées.

Pendant ma thèse, je me suis intéressée aux enzymes de synthèse des phospholipides qui sont pour la plupart des protéines de la membrane interne (Cronan, 2003). Ces protéines de relativement faible quantité sont essentielles à la croissance de la cellule.

Au laboratoire, afin d'étudier les interactions protéine-protéine, nous utilisons en routine les techniques de BACTH et de (co-)purifications par affinité (TAP ou autre). Pendant sa thèse, Djamel Gully avaient mis en évidence par ces techniques plusieurs interactions protéine-protéine impliquant des enzymes de synthèse des phospholipides (Gully *et al.*, 2003 ; Gully *et al.*, 2006 ; Guly *et al.*, non publié). Nous voulions mettre en évidence les complexes protéiques correspondant dans la membrane, en utilisant des conditions de purifications

natives. Nous avons pour cela voulu développer la technique v-TAP. Le but recherché était de (co-)purifier les protéines de la synthèse des phospholipides dans des conditions natives (sans détergent) et physiologiques (expression des gènes par leur promoteur naturel). L'étiquette TAP a été fusionnée sur le chromosome avec plusieurs enzymes de synthèse des phospholipides. Nous avons pu vérifier qu'elles étaient produites et localisées correctement dans la membrane. En revanche, nous n'avons pas réussi à purifier de protéine cible. Les problèmes rencontrés ont été la perte de matériel au cours de la purification et la faible quantité des protéines produites physiologiquement. En perspective à ce travail, la méthode du v-TAP est toujours en cours de développement au laboratoire. Nous recherchons une meilleure séparation des membranes externe et interne, et de nouvelles étiquettes d'affinité et d'autres résines sont testées qui permettraient une meilleure fixation des protéines étiquetées, ancrées dans les vésicules.

Une autre approche pour détecter les interactions entre protéines membranaires pourrait être l'utilisation des techniques du FRET ou BRET sur des cellules vivantes produisant les protéines fluorescentes ou luminescentes (Xu *et al.*, 1999). Je n'ai pas entamé cette approche durant ma thèse, mais j'ai construit de nombreuses souches produisant les enzymes de synthèse des phospholipides fusionnées à des protéines fluorescentes ou luminescentes. Ceci m'a permis d'étudier la stœchiométrie et la localisation de ces enzymes. Les protéines fusions sont produites, mais leur faible quantité rend le signal de fluorescence ou de luminescence très faible et difficile à détecter, que ce soit par microscopie, ou en utilisant un fluorimètre de type TECAN. De plus, de nombreuses protéines fusion perdent leur fonctionnalité. Ceci est facilement mis en évidence par l'apparition de graves défauts de croissance, car la plupart des enzymes de synthèse des phospholipides sont essentielles. De nombreux essais sont donc encore à réaliser : nous devons sélectionner de meilleures fusions afin de préserver la fonctionnalité des protéines et afin d'améliorer le signal. On pourra ainsi essayer de nouveaux rapporteurs fluorescents, et surtout mettre au point une cassette qui fonctionne pour fusionner les protéines à leur extrémité N-terminale. Nous n'abandonnons pas la possibilité de réaliser alors des expériences de FRET ou de BRET.

Toutefois, j'ai pu étudier la localisation de plusieurs enzymes de synthèse des phospholipides en microscopie par fluorescence. Suivant les enzymes, j'ai observé un signal homogène sur tout le pourtour de la bactérie, ce qui suggère une localisation homogène dans la membrane. C'est le cas de PgsA. Pour d'autres, j'ai observé de façon répétée une localisation membranaire mais non homogène, avec l'apparition de 'patchs' irréguliers. C'est le cas de PlsB et Psd. Il serait nécessaire d'étudier plus en détail ces images afin de

caractériser cette localisation. La solubilisation correcte des protéines fusions suggère que cet aspect ne serait pas dû à l'aggrégation des protéines. On aurait ainsi deux types d'organisation des enzymes de synthèse des phospholipides dans la membrane. Deux études seulement ont déjà été publiées sur la localisation de ces enzymes, et uniquement dans *B. subtilis* (Nishibori *et al.*, 2005 ; Paoletti *et al.*, 2007). La première réalisée sur de nombreuses protéines fusion a montré une localisation préférentielle au septum et aux pôles, mais les auteurs avaient utilisé une expression à partir d'un promoteur inductible. La deuxième, beaucoup plus physiologique (immunofluorescence sur une souche sauvage avec des anticorps spécifiques), a montré que PlsX était associée à la membrane, avec un pattern ponctué qui ressemble à ce que nous observons pour PlsB. Malgré des résultats très préliminaires, on peut suggérer qu'il existe une organisation ponctuée des enzymes effectuant les premières étapes des synthèse (étapes d'acylation) qui doivent de plus faire un contact avec la synthèse des acides gras qui se déroule dans le cytoplasme. L'existence d'une machinerie dédiée est toujours à démontrer, mais dans tous les cas, la localisation des enzymes n'est pas restreinte à certaines positions (septum ou pôle).

Comment la synthèse des phospholipides est-elle régulée en réponse aux différents stress ?

J'ai montré que le locus génétique *plsB-dgkA* est régulé en réponse à trois différents stress: le système à deux composants BasRS, le facteur sigma alternatif RpoE et le ppGpp. Ces trois signaux doivent être intégrés sur ce locus génétique pour enfin activer ou inhiber soit *plsB* et la synthèse *de novo*, soit *dgkA* et le recyclage des phospholipides. De plus, nos résultats et ceux décrits dans la littérature suggèrent qu'ils existent de nombreuses interconnections entre ces trois voies de régulation, assurées par exemple par de petits ARNs non-codants.

DgkA recycle le diacylglycérol produit lors des modifications du LPS avec un groupement phosphoethanolamine par EptA (Lee *et al.*, 2004). De façon consistante, nos résultats démontrent que *dgkA* est co-régulé avec tous les gènes de modifications du LPS, dont *eptA*. On peut se demander pourquoi *dgkA* est spécifiquement activé par cette réponse, alors qu'il ne l'est pas dans le cas d'autres réponses conduisant à la production de diacylglycérol, comme la synthèse des OPGs ou lors de l'activation de EptB, un homologue de EptA, activé par RpoE (Reynolds *et al.*, 2005 ; Figuerroa-Bossi *et al.*, 2006). Au contraire, DgkA semble être inhibé par RpoE. De plus, le signal détecté par le TCS BasRS serait une trop forte concentration en fer ou autres cations, mais cette réponse est mal comprise (Hagiwara *et al.*, 2004). Nos premiers résultats sur la régulation de la synthèse des phospholipides soulèvent ainsi de nombreuses questions, et il apparaît que les mécanismes

sont complexes, afin de finement réguler la composition de l'enveloppe en réponse aux conditions extérieures.

A la suite des travaux présentés dans l'article 2, nous aimerions particulièrement comprendre comment les trois voies de signalisation du TCS BasRS, du facteur sigma alternatif RpoE et du ppGpp, s'interconnectent au niveau de la régulation du locus *plsB-dgkA*. En effet, il existe de nombreux cross-talk. Il a été proposé par exemple que des modifications du LPS pourraient constituer un signal pour déclencher une réponse RpoE-dépendante (Tam & Missiakas, 2005). Ceci suggère que le TCS BasRS et RpoE sont connectés d'une façon complexe via les modifications du LPS. Par ailleurs, il est connu que RpoE requiert pour son induction l'activité du ppGpp (Costanzo & Ades, 2006). Mais dans ce contexte, comment les signaux des deux régulateurs ppGpp et RpoE, ayant un effet inverse sur l'expression de *plsB* et *dgkA*, sont-ils intégrés et quel est le signal résultant ? Le promoteur de *dgkA* que nous avons mis en évidence, activé par BasR, est loin en amont de l'orf (170 bp). On ne peut pas exclure que d'autres mécanismes de régulation, et peut-être d'autres promoteurs contrôlent *dgkA* dans cette région intergénique. Toutefois, nous n'avons pas détecté pour l'instant d'autres régions permettant la transcription de *dgkA*. Il faudrait donc étudier plus en détail chacune des trois régulations mises en évidence, et comment elles sont influencées par les deux autres réponses au stress.

Le deuxième résultat important de notre étude a été de montrer que *plsB* était contrôlé par deux promoteurs, un promoteur fort basal responsable de l'expression constitutive, et un promoteur activé par RpoE, uniquement en réponse à un stress extracytoplasmique. Il est possible que cette organisation soit retrouvée pour d'autres gènes régulés par RpoE. En particulier, il serait intéressant d'étudier la régulation du gène *psd* responsable de la synthèse de PE. Non seulement *psd* est activé par RpoE (Rhodius *et al.*, 2006), mais son promoteur contient également un site de fixation pour le régulateur CpxR du TCS CpxRA (De Wulf *et al.*, 2002). Le TCS CpxRA est, comme RpoE, impliqué dans la régulation en réponse à un stress de l'enveloppe, mais leurs rôles distincts dans la dégradation et dans le repliement des OMPs ne sont pas entièrement compris. Le gène *psd* est essentiel et devrait donc, comme dans le cas de *PlsB*, être sous le contrôle d'un deuxième promoteur responsable de son expression constitutive. Il faudrait alors caractériser les promoteurs de *psd* et comprendre leur régulation croisée par RpoE et CpxR, et peut-être également par la réponse stringente.

Deux régulateurs potentiels de la synthèse des phospholipides avaient été décrits, *dgkR* et *pssR* régulant respectivement l'activité diacylglycerol kinase et phosphatidylserine synthase

(Raetz *et al.*, 1981 ; Sparrow & Raetz, 1983). Nos travaux nous ont permis d'identifier le régulateur DgkR, qui est en fait le TCS BasRS. De la même façon, il serait intéressant d'identifier le régulateur PssR qui n'a toujours pas de gène assigné. Par la même approche que celle suivie pour *dgkR*, on pourra déjà vérifier dans la souche contenant la mutation *pssR*1 si la transcription du gène *pssA* ou celle d'autres gènes de synthèse des phospholipides est effectivement affectée. Ensuite, le gène devra être identifié, sachant que là encore, la mutation *pssR1* a été localisée grossièrement à 85 minutes sur le chromosome de *E. coli* (Sparrow & Raetz, 1983).

Notre projet de recherche était parti du constat qu'il n'existait pratiquement pas de données sur la régulation génétique de la synthèse des phospholipides. Les résultats obtenus sur seulement deux gènes, *plsB* et *dgkA*, indiquent qu'il existe une régulation complexe de ces gènes, en réponse au stress, et suggèrent qu'il reste de nombreux autres mécanismes de régulation à découvrir dans la voie de synthèse des phospholipides, non seulement dans *E. coli* mais également chez toutes les bactéries. Un des aspects, et non le moindre, concerne le nombre important de gènes prédits pour être impliqués dans le métabolisme des phospholipides.

Quels rôles pour les protéines de fonction inconnue homologues aux enzymes de la synthèse des phospholipides?

Toutes les enzymes nécessaires à la synthèse des phospholipides ont été identifiées et sont très conservées parmi les bactéries (Lu *et al.*, 2006). Chez *E. coli*, il existe plusieurs protéines homologues à des enzymes de la synthèse des phospholipides, mais dont la fonction reste inconnue (figure 24). Pour comprendre leur rôle physiologique, il faudrait dans un premier instant caractériser précisément leur activité biochimique et identifier leur substrat lipidique. De plus, il faudrait déterminer si ces enzymes sont responsables de la synthèse d'espèces lipidiques minoritaires, ou si elles jouent un rôle dans des réponses spécifiques au stress. En effet, des études transcriptomiques suggèrent que certains de ces gènes codant pour des enzymes de fonction inconnue seraient régulés en réponse au stress, par exemple par la réponse stringente ou par RpoS (Traxler *et al.*, 2008).

Un exemple est YbhO, la cardiolipine synthase 2, qui possède comme Cls et PssA les deux motifs HKD caractéristiques de la superfamille des phospholipases D (Pfam PF00614) (Guo & Tropp, 2000). YbhO catalyse la formation de CL *in vitro*, mais pas *in vivo* (Guo & Tropp, 2000 ; Quigley & Tropp, 2009), suggérant un autre rôle physiologique pour YbhO. De manière intéressante, il a été trouvé dans une étude de transcriptome que l'expression du gène

ybhO est activée par le ppGpp (Traxler *et al.*, 2008). Cela suggère que *ybhO* serait impliqué dans le métabolisme des phospholipides durant la réponse stringente. YbhO n'a pas été incluse dans notre étude dans laquelle nous nous sommes concentrées sur la voie de biosynthèse établie des phospholipides. Il reste donc à vérifier si l'expression de *ybhO* varie avec le taux de croissance et le ppGpp. Une fonction possible de YbhO pourrait être de produire un lipide à présent inconnu important en réponse au stress. Plus simplement, l'activation de *ybhO* pourrait être responsable de l'augmentation en proportion de la CL dans la membrane en phase stationnaire (Hiraoka *et al.*, 1993) tandis que l'expression du gène *cls* serait constitutive. La CL est importante pour la survie de la cellule (Hiraoka *et al.*, 1993) et pour des localisations membranaires de certaines protéines (Romantsov *et al.*, 2008 ; Romantsov *et al.*, 2010). Il faudrait donc tester le phénotype d'un mutant Δ*ybhO* pour la survie en phase stationnaire.

Pour une autre protéine de fonction inconnue, YihG, il a été proposé que l'expression du gène *yihG* est induite par le facteur sigma alternatif RpoS en phase stationnaire (Mohanty & Kushner, 1999). Cela suggère un rôle de YihG en réponse au stress. YihG possède un domaine acyltransférase homologue à ceux de PlsC et PlsB (Pfam 01553) et des résultats obtenus au laboratoire indiquent que YihG est une acyltransférase du type PlsC (Bouveret *et al.*, non-publié). Il nous reste à trouver précisément dans quelles conditions l'expression est induite et quelle fonction YihG possède dans la cellule. YihG pourrait catalyser la réaction de PlsC en phase stationnaire quand l'expression de *plsC* est réprimée. Alternativement, YihG pourrait catalyser une acylation acceptant des substrats différents de ceux de PlsC. Là encore, la solution pourrait provenir de l'identification des conditions dans lesquelles un mutant Δ*yihG* serait affecté, afin d'obtenir des indications sur son rôle physiologique.

Finalement, certains gènes codants pour des protéines de fonction totalement inconnue sont exprimés en opéron avec des gènes de synthèse des phospholipides. Il serait important de savoir si ces gènes sont directement impliqués dans le métabolisme des lipides, et quels sont leurs rôles. Est-ce qu'ils participent aux activités enzymatiques ou bien ont-ils un rôle dans la régulation ? Nous nous sommes intéressées pendant ma thèse au gène *yciU* qui serait en opéron avec *cls*, et au gène *yjeP*, qui est en opéron avec *psd* (Rhodius *et al.*, 2006). Pour étudier YciU et YjeP, plusieurs approches sont envisageables. Tout d'abord, il faut vérifier leur co-expression avec *cls* et *psd*, et étudier leur régulation. En ce sens, nous avons confirmé la co-régulation par RpoE de *yjeP* avec *psd*. *yjeP* code pour une protéine homologue à des canaux mécanosensitifs. Chez *Erwinia chrysanthemi*, le gène *bspA*, qui est homologue à *yjeP* et situé en aval de *psd*, code pour une protéine qui joue un rôle dans l'osmoprotection de la

cellule (Touzé *et al.,* 2001). Mais chez *E. coli*, YjeP semble avoir une autre fonction et son rôle (en connexion avec Psd) reste mystérieux. Ensuite, on pourrait tester si les protéines YciU et YjeP interagissent avec des enzymes de la synthèse des phospholipides, en particulier Cls et Psd. Nous avons effectué quelques tests par BACTH, malheureusement sans succès. La technique v-TAP pourrait être envisagées, ou la technique TAP simple dans le cas de YciU qui est prédite pour être une protéine soluble. Enfin, on pourra tester si les gènes *yciU* et *yjeP* ont un effet sur le métabolisme des phospholipides en testant l'effet de leur surexpression ou au contraire de leur délétion. Là encore, il est important de pouvoir identifier des conditions où les mutants ont un phénotype.

En conclusion, ces études préliminaires indiquent que certaines protéines de fonction inconnue homologues aux enzymes de synthèse des phopholipides pourraient avoir des rôles à jouer dans des réponses au stress. Ceci n'est qu'un aperçu (figure 24 qui présente les homologues dans *E. coli*) et suggère que l'étude de la biosynthèse des phospholipides chez les bactéries peut encore révéler de nombreux secrets.

MATERIALS & METHODS

I. RECOMBINATION ON THE CHROMOSOME OF *E.COLI* BY THE λRED METHOD

In order to delete genes or to insert tags, such as TAP, SPA or fluorescent proteins, at the 3′ end of genes on the *E. coli* chromosome we used he λRed system [Datensko & Wanner, 2000] (figure 111). The λRed genes (*γ*, *β*, *exo*), which are over-expressed from a thermosensitive plasmid (pKD46), promote a greatly enhanced rate of recombination in any *E. coli* strain.

First, the oligonucleotides need to be designed that amplify the cassette and contain 45 bp on both extremities homologous to the region of insertion on the chromosome.

In the case of TAP, SPA, CBP-EGFP, -EYFP, -mRFP, and -Rluc cassettes, the primer pairs are as follows:

• FW: 5'-[45 bp before stop] + TCCATGGAAAAGAGAAG-3'

• RV: 5'-[complement-reverse of 45 bp after stop] + CATATGAATATCCTCCTTAG-3'

• without the CBP cassette FW: 5'-[45 bp before stop] + ATTCCAACTACTGCTAGC-3'

In this case, plasmids pJL72 (TAP), pJL148 (SPA), p(CBP)EGFP::*kana*^{R}, p(CBP)EYFP::*kana*^{R}, p(CBP)ECFP::*kana*^{R}, p(CBP)mRFP::*kana*^{R}, and p(CBP)Rluc::*kana*^{R} can be used as a matrix containing the tag of interest and the cassette FRT-Kana^R-FRT (table 1).

In the case of a gene deletion, the primer pairs are as follows:

VFTF: 5'- [45 pb before the stop] + ATTCCGGGGATCCGTCGACC-3'

VRTR: 5'-[complement reverse of 45pb after the stop] + TGTAGGCTGGAGCTGCTTCG-3'

In this case, the plasmid pKD13 (pEB270) (Datsenko & Wanner, 2000) is used as a matrix containing the cassette FRT-Kana^R-FRT (table 1).

The oligonucleotides were ordered at Eurogentec with HPLC-RP purification to ensure full length. The amplification is performed with a high fidelity DNA polymerase. The matrix is either a plasmid (figure 111) or a colony from a strain already containing the cassette in the chromosome.

The PCR product is purified using the Purification kit Qiagen and eluted in 50 µl water. This elution is digested by 0.5µl DpnI in buffer 4 1X adjusted (this step is not necessary when the amplification was done on a colony of an already existing strain). The PCR product is then again purified with the Qiagen kit and eluted in a minimum of water (25 µl).

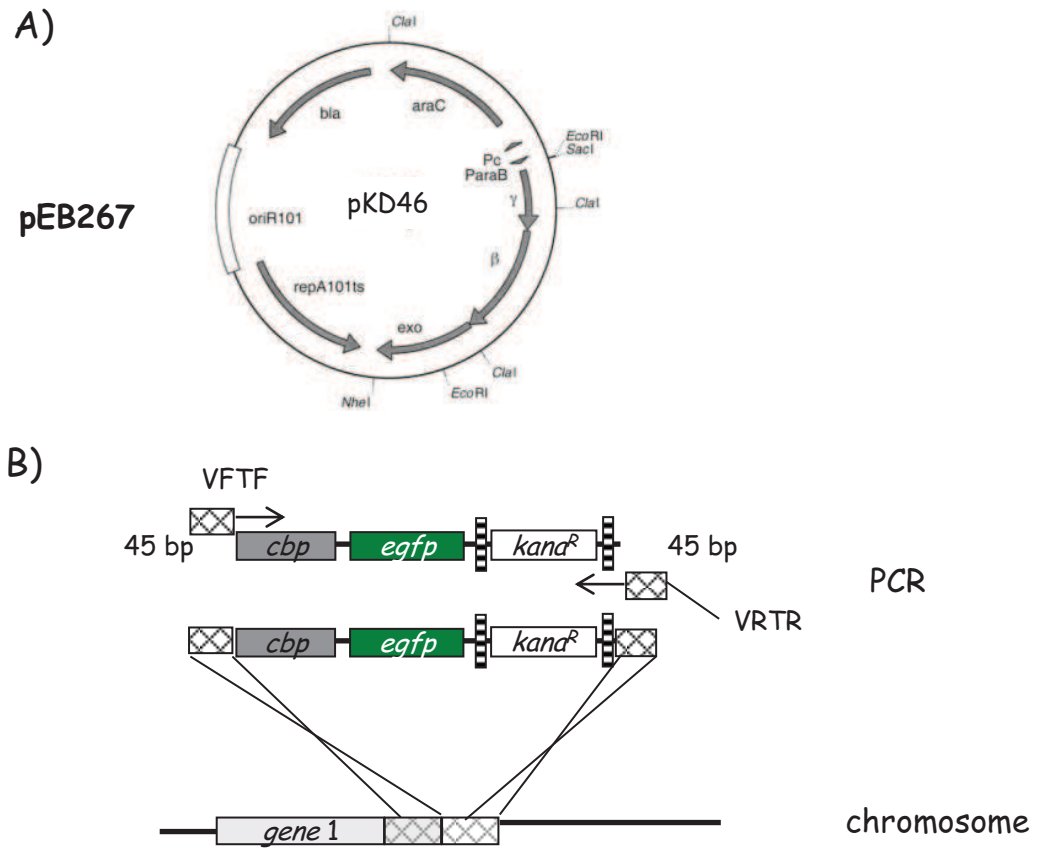

Figure 111: Chromosomal tagging with the λRed system in *E. coli*. **A)** Map of plasmid pKD46: Red recombinase expression plasmids that includes 2,154 nt (31088–33241) of phage λ (GenBank accession no. J02459). **B)** Transformation by electroporation of BW25113 strain expressing λRed recombinase (pKD46, ts) with a PCR product. The hatched boxes indicate regions of homology. VFTF: forward primer; VRTR: reverse primer.

Electrocompetent cells of BW25113 transformed with pKD46 (ts) (pEB267) are prepared by diluting 100 times a starter culture (30 °C) from an isolated colony in 100 ml of LB supplemented with ampicillin. This culture is then incubated at 30°C till it reaches an OD_{600nm} = 0,2. The production of the λRed proteins is induced with 0,2% arabinose. When the culture reaches an OD_{600nm} = 1, it is placed on ice/water during 10 minutes. The whole preparation is done from now on in the cold room and with cold material (4 °C). The cells are centrifuged for 10 minutes at 4000 rpm at 4°C, resuspended in 50 ml of icecold water and centrifuged again. This procedure is repeated 2 times. After the last centrifugation step, the pellet is resuspended in 10 ml icecold water with 10% glycerol and centrifuged a last time. The cells are aliquoted by 60 µl and can be stocked at -80°C, but it is better to use freshly prepared cells.

60 µl of electrocompetent cells are transformed by electroporation with 1 to 100ng of the PCR product (ca. 5µl) using the Biorad Micro Pulser™ with cuvettes of 2 mm and standard bacteria settings. Immediately after the electroporation 1 ml of LB preheated at 37 °C is added and the cells are regenerated for at least 1 h at 37 °C. Half of the cells are then plated on LB supplemented with kanamycin (25 µg/ml), the other half is left at RT for plating after overnight. The LB plates are incubated 24 h at 37°C. Colonies are restriked on LB supplemented with kanamycine at 37°C for 24 h. Isolated colonies are replicated on LB supplemented with ampicillin (100 µg/mL) or kanamycine (25 µg/mL) to select for clones that are $Kana^R$ (cassette insertion) and Amp^S (lost pKD46 plasmid).

The correct deletion of a gene by insertion of the FRT-$Kana^R$-FRT cassette is verified by PCR on colony (primer pair: 5' ORF and Ebm283 (in the $Kana^R$ cassette); or 3' ORF and Ebm282 (in the $Kana^R$ cassette). The correct insertion of a cassette on the chromosome is verified by PCR on colony (primer pair: 5' ORF and Ebm25 (in CBP tag); or 3' ORF and Ebm282 (in the $Kana^R$ cassette)). Additionally, the production of the tagged protein can be checked by Western blot (PAP, anti-Flag, anti-GFP) and/or with fluorescent techniques (TECAN; microscope).

To work in a "clean" strain, that is a strain of a known genetic background, one should transduce the construction in an *E. coli* wild type strain (W3110, MG1655) (cf. II). After transduction, the kanamycine cassette can be removed by transforming the strain with the pCP20 (pEB266) or pEB220 plasmids that contain a flipase recognizing the FRT sites. The transformation is performed at 30°C and the cells are plated on LB supplemented with ampicillin. The strain is cured from the plasmid by isolating clones and growing them overnight on LB plates at 37°C. Some clones are then replicated on three plates, successively

kanamycine, ampicillin, and LB, in order to select clones that are Amp^S and $Kana^S$. They are verified by PCR on colony.

II. PHAGE P1 TRANSDUCTION

The transduction by phage P1 permits to transfer chromosomal DNA (approx. 100 kb) from one strain to another (Miller, 1972). Then, a screen for a marker, such as a mutation, an antibiotic resistance, or a phenotype selects for the desired recombination event. In our case, the goal was to transduce tagged or deleted genes (with a kanamycine resistance marker) from one strain to a strain with a clean genetic background or to combine two different cassettes in one cell.

Lysate preparation:

An overnight culture of the donor strain is diluted 1:100 in 3 mL of fresh LB supplemented with 5 mM $CaCl_2$ and appropriate antibiotic. The culture is grown with aeration at 37 ˚C till it reaches an OD=0,5. 100 µL of a wild type P1 phage lysate are added to the culture which is incubated at 37 ˚C for 1–3 hrs until the culture has lysed completely. Then, 300 µL of chloroform are added to the lysate and vortexed. The debris is centrifuged (6,000 rpm, 10 min) and the supernatant is transfered to a fresh tube. 20 µL of chloroform are added to the lysate that can be stored at 4 ˚C.

Titration:

A culture of a wild type strain (MG1655) grown overnight in LB medium is diluted 1:100 in 3 mL fresh LB medium supplemented with 5 mM $CaCl_2$. The culture is grown with aeration at 37 ˚C till it reaches an OD=0,2-0,5. A cascade dilution of the lysate is prepared between 10^{-1} and 10^{-9}. 100 µL of dilutions 10^{-4} till 10^{-9} are then mixed with 100 µL of the MG1655 culture, which is incubated for 15 min at 37 °C. 3 mL of soft agar are added to the lysate/culture mix and plated on LB plates, which are incubated overnight at 37 °C. The next day the titer of the lysate is determined that should be: phage forming unit/mL between 10^{-8} and 10^{-10}.

Transduction:

An overnight culture of the recipient strain grown in LB medium is diluted 1:100 in 3 mL fresh LB medium supplemented with 5 mM $CaCl_2$. The culture is grown with aeration at 37˚C till it reaches an OD=1. Different MOI (in general from 0,1 till 0,5) are then set up of the culture with the lysate. The tubes are incubated at 37 ˚C for 15-20 min without shaking. Then, 1 mL LB supplemented with 5mM citrate is added and incubated at 37 ˚C for 1 hr with shaking to allow expression of the antibiotic resistance marker. The cells are harvested by centrifugation at 5,000 rpm for 5 min and washed with LB supplemented with 5 mM citrate (pH 5.5). Finally, the cells are resuspended in 100 µL LB supplemented with 5 mM citrate and plated on a LB plate supplemented with kanamycine (25 µg/mL) and 2 mM citrate, which is incubated overnight at 37 °C. The colonies are re-isolated on a LB plate supplemented with

kanamycin (25 µg/mL) and 2 mM citrate (pH 5.5) and incubate overnight at 37 °C. When possible, the correct acquisition of the allele is verified by PCR on colony.

A)

pEB227

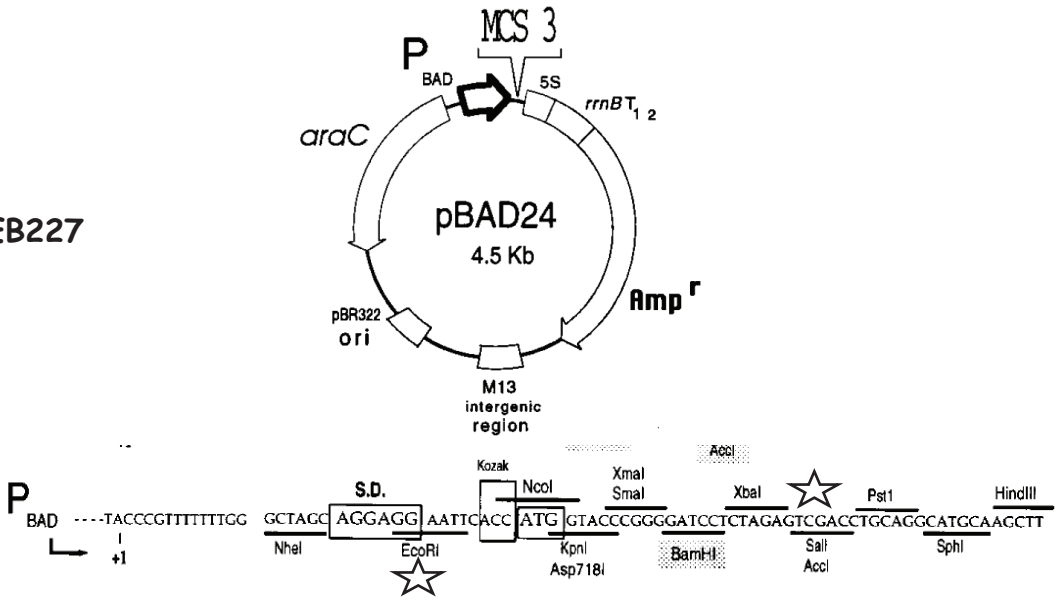

B)

pEB1188

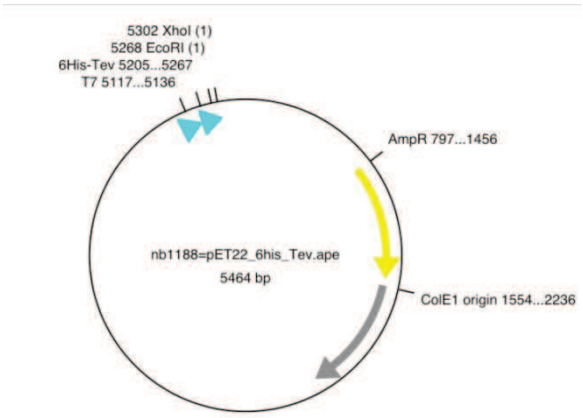

Figure 112: Maps of plasmids pBAD24 and pET22-6his-tev. A) Map of the overexpression plasmid pBAD24 (Guzman *et al.*, 1995). The plasmid contains a with arabinose inducible P_{BAD} promoter and an ampicillin resistance (*amp*^{R}) gene. **B)** Map of the overexpression plasmid pET22-6his-tev. The plasmid contains a with IPTG inducible T7 promoter and an ampicillin resistance (*amp*^{R}) gene. Arrows in the circular plasmid indicate the direction of transcription.

III. PLASMID AND STRAIN CONSTRUCTIONS

Name	Lab code[a]	Relevant characteristics[a], primers used for construction	Reference
pCP20	pEB266	ts, Cm^R, Amp^R, FLP recombinase gene to remove *kana*^{R} cassette	Cherepanov & Wackernagel (1995)
pKD46	pEB267	ts, Amp^R, recombination requires the phage lambda Red recombinase	Datsenko & Wanner (2000)
pJL72	pEB793	Amp^R, Km^R, TAP-$Kana^R$	Zeghouf et al. (2003)
pJL148	pEB794	Amp^R, Km^R, TAP-$Kana^R$	Zeghouf et al. (2003)
pBAD-NtermTAPlinker	pEB587		Battesti & Bouveret (2008)
pBAD24	pEB227	Amp^R, ColE1 replication origin, P_{BAD} promotor; cloning usually: PCR (EcoRI/XhoI) in pBAD24 (EcoRI/SalI)	Guzman et al. (1995)
pBAD-*ymcE*	pEB1111	ebm421/422	this work
pBAD-*gnsA*	pEB1112	ebm423/424	this work
pBAD-*rpoE*	pEB1102	ebm399/400	this work
pBAD-*rseAB*	pEB1204	ebm588/589	this work
pBAD-*basR*	pEB1149	ebm516/517	this work
pBAD-*basR53*	pEB1165	ebm542/543on pEB1149; mutation Gly53Val	this work
pBAD-*basS*	pEB1195	ebm582/583	this work
pBAD-*basS**	pEB1276	ebm582/583 on strain EB652 (D312N)	this work
pBAD-d*cuR*	pEB1150	ebm519/520	this work
pBAD-*dcuS*	pEB1203	ebm551/552	this work
pBAD-*yedW*	pEB1181	ebm549/550	this work
pBAD-*yjeP*	pEB1148	ebm506/507	this work
pET6hisTev	pEB1188	Amp^R, F1 replication origin, T7 promotor; cloning usually: PCR (EcoRI/XhoI) in pET6hisTev (EcoRI/XhoI)	this work
pET6hisTev-*basR*	pEB1189	ebm516/517	this work
pET6hisTev-*basR53*	pEB1192	ebm542/543 on pEB1189	this work
pET6hisTev-*dcuR*	pEB1190	ebm519/520	this work
pET6his-*tev*$^+$	pEB570		Séraphin's laboratory
p(CBP)EGFP::*kana*^{R}	pEB857	ebm328/329 (EcoRV/NheI) in pJL72 (EcoRV/NheI)	this work
p(CBP)EYFP::*kana*^{R}	pEB1008	ebm328/329 (EcoRV/NheI) in pJL72 (EcoRV/NheI)	this work
p(CBP)ECFP::*kana*^{R}	pEB1009	ebm328/329 (EcoRV/NheI) in pJL72 (EcoRV/NheI)	this work
p(CBP)mRFP::*kana*^{R}	pEB1050	ebm 376/377 (EcoRV/NheI) in pJL72 (EcoRV/NheI)	this work

A)

pEB898

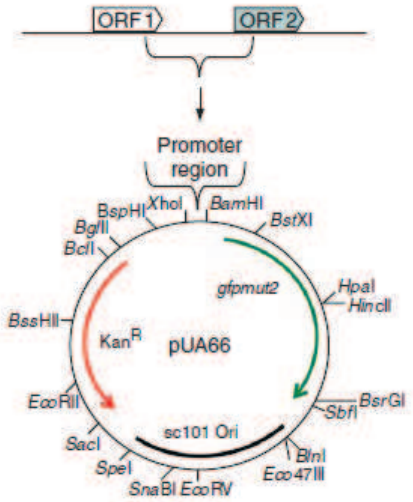

B)

pEB1121

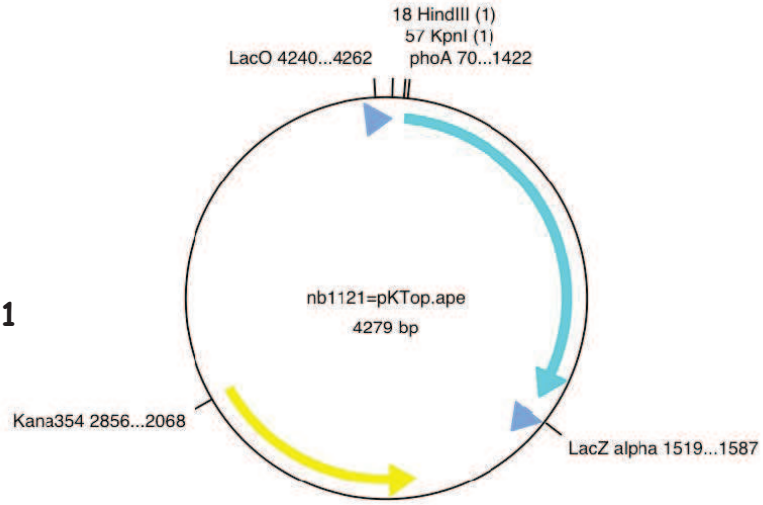

Figure 113: Maps of plasmids pUA66 and pKTOP. A) Map of the low copy plasmid pUA66 (Zaslaver *et al.*, 2007). The plasmid contains a kanamycin resistance gene (*kana*^{R}) and a fast folding *gfpmut*2 gene as a reporter gene with a strong ribosome binding site. The second plasmid, pUA139 (not shown), is similar to pUA66, except that the restriction sites are switched. **B)** Map of plasmid pKTOP expressing a dual reporter PhoA22-472/LacZ4-60 (Karimova *et al.*, 2009). The plasmid contains a with IPTG inducible *lac* promoter and a kanamycin resistance (*kana*^{R}) gene. ori, origin of replication. Arrows in the circular plasmid indicate the direction of transcription.

p(CBP)Rluc::*kana*^{R}	pEB1082	ebm 395/396 (EcoRV/NheI) in pJL72 (EcoRV/NheI)	this work
pUA66	pEB898	Kana^R, transcriptional GFP fusion, cloning usually: PCR (BamHI/XhoI) in pUA66 (BamHI/XhoI)	Zaslaver et al. (2006)
pUA139	pEB987	As pUA66, but cloning usually: PCR (XhoI /BamHI) in pUA139 (XhoI/BamHI)	Zaslaver et al. (2006)
pUA66-*dgkA*	-		Zaslaver et al. (2006)
pUA66-*psd*2	pEB1120	Ebm435/436	this work
pUA66-*pssA*	pEB1114	ebm427/428	this work
pUA66-*dgkA*2	pEB1115	ebm431/432	this work
pUA66-*dgkA*mut*P_{rpoE}	pEB1117	ebm433/434 on pUA66-*dgkA*	this work
pUA66-*dgkA*2mut*P_{rpoE}	pEB1158	ebm433/434 on pEB1115	this work
pUA66-*dgkA*2mut#1	pEB1166	mutation mut#1 in the BasR consensus motif	this work
pUA66-*dgkA*bis*#1	pEB1167	mutations in the RpoE and BasR consensus motifs	this work
pUA66-*dgkA*2mut#2	pEB1174	ebm547/548 on pEB1115	this work
pUA66-*dgkA2*mutT	pEB1176	ebm545/546 on pEB1115	this work
pUA66-*dgkA*3	pEB1171	ebm432/541	this work
pUA66-*dgkA*3mut#1	pEB1173	ebm432/541 on pEB1166	this work
pUA66-*dgkA*3mut#2	pEB1175	ebm547/548 on pEB1171	this work
pUA66-*dgkA*mutT	pEB1176	ebm545/546 on pEB1115	this work
pUA66-*dgkA*3mutT	pEB1177	ebm545/546 on pEB1171	this work
pUA66-*dgkA*3mutP2	pEB1208	ebm586/587 on pEB1171	this work
pUA66-*dgkA*4	pEB1241	ebm432/647	this work
pUA66-*dgkA*4mut#1	pEB1248	ebm432/541 on pEB1241	this work
pUA66-*dgkA*4mut#2	pEB1249	ebm547/548 on pEB1171	this work
pUA66-*dgkA*4mutT	pEB1250	ebm545/546 on pEB1171	this work
pUA139-*plsB*	-		Zaslaver et al. (2006)
pUA139-*plsB*mut* P_{rpoE}	pEB1116	Point mutation in the RpoE consensus motif	this work
pUA139-*plsB*Δ	pEB1172	ebm432/541	this work
pUA139-P*plsB*ΔmutP2	pEB1200	ebm586/587 on pEB1172	this work
pUA139-*plsB*mutP2	pEB1201	ebm586/587 on pUA139-*plsB*	this work
pUA66-*rpoE*	-		Zaslaver et al. (2006)
pUA66-*pmrH*	-		Zaslaver et al. (2006)
pUA66-*eptA*2	pEB1244	ebm648/649	This work
pKTop	pEB1121	dual reporter PhoA22-472/LacZ4-60, p15 replication origin, Kana^R ;	Karimova et al. (2009)

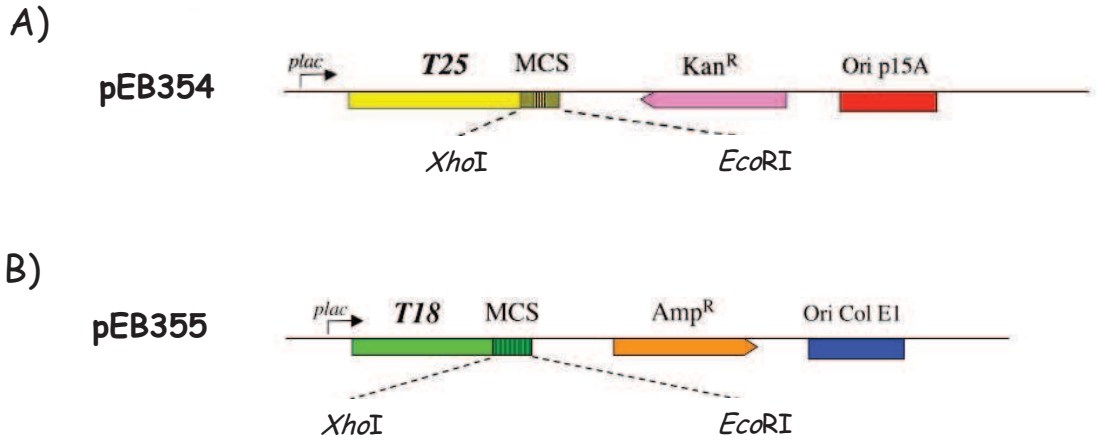

Figure 114: Maps of plasmids pKT25linker (pEB354) and pUT18Clinker (pEB355) (Gully *et al.*, 2006). **A)** Map of the low copy plasmid pKT25linker. pKT25 encodes the T25 fragment (corresponding to the first 224 amino acids of CyaA) that is expressed under the transcriptional control of a lac promoter. The plasmid contains a with IPTG inducible *lac* promoter and a kanamycin resistance (*kana*^{R}) gene. **B)** Map of the high copy plasmid pUT18linker. The plasmid contains an ampicillin resistance (*amp*^{R}) gene and encodes the T18 fragment (amino acids 225 to 399 of CyaA) that is expressed under the transcriptional control of a lac promoter. These plasmids are designed to express chimeric proteins in which a heterologous polypeptide is fused to the N-terminal end of T18. Ori: origin of replication.

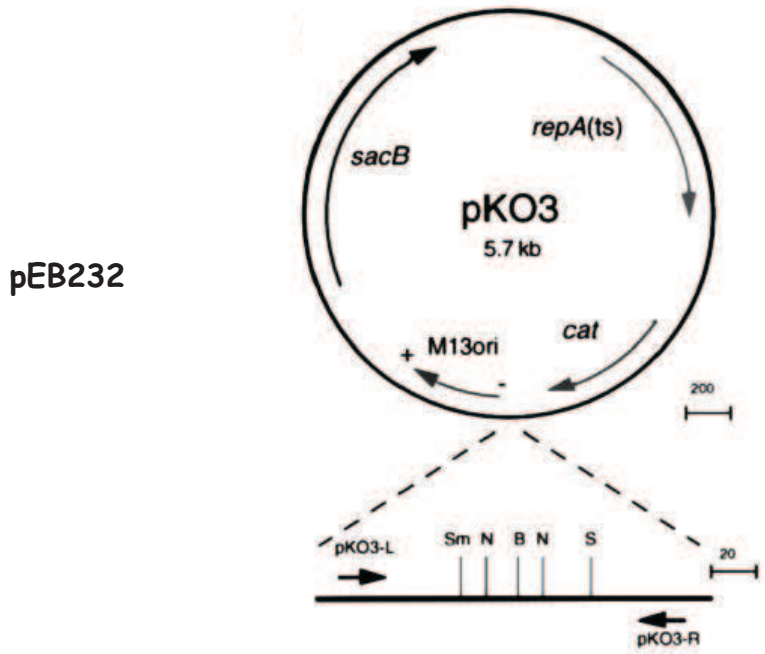

Figure 115: Map of plasmids pKO3 (Link & Church, 1997). Map of the "suicide" plasmid pKO3, which is used for clean gene deletions. It contains a counterselectable *sacB* marker that is used to select for loss of plasmid sequences after excision from the chromosome. The cloning region is enlarged. Arrows in the circular plasmid indicate the direction of transcription and the direction of M13 replication. The arrows in the enlarged region are the DNA primer sites. Unique restriction sites are shown (B, *BamH*I; N, *NotI*; S, *Sal*I; Sm, *Sma*I). ori, origin of replication.

		cloning usually: PCR (HindIII/KpnI) in pKTop (HindIII/KpnI)	
pKTop-*pgsA*	pEB1182	ebm473/479 (full length protein)	this work
pKTop-*pgsA*37	pEB1277	ebm473/474	this work
pKTop-*pgsA*61	pEB1278	ebm473/475	this work
pKTop-*pgsA*85	pEB1279	ebm473/476	this work
pKTop-*pgsA*107	pEB1280	ebm473/477	this work
pKTop-*pgsA*146	pEB1281	ebm473/478	this work
pKTop-*pgsA*50	pEB1283	ebm473/485	this work
pKTop-*pgsA*127	pEB1284	ebm473/486	this work
pKTop-*pgsA*166	pEB1285	ebm473/487	this work
pKTop-*plsC*	pEB1125	ebm453/454 (full length protein)	this work
pKTop-*plsC*30	pEB1286	ebm453/459	this work
pKTop-*plsC*123	pEB1287	ebm453/460	this work
pKTop-*plsC*185	pEB1127	ebm453/461	this work
pKTop-*plsC*70	pEB1289	ebm453/462	this work
pKTop-*plsC*210	pEB1290	ebm453/463	this work
pSC-*kana*P_{BAD}	pEB1124		this work
pSC-*kana*P_{BAD}-*egfp*	pEB1129	ebm470/471 in pEB1124 (BsrGI/HindIII)	this work
pUT18Clinker	pEB355	Amp^R, N-terminal fusion of a given protein with T18 fragment, ColE1 replication origin; cloning usually: PCR (EcoRI/XhoI) in pUT18linker (EcoRI/XhoI)	Gully et al. (2006)
pUT18linker-*plsB*	pEB621	ebm125/126	Gully et al., unpublished
pUT18linker-Ntr*plsB*	pEB689	ebm125/150 (N-terminal residues 1 to 279)	Gully et al., unpublished
pUT18linker-Ctr*plsB*	pEB691	ebm126/151 (C-terminal residues 280 to 807)	Gully et al., unpublished
pUT18linker-*dgkA*	pEB954	ebm298/299	Gully et al., unpublished
pUT18linker-*yciU*	pEB1152	ebm523/524	this work
pUT18Clinker-*cls*	pEB1178	ebm521/522	this work
pUT18linker-*acp*	pEB379	ebm76/77	Gully et al. (unpublished)
pKT25linker	pEB354	N-terminal fusion of a given protein with T25 fragment, p15 replication origin, $Kana^R$; cloning usually: PCR (EcoRI/XhoI) in pUT18linker (EcoRI/XhoI)	Gully et al. (2006)
pKT25linker-*plsB*	pEB622	ebm125/126	Gully et al., unpublished
pKT25linker-Ntr*plsB*	pEB690	ebm125/150 (N-terminal residues 1 to 279)	Gully et al., unpublished
pKT25linker-Ctr*plsB*	pEB692	ebm126/151 (C-terminal residues 280 to 807)	Gully et al., unpublished
pKT25linker-*dgkA*	pEB952	ebm298/299	Gully et al., unpublished
pKT25linker-*yciU*	pEB1151	ebm523/524	this work

pKT25linker-*cls*	pEB1180	ebm521/522	this work
pKO3	pEB232	Cat^R – ori (ts) – *sacB*; cloning usually: PCR (BamHI/SalI) in pKO3 (BamHI/SalI)	Link & Church (1997)
pKO3-*plsBdgkA*	pEB1207	ebm592/593	this work
pKO3-*plsBdgkA*mut#1	pEB1264	ebm592/593	this work
pKO3-*plsBdgkA*mut*P_{rpoE}	pEB1265	ebm592/593	this work
pKO3-*plsBdgkA*mut*P2	pEB1266	ebm592/593	this work
pKO3-*plsBdgkA*mut#2	pEB1267	ebm592/593	this work
pKO3-*plsBdgkA*mutT	pEB1268	ebm592/593	this work

Table 1: Plasmids. ts : thermosensitive. [a]: Lab codes correspond to our stock numbering. [b]: the characteristics are given only for the vectors or the reference plasmids.

Name	Relevant characteristics	Reference
BW25113	rrnB3 ΔlacZ4787 hsdR514 Δ(araBAD) Δ(rhaBAD)568 rph-1	Datsenko & Wanner (2000)
EB241	BW25113 Δ*dgkA::kana*^{R}	Baba et al. (2006)
EB261	BW25113 *pgsA*-tap::*kana*^{R}; VFTF/VRTR	this work
EB262	BW25113 *pgsA*-cbp-egfp::*kana*^{R}; VFTF/VRTR	this work
EB275	BW25113 *acp*-tap::*kana*^{R}; ebm344/345	this work
EB276	BW25113 *acp*-cbp-egfp::*kana*^{R}; ebm344/345	this work
EB278	BW25113 *plsB*-tap::*kana*^{R}; ebm264/265	this work
EB293	BW25113 *plsB*-cbp-eyfp::*kana*^{R}; ebm264/265	this work
EB322	BW25113 *acp*-cbp-eyfp::*kana*^{R}; ebm344/345	this work
EB356	BW25113 *dgkA*-spa*::kana*^{R}; ebm397/398	this work
EB357	BW25113 *dgkA*-tap*::kana*^{R}; ebm397/398	this work
EB361	BW25113 *pgsA*-cbp-mrfp::*kana*^{R}; VFTF/VRTR	this work
EB363	BW25113 *acp*-cbp-mrfp::*kana*^{R}; ebm344/345	this work
EB373	BW25113 *pgsA*-cbp-rluc::*kana*^{R}; VFTF/VRTR	this work
EB378	BW25113 *dgkA*-protA*::kana*^{R}; ebm397/409	this work
EB379	BW25113 *dgkA*-flag*::kana*^{R}; ebm397/409	this work
EB384	BW25113 *acp*-cbp-rluc::*kana*^{R}; ebm344/345	this work
EB389	BW25113 *plsB*-cbp-mrfp::*kana*^{R}; ebm264/265	this work
EB391	BW25113 *plsY*-cbp-egfp::*kana*^{R}; ebm334/335	this work

EB394	BW25113 *plsY*-cbp-mrfp::*kana*^{R}; ebm334/335	this work
EB396	BW25113 *plsX*-cbp-rluc::*kana*^{R}; ebm255/256	this work
EB398	BW25113 *plsX*-cbp-eyfp::*kana*^{R}; ebm255/256	this work
EB402	BW25113 *plsX*-cbp-egfp::*kana*^{R}; ebm255/256	this work
EB405	BW25113 *plsB*-cbp-rluc::*kana*^{R}; ebm264/265	this work
EB422	BW25113 *plsY*-cbp-rluc::*kana*^{R}; ebm334/335	this work
EB427	BW25113 Δ*basS::kana*^{R}	Baba et al. (2006)
EB428	BW25113 Δ*basR::kana*^{R}	Baba et al. (2006)
EB430	BW25113 Δ*basS*°- pCP20	this work
EB431	BW25113 Δ*basR*°- pCP20	this work
EB440	BW25113 Δ*dcuR::kana*^{R}	Baba et al. (2006)
EB441	BW25113 Δ*dcuS::kana*^{R}	Baba et al. (2006)
EB493	BW25113 *plsB*-cbp-egfp::*kana*^{R}; ebm264/265	this work
EB498	BW25113 *psd*-cbp-mrfp::*kana*^{R}; ebm447/448	this work
EB515	BW25113 *psd*-egfp::*kana*^{R}; ebm447/472	this work
EB518	BW25113 *pssA*-cbp-mrfp::*kana*^{R}; ebm425/426	this work
EB519	BW25113 *yjeP*-cbp-egfp::*kana*^{R}; ebm488/489	this work
EB536	BW25113 P_{BAD}-*kana*^{R}::egfp-*dgkA*; ebm490/494	this work
EB537	BW25113 °egfp-*dgkA* – pCP20	this work
EB126	BW25113 Δ*relA::kana*^{R}	Baba et al. (2006)
EB146	W3110 Δ*relA::kana*$^{R\,-}$ P1 transduction of EB126 in W3110	this work
EB132	BW25113 Δ*dksA::kana*^{R}	Baba et al. (2006)
W3110	F- LAM-IN(rrnD-rrnE)1 rph-1	Bachmann (1987)
EB182	W3110 *plsC*-cbp-rluc:: *kana*^{R}; shuffling technique ebm415/416	Wahl et al. (2009)
EB258	W3110 *plsY*-tap:: *kana*^{R}; ebm334/335	this work
EB263	W3110 *pgsA*-tap::*kana*^{R}- P1 transduction of EB261 in W3110	this work
EB264	W3110 *pgsA*-cbp-egfp::*kana*^{R}- P1 transduction of EB262 in W3110	this work
EB265	W3110 *pgsA*-tap° - pCP20	this work
EB271	W3110 *pgsA*-cbp-egfp° - pCP20	this work
EB286	W3110 *plsB*-tap::*kana*^{R}- P1 transduction of EB278 in W3110	this work
EB300	W3110 *plsB*-cbp-eyfp:: *kana*^{R} – P1 transduction of EB286 in W3110	Wahl et al. (2009)
EB342	W3110 *acp*-cbp-egfp::*kana*^{R} – P1 transduction of EB322 in W3110	Wahl et al. (2009)
EB344	W3110 *acp*-cbp-eyfp::*kana*^{R}; - P1 transduction of EB322 in W3110	Wahl et al. (2009)
EB345	W3110 *acp*-cbp-eyfp° - pCP20	this work
EB358	W3110 *dgkA*-spa*::kana*^{R}- P1 transduction of EB356 in W3110	this work

EB359	W3110 *dgkA*-tap*::kana*^{R}- P1 transduction of EB357 in W3110	this work
EB360	W3110 *acp*-cbp-eyfp°/ *pgsA*-cbp-egfp::*kana*^{R}- P1 transduction of EB262 in EB345	this work
EB362	W3110 *pgsA*-cbp-mrfp::*kana*^{R}- P1 transduction of EB361 in W3110	Wahl et al. (2009)
EB364	W3110 *acp*-cbp-mrfp::*kana*^{R} – P1 transduction of EB363 in W3110	this work
EB367	W3110 p*lsB*-TAP° - pCP20	this work
EB368	W3110 *acp*-cbp-mrfp° – pCP20	this work
EB371	W3110 *acp*-cbp-mrfp°/*pgsA*-cbp-egfp::*kana*^{R} – P1 transduction of EB262 in W3110	this work
EB376	W3110 *pgsA*-cbp-rluc::*kana*^{R}- P1 transduction of EB373 in W3110	this work
EB382	W3110 *plsB*-cbp-eyfp°- pCP20	this work
EB388	W3110 *dgkA*-ProtA:: *kana*^{R}- P1 transduction of EB378 in W3110	this work
EB392	W3110 *acp*-cbp-rluc::*kana*^{R}- P1 transduction of EB384 in W3110	Wahl et al. (2009)
EB393	W3110 *plsB*-cbp-mrfp::*kana*^{R}- P1 transduction of EB389 in W3110	this work
EB395	W3110 *dgkA*-ProtA°- pCP20	this work
EB399	W3110 *plsY*-cbp-egfp::*kana*^{R}- P1 transduction of EB391 in W3110	this work
EB381	W3110 *dgkA*-Flag:: *kana*^{R}-	this work
EB401	W3110 *dgkA*-Flag°- pCP20	this work
EB403	W3110 *plsX*-cbp-eyfp::*kana*^{R}- P1 transduction of EB398 in W3110	this work
EB407	W3110 *acp*-cbp-rluc° - pCP20	this work
EB409	W3110 *plsB*-cbp-mrfp° - pCP20	this work
EB410	W3110 *plsB*-cbp-rluc::*kana*^{R} – P1 transduction of EB405 in W3110	Wahl et al. (2009)
EB411	W3110 *plsY*-cbp-rluc::*kana*^{R} – P1 transduction of EB422 in W3110	this work
EB414	W3110 *plsY*-cbp-egfp° - pCP20	this work
EB416	W3110 *plsC*-cbp-ecfp:: *kana*^{R}; shuffling technique ebm415/416	this work
EB417	W3110 *plsC*-cbp-egfp:: *kana*^{R}; shuffling technique ebm415/416	Wahl et al. (2009)
EB418	W3110 *plsC*-cbp-eyfp:: *kana*^{R}; shuffling technique ebm415/416	this work
EB419	W3110 *plsX*-cbp-egfp:: *kana*^{R}- P1 transduction of EB402 in W3110	this work
EB431	W3110 Δ*basR::kana*^{R} - P1 transduction of EB428 in W3110	this work
EB495	W3110 *plsB*-cbp-egfp::*kana*^{R}- P1 transduction of EB493 in W3110	this work
EB497	W3110 *plsB*-cbp-egfp° - pCP20	this work
EB499	W3110 *psd*-cbp-mrfp::*kana*^{R} - P1 transduction of EB498 in W3110	this work
EB531	W3110 *psd*-egfp::*kana*^{R} - P1 transduction of EB515 in W3110	this work
EB523	W3110 *pssA*-cbp-mrfp::*kana*^{R}- P1 transduction of EB518 in W3110	this work
EB521	W3110 *yjeP*-cbp-egfp::*kana*^{R}- P1 transduction of EB519 in W3110	this work
EB566	W3110 *dgkA*-flag°/ Δ*basR*	this work

EB611	W3110 *dgkA*-protA°/mut#1; pKO3mut#1 on EB395	this work
EB612	W3110 *dgkA*-protA°/mut#2; pKO3mut#2 on EB395	this work
EB613	W3110 *plsB*-tap°/mutP_{rpoE}; pKO3mutP_{rpoE} on EB367	this work
EB625	W3110 *plsB*-tap°/mut*plsB*P2; pKO3mut *plsB*P2 on EB367	this work
MG1655	F- lambda- ilvG- rfb-50 rph-1	Bachmann (1996)
EB421	MG1655 ΔrelA°	this work
EB425	MG1655 Δ*relA*° *spoT*207 – transduction spoT207 (CF1693) in EB421	this work
EB559	MG1655 ΔdksA° - P1 transduction of EB132 in MG1655	this work
EB633	MG1655 Δ*basR*°- pCP20	this work
EB634	MG1655 Δ*basS*°- pCP20	this work

Table 2: *E. coli* K12 strains. The ° character after a strain name means that the kanamycin cassette has been removed using the pCP20 plasmid.

Lab code	Sequence 5' – 3'
Ebm125	GACA**GAATTC**ATGTCCGGCTGGCCACG
Ebm126	ACCG**CTCGAG**AAGCTTACCCTTCGCCCTGCGTCGC
Ebm150	ACCG**CTCGAG**AAGCTTAGAAATTCGCCGCAATCTC
Ebm151	CACC**GAATTC**TCTTACGAGATGATTCGC
Ebm255	agctggttttgagctgctggacggtggcaaaagcggaactctgcggTCCATGGAAAAGAGAAG
Ebm256	gttatataccgtcacttgcaaactgcgagttcgctggcagcgtcctgCATATGAATATCCTCCTTAG
Ebm264	ATGACTTTCTGCTATCCTTGCCGCGCATTTGCATTATTAACCAGattccggggatccgtcgacc
Ebm265	TTACCCTTCGCCCTGCGTCGCACTCTCAATCGTCAAACGCACGTtgtaggctggagctgcttcg
Ebm298	CACC**GAATTC**ATGGCCAATAATACCACTGGATTC
Ebm299	CTA**CTCGAGAAGC**TTATCCAAAATGCGACCATAACAG
Ebm332	TCAGACGTGCGTTTGACGATTGAGAGTGCGACGCAGGGCGAAGGGTCCATGGAAAAGAGAAG
Ebm333	AAGGCCGGATAAGGCGTTTTCGCCGCATCCGGCAATTCTCTCTGACATATGAATATCCTCCTTAG
Ebm344	ACCACCGTTCAGGCTGCCATTGATTACATCAACGGCCACCAGGCGTCCATGGAAAAGAGAAG
Ebm345	AaagataaaactcaggcggtcgaacgaccgcctggagatgttcacCATATGAATATCCTCCTTAG
Ebm397	GTCGCCGTGATTACCTGGTGCATTCTGTTATGGTCGCATTTTGGA**TCCATGGAAAAGAGAAG**
Ebm398	CATAAACTGCACAATAAACCAGAGATTTATCGAATTCTGGAAGGGCATATGAATATCCTCCTTA G
Ebm399	ACC**GAATTC**ATGAGCGAGCAGTTAACGGACC
Ebm400	ACG**CTCGAG**TCAACGCCTGATAAGCGGTTG
Ebm409	GTCGCCGTGATTACCTGGTGCATTCTGTTATGGTCGCATTTTGGAATTCCAACTACTGCTAGC
Ebm421	ACC**GAATTC**atgCGCCGCTGGATTTCAC

Ebm422	ACG**CTCGAG**TCAATATTCACTGTTAACCTCTTC
Ebm425	CGTTTGCGCCGTATCCGCATCGACCGATTAATTAGCCGCATCCTG**TCCATGGAAAAGAGAAG**
Ebm426	AACGTGGCCTCCAAAAAACAAACCCCGTACAGGACGGGGTTGTGA**CATATGAATATCCTCCTTAG**
Ebm427	ACC**CTCGAG**ATGGTGGCGCTAGCCCGCAAG
Ebm428	ACG**GGATCC**TCCAGCAGCGTCTCCCGGAAG
Ebm431	CG**GGATCC**TCGGGTGAATCCAGTGGT
Ebm432	CCG**CTCGAG**GACGAGAGGTATCCAGCCC
Ebm433	TTACATTATGAGCGTacgTATCAGTGTACCGTTA
Ebm434	TAACGGTACACTGATAcgtACGCTCATAATGTAA
Ebm435	CCG**CTCGAG**TCGGCTGTATCACTTCCCGC
Ebm436	CG**AGATCT**GCGAGTAAGCCATAGTTTCGGC
Ebm447	GAACACGACGCCAGCCCATTGGTTGACGACAAAAAAGACCAGGTC**TCCATGGAAAAGAGAAG**
Ebm448	CAGAAAAGTGATAATCAGGCGCACGTCAGCGTTTCCTTTGATGGA**CATATGAATATCCTCCTTAG**
Ebm453	CGCC**AAGCTT**GCTATATATCTTTCGTCTTATTATTACC
Ebm454	GCTC**GGTACC**ACTTTTCCGGCGGCTTCGC
Ebm459	GCTC**GGTACC**CGCGGGCTGAAAAGGCAG
Ebm460	GCTC**GGTACC**TTAGTGCGATTGTTTCTGTCGATC
Ebm461	GCTC**GGTACC**TTATTCGAAGTTGTAGAGACGCAC
Ebm462	GCTC**GGTACC**ATATAGATAGCATTGCCG
Ebm463	GCTC**GGTACC**TGACTGACGTCAATTGGCGG
Ebm468	AGC**TGTACA**TGGCAGGCCTTGCGCAAC
Ebm469	CGAT**AAGCTT**ATCGTCATCATCAAGTGCCCC
Ebm470	AGC**TGTACA**TGGTGAGCAAGGGCGAGGAG
Ebm471	GAT**AAGCTT**gtcatcCTTATACAGCTCGTCCATGCCGAGAG
Ebm472	GAACACGACGCCAGCCCATTGGTTGACGACAAAAAAGACCAGGTC**ATTCCAACTACTGCTAGC**
Ebm473	TAGA**GGATCC**CATGCAATTTAATATCCCTACGTTGC
Ebm474	GCTC**GGTAC C**GC GGC GGC AAACGGCGA
Ebm475	GCTC**GGTAC**CCGGGTACTCTGGTTCCAGCG
Ebm476	GCTC**GGTAC**CTCGGTTACCAGCACCATGGCG
Ebm477	GCTC**GGTAC**CGCAGAAATAATAATTTCACGGGCG
Ebm478	GCTC**GGTAC**CGGACGCCACAGCAGCCAT
Ebm479	GCTC**GGTACC**TGATCAAGCAAATCTGCACGCG
Ebm485	GCTC**GGTACC**CCATCGAACCAGTCAGTCACCG
Ebm486	GCTC**GGTAC**CCCAATCCAGGAGACGGCCACG

Ebm487	GCTC**GGTAC**CAGAGTCAGTACCGCAGCCACAAAG
Ebm488	AGAACGCTGACGTCTGCGGGCAAAGGTCGTCAGGCGGGAAGTTTG**TCCATGGAAAAGAGAAG**
Ebm489	ATCAGTTTTGTTTGTGAGCCGGATTGGTTCATCCGGCACACAAAC**CATATGAATATCCTCCTTAG**
Ebm490	ACGGTACACTGATATTGACGCTCATAATGTAAAAAGGTTCTTTCATCCTTAGTTCCTATTCCGAAG
Ebm493	CGTTTGCGCCGTATCCGCATCGACCGATTAATTAGCCGCATCCTG**ATTCCAACTACTGCTAGC**
Ebm494	AGCAGCTTTGATAATTCGGGTGAATCCAGTGGTATTATTGGCCATTCCCTTATACAGCTCGTCCATGCCGAG
Ebm505	ACC**TCTAGA**CGTGCGCCTGATTATCACTTTTC
Ebm506	ACCCCATGGTGCGCCTGATTATCACTTTTC
Ebm507	ACG**CTCGAG**TTACAAACTTCCCGCCTGACG
Ebm508	AGCAGCTTTGATAATTCGGGTGAATCCAGTGGTATTATTGGCCATAAGTGCCCCGGAGGATGAG
Ebm509	GACAAAAAAGACCAGGTCTAATCCATCAAAGGAAACGCTGACGTGATTCCGGGGATCCGTCGACC
Ebm516	ACC**GAATTC**ATGAAAATTCTGATTGTTGAAGACG
Ebm517	ACG**CTCGAG**TTAGTTTTCCTCATTCGCGAC
Ebm519	ACC**GAATTC**ATGATCAATGTATTAATTATCGATG
Ebm520	ACG**CTCGAG**TTATTGGCAATATTGTTTCAGTAG
Ebm521	ACC**GAATT**CATGACAACCGTTTATACGTTGG
Ebm522	ACG**CTCGAG**TTACAGCAACGGACTGAAGAAG
Ebm523	ACC**GAATTC**ATGGATATGGATCTAAACAATCG
Ebm524	ACGC**TCGAG**TTATTCCCGCCAGATGATATG
Ebm538	TGCTTTTTACCAGGATGCcaatTGGTAAATTCAGTAATTTGTA
Ebm539	ACAAATTACTGAATTTACCAattgGCATCCTGGTAAAAAGCA
Ebm541	CG**GGATCC**CGAAACATGAGCGGATACCAC
Ebm542	GGTGGTACTGGATTTAGtacTACCCGACGAAGATGG
Ebm543	CCATCTTCGTCGGGTAgtaCTAAATCCAGTACCACC
Ebm545	GCCGGAATAGACTTGC**gca**TTACCAGGATGCTTAATGG
Ebm546	CCATTAAGCATCCTGGTAA**tgc**GCAAGTCTATTCCGGC
Ebm547	TGCTTTTTACCAGGATGC**gc**A**c**TGGTAAATTCAGTAATTTGTA
Ebm548	TACAAATTACTGAATTTACCagT**gC**GCATCCTGGTAAAAAGCA
Ebm549	CGA**CAATTG**ATGAAGATTCTACTTATTGAAGATAATC
Ebm550	ACG**CTCGAG**ttaTTTTTTTACCGCTACGAATGAATAG
Ebm551	ACC**GAATTC**ATGAGACATTCATTGCCCTACC
Ebm552	ACG**CTCGAG**TCATCTGTTCGACCTCTCCC
Ebm586	cccATGACTTTCtgcAGGcctTGCCGCGCATTTG
Ebm587	CAAATGCGCGGCAaggCCTgcaGAAAGTCATggg

Ebm588	CA**CCATGG**TAATGCAGAAAGAACAACTTTCCGC
Ebm589	GCC**AAGCTT**TCATTGCGCTGCCCCGAAC
Ebm592	TTC**GGATCC**AGCAAACGCCC
Ebm593	TTC**GTCGAC**CATATCTTTTGCGCGTCCGG
Ebm600	C**GGGATCC**GACTTCAACGAAGAGCGG
Emb601	CCG**CTCGAG**CATTGCTTTTCCTTCCGC
Ebm647	CG**GGATCC**GCCGCGCATTTGCATTATTAAC
Ebm648	CCG**CTCGAG**GTCACCCTGATGGTCATCACCGC
Ebm649	CG**GGATCC**TTAGGCCAACAATAGCCAAGGCG

Table 3. Oligodeoxynucleotides used in this study. Restriction sites used for construction are indicated in bold; changes in nucleotide sequence inserting point mutations are indicated in small type.

IV. FRACTIONATION OF *E. COLI* BY THE SPHAEROPLAST METHOD

The fractionation by the sphaeroplast method enables to separate the periplasmic, membrane, and cytoplasmic cellular fractions (Isnard *et al.*, 1994). An overnight culture supplemented with appropriate antibiotic is diluted in 3 mL of fresh LB and grown at 37 °C till an OD_{600nm}=1. 1 mL of the culture is centrifuged 3 min at 8,000 rpm; the pellet corresponds to total cells (fraction 1). 1 mL of the culture is centrifuged 7 min at 6000 rpm. The supernatant is kept (fraction 2) and the next steps of the fractionation are realized on this cell pellet. The pellet is resuspended in 250 µL Tris 10 mM (pH 6,8), 30 % sucrose. 5 µL of lysozyme (10 mg/mL) are added and the cells are kept on ice for 2 min before adding 250 µL Tris 10 mM (pH 6,8) and EDTA 1 mM. The cells are then kept on ice for 10 min. After incubation, the cells are centrifuged 10 min at 4000 rpm (4 °C) and the supernatant corresponding to the periplasmic material (fraction 3) is kept. The sphaeroplasts are resuspended in 500 µL Tris 10 mM, EDTA 0,5 mM MgCl2 10 mM supplemented with 5 µL of DNAse (100 µg/mL). The sphaeroplasts are lysed with 5 cycles of freezing/defreezing in liquid N_2 and a water bath (37 °C) and then centrifuged 15 min at 15300 rpm (4 °C). The supernatant corresponds to the cytoplasme (fraction 4). The pellet is resuspended in 500 µL Tris 10 mM, EDTA 0,5 mM, and 2 % Triton and then incubated during 2 h on a wheel in the cold room (4 °C). After centrifugation 30 min at 15300 rpm (4 °C), the supernatant corresponds to the solubilized membranes (fraction 5) and the pellet corresponds to unsoluble material (aggregates; fraction 6). The samples of fraction 1, 2, 3, 4, and 5 are precipitated with trichloroacetic acid 100 % (1/10th), placed on ice for 30 min, and finally centrifuged 5 min at 15300 rpm (4 °C). All samples are then denaturated in Laemmli buffer (1X) and heated 5 min at 96 °C before loading onto a SDS-PAGE for analysis.

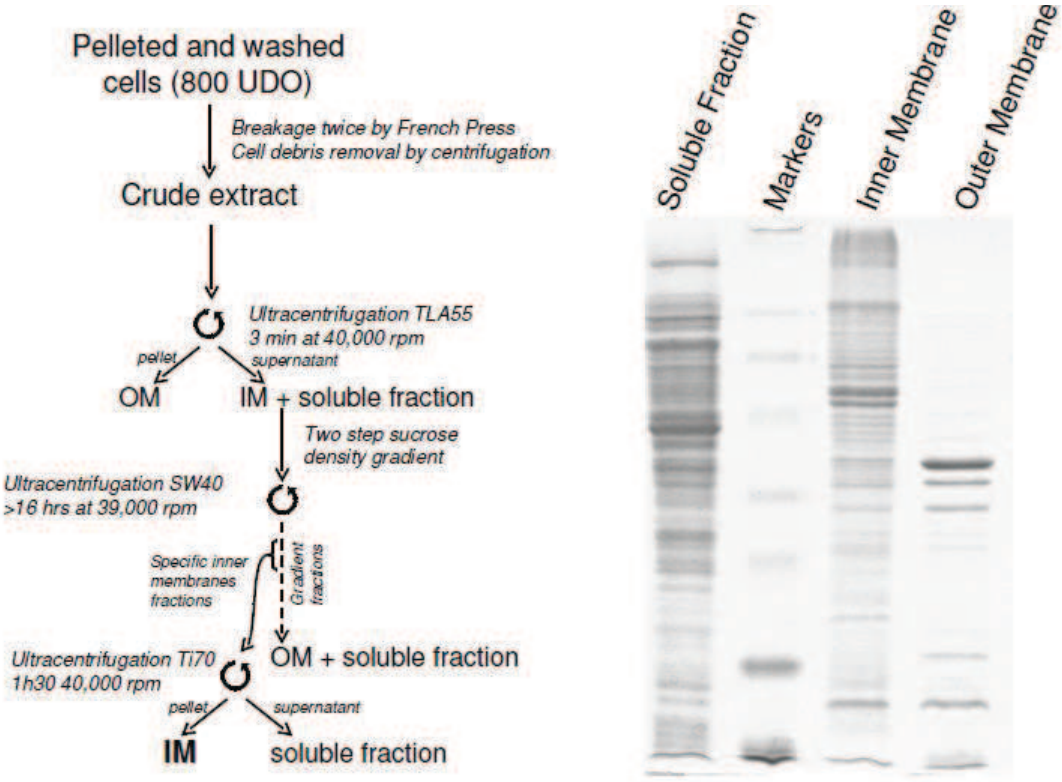

Figure 116: Differential centrifugation to separate inner and outer membrane (Duquesne & Sturgis, 2008). IM= inner membrane; OM= outer membrane.

V. INNER AND OUTER MEMBRANE SEPARATION

The inner and outer membranes are crudely separated by differential centrifugation (figure 83 and 116) (Duquesne & Sturgis, 2008). The cells of 1 or 2 L cultures are harvested at 6300 rpm (15 min at 4 °C), then the pellet is washed with 50 ml icecold buffer TRIS (10 mM, pH 8,0) and transferred to a Falcon tube (50 ml). Then the cells are centrifugated at 4000 rpm for 30 min at 4 °C and the pellets can be frozen in liquid N_2 and kept at - 80°C.

The pellet is resuspended in 20 ml buffer K (50 mM TEA acetate, 250 mM sucrose, 1 mM EDTA, 1 mM DTT; + DNase 100 µl/ml (stock 100X), + Roche© cocktail anti-protease 1X (stock 50 X) + lysozyme (80 µg/20 uOD) (to digest peptidoglycan)). The cells in this extract are passed 2 times through a French Press (1200 psi) to break them physically and give a translucide lysate. This lysate is centrifugated at 4000 rpm for 15 min at 4 °C to eliminate unbroken cells. Then, the supernatant is centrifuged for two times 5 min at 40 K (ultracentrifuge with vacuum) to eliminate the outer membrane (OM) fragments. The supernatant of the last ultracentrifugation is finally centrifuged 1h30 at 40 K at 4 °C (ultracentrifuge with vacuum) and the pellet corresponds to the inner membrane (IM) fragments. The soluble fraction (cytoplasm and periplasm) is discarded. The IM and OM pellets are gently resuspended in 1 ml of Ammonium bicarbonate (10 mM pH 8,0) with anti-protease (1X). Generally, the pellet is kept overnight on ice or on a wheel at 4 °C in the cold room with the Ammonium bicarbonate buffer.

VI. VESICLE TANDEM AFFINITY PURIFICATION (V-TAP)

Culture:

An overnight preculture (20 ml LB) supplemented with appropriate antibiotic is incubated under aeration at 37 °C. The next day this preculture is added to 1 or 2L fresh medium and incubated at 37 °C. If the TAP tagged protein is expressed from a plasmid (ampicillin resistance), the expression is induced at $OD_{600\ nm}$= 0,8 for 1h at 37 °C with 0,005 % of arabinose (to final OD ~ 2). If the TAP tagged protein is expressed from the chromosome (kanamycin resistance), the culture is grown till it reaches an $OD_{600\ nm}$ = 2.

Cell fractionation:

For details of the separation of outer and inner membranes see V.

Vesicles prepared by extrusion:

The extruder (Avanti® Mini-Extruder) was designed to prepare lyposomes of defined size. In our case it is used to prepare membrane vesicles (figure 83). The polycarbonate membranes and filters, which were purchased from Avanti® Polar Lipids Inc, USA, are pre-soaked in ammonium bicarbonate (10 mM) buffer. The 1 mL IM extract makes then 11 passages through the extruder for each diameter (membranes with pore size: 1 µm → 0,4 µm and 0,1 µm). The protein amount can be estimated by taking the $OD_{280\ nm}$= of 5 µl of the vesicle suspension in 995 µl SDS 0,6 % (blank: 935 µl H_20 + 60 µl SDS 10 %). An absorbance of 0,2 corresponds to ~ 20 mg/ml of protein.

TAP purification

Materiels and buffers:

- Beads coated with antibody anti-rabbit IgG MagnaBind (Pierce 21356) should be mixed well before use.
- Support for the paramagnetic beads (IBA)
- Calmodulin beads (Stratagene 214303)
- Cocktail anti-protease EDTA free (Roche©)

IPP150protA: 10mM Tris-HCl (pH8.0), 150mM NaCl, water qsp 100ml.

TEV cleavage buffer: 10mM Tris-HCl (pH8.0), 150mM NaCl, 0,5mM EDTA, 1mM DTT, water qsp 10ml.

note: DTT is added just before the experiment. It is necessary for TEV activity.

IPP150 Calmodulin binding buffer: 10mM ß-mercaptoethanol, 10mM Tris-HCl (pH8.0), 150mM NaCl, 2mM $CaCl_2$, water qsp 100ml.

IPP150 Calmodulin elution buffer: 10mM ß-mercaptoethanol, 10mM Tris-HCl (pH8.0), 150mM NaCl, 2mM EGTA, water qsp 100ml.

note: ß-mercaptoethanol is added just before the experiment.

The principle of the v-TAP purification is shown in figure 82. 1,5 mL of paramagnetic IgG beads are pre-washed 3 times with 1,5 mL IPP150-ProteinA buffer by rotation of the wheel in the cold room (4°C). 75 to 100 mg (usually 1 mL) of protein is then incubated on the beads with 1 mL IPP150-ProteinA buffer during 2 h at 4°C on the wheel. After the incubation, the beads are washed 3 times with 1,5 mL IPP150-ProteinA buffer. The beads are then incubated with 1 mL TEV cleavage buffer and 45 µL 6His-TEV$^+$ enzyme (homemade) during 1 h at 16°C and 1 h at 25°C on the wheel. The eluted extract is recovered and 3 mL IPP150-Calmodulin binding buffer is added together with 30 µL of $CaCl_2$ (0,1 M) to block the EDTA of the buffer TEV cleavage.

200 µL Calmodulin beads are pre-washed with 1,5 mL of IPP150-Calmodulin binding buffer and incubated with the eluted extract during 1 h on the wheel at 4 °C. The beads are washed 5 times with 20 mL IPP150-Calmodulin binding buffer. Finally, the bound proteins are eluted with 5 times 200 µL IPP150-Calmodulin elution buffer. The 5 elutions are pooled together and centrifuged 2 h with an ultracentrifuge at 40K and 4 °C. The transparent pellet is resuspended in 30 µL of ammonium bicarbonate (10 mM).

The whole cells, extract, unbound, and the pooled elution fraction are finally analysed on a SDS-PAGE with Coomassie staining. Then bands are cut, conserved in ammonium bicarbonate (10 mM) buffer and sent to mass spectrometry analyses.

VII. PROTEIN PURIFICATION WITH 6HIS TAG

For each purification BL21(DE3)LYS competent *E. coli* cells are transformed by a plasmid pET6his-tev (figure 112B) containing the gene coding for the protein of interest or pEB570 for TEV^+ preparation and incubated overnight at 37°C on LB plates supplemented with ampicillin (100 µg/ml). From this transformation plate an isolated colony is incubated in 25 ml LB supplemented with ampicillin (100 µg/ml) and incubated overnight at 37°C. The next morning, 500 mL of fresh LB supplemented with ampicillin (100 µg/ml) is inoculated with 12,5 mL of the starter culture and grown at 30 °C till the culture reaches OD_{600nm}=0,9. The expression is induced by adding 0,1 mM IPTG to the culture which is then grown during 6 h at 23 °C with 180 rpm shaking. The culture is centrifuged 20 min at 4000 rpm at 4 °C and the pellet is then washed with 50 mL PBS (1X, pH 7) and transferred to a 50 mL falcon tube. The cells are harvested by centrifugation for 30 min at 4000 rpm at 4 °C, frozen with liquid N_2, and can be kept at -80 °C.

The frozen pellet is then resuspended in 15 mL of buffer 1 and 1 X anti-protease inhibitor cocktail (Roche©) is added. The cells are then broken by sonication with a Branson Sonifier450 (keep at 4°C) at intensity of 8 during 2 min at 80 %. The total extract is centrifuged during 30 min at 15400 rpm at 4 °C. In the meantime, 500µl of resin (Talon®) is pre-washed with 10 mL of buffer 1 in a 10 mL BIO-RAD column. After the centrifugation, the soluble extract is transferred in the column and incubated during 1 h on a wheel in the cold room (4 °C). The unbound extract is kept in a 15 mL falcon on ice. The resin is washed successively with 10 mL buffer 1, with 5 mL buffer 2, and finally, with 10 mL buffer 1.

The bound protein fraction is eluted with 5 times 500 µL buffer 3 in 5 1,5 mL eppendorff tubes filled already with icecold 500 µL glycerol (80 %). The whole cells, extract, unbound, and the 5 elution fractions are finally analysed on a SDS-PAGE with Coomassie staining.

Materials and buffers:

BIO-RAD Poly-Prep® Chromatography Column

TALON® Metal Affinity Resin purchased from Clontech

Buffer 1: 20 mM Tris-HCl (pH 8), 10 mM imidazole, 200 mM NaCl, 2 mM β-mercaptoethanol, 0,2 % NP40, qsp water.

Buffer 2: 20 mM Tris-HCl (pH 8), 10 mM imidazole, 1 M NaCl, 2 mM β-mercaptoethanol, 0,2 % NP40, qsp water.

Buffer 3: 20 mM Tris-HCl (pH 8), 200 mM imidazole, 200 mM NaCl, 2 mM β -mercaptoethanol, 0,2 % NP40, qsp water.

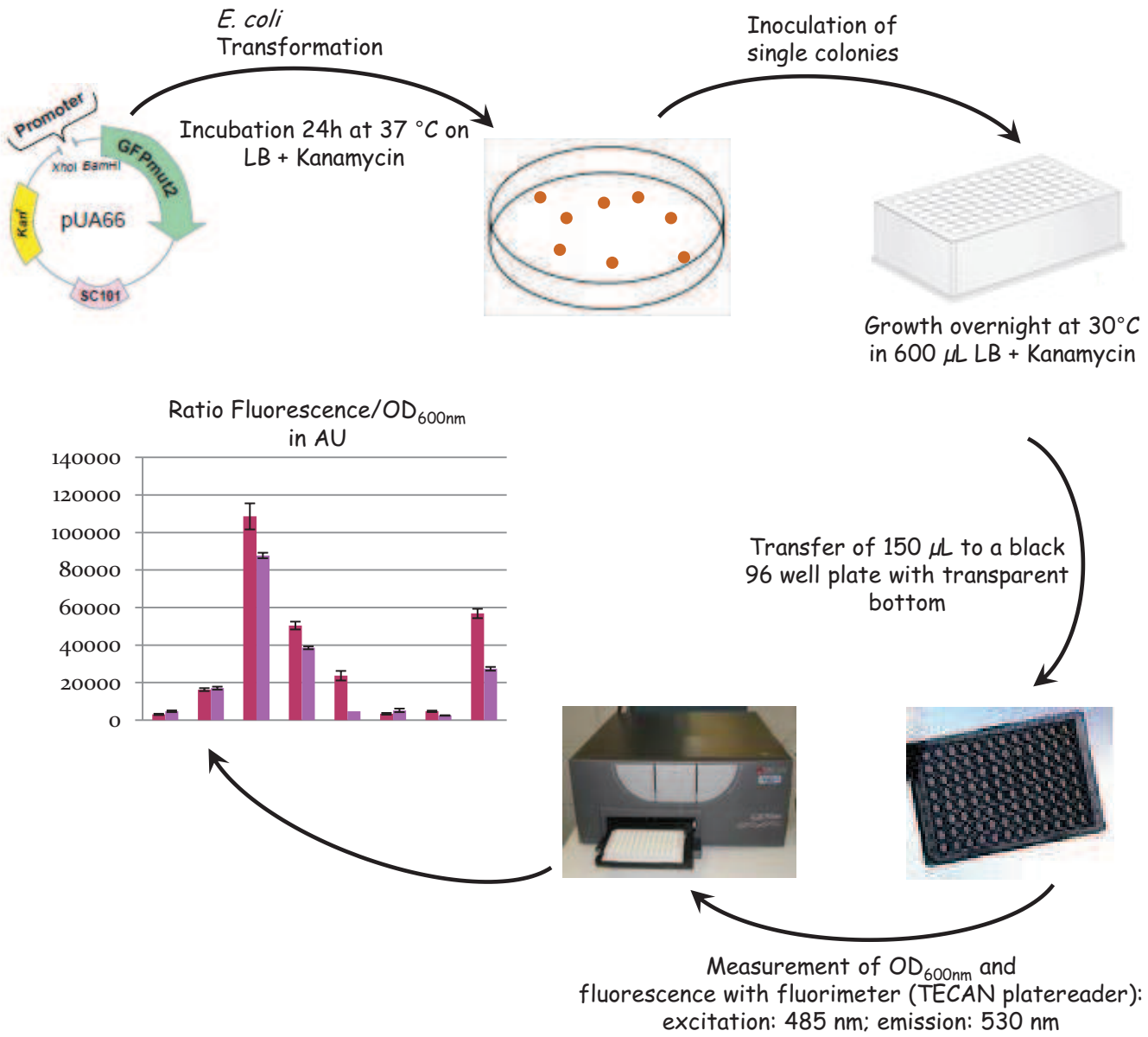

Figure 117: Measurement of expression of transcriptional fusions with GFP. *E. coli* MG1655 strain (or isogenic strains) is transformed with plasmids carrying the *gfp* transcriptional fusion that are maintained with kanamycin (25 µg/mL). The activity is measured as follows: sterile 2.2ml storage 96-well plates are used (Dutscher #016025) for cultures covered with porous sterile film (Aeraseal Dutscher #760215). 600µl LB supplemented with required antibiotics are distributed, with or without induction, using a distributer. Single clones (ideally 4-6 replicas) are picked with a toothpick in the culture. The culture plate is then incubated under aeration overnight at 30°C. For measurement in a TECAN© infinite M200, 150 µL of each well are transferred by a multichannel pipette into a black 96 well plate with transparent bottom permitting parallel reading of absorbance (600 nm) and fluorescence (excitation: 485 nm; emission: 530 nm).

VIII. TRANSCRIPTIONAL FUSIONS WITH GFP

Two cloning vectors are provided with the transcriptional fusion library (Zaslaver *et al.*, 2006), pUA66 (pEB898) which is used for promoters localized on the forward strand of the chromosome, or pUA139 (pEB987) for the reverse orientation (figure 113A). In these vectors, only the BamHI and XhoI restriction sites are changed in their orientation. *E. coli* MG1655 or a strain (for exemple ppGpp° (EB425) or another mutant strain) that shall be compared with a wild type strain, are transformed with plasmids carrying the *gfp* transcriptional fusions that are maintained with kanamycin (25 µg/mL). In an approach to see the effect of the overproduction of a protein on gene expression, *E. coli* MG1655 strain is co-transformed with the transcriptional fusions and a plasmid permitting overexpression, such a pBAD24.

600µl LB supplemented with required antibiotics are inoculated with 4 to 6 replica for each transformation in a 96-well plate (figure 117). The culture plate is then incubated under aeration overnight at 30°C.

For measurement in a TECAN© infinite M200, 150 µL of each well are transferred by a multichannel pipette into a black 96 well plate with transparent bottom permitting parallel reading of absorbance (600 nm) and fluorescence (excitation: 485 nm; emission: 530 nm). The expression profiles of each reporter strain are calculated by dividing the background (= medium) subtracted GFP by OD: [Fluo - Fluo(blank)] / [OD - OD(blank)]. The values presented are the mean of four or six independent cultures.

IX. FLUORESCENCE MICROSCOPY

Bacterial cells were immobilized either with poly-lysinated microscopy slides which are charged positively and attract the negatively charged cells or physically with 0,25 % agarose. For imaging, either a Zeiss Axiovert 200M or a confocal Olympus FV1000 microscope was used. In both cases, a 100X oil immersion inverted objective was used.

Default settings for Zeiss Axiovert that has a mercure lamp:

Experiment	Excitation and Emission[a]	Exposure time
GFP	excitation: BP450-490 nm beamspliter 510 nm emission : BP515-565 nm	20 ms to 1 sec
Rhodamine (mRFP)	excitation: BP534-558 nm beamspliter 580 nm emission : LP590 nm	20 ms to 1 sec
CFP/YFP	excitation: BP480-520 nm beamspliter 515 nm emission : BP505-565 nm	20 ms to 1 sec
Phase contrast	–	5-7 ms

[a] BP: band passage; LP: long passage (≥ x nm).

There are various laser and filter settings possible for the Olympus FV1000 microscope that can be customized for each experiment.

Finally, images and artificially added colours were treated with the programme ImageJ.

X. GEL MOBILITY SHIFT ASSAY

Gel mobility shift assay (GMSA) is an *in vitro* technique to determine if a regulatory protein binds directly to a promoter region.

The concentration and molarity of the purified protein (i.e. 6his tag) in an adequate buffer is determined by using a Bradford assay. The promoter region of interest is amplified by PCR: in general 8x50 µL PCR are prepared using Dynazyme (Finnzym) on 0,5 µL MG1655 genomic DNA or plasmid, then pooled together and purified with NucleoSpin kit (elution with water). The concentration is determined by absorbance 280/260 nm with Spectrometer and the molarity is calculated.

A buffer (5X) is prepared with Tris-HCl (pH 7,2, 25 mM) , $MgCl_2$ (10 mM), $CaCl_2$ (1 mM), EDTA (pH 8, 0,5 mM), KCl (50 mM), and glycerol (5 %). A native PAGE is prepared (6 - 10 %) using an Acrylamid/bis mix (29:1) purchased from Sigma with a 4 % stacking gel. The reaction mix (final 20 µL) is prepared on ice (4 °C) by adding different ratios of molarity of DNA : protein. Usually, ratios 1:1, 1:10, 1:20 till 1:200 are used. The reaction mix is then incubated 30 min at a constant temperature of 20 °C. During this incubation, the empty PAGE gel is run 30 min at 80 V (in 0,5X TBE) to equilibrate buffers and temperature. Then, the reaction mixes are loaded and run at 80 V in TBE 0,5X (other low-salt buffers like TAE can be used). The PAGE gel is finally developed in GelRed™ (Fluoprobes®) Nucleic Acid gel staining solution for 10 min to visualize the DNA bands.

Aberg, A., Fernández-Vázquez, J., Cabrer-Panes, J. D., Sánchez, A.et al. (2009) Similar and divergent effects of ppGpp and DksA deficiencies on transcription in Escherichia coli. *J Bacteriol*, **191**, 3226-3236.

Ahn, V. E., Lo, E. I., Engel, C. K., Chen, L.et al. (2004) A hydrocarbon ruler measures palmitate in the enzymatic acylation of endotoxin. *EMBO J*, **23**, 2931-2941.

Alexeyev, M. F. & Winkler, H. H. (1999) Membrane topology of the Rickettsia prowazekii ATP/ADP translocase revealed by novel dual pho-lac reporters. *J Mol Biol*, **285**, 1503-1513.

Asai, Y., Katayose, Y., Hikita, C., Ohta, A.et al. (1989) Suppression of the lethal effect of acidic-phospholipid deficiency by defective formation of the major outer membrane lipoprotein in Escherichia coli. *J Bacteriol*, **171**, 6867-6869.

Azizan, A., Sherin, D., DiRusso, C. C. & Black, P. N. (1999) Energetics underlying the process of long-chain fatty acid transport. *Arch Biochem Biophys*, **365**, 299-306.

Babu, M., Butland, G., Pogoutse, O., Li, J.et al. (2009) Sequential peptide affinity purification system for the systematic isolation and identification of protein complexes from Escherichia coli. *Methods Mol Biol*, **564**, 373-400.

Bader, M. W., Sanowar, S., Daley, M. E., Schneider, A. R.et al. (2005) Recognition of antimicrobial peptides by a bacterial sensor kinase. *Cell*, **122**, 461-472.

Bakali, H. M. A., Herman, M. D., Johnson, K. A., Kelly, A. A.et al. (2007) Crystal structure of YegS, a homologue to the mammalian diacylglycerol kinases, reveals a novel regulatory metal binding site. *J Biol Chem*, **282**, 19644-19652.

Bakali, M. A., Nordlund, P. & Hallberg, B. M. (2006) Expression, purification, crystallization and preliminary diffraction studies of the mammalian DAG kinase homologue YegS from Escherichia coli. *Acta Crystallogr Sect F Struct Biol Cryst Commun*, **62**, 295-297.

Battesti, A. & Bouveret, E. (2009) Bacteria possessing two RelA/SpoT-like proteins have evolved a specific stringent response involving the acyl carrier protein-SpoT interaction. *J Bacteriol*, **191**, 616-624.

Bell, R. M. (1974) Mutants of Escherichia coli defective in membrane phospholipid synthesis: macromolecular synthesis in an sn-glycerol 3-phosphate acyltransferase Km mutant. *J Bacteriol*, **117**, 1065-1076.

Bishop, R. E., Gibbons, H. S., Guina, T., Trent, M. S.et al. (2000) Transfer of palmitate from phospholipids to lipid A in outer membranes of gram-negative bacteria. *EMBO J*, **19**, 5071-5080.

Black, P. N. (1990) Characterization of FadL-specific fatty acid binding in Escherichia coli. *Biochim Biophys Acta*, **1046**, 97-105.

Black, P. N. & DiRusso, C. C. (2003) Transmembrane movement of exogenous long-chain fatty acids: proteins, enzymes, and vectorial esterification. *Microbiol Mol Biol Rev*, **67**, 454-72, table of contents.

Black, P. N., Said, B., Ghosn, C. R., Beach, J. V.et al. (1987) Purification and characterization of an outer membrane-bound protein involved in long-chain fatty acid transport in Escherichia coli. *J Biol Chem*, **262**, 1412-1419.

Bogdanov, M., Heacock, P. N. & Dowhan, W. (2002) A polytopic membrane protein displays a reversible topology dependent on membrane lipid composition. *EMBO J*, **21**, 2107-2116.

Bogdanov, M., Sun, J., Kaback, H. R. & Dowhan, W. (1996) A phospholipid acts as a chaperone in assembly of a membrane transport protein. *J Biol Chem*, **271**, 11615-11618.

Bogdanov, M., Xie, J., Heacock, P. & Dowhan, W. (2008) To flip or not to flip: lipid-protein charge interactions are a determinant of final membrane protein topology. *J Cell Biol*, **182**, 925-935.

Bradley, M. D., Beach, M. B., de Koning, A. P. J., Pratt, T. S.et al. (2007) Effects of Fis on Escherichia coli gene expression during different growth stages. *Microbiology*, **153**, 2922-2940.

Bulieris, P. V., Behrens, S., Holst, O. & Kleinschmidt, J. H. (2003) Folding and insertion of the outer membrane protein OmpA is assisted by the chaperone Skp and by lipopolysaccharide. *J Biol Chem*, **278**, 9092-9099.

Butland, G., Peregrín-Alvarez, J. M., Li, J., Yang, W.et al. (2005) Interaction network containing conserved and essential protein complexes in Escherichia coli. *Nature*, **433**, 531-537.

Byers, D. M. & Gong, H. (2007) Acyl carrier protein: structure-function relationships in a conserved multifunctional protein family. *Biochem Cell Biol*, **85**, 649-662.

Campbell, J. W., Morgan-Kiss, R. M. & Cronan, J. E. J. (2003) A new Escherichia coli metabolic competency: growth on fatty acids by a novel anaerobic beta-oxidation pathway. *Mol Microbiol*, **47**, 793-805.

Campbell, R. E., Tour, O., Palmer, A. E., Steinbach, P. A.et al. (2002) A monomeric red fluorescent protein. *Proc Natl Acad Sci U S A*, **99**, 7877-7882.

Cheung, J., Bingman, C. A., Reyngold, M., Hendrickson, W. A.et al. (2008) Crystal structure of a functional dimer of the PhoQ sensor domain. *J Biol Chem*, **283**, 13762-13770.

Cho, B., Knight, E. M. & Palsson, B. Ø. (2006) Transcriptional regulation of the fad regulon genes of Escherichia coli by ArcA. *Microbiology*, **152**, 2207-2219.

Coleman, J. (1990) Characterization of Escherichia coli cells deficient in 1-acyl-sn-glycerol-3- phosphate acyltransferase activity. *J Biol Chem*, **265**, 17215-17221.

Cooper, C. L., Hsu, L., Jackowski, S. & Rock, C. O. (1989) 2-Acylglycerolphosphoethanolamine acyltransferase/acyl-acyl carrier protein synthetase is a membrane-associated acyl carrier protein binding protein. *J Biol Chem*, **264**, 7384-7389.

Coornaert, A., Lu, A., Mandin, P., Springer, M.et al. (2010) MicA sRNA links the PhoP regulon to cell envelope stress. *Mol Microbiol*, **76**, 467-479.

Costanzo, A. & Ades, S. E. (2006) Growth phase-dependent regulation of the extracytoplasmic stress factor, sigmaE, by guanosine 3',5'-bispyrophosphate (ppGpp). *J Bacteriol*, **188**, 4627-4634.

Costanzo, A., Nicoloff, H., Barchinger, S. E., Banta, A. B.et al. (2008) ppGpp and DksA likely regulate the activity of the extracytoplasmic stress factor sigmaE in Escherichia coli by both direct and indirect mechanisms. *Mol Microbiol*, **67**, 619-632.

Cronan, J. E. (2003) Bacterial membrane lipids: where do we stand?. *Annu Rev Microbiol*, **57**, 203-224.

Cronan, J. E. J. (1997) In vivo evidence that acyl coenzyme A regulates DNA binding by the Escherichia coli FadR global transcription factor. *J Bacteriol*, **179**, 1819-1823.

Cronan, J. E. J., Li, W. B., Coleman, R., Narasimhan, M.et al. (1988) Derived amino acid sequence and identification of active site residues of Escherichia coli beta-hydroxydecanoyl thioester dehydrase. *J Biol Chem*, **263**, 4641-4646.

Cronan, J. E. J., Reed, R., Taylor, F. R. & Jackson, M. B. (1979) Properties and biosynthesis of cyclopropane fatty acids in Escherichia coli. *J Bacteriol*, **138**, 118-121.

Crooke, E. (2001) Escherichia coli DnaA protein--phospholipid interactions: in vitro and in vivo. *Biochimie*, **83**, 19-23.

Cullen, T. W. & Trent, M. S. (2010) A link between the assembly of flagella and lipooligosaccharide of the Gram-negative bacterium Campylobacter jejuni. *Proc Natl Acad Sci U S A*, **107**, 5160-5165.

Daley, D. O., Rapp, M., Granseth, E., Melén, K.et al. (2005) Global topology analysis of the Escherichia coli inner membrane proteome. *Science (80-)*, **308**, 1321-1323.

Dartigalongue, C., Missiakas, D. & Raina, S. (2001) Characterization of the Escherichia coli sigma E regulon. *J Biol Chem*, **276**, 20866-20875.

Dathe, M. & Wieprecht, T. (1999) Structural features of helical antimicrobial peptides: their potential to modulate activity on model membranes and biological cells. *Biochim Biophys Acta*, **1462**, 71-87.

De Las Peñas, A., Connolly, L. & Gross, C. A. (1997) SigmaE is an essential sigma factor in Escherichia coli. *J Bacteriol*, **179**, 6862-6864.

De Lay, N. R. & Cronan, J. E. (2006) A genome rearrangement has orphaned the Escherichia coli K-12 AcpT phosphopantetheinyl transferase from its cognate Escherichia coli O157:H7 substrates. *Mol Microbiol*, **61**, 232-242.

DeChavigny, A., Heacock, P. N. & Dowhan, W. (1991) Sequence and inactivation of the pss gene of Escherichia coli. Phosphatidylethanolamine may not be essential for cell viability. *J Biol Chem*, **266**, 5323-5332.

Dekker, N. (2000) Outer-membrane phospholipase A: known structure, unknown biological function. *Mol Microbiol*, **35**, 711-717.

DiRusso, C. C. & Nyström, T. (1998) The fats of Escherichia coli during infancy and old age: regulation by global regulators, alarmones and lipid intermediates. *Mol Microbiol*, **27**, 1-8.

DiRusso, C. C., Black, P. N. & Weimar, J. D. (1999) Molecular inroads into the regulation and metabolism of fatty acids, lessons from bacteria. *Prog Lipid Res*, **38**, 129-197.

Dillon, D. A., Wu, W. I., Riedel, B., Wissing, J. B.et al. (1996) The Escherichia coli pgpB gene encodes for a diacylglycerol pyrophosphate phosphatase activity. *J Biol Chem*, **271**, 30548-30553.

Dirusso, C. C. & Black, P. N. (2004) Bacterial long chain fatty acid transport: gateway to a fatty acid-responsive signaling system. *J Biol Chem*, **279**, 49563-49566.

Doerrler, W. T., Gibbons, H. S. & Raetz, C. R. H. (2004) MsbA-dependent translocation of lipids across the inner membrane of Escherichia coli. *J Biol Chem*, **279**, 45102-45109.

Dowhan, W. (1997) CDP-diacylglycerol synthase of microorganisms. *Biochim Biophys Acta*, **1348**, 157-165.

Dowhan, W. & Hirabayashi, T. (1981) Phosphatidylglycerophosphate synthase from Escherichia coli. *Methods Enzymol*, **71 Pt C**, 555-561.

Dowhan, W. & Li, Q. X. (1992) Phosphatidylserine decarboxylase from Escherichia coli. *Methods Enzymol*, **209**, 348-359.

Duquesne, K., Sturgis, J. N. (2008) Membrane Protein Solubilization. *Meth in Mol Biol.*

Durfee, T., Hansen, A., Zhi, H., Blattner, F. R.et al. (2008) Transcription profiling of the stringent response in Escherichia coli. *J Bacteriol*, **190**, 1084-1096.

Eckford, P. D. W. & Sharom, F. J. (2010) The reconstituted Escherichia coli MsbA protein displays lipid flippase activity. *Biochem J*, **429**, 195-203.

El Ghachi, M., Derbise, A., Bouhss, A. & Mengin-Lecreulx, D. (2005) Identification of multiple genes encoding membrane proteins with undecaprenyl pyrophosphate phosphatase (UppP) activity in Escherichia coli. *J Biol Chem*, **280**, 18689-18695.

Farewell, A., Diez, A. A., DiRusso, C. C. & Nyström, T. (1996) Role of the Escherichia coli FadR regulator in stasis survival and growth phase-dependent expression of the uspA, fad, and fab genes. *J Bacteriol*, **178**, 6443-6450.

Feilmeier, B. J., Iseminger, G., Schroeder, D., Webber, H.et al. (2000) Green fluorescent protein functions as a reporter for protein localization in Escherichia coli. *J Bacteriol*, **182**, 4068-4076.

Feng, Y. & Cronan, J. E. (2010) Overlapping repressor binding sites result in additive regulation of Escherichia coli FadH by FadR and ArcA. *J Bacteriol*, **192**, 4289-4299.

Fiedler, W. & Rotering, H. (1985) Characterization of an Escherichia coli mdoB mutant strain unable to transfer sn-1-phosphoglycerol to membrane-derived oligosaccharides. *J Biol Chem*, **260**, 4799-4806.

Figueroa-Bossi, N., Lemire, S., Maloriol, D., Balbontín, R.et al. (2006) Loss of Hfq activates the sigmaE-dependent envelope stress response in Salmonella enterica. *Mol Microbiol*, **62**, 838-852.

Flint, D. H., Tuminello, J. F. & Miller, T. J. (1996) Studies on the synthesis of the Fe-S cluster of dihydroxy-acid dehydratase in escherichia coli crude extract. Isolation of O-acetylserine sulfhydrylases A and B and beta-cystathionase based on their ability to mobilize sulfur from cysteine and to participate in Fe-S cluster synthesis. *J Biol Chem*, **271**, 16053-16067.

Froelich, J. M., Tran, K. & Wall, D. (2006) A pmrA constitutive mutant sensitizes Escherichia coli to deoxycholic acid. *J Bacteriol*, **188**, 1180-1183.

Funk, C. R., Zimniak, L. & Dowhan, W. (1992) The pgpA and pgpB genes of Escherichia coli are not essential: evidence for a third phosphatidylglycerophosphate phosphatase. *J Bacteriol*, **174**, 205-213.

Ganz, T. (2003) Defensins: antimicrobial peptides of innate immunity. *Nat Rev Immunol*, **3**, 710-720.

Gavin, A. L., Hoebe, K., Duong, B., Ota, T.et al. (2006) Adjuvant-enhanced antibody responses in the absence of toll-like receptor signaling. *Science (80-)*, **314**, 1936-1938.

Gavin, A., Aloy, P., Grandi, P., Krause, R.et al. (2006) Proteome survey reveals modularity of the yeast cell machinery. *Nature*, **440**, 631-636.

Gavin, A., Bösche, M., Krause, R., Grandi, P.et al. (2002) Functional organization of the yeast proteome by systematic analysis of protein complexes. *Nature*, **415**, 141-147.

Gibbons, H. S., Kalb, S. R., Cotter, R. J. & Raetz, C. R. H. (2005) Role of Mg2+ and pH in the modification of Salmonella lipid A after endocytosis by macrophage tumour cells. *Mol Microbiol*, **55**, 425-440.

Gibbons, H. S., Lin, S., Cotter, R. J. & Raetz, C. R. (2000) Oxygen requirement for the biosynthesis of the S-2-hydroxymyristate moiety in Salmonella typhimurium lipid A. Function of LpxO, A new Fe2+/alpha-ketoglutarate-dependent dioxygenase homologue. *J Biol Chem*, **275**, 32940-32949.

Gonzalez-Baro, M. R., Granger, D. A. & Coleman, R. A. (2001) Mitochondrial glycerol phosphate acyltransferase contains two transmembrane domains with the active site in the N-terminal domain facing the cytosol. *J Biol Chem*, **276**, 43182-43188.

Green, P. R., Merrill, A. H. J. & Bell, R. M. (1981) Membrane phospholipid synthesis in Escherichia coli. Purification, reconstitution, and characterization of sn-glycerol-3-phosphate acyltransferase. *J Biol Chem*, **256**, 11151-11159.

Greenway, D. L. & Silbert, D. F. (1983) Altered acyltransferase activity in Escherichia coli associated with mutations in acyl coenzyme A synthetase. *J Biol Chem*, **258**, 13034-13042.

Grogan, D. W. & Cronan, J. E. J. (1997) Cyclopropane ring formation in membrane lipids of bacteria. *Microbiol Mol Biol Rev*, **61**, 429-441.

Gully, D. & Bouveret, E. (2006) A protein network for phospholipid synthesis uncovered by a variant of the tandem affinity purification method in Escherichia coli. *Proteomics*, **6**, 282-293.

Gully, D., Moinier, D., Loiseau, L. & Bouveret, E. (2003) New partners of acyl carrier protein detected in Escherichia coli by tandem affinity purification. *FEBS Lett*, **548**, 90-96.

Gunn, J. S. (2008) The Salmonella PmrAB regulon: lipopolysaccharide modifications, antimicrobial peptide resistance and more. *Trends Microbiol*, **16**, 284-290.

Guo, D. & Tropp, B. E. (2000) A second Escherichia coli protein with CL synthase activity. *Biochim Biophys Acta*, **1483**, 263-274.

Hagiwara, D., Yamashino, T. & Mizuno, T. (2004) A Genome-wide view of the Escherichia coli BasS-BasR two-component system implicated in iron-responses. *Biosci Biotechnol Biochem*, **68**, 1758-1767.

Hancock, R. E. & Diamond, G. (2000) The role of cationic antimicrobial peptides in innate host defences. *Trends Microbiol*, **8**, 402-410.

Hancock, R. E. W. & McPhee, J. B. (2005) Salmonella's sensor for host defense molecules. *Cell*, **122**, 320-322.

Hara, Y., Seki, M., Matsuoka, S., Hara, H.et al. (2008) Involvement of PlsX and the acyl-phosphate dependent sn-glycerol-3-phosphate acyltransferase PlsY in the initial stage of glycerolipid synthesis in Bacillus subtilis. *Genes Genet Syst*, **83**, 433-442.

Harvat, E. M., Zhang, Y., Tran, C. V., Zhang, Z.et al. (2005) Lysophospholipid flipping across the Escherichia coli inner membrane catalyzed by a transporter (LplT) belonging to the major facilitator superfamily. *J Biol Chem*, **280**, 12028-12034.

Hayden, J. D. & Ades, S. E. (2008) The extracytoplasmic stress factor, sigmaE, is required to maintain cell envelope integrity in Escherichia coli. *PLoS ONE*, **3**, e1573.

He, X. Y., Yang, S. Y. & Schulz, H. (1997) Cloning and expression of the fadH gene and characterization of the gene product 2,4-dienoyl coenzyme A reductase from Escherichia coli. *Eur J Biochem*, **248**, 516-520.

Heacock, P. N. & Dowhan, W. (1987) Construction of a lethal mutation in the synthesis of the major acidic phospholipids of Escherichia coli. *J Biol Chem*, **262**, 13044-13049.

Hearn, E. M., Patel, D. R., Lepore, B. W., Indic, M.et al. (2009) Transmembrane passage of hydrophobic compounds through a protein channel wall. *Nature*, **458**, 367-370.

Heath, R. J. & Rock, C. O. (1996) Inhibition of beta-ketoacyl-acyl carrier protein synthase III (FabH) by acyl-acyl carrier protein in Escherichia coli. *J Biol Chem*, **271**, 10996-11000.

Heath, R. J. & Rock, C. O. (1996) Roles of the FabA and FabZ beta-hydroxyacyl-acyl carrier protein dehydratases in Escherichia coli fatty acid biosynthesis. *J Biol Chem*, **271**, 27795-27801.

Heath, R. J. & Rock, C. O. (1998) A conserved histidine is essential for glycerolipid acyltransferase catalysis. *J Bacteriol*, **180**, 1425-1430.

Heath, R. J., Jackowski, S. & Rock, C. O. (1994) Guanosine tetraphosphate inhibition of fatty acid and phospholipid synthesis in Escherichia coli is relieved by overexpression of glycerol-3-phosphate acyltransferase (plsB). *J Biol Chem*, **269**, 26584-26590.

Heber, S. & Tropp, B. E. (1991) Genetic regulation of cardiolipin synthase in Escherichia coli. *Biochim Biophys Acta*, **1129**, 1-12.

Helbig, A. O., Heck, A. J. R. & Slijper, M. (2010) Exploring the membrane proteome--challenges and analytical strategies. *J Proteomics*, **73**, 868-878.

Henry, M. F. & Cronan, J. E. J. (1992) A new mechanism of transcriptional regulation: release of an activator triggered by small molecule binding. *Cell*, **70**, 671-679.

Herrera, C. M., Hankins, J. V. & Trent, M. S. (2010) Activation of PmrA inhibits LpxT-dependent phosphorylation of lipid A promoting resistance to antimicrobial peptides. *Mol Microbiol*.

Hill, R. B., MacKenzie, K. R., Flanagan, J. M., Cronan, J. E. J.et al. (1995) Overexpression, purification, and characterization of Escherichia coli acyl carrier protein and two mutant proteins. *Protein Expr Purif*, **6**, 394-400.

Hirabayashi, T., Larson, T. J. & Dowhan, W. (1976) Membrane-associated phosphatidylglycerophosphate synthetase from Escherichia coli: purification by substrate affinity chromatography on cytidine 5'-diphospho-1,2-diacyl-sn-glycerol sepharose. *Biochemistry*, **15**, 5205-5211.

Hiraoka, S., Matsuzaki, H. & Shibuya, I. (1993) Active increase in cardiolipin synthesis in the stationary growth phase and its physiological significance in Escherichia coli. *FEBS Lett*, **336**, 221-224.

Hu, P., Janga, S. C., Babu, M., Díaz-Mejía, J. J.et al. (2009) Global functional atlas of Escherichia coli encompassing previously uncharacterized proteins. *PLoS Biol*, **7**, e96.

Huang, K. C., Mukhopadhyay, R. & Wingreen, N. S. (2006) A curvature-mediated mechanism for localization of lipids to bacterial poles. *PLoS Comput Biol*, **2**, e151.

Huerta, A. M. & Collado-Vides, J. (2003) Sigma70 promoters in Escherichia coli: specific transcription in dense regions of overlapping promoter-like signals. *J Mol Biol*, **333**, 261-278.

Hwang, P. M., Choy, W., Lo, E. I., Chen, L.et al. (2002) Solution structure and dynamics of the outer membrane enzyme PagP by NMR. *Proc Natl Acad Sci U S A*, **99**, 13560-13565.

Icho, T. (1988) Membrane-bound phosphatases in Escherichia coli: sequence of the pgpB gene and dual subcellular localization of the pgpB product. *J Bacteriol*, **170**, 5117-5124.

Icho, T. & Raetz, C. R. (1983) Multiple genes for membrane-bound phosphatases in Escherichia coli and their action on phospholipid precursors. *J Bacteriol*, **153**, 722-730.

Isnard, M., Rigal, A., Lazzaroni, J. C., Lazdunski, C.et al. (1994) Maturation and localization of the TolB protein required for colicin import. *J Bacteriol*, **176**, 6392-6396.

Jackowski, S. & Rock, C. O. (1986) Transfer of fatty acids from the 1-position of phosphatidylethanolamine to the major outer membrane lipoprotein of Escherichia coli. *J Biol Chem*, **261**, 11328-11333.

Joshi, A. K., Witkowski, A., Berman, H. A., Zhang, L.et al. (2005) Effect of modification of the length and flexibility of the acyl carrier protein-thioesterase interdomain linker on functionality of the animal fatty acid synthase. *Biochemistry*, **44**, 4100-4107.

Kameda, K. & Nunn, W. D. (1981) Purification and characterization of acyl coenzyme A synthetase from Escherichia coli. *J Biol Chem*, **256**, 5702-5707.

Karimova, G., Dautin, N. & Ladant, D. (2005) Interaction network among Escherichia coli membrane proteins involved in cell division as revealed by bacterial two-hybrid analysis. *J Bacteriol*, **187**, 2233-2243.

Karimova, G., Pidoux, J., Ullmann, A. & Ladant, D. (1998) A bacterial two-hybrid system based on a reconstituted signal transduction pathway. *Proc Natl Acad Sci U S A*, **95**, 5752-5756.

Karimova, G., Robichon, C. & Ladant, D. (2009) Characterization of YmgF, a 72-residue inner membrane protein that associates with the Escherichia coli cell division machinery. *J Bacteriol*, **191**, 333-346.

Kato, A. & Groisman, E. A. (2004) Connecting two-component regulatory systems by a protein that protects a response regulator from dephosphorylation by its cognate sensor. *Genes Dev*, **18**, 2302-2313.

Keating, D. H., Zhang, Y. & Cronan, J. E. J. (1996) The apparent coupling between synthesis and posttranslational modification of Escherichia coli acyl carrier protein is due to inhibition of amino acid biosynthesis. *J Bacteriol*, **178**, 2662-2667.

Keatinge-Clay, A. T., Shelat, A. A., Savage, D. F., Tsai, S. C.et al. (2003) Catalysis, specificity, and ACP docking site of Streptomyces coelicolor malonyl-CoA:ACP transacylase. *Structure*, **11**, 147-154.

Kennedy, E. P. (1982) Osmotic regulation and the biosynthesis of membrane-derived oligosaccharides in Escherichia coli. *Proc Natl Acad Sci U S A*, **79**, 1092-1095.

Kennedy, E. P., Rumley, M. K., Schulman, H. & Van Golde, L. M. (1976) Identification of sn-glycero-1-phosphate and phosphoethanolamine residues linked to the membrane-derived Oligosaccharides of Escherichia coli. *J Biol Chem*, **251**, 4208-4213.

Kikuchi, S., Shibuya, I. & Matsumoto, K. (2000) Viability of an Escherichia coli pgsA null mutant lacking detectable phosphatidylglycerol and cardiolipin. *J Bacteriol*, **182**, 371-376.

Kim, Y. & Prestegard, J. H. (1989) A dynamic model for the structure of acyl carrier protein in solution. *Biochemistry*, **28**, 8792-8797.

Kim, Y. & Prestegard, J. H. (1990) Refinement of the NMR structures for acyl carrier protein with scalar coupling data. *Proteins*, **8**, 377-385.

Kivistik, P. A., Kivi, R., Kivisaar, M. & Hõrak, R. (2009) Identification of ColR binding consensus and prediction of regulon of ColRS two-component system. *BMC Mol Biol*, **10**, 46.

Kleinschmidt, J. H. (2003) Membrane protein folding on the example of outer membrane protein A of Escherichia coli. *Cell Mol Life Sci*, **60**, 1547-1558.

Kloser, A., Laird, M., Deng, M. & Misra, R. (1998) Modulations in lipid A and phospholipid biosynthesis pathways influence outer membrane protein assembly in Escherichia coli K-12. *Mol Microbiol*, **27**, 1003-1008.

Koonin, E. V. (1996) A duplicated catalytic motif in a new superfamily of phosphohydrolases and phospholipid synthases that includes poxvirus envelope proteins. *Trends Biochem Sci*, **21**, 242-243.

Kunau, W. H., Dommes, V. & Schulz, H. (1995) beta-oxidation of fatty acids in mitochondria, peroxisomes, and bacteria: a century of continued progress. *Prog Lipid Res*, **34**, 267-342.

Kvint, K., Hosbond, C., Farewell, A., Nybroe, O.et al. (2000) Emergency derepression: stringency allows RNA polymerase to override negative control by an active repressor. *Mol Microbiol*, **35**, 435-443.

Kvint, K., Nachin, L., Diez, A. & Nyström, T. (2003) The bacterial universal stress protein: function and regulation. *Curr Opin Microbiol*, **6**, 140-145.

Lange, R. & Hengge-Aronis, R. (1994) The cellular concentration of the sigma S subunit of RNA polymerase in Escherichia coli is controlled at the levels of transcription, translation, and protein stability. *Genes Dev*, **8**, 1600-1612.

Larson, T. J. & Dowhan, W. (1976) Ribosomal-associated phosphatidylserine synthetase from Escherichia coli: purification by substrate-specific elution from phosphocellulose using cytidine 5'-diphospho-1,2-diacyl-sn-glycerol. *Biochemistry*, **15**, 5212-5218.

Larson, T. J., Ludtke, D. N. & Bell, R. M. (1984) sn-Glycerol-3-phosphate auxotrophy of plsB strains of Escherichia coli: evidence that a second mutation, plsX, is required. *J Bacteriol*, **160**, 711-717.

Lau, F. W., Chen, X. & Bowie, J. U. (1999) Active sites of diacylglycerol kinase from Escherichia coli are shared between subunits. *Biochemistry*, **38**, 5521-5527.

Lee, H., Hsu, F., Turk, J. & Groisman, E. A. (2004) The PmrA-regulated pmrC gene mediates phosphoethanolamine modification of lipid A and polymyxin resistance in Salmonella enterica. *J Bacteriol*, **186**, 4124-4133.

Lee, L. J., Barrett, J. A. & Poole, R. K. (2005) Genome-wide transcriptional response of chemostat-cultured Escherichia coli to zinc. *J Bacteriol*, **187**, 1124-1134.

Leibundgut, M., Maier, T., Jenni, S. & Ban, N. (2008) The multienzyme architecture of eukaryotic fatty acid synthases. *Curr Opin Struct Biol*, **18**, 714-725.

Lewin, T. M., Wang, P. & Coleman, R. A. (1999) Analysis of amino acid motifs diagnostic for the sn-glycerol-3-phosphate acyltransferase reaction. *Biochemistry*, **38**, 5764-5771.

Li, Q. X. & Dowhan, W. (1988) Structural characterization of Escherichia coli phosphatidylserine decarboxylase. *J Biol Chem*, **263**, 11516-11522.

Li, Q. X. & Dowhan, W. (1990) Studies on the mechanism of formation of the pyruvate prosthetic group of phosphatidylserine decarboxylase from Escherichia coli. *J Biol Chem*, **265**, 4111-4115.

Liu, X. & De Wulf, P. (2004) Probing the ArcA-P modulon of Escherichia coli by whole genome transcriptional analysis and sequence recognition profiling. *J Biol Chem*, **279**, 12588-12597.

Lonetto, M., Gribskov, M. & Gross, C. A. (1992) The sigma 70 family: sequence conservation and evolutionary relationships. *J Bacteriol*, **174**, 3843-3849.

Louie, K., Chen, Y. C. & Dowhan, W. (1986) Substrate-induced membrane association of phosphatidylserine synthase from Escherichia coli. *J Bacteriol*, **165**, 805-812.

Lu, Y., Zhang, F., Grimes, K. D., Lee, R. E.et al. (2007) Topology and active site of PlsY: the bacterial acylphosphate:glycerol-3-phosphate acyltransferase. *J Biol Chem*, **282**, 11339-11346.

Lu, Y., Zhang, Y., Grimes, K. D., Qi, J.et al. (2006) Acyl-phosphates initiate membrane phospholipid synthesis in Gram-positive pathogens. *Mol Cell*, **23**, 765-772.

Maekawa, T., Yanagihara, K. & Ohtsubo, E. (1996) Specific nicking at the 3' ends of the terminal inverted repeat sequences in transposon Tn3 by transposase and an E. coli protein ACP. *Genes Cells*, **1**, 1017-1030.

Malinverni, J. C. & Silhavy, T. J. (2009) An ABC transport system that maintains lipid asymmetry in the gram-negative outer membrane. *Proc Natl Acad Sci U S A*, **106**, 8009-8014.

Marchal, K., De Keersmaecker, S., Monsieurs, P., van Boxel, N.et al. (2004) In silico identification and experimental validation of PmrAB targets in Salmonella typhimurium by regulatory motif detection. *Genome Biol*, **5**, R9.

Mascher, T., Helmann, J. D. & Unden, G. (2006) Stimulus perception in bacterial signal-transducing histidine kinases. *Microbiol Mol Biol Rev*, **70**, 910-938.

Masuda, N. & Church, G. M. (2003) Regulatory network of acid resistance genes in Escherichia coli. *Mol Microbiol*, **48**, 699-712.

Matsumoto, K. (2001) Dispensable nature of phosphatidylglycerol in Escherichia coli: dual roles of anionic phospholipids. *Mol Microbiol*, **39**, 1427-1433.

Merlie, J. P. & Pizer, L. I. (1973) Regulation of phospholipid synthesis in Escherichia coli by guanosine tetraphosphate. *J Bacteriol*, **116**, 355-366.

Mileykovskaya, E. & Dowhan, W. (2000) Visualization of phospholipid domains in Escherichia coli by using the cardiolipin-specific fluorescent dye 10-N-nonyl acridine orange. *J Bacteriol*, **182**, 1172-1175.

Mileykovskaya, E., Ryan, A. C., Mo, X., Lin, C.et al. (2009) Phosphatidic acid and N-acylphosphatidylethanolamine form membrane domains in Escherichia coli mutant lacking cardiolipin and phosphatidylglycerol. *J Biol Chem*, **284**, 2990-3000.

Mileykovskaya, E., Zhang, M. & Dowhan, W. (2005) Cardiolipin in energy transducing membranes. *Biochemistry (Mosc)*, **70**, 154-158.

Miller, K. J. & Kennedy, E. P. (1987) Transfer of phosphoethanolamine residues from phosphatidylethanolamine to the membrane-derived oligosaccharides of Escherichia coli. *J Bacteriol*, **169**, 682-686.

Missiakas, D., Betton, J. M. & Raina, S. (1996) New components of protein folding in extracytoplasmic compartments of Escherichia coli SurA, FkpA and Skp/OmpH. *Mol Microbiol*, **21**, 871-884.

Mogensen, J. E. & Otzen, D. E. (2005) Interactions between folding factors and bacterial outer membrane proteins. *Mol Microbiol*, **57**, 326-346.

Mohanty, B. K. & Kushner, S. R. (1999) Residual polyadenylation in poly(A) polymerase I (pcnB) mutants of Escherichia coli does not result from the activity encoded by the f310 gene. *Mol Microbiol*, **34**, 1109-1119.

Moon, K. & Gottesman, S. (2009) A PhoQ/P-regulated small RNA regulates sensitivity of Escherichia coli to antimicrobial peptides. *Mol Microbiol*, **74**, 1314-1330.

Morgan-Kiss, R. M. & Cronan, J. E. (2004) The Escherichia coli fadK (ydiD) gene encodes an anerobically regulated short chain acyl-CoA synthetase. *J Biol Chem*, **279**, 37324-37333.

Nichols, C. E., Lamb, H. K., Lockyer, M., Charles, I. G.et al. (2007) Characterization of Salmonella typhimurium YegS, a putative lipid kinase homologous to eukaryotic sphingosine and diacylglycerol kinases. *Proteins*, **68**, 13-25.

Niki, H., Imamura, R., Kitaoka, M., Yamanaka, K.et al. (1992) E.coli MukB protein involved in chromosome partition forms a homodimer with a rod-and-hinge structure having DNA binding and ATP/GTP binding activities. *EMBO J*, **11**, 5101-5109.

Nishibori, A., Kusaka, J., Hara, H., Umeda, M.et al. (2005) Phosphatidylethanolamine domains and localization of phospholipid synthases in Bacillus subtilis membranes. *J Bacteriol*, **187**, 2163-2174.

Nishijima, S., Asami, Y., Uetake, N., Yamagoe, S.et al. (1988) Disruption of the Escherichia coli cls gene responsible for cardiolipin synthesis. *J Bacteriol*, **170**, 775-780.

Nunn, W. D. & Cronan, J. E. J. (1974) rel Gene control of lipid synthesis in Escherichia coli. Evidence for eliminating fatty acid synthesis as the sole regulatory site. *J Biol Chem*, **249**, 3994-3996.

Nunn, W. D., Giffin, K., Clark, D. & Cronan, J. E. J. (1983) Role for fadR in unsaturated fatty acid biosynthesis in Escherichia coli. *J Bacteriol*, **154**, 554-560.

Nyström, T. & Neidhardt, F. C. (1992) Cloning, mapping and nucleotide sequencing of a gene encoding a universal stress protein in Escherichia coli. *Mol Microbiol*, **6**, 3187-3198.

Nyström, T. & Neidhardt, F. C. (1994) Expression and role of the universal stress protein, UspA, of Escherichia coli during growth arrest. *Mol Microbiol*, **11**, 537-544.

Overath, P., Pauli, G. & Schairer, H. U. (1969) Fatty acid degradation in Escherichia coli. An inducible acyl-CoA synthetase, the mapping of old-mutations, and the isolation of regulatory mutants. *Eur J Biochem*, **7**, 559-574.

Overgaard, M., Kallipolitis, B. & Valentin-Hansen, P. (2009) Modulating the bacterial surface with small RNAs: a new twist on PhoP/Q-mediated lipopolysaccharide modification. *Mol Microbiol*, **74**, 1289-1294.

Paoletti, L., Lu, Y., Schujman, G. E., de Mendoza, D.et al. (2007) Coupling of fatty acid and phospholipid synthesis in Bacillus subtilis. *J Bacteriol*, **189**, 5816-5824.

Pawar, S. & Schulz, H. (1981) The structure of the multienzyme complex of fatty acid oxidation from Escherichia coli. *J Biol Chem*, **256**, 3894-3899.

Perez, J. C. & Groisman, E. A. (2007) Acid pH activation of the PmrA/PmrB two-component regulatory system of Salmonella enterica. *Mol Microbiol*, **63**, 283-293.

Pizer, L. I. & Merlie, J. P. (1973) Effect of serine hydroxamate on phospholipid synthesis in Escherichia coli. *J Bacteriol*, **114**, 980-987.

Podkovyrov, S. & Larson, T. J. (1995) Lipid biosynthetic genes and a ribosomal protein gene are cotranscribed. *FEBS Lett*, **368**, 429-431.

Podkovyrov, S. M. & Larson, T. J. (1996) Identification of promoter and stringent regulation of transcription of the fabH, fabD and fabG genes encoding fatty acid biosynthetic enzymes of Escherichia coli. *Nucleic Acids Res*, **24**, 1747-1752.

Polakis, S. E., Guchhait, R. B. & Lane, M. D. (1973) Stringent control of fatty acid synthesis in Escherichia coli. Possible regulation of acetyl coenzyme A carboxylase by ppGpp. *J Biol Chem*, **248**, 7957-7966.

Potrykus, K. & Cashel, M. (2008) (p)ppGpp: still magical?. *Annu Rev Microbiol*, **62**, 35-51.

Puig, O., Caspary, F., Rigaut, G., Rutz, B.et al. (2001) The tandem affinity purification (TAP) method: a general procedure of protein complex purification. *Methods*, **24**, 218-229.

Quigley, B. R. & Tropp, B. E. (2009) E. coli cardiolipin synthase: function of N-terminal conserved residues. *Biochim Biophys Acta*, **1788**, 2107-2113.

Raben, D. M. & Wattenberg, B. W. (2009) Signaling at the membrane interface by the DGK/SK enzyme family. *J Lipid Res*, **50 Suppl**, S35-9.

Raetz, C. R. (1986) Molecular genetics of membrane phospholipid synthesis. *Annu Rev Genet*, **20**, 253-295.

Raetz, C. R. & Dowhan, W. (1990) Biosynthesis and function of phospholipids in Escherichia coli. *J Biol Chem*, **265**, 1235-1238.

Raetz, C. R. & Newman, K. F. (1978) Neutral lipid accumulation in the membranes of Escherichia coli mutants lacking diglyceride kinase. *J Biol Chem*, **253**, 3882-3887.

Raetz, C. R. H. & Whitfield, C. (2002) Lipopolysaccharide endotoxins. *Annu Rev Biochem*, **71**, 635-700.

Raetz, C. R. H., Reynolds, C. M., Trent, M. S. & Bishop, R. E. (2007) Lipid A modification systems in gram-negative bacteria. *Annu Rev Biochem*, **76**, 295-329.

Raetz, C. R., Kantor, G. D., Nishijima, M. & Jones, M. L. (1981) Isolation of Escherichia coli mutants with elevated levels of membrane enzymes. A trans-acting mutation controlling diglyceride kinase. *J Biol Chem*, **256**, 2109-2112.

Ragolia, L. & Tropp, B. E. (1994) The effects of phosphoglycerides on Escherichia coli cardiolipin synthase. *Biochim Biophys Acta*, **1214**, 323-332.

Reynolds, C. M., Kalb, S. R., Cotter, R. J. & Raetz, C. R. H. (2005) A phosphoethanolamine transferase specific for the outer 3-deoxy-D-manno-octulosonic acid residue of Escherichia coli lipopolysaccharide. Identification of the eptB gene and Ca2+ hypersensitivity of an eptB deletion mutant. *J Biol Chem*, **280**, 21202-21211.

Reynolds, C. M., Ribeiro, A. A., McGrath, S. C., Cotter, R. J.et al. (2006) An outer membrane enzyme encoded by Salmonella typhimurium lpxR that removes the 3'-acyloxyacyl moiety of lipid A. *J Biol Chem*, **281**, 21974-21987.

Rezuchova, B., Miticka, H., Homerova, D., Roberts, M.et al. (2003) New members of the Escherichia coli sigmaE regulon identified by a two-plasmid system. *FEMS Microbiol Lett*, **225**, 1-7.

Rhodius, V. A., Suh, W. C., Nonaka, G., West, J.et al. (2006) Conserved and variable functions of the sigmaE stress response in related genomes. *PLoS Biol*, **4**, e2.

Ried, G., Hindennach, I. & Henning, U. (1990) Role of lipopolysaccharide in assembly of Escherichia coli outer membrane proteins OmpA, OmpC, and OmpF. *J Bacteriol*, **172**, 6048-6053.

Rigaut, G., Shevchenko, A., Rutz, B., Wilm, M.et al. (1999) A generic protein purification method for protein complex characterization and proteome exploration. *Nat Biotechnol*, **17**, 1030-1032.

Riley, M., Abe, T., Arnaud, M. B., Berlyn, M. K. B.et al. (2006) Escherichia coli K-12: a cooperatively developed annotation snapshot--2005. *Nucleic Acids Res*, **34**, 1-9.

Rock, C. O. & Cronan, J. E. (1996) Escherichia coli as a model for the regulation of dissociable (type II) fatty acid biosynthesis. *Biochim Biophys Acta*, **1302**, 1-16.

Rock, C. O. & Jackowski, S. (1982) Regulation of phospholipid synthesis in Escherichia coli. Composition of the acyl-acyl carrier protein pool in vivo. *J Biol Chem*, **257**, 10759-10765.

Rock, C. O. & Jackowski, S. (1985) Pathways for the incorporation of exogenous fatty acids into phosphatidylethanolamine in Escherichia coli. *J Biol Chem*, **260**, 12720-12724.

Rock, C. O., Cronan, J. E. J. & Armitage, I. M. (1981) Molecular properties of acyl carrier protein derivatives. *J Biol Chem*, **256**, 2669-2674.

Rock, C. O., Goelz, S. E. & Cronan, J. E. J. (1981) Phospholipid synthesis in Escherichia coli. Characteristics of fatty acid transfer from acyl-acyl carrier protein to sn-glycerol 3-phosphate. *J Biol Chem*, **256**, 736-742.

Rock, C. O., Tsay, J. T., Heath, R. & Jackowski, S. (1996) Increased unsaturated fatty acid production associated with a suppressor of the fabA6(Ts) mutation in Escherichia coli. *J Bacteriol*, **178**, 5382-5387.

Romantsov, T., Battle, A. R., Hendel, J. L., Martinac, B.et al. (2010) Protein localization in Escherichia coli cells: comparison of the cytoplasmic membrane proteins ProP, LacY, ProW, AqpZ, MscS, and MscL. *J Bacteriol*, **192**, 912-924.

Romantsov, T., Stalker, L., Culham, D. E. & Wood, J. M. (2008) Cardiolipin controls the osmotic stress response and the subcellular location of transporter ProP in Escherichia coli. *J Biol Chem*, **283**, 12314-12323.

Rosenthal, A. Z., Kim, Y. & Gralla, J. D. (2008) Poising of Escherichia coli RNA polymerase and its release from the sigma 38 C-terminal tail for osmY transcription. *J Mol Biol*, **376**, 938-949.

Rotering, H. & Raetz, C. R. (1983) Appearance of monoglyceride and triglyceride in the cell envelope of Escherichia coli mutants defective in diglyceride kinase. *J Biol Chem*, **258**, 8068-8073.

Ruiz, N., Kahne, D. & Silhavy, T. J. (2009) Transport of lipopolysaccharide across the cell envelope: the long road of discovery. *Nat Rev Microbiol*, **7**, 677-683.

Sankaran, K. & Wu, H. C. (1994) Lipid modification of bacterial prolipoprotein. Transfer of diacylglyceryl moiety from phosphatidylglycerol. *J Biol Chem*, **269**, 19701-19706.

Schmelter, T., Trigatti, B. L., Gerber, G. E. & Mangroo, D. (2004) Biochemical demonstration of the involvement of fatty acyl-CoA synthetase in fatty acid translocation across the plasma membrane. *J Biol Chem*, **279**, 24163-24170.

Schmitzberger, F., Kilkenny, M. L., Lobley, C. M. C., Webb, M. E.et al. (2003) Structural constraints on protein self-processing in L-aspartate-alpha-decarboxylase. *EMBO J*, **22**, 6193-6204.

Sharpe, P. L. & Craig, N. L. (1998) Host proteins can stimulate Tn7 transposition: a novel role for the ribosomal protein L29 and the acyl carrier protein. *EMBO J*, **17**, 5822-5831.

Shibuya, I., Miyazaki, C. & Ohta, A. (1985) Alteration of phospholipid composition by combined defects in phosphatidylserine and cardiolipin synthases and physiological consequences in Escherichia coli. *J Bacteriol*, **161**, 1086-1092.

Siarheyeva, A., Liu, R. & Sharom, F. J. (2010) Characterization of an asymmetric occluded state of P-glycoprotein with two bound nucleotides: implications for catalysis. *J Biol Chem*, **285**, 7575-7586.

Smith, R. L., O'Toole, J. F., Maguire, M. E. & Sanders, C. R. 2. (1994) Membrane topology of Escherichia coli diacylglycerol kinase. *J Bacteriol*, **176**, 5459-5465.

Snell, K. D., Feng, F., Zhong, L., Martin, D.et al. (2002) YfcX enables medium-chain-length poly(3-hydroxyalkanoate) formation from fatty acids in recombinant Escherichia coli fadB strains. *J Bacteriol*, **184**, 5696-5705.

Soncini, F. C. & Groisman, E. A. (1996) Two-component regulatory systems can interact to process multiple environmental signals. *J Bacteriol*, **178**, 6796-6801.

Sperandeo, P., Dehò, G. & Polissi, A. (2009) The lipopolysaccharide transport system of Gram-negative bacteria. *Biochim Biophys Acta*, **1791**, 594-602.

Srivatsan, A. & Wang, J. D. (2008) Control of bacterial transcription, translation and replication by (p)ppGpp. *Curr Opin Microbiol*, **11**, 100-105.

Stenberg, F., Chovanec, P., Maslen, S. L., Robinson, C. V.et al. (2005) Protein complexes of the Escherichia coli cell envelope. *J Biol Chem*, **280**, 34409-34419.

Stingl, K., Schauer, K., Ecobichon, C., Labigne, A.et al. (2008) In vivo interactome of Helicobacter pylori urease revealed by tandem affinity purification. *Mol Cell Proteomics*, **7**, 2429-2441.

Stofko-Hahn, R. E., Carr, D. W. & Scott, J. D. (1992) A single step purification for recombinant proteins. Characterization of a microtubule associated protein (MAP 2) fragment which associates with the type II cAMP-dependent protein kinase. *FEBS Lett*, **302**, 274-278.

Sugai, R., Shimizu, H., Nishiyama, K. & Tokuda, H. (2001) Overexpression of yccL (gnsA) and ydfY (gnsB) increases levels of unsaturated fatty acids and suppresses both the temperature-sensitive fabA6 mutation and cold-sensitive secG null mutation of Escherichia coli. *J Bacteriol*, **183**, 5523-5528.

Sugai, R., Shimizu, H., Nishiyama, K. & Tokuda, H. (2004) Overexpression of gnsA, a multicopy suppressor of the secG null mutation, increases acidic phospholipid contents by inhibiting phosphatidylethanolamine synthesis at low temperatures. *J Bacteriol*, **186**, 5968-5971.

Suits, M. D. L., Sperandeo, P., Dehò, G., Polissi, A.et al. (2008) Novel structure of the conserved gram-negative lipopolysaccharide transport protein A and mutagenesis analysis. *J Mol Biol*, **380**, 476-488.

Suzuki, M., Hara, H. & Matsumoto, K. (2002) Envelope disorder of Escherichia coli cells lacking phosphatidylglycerol. *J Bacteriol*, **184**, 5418-5425.

Sánchez, A. M., Bennett, G. N. & San, K. (2005) Effect of different levels of NADH availability on metabolic fluxes of Escherichia coli chemostat cultures in defined medium. *J Biotechnol*, **117**, 395-405.

Taguchi, M., Izui, K. & Katsuki, H. (1980) Augmentation of cyclopropane fatty acid synthesis under stringent control in Escherichia coli. *J Biochem*, **88**, 1879-1882.

Takiff, H. E., Baker, T., Copeland, T., Chen, S. M.et al. (1992) Locating essential Escherichia coli genes by using mini-Tn10 transposons: the pdxJ operon. *J Bacteriol*, **174**, 1544-1553.

Tam, C. & Missiakas, D. (2005) Changes in lipopolysaccharide structure induce the sigma(E)-dependent response of Escherichia coli. *Mol Microbiol*, **55**, 1403-1412.

Tanaka, Y., Tsujimura, A., Fujita, N., Isono, S.et al. (1989) Cloning and analysis of an Escherichia coli operon containing the rpmF gene for ribosomal protein L32 and the gene for a 30-kilodalton protein. *J Bacteriol*, **171**, 5707-5712.

Taylor, F. R. & Cronan, J. E. J. (1979) Cyclopropane fatty acid synthase of Escherichia coli. Stabilization, purification, and interaction with phospholipid vesicles. *Biochemistry*, **18**, 3292-3300.

Tefsen, B., Bos, M. P., Beckers, F., Tommassen, J.et al. (2005) MsbA is not required for phospholipid transport in Neisseria meningitidis. *J Biol Chem*, **280**, 35961-35966.

Therisod, H. & Kennedy, E. P. (1987) The function of acyl carrier protein in the synthesis of membrane-derived oligosaccharides does not require its phosphopantetheine prosthetic group. *Proc Natl Acad Sci U S A*, **84**, 8235-8238.

Torrents, E., Grinberg, I., Gorovitz-Harris, B., Lundström, H.et al. (2007) NrdR controls differential expression of the Escherichia coli ribonucleotide reductase genes. *J Bacteriol*, **189**, 5012-5021.

Touzé, T., Gouesbet, G., Boiangiu, C., Jebbar, M.et al. (2001) Glycine betaine loses its osmoprotective activity in a bspA strain of Erwinia chrysanthemi. *Mol Microbiol*, **42**, 87-99.

Touzé, T., Tran, A. X., Hankins, J. V., Mengin-Lecreulx, D.et al. (2008) Periplasmic phosphorylation of lipid A is linked to the synthesis of undecaprenyl phosphate. *Mol Microbiol*, **67**, 264-277.

Travers, A. A. (1980) Promoter sequence for stringent control of bacterial ribonucleic acid synthesis. *J Bacteriol*, **141**, 973-976.

Traxler, M. F., Summers, S. M., Nguyen, H., Zacharia, V. M.et al. (2008) The global, ppGpp-mediated stringent response to amino acid starvation in Escherichia coli. *Mol Microbiol*, **68**, 1128-1148.

Trent, M. S., Pabich, W., Raetz, C. R. & Miller, S. I. (2001) A PhoP/PhoQ-induced Lipase (PagL) that catalyzes 3-O-deacylation of lipid A precursors in membranes of Salmonella typhimurium. *J Biol Chem*, **276**, 9083-9092.

Tropp, B. E. (1997) Cardiolipin synthase from Escherichia coli. *Biochim Biophys Acta*, **1348**, 192-200.

Turnbull, A. P., Rafferty, J. B., Sedelnikova, S. E., Slabas, A. R.et al. (2001) Crystallization and preliminary X-ray analysis of the glycerol-3-phosphate 1-acyltransferase from squash (Cucurbita moschata). *Acta Crystallogr D Biol Crystallogr*, **57**, 451-453.

Usui, M., Sembongi, H., Matsuzaki, H., Matsumoto, K.et al. (1994) Primary structures of the wild-type and mutant alleles encoding the phosphatidylglycerophosphate synthase of Escherichia coli. *J Bacteriol*, **176**, 3389-3392.

Van Horn, W. D., Kim, H., Ellis, C. D., Hadziselimovic, A.et al. (2009) Solution nuclear magnetic resonance structure of membrane-integral diacylglycerol kinase. *Science*, **324**, 1726-1729.

Veyron-Churlet, R., Bigot, S., Guerrini, O., Verdoux, S.et al. (2005) The biosynthesis of mycolic acids in Mycobacterium tuberculosis relies on multiple specialized elongation complexes interconnected by specific protein-protein interactions. *J Mol Biol*, **353**, 847-858.

Veyron-Churlet, R., Guerrini, O., Mourey, L., Daffé, M.et al. (2004) Protein-protein interactions within the Fatty Acid Synthase-II system of Mycobacterium tuberculosis are essential for mycobacterial viability. *Mol Microbiol*, **54**, 1161-1172.

Voelker, D. R. (1997) Phosphatidylserine decarboxylase. *Biochim Biophys Acta*, **1348**, 236-244.

Wang, A. Y. & Cronan, J. E. J. (1994) The growth phase-dependent synthesis of cyclopropane fatty acids in Escherichia coli is the result of an RpoS(KatF)-dependent promoter plus enzyme instability. *Mol Microbiol*, **11**, 1009-1017.

Wang, A. Y., Grogan, D. W. & Cronan, J. E. J. (1992) Cyclopropane fatty acid synthase of Escherichia coli: deduced amino acid sequence, purification, and studies of the enzyme active site. *Biochemistry*, **31**, 11020-11028.

Ward, A., Reyes, C. L., Yu, J., Roth, C. B.et al. (2007) Flexibility in the ABC transporter MsbA: Alternating access with a twist. *Proc Natl Acad Sci U S A*, **104**, 19005-19010.

Weber, H., Polen, T., Heuveling, J., Wendisch, V. F.et al. (2005) Genome-wide analysis of the general stress response network in Escherichia coli: sigmaS-dependent genes, promoters, and sigma factor selectivity. *J Bacteriol*, **187**, 1591-1603.

Weimar, J. D., DiRusso, C. C., Delio, R. & Black, P. N. (2002) Functional role of fatty acyl-coenzyme A synthetase in the transmembrane movement and activation of exogenous long-chain fatty acids. Amino acid residues within the ATP/AMP signature motif of Escherichia coli FadD are required for enzyme activity and fatty acid transport. *J Biol Chem*, **277**, 29369-29376.

White, S. W., Zheng, J., Zhang, Y. & Rock (2005) The structural biology of type II fatty acid biosynthesis. *Annu Rev Biochem*, **74**, 791-831.

Wickner, W. (1989) Secretion and membrane assembly. *Trends Biochem Sci*, **14**, 280-283.

Wilkison, W. O. & Bell, R. M. (1997) sn-Glycerol-3-phosphate acyltransferase from Escherichia coli. *Biochim Biophys Acta*, **1348**, 3-9.

Winfield, M. D. & Groisman, E. A. (2004) Phenotypic differences between Salmonella and Escherichia coli resulting from the disparate regulation of homologous genes. *Proc Natl Acad Sci U S A*, **101**, 17162-17167.

Wösten, M. M. & Groisman, E. A. (1999) Molecular characterization of the PmrA regulon. *J Biol Chem*, **274**, 27185-27190.

Wösten, M. M., Kox, L. F., Chamnongpol, S., Soncini, F. C.et al. (2000) A signal transduction system that responds to extracellular iron. *Cell*, **103**, 113-125.

Xu, Y., Piston, D. W. & Johnson, C. H. (1999) A bioluminescence resonance energy transfer (BRET) system: application to interacting circadian clock proteins. *Proc Natl Acad Sci U S A*, **96**, 151-156.

Yan, A., Guan, Z. & Raetz, C. R. H. (2007) An undecaprenyl phosphate-aminoarabinose flippase required for polymyxin resistance in Escherichia coli. *J Biol Chem*, **282**, 36077-36089.

Yang, S. Y., He Yang, X. Y., Healy-Louie, G., Schulz, H.et al. (1991) Nucleotide sequence of the fadA gene. Primary structure of 3-ketoacyl-coenzyme A thiolase from Escherichia coli and the structural organization of the fadAB operon. *J Biol Chem*, **266**, 16255.

Yang, X. Y., Schulz, H., Elzinga, M. & Yang, S. Y. (1991) Nucleotide sequence of the promoter and fadB gene of the fadBA operon and primary structure of the multifunctional fatty acid oxidation protein from Escherichia coli. *Biochemistry*, **30**, 6788-6795.

Yoshimura, M., Oshima, T. & Ogasawara, N. (2007) Involvement of the YneS/YgiH and PlsX proteins in phospholipid biosynthesis in both Bacillus subtilis and Escherichia coli. *BMC Microbiol*, **7**, 69.

Zaslaver, A., Bren, A., Ronen, M., Itzkovitz, S.et al. (2006) A comprehensive library of fluorescent transcriptional reporters for Escherichia coli. *Nat Methods*, **3**, 623-628.

Zeghouf, M., Li, J., Butland, G., Borkowska, A.et al. (2004) Sequential Peptide Affinity (SPA) system for the identification of mammalian and bacterial protein complexes. *J Proteome Res*, **3**, 463-468.

Zhang, Y. & Cronan, J. E. J. (1996) Polar allele duplication for transcriptional analysis of consecutive essential genes: application to a cluster of Escherichia coli fatty acid biosynthetic genes. *J Bacteriol*, **178**, 3614-3620.

Zhang, Y. & Cronan, J. E. J. (1998) Transcriptional analysis of essential genes of the Escherichia coli fatty acid biosynthesis gene cluster by functional replacement with the analogous Salmonella typhimurium gene cluster. *J Bacteriol*, **180**, 3295-3303.

Zhang, Y. & Rock, C. O. (2008) Thematic review series: Glycerolipids. Acyltransferases in bacterial glycerophospholipid synthesis. *J Lipid Res*, **49**, 1867-1874.

Zhang, Y. & Rock, C. O. (2008) Membrane lipid homeostasis in bacteria. *Nat Rev Microbiol*, **6**, 222-233.

Zhang, Y., Wu, B., Zheng, J. & Rock, C. O. (2003) Key residues responsible for acyl carrier protein and beta-ketoacyl-acyl carrier protein reductase (FabG) interaction. *J Biol Chem*, **278**, 52935-52943.

Zhou, Z., Lin, S., Cotter, R. J. & Raetz, C. R. (1999) Lipid A modifications characteristic of Salmonella typhimurium are induced by NH4VO3 in Escherichia coli K12. Detection of 4-amino-4-deoxy-L-arabinose, phosphoethanolamine and palmitate. *J Biol Chem*, **274**, 18503-18514.

Zhou, Z., Ribeiro, A. A., Lin, S., Cotter, R. J.et al. (2001) Lipid A modifications in polymyxin-resistant Salmonella typhimurium: PMRA-dependent 4-amino-4-deoxy-L-arabinose, and phosphoethanolamine incorporation. *J Biol Chem*, **276**, 43111-43121.

Zhu, K., Zhang, Y. & Rock, C. O. (2009) Transcriptional regulation of membrane lipid homeostasis in Escherichia coli. *J Biol Chem*, **284**, 34880-34888.

van Aalten, D. M., DiRusso, C. C., Knudsen, J. & Wierenga, R. K. (2000) Crystal structure of FadR, a fatty acid-responsive transcription factor with a novel acyl coenzyme A-binding fold. *EMBO J*, **19**, 5167-5177.

van Klompenburg, W., Nilsson, I., von Heijne, G. & de Kruijff, B. (1997) Anionic phospholipids are determinants of membrane protein topology. *EMBO J*, **16**, 4261-4266.

van den Berg, B., Black, P. N., Clemons, W. M. J. & Rapoport, T. A. (2004) Crystal structure of the long-chain fatty acid transporter FadL. *Science (80-)*, **304**, 1506-1509.

von Heijne, G. (1989) Control of topology and mode of assembly of a polytopic membrane protein by positively charged residues. *Nature*, **341**, 456-458.